

L. I. Yastrebov and A. A. Katsnelson

Foundations
of one-electron theory
of solids

$C_0 V V C_0 V C_0 V$

$$Z_{*}^2 \left\{ \frac{4\pi}{\Omega} \sum_q \frac{1}{q^2} \exp\left(-\frac{q^2}{4\eta}\right) \right.$$

Mir Publishers Moscow

Foundations of one-electron theory of solids

L.I. Yastrebov and A.A. Katsnelson

Foundations of one-electron theory of solids



Mir Publishers Moscow

Translated from Russian by E. Strelchenko

First published 1987
Revised from the 1981 Russian edition

ISBN 0-88318-540-7

Printed in the Union of Soviet Socialist Republics

© Издательство «Наука», Главная редакция
физико-математической литературы, 1981
© English translation, Mir Publishers, 1987

Contents

Preface 7

Introduction 11

Chapter 1. Principles of the one-electron theory

Part 1

Theoretical principles of the pseudopotential method

Chapter 2. Scattering theory for "solid-state people"

- 2.1. Mathematical formalism 23
- 2.2. Scattering on an isolated potential 31
- 2.3. Pseudism and scattering 46
- 2.4. Bound states, pseudopotentials and the convergence of series 54
- 2.5. Scattering theory and potential formfactors 61

Chapter 3. Theory of potential

- 3.1. Potential seen by an atomic electron 69
- 3.2. Dielectric screening 83
- 3.3. The self-consistency of pseudopotential and additive screening 99
- 3.4. Muffin-tin potential 107
- 3.5. Average value of the screened potential 124

Chapter 4. Theory of pseudopotential formfactors

- 4.1. Nonlocality, the energy dependence of formfactors and perturbation theory 132
- 4.2. The OPW formfactor 144
- 4.3. Phase-shift formfactors 157
- 4.4. Effective medium and pseudopotential formfactors 173

Chapter 5. Pseudism and the secular equations of band theory

- 5.1. The Green's function (or KKR) method 181
- 5.2. Pseudopotential secular equations 196

Part 2

The use of pseudopotential theory for crystal-structure calculations

Chapter 6. Formalism of crystal-structure energy calculations

- 6.1. Basic assumptions 205
- 6.2. Band structure energy of pure metals and binary alloys 205
- 6.3. Electrostatic energy 223

6.4. The total internal energy of an alloy: second-order perturbation theory and the locality approximation	227
6.5. Higher-order perturbation analysis	232
6.6. OPW nonlocal alloy theory	236
Chapter 7. Pseudopotential theory of alloys. Structure stability application	
7.1. Phase boundaries in terms of pseudopotential theory	241
7.2. Ordered phases, their structures, and existence conditions	245
7.3. Short-range order problems	256
7.4. Crystal structure stability in the OPW approach	261
Chapter 8. Pseudopotential theory and imperfections in crystals	
8.1. Introductory remarks	267
8.2. Crystal lattice vibrations	267
8.3. Static imperfections	279
Chapter 9. Principles of pseudopotential calculations of the properties of metals	
9.1. General	287
9.2. Calculation of the atomic properties of crystalline metals and alloys	287
9.3. Transport properties of noncrystalline metals and alloys	297
References	317
Index	331

Preface

In this book the behavior of electrons in a crystal is described in terms of the one-electron model. Clearly, such a system would be best approached by a many-body formalism but because of mathematical complexities only a very few real problems can be solved in this way. In the one-electron model, each electron is considered separately as moving in the averaged field of the nuclei and all the other electrons. The resulting picture is simpler conceptually, much more tractable mathematically and, at the same time, is quite comprehensive, which makes the one-electron model the most popular approach currently in use in solid state physics.

The concept of pseudopotential that has been developed within the one-electron model over the past 15 to 20 years appears at first sight artificial and inconsistent. It is stated that the interaction potential between an atom and an electron, with its notorious Coulomb singularity at the nucleus, may be replaced with a non-singular potential (or "pseudopotential") without the electron so much as noticing the change. What is more, quite a number of such pseudopotentials are possible for a given atom, each leading to essentially the same overall picture. This seems rather strange because the properties of crystals are uniquely determined by the element's position in the periodic table, that is to say, by the charge of the nucleus that is "left out" in the pseudopotential method.

Naturally enough, many of today's materials scientists are skeptical of the pseudopotential method and consider its predictions unreliable or at least difficult to interpret. Some physicists avoid the use of the method in their work and some use the technique without properly understanding it (which is not an error-proof attitude). It would be desirable therefore to have available an up-to-date solid state theory formulated in terms of "pseudism".

The pseudopotential method was first put forward in the framework of the nearly-free-electron model and it is in these terms that it is mostly discussed in textbooks. However, the method extends far beyond one particular model, indeed it provides insights into virtually every aspect of the behavior of electrons in a crystal. Today, a knowledge of pseudism is mandatory for anyone interested

in a thorough understanding of the properties of solids and their dependence on external conditions and composition.

Although conceptually the pseudopotential method is closely related to and, indeed, originates from scattering theory (to show this is, more or less, the *raison d'être* of this book), up to now there has been no other way to see this than by searching for scraps of relevant information through innumerable journal papers. This is another example of what often happens in science: a theory has been worked out and is already well in use before theorists manage to systematize the material into a consistent form. Surprising as it may seem, we have not even been able to find a definition for pseudism. In our view, the following one would be comprehensive: Pseudism is a system of ideas stemming from the fact that a short-range "compensatory" term may be added to the electron-ion interaction potential which will model the combined action of the nucleus and the core electrons while leaving unchanged the long-range part of the potential. The resulting potential is called a pseudopotential. This interpretation of pseudism is not only valid for model or augmented-plane-wave pseudopotentials but is also suitable for the pseudopotentials in scattering theory and for those involved in band-theory secular equations.

Even such a fundamental phenomenon as the periodicity of chemical elements can be interpreted in terms of pseudism. As the number of atomic electrons increases, the outer uncompleted shell of the atom eventually fills to become what is called a core shell. It may then be dropped from consideration. This means that as the atomic number (and, accordingly, the number of valence electrons) increases, progressively higher shells will be neglected in this manner and the structure of the atom—in terms of its interaction with an external electron—will indeed show periodicity.

Even though we have given the techniques of the one-electron theory a good deal of attention, our primary concern was to provide the reader with an understanding of the underlying physics. Since we did not intend the book to be a literature review, we usually start each new topic with references to the main works on the subject (both original papers and, if need be, reviews) and in the subsequent discussion we only mention the papers we considered the most interesting. We hope that in doing so we have been more or less objective, though admittedly this was not always an easy task.

We found it appropriate to illustrate some applications of the one-electron theory. One example is the relative stability of different crystal structures of metals and alloys, a significant part of the more general and, from the practical point of view, important problem of phase transitions. For those about to study solid state physics, the stability problem is certainly a promising start. All the relevant material presented in Chapter 1 in analytical form, will be found in

Chapter 2 in its “numerical” interpretation. Since crystal stability is still an area of research, the reader is thus invited to see—from inside, as it were—a solid state problem still in its evolution.

In presenting the material, we have tried to show the logic the theory followed as it was developed and, to some extent at least, to show the “scaffolding” used to build it. Whether or not we have succeeded is for the reader to judge.

The concept of pseudopotential, as we believe the reader will become convinced, is a direct consequence of quantum-mechanical scattering theory and we hope therefore that the book will be of interest not only for solid state specialists but also for a reader involved in other “quantum” activities.

The intended reader need have no more background in quantum mechanics and atomic structure than is provided by, say, Shiff's *Quantum Mechanics*. Scattering theory and some other necessary information will be found in the book itself. An elementary knowledge of solid state physics is, of course, desirable, although not necessary.

It should be noted that, as is characteristic of science in general, the literature in this field abounds in jargon. The term “exchange”, for example, is often used instead of the more correct “exchange potential” which, in turn, is an abbreviation for “the potential of the exchange interaction”; “potential” often replaces “pseudopotential” or is sometimes supposed to mean “the potential formfactor”. Whenever appropriate, we have tried to accustom the reader to the jargon, though not of course at the expense of the clarity and cohesion of the material. The same is true of equations: in journal papers indices are frequently omitted and arguments or variables are not meticulously specified. Although a self-evident simplification for a specialist, this is often a stumbling block for a beginner.

The book should be read more than once, though some places can perhaps be skipped over. Some of the topics were chosen because they are likely to be important in the future development of the one-electron model (these topics include scattering outside isoenergetic surfaces, the concept of effective medium, and higher-order perturbation corrections). Some problems are left, unobtrusively, for the reader to solve. For example, will a self-consistent calculation yield wider or narrower energy bands than those resulting from the non-self-consistent treatment? To answer this question, the reader will have to master the material in Chapter 3. Our hope is that in the course of the book the reader will himself pose problems like this and we foresee the satisfaction he (or she) will take in solving them.

We hope that this book will be helpful for both theorists and experimentalists.

The Introduction and Part 1 were written by L.I. Yastrebov (who would like to use an opportunity to express his gratitude to his co-

author for enlightening discussions about pseudopotential secular equations (Sec. 5.2)). Part 2 was written by A.A. Katsnelson.

Members of Solid State Physics Department of the Physics Faculty at Moscow State University were of great help in preparing the manuscript, as were the members of the Metals Science Department at the Moscow Aviation Technology Institute. We gratefully acknowledge their continuous support and valuable comments.

Since the first (Russian) edition of this book was published in 1981, evidence has built up to support the theoretical principles presented therein and to strengthen our confidence in their usefulness for solid state physics. In the first edition our discussion of the applications of the theory was limited to the crystal stability of metals and alloys. Since a great deal of work has been done in other areas in recent years along the same principles, we believed it appropriate, when the English translation was being prepared, to illustrate the theory with more examples of its computational value.

Introduction

Chapter 1

Principles of the one-electron theory

This is the introductory chapter and it is written therefore in a very concise manner. For more details see, for example, [1-5].

1.1.1. The assumptions of the theory. In principle, we should be able to find out everything about a (stationary) crystal by solving Schrödinger's equation for a system of interacting nuclei and electrons that form the crystal. This problem, however, is too hard to solve and some simplifications are therefore unavoidable.

First, it is generally assumed that the nuclei are too massive to follow the rapidly changing spatial distribution of the electrons (the adiabatic approximation). For this reason we actually consider two Schrödinger equations, one for the electrons and the other for the nuclei. In the following we shall only be concerned with the behavior of electrons.

It is further assumed that instead of treating the electronic subsystem as a whole, it is possible to consider separately the motions of individual electrons. Each of them is then thought of as moving in the effective field of the (stationary) nuclei and all the other electrons (hence the name—the effective field approximation). Accordingly, the total electron wave function is expressed in terms of individual electron wave functions, Ψ_i .

Further approximations are made in the actual evaluation of the total function and in the consequent determination of the effective potential as seen by a single electron. It is customary to use Slater's determinant which automatically incorporates the Pauli exclusion principle [6, 7]. This leads to a system of one-electron Schrödinger equations in the Hartree-Fock approximation; the crystal potential includes both Coulomb and exchange interactions between the electrons. The theory discussed in Secs. 2.2-5 and 3.1 is valid, in fact, for any effective potential, that is, in order to develop a general form of the one-electron theory of crystals, the first two approximations are quite sufficient.

1.1.2. Bloch's theorem. The potential acting on an electron in the crystal must possess the periodicity of the crystal:

$$\mathcal{V}(\mathbf{r} + \mathbf{t}_\mathbf{v}) = \mathcal{V}(\mathbf{r}), \quad (1.1)$$

where \mathbf{t}_v is a translation vector (the radius-vector of the v th lattice site). It can be proved that, under the translation \mathbf{t}_v , a one-electron wave function Ψ obeys Bloch's theorem:

$$\Psi(\mathbf{r} + \mathbf{t}_v) = e^{i\mathbf{k}\mathbf{t}_v} \Psi(\mathbf{r}). \quad (1.2)$$

Introducing $u_{\mathbf{k}}(\mathbf{r}) = \Psi(\mathbf{r}) \exp(-i\mathbf{k}\mathbf{t}_v)$, it is easily seen that $u_{\mathbf{k}}(\mathbf{r} + \mathbf{t}_v) = u_{\mathbf{k}}(\mathbf{r})$, so that Ψ may be written in the form

$$\Psi_{\mathbf{k}}(\mathbf{r}) = u_{\mathbf{k}}(\mathbf{r}) e^{i\mathbf{k}\mathbf{r}}, \quad (1.3)$$

where $u_{\mathbf{k}}(\mathbf{r})$ has the periodicity of the crystal lattice. The wave function of an electron in a crystal is thus a plane wave modulated by a periodic factor.

The vector \mathbf{k} is known as a wave vector; for electrons in a vacuum, $E = \hbar^2 k^2 / 2m$, for electrons in a crystal the \mathbf{k} -dependence of E is more complicated. Its actual form (the dispersion law) may be calculated by using the band theory of crystals.

In the following, the crystal potential \mathcal{V} is represented as the sum of the potentials $V(\mathbf{r} - \mathbf{t}_v)$, which are centered at the sites of the crystal lattice. This allows us to write a Schrödinger equation for each such (single-site) potential.* For the information about the crystal to be retained the wave function of this single-site Schrödinger equation must obey Bloch's theorem (1.2).

Bloch's theorem (1.2) may therefore be considered as boundary conditions for a single-site Schrödinger equation.

1.1.3. Reciprocal space. The wave vector \mathbf{k} has a dimension of reciprocal length and is therefore defined not in the coordinate space of the crystal but rather in reciprocal space.

In reciprocal space we can set up a reciprocal lattice: its sites will be specified by radius-vectors \mathbf{g}_n . The vectors \mathbf{t}_v and \mathbf{g}_n are related by the important relationship:

$$\mathbf{t}_v \mathbf{g}_n = 2\pi f_{vn},$$

where f_{vn} 's are integers. It is known that in real space each site can be surrounded by a polyhedron with the property that all points within it are nearer to the given site than to any other one. Such a construction is called the Wigner-Seitz cell. Its analog in reciprocal space is also known as the first Brillouin zone. Calculations of dispersion laws are carried out in band theory only for the wave vectors inside this zone.

If a face of a Brillouin zone is the perpendicular bisector of a vector \mathbf{g}_n (of which there are an infinite number), we may write an obvious

* Throughout the book, the script letters \mathcal{V} and \mathcal{W} denote the potentials and pseudopotentials, respectively, that result from the superposition of the single-site potentials, V , and pseudopotentials, W .

relationship for any vector \mathbf{k} ending at the face:

$$|\mathbf{k}| = |\mathbf{k} - \mathbf{g}_n|. \quad (1.4)$$

A crystal under study is usually assumed to be a large one, with the wave functions having the same values at opposite faces. This means that the vector \mathbf{k} can only take on fixed values, but these are so closely spaced that, if needed, a summation over the allowed \mathbf{k} values may be replaced by a d^3k -integration.

1.1.4. Measurement units. Planck's constant is taken to be unity. The Bohr radius is adopted as the length unit, viz. $a_0 = 0.529177 \text{ \AA}$, the unit of mass is twice the mass of an electron m , and the energy unit is the rydberg, the ionization potential for the hydrogen atom: $1 \text{ Ry} = 13.6 \text{ eV}$. We thus have in atomic units:

$$\begin{aligned} \hbar &= 1, \quad \hbar^2/(me^2) = a_0 = 1, \quad me^2 = 1, \\ m &= 1/2, \quad e^2 = 2, \quad 1 \text{ Ry} = e^2/(2a_0) = 1. \end{aligned}$$

The unit of length in reciprocal space is $2\pi/a$ (a being the lattice constant of the crystal); $k = 2\pi/a (x, y, z)$, with $x \leq y \leq z$; and $\mathbf{g}_n = 2\pi/a (A, B, C)$, where A, B, C are integers. In this system of units, Schrödinger's equation for an electron takes the form:

$$(\hat{H} - E) \Psi_{\mathbf{k}}(\mathbf{r}) \equiv (-\nabla^2 + \mathcal{V}(\mathbf{r}) - E) \Psi_{\mathbf{k}}(\mathbf{r}) = 0. \quad (1.5)$$

1.1.5. General approach to a band problem. For all existing methods of solving Schrödinger's equation (1.5), the underlying principle is virtually the same. First, a set of trial (initial) functions Φ_i is chosen. The unknown function $\Psi_{\mathbf{k}}$ is then presented as an expansion in Φ_i in terms of unknown coefficients $B_i^{\mathbf{k}}$:

$$\Psi_{\mathbf{k}}(\mathbf{r}) = \sum_i B_i^{\mathbf{k}} \Phi_i(\mathbf{r}). \quad (1.6)$$

Substituting (1.6) in (1.5), multiplying on the left by Φ_j^* and integrating over all space, we arrive at a system of equations for $B_i^{\mathbf{k}}$:

$$\sum_i (H_{ji} - ES_{ji}) B_i^{\mathbf{k}} = 0, \quad (1.7)$$

where

$$\begin{aligned} H_{ji} &= \int \Phi_j^*(\mathbf{r}) \hat{H} \Phi_i(\mathbf{r}) d^3r, \\ S_{ji} &= \int \Phi_j^*(\mathbf{r}) \Phi_i(\mathbf{r}) d^3r. \end{aligned} \quad (1.8)$$

The system of linear homogeneous equations (1.7) has nonvanishing solutions if (and only if) its determinant vanishes:

$$\det |H_{ji} - ES_{ji}| = 0. \quad (1.9)$$

Equation (1.9) is called the secular equation, and the determinant in (1.9) the secular determinant. The E values that satisfy (1.9) are the quantities $E(\mathbf{k})$ that we require. Having obtained them, we solve (1.7) for the B_i^k and, at the next step, get $\Psi_k(\mathbf{r})$ by using (1.6).

A secular equation may be very complicated in practice, but the expansion of Ψ_k in terms of trial functions is a common feature for all band theory methods. Sometimes it is convenient to take as trial functions the solutions of a certain auxiliary problem:

$$\hat{H}_0 \Phi_i = \varepsilon_i \Phi_i, \quad (1.10)$$

where \hat{H}_0 is the "initial" Hamiltonian and ε_i —the "initial" dispersion law. Introducing the difference

$$\Delta \equiv \hat{H} - \hat{H}_0, \quad (1.11)$$

we obtain the equation

$$\det |(\varepsilon_i - E) \delta_{ji} + \Delta_{ji}| = 0, \quad (1.12)$$

in which the orthonormality of the functions Φ_i has been taken into account.

When Eq. (1.6) has only two significant terms, Eq. (1.12) can be solved analytically, i.e.

$$E_{\pm} = \bar{E} \pm E_2, \quad (1.13)$$

where

$$\begin{aligned} \bar{E} &= E_0 + E_1, \quad E_0 = (1/2)(\varepsilon_a + \varepsilon_b), \quad E_1 = (1/2)(\Delta_{aa} + \Delta_{bb}), \\ E_2 &= (1/2) \sqrt{(\varepsilon_a + \Delta_{aa} - \varepsilon_b - \Delta_{bb})^2 + 4|\Delta_{ab}|^2}. \end{aligned} \quad (1.14)$$

To see the meaning of this result, consider a system with two quantum levels, ε_a and ε_b . Switching on the interaction Δ between

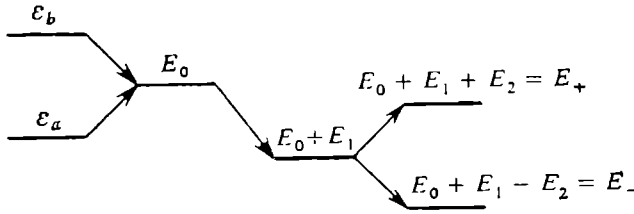


Fig. 1.1. Old levels ε_a and ε_b are hybridized into new levels E_+ and E_- . The E_0 level is introduced to emphasize the inadequacy of the old quantum numbers.

them gives rise to an "intermediate" twofold degenerate level E_0 . The latter then shifts in energy by the amount E_1 (upwards or downwards) and splits into a pair of new levels, E_+ and E_- , separated from the level $\bar{E} = E_0 + E_1$ by $\pm E_2$, as shown in Fig. 1.1.

It can be seen from Eqs. (1.13) and (1.14) that it is impossible to label the new levels with the old quantum numbers (a and b), since hybridization has taken place and new “numbers” have emerged (denoted by $+$ and $-$).

If $\Delta_{ab} (= \Delta_{ba}^*)$ is set to zero, there is no level hybridization and we are simply left with two displaced levels, $\varepsilon_a + \Delta_{aa}$ and $\varepsilon_b + \Delta_{bb}$.

1.1.6. Linear combination of atomic orbitals (LCAO). Let us apply the above formalism to the formation of a crystal by bringing together N atoms, each of which has M levels described by the quantum numbers α (rather, these are sets of quantum numbers). The quantum number i in the expansion (1.6), in fact, includes not only the number α but also the index of each atom ν , which makes the dimensionality of the secular equation (1.9) enormously large. To avoid this the Bloch boundary conditions (1.2) are incorporated into the trial functions themselves which are written for this purpose as (Bloch's) linear combination of atomic orbitals $\varphi_\alpha(\mathbf{r})$, viz.

$$\Phi_\alpha(\mathbf{k}, \mathbf{r}) = \frac{1}{\sqrt{N}} \sum_{\nu} e^{i\mathbf{k}\cdot\mathbf{t}_\nu} \varphi_\alpha(\mathbf{r} - \mathbf{t}_\nu). \quad (1.15)$$

It then turns out that the matrix elements in the secular equation (1.7) are labeled by atomic quantum numbers while the summation over the crystal sites has already been performed within the equation which greatly reduces its size:

$$H_{\beta\alpha} = \sum_{\nu} e^{i\mathbf{k}\cdot\mathbf{t}_\nu} \int \varphi_\beta^*(\mathbf{r}) \hat{H} \varphi_\alpha(\mathbf{r} - \mathbf{t}_\nu) d^3r = H_{\beta\alpha}(\mathbf{k}). \quad (1.16)$$

In the tight-binding limit when the electron interacts, in effect, with only one atom (the central one) the hybridization of the initial dispersion laws (atomic levels) occurs even if the functions of neighboring atoms are orthogonal. The point is that the initial atomic levels are affected by the matrix elements of the central atom's potential, taken between the functions of the central atom and its neighbors. A change in the boundary conditions imposed on the wave function acts as a “perturbation potential” and the requirement that it vanish at infinity is replaced by condition (1.2), which is easily seen to be satisfied by LCAO, Eq. (1.15).

When the functions of the central and neighboring atoms do not overlap (if, for example, the lattice constant goes to infinity), Eq. (1.12) automatically reduces to the equation for the energy levels of a free atom, viz.

$$\det | (\varepsilon_\alpha^{\text{at}} - E) \delta_{\beta\alpha} | = 0. \quad (1.17)$$

1.1.7. Nearly-free-electron model (NFE). In this model a crystal is viewed as a spatial lattice of ions embedded in an electron gas. While in LCAO the perturbation in the eigenvalue problem is the departure of the true potential from the *atomic* potential, in an NFE model it is the departure from *zero*. For a zero potential (in, say, a vacuum) an electron wave function is a plane wave normalized to all space. In a crystal, the normalization integral may be conveniently presented as the sum of contributions from all the lattice sites. Since these contributions are all the same, they can be taken out of the sum and what remains is simply the total number of sites, N . If we introduce the volume of the Wigner-Seitz cell, $\Omega_0 = \Omega/N$, where Ω is the volume of the crystal, we find that the plane waves may just as well be normalized to the Wigner-Seitz cell.

The function $u_{\mathbf{k}}(\mathbf{r})$, which has the periodicity of the crystal, may be expanded in Fourier series over the reciprocal lattice vectors \mathbf{g}_n [8]. As a result, the function $\Psi_{\mathbf{k}}(\mathbf{r})$, Eq. (1.3), then takes the form of an expansion in terms of the plane waves $|\mathbf{k} + \mathbf{g}_n\rangle$:

$$\Psi_{\mathbf{k}}(\mathbf{r}) = \frac{1}{\sqrt{\Omega}} \sum_n B_n e^{i(\mathbf{k} + \mathbf{g}_n)\mathbf{r}}. \quad (1.18)$$

The secular equation (1.12) in the NFE model may be written as

$$\det |(\varepsilon_n - E) \delta_{nn'} + \langle \mathbf{k} + \mathbf{g}_{n'} | \mathcal{T}^{\text{cr}} | \mathbf{k} + \mathbf{g}_n \rangle| = 0, \quad (1.19)$$

where $\varepsilon_n = (\mathbf{k} + \mathbf{g}_n)^2$ and

$$\langle \mathbf{k}' | \mathcal{T}^{\text{cr}} | \mathbf{k} \rangle = \frac{1}{\Omega} \int e^{-i\mathbf{k}'\mathbf{r}} \mathcal{T}^{\text{cr}}(\mathbf{r}) e^{i\mathbf{k}\mathbf{r}} d^3r \quad (1.20)$$

is the matrix element of the crystal potential.

The crystal potential can always be written as the sum of the contributions from all the lattice sites. Since these contributions (or single-site potentials $V(\mathbf{r})$) are all equal, the corresponding integrals are independent of the site index and we have a general expression:

$$\begin{aligned} \langle \mathbf{k}' | \mathcal{T}^{\text{cr}} | \mathbf{k} \rangle &= \frac{1}{\Omega} \sum_{\mathbf{v}} \int V(\mathbf{r} - \mathbf{t}_{\mathbf{v}}) e^{i(\mathbf{k} - \mathbf{k}')\mathbf{r}} d^3r \\ &= S(\mathbf{k} - \mathbf{k}') \langle \mathbf{k}' | V | \mathbf{k} \rangle = S(\mathbf{q}) V(\mathbf{q}). \end{aligned} \quad (1.21)$$

Here we have denoted $\mathbf{q} = \mathbf{k}' - \mathbf{k}$ and introduced the structure factor $S(\mathbf{q})$ and the formfactor of the single-site potential $V(\mathbf{q}) = \langle \mathbf{k} + \mathbf{q} | V | \mathbf{k} \rangle$. Note that, unlike plane wave normalization, the integration in the formfactor is over all space rather than over a

Wigner-Seitz cell alone:

$$S(\mathbf{q}) = \frac{1}{N} \sum_{\mathbf{v}} e^{-i\mathbf{q}\cdot\mathbf{t}_{\mathbf{v}}}, \quad (1.22)$$

$$\langle \mathbf{k} + \mathbf{q} | V | \mathbf{k} \rangle = \frac{1}{\Omega_0} \int_{\text{over all space}} e^{-i(\mathbf{k}+\mathbf{q})\cdot\mathbf{r}} V(\mathbf{r}) e^{i\mathbf{k}\cdot\mathbf{r}} d^3r. \quad (1.23)$$

The structure factor $S(\mathbf{q})$ is defined for any vector \mathbf{q} . For a periodic lattice, $S(\mathbf{q})$ is zero unless \mathbf{q} happens to coincide with any of the vectors of the reciprocal lattice, i.e. $S(\mathbf{q} = \mathbf{g}_n) = 1$.

The potential formfactor (1.23) is also defined for all \mathbf{q} 's. If the potential operator V is merely a multiplication operator, the formfactor depends solely on \mathbf{q} and is called local. In the following we shall introduce more complicated effective potentials (pseudopotentials), with formfactors dependent both on \mathbf{q} and on \mathbf{k} . These formfactors and potentials are called nonlocal.

Let us now consider a few simple examples. Let $V(r)$ be a screened Coulomb attraction potential:

$$V_C^{\text{scr}} = -\frac{Ze^2}{r} e^{-Cr}. \quad (1.24)$$

To calculate its formfactor, we direct the polar axis along the vector \mathbf{q} [8]. We find

$$V_C^{\text{scr}}(q) = -\frac{4\pi Ze^2}{\Omega_0} \frac{1}{q^2 + C^2}. \quad (1.25)$$

In the limit when C vanishes, (1.24) is replaced by the familiar (nonscreened) Coulomb potential V_C , and (1.25) is replaced by its formfactor:

$$V_C(r) = -\frac{Ze^2}{r}, \quad V_C(q) = -\frac{4\pi Ze^2}{\Omega_0} \frac{1}{q^2}. \quad (1.26)$$

Comparing V_C and V_C^{scr} shows that the screening of the Coulomb potential removes the singularity of the formfactor at small q while leaving its behavior at large q ($V(q) \propto q^{-2}$) unchanged. This is typical of most formfactors, as will be shown in Secs. 4.1-3.

Let the potential $V(r)$ be vanishingly small. In this case the crystal is what may be called an empty lattice: electrons move within an imaginary crystalline lattice with no potentials on its sites.

The secular equation (1.19) for the empty lattice model is very similar to Eq. (1.17), which was obtained for the LCAO model in the limit of large interatomic separations:

$$\det |(\epsilon_n - E) \delta_{nn'}| = 0. \quad (1.27)$$

The empty lattice model is equivalent to a free electron gas subject to periodic boundary conditions. The band structure for the model is discussed in [9-11].

1.1.8. Perturbation theory. The secular equation (1.19) may be approximated by a perturbation theory expansion. To see this, we employ a version of Löwdin's method of "folding" secular equations [12-14].

Let us write a matrix X in block notation:

$$X = \begin{pmatrix} A & B \\ C & D \end{pmatrix}. \quad (1.28)$$

Next we introduce the unit matrix I and matrices Y and Z :

$$Y = \begin{pmatrix} I & 0 \\ -D^{-1}C & I \end{pmatrix}, \quad Z = \begin{pmatrix} D & 0 \\ 0 & D^{-1} \end{pmatrix}.$$

It can be seen that $\det Y = \det Z = 1$ (this is proved by decomposing the determinants in terms of their minors, starting from the upper left-hand corner). Now consider the matrix product $P = XYZ$. Clearly, $\det P = \det X$. We obtain

$$\det X = \det D \cdot \det (A - BD^{-1}C). \quad (1.29)$$

We have thus succeeded in expressing the determinant of a large-dimension matrix X in terms of the determinants of small-dimension matrices.

We now can use Löwdin's method to rewrite Eq. (1.19) as a single line. Let the diagonal perturbation matrix element $\langle \mathbf{k} | V | \mathbf{k} \rangle$ be first order relative to k^2 , $\langle \mathbf{k} + \mathbf{g}_n | V | \mathbf{k} \rangle$ second order in k^2 , and $\langle \mathbf{k} + \mathbf{g}_n | V | \mathbf{k} + \mathbf{g}_n \rangle$ third order in k^2 , though for the moment we shall ignore third-order terms. Block A in (1.28) only contains one element, $k^2 - E + \langle \mathbf{k} | V | \mathbf{k} \rangle$; blocks B and C are Hermitian-conjugate with matrix elements $\langle \mathbf{k} + \mathbf{g}_n | V | \mathbf{k} \rangle$; and block D is diagonal. When $\det D$ is zero, Eq. (1.19) is satisfied on account of (1.29), but its solutions are of no physical interest since they only describe high-lying empty lattice dispersion laws. As a result, we get from Eqs. (1.19) and (1.29):

$$E(\mathbf{k}) = \mathbf{k}^2 + \langle \mathbf{k} | V | \mathbf{k} \rangle - \sum_{n \neq 0} \frac{|\langle \mathbf{k} + \mathbf{g}_n | V | \mathbf{k} \rangle|^2}{\epsilon_n + \langle \mathbf{k} + \mathbf{g}_n | V | \mathbf{k} + \mathbf{g}_n \rangle - E} + (\dots) \quad (1.30)$$

where (\dots) indicates higher-order terms arising from the nondiagonality of D .

We have thus obtained the Brillouin-Wigner form of the perturbation theory expansion [15]. Now we shall take E in the denominator of (1.30) as the dispersion law given by the first-order perturbation theory ($E = \mathbf{k}^2 + \langle \mathbf{k} | V | \mathbf{k} \rangle$). Taking into account that, by (1.20), the local potential formfactor $\langle \mathbf{k} + \mathbf{g}_n | V | \mathbf{k} + \mathbf{g}_n \rangle$ is independent of n , we arrive at the perturbation theory expansion in the Rayleigh-

Schrödinger form [15]:

$$E(\mathbf{k}) = \mathbf{k}^2 + \langle \mathbf{k} | V | \mathbf{k} \rangle - \sum_{n \neq 0} \frac{|\langle \mathbf{k} + \mathbf{g}_n | V | \mathbf{k} \rangle|^2}{\varepsilon_n - \mathbf{k}^2} + \dots \quad (1.31)$$

Even though less exact, Eq. (1.31) is extremely valuable in that it allows analytical expression for dispersion laws. In fact, it is the basis for the present-day theory of the atomic properties of solids. We shall see later that this expansion is used for calculating the total energy of a crystal.

There are two types of sums in Eq. (1.31): infinite sums over the vectors of the reciprocal lattice, that form m th order contributions and the infinite sum of these contributions, usually restricted to the second- or third-order perturbation terms. One should be confident that the sums of both types are convergent.

Consider a sum over \mathbf{g}_n . In view of Eq. (1.25), each term of the sum is proportional to \mathbf{g}_n^{-6} at large \mathbf{g}_n . The density of points in reciprocal space increases as \mathbf{g}_n^2 , that is, the \mathbf{g}_n -sum does converge, each term giving a finite contribution.

The convergence of (1.31) as a whole requires much more careful analysis and in Sec. 2.5 we take up this subject in more detail. For the moment we restrict ourselves to a generally accepted statement: a perturbation expansion diverges if the perturbing potential produces at least one bound state.

This is a point of extreme importance. It is stated in fact that whether or not the continuum spectrum ($E > 0$) may be treated by perturbation theory depends on the presence or absence of bound states (which are only possible at $E < 0$). The existence of bound states is known to depend on the depth of the potential. If the potential is too strong (what exactly this means is determined by some criteria), the m th order contribution equals or exceeds that of the $(m - 1)$ th order and the perturbation expansion fails to converge.

Every atomic potential has bound states. Hence, to make perturbation theory applicable, a new and rather peculiar potential has to be constructed. It has to be weaker than the original one, but it must still affect the continuum electrons in exactly the same way. The contribution of these potentials is discussed in Secs. 2.3-4, 4.1-4, 5.2.

1.1.9. The Fermi free-electron gas. In this model the crystal formation process is as follows: N neutral isolated atoms are each stripped of Z outer (valence) electrons. The resulting ions are then brought together to form a crystal lattice, with a volume of Ω_0 per ion. An electron gas is then allowed into the lattice, its spatial distribution being assumed uniform, so that its density is Z/Ω_0 .

If we ignore the fact that the lattice potential is not constant, the electron dispersion law is simply $E = k^2$. The energy levels occupied by the electrons range from zero to a maximum, which is known as the Fermi level of a free electron gas:

$$E_F^0 = (3\pi^2 Z / \Omega_0)^{2/3} = k_F^2. \quad (1.32)$$

It was shown in [8] that a dispersion law is not altered if electron-electron Coulomb interactions are allowed. Including exchange interactions, we obtain [8]:

$$E(k) = k^2 - e^2 \frac{k_F}{\pi} \left(1 + \frac{1-y^2}{2y} \ln \left| \frac{1+y}{1-y} \right| \right), \quad (1.33)$$

where $y = k/k_F$. The exchange interaction strongly affects the states within the Fermi sphere. At $k = k_F$ the gradient of $E(k_F)$ goes to infinity, which is physical nonsense, although this singularity disappears in more elaborate theories. In Secs. 3.1,3,4 the exchange interaction is discussed in more detail. For the moment, note that the exchange correction term in Eq. (1.33) (corresponding to the $\langle \mathbf{k} | V | \mathbf{k} \rangle$ term of (1.31) is at a maximum at $k = 0$ and decreases with increasing k .

1.1.10. Total crystal energy in the NFE model. To calculate the total energy of a crystal, the dispersion laws are summed over all the occupied states. This is performed by integrating (1.31) over all the wave vectors within the Fermi sphere. As a result, the total crystal energy, Σ_{cr} , takes the form

$$\Sigma_{cr} = U_0 + U_{bs} + U_{lat}, \quad (1.34)$$

where U_{lat} takes account of the Coulomb repulsion between the ion cores; U_0 and U_{bs} are respectively the volume- and structure-dependent electronic contributions to the total energy:

$$U_0 = 2 \frac{\Omega}{(2\pi)^3} \int_{\text{inside the Fermi sphere}} (k^2 + \langle \mathbf{k} | V | \mathbf{k} \rangle) d^3k, \quad (1.35)$$

$$U_{bs} = -2 \frac{\Omega}{(2\pi)^3} \sum_{\mathbf{q}} |S(\mathbf{q})|^2 \int_{\text{inside the Fermi sphere}} \frac{|\langle \mathbf{k} + \mathbf{q} | V | \mathbf{k} \rangle|^2}{(\mathbf{k} + \mathbf{q})^2 - k^2} d^3k - U_{el}^{int}, \quad (1.36)$$

where the \mathbf{g}_n are replaced, for generality, by the ordinary position vectors \mathbf{q} .

The U_0 term describes a "free" electron gas with the inclusion of electron-electron interaction; U_{bs} is associated with band characteristics and is therefore called the band-structure energy (or simply band

energy). The term $U_{\text{el}}^{\text{int}}$ takes care of the fact that when calculating $E(\mathbf{k})$ the interaction energy of each electron pair contributes to the energy of each electron, that is, in summing the one-electron energies in (1.34), the electron-electron interaction energy is counted twice.

The calculation of U_0 and U_{lat} may be found in many textbooks (see [16-18] and [19]). It is instructive to discuss U_{bs} .

If a potential V is local, its formfactor is \mathbf{k} -independent and can be taken out of the \mathbf{k} -integral. The \mathbf{k} -integral that appears then in Eq. (1.36) is known as Lindhard's function [3]:

$$\chi(\mathbf{q}) = -2 \frac{\Omega}{(2\pi)^3} \frac{1}{N} \int_{\text{inside the Fermi sphere}} \frac{d^3k}{(\mathbf{k} + \mathbf{q})^2 - k^2}. \quad (1.37)$$

By assuming a spherical Fermi surface, one gets

$$\chi(\mathbf{q}) = -\frac{Z}{4} \left(\frac{2}{3} E_F^0 \right)^{-1} \left(1 + \frac{1-x^2}{2x} \ln \left| \frac{1+x}{1-x} \right| \right), \quad (1.38)$$

where $x = k/(2k_F)$. There is a similarity between Eq. (1.38) and the exchange correction term to the dispersion law (1.33), the only difference being that in $\chi(\mathbf{q})$ the singularity occurs at $k = 2k_F$ instead of $k = k_F$ as in Eq. (1.33).

The electron-electron interaction energy $U_{\text{el}}^{\text{int}}$ may be represented [17] as a result of interactions between the nonuniform part of the crystal's electron density and the potential which is the difference between the crystal potential \mathcal{V}^{cr} and the initial potential \mathcal{V}^{ion} of the system of ions. By formally setting up a function by which to characterize this potential, $\alpha(\mathbf{q}) = \mathcal{V}^{\text{ion}}(\mathbf{q})/\mathcal{V}^{\text{cr}}(\mathbf{q})$, we can express $U_{\text{el}}^{\text{int}}$ in terms of the formfactor of $\mathcal{V}^{\text{cr}}(\mathbf{q})$, Eq. (1.21):

$$U_{\text{el}}^{\text{int}} = \sum_{\mathbf{q}} |S(\mathbf{q})|^2 |V(\mathbf{q})|^2 \chi(\mathbf{q}) (1 - \alpha(\mathbf{q})), \quad (1.39)$$

$$U_{\text{bs}} = \sum_{\mathbf{q}} |S(\mathbf{q})|^2 |V(\mathbf{q})|^2 \chi(\mathbf{q}) - U_{\text{el}}^{\text{int}} = \sum_{\mathbf{q}} |S(\mathbf{q})|^2 |V(\mathbf{q})|^2 \chi(\mathbf{q}) \alpha(\mathbf{q}). \quad (1.40)$$

Note that, in deriving this equation, we made no assumptions about the nature of the potential (except for its locality) or about the way in which the crystal potential is composed of the ionic potentials (that is, about the screening mechanism). $\chi(\mathbf{q})$ is a function arising from perturbation theory whereas $\alpha(\mathbf{q})$ is the ratio of the original potential of the ions to the crystal potential. In Sec. 3.2 we shall encounter dielectric screening, in which case Lindhard's function $\chi(\mathbf{q})$ will also be needed and α will be interpreted as the system's "response" to a perturbation. This, however, will only be a matter of elaborating the technique: the meaning of Eqs. (1.34)-(1.40) will remain intact.

A frequently used characteristic function $\Phi_{bs}(\mathbf{q})$ is defined as

$$\Phi_{bs}(\mathbf{q}) = |V(\mathbf{q})|^2 \chi(\mathbf{q}) \propto (\mathbf{q}). \quad (1.41)$$

Using Eq. (1.41), U_{bs} can be rewritten as a sum, over the lattice sites, of Fourier transforms $\Phi_{bs}(\mathbf{t}_v)$ which are defined as

$$\Phi_{bs}(\mathbf{t}) = 2 \frac{\Omega}{(2\pi)^3} \int \Phi_{bs}(\mathbf{q}) e^{i\mathbf{q}\mathbf{t}} d^3q. \quad (1.42)$$

$\Phi_{bs}(\mathbf{t})$ may be thought of as the potential of the interaction between ions through the electron gas (the same electron is simultaneously attracted by all the ions, hence their mutual attraction). It is this interaction that must compensate for the direct Coulomb repulsion of the ions. The total potential for interatomic interaction is

$$\Phi(\mathbf{t}) = \frac{(Ze)^2}{t} + \Phi_{bs}(\mathbf{t}). \quad (1.43)$$

Note that $\Phi(\mathbf{t})$ describes the interaction between atoms given that the system's volume is constant. In other words, $\Phi(\mathbf{t})$ is the redistribution of the atoms.

Part 1

Theoretical principles of the pseudopotential method

Chapter 2

Scattering theory for “solid-state people”

2.1. Mathematical formalism

The subject of this chapter is quantum mechanical scattering theory. Although the concepts of the theory are widely used within the one-electron approach, the relevant mathematics can nowhere be found in a compact form and often many books, sometimes very obscure ones, have to be consulted before a needed formula is located. This makes things difficult for someone interested in band-theory computational methods and, especially, in how the methods are related to each other. We have therefore attempted to compile all the necessary information, avoiding whenever possible asking the reader to take anything “on trust”.

This chapter may thus be considered as an introduction to the modern formalism of the one-electron approximation.

2.1.1. δ -function. This frequently used function has the following property: for a continuous function $f(\mathbf{x})$

$$\int f(\mathbf{x}) \delta(\mathbf{x} - \mathbf{x}_0) d^3x = f(\mathbf{x}_0). \quad (2.1)$$

the integral extending over all space.

2.1.2. Green’s function method (GF). This is a powerful tool for treating differential equations which can be described briefly as follows [20]. Consider the differential equation

$$(-\nabla^2 - E) \psi(\mathbf{r}) = f(\mathbf{r}). \quad (2.2)$$

We chose Schrödinger’s equation for the sake of concreteness but the GF method in fact applies to any equation.

Green’s function $G(\mathbf{r}, \mathbf{r}')$ is defined as the solution of (2.2) whose right-hand side is replaced by a source function

$$(-\nabla^2 - E) G(\mathbf{r}, \mathbf{r}') = -\delta(\mathbf{r} - \mathbf{r}'). \quad (2.3)$$

In terms of Green's function, the solution of (2.2) is given by

$$\psi(\mathbf{r}) = A\varphi(\mathbf{r}) + \int_{\text{over all space}} G(\mathbf{r}, \mathbf{r}') f(\mathbf{r}') d^3r', \quad (2.4)$$

where A is an arbitrary constant and φ satisfies equation (2.2) for a zero right-hand side,

$$(-\nabla^2 - E)\varphi(\mathbf{r}) = 0. \quad (2.5)$$

To prove equation (2.4), we apply the operator $(-\nabla^2 - E)$. Since ∇^2 acts on the coordinate \mathbf{r} , it may be introduced into the integrand. The first term in (2.4) is, by (2.5), zero. We use Eqs. (2.3) and (2.1) for the integrand, and this completes the proof.

The integral equation (2.4) is more convenient to deal with than a differential equation since the boundary conditions needed for calculating ψ are already included in $\varphi(\mathbf{r})$ and $G(\mathbf{r}, \mathbf{r}')$.

2.1.3. Spectral expansion of Green's function. Let ε_n be the eigenvalues of Eq. (2.5), and φ_n the corresponding eigenfunctions. Since, by definition, GF obeys the same boundary conditions that $\varphi_n(\mathbf{r})$ does, it can be expanded in terms of these functions (which form a complete set for GF):

$$G(\mathbf{r}, \mathbf{r}') = \sum_n a_n \varphi_n(\mathbf{r}). \quad (2.6)$$

Insertion of (2.6) in (2.3) leads to

$$\sum_n a_n (\varepsilon_n - E) \varphi_n(\mathbf{r}) = -\delta(\mathbf{r} - \mathbf{r}'). \quad (2.7)$$

Multiplying this equation by $\varphi_n^*(\mathbf{r})$ and integrating over \mathbf{r} we find after using the orthogonality of φ_n that

$$a_n = -\frac{\varphi_n^*(\mathbf{r}')}{\varepsilon_n - E}, \quad (2.8)$$

$$G(\mathbf{r}, \mathbf{r}') = -\sum_n \frac{\varphi_n(\mathbf{r})\varphi_n^*(\mathbf{r}')}{\varepsilon_n - E}. \quad (2.9)$$

In deriving (2.9) we have used the fact that the left-hand side of (2.3) is a self-conjugate operator.

Expression (2.9) allows us to determine GF. It follows from (2.9) that GF is Hermitian:

$$G(\mathbf{r}, \mathbf{r}') = G^*(\mathbf{r}', \mathbf{r}).$$

Combining Eqs. (2.7) and (2.8), we arrive at an important result characteristic of all complete sets of functions, i.e.

$$\sum_n \varphi_n(\mathbf{r}) \varphi_n^*(\mathbf{r}') = \delta(\mathbf{r} - \mathbf{r}'). \quad (2.10)$$

2.1.4. Free-electron Green's function. In the special case of free electrons the eigenfunctions of equation (2.5) are plane waves:

$$\begin{aligned}\varphi_{\mathbf{k}} &= \frac{1}{V(2\pi)^3} e^{i\mathbf{k}\mathbf{r}}, \\ G_0(\mathbf{r}, \mathbf{r}') &= -\frac{1}{(2\pi)^3} \int \frac{e^{i\mathbf{k}(\mathbf{r}-\mathbf{r}')}}{k^2 - \kappa^2} d^3k,\end{aligned}\quad (2.11)$$

where $\kappa = +\sqrt{E}$. This integral is known to be [20, 21]

$$G_0(\mathbf{r}, \mathbf{r}') = -\frac{1}{4\pi} \frac{e^{i\kappa|\mathbf{r}-\mathbf{r}'|}}{|\mathbf{r}-\mathbf{r}'|}. \quad (2.12)$$

It can be easily seen that at $\mathbf{r} = \mathbf{r}'$ GF has a singularity. Consequently, the derivative dG/dr is discontinuous at $r = r'$:

$$\left(\frac{\partial G}{\partial r} - \frac{\partial G}{\partial r'} \right) \Big|_{r \rightarrow r'} \neq 0.$$

2.1.5. Spherical harmonics. Coming back to Eq. (2.2), let us set $f(\mathbf{r}) = -V(\mathbf{r})\psi(\mathbf{r})$ where the potential $V(\mathbf{r})$ is spherically symmetrical. It is then convenient, in Eqs. (2.2) and (2.5), to change to polar coordinates:

$$\begin{aligned}x &= r \sin \theta \cdot \cos \varphi, & y &= r \sin \theta \cdot \sin \varphi, & z &= r \cos \theta; \\ 0 &\leq \theta \leq \pi, & 0 &\leq \varphi \leq 2\pi.\end{aligned}$$

The operator ∇^2 is the sum of two operators:

$$\nabla^2 = \nabla_r^2 + \frac{1}{r^2} \nabla_{\theta, \varphi}^2, \quad (2.13)$$

where the operator ∇_r^2 only acts on the absolute value of the vector \mathbf{r} and $\nabla_{\theta, \varphi}^2$ only acts on the angles between \mathbf{r} and the coordinate axes. We shall need the explicit form of ∇_r^2 :

$$\nabla_r^2 = \frac{1}{r^2} \frac{\partial}{\partial r} r^2 \frac{\partial}{\partial r}. \quad (2.14)$$

The eigenfunctions of this operator, $Y_{lm}(\theta, \varphi)$, are called spherical harmonics:

$$-\nabla_{\theta, \varphi}^2 Y_{lm}(\theta, \varphi) = l(l+1) Y_{lm}(\theta, \varphi), \quad (2.15)$$

$$Y_{lm}(\theta, \varphi) = N_{lm} P_l^{|m|}(\cos \theta) e^{im\varphi}, \quad (2.16)$$

where N_{lm} is a normalization factor and $P_l^{|m|}$ is the associated Legendre polynomial of degree $|m|$, which is dependent solely on the angle θ . It can be seen from (2.15) that the solutions Y_{lm} are degenerate with respect to the index m .

The spherical harmonics obey the addition theorem:

$$\sum_m Y_{lm}^*(\mathbf{r}) Y_{lm}(\mathbf{r}') = \frac{2l+1}{4\pi} P_l(\cos \theta_{\mathbf{r}, \mathbf{r}'}), \quad (2.17)$$

where $Y_{lm}(\mathbf{r})$ is a harmonic dependent on the angles between the vector \mathbf{r} and the coordinate axes, and P_l is a Legendre polynomial dependent on the angle between \mathbf{r} and \mathbf{r}' :

$$P_l^{[m=0]} = P_l, \quad P_l(\cos \theta) |_{\cos \theta=1} = 1.$$

The spherical harmonics are orthonormal:

$$\int Y_{lm}^*(\mathbf{r}) Y_{l'm'}(\mathbf{r}) d\Omega_{\mathbf{r}} = \delta_{ll'} \delta_{mm'}, \quad (2.18)$$

where the integration is over the angles between \mathbf{r} and the coordinate axes, and $\delta_{pp'}$ is the Kronecker delta:

$$\delta_{pp'} = \begin{cases} 1 & \text{if } p = p', \\ 0 & \text{if } p \neq p'. \end{cases}$$

The harmonics are thus "normalized to unity"; the normalization factor N_{lm} includes a factor of $1/\sqrt{4\pi}$, so that, as a special case, we have

$$Y_{l=0, m=0} = \frac{1}{\sqrt{4\pi}} \quad (2.19)$$

There exists the addition theorem for harmonics with different l, m and l', m' :

$$Y_L(\mathbf{r}) Y_{L'}(\mathbf{r}) = \sum_{L_1} C_{L_1 L'}^L Y_{L_1}(\mathbf{r}), \quad (2.20)$$

where the quantities $C_{L_1 L'}^L$ are known as Gaunt's coefficients. They are, in fact, the matrix elements of Y_L between $Y_{L_1}^*$ and $Y_{L'}$, i.e. $L_1 | L | L'$:

$$C_{L_1 L'}^L = \int Y_{L_1}^*(\mathbf{r}) Y_L(\mathbf{r}) Y_{L'}(\mathbf{r}) d\Omega_{\mathbf{r}}. \quad (2.21)$$

Here and often in the following we use L as a shorthand for $\{l, m\}$.

The spherical harmonics Y_L are complex. We may also define real harmonics [22]:

$$y_{l|m|}^+ = \frac{Y_{lm} + Y_{l,-m}}{2}, \quad y_{l|m|}^- = \frac{Y_{lm} - Y_{l,-m}}{2i}. \quad (2.22)$$

These are also called "cubic harmonics" since, under symmetry operations, they transform as cubic symmetry eigenfunctions.

The $l = 0, 1, 2, 3, 4$ harmonics are usually referred to as the s, p, d, f and g functions, respectively. In many textbooks angular dependences for s, p and d functions are plotted in Cartesian coordi-

nates. These are, of course, the cubic harmonics because the spherical ones have imaginary components and cannot therefore be plotted.

Formally, the cubic harmonics can be labeled* by certain p indices instead of m indices; the cubic harmonics will then be orthogonal with respect to both m and p .

The functions used in band-structure applications (see for example, Sec. 5.1 for a discussion of GF structure constants) are usually the cubic harmonics, since matrix elements between them are convenient in being real. This is, in fact, achieved by simply changing notation, and so in what follows we only use spherical harmonics because they make the Hermitian property more transparent.

Spherical (cubic) harmonics, since they are the eigenfunctions of the operator $\nabla_{\theta,\phi}^2$, form a complete set of functions on sphere and therefore any angle-dependent function can be expanded in terms of $Y_L(\mathbf{r})$:

$$f(\mathbf{r}) = \sum_L f_L(|\mathbf{r}|) Y_L(\mathbf{r}). \quad (2.23)$$

2.1.6. Radial equation. Let us consider Eq. (2.2) with $-V(r)\psi$ on the right. By (2.23), its solution ψ can be expanded in terms of Y_L :

$$\psi(\mathbf{r}) = \sum_L \mathcal{R}_{lm}(|\mathbf{r}|) Y_L(\mathbf{r}). \quad (2.24)$$

Substituting (2.24) in (2.2), changing over to spherical coordinates, and using Eqs. (2.14) and (2.15) we obtain a differential equation for \mathcal{R}_{lm} :

$$-\frac{1}{r^2} \frac{\partial}{\partial r} r^2 \frac{\partial}{\partial r} \mathcal{R}_{lm}(r) + \left[V(r) + \frac{l(l+1)}{r^2} - E \right] \mathcal{R}_{lm}(r) = 0. \quad (2.25)$$

Obviously, \mathcal{R}_{lm} is independent of m and this index may therefore be dropped. Since Eq. (2.25) is linear, the function \mathcal{R}_l will be defined in terms of a multiplicative constant independent of r which will be determined by the boundary conditions (e.g., by normalization). Equation (2.24) will therefore be replaced by the more correct expression

$$\psi(\mathbf{r}) = \sum_L B_L \mathcal{R}_l(r) Y_L(\mathbf{r}) \quad (2.26)$$

with \mathcal{R}_l satisfying Eq. (2.25).

2.1.7. Bessel, Neumann and Hankel spherical functions. Equation (2.25) always has two linearly independent solutions, one regular

* It is clear from (2.22) that cubic harmonics cannot be labeled by the old indices m . This "prohibition" results from the mixing of quantum numbers which is caused by the same kind of perturbation we saw in LCAO and NFE models. In this particular case the "perturbation" is due to the change in symmetry.

and the other irregular at the origin. For a zero potential, they are well known and are called, respectively, the Bessel and the Neumann spherical functions, $j_l(x)$ and $n_l(x)$, where $x = \kappa r$ (see [20, 21]). For the first few l their explicit forms are:

$$\begin{aligned} j_0(x) &= \frac{\sin x}{x}, \quad n_0(x) = -\frac{\cos x}{x}, \\ j_1(x) &= \frac{\sin x}{x^2} - \frac{\cos x}{x}, \quad n_1(x) = -\frac{\cos x}{x^2} - \frac{\sin x}{x}, \\ j_2(x) &= \left(\frac{3}{x^3} - \frac{1}{x}\right) \sin x - \frac{3}{x^2} \cos x, \quad n_2(x) = -\left(\frac{3}{x^3} - \frac{1}{x}\right) \cos x \\ &\quad - \frac{3}{x^2} \sin x. \end{aligned} \quad (2.27)$$

In the small- x limit the asymptotic values are:

$$j_l(x) \xrightarrow{x \rightarrow 0} \frac{x^l}{(2l+1)!!}, \quad n_l(x) \xrightarrow{x \rightarrow 0} -\frac{|(2l-1)!!|}{x^{l+1}}, \quad (2.28)$$

where the l in $(2l \pm 1)!!$ is a positive integer or zero. These formulas provide a good approximation to j_l for $x^2 < 4l + 6$ and to n_l for $x^2 < 2$ [21].

At large x the asymptotic values are [23]:

$$j_l(x) \xrightarrow{x \rightarrow \infty} \frac{\sin(x - l\pi/2)}{x}, \quad n_l(x) \xrightarrow{x \rightarrow \infty} -\frac{\cos(x - l\pi/2)}{x}. \quad (2.29)$$

These formulas are good for $x > l(l+1)/2$. The oscillation amplitude is already within 10% of the asymptotic value for $x \gtrsim 2l$ [23].

Both functions obey the recurrence relations for j_l

$$\begin{aligned} j_{l+1}(x) &= -x^{-l} \frac{d}{dx} [x^{-l} j_l(x)], \\ j_{l-1}(x) + j_{l+1}(x) &= \frac{2l+1}{x} j_l(x) \quad (l > 0) \end{aligned}$$

and similarly for n_l .

The Wronskian of the functions j_l and n_l is nonzero:

$$j_l(x) \frac{d}{dr} n_l(x) - n_l(x) \frac{d}{dr} j_l(x) = \frac{1}{\kappa r^2}. \quad (2.30)$$

The functions j_l and n_l are related to the ordinary (cylindrical) Bessel and Neumann functions, $\mathcal{J}_l(x)$ and $\mathcal{Y}_{-l}(x)$, by

$$j_l(x) = \sqrt{\frac{\pi}{2x}} \mathcal{J}_{l+1/2}(x), \quad n_l(x) = (-1)^{l+1} \sqrt{\frac{\pi}{2x}} \mathcal{Y}_{-l-1/2}(x).$$

It is often convenient to work with a complex combination of j_l and n_l , which is known as the Hankel function:

$$\gamma_l^\pm = j_l(x) \pm i n_l(x). \quad (2.31)$$

For large x its asymptotic value is

$$\gamma_l^\pm \xrightarrow{x \rightarrow \infty} \frac{1}{x} e^{\pm i(x - l\pi/2)}$$

The functions γ_l^+ and γ_l^- correspond to the incoming and outgoing waves, respectively. For a more detailed discussion of j_l and n_l , see [21, 24].

2.1.8. Useful formulas. A good example to illustrate the use of Eqs. (2.23) and (2.26) is the plane-wave expansion in $Y_L(\mathbf{r})$

$$\frac{1}{V\Omega_0} e^{i\mathbf{k}\mathbf{r}} = \frac{4\pi}{V\Omega_0} \sum_L i^l j_l(kr) Y_L^*(\mathbf{k}) Y_L(\mathbf{r}) \equiv \sum_L h_L(\mathbf{k}, \mathbf{r}) Y_L(\mathbf{r}), \quad (2.32)$$

where Ω_0 is the normalization volume and

$$h_L(\mathbf{k}, \mathbf{r}) = \frac{4\pi}{V\Omega_0} i^l j_l(kr) Y_L^*(\mathbf{k}). \quad (2.33)$$

A comparison of Eqs. (2.32) and (2.26) shows that, for a plane wave, the coefficient B_L in (2.26) is $4\pi i^l Y_L^*(\mathbf{k})$ and it can by no means be omitted.

By using Eq. (2.32) we obtain a re-expansion of the spherical functions relative to another origin of coordinates:

$$j_l(\kappa |\mathbf{r} - \mathbf{t}|) Y_L(\mathbf{r} - \mathbf{t}) = \sum_{L'} F_{LL'} j_{l'}(\kappa r) Y_{L'}(\mathbf{r}), \quad (2.34)$$

$$F_{LL'} = \sum_{L_1} C_{L'L_1}^L j_{l_1}(\kappa t) Y_{L_1}^*(\mathbf{t}).$$

The following formula [25, 26] is more difficult to derive

$$n_l(\kappa |\mathbf{r} - \mathbf{t}|) Y_L(\mathbf{r} - \mathbf{t}) = \sum_{L'} K_{LL'} j_{l'}(\kappa r) Y_{L'}(\mathbf{r}), \quad (2.35)$$

$$K_{LL'} = \sum_{L_1} C_{L'L_1}^L n_{l_1}(\kappa t) Y_{L_1}^*(\mathbf{t}).$$

Equation (2.35) is valid for $|\mathbf{r}| < |\mathbf{t}|$.

If cubic harmonics are used, Eqs. (2.34) and (2.35) yield an analogous result for the γ_l^\pm functions.

Another useful formula for GF (2.12) is

$$\frac{1}{4\pi} \frac{e^{i\kappa|\mathbf{r} - \mathbf{r}'|}}{|\mathbf{r} - \mathbf{r}'|} = i\kappa \sum_L j_l(\kappa r_{<}) \gamma_l^+(\kappa r_{>}) Y_L^*(\mathbf{r}) Y_L(\mathbf{r}'), \quad (2.36)$$

where $r_<$ ($r_>$) is the smaller (larger) of the lengths r and r' . (It is due to these restrictions on r and r' that a GF remains finite at r when r' tends to zero.)

A Green function can be divided into two parts, one regular at $r = r'$ (G_0^{reg}) and the other singular (G_0^{sing}):

$$\begin{aligned} G_0^{\text{reg}} &= -\frac{1}{4\pi} \frac{\sin(\kappa |\mathbf{r} - \mathbf{r}'|)}{|\mathbf{r} - \mathbf{r}'|} = \text{Im } G_0, \\ G_0^{\text{sing}} &= -\frac{1}{4\pi} \frac{\cos(\kappa |\mathbf{r} - \mathbf{r}'|)}{|\mathbf{r} - \mathbf{r}'|} = \text{Re } G_0. \end{aligned} \quad (2.37)$$

The function G_0^{reg} satisfies Eq. (2.5) and G_0^{sing} satisfies Eq. (2.3). If the full G_0 is replaced by G_0^{sing} , Eq. (2.4) is still a solution to (2.2). In this case, known as the standing wave representation (note that this is not an approximation), the solution of Eq. (2.4) is real.

With the help of (2.32) we find that

$$\sum_{l=0}^{\infty} (2l+1) j_l^2(x) = 1. \quad (2.38)$$

It is also noteworthy that, as follows from (2.10), the spherical harmonics form a complete set:

$$\sum_{L=0}^{\infty} Y_L^*(\mathbf{r}) Y_L(\mathbf{r}') = \delta\left(\frac{\mathbf{r}}{|\mathbf{r}|} - \frac{\mathbf{r}'}{|\mathbf{r}'|}\right). \quad (2.39)$$

2.1.9. Projection operators. The concepts of orthogonality and completeness are closely related to projection operators which are used in pseudopotential theory. For an orthonormal set of functions $|\alpha\rangle$, we can write an operator that "projects" a function $f(\mathbf{r})$ onto the space of the $|\alpha\rangle$ functions:

$$\hat{P} = \sum_{\alpha} \hat{P}_{\alpha}, \quad \hat{P}_{\alpha} = |\alpha\rangle \langle \alpha| \quad (2.40)$$

in the sense that

$$\hat{P} |f\rangle = \sum_{\alpha} \hat{P}_{\alpha} |f\rangle = \sum_{\alpha} |\alpha\rangle \langle \alpha | f \rangle.$$

Here the right-hand side is clearly recognized as an expansion of f in terms of the $|\alpha\rangle$ functions, that is the projection operator is simply an expansion operator over a basis set.

A simple example is the operator that singles out the L th component of $f(\mathbf{r})$, i.e.

$$\begin{aligned} \hat{P}_L &= |L\rangle \langle L|, \\ \hat{P}_L |f\rangle &= |L\rangle \langle L | f \rangle = Y_L(\mathbf{r}) \int Y_L^*(\mathbf{r}') f(\mathbf{r}') d\Omega_{\mathbf{r}'}. \end{aligned} \quad (2.41)$$

By applying (2.41) to the plane wave (2.32) we get

$$\hat{P}_L | \mathbf{k} \rangle = h_L(\mathbf{k}, r) Y_L(\mathbf{r}).$$

It can easily be proved that any projection operator is idempotent, i.e. $\hat{P}\hat{P} = \hat{P}$.

2.2. Scattering on an isolated potential

2.2.1. Phase shifts, analysis in terms of Green's functions. We can now apply* the GF method to scattering on an isolated spherically symmetrical potential $V(r)$. We employ the standing wave representation (2.37):

$$G_0^{\text{sing}} = \kappa \sum_L j_l(\kappa r_<) n_l(\kappa r_>) Y_L(\mathbf{r}) Y_L(\mathbf{r}'). \quad (2.42)$$

Substituting (2.42) into (2.4) and taking into account that, for free electrons, $k^2 = \kappa^2 = E$, we obtain using (2.32)

$$\begin{aligned} \psi = A \sum_L h_L(\kappa, r) Y_L(\mathbf{r}) \\ + \kappa \sum_L \int j_l(\kappa r_<) n_l(\kappa r_>) V(r') \psi(\mathbf{r}') Y_L(\mathbf{r}') d^3r' \cdot Y_L(\mathbf{r}) \end{aligned}$$

We now change to spherical coordinates, use (2.26) and integrate over the angles between the vectors \mathbf{r} and \mathbf{r}' . We choose B_L to be of the form

$$B_L = b_L \frac{4\pi}{\sqrt{\Omega_0}} i^l Y_l(\kappa).$$

This allows us to eliminate the dependence on the direction of κ in final formulas. As a result,

$$\begin{aligned} \mathcal{R}_l = \left\{ \frac{A}{b_L} + \kappa \int_r^\infty n_l(\kappa r_1) V(r_1) \mathcal{R}_l(r_1) r_1^2 dr_1 \right\} j_l(\kappa r) \\ + \left\{ \kappa \int_0^r j_l(\kappa r_1) V(r_1) \mathcal{R}_l(r_1) r_1^2 dr_1 \right\} n_l(\kappa r). \end{aligned}$$

It is an easy matter to obtain the same expression in the running wave representation (which only means replacing n_l by $i\gamma_l^+$).

* The same approach is used in Sec. 5.1 to treat energy spectra in crystals. This leads to the secular equation of the Korringa-Kohn-Rostoker (KKR) method.

Let us define the functions:

$$S_l(r) = -\kappa \int_0^r j_l(\kappa r_1) V(r_1) \mathcal{R}_l(E, r_1) r_1^2 dr_1, \quad (2.43)$$

$$C_l(r) = \frac{A}{b_L} + \kappa \int_r^\infty n_l(\kappa r_1) V(r_1) \mathcal{R}_l(E, r_1) r_1^2 dr_1. \quad (2.44)$$

Note that $S_l(0) = 0$, $C_l(\infty) = A/b_L$. Using Eqs. (2.43) and (2.44), we find

$$\mathcal{R}_l(r) = C_l(r) j_l(\kappa r) - S_l(r) n_l(\kappa r). \quad (2.45)$$

The presence of a potential has thus resulted in mixing the regular and irregular solutions of the homogeneous equation.

In the limiting case of small r

$$C_l(r \rightarrow 0) = \text{const}_l^0, \quad (2.46)$$

$$\mathcal{R}_l(r \rightarrow 0) = \text{const}_l^0 \cdot j_l(\kappa r). \quad (2.47)$$

For a potential that decreases rapidly enough (say, dropping to zero at $r > R$), the functions C_l and S_l at large r are independent of r . Let us introduce

$$\text{const}_l^\infty = \sqrt{C_l^2 + S_l^2}$$

and define an angle $\eta_l(E)$:

$$\eta_l(E) = \arctan [S_l(r \rightarrow \infty)/C_l(r \rightarrow \infty)]. \quad (2.48)$$

Eq. (2.48) is equivalent to

$$S_l(r \rightarrow \infty) = \text{const}_l^\infty \cdot \sin \eta_l, \quad (2.49)$$

$$C_l(r \rightarrow \infty) = \text{const}_l^\infty \cdot \cos \eta_l, \quad (2.50)$$

$$\mathcal{R}_l(E, r \rightarrow \infty) = \text{const}_l^\infty (\cos \eta_l \cdot j_l(\kappa r) - \sin \eta_l \cdot n_l(\kappa r)). \quad (2.51)$$

The angle η_l is called the scattering phase or the phase shift. To see where the name comes from, note that by using (2.29) we obtain for $r \rightarrow \infty$

$$\mathcal{R}_l(r \rightarrow \infty) = \text{const}_l^\infty \frac{\sin(\kappa r - l\pi/2 + \eta_l)}{\kappa r}. \quad (2.52)$$

It can then be seen that the solution (2.52) is, in a way, shifted by an angle η_l relative to the $j_l(\kappa r)$ (2.29). Note, however, that there is no phase shift in the denominator of (2.52), which means that this interpretation can only be made with caution.

The magnitude of the phase shift can be found from

$$\tan \eta_l(E) = \frac{S_l(E, r=\infty)}{\text{const}_l^0 - \kappa \int_0^\infty n_l(\kappa r) V(r) \mathcal{R}_l(r) r^2 dr} = \frac{b_L}{A} S_l(E, r=\infty). \quad (2.53)$$

One more useful relation is

$$\text{const}_l^\infty \cdot \cos \eta_l = A/b_L. \quad (2.54)$$

2.2.2. Normalization conditions for the wave functions. It is a usual textbook statement that the normalization of a wave function is arbitrary in scattering problems and it is only relative quantities which matter, such as reflectivity or transmissivity. This is undoubtedly true. However, it is the particular choice of normalization that specifies the form of the wave function of relevance. Moreover, as the following examples show, the choice of normalization determines the way in which the phase shift is expressed in terms of \mathcal{R}_l .

(A) Plane-wave normalization:

$$b_L = A. \quad (2.55)$$

Then, by (2.53),

$$\tan \eta_l = -\kappa \int_0^\infty j_l(\kappa r) V(r) \mathcal{R}_l(r) r^2 dr, \quad (2.56)$$

$$\mathcal{R}_l(r) = j_l(\kappa r) - \tan \eta_l(E) n_l(\kappa r). \quad (2.57)$$

(B) Normalization at the origin:

$$\text{const}_l^0 = 1, \quad (2.58)$$

$$\tan \eta_l = -\kappa \int_0^\infty j_l V \mathcal{R}_l r^2 dr \bigg/ \left(1 - \kappa \int_0^\infty n_l V \mathcal{R}_l r^2 dr \right). \quad (2.59)$$

The radial function \mathcal{R}_l is given by (2.51) with the phases determined by (2.59). Note that it is this normalization which is adopted in books on the phase function method [27, 28] (see Sec. 2.3). Expression (2.59) is identical, for example, with Eq. (6.18) of [28] (note, though, that \mathcal{R}_l is replaced in [28] by $u_l = \mathcal{R}_l/r$).

(C) Normalization at infinity:

$$\text{const}_l^\infty = 1, \quad (2.60)$$

$$\sin \eta_l = -\kappa \int_0^\infty j_l V \mathcal{R}_l r^2 dr, \quad (2.61)$$

$$\mathcal{R}_l = \cos \eta_l \cdot j_l(\kappa r) - \sin \eta_l \cdot n_l(\kappa r). \quad (2.62)$$

This normalization is used when the behavior of electrons is studied far away from a scatterer at the origin (e.g., an impurity atom, see [29]).

(D) Scattering-oriented normalization:

$$b_L = -\frac{\kappa A}{S_L(r \rightarrow \infty)} \int_0^\infty n_l(\kappa r) V(r) \mathcal{R}_l(r) r^2 dr. \quad (2.63)$$

Then we have

$$\tan \eta_l = -\kappa \int_0^\infty n_l(\kappa r) V(r) R_l(r) r^2 dr,$$

and finally

$$\begin{aligned} \text{const}_l^0 &= \frac{A}{b_L} - \tan \eta_l, \quad \text{const}_l^0 = \text{const}_l^\infty \cdot \cos \eta_l - \tan \eta_l, \\ \mathcal{R}_l &= (\text{const}_l^0 + \tan \eta_l) (j_l(\kappa r) - \tan(\eta_l \cdot n_l(\kappa r))). \end{aligned} \quad (2.64)$$

If the amplitude of the function is known for both small and large distances, we can evaluate the phase shift. Conversely, from the large-distance amplitude and shift we can determine the function at the origin and ignore its intermediate behavior. This is, in fact, a manifestation of the principle underlying the concept of the pseudopotential: the phase shift contains a “memory” of the interaction times $n\pi$, where n is an integer. Note that for the asymptotic value (2.52) the phase is needed to within $2n\pi$, which is exactly the accuracy provided by Eq. (2.64).

2.2.3. Logarithmic derivatives of the radial functions. We thus know that far away from a force center (or at $r > R$, for a potential of (finite) range R) the wave function \mathcal{R}_l is given by (2.51). The expressions we derived for η_l are in an integral form and for this reason are not very practical. There are a large number of methods (both variational [30-32] and not [33-37]) with which to calculate the phase shifts. The one that follows is the most commonly used.

If no boundary conditions are imposed, Eq. (2.25) can be solved numerically for any value of E . We can therefore integrate* Eq. (2.25) to a certain r_0 (which may, for example, be the range R) and then demand that \mathcal{R}_l join smoothly to (2.51):

$$\begin{aligned} \lim_{\delta \rightarrow 0} \mathcal{R}_l(r = R - \delta) &= \text{const}_l^\infty (\cos \eta_l \cdot j_l(\kappa R) - \sin \eta_l \cdot n_l(\kappa R)), \\ \lim_{\delta \rightarrow 0} \mathcal{R}_l'(r = R - \delta) &= \text{const}_l^\infty (\cos \eta_l \cdot j_l'(\kappa R) - \sin \eta_l \cdot n_l'(\kappa R)). \end{aligned} \quad (2.65)$$

* Any differential equation can be numerically integrated without boundary conditions being specified. Initial conditions are, of course, necessary.

Introducing the logarithmic derivative of the radial wave function,

$$\lambda_l(E) = \left[\frac{1}{\mathcal{R}_l(E)} \frac{d}{dr} \mathcal{R}_l(E) \right]_{r=R}, \quad (2.66)$$

we obtain for the phase shift

$$\tan \eta_l(E) = \frac{j'_l(\kappa R) - j_l(\kappa R) \cdot \lambda_l(E)}{n'_l(\kappa R) - n_l(\kappa R) \cdot \lambda_l(E)}, \quad (2.67)$$

where the primes denote differentiation with respect to r .

Let us discuss the E dependence of the function λ_l . The function $\lambda_l(E)$ has zeroes at energies E_l^0 and it has singularities at energies ε_l determined by*

$$\frac{d}{dr} \mathcal{R}_l(r, E_l^0) |_{r=R} = 0, \quad (2.68)$$

$$\mathcal{R}_l(r, \varepsilon_l) |_{r=R} = 0. \quad (2.69)$$

To see whether λ_l is a decreasing or increasing function of E , we write out (2.25) for energy E_1 , multiply it by $\mathcal{R}_l(E_2) r^2$ and integrate over r from 0 to R . Next we take (2.25) for energy E_2 , multiply it by $\mathcal{R}_l(E_1) r^2$ and integrate over r . Subtracting the second integral from the first, we get

$$\begin{aligned} & [r^2 (\mathcal{R}_l(E_2) \mathcal{R}'_l(E_1) - \mathcal{R}_l(E_1) \mathcal{R}'_l(E_2))]_0^R \\ &= (E_1 - E_2) \int_0^R \mathcal{R}_l(E_1) \mathcal{R}_l(E_2) r^2 dr, \end{aligned}$$

where use has been made of Eq. (2.14). Now let E_2 tend to E_1 :

$$E_1 - E_2 = 2\kappa \delta\kappa, \quad \mathcal{R}_l(E_2) = \mathcal{R}_l(E_1) + (\partial \mathcal{R}_l / \partial \kappa) \delta\kappa,$$

$$\left[-r^2 \mathcal{R}_l^2 \frac{d}{dE} \lambda_l(r, E) \right]_0^R = \int_0^R \mathcal{R}_l^2(r, E) r^2 dr.$$

As r tends to zero, $\mathcal{R}_l \propto r^l$, in accordance with Eqs. (2.47) and (2.28); consequently,

$$\lambda_l(r \rightarrow 0) \propto l r^{-1}, \quad (2.70)$$

and we have

$$\frac{d}{dE} \lambda_l(R, E) = - \frac{1}{R^2 \mathcal{R}_l^2(R, E)} \int_0^R \mathcal{R}_l^2(r, E) r^2 dr. \quad (2.71)$$

Since the right-hand side of (2.71) is negative we conclude that $\lambda_l(E)$ is a monotonically decreasing function apart from the point ε_l where it changes from minus to plus infinity (see Fig. 2.1).[†]

* Note that these conditions are similar to those used for the bonding and antibonding functions in diatomic molecules (cf Chapter 4 in [37]).

2.2.4. The behavior of $\tan \eta_l$ as a function of E . Since λ_l may assume any value, it should be expected that at certain energies either the numerator or denominator in (2.67) will vanish and $\tan \eta_l(E)$

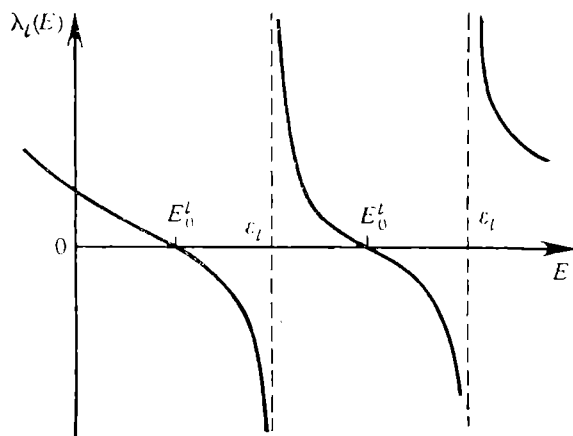


Fig. 2.1. Logarithmic derivative λ_l versus energy. (See Fig. 4.7 for actual dependence.)

will have zeroes and singularities similar and related to those of $\lambda_l(E)$.

The position of a singularity of $\tan \eta_l(E)$ (or a resonance energy, to use the accepted term) can be found by solving the nonlinear equation

$$\lambda_l(E) = n_l^{-1}(\kappa R) \frac{d}{dr} n_l(\kappa R). \quad (2.72)$$

In other words, when \mathcal{R}_l is matched to an irregular solution n_l of the homogeneous equation, the scattering gives rise to a resonance.

Let us define a hard-sphere potential as being infinite at $r \leq R$ (R being the radius of the sphere) and zero at $r > R$. (We shall see later that this is an "MT-type" potential.) In this case the solution of Eq. (2.25) for $r \leq R$ is zero at any energy: $\mathcal{R}_l(E, r) = 0$, which means that, whatever the energy, the logarithmic derivative $\lambda_l(E, r)$ is infinite. Equation (2.67) then gives the phase β_l for hard-sphere scattering:

$$\tan \beta_l(E) = j_l(\kappa R)/n_l(\kappa R). \quad (2.73)$$

On the other hand, if for an arbitrary scattering potential and an energy $E = \epsilon_l$ Eq. (2.69) is valid, then we have a singularity in $\lambda_l(E = \epsilon_l)$ by (2.66). This means, in turn, that at $E = \epsilon_l$ the potential acts as a hard sphere, or

$$\eta_l(\epsilon_l) = \beta_l(\epsilon_l). \quad (2.74)$$

It follows that at $E = \varepsilon_l$ the true potential may be replaced by an infinite repulsive one, which supports our earlier conclusion that, provided a new potential is appropriately chosen, it may be substituted for the true potential $V(r)$ without distorting the description of the scattering process.

We have thus discussed the behavior of $\tan \eta_l$ near $E = \varepsilon_l$. With regard to its low-energy behavior let us consider the scattering problem for a square well of depth V_0 and radius R . We denote $\kappa_0 = \sqrt{E + V_0}$ to obtain the solution of (2.25) as spherical Bessel functions $j_l(\kappa_0 R)$ and

$$\tan \eta_l(E) = \frac{j'_l(\kappa R) - j_l(\kappa R) j'_l(\kappa_0 R)/j_l(\kappa_0 R)}{n'_l(\kappa R) - n_l(\kappa R) j'_l(\kappa_0 R)/j_l(\kappa_0 R)}. \quad (2.75)$$

To study the low-energy behavior of $\tan \eta_l$ we may use the asymptotic values (2.28). It can be seen from (2.73) and (2.75) that in both cases considered above the low-energy behavior of $\tan \eta_l$ is the same; indeed, it is the same for all finite-range potentials, viz.

$$\lim_{E \rightarrow 0} \tan \eta_l(E) \propto E^{l + \frac{1}{2}}. \quad (2.76)$$

Next we turn to the behavior of $\tan \eta_l$ near a resonance. It is tempting to interpret the conditions for "bonding and antibonding", Eqs. (2.68) and (2.69), as arising from the interaction between a certain level (of, say, energy E_l^{res}) and a perturbation. The perturbation may result, for example, from a change in boundary conditions: a previously discrete level appears, "all of a sudden", above the energy zero and therefore becomes quasi-discrete. The electrons may then leave this level and spread throughout space or, to put it another way, the electron lifetime at the level becomes finite instead of being infinite as in the discrete case. For the rest of our discussion we shall use the Schrödinger representation [7, 38] in which the wave function depends harmonically on time:

$$\psi(t) = \psi(t=0) e^{iEt/\hbar}.$$

To describe the time decay of this quasi-discrete state, its energy should be considered a complex variable (in distinction to a discrete level):

$$E_l^{\text{res}} = E_l + i\Delta_l. \quad (2.77)$$

The quantity Δ_l , known as the level width, is related to the electron lifetime τ_l at the (quasi-discrete) level by

$$\tau_l \cdot \Delta_l \simeq 1.$$

Instead of the width Δ_l , it is customary to use the halfwidth $\Gamma_l = \Delta_l/2$. Assuming the existence of a quasi-discrete level of energy E_l

and the halfwidth Γ_l , we obtain [39]:

$$\tan \eta_l = \frac{\tan \eta_l^0 + \Gamma_l / (E_l - E)}{1 - \tan \eta_l^0 \cdot \Gamma_l / (E_l - E)}. \quad (2.78)$$

From this (see [39], Eq. (134.10)) there follows a relationship for the phases:

$$\eta_l = \eta_l^0 + \arctan \frac{\Gamma_l}{E_l - E}, \quad (2.79)$$

where $\eta_l^0(E)$ is the scattering phase for energies far away from E_l . Equation (2.78) can be rewritten formally as

$$\tan \eta_l = \tan \eta_l^0 + \frac{\Gamma_l'}{E_l' - E}, \quad (2.80)$$

where

$$\begin{aligned} \Gamma_l' &= \Gamma_l (1 + \tan^2 \eta_l^0), \\ E_l' &= E_l - \Gamma_l \tan \eta_l^0. \end{aligned} \quad (2.81)$$

We are now in a position to determine the behavior of $E_l'(E)$, taking into account, of course, that for (2.76) to hold at low energies, we must have

$$\Gamma_l = \Gamma_l(E) \propto E^{l+\frac{1}{2}}. \quad (2.82)$$

It follows from (2.80) that the energy of a singularity of $\tan \eta_l$ is not identical to a resonance-level energy. The presence of the potential-scattering phase (denoted η_l^0 to distinguish it from the resonance case) renormalizes the resonance energy much in the same way as friction affects mechanical resonance. This means that E_l' can be shifted relative to E_l by $\Gamma_l \tan \eta_l^0$ (or about 0.1 Ry to 0.3 Ry). In the theory of the transition metals (see Figs. 6.4, 6.5 and Secs. 2.3, 5.1) a d band arises from a quasi-discrete level, the energy of which is usually thought to be the average energy of the band. This is not the case, however: we shall see in Sec. 5.1 that the average energy is actually E_l' .

Equation (2.81) may be regarded as the first-order result obtained in the LCAO model: the role of the perturbation is played by the deviation of Γ_l from zero and the perturbation itself is caused by a change in boundary conditions. The level is shifted by the magnitude of the "perturbing" potential.

2.2.5. The relationship between the energies of the singularities of $\tan \eta_l$ and λ_l . To find this relationship we first write out the energy as a function of the phase shift. It follows from (2.79) that

$$E = E_l + \Gamma_l \cot(\eta_l^0 - \eta_l).$$

The singularity in λ_l implies that Eq. (2.74) is satisfied. This means that at $E = \varepsilon_l$ the phase η_l equals β_l . The desired equation thus is

$$\varepsilon_l = E_l + \Gamma_l \cot(\eta_l^0 - \beta_l), \quad (2.83)$$

where all the quantities are evaluated for the energy ε_l . The closer the scattering is to the hard-sphere case, the farther ε_l is from E_l . This means that in the energy range under study one of the two singularities may be present and the other not. It should be noted that the hard-sphere scattering need not always be strong: the phase β_l is small when j_l approaches zero. With d electrons, the asymptotic form (2.29) is correct for $\kappa R > 3$, the zeroes of j_l are determined from the condition $\kappa R - \pi = n\pi$ and, accordingly, the asymptotic value (2.29) may be helpful in locating even the first zero. In band calculations, κR is ordinarily somewhat less than 3 so that the hard-sphere d scattering must be weak for energies of about 1 Ry which is, typically, the upper energy limit for such calculations.

2.2.6. Levinson's theorem. The above formalism is also applicable at negative energies because Eq. (2.25) is integrable for any E , including $E = -\kappa^2$, the only difference from the $E = +\kappa^2$ case being in boundary conditions for \mathcal{R}_l at infinity.

The negative-energy solution of Eq. (2.25) is again a superposition of regular (j_l) and irregular (n_l) solutions, regarded as functions of the imaginary argument $i\kappa R$. The boundary condition corresponding to a bound state is that the normalization integral is finite. This implies that as r tends to infinity, \mathcal{R}_l should go to zero faster than r^{-3} . The only combination to satisfy this condition is the function γ_l^+ , which represents an outgoing wave (see (2.31)). Comparing (2.31) and (2.57) yields the condition for the existence of a bound state:

$$\tan \eta_l = -i. \quad (2.84)$$

Let us set up the function $\varphi_l = i\kappa f_l$, where

$$f_l = \frac{1/\kappa}{\cot \eta_l - i} \equiv \frac{1}{\kappa} e^{i\eta_l} \sin \eta_l \equiv \frac{1}{2\kappa i} (e^{2i\eta_l} - 1). \quad (2.85)$$

The function f_l is called the partial scattering amplitude and its elements between $|\mathbf{k}\rangle$ and $|\mathbf{k} + \mathbf{q}\rangle$ form the t -matrix. In the complex energy plane the scattering amplitude has poles at the energies of the bound levels.

Let us introduce the function

$$\tilde{f}_l = \frac{d}{d\kappa} \ln |2\varphi_l + 1|$$

and integrate it over the interval $0 \leq \kappa \leq +\infty$. As usual, the integration contour must enclose all the poles of the function \tilde{f}_l ,

which coincide with those of f_l . The integral will be $-2\pi i$ times the number of singularities of the integrand (alias the number of bound states, N_l) (see [40]). On the other hand, the definition of \tilde{f}_l and Eq. (2.85) indicate that this integral must be $2i (\eta_l(0) - \eta_l(\infty))$. We thus have arrived at Levinson's theorem [41], namely

$$\eta_l(0) - \eta_l(\infty) = \pi N_l. \quad (2.86)$$

Although, it must be admitted, our derivation is not perfectly strict, the theorem has been rigorously proved elsewhere [42-44].

The phases involved in (2.86) are the usual phases for positive (that is, $E = +\kappa^2$) energies.*

There are two conclusions to be drawn from the above discussion. Firstly, scattering theory can yield the energies of bound states. Secondly, Levinson's theorem reveals that the number of levels at $E < 0$ is related to the behavior of the phase at $E > 0$. It is this remarkable fact that will allow us to introduce the concept of the pseudopotential.

Since it is clear that at high energies $V(r)$ is negligible as compared to E and equation (2.25) therefore becomes homogeneous, the phase shift is usually subjected to an additional condition, namely $\eta_l(\infty) = 0$. In this case Levinson's theorem states that

$$\eta_l(0) = \pi N_l, \quad (2.87)$$

except for the $l = 0$, $E_l = 0$ case, when $\eta_l(0) = \pi (N_l + 1/2)$.

2.2.7. True and spurious quasi-stationary levels. The quasi-discrete (resonant) level becomes a discrete one when the attractive potential gets stronger: the E_l level goes down and the quantity Γ_l decreases, that is, the energy E_l^{res} appears on the real axis. At $E_l = 0$ the resonance width is also zero and the potential gives rise to a bound state, thus affecting the phase (see Fig. 2.2d).

It can be seen from Fig. 2.2b, c that the phase passes through $\pi/2$ (at energy E_x) either when increasing or decreasing. But as the potential increases still further, the low-energy part of the $\eta_l(E)$ curve "bulges out" and E_x moves toward higher energies (see Fig. 2.2d, e). The picture then repeats itself, this time shifted upward by π . The energy E_x will thus never fall into the region of bound states. This may be seen from Fig. 2.2f where a zero-energy bound state is shown: for E_x to reach (at least) zero, the phase shifts must

* We have considered an individual local potential for which bound states are only possible at negative energies. Levinson's theorem has not yet been proved for nonlocal potentials capable of producing positive-energy bound states. Recent attempts [45, 46] to interpret N_l in Eq. (2.86) as the total number of bound states (at both negative and positive energies) have proved to be incorrect [47]. See also [48, 49].

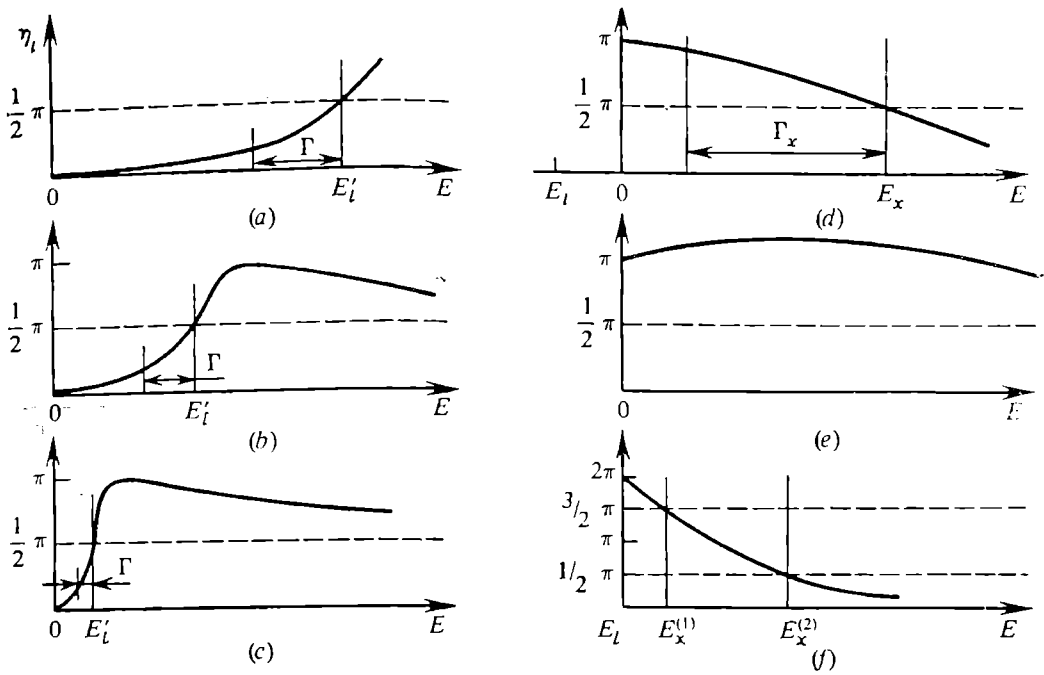


Fig. 2.2. Phase shift η_l versus energy E for potentials of different strengths. The potential deepens from (a) to (e).

vanish at $E = 0$. It is clear intuitively that this is impossible and indeed it has been shown [50, 42] that the magnitude of the derivative $d\eta_l/dE$ is bounded from below, i.e.

$$-\kappa R \leq \tau_l \equiv 2d\eta_l(E)/dE \leq +\infty \quad (2.88)$$

The quantity τ_l is called the electron's scattering time delay. The negative values imply that a scattered electron sort of outruns a free one instead of being retarded as before (this may be seen from Eq. (2.52)). The lower bound is due to the causality [42].

The resonances of $\tan \eta_l$ at E_x has thus nothing to do with the presence of a quasi-discrete level.

The resonances at E_l and E_x may be distinguished by their width. The minimum resonances width $\Gamma_{l,x}^{\min}$ is of the order of $1/\tau_l^\infty$. It follows from (2.88) that $\Gamma_{l,x}^{\min} \simeq (R\sqrt{E_x})^{-1}$ and if the resonance width of $\tan \eta_l$ is less than $\Gamma_{l,x}^{\min}$, we may be confident that the resonance occurs at a quasi-discrete level. This argument may be helpful in interpreting atomic physics experiments or in a preliminary analysis of the band structure of a solid. Figure 2.3, for example, shows the phase shifts found in [51] for crystalline Al (the shifts are given in radians; the s shift is diminished by 2π and the p shift by π). Note that there are d and f scattering shifts in this case, even though the Al atom contains neither d nor f electrons.

The difference between the phase shifts of s and d electrons can be clearly seen. It may be argued that the d electrons must be scattered by a quasi-discrete level, that is, a d band is described in terms of the LCAO method. At the same time it is clear that even though the s phase will pass through $\pi/2$ this is actually an x -type resonance, so that the LCAO scheme is not suitable for describing the s band (because of the lack of the original level) and instead the NFE model is needed. A calculation of the Fermi energy in Al by Eq. (1.32) shows that $E_F^0 < E_{l=2}$, that is, in crystalline Al only s and p scattering is significant and the Al band structure must be calculated by the NFE model. This latter circumstance is confirmed by practice.

Note that the low-energy phase shifts obey the rule:

$$\eta_0 > \eta_1 > \eta_2 > \eta_3 \quad (2.89)$$

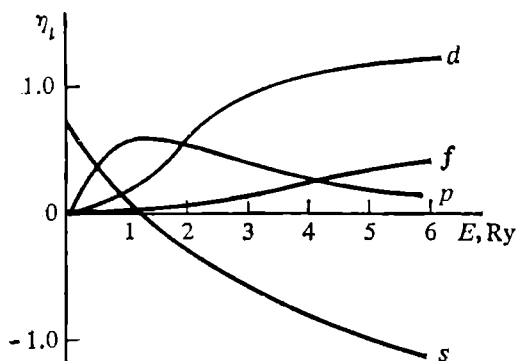


Fig. 2.3. Phase shifts for Al as derived from a crystal potential [51].

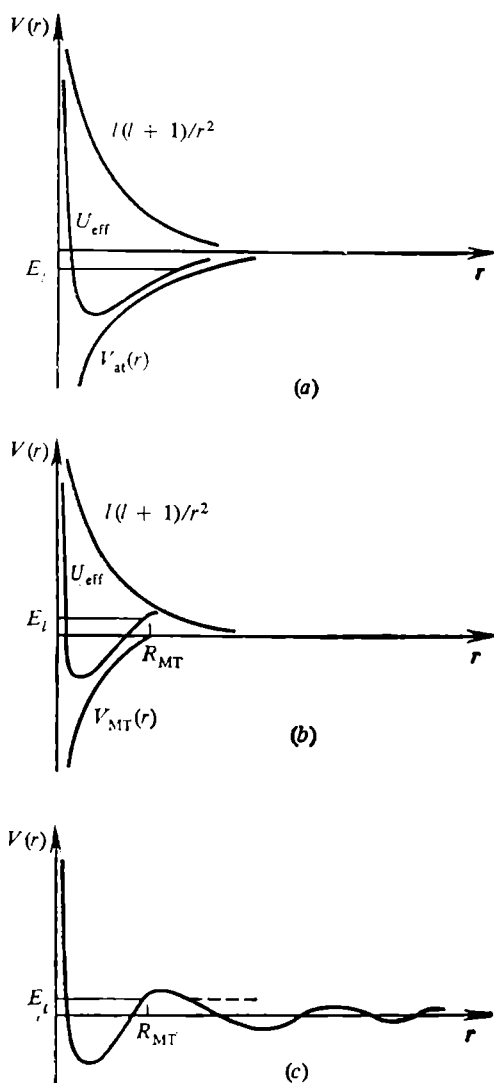


Fig. 2.4. Formation of a quasi-bound state: (a) the minimum of a free-atom potential, (b) the minimum of a short-range potential, (c) Friedel oscillations on the tail of an MT potential.

which follows from the asymptotic behavior given by Eq. (2.76). Physically, the explanation for this is that the centrifugal potential $U_l = l(l+1)r^{-2}$ in Eq. (2.25) is a repulsive one: it prevents the electron from approaching the origin. As l increases so does the inac-

cessible area, the effect of the potential on the electron weakens and hence the phase shift gets smaller. Clearly, the inaccessible area should be smaller for higher-energy electrons.

Although the centrifugal potential is of a purely classical nature, it leads to a very interesting quantum mechanical consequence. When $r \rightarrow 0$, the total potential $U_{\text{eff}} = V(r) + U_l(r) \propto +r^{-2}$, when $r \rightarrow \infty$, $U_{\text{eff}} \propto -r^{-1}$. Obviously, U_{eff} has a minimum (see Fig. 2.4a). If, however, $V(r)$ decreases faster than r^{-2} at $r \rightarrow \infty$, then $U_{\text{eff}} \propto +r^{-2}$ which means that the function $U_{\text{eff}}(r)$ must

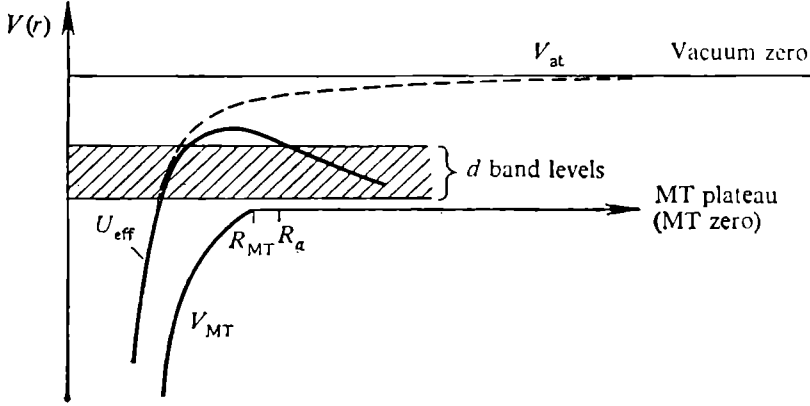


Fig. 2.5. Characteristic contributions to the crystal potential. The example shown is Pt [52].

also have a maximum, as shown in Fig. 2.4b. The quasi-discrete level from the above discussion may then be viewed as a resonance state in this potential (Fig. 2.4b).

The actual relationship between the characteristic contributions to the crystal potential is shown in Fig. 2.5 for Pt [52]. We can see both the radius of the sphere inscribed within a Wigner-Seitz cell ("muffin-tin" or MT sphere and hence the MT-radius) and the radius of the Wigner-Seitz sphere. The atomic potential is shown for comparison. The shaded area indicates the approximate location of the d band levels.

2.2.8. Friedel's sum rule. We have thus established that depending on the energy of the scattered electron, the potential may act either attractively or repulsively. It would thus be appropriate to characterize a potential by the difference between the total number of electrons it scatters and the number of electrons that would be present in the absence of the potential. To evaluate this parameter we employ Eq. (2.71), which yields the number of electrons with energy E that are contained within a sphere of radius R . When R is large enough, we can use the asymptotic value (2.52) with the normalization

(2.59), i.e.

$$\begin{aligned} & \frac{4\pi}{\Omega_0} \int_0^R R_l^2(r, E) r^2 dr \\ &= \frac{4\pi}{\Omega_0} (\text{const}_l^\infty)^2 \frac{1}{2E} \left[R + \frac{d\eta_l}{d\kappa} - \frac{1}{2\kappa} \sin \left(2 \left(\kappa R - \frac{l\pi}{2} + \eta_l \right) \right) \right]. \end{aligned}$$

Setting $\eta_l = 0$ we obtain the number of free electrons formerly within the sphere. Subtracting one from the other, we have

$$\Delta\rho_l(E) = \frac{2\pi}{\kappa} \left[\tau_l(E) - \frac{\sin \eta_l}{E} \cos(2\kappa R - l\pi + \eta_l(E)) \right].$$

This is the number of electrons that were in the state with energy E . To find the total number of electrons scattered by the potential, we must multiply $\Delta\rho_l(E)$ by the unperturbed density of states, sum over all l , and integrate the result over the energy range from 0 to E_F^0 . Taking spin into account gives

$$\begin{aligned} \Delta Z &= 2 \frac{\Omega_0}{4\pi^2} \int_0^{E_F^0} V \bar{E} \sum_l (2l+1) \Delta\rho_l(E) dE = [\mathcal{F}(E_F^0) - \mathcal{F}(0)] \\ &\quad - \frac{1}{\pi} \int_0^{E_F^0} \sum_l (2l+1) \frac{\sin \eta_l}{E} \cos(2\kappa R - l\pi + \eta_l) dE, \quad (2.90) \end{aligned}$$

where we used the Friedel sum:

$$\mathcal{F}(E) = \frac{2}{\pi} \sum_l (2l+1) \eta_l(E). \quad (2.91)$$

The integral in Eq. (2.90) cannot be carried out analytically unless the $\eta_l(E)$ function is specified, but at large R it can be shown to be proportional to $1/R$. This can easily be verified for small phase shifts.

If a potential does not produce bound states then, by the Levinson theorem, $\mathcal{F}(0) = 0$. If it does, then the choice of energy zero becomes important. If the bound states are not relevant to the problem, the energy zero should be chosen so as to place them below the energy range of interest. We may then use the degree of freedom in the definition of the phase shifts to subtract πN_l from each shift. This, in a sense, is a change from the original potential to another potential (or, more properly, pseudopotential) that has no bound states. But then, by the Levinson theorem, $\mathcal{F}(0)$ will again go to zero. Thus,

$$\Delta Z = \mathcal{F}(E_F^0). \quad (2.92)$$

Equation (2.92) is usually employed for impurity studies in crystals. In this case, ΔZ is, by definition, the difference between the numbers of valence electrons in the host and impurity atoms. The E_F^0 in (2.92) is the matrix Fermi energy and (2.92) is then a certain condition imposed on the phase shifts for impurity scattering. This condition is known as the Friedel sum rule. Using this rule in the form of (2.90) we can find (provided we have correct phase shifts) a quantity R which may be regarded as the effective impurity radius or the maximum distance at which the impurity potential is still felt. A knowledge of the effective radius makes it possible to find the maximum impurity concentration beyond which the impurities start interacting with each other to form impurity bands (at which point the alloy may no longer be considered a dilute solid solution).

An impurity atom is sometimes modeled by a square well with a depth chosen to satisfy the Friedel sum rule, Eq. (2.92). The phase shifts so obtained are then used for calculating the residual resistance due to impurities. The results [53-56] were in qualitative agreement with experiment. The Friedel sum rule turns out to be quite a reliable computational tool, even if the integral in (2.90) is disregarded.

Now it is natural to ask what the Friedel sum is for a pure crystal. On the one hand, this must be the difference between the valencies of the host and impurity atoms—which is zero. On the other hand, this is the number of electrons that, in the NFE model, must be removed from an atom in the ion formation process, to be given back when the ion enters the crystal. This means that the Friedel sum is by no means zero but rather equals the valency of the atom, Z . With this approach, the Friedel sum rule is also valid for an impurity. We thus encounter a paradox whose resolution will be postponed until Sec. 3.5.

Since the integral in Eq. (2.90) is an alternating sign function of R , ΔZ oscillates with R . To see how this arises, let us consider the r dependence of the l th component of the electron density. We start from the free electron case.

Far from the origin, the number of electrons with a given l may be written

$$\begin{aligned} \rho_{\text{free}}^l(r) &\simeq \int_0^{E_F^0} V \overline{E} j_l^2(\kappa r) dE \\ &= \frac{1}{r^3} \left(r \sqrt{E_F^0} - \frac{1}{2} \sin(2r \sqrt{E_F^0} - \delta_l) - \frac{1}{2} \sin \delta_l \right), \end{aligned} \quad (2.93)$$

where we have introduced the phase $\delta_l = (1/2) l\pi$. Apart from the leading term, which is of the order of r^{-2} , there is an oscillating additive term that decreases as r^{-3} .

Now if a scatterer is placed at the origin, ρ_{scat}^l is given by an equation like (2.93) but with the δ_l replaced by $(1/2) l\pi - \eta_l$, hence

$$\Delta\rho^l(r) = \rho_{\text{scat}}^l - \rho_{\text{free}}^l \\ \simeq \frac{(-1)^l}{r^3} \sin \eta_l [\cos(2r \sqrt{E_F^0} + \eta_l) + \cos \eta_l (E_F^0)]. \quad (2.94)$$

The excess density due to the presence of the scatterer falls off as r^{-3} and has a term that oscillates with distance, being known as Friedel oscillations. It is this term that causes the ΔZ oscillations. It should be remarked that Eq. (2.94) also contains a term which does not oscillate but which is disregarded in most books on band theory. A similar result was obtained in [57].

The density distribution as given by (2.94) is associated with the Coulomb potential $V_{\text{el}}(r)$. The potential must also affect the electrons including those producing it. We have thus started with a finite-range potential and arrived at a long-range one (see Fig. 2.4c). Our calculations thus lack self-consistency. What is more, we can no longer, with the potential V_{el} , consider η_l to be an assumption used in the derivation of Eqs. (2.90) and (2.94).

That there can be no short-range potentials in an electron gas is important in solid state theory, for analogous potentials are the ones used to model all interatomic interactions. We shall see in Sec. 3.2 that the interatomic interaction potential of Chapter 1 also yields characteristic Friedel oscillations.

2.3. Pseudism and scattering

From now on we shall frequently use the word "pseudism" as proposed in [17] as a general term to denote all phenomena associated with pseudopotentials.

2.3.1. Pseudism and the periodicity in the properties of the chemical elements. For the sake of simplicity, consider a one-dimensional square well of depth V_0 . The wave function in this case is a plane wave $\exp(ikx)$, for which $\sqrt{E} = k$ outside the well and inside $k = \sqrt{E + V_0}$. Thus the wavelength inside the well is shorter (and the oscillation frequency higher) than outside. This then is the reason for a path difference (or phase shift) between an electron surmounting the well and the free motion case.*

A rise in the oscillation frequency indicates the greater wave function curvatures and hence larger $\nabla^2\Psi$. Thus oscillations reflect

* The effect of bound states on scattering is for the moment neglected; we shall discuss it later.

increases in the electron's kinetic energy due to increases in the (absolute) magnitude of its potential energy. A phase shift is thus a manifestation of the virial theorem (for more details, see [29]).

Now if the well is made deeper the curvature of the oscillations increases, the time delay gets longer and the scattering stronger until at a certain value $V_0^{(1)}$ a zero-energy bound state is produced. The situation may then be described by saying that the level "traps" the electron and "holds" it for a time (hence the time delay) the duration of which is related to the energy of the level by

$$\tau_l \propto (E + |E_l|)^{-1}. \quad (2.95)$$

Further increases in V_0 push the level in the well to lower energies, the quantity τ_l in (2.95) is made smaller and the scattering weaker.

When the potential becomes strong enough to contain another bound state, the scattering becomes stronger and the situation is repeated. As bound states with new orbital numbers are produced, the scattering process involves higher partial components of the plane wave. Resonances will be observed for the $l > 0$ components.

If the square-well atomic model is adopted, atoms with larger nuclear charges will be approximated by deeper wells. By varying the well depth, potentials for all the chemical elements may be modeled.

The variation of the phase shift with well depth (for square-well scattering) is illustrated in Fig. 2.6. The figure shows the wave function in the absence of scattering (Fig. 2.6a), weak scattering by a shallow well (Fig. 2.6b), strong scattering by a middle-depth well (Fig. 2.6c). Finally, Figure 2.6d shows that as the well is deepened still further, the scattering may again become as weak as that in Fig. 2.6b. If the function's behavior inside the well is ignored, then Figure 2.6b and Figure 2.6d are the same. It can be seen that the wave function is "pulled in" as the well gets deeper.

In Fig. 2.6d the shallow potential of Fig. 2.6b is also shown. The shaded area affects the magnitude of the formfactor by contributing to the integral, but it has no effect on the scattering or, to put it another way, on the formation of the crystal energy spectrum.

The above discussion is important enough to deserve a review. As illustrated in Fig. 2.6, the periodic change in the scattering pattern with increasing well depth is associated with the wave function being "pulled" into the well, or, in other words, with the phase shift being only determined modulo π . This indeterminacy suggests, as we have already remarked, that the true potential may be replaced by a pseudopotential. On the other hand, the periodicity in the strength of scattering implies periodicity in physical properties.

The NFE model depicts a metal as a gas of free electrons scattered by an atomic lattice and, as follows from the factorization of the

matrix element, Eq. (1.21), the interaction of an electron with a given atom is, in effect, independent of the rest of the atoms.

Around each of these atoms oscillations in charge density (see Sec. 2.2) and hence in screening potential will arise. Each atomic cell is, by definition, electrically neutral. It then follows that the inter-atomic interaction, which is the sum of a direct term (Coulomb

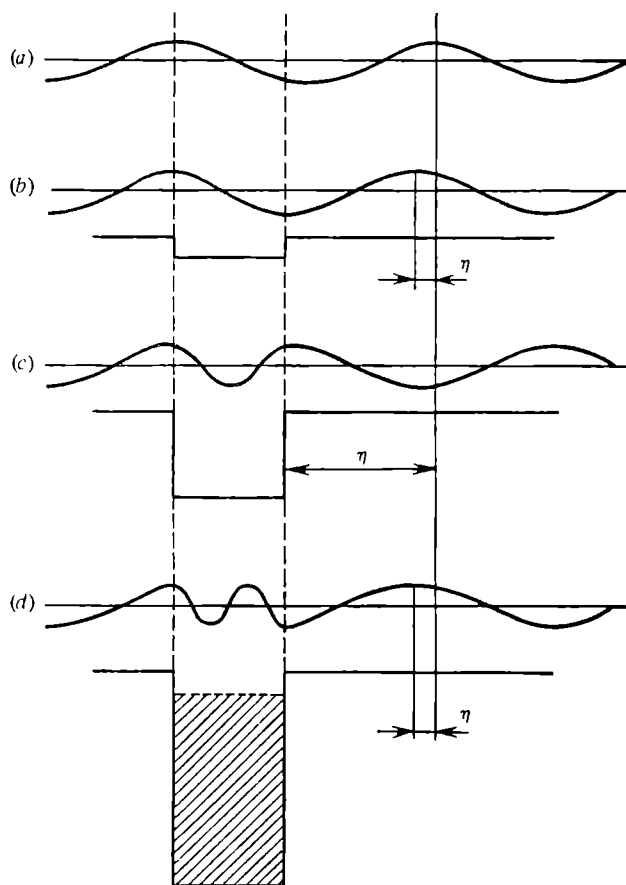


Fig. 2.6. Variation of the phase shift with the depth of the square well.

repulsion) and an indirect one (the interaction via conduction electrons), reduces to the indirect term alone, i.e., to the oscillating potential V_{el} .

Suppose that at some moderate distance r_0 from a given atom (A) there is another atom (B). Generally, the atom B experiences a force $F_{at} = -\text{grad } V_{el}$. Depending on the sign of F_{at} , the atom B will be either attracted to atom A (the equilibrium separation a is then smaller than the initial r_0) or repelled from it, whence $a > r_0$. As the atomic number of A increases (or the square well deepens) the quantity $V_{el}(r = r_0)$ oscillates, since the wave function is "pulled in" by the atom A . Consequently, F_{at} changes sign. This means that

the equilibrium interatomic distance (the lattice parameter) is an oscillating function of atomic number, a phenomenon which has indeed been observed [58-60].

In the same manner pseudism manifests itself in the oscillatory behavior of other macroscopic crystal properties. The moduli of elasticity, for example, are determined by the slope of V_{el} at atomic sites (i.e., by the elastic forces F_{at}) and therefore oscillate with increasing atomic number. The same forces determine the elasticity of a vibrating lattice, that is, the phonon characteristics of crystals. For example, the Debye temperature varies periodically with atomic number [58-60].

Since, by the Lindeman criterion, the melting point is related to the Debye temperature [3], some correlation should exist between the melting temperature and the cohesion energy. This is indeed the case [58].

The same elastic forces determine the thermal expansion coefficient which, accordingly, also shows periodicity (for example, its correlation with melting point is reported in [58, 61]).

The concepts of pseudopotential and of a "pulled-in" wave function have thus proved to be effective tools for interpreting crystal properties (for more examples, see [17]).

We pointed out in the Introduction that even the periodicity in the properties of the elements can be readily explained in terms of pseudism.

As the atomic number increases, the outer shell is gradually filled by electrons until at some moment it becomes a "core" shell. The atomic core is thus periodically re-defined, which means that the potential felt by a valence electron is repeated within the periodic table (with some variations in detail though).

It should be emphasized that the mere existence of bound states does not necessarily imply that the scattering is strong. It is however strong if (a) these states are close to the zero energy (see Eq. (2.95)) or (b) they result from a small variation in the potential (virtual states in the terminology of [39]) or (c) the scattering potential has quasi-bound (or resonant) states. The last condition follows from the definition of the time delay, Eq. (2.88), combined with Eq. (2.79):

$$\tau_l(E) = \tau_l^0(E) + 2 \frac{\Gamma_l}{(E_l - E)^2 + \Gamma_l^2}. \quad (2.96)$$

The time delay is given by the classical Breit-Wigner formula and is therefore a Lorentzian curve superimposed on the smooth background due to the potential scattering with phase $\eta_l^0(E)$.

Thus, from the point of view of scattering theory not every potential with bound states gives large corrections to the free-electron dispersion law $E = k^2$ (see Eq. (1.31)). But then a paradox arises:

on the one hand, these corrections clearly must be small, on the other the corresponding perturbation expansion must diverge.

It is intuitively clear that the shaded area on the potential curve of Fig. 2.6*d*, while not contributing to the phase shift, must lead to the divergence of the perturbation series. This area may not simply be “cut off”, and the origin of the phase shift should therefore be discussed in more detail.

2.3.2. Phase function method and pseudopotentials. Let us define the phase function $\eta_l(r)$ for all r by demanding that the solution \mathcal{R}_l of the Schrödinger equation have the form (2.45) for all r , the phase shift $\eta_l(r)$ being defined as in (2.48). The ambiguity due to the appearance of two unknown functions ($C_l(r)$ and $S_l(r)$) instead of one ($\mathcal{R}_l(r)$) can be removed by imposing an additional condition on \mathcal{R}_l . It is convenient to write this condition in accordance with (2.65):

$$\frac{d}{dr} \mathcal{R}_l(r) = C_l(r) \frac{d}{dr} j_l(\kappa r) - S_l(r) \frac{d}{dr} n_l(\kappa r). \quad (2.97)$$

Then, by substituting (2.45) into (2.25), and expressing C_l in terms of S_l , we obtain differential equations for C_l and S_l leading, in turn, to an equation for the phase function $\eta_l(r)$:

$$\frac{d}{dr} \tan \eta_l(r, E) = -\kappa V(r) r^2 [j_l(\kappa r) - \tan \eta_l(r, E) n_l(\kappa r)]^2. \quad (2.98)$$

This is the basic equation for the quantum-mechanical phase-function method [27, 28].

By performing mentally a numerical integration of Eq. (2.98) we can get an idea of the r -dependence of the phase shift.

Let the energy of the electron be close to zero. At $r = 0$ the right-hand side of Eq. (2.98) is zero. From Eq. (2.47) it follows that $\eta_l(r = 0) = 0$. Increasing r means that increasingly more regions of the potential are made to participate in the scattering process, causing thereby a gradual increase in the phase.

At a certain value of R_l , the “already integrated” region of the potential produces a zero-energy bound state ($E_l = -0$) on which the incoming electron ($E_l = +0$) is resonantly scattered. The right-hand side of Eq. (2.98) (which is the derivative $(d/dr)(\tan \eta_l)$) must then be large. At the point where the bound state “appears” the phase shift jumps. In accordance with the Levinson theorem (2.87) the phase must be πN_l .

As the integration goes on, the phase shift jumps each time a bound state with a given l “appears” (see Fig. 2.7).

When, for example, the potential well defined by the curve between the points $-\infty, V^{(1)}, R_l^{(1)}$, gives rise to a zero-energy bound state, then, by the Levinson theorem, $\eta_l = \pi$. We can introduce three pseudopotentials ($i = 1, 2, 3$) which lead to the same (modulo π)

small phase. Each pseudopotential is zero for $r < R_l^{(i)}$ while, for larger r , they coincide with $V(r)$ from $V^{(i)}$ on. The most suitable potential is $i = 3$, shown by the bold line.

If the scattered electron has a nonzero energy, the jumps in phase are rounded off, which means that the positions of R_l depend on the electron's energy.

Instead of the true potential, we may consider, at a given energy, a corresponding pseudopotential:

$$W_l(r, E) = \begin{cases} 0, & r \leq R_l(E), \\ V(r), & r > R_l(E). \end{cases} \quad (2.99)$$

This may be seen by noting that, according to (2.98), the phase shift does not depend on r in the zero potential. For both the true potential $V(r)$ and the pseudopotential $W_l(r, E)$ the scattering phase shift accumulated to the point $r = R_l$ is πN_l and the wave functions \mathcal{R}_l^V and \mathcal{R}_l^W at this point (as well as their derivatives) will coincide. At $r > R_l$ the phase equations for the potential and pseudopotential will be the same, which means that the wave functions will be also the same. We conclude that the removal of the core region of the potential does not alter its scattering characteristics. This allows us to introduce a pseudopotential [62, 66]*.

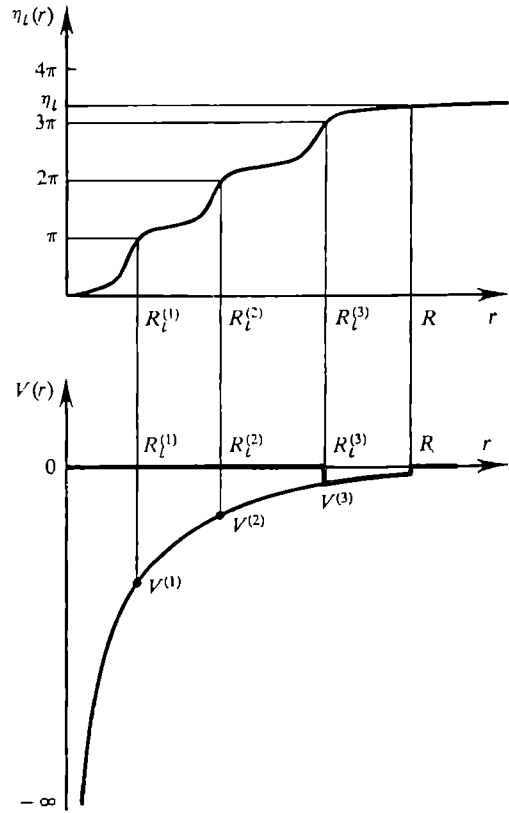


Fig. 2.7. Above: the build-up of phase shift with gradual integration of the radial Schrödinger equation. Below: the potential V of the radial equation (normal line) and the pseudopotential (bold line).

* The variations in R_l with energy turn out to be small. For Li^+ , Na^+ , and K^+ they are negligible [63], for di- and trivalent elements they are larger. For Mg^{++} , for example, they are 1.4% for the $l = 0$ electrons within about 0.17 Ry of the Fermi energy (as calculated for Mg in the NFE approximation). For Ca^{++} the variations in $R_{l=0}$ are 3.3%, in $R_{l=1}$ about 1.7%. The variations for Al^{+++} turned out to be smaller than those for Ca^{++} [64]. Note that the calculations were carried out for ions rather than for neutral atoms. To our knowledge, the phase function method has not yet been employed in pseudopotential theory.

The qualitative ideas developed at the beginning of this section may now be complemented by the following remark which is obvious in the context of the phase function method. Even though elements in the same groups but in different periods have identical valence shells, they differ in their pseudopotentials because of the different numbers of bound states. Therefore, the elements in a new period are always different (however little) from those in the old one.

In the $3d$ transition metals, for example, the d electrons are affected by the whole of the potential. As a result, the width Γ_l of a resonant level will be smaller in $3d$ metals than in $4d$ metals, which have core d levels. Since Γ_l is a measure of the disturbance felt by the electrons (see Sec. 2.2) the d bands of $3d$ -metal will be narrower than their $4d$ counterparts. On the other hand, narrow bands favor ferromagnetism and it is the $3d$ metals Fe, Co and Ni which are ferromagnetics. Note that these are end-period metals and their E_l level is therefore low (by the argument of Secs. 2.2.7 and 2.3.1, E_l moves to lower values along a d period because as Z grows this level must be bounded, so that Γ_l also decreases toward the end of a period (Eq. (2.82)) and the d bands get narrower. For metals of other d periods, Γ_l is greater and, accordingly, they are less inclined to ferromagnetism. Amongst the elements of a given d period the most probable candidates for ferromagnetics are those at the end where Γ_l is relatively small. Both these conclusions are in good agreement with experiment.*

It can be easily shown [65] that the wider the band resulting from an atomic (or, in this case, quasi-atomic) level, the higher is the cohesion energy of the metal. Since d bands get wider from $3d$ to $4d$ and then to $5d$ metals, the cohesion energy should increase from one period to another. This is also confirmed by experiment [58, 60].

The pseudopotential (2.99) shown in Fig. 2.7 is not the only one to derive from the phase function method. Instead of an "empty core" with an energy-dependent radius, we could also consider a square well with an energy-dependent depth. Then

$$W_l(r, E) = \begin{cases} -A_l(E), & r \leq R_l, \\ V(r), & r > R_l. \end{cases} \quad (2.100)$$

The well depth A_l should be chosen for each energy by matching, at $r = R_l$, the inside and outside solutions:

$$\frac{j_l'(R_l \sqrt{E + A_l(E)})}{j_l(R_l \sqrt{E + A_l(E)})} = \lambda_l(r = R_l, E). \quad (2.101)$$

The only thing, in fact, needed to carry through this procedure is to know how to construct the potential "seen" by the electrons in

* A similar, if more complicated, situation occurs in f metals where relativistic corrections seem to be of importance.

the crystal. A suitable procedure may be borrowed from the band-calculation method and is based on the use of secular equations (it is described in Sec. 3.5). The calculation of the function $\lambda_l(E)$ and determination of A_l from (2.101) present no computational difficulties. We can therefore introduce a model pseudopotential that automatically incorporates the free-electron-gas screening of the atom (since screened potentials are used in band calculations).

For a potential of (finite) range R , an equivalent square well may be constructed by using the matching procedure of (2.101) at $r = R$. The computation of the corresponding formfactor is then drastically simplified since there is no need to do a numerical integration outside R_l .

Finally, it should be noted that applying the above argument to the NFE model makes the construction of a pseudopotential particularly easy since outside the ion core the $V(r)$ function has, of course, the form (1.26), where Z is the number of valence electrons. For such a potential, the solutions \mathcal{J}_l are known: they are Coulomb functions [67, 68]. The right-hand side of Eq. (2.101) becomes analytical and the evaluation of A_l is then straightforward.

2.3.3. The Lloyd pseudopotential. Scattering theory allows still another type of pseudopotential, which will be important later.

Consider the difference $\lambda_l(E) - \mathcal{J}_l(E)$, where $\mathcal{J}_l(E)$ is the logarithmic derivative of the electronic wave function in the absence of a scatterer. The difference logarithmic derivative $\lambda_l - \mathcal{J}_l$ reflects the strength of scattering. Thus we have (cf. (2.66)):

$$\mathcal{J}_l(E) = \left[\frac{1}{j_l(\kappa r)} \frac{d}{dr} j_l(\kappa r) \right]_{r=R}, \quad (2.102)$$

$$\lambda_l - \mathcal{J}_l = (\mathcal{R}'_l j_l - \mathcal{J}_l j'_l) / (j_l \mathcal{R}_l) = -\frac{\tan \eta_l}{\kappa R^2 \mathcal{R}_{lj_l}}. \quad (2.103)$$

Here use has been made of the normalization (2.55)-(2.57). Finally:

$$R^2 (\lambda_l - \mathcal{J}_l) = \int_0^\infty \frac{j_l(\kappa r)}{j_l(\kappa R)} V(r) \frac{\mathcal{R}_l(r, E)}{\mathcal{R}_l(R, E)} r^2 dr. \quad (2.104)$$

This equation links the difference logarithmic derivative with the potential that determines it. This equation is for λ_l like equation (2.56) is for $\tan \eta_l$.

It is clear that Eq. (2.104) is satisfied not only by the true $V(r)$ but also by the pseudopotential

$$W_l(r, E) = [\lambda_l(R, E) - \mathcal{J}_l(R, E)] \delta(r - R). \quad (2.105)$$

It can readily be seen that substituting (2.105) into both Eq. (2.104) and Eq. (2.57) leads to identities.

The pseudopotential (2.105) was obtained by Lloyd [69] in the framework of band theory, and we have also come to it in a discussion of the isolated-center scattering problem. The Lloyd pseudopotential suggests that a crystal may be described by models other than the LCAO or NFE. This can be seen by combining Eqs. (2.103), (2.67) and (2.57) to give an exact equation

$$\lambda_l(E) - j_l(E) = - \frac{\tan \eta_l^z(E)}{\kappa R^2 j_l^2(\kappa R)}, \quad (2.106)$$

in which we used the phase shift η_l^z introduced by Ziman [70], i.e.

$$\cot \eta_l^z(E) = \cot \eta_l - n_l(\kappa R)/j_l(\kappa R). \quad (2.107)$$

Note that the phase η_l^z describes the difference between the scattering patterns produced by the potential $V(r)$ and the hard-sphere potential (2.73). The more η_l differs from β_l , the larger $\cot \eta_l^z$ becomes and the less the pseudopotential (2.105) affects the electron gas. This disturbance is the greatest for a hard-sphere-like potential. In this sense, a hard sphere is the strongest scatterer possible and any deviation from it means less effective scattering.

We can follow this approach to develop a pseudopotential theory for a strong scatterer. The first step will be to calculate the band structure for a crystal whose actual atoms are substituted for by hard spheres. Next, we will consider the departure of the scattering potential from the hard sphere model as a perturbation and correct the solutions. Clearly, the solutions for the initial model will only depend on the lattice type and lattice constant. The solutions can be tabulated and then easily recalculated to a new lattice constant.

Certainly, the band-structure problem for the initial crystal is not easy, but the formalism is available: this is the secular equation of the Green function method (see Sec. 5.1) involving only the quantity $\cot \eta_l^z$ (see Eqs. (5.3) and (4.56)).

2.4. Bound states, pseudopotentials and the convergence of series

2.4.1. Bargmann's criterion for the existence of bound states. Scattering theory thus helps us in choosing an initial pseudopotential. We are still at a loss, however, as to why the perturbation series is divergent for a potential producing bound states. Furthermore, we cannot be confident that the scattering-theory pseudopotential may be treated by perturbation theory. In other words, we do not yet know how scattering theory is related to NFE-model perturbation theory. These are the questions we take up in this section (which may safely be skipped by a reader not interested in the subject).

First, let us establish a criterion by which to judge whether or not a potential can produce bound states. To do this, note that Eq. (2.59) for a phase function may be rewritten for all r by changing the upper integration limit from infinity to r .

If the electron's energy is zero, the appearance of a bound state leads to resonance scattering, that is, $\tan \eta_l$ goes to infinity, which is only possible if

$$\kappa \int_0^r n_l(\kappa r) V(r) \mathcal{R}_l(r, E) r^2 dr = 1. \quad (2.108)$$

We introduce the n th moment of a potential:

$$B_n = \int_0^\infty V(r) r^n dr, \quad \tilde{B}_n = \int_0^\infty \tilde{V}(r) r^n dr, \quad (2.109)$$

where \tilde{V} denotes the attractive part of $V(r)$.

If E goes to zero, $\mathcal{R}_l \propto j_l(\kappa r)$. Substituting the asymptotic values (2.28) into (2.108) yields a condition for there being no bound states with a given l in the potential, i.e.

$$\frac{1}{2l+1} |\tilde{B}_1| < 1. \quad (2.110)$$

This expression is closely related to Bargmann's theorem [28, 71], which states that the number of bound states N_l obeys the condition

$$N_l \leq \frac{1}{2l+1} |\tilde{B}_1|. \quad (2.111)$$

Our next concern is to find out a relation between the formulas of scattering theory and those of NFE perturbation theory. In other words, we wish to reformulate scattering theory in such a way that, instead of phase shifts or logarithmic derivatives, it contains pseudo-potential formfactors. Then, hopefully, the formalism of scattering theory might be used to develop pseudopotential theory further.

Consider the scattering-theory integral equation (2.4). It can be rewritten formally as

$$\Psi = \varphi + G_0 V \Psi, \quad (2.112)$$

where Ψ is the wave function to be found, V is the scattering potential $V(r)$ and G_0 is the free motion Green's function (2.12). This equation is known in scattering theory as the Lippmann-Schwinger equation.

Solving equation (2.112) by successive approximations (i.e. using perturbation theory), we obtain the Born series:

$$\Psi = \varphi + G_0 V (\varphi + G_0 V \Psi) = \varphi + G_0 V \varphi + G_0 V \varphi G_0 V \varphi + \dots \quad (2.113)$$

This expression can be obtained by formally rewriting (2.112) in the form

$$\Psi = (1 - G_0 V)^{-1} \varphi \quad (2.114)$$

and then expanding in powers of $G_0 V$. The convergence condition for this series is therefore given by the operator inequality:

$$G_0 V < 1, \quad (2.115)$$

which is only meaningful when it operates on φ . The convergence condition for the perturbation theory approach in scattering problems is thus

$$|\varphi(\mathbf{r})| > \left| \int G_0(\mathbf{r}, \mathbf{r}') V(\mathbf{r}') \varphi(\mathbf{r}') d^3 r' \right|. \quad (2.116)$$

Note that $|\varphi| = 1$ because $\varphi = e^{i\mathbf{k}\cdot\mathbf{r}}$. The inequality (2.116) holds for any \mathbf{r} , so that we can set $r = 0$ without losing generality. For a spherically symmetrical potential, a coordinate system may be chosen in such a way that the vector \mathbf{k} points in the z direction. Integrating over angles, we get [6]:

$$\left| \int_0^\infty V(r) (e^{2i|\mathbf{k}|r} - 1) dr \right| < 2k. \quad (2.117)$$

At low energies (for scattering from an isolated center, $E = k^2$) the exponential can be expanded. By making use of (2.109), we find

$$\sqrt{B_1^2 + EB_2^2} < 1. \quad (2.118)$$

At $E = 0$ we have thus obtained a convergence condition analogous to (2.110). Note that in Eq. (2.110) only the attractive part of the potential is involved, whereas in Eq. (2.118) the whole potential is.

If the potential has a repulsive part, Eq. (2.110) cannot be used as the convergence condition for the Born series (2.113).

We can easily construct a model potential such that, on the one hand, it will produce bound states, and on the other it will ensure the convergence of (2.113) by criterion (2.118). The reverse case is also possible and it is important for the potentials that are chosen to ensure smooth wave functions (\mathcal{R}_l does not oscillate and has no zeroes, hence there are no λ_l singularities at $r < R$ and no bound states in the potential). Such a pseudopotential may have a significant repulsive part (equal, for example, to the average energy of the scattered electron): in this region the wave function is virtually constant and, by (2.118), the series will diverge.

Note that $4\pi B_2/\Omega_0$ (cf. (2.109)) is, on the one hand, the average value of the potential $V(r)$ and on the other, the long-wavelength

limit ($q \rightarrow 0$) of its formfactor (1.23). It may therefore be said *a priori* that if

$$k|B_2| > 1, \text{ i.e., } k|\langle \mathbf{k} | V | \mathbf{k} \rangle| > 4\pi/\Omega_0, \quad (2.119)$$

then the Born series will diverge.*

2.4.2. Born series in scattering and perturbation theories. Our next concern is to demonstrate that the scattering theory in the form of (2.113) is equivalent to the perturbation theory in the form of (1.31). We consider the first Born approximation for the wave functions:

$$\Psi = e^{i\mathbf{k}\mathbf{r}} + \int G_0(\mathbf{r}, \mathbf{r}') V(\mathbf{r}') e^{i\mathbf{k}\mathbf{r}'} d^3r'. \quad (2.120)$$

It is easily seen that by (2.11)

$$\begin{aligned} & \int G_0(\mathbf{r}, \mathbf{r}') V(\mathbf{r}') e^{i\mathbf{k}\mathbf{r}'} d^3r' \\ &= \int \sum_{\mathbf{q}} \frac{e^{i\mathbf{q}(\mathbf{r}-\mathbf{r}')}}{q^2 - k^2} V(\mathbf{r}') e^{i\mathbf{k}\mathbf{r}'} d^3r' = \sum_{\mathbf{q}} \frac{e^{i\mathbf{q}\mathbf{r}}}{q^2 - k^2} \langle \mathbf{q} | V | \mathbf{k} \rangle. \end{aligned} \quad (2.121)$$

It is convenient here to separate out the vector \mathbf{k} explicitly by shifting the origin. Taking into account that the order of summation in (2.121) is immaterial, we have

$$\int G_0(\mathbf{r}, \mathbf{r}') V(\mathbf{r}') e^{i\mathbf{k}\mathbf{r}'} d^3r' = \sum_{\mathbf{q}} \frac{\langle \mathbf{k} + \mathbf{q} | V | \mathbf{k} \rangle}{(\mathbf{k} + \mathbf{q})^2 - k^2} e^{i(\mathbf{k} + \mathbf{q})\mathbf{r}}, \quad (2.122)$$

where the right-hand side is nothing but the first-order NFE wave function.

We have thus proved that for weak potentials satisfying (2.115), scattering theory becomes equivalent to NFE perturbation theory. Since the convergence conditions are the same for perturbation theory and for the Born series (2.113), it follows that we have also proved the validity of (2.118) for pseudopotential perturbation theory: the series (1.31) diverges for an everywhere attractive potential having bound states.

2.4.3. The Austin-Heine-Sham theorem. Let us prove now a remarkable theorem which shows that in Eq. (2.112) (or, equivalently, in Eqs. (2.113) and (1.30)) a part of the potential may be "thrown away" without invalidating the equation.

Let Ψ in Eq. (2.112) be an eigenfunction of a continuum state of the Hamiltonian $H = -\nabla^2 + V(\mathbf{r})$. It must be orthogonal to the

* We shall see later that typically in pseudopotential theory $\langle \mathbf{k} | W | \mathbf{k} \rangle = -(2/3) E_F^0$. This means according to (2.119) that the perturbation expansion for a single scatterer can only converge if $Z < (2/\pi) (k_F/k) \approx 0.6 (k_F/k)$. For scattering in crystals, the situation is much more complicated.

bound (discrete) states $\Phi_\alpha(r)$ of the same Hamiltonian, with quantum numbers $\alpha = \{n, l, m\}$:

$$\langle \alpha | \Psi \rangle \equiv \int \Phi_\alpha^*(r) \Psi(r) d^3r = 0. \quad (2.123)$$

We set up a potential involving a projection operator (see (2.40)) onto the bound states Φ_α :

$$\hat{V}^{\text{bound}} = \sum_\alpha U_\alpha \hat{P}_\alpha = \sum_\alpha U_\alpha |\alpha\rangle \langle \alpha|. \quad (2.124)$$

By (2.123) we have

$$\hat{V}^{\text{bound}} \Psi = 0. \quad (2.125)$$

Consequently, if (2.125) is added to the right-hand side of (2.112), the equation will still hold, and we may write

$$\Psi = \varphi + G_0 W \Psi \quad (2.126)$$

where we have introduced the pseudopotential $W(r)$:

$$W(r) = V(r) + \sum_\alpha U_\alpha(r) |\alpha\rangle \langle \alpha|. \quad (2.127)$$

From the point of view of scattering theory, this pseudopotential has the same properties as the original one had (the resulting wave function is the same), but it may be much weaker by perturbation theory standards. To make this clear, we evaluate its formfactor (see Eq. (1.23)):

$$\langle \mathbf{k} + \mathbf{q} | W | \mathbf{k} \rangle = \langle \mathbf{k} + \mathbf{q} | V | \mathbf{k} \rangle + \sum_\alpha \langle \mathbf{k} + \mathbf{q} | U_\alpha | \alpha \rangle \langle \alpha | \mathbf{k} \rangle. \quad (2.128)$$

Suppose we can separate out a region (of radius R_c) where the functions Φ_α are localized; this is in fact the ion core formed by bound states. Inside this core region the functions Φ_α form a complete set in the sense that for $r \leq R_c$ and $r' \leq R_c$ (cf. (2.10))

$$\sum_\alpha \Phi_\alpha^*(\mathbf{r}') \Phi_\alpha(\mathbf{r}) = \delta(\mathbf{r}' - \mathbf{r}). \quad (2.129)$$

Let us define $U_\alpha(r)$ as

$$U_\alpha(r) = U(r) = \begin{cases} -V(r), & r \leq R_c, \\ 0, & r > R_c. \end{cases}$$

As a result, we obtain

$$\begin{aligned} \langle \mathbf{k} + \mathbf{q} | W | \mathbf{k} \rangle &= \langle \mathbf{k} + \mathbf{q} | V | \mathbf{k} \rangle + \langle \mathbf{k} + \mathbf{q} | U | \mathbf{k} \rangle \\ &= \frac{4\pi}{\Omega_0} \int_{\text{outside the ion core}} e^{-i(\mathbf{k} + \mathbf{q})\mathbf{r}} V(\mathbf{r}) e^{i\mathbf{k}\mathbf{r}} d^3r, \end{aligned} \quad (2.130)$$

that is, the potential has indeed been stripped of all its interior region, which is responsible for the bound states!

We have thus proved the following existence theorem for pseudopotentials: an original potential may be modified by adding a more or less arbitrary potential but from the scattering theory point of view it will remain the same.

A similar theorem for conventional pseudopotential theory states that adding an expression of the form (2.124) does not change the eigenvalues of the Schrödinger equation. This is the Austin-Heine-Sham theorem [3, 72, 73].

2.4.4. Pseudopotential optimization. Because of the arbitrariness of U_α , a great many pseudopotentials are possible. The Austin-Heine-Sham theorem only tells us that a pseudopotential can be found but it says nothing about how it affects the electron gas. In the literature, it is often stated that an optimal pseudopotential should be chosen. One of the various optimization criteria is that there be no bound states.

It follows from the argument in Sec. 2.3 that wave function oscillations inside the potential are due to the presence of bound states. But then if we require that there be no such oscillations and set up a corresponding pseudopotential, this will be suitable. If, further, we require that the function be as smooth as possible, the pseudopotential will be the best achievable. This will also secure a good convergence of the perturbation theory series.

This optimization criterion was suggested in 1961 by Cohen and Heine [74]. It may be applied both to model pseudopotentials and to the OPW pseudopotential (see Secs. 2.5 and 4.2). In the latter case the optimization procedure leads to a replacement of the unknown energy E in Eq. (4.31) by an approximation [73] (Cohen and Heine, for example, derived a first-order dispersion law). Note that the difference between OPW pseudopotentials due to the difference between the initial dispersion laws can be ascribed to (or rather described by) movements of the ion-core levels E_α caused by neighboring atoms [75]. These displacements do exist and are sometimes quite large [76-78].

Unfortunately, the smoothness of wave functions is not an entirely satisfactory criterion. The point is that a potential which is weak from the point of view of perturbation theory may still not yield smooth wave functions. This was first noted by Pendry [79]. Consider the Schrödinger equation

$$(-\nabla^2 + V(r))\Psi = E\Psi \quad (2.134)$$

where V is the crystal original potential. Let us replace V by an arbitrary model pseudopotential (2.124):

$$V \rightarrow V + \hat{V}_R, \quad (2.132)$$

$$\hat{V}_R \Psi = \sum_{\alpha} |\alpha\rangle \langle F_{\alpha} | \Psi \rangle \quad (2.133)$$

where F_{α} is an arbitrary function and $|\alpha\rangle$ are core states. Now by substituting Eqs. (2.132) and (2.133) into (2.131), multiplying by Ψ^* , integrating over all space, and using the orthogonality of Ψ (a conduction band function!) to the core states, we find that when calculating $E(\mathbf{k})$ the result is the same as if we were dealing with the initial Schrödinger equation (2.131). Thus the Schrödinger equation even with the best possible of the (2.132) type pseudopotentials leads to the same oscillatory crystalline function.

Pendry showed [79] that the smoothness criterion is only valid for a non-Hermitian pseudopotential, for which the weakness of the perturbation turns out to be uniquely related to the smoothness of the wave function. The optimization criterion he proposed can be described briefly as follows. The replacement of the true potential by a general pseudopotential (2.133) displaces the Hamiltonian's eigenvalues including the core ones. The new core levels are

$$E'_{\alpha} = E_{\alpha} + \langle F_{\alpha} | \alpha \rangle. \quad (2.134)$$

This is simply the expectation value for the pseudo-Hamiltonian $(-\nabla^2 + \hat{V} + \hat{V}_R)$ taken for the $|\alpha\rangle$ states.

The perturbation series will converge most quickly if the bound states are eliminated. Thus, for a pseudopotential having a single core state, a sufficient optimization condition is

$$E'_{\alpha} = 0, \quad (2.135)$$

which leads to the pseudopotential given in [79].

$$\hat{W} = V - E_{\alpha} |\alpha\rangle \langle \alpha|. \quad (2.136)$$

This potential is energy-dependent and Hermitian.

Some other criteria have also been proposed. In [80] all the criteria except Pendry's are comprehensively discussed and yet another criterion is proposed, namely, the electron density deviates least from its mean value. On the one hand, this is closely related to the idea of a smooth pseudowave function, on the other it is associated with the pseudopotential that least affects the electron gas (the 'minimum perturbation' pseudopotential, see Sec. 3.5). Perhaps the best approach would be to minimize the deviation from the mean

of the crystal density (taking screening into account). Such a pseudopotential would have a minimum effect on the electron gas. So far this criterion has not been used.

In Sec. 4.1 we introduce Pendry's pseudopotential (2.136) without explicitly optimizing it.

2.5. Scattering theory and potential formfactors

It was shown in Sec. 2.3 that the true potential can be replaced by a pseudopotential exactly, approximations only come with perturbation theory.

While scattering theory does not involve formfactors, they are used in the band theory applications of the pseudopotential method. In Sec. 2.4 we derived (2.122) with formfactors inside the sum. The formula has already done its job, and we shall now discuss the use of formfactors in scattering theory from a somewhat different angle.

2.5.1. Scattering amplitude. Let us reconsider the integral equation (2.4). The Green's function (2.12) may be approximated for large r by

$$G_0(\mathbf{r}, \mathbf{r}') = -\frac{1}{4\pi} \frac{1}{r} e^{i\kappa r - i\kappa' r'}, \quad (2.137)$$

where we have introduced a wave vector for a scattered state, i.e.

$$\kappa' = \kappa \frac{\mathbf{r}}{|\mathbf{r}|}. \quad (2.138)$$

Using (2.137) and denoting $\varphi_\kappa \equiv |\kappa\rangle$, we obtain from (2.4):

$$\Psi_\kappa = \varphi_\kappa + f(\kappa, \kappa') \frac{e^{i\kappa r}}{|\mathbf{r}|}, \quad (2.139)$$

$$f(\kappa, \kappa') = -\frac{\sqrt{\Omega}}{4\pi} \langle \kappa' | V | \Psi_\kappa \rangle, \quad (2.140)$$

where the factor $\sqrt{\Omega}$ comes from the definition: $|\kappa\rangle = \Omega^{-1/2} \times \exp(i\kappa r)$.

Equation (2.139) is a typical example of the "mixing" of an irregular solution (at $r \rightarrow 0$) with a regular one. The strength of scattering is characterized by the function $f(\kappa, \kappa')$ which is known as the scattering amplitude [38, 42]. This is a fundamental concept of scattering theory.

Let us define the l th component of the scattering amplitude (or the partial scattering amplitude) f_l as

$$f(\kappa, \kappa') = \sum_l (2l+1) f_l(E) P_l(\cos \theta_{\kappa\kappa'}) \quad (2.144)$$

where we have used the normalization (2.56) and the fact that $\kappa^2 = (\kappa')^2 = E$. It can easily be seen that $f_l(E)$ is defined by

$$f_l(E) = \frac{1}{\sqrt{E}} \tan \eta_l(E). \quad (2.142)$$

If Ψ_κ is taken in the complex (i.e., running wave) representation, the quantity f_l becomes complex and is determined by Eq. (2.85). This is what is customarily done in works on scattering, although the right-hand side of (2.142) is then called the K -matrix instead of the scattering amplitude; the reader should not be confused by this conflicting terminology.

We now return to the Born approximation. It is clear from Eq. (2.140) that by replacing Ψ_κ by φ_κ we have introduced a potential formfactor into scattering theory. If somewhat loosely, the Born approximation may be interpreted as replacement of the tangent of the scattering phase for a given potential by the formfactor of the potential:

$$f^B(\kappa, \kappa') = -\frac{\Omega}{4\pi} \langle \kappa' | V | \kappa \rangle. \quad (2.143)$$

Equation (2.140) holds for both weak and strong scattering, but to go from (2.140) to (2.143) is only possible for weak scattering. In order to justify the pseudopotential method in terms of scattering theory, a formula with a formfactor must be derived for strong scattering as well. How is this possible?

2.5.2. The t -matrix. Let us define an operator t such that its action on an unperturbed function φ_κ gives the same result as that for the operator V acting on the perturbed function Ψ_κ :

$$t\varphi_\kappa = V\Psi_\kappa. \quad (2.144)$$

The scattering amplitude can then always be expressed in terms of a formfactor:

$$f(\kappa, \kappa') = -\frac{\Omega}{4\pi} \langle \kappa' | t | \kappa \rangle. \quad (2.145)$$

Obviously, t is a generalization of the concept of the pseudopotential.

The formfactors $\langle \kappa' | t | \kappa \rangle$ form the t -matrix (though the same name is also applied to the t -operator).

The t -operator obeys the integral equation

$$t\varphi_\kappa \equiv V(\varphi_\kappa + G_0 V \Psi_\kappa) = V\varphi_\kappa + V G_0 t\varphi_\kappa \quad (2.146)$$

which can be solved by perturbation theory:

$$t = V + V G_0 V + V G_0 V G_0 V + \dots \quad (2.147)$$

In view of (2.144), the Born approximation for t coincides with the original potential:

$$t^B = V. \quad (2.148)$$

By introducing a partial t -operator t_l we obtain from (2.145)

$$\begin{aligned} \langle \kappa' | t | \kappa \rangle &= -\frac{4\pi}{\Omega} \frac{1}{\kappa} \sum_l (2l+1) \tan \eta_l P_l(\cos \Theta_{\kappa, \kappa'}) \\ &\equiv \sum_l (2l+1) t_l(E) P_l(\cos \theta_{\kappa, \kappa'}), \end{aligned} \quad (2.149)$$

$$t_l(E) = -\frac{4\pi}{\Omega} \frac{1}{\kappa} \tan \eta_l(E) = -\frac{4\pi}{\Omega \kappa} \frac{1}{\cot \eta_l}. \quad (2.150)$$

In the standing-wave representation, the t -matrix has singularities due to $\tan \eta_l$. In the running-wave representation, these singularities are only important for bound states since, by (2.145), the t -matrix has the form (2.85):

$$t_l(E) = -\frac{4\pi}{\Omega \kappa} e^{i\eta_l} \sin \eta_l = -\frac{4\pi}{\Omega \kappa} \frac{1}{\cot \eta_l - i}. \quad (2.151)$$

This equation only has singularities when $\cot \eta_l = i$, that is, according to (2.84), when bound states arise.

Unfortunately, in the running-wave representation the t -matrix is not Hermitian

$$\langle \kappa' | t | \kappa \rangle \neq (\langle \kappa | t | \kappa' \rangle)^*,$$

even though with standing waves it is (cf. (2.150)).

We thus run into difficulties in trying to use the t -operator as a pseudopotential, since in the standing-wave representation the perturbation series may diverge because of the t -matrix singularities while in the running-wave case the band structure energy (1.40) becomes a complex quantity.

We thus have the paradox that although pseudopotential theory is clearly a special case of scattering theory, we do not yet understand how to use the more general form (see also [17]). It is for this reason that pseudopotential theory is as yet a distinct discipline.

2.5.3. The OPW pseudopotential in scattering theory. The difficulties in using the t -matrix as a perturbation pseudopotential arise because the t -operator is actually an *exact* solution of the problem. If the solutions were *modeled* the operators could be Hermitian at each step of the procedure (as may be seen from Eq. (2.147)).

Let us consider therefore the model approach to the scattering problem.

It can be seen from Eq. (2.148) that in the first Born approximation the t -matrix coincides with the potential. In Sec. 2.3 we used an integral equation to introduce the scattering phase (2.56) expressed in terms of \mathcal{R}_l , the l th component of the true wave function Ψ . In the first Born approximation Ψ is replaced by the plane wave:

$$\Psi = \frac{1}{\sqrt{\Omega}} e^{i\mathbf{k}\cdot\mathbf{r}}. \quad (2.152)$$

Consequently, the \mathcal{R}_l in the definition of the phase is replaced by j_l and we get

$$\tan \eta_l^B = -\kappa \int j_l^2(\kappa r) V(r) r^2 dr. \quad (2.153)$$

There are two ways we can improve on the first Born approximation. We can either include higher terms in (2.147) one by one or improve the zeroth order approximation (2.152) by somehow including some information about the potential. The remainder will then act as a perturbation. The better we make the zeroth-order model, the smaller the perturbation will be and the more workable the pseudopotential.

This is another illustration of an approach generally used in physics: an initial model is chosen so as to make the subsequent perturbation treatment most effective. (In band calculations, for example, this occurs when choosing the best trial functions with which to form the secular matrix.) So can we improve the approximation (2.152)?

Let us consider elastic scattering on a potential containing bound states; these latter are occupied and therefore unavailable for electrons. The true wave function Ψ is the continuum state of the same Hamiltonian whose discrete spectrum contains the bound states. We can therefore require that the Ψ function be orthogonal to the inner states Φ_α (α being a set of quantum numbers n, l, m). The effect of the potential will then be taken, if partly, into account.

The required zeroth approximation will thus be an orthogonalized to the inner states) plane wave (OPW):

$$\chi_{\mathbf{k}} = \frac{1}{\sqrt{\Omega}} e^{i\mathbf{k}\cdot\mathbf{r}} + \sum_{\alpha} \mu_{\alpha, \mathbf{k}} \Phi_{\alpha}(\mathbf{r}). \quad (2.154)$$

The coefficient $\mu_{\mathbf{k}, \alpha}$ is chosen from the orthogonality condition

$$\int \Phi_{\alpha}^*(\mathbf{r}) \chi_{\mathbf{k}}(\mathbf{r}) d^3r = 0,$$

which gives

$$\mu_{\alpha, \mathbf{k}} = -\frac{1}{\sqrt{\Omega}} \int \Phi_{\alpha}^*(\mathbf{r}) e^{i\mathbf{k}\cdot\mathbf{r}} d^3r = -\langle \alpha | \mathbf{k} \rangle. \quad (2.155)$$

The l th component of (2.154) with respect to \mathbf{k} and \mathbf{r} is

$$\mathcal{R}_l(r) \approx j_l(\kappa r) + \sum_n \mu_{n,|\mathbf{k}|,l} \phi_{nl}(|\mathbf{r}|), \quad (2.156)$$

where the radial function ϕ_{nl} is defined as $\Phi_{nlm}(\mathbf{r}) = \phi_{nl}(|\mathbf{r}|) Y_L(r)$.

Substituting (2.156) into (2.56) yields [81]

$$\tan \eta_l(E) = \tan \eta_l^B - \kappa \sum_n \mu_{n,|\mathbf{k}|,l} \int j_l(\kappa r) V(r) \phi_{nl}(r) r^2 dr. \quad (2.157)$$

This expression may be rewritten in a generalized Born form:

$$\tan \eta_l(E) = -\kappa \int \int j_l(\kappa r) r^2 W_l(r, r_1) j_l(\kappa r_1) r_1^2 dr dr_1, \quad (2.158)$$

where we have introduced the nonlocal pseudopotential

$$W_l(r, r_1) = V(r) \left[\frac{\delta(r-r_1)}{rr_1} - \sum_n \phi_{nl}(r) \phi_{nl}(r_1) \right]. \quad (2.159)$$

This is the same pseudopotential that we obtained from the Austin-Heine-Sham theorem and to show this, it suffices to evaluate the formfactor of expression (2.159):

$$W(r, r_1) = \sum_L W_l(r, r_1) Y_L(r) Y_L(r_1), \quad (2.160)$$

$$\langle \mathbf{k} + \mathbf{q} | W | \mathbf{k} \rangle = \langle \mathbf{k} + \mathbf{q} | V | \mathbf{k} \rangle - \sum_\alpha \langle \mathbf{k} + \mathbf{q} | V | \alpha \rangle \langle \alpha | \mathbf{k} \rangle \quad (2.161)$$

We observe once again that the (exact) scattering problem for the true potential may be treated as a Born-approximated scattering on a pseudopotential.

Using the equation for Φ_α and the Hermitian property, we find that

$$\begin{aligned} \langle \mathbf{k} + \mathbf{q} | V | \alpha \rangle \\ = \langle \langle \alpha | \nabla^2 + E_\alpha | \mathbf{k} + \mathbf{q} \rangle \rangle^* = -(\varepsilon_{\mathbf{q}} - E_\alpha) \langle \mathbf{k} + \mathbf{q} | \alpha \rangle, \end{aligned} \quad (2.162)$$

$$\begin{aligned} \langle \mathbf{k} + \mathbf{q} | W | \mathbf{k} \rangle \\ = \langle \mathbf{k} + \mathbf{q} | V | \mathbf{k} \rangle - \sum_\alpha (E_\alpha - \varepsilon_{\mathbf{q}}) \langle \mathbf{k} + \mathbf{q} | \alpha \rangle \langle \alpha | \mathbf{k} \rangle \end{aligned} \quad (2.163)$$

The expression for the formfactor is now simpler but, as can readily be verified, the formfactor remains non-Hermitian.

Interestingly, this pseudopotential is independent of energy. This is due here to the model we adopted for \mathcal{R}_l : had the orthogonalization coefficient been energy-dependent, so would the pseudopotential.

2.5.4. R-matrix pseudopotential. In the (approximate) formula (2.156) no account is taken of the phase shift: for $r > R_c$, R_c being

the ion core radius, \mathcal{R}_l tends to $j_l(\kappa r)$. A more rigorous treatment by Hubbard [81] employed artificial extra orbitals [82]. This approach was proposed in [83] and is now known as the R -matrix method [84, 85]. The idea is straightforward. If in the continuous spectrum the expansion in terms of bound-state eigenfunctions is impossible and hence the powerful method of trial functions (see Chapter 1) is inapplicable, we assume bound states to be introduced! To do this, the solutions of the radial Schrödinger equation (2.25) must be subjected to an appropriate boundary condition at the edge of the potential (cf. Sec. 5.2). The continuum will then acquire bound states, these will form the basis set to expand Ψ and the variation principle will then be used to find the best solutions.

It is reasonable to specify this boundary condition by requiring that the $\tilde{\phi}_\alpha$ orbitals smoothly join to the irregular solutions, i.e., spherical Neumann functions:

$$\frac{1}{\tilde{\phi}_\alpha(R)} \left. \frac{d}{dr} \tilde{\phi}_\alpha \right|_{r=R} = \frac{1}{n_l(\kappa R)} \left. \frac{d}{dr} n_l(\kappa r) \right|_{r=R}, \quad (2.164)$$

where α includes both l and an analog of the principal quantum number, namely, the index of the level which satisfies (2.164).

According to (2.164), the eigenvalues of this problem, E_α , are energy-dependent, that is, for each energy of a scattered particle there exists a special set of functions $\tilde{\phi}_\alpha(E)$. For a given E -value, the corresponding set is complete on $(0, R)$ for functions that behave well at zero and smoothly join to $n_l(\kappa r)$ at $r = R$. To appreciate the elegance of the boundary condition (2.164), note that $\mathcal{R}_l(r, E) = j_l(\kappa r)$ is one of the functions that smoothly join to n_l at $r = R$, and, as such, it can be expanded in terms of $\tilde{\phi}_\alpha(r)$:

$$\mathcal{R}_l(r, E) = j_l(\kappa r) + \sum_\alpha C_\alpha \tilde{\phi}_\alpha(r, E). \quad (2.165)$$

There is a close analogy between (2.165) and the OPW as given by (2.156). Substituting (2.165) into the Schrödinger equation (2.25) and using the orthonormality of $\tilde{\phi}_\alpha$, we obtain

$$C_\alpha = \frac{B_\alpha(E)}{E - E_\alpha}, \quad (2.166)$$

where

$$B_\alpha = \int_0^R j_l(\kappa r) V(r) \tilde{\phi}_\alpha^*(r) r^2 dr. \quad (2.167)$$

From (2.165), (2.166) and (2.56) we find

$$\tan \eta_l(E) = \tan \eta_l^B(E) - \kappa \sum_\alpha \frac{|B_\alpha|^2}{E - E_\alpha}. \quad (2.168)$$

This expression has a strong formal similarity to Eq. (2.80). The role of the resonance halfwidth is played here by the quantity $\kappa |B_\alpha|^2$, with a correct low-energy behavior of $\sim \kappa^{2l+1}$ (cf. (2.82)). Note that E_α is a function of energy, in accordance with (2.81).

Transforming, once again, the tangent of the phase shift to the generalized Born form (2.158), we obtain, instead of (2.159), a new pseudopotential

$$W(r, r_1) = V(r) \frac{\delta(r-r_1)}{rr_1} - \sum_{\alpha} \frac{V(r) \phi_{\alpha}(r) \phi_{\alpha}^*(r_1) V(r_1)}{E_{\alpha} - E} \quad (2.169)$$

with a Hermitian but energy-dependent formfactor

$$\langle \mathbf{k} + \mathbf{q} | W | \mathbf{k} \rangle = \langle \mathbf{k} + \mathbf{q} | V | \mathbf{k} \rangle - \sum_{\alpha} \frac{\langle \mathbf{k} + \mathbf{q} | V | \alpha \rangle \langle \alpha | V | \mathbf{k} \rangle}{E_{\alpha} - E}. \quad (2.170)$$

By transforming B_α , we may obtain an expression with orthogonalization coefficients similar to those of (2.155). To do this, we use the equation for $\tilde{\phi}_\alpha$, integrate in (2.167) by parts and take into account (2.164). This gives

$$B_\alpha = \frac{1}{\kappa} \frac{\tilde{\phi}_\alpha(R, E)}{n_l(\kappa R)} + (E_\alpha - E) \int j_l(\kappa r) \tilde{\phi}_\alpha^*(r) r^2 dr. \quad (2.171)$$

Suppose, all the states $\tilde{\phi}_\alpha$ of the original potential are deep, so that at the edge of the potential $\tilde{\phi}_\alpha(R) = 0$. It can easily be seen that the formfactor for such a potential is

$$\langle \mathbf{k} + \mathbf{q} | W | \mathbf{k} \rangle = \langle \mathbf{k} + \mathbf{q} | V | \mathbf{k} \rangle - \sum_{\alpha} (E_\alpha - E) \langle \mathbf{k} + \mathbf{q} | \alpha \rangle \langle \alpha | \mathbf{k} \rangle. \quad (2.172)$$

In the general case, the original potential V contains both deep and quasi-discrete levels, so that the α -sum in (2.170) includes both terms linear in $(E_\alpha - E)$ and singular at $E = E_\alpha$, that is, proportional to $(E_\alpha - E)^{-1}$.

It is interesting to note that (2.172) looks like a generalization of (2.163).

We recapitulate our discussion. First, the Born approximation (2.152) (cf. (2.113)) was shown to be equivalent to the perturbation theory approach. Using Eqs. (2.152) and (2.156), we then proceeded by modeling the scattering on the original potential; this is a very important point for a proper understanding of how the theories are related to each other. When substituting these equations into the exact scattering-theory expression (2.56), we required that it become a Born approximation or, in other words, that perturbation theory be applicable. It is this requirement that led us to the pseudopotentials (2.163), (2.170), and (2.172).

2.5.5. Other pseudopotentials. The above procedure clearly suggests two more ways for constructing pseudopotential formfactors. One is to evaluate the Lloyd-pseudopotential's formfactor (see (2.105)) directly. This will be the exact formfactor because perturbation theory will not be involved in the derivation.

Alternatively, we can employ scattering-theory model functions as the functions in terms of which to expand the required wave function Ψ ; when substituted into the Schrödinger equation for Ψ , this expansion will automatically lead to a pseudopotential.

The first method gives rise to the KKRZ-formfactor (the formfactor of the Korringa-Kohn-Rostoker-Ziman method, see Secs. 4.3 and 5.1), the second (using the OPW of (2.154)) leads to the OPW-formfactor (the formfactor of the orthogonalized plane wave method, see Sec. 4.2). Interestingly enough, the two approaches are generally considered to be entirely different whereas we have just seen both of them to originate from scattering theory.

In Chapter 4 both methods are used and compared.

Theory of potential

3.1. Potential seen by an atomic electron

3.1.1. Hartree-Fock equations. The motion of an atomic electron is usually described in the Hartree-Fock approximation as outlined in Chapter 1. The Schrödinger equation for the i th electron takes the form [86, 87]:

$$-\nabla^2 \Psi_i(\mathbf{r}) + \hat{V}_i^{\text{HF}} \Psi_i(\mathbf{r}) = E_i^{\text{HF}} \Psi_i(\mathbf{r}), \quad (3.1)$$

where

$$\begin{aligned} \hat{V}_i^{\text{HF}} \Psi_i(\mathbf{r}) = & -\frac{Ze^2}{r} \Psi_i(\mathbf{r}) + \left[\sum_j \int \frac{|\Psi_j(\mathbf{r}_1)|^2}{|\mathbf{r} - \mathbf{r}_1|} d^3r_1 \right] \Psi_i(\mathbf{r}) \\ & - \sum_j \Psi_j(\mathbf{r}) \int \frac{\Psi_j^*(\mathbf{r}_1) \Psi_i(\mathbf{r}_1)}{|\mathbf{r} - \mathbf{r}_1|} d^3r_1. \end{aligned} \quad (3.2)$$

The first term in (3.2) describes the attraction by the nucleus. The second is for the Coulomb repulsion from the rest of the electrons; this is an ordinary multiplication operator where the summation is over all the quantum numbers of the occupied orbitals (principal quantum number n , orbital angular momentum l , magnetic momentum m , and spin quantum number σ) or, for short, over all spin-orbitals. (At $j = i$ we have what is called Coulomb self-action: the electron, as it were, repels itself.)

The third term in (3.2), called the exchange potential, is again attractive and is an integral operator because the function Ψ_i appears inside the integrand. The j th summation only includes the spin-orbitals of the same spin as the orbital Ψ_i . The term is known as the exchange self-action term.

It can readily be seen that the $j = i$ terms in the second and third sums of (3.2) are equal in magnitude but opposite in sign so that in the Hartree-Fock approach the Coulomb and exchange self-actions cancel each other. A valence electron of a neutral atom may thus be said to move in the field of a singly-ionized atom, the potential it feels being produced by all the electrons except itself.

Equation (3.2) can be written for each function Ψ_i . Each Ψ_i depends on all the other orbitals. Equation (3.1) is solved iteratively until self-consistency is attained.

3.1.2. Orbital relaxation and electronegativity. Suppose an electron moves from one orbital to another. Since one of the spin-orbitals is thus changed, the potential (3.2) and, accordingly, all the other functions will also change. The change in atomic orbitals due to the transition of an electron from one to another is called orbital relaxation.

That electron transitions are accompanied by orbital relaxation is a major point in the physics of the atom. It is usually said that the energy needed to move an electron from the i th orbital (energy E_i) to the j th (energy E_j) is $\Delta = E_j - E_i$. This, however, is only true if the energy of orbital relaxation is neglected (this energy is of order $1/Z$ and may therefore be quite significant). The statement is known as Koopmans' theorem [88-90].

Orbital relaxation is of particular importance in light and hence low Z atoms. This is clearly illustrated by hydrogen. The hydrogen electron has an energy of 1 Ry. Supposing an H atom captures another electron, what energy will be released?

With the orbital relaxation ignored, the number is: 1 Ry. The correct answer is 0.055 Ry [91], an order and a half less.

The effects of orbital relaxation are exceptionally important in the study of chemical bonds in a molecule or crystal. Consider, for example, the formation of the palladium hydride (PdH) crystal. One of the two atoms will "pull" the electron charge onto itself. But which atom? The hydrogen level is lower than the upper vacant level in palladium, hence an electron transition from hydrogen to palladium is energetically unfavorable. But so is the reverse transition, since the hydrogen level would then be raised above palladium's. Still the atoms are different and the electron charge is bound to move one way or the other.

The ability of an atom to hold an extra electron may be characterized by half the sum of the electron's energy in the neutral atom, I (i.e., the ionization potential of the neutral atom) and its energy in the negative ion, S (i.e., the ionization potential of the negative ion). This quantity is called the atomic electronegativity:

$$\mathcal{E} = (I + S)/2. \quad (3.3)$$

Hydrogen, for example, has $I = 13.6$ eV and $S = 0.75$ eV, hence $\mathcal{E} = 7.18$ eV $= 0.528$ Ry $\approx I/2$.

If two atoms react, the electrons will move toward the more electronegative one. There are several definitions of electronegativity now in use; the one expressed by (3.3) is due to Mulliken [92].

Note that we have implicitly introduced the notion of a fractional electron charge. The electron is thought of as a liquid that can flow from one atom to another thereby equalizing the atomic levels. The concept of electronegativity is thus closely related (although not identical) to that of chemical potential.

For atoms and molecules, the “liquid electron” is perhaps too rough a notion since their wave functions and, accordingly, their densities have atom-like oscillations or, in other words, the density of the electron liquid is highly nonuniform. For crystals, however, this model may prove quite reasonable, the more so since it forms, in fact, the ideological basis for the NFE model.

3.1.3. Statistical approach. The atom-like nature of the wave function may be taken into account (if partially) by replacing Ψ by the φ model functions such that the integrals in (3.2) become analytically computable. The answer is rewritten in terms of the model’s electron density $\rho_{\text{mod}}(\mathbf{r})$, which is then replaced by the true density $\rho(\mathbf{r})$. We thus take into account both the liquid-like nature of the electrons and their localization.

If the model functions are taken to be plane waves, we shall actually be dealing with an electron gas and shall be led to the so-called statistical model. This model, however, is not to be confused with the Thomas-Fermi approximation. In the latter, the (potential-forming) electron wave functions are (or remained) plane waves, whereas in the statistical model they are nearly Hartree-Fock atomic orbitals. “Nearly”—because the potential seen by the electrons is not a Hartree-Fock one.

In the past 20-25 years, the statistical approximation has become very popular and is now used in about 90-95% of all first-principle band-structure calculations. The reason is that the approximation dramatically simplifies the potential (3.2) while the error it introduces into the band structure is small.

The value of any simplification depends on the extent to which the calculations are made easier. Looking at Eq. (3.2), which terms should be simplified?

Let us rewrite the potential (3.2) as a multiplication operator:

$$V_i^{\text{HF}}(\mathbf{r}) = -\frac{Ze^2}{r} + \sum_j \int \frac{|\Psi_j(\mathbf{r}_1)|^2}{|\mathbf{r}-\mathbf{r}_1|} d^3r_1 - \sum_j \frac{\Psi_j(\mathbf{r})}{\Psi_i(\mathbf{r})} \int \frac{\Psi_j^*(\mathbf{r}_1) \Psi_i(\mathbf{r}_1)}{|\mathbf{r}-\mathbf{r}_1|} d^3r_1. \quad (3.4)$$

In the Hartree-Fock approximation, a potential depends on the state it acts upon. This dependence is due to the exchange term. What is more, the exchange potential V^{ex} is singular where $\Psi_i(\mathbf{r}) = 0$, which makes it very inconvenient to use as a local potential.

Clearly, V^{ex} should be the first term to be simplified. In the statistical approximation, this turns out to be a rather easy task. Let Ψ_j be replaced by the plane wave $|\mathbf{k}_j\rangle$. The exchange potential (the

third term in Eq. (3.4)) then takes the form

$$V_i^{\text{ex}}(\mathbf{r}) = -\frac{1}{\Omega_0} \sum_j e^{i(\mathbf{k}_j - \mathbf{k}_i)\mathbf{r}} \int \frac{e^{i(\mathbf{k}_i - \mathbf{k}_j)\mathbf{r}_1}}{|\mathbf{r} - \mathbf{r}_1|} d^3r_1, \quad (3.5)$$

where the j -summation is over all the vectors within the Fermi sphere. The integration over \mathbf{r}_1 is over all space, which allows us to change the variable while leaving the integration limits the same. Formally, the integral will take the form of a Fourier transform of the Coulomb potential, which we discussed in Chapter 1. Making use of (1.26) we get

$$V_i^{\text{ex}}(\mathbf{r}) = -\frac{4\pi}{\Omega_0} \sum_j \frac{1}{(\mathbf{k}_i - \mathbf{k}_j)^2} \quad (3.6)$$

There being no preferred point in a free-electron gas, it is only natural that its exchange potential is thus independent of coordinates. (For a crystal, the translational invariance also makes this approximation reasonable, although we should, in principle, take into account the nonuniformity of the electron gas near a nucleus.)

For an atomic electron, the statistical approximation with its \mathbf{r} -independent potential is unsatisfactory. We must therefore continue with our program of transforming V^{ex} into a form containing the electron gas density (to be later replaced by the "true" density).

We start by evaluating the sum in Eq. (3.6). Let us replace the \mathbf{k}_j -summation by integration. The coordinate axes in the \mathbf{k} -space may be chosen so that \mathbf{k}_i will point in the z -direction. Changing to spherical coordinates, we get the integral

$$\int_{\text{inside the Fermi sphere}} \frac{d^3k}{(\mathbf{k} - \mathbf{k}_i)^2} = 2\pi \int_0^{k_F} \int_{-1}^1 \frac{d(\cos \Theta) k^2 dk}{k^2 + k_j^2 - 2k_j k \cos \Theta}.$$

The integral over $d(\cos \Theta)$ will lead to one-dimensional k -integrals containing logarithms that can be integrated by parts. Using the substitution

$$F(x) = \frac{1}{2} + \frac{1-x^2}{4x} \ln \left| \frac{1+x}{1-x} \right|, \quad (3.7)$$

(cf. (1.38)), we have

$$V_i^{\text{ex}} = -\frac{4k_F}{\pi} F\left(\frac{k_i}{k_F}\right). \quad (3.8)$$

This is a k -dependent potential. It has a singularity at $k = k_F$ which makes it inconvenient to work with and necessitates further simplifications of the exchange potential.

The first thing that comes to mind is simply to average V^{ex} over all occupied states (i.e., over the Fermi sphere). As a result, we come to the Slater approximation for the exchange potential [93]:

$$V_{\text{Sl}}^{\text{ex}} = -3 \frac{k_F}{\pi}. \quad (3.9)$$

If the potential is only averaged over the Fermi surface (i.e., the exchange interaction over the whole zone is assumed to be equal to that of the Fermi-surface electrons) we obtain the Gaspar-Kohn-Sham exchange potential [94, 95]:

$$V_{\text{GKS}}^{\text{ex}} = \frac{2}{3} V_{\text{Sl}}^{\text{ex}} = -2 \frac{k_F}{\pi}. \quad (3.10)$$

The $F(x)$ function decreases with x , so that the Gaspar-Kohn-Sham exchange is smaller than Slater's.

Since other averaging procedures are also possible, it seems reasonable to take this into account by introducing an adjustable parameter α

$$V_{\alpha}^{\text{ex}} = -3\alpha \frac{k_F}{\pi}. \quad (3.11)$$

For $\alpha = 1$ we retrieve the Slater exchange potential and at $\alpha = 2/3$ we obtain the Gaspar-Kohn-Sham potential. The "correct" value of α lies somewhere in-between.

We can now return from the model functions to the initial spin-orbitals. To do this we must set $k_F = k_F(r)$, by analogy with the procedure customary in all statistical methods. Specifically, we express k_F in terms of the average electron density (we denote it as ρ_{mod}) and replace it by the true one:

$$k_F = (3\pi^2 Z/\Omega_0)^{1/3} = (3\pi^2 \rho_{\text{mod}})^{1/3} = (3\pi^2 \rho(r))^{1/3}.$$

The resulting expression is known as Slater's [96, 97] X_{α} approximation for the exchange potential (the letter X indicates that the parameter α is unknown), that is

$$V_{\alpha}^{\text{ex}}(\mathbf{r}) = -\frac{3}{\pi} \alpha \left[3\pi^2 \sum_j \Psi_j(\mathbf{r}) \Psi_j^*(\mathbf{r}) \right]^{1/3}. \quad (3.12)$$

Starting with the nonlocal state-dependent exchange potential (3.2) we have thus ended up with a local potential (3.12), which is the same for all the states.

We have derived (3.12) very much on the basis of intuition and following, in fact, the original argument of Slater [93]. He performed averaging over the volume of the Fermi sphere, which corresponds to $\alpha = 1$ in (3.12). To justify this approach, a rather complicated formalism was later developed [94, 95]. It turned out that the variational formalism [95] leads strictly to $\alpha = 2/3$ and never to $\alpha = 1$.

This discrepancy turned out to be associated with the order of actions taken in the modeling process.

Let us discuss this point in more detail. The Hartree-Fock equation (3.1) is obtained by varying the total energy. The order of the calculations when deriving (3.9) was therefore first to take a variation of the total energy, and then to apply the statistical approximation (thereby averaging over all states). By contrast, Kohn and Sham [95] started by writing down the total energy in the statistical approximation and then proceeded variationally by constructing a one-electron equation with a potential averaged over all the states within the Fermi sphere. These two operations, namely the variation of the total energy and replacing the exchange potential by its statistical approximation, are thus not “commutative” [87].

The Gaspar-Kohn-Sham approach is internally consistent and rigorous and is therefore being extensively used at present in various modifications of the X_α approximation.

Naturally we want to know how the state-dependent Hartree-Fock potential of (3.2) can be replaced by the state-independent X_α potential, for these potentials have long been known [98] to be very different from each other due to the large differences among the Hartree-Fock potentials that are defined for different states. The answer [87] is that a change in potential changes the wave functions and energy eigenvalues, but a Coulomb potential is not much affected by variations in the wave functions because the average density (hence the Coulomb repulsion) remains virtually unaltered. For the exchange potential we have, approximately,

$$[V_\alpha^{\text{ex}}(\mathbf{r}) - E_i^{X_\alpha}] \Psi_i^{X_\alpha}(\mathbf{r}) = [V_i^{\text{HF}}(\mathbf{r}) - E_i^{\text{HF}}] \Psi_i^{\text{HF}}(\mathbf{r}) \quad (3.13)$$

which in fact answers our question.

We have thus encountered once again the idea of a pseudopotential. In particular, we see again that a potential and a pseudopotential are not directly comparable; but their effects on the corresponding wave functions are comparable.

It is interesting that whatever α the kinetic and potential energies in the X_α approximation satisfy the virial theorem [87]. This is very important for we can thus be confident that the approximations made do not “violate the equilibrium” of the system.

It should be remarked that the X_α method has several serious disadvantages. To begin with, the application of the statistical approximation to the exchange potential violates the compensation between the Coulomb and exchange potential self-actions. Even the hydrogen atom (with a single electron) acquires an exchange potential! Certainly, the Coulomb potential for the electron “self-repulsion” is also considered, but the r -dependences of these potentials are different. Near the nucleus, the Coulomb repulsion always exceeds

the exchange X_α attraction (for reasonable α 's) while at large distances the X_α exchange potential falls off more slowly than the Hartree-Fock one. As a result, the large-distance potential due to an atom is not a Coulomb one.

In the X_α approximation for the total energy, the two self-action contributions cancel out, but the difference between the potentials affects the energy eigenvalues. In the hydrogen atom, for example, the X_α approximation, even at $\alpha = 1$, yields an energy of about 0.6 Ry for the ground level instead of 1.0 Ry as it should. At lower α 's the exchange attraction is weaker, the Coulomb repulsion being unchanged, which raises the level still higher.

To improve the X_α approximation, Latter [99] proposed to cut off the exchange potential at large distances while somewhat renormalizing it at small distances. With Latter's correction, the levels are markedly depressed (see below) even though they fail to reach the Hartree-Fock positions. Regrettably, the correction violates the virial theorem, i.e., it strongly affects the average shape of the wave functions. At present, Latter's correction is considered unsatisfactory [100] for calculating the atomic wave functions to be used for constructing molecular and crystal potentials. That the Latter correction affects the eigenvalues should be remembered when comparing a band structure with the corresponding atomic levels, because the correction changes both the absolute and relative values of the atomic energies (for example, the separation between the s and d levels in transition metal atoms, see below).

3.1.4. Electronic levels in the X_α approximation. The literature provides tables of atomic wave functions, and potentials and energy levels for all the elements, calculated by the self-consistent X_α method with the Slater exchange ($\alpha = 1$) and Latter's correction [101]. The computed one-electron energies are in reasonable agreement with the Hartree-Fock eigenvalues throughout the periodic table. As to the wave functions, however, it turns out [87] that the agreement is only achievable for $\alpha < 1$.

The implication is that the X_α method is not self-consistent. It should be noted that even in the Hartree-Fock model the difference between energy eigenvalues is not identical to the energy of the transition between the levels. The more so in X_α method where the eigenvalues obey the "pseudopotential" condition (3.13). But then the eigenvalues in the X_α and Hartree-Fock methods have different meanings and, accordingly, cannot be compared.

To see the physical meaning of X_α electron energy levels, it should be remembered that we are dealing with the statistical approximation in which, unlike the Hartree-Fock scheme, the occupancy of the states is described by continuous variables. It follows that the one-electron energy of the i th level $E_i^{X_\alpha}$ is determined as the derivative

of the total energy $U_{\Sigma}^{X\alpha}$ with respect to the occupancy of this level, n_i :

$$E_i^{X\alpha} = \frac{\partial}{\partial n_i} U_{\Sigma}^{X\alpha}. \quad (3.14)$$

But this means that we come back to the notion of electronegativity. To see this, note that, by definition,

$$\begin{aligned} I_i &= U_{\Sigma}^{X\alpha}(n_1, \dots, n_i, \dots) - U_{\Sigma}^{X\alpha}(n_1, \dots, n_i - \delta, \dots), \\ S_i &= U_{\Sigma}^{X\alpha}(n_1, \dots, n_i + \delta, \dots) - U_{\Sigma}^{X\alpha}(n_1, \dots, n_i, \dots), \end{aligned}$$

where δ is unity in the Hartree-Fock method and may be small in the statistical approximation. We have

$$I_i + S_i = U_{\Sigma}^{X\alpha}(n_1, \dots, n_i + \delta, \dots) - U_{\Sigma}^{X\alpha}(n_1, \dots, n_i - \delta, \dots). \quad (3.15)$$

Expanding the right-hand side around $\delta = 0$ we see that the X_{α} eigenvalues may indeed be interpreted as the electronegativities of given states:

$$E_i^{X\alpha} = \frac{I_i + S_i}{2} = \mathcal{E}_i. \quad (3.16)$$

This means, in particular, that in numerical estimates, the X_{α} energies of the valence levels cannot be identified with the centers of gravity of bands in crystals, nor with the positions of the quasi-bound states. Even so correlations between these energies do exist and may be useful for qualitative estimates.

In X_{α} calculations of level-to-level transition energies one should take into account orbital relaxation. The needed formalism turns out to be quite simple. It may be shown [87] that the transition energy is determined very accurately if the electron is thought of as being "smeared" between the initial and final states. It is assumed that "half" the electron has already moved, as it were, to the j th level so that we have $n_j + 1/2$ instead of n_j , while the other remains on the i th level ($n_i - 1/2$ instead of n_i). This fractional occupancy of orbitals is then used for a self-consistent energy-structure calculation for an atom or molecule. The difference $\Delta = E_j - E_i$ will give the transition energy between the i th and j th levels with a better accuracy than the analogous difference between the Hartree-Fock values. This approach is known as transition state theory [87]. The notion of a transition state is closely related to the interpretation of the energies as orbital electronegativities, since it takes into account that all the levels are, on the one hand, lowered because the i th electrons weaken the screening of the nucleus and, on the other, raised because the j th electrons make it stronger (cf. Sec. 3.4.7; also see [102]).

A self-consistent calculation using fractional occupancies might seem a painstaking task. Our experience shows, however, that even

with a relatively low-speed computer (such as an IBM-360/44, about 80,000 operations per second), the calculation takes no more than 5 to 7 minutes even for a transition element.

3.1.5. Sensitivity to α . The values of α are either determined from some optimization criteria or fitted to experiment. As yet, no semi-empirical calculations of this sort have been performed for atoms, for crystals there are a number of results. The determination of α by "optimization" may be carried out in a number of ways (see [103-107]). The most frequently used are $\alpha = 2/3$, $\alpha = 1$ and the values given in [105, 106]. It is interesting to note that, whichever way α is chosen, its value decreases across the periodic table from about unity to about $2/3$.

Note that due to the way it was introduced the exchange potential (3.12) includes the exchange of both the valence and core electrons. Strictly speaking, the exchange interaction between valence electrons alone and that between valence and core electrons should be described by different α -values [108, 109]. As a rule, however, this is not the case.

In the theory of solids, the subtleties of the X_α approximation are usually given little or no attention. The choice of α is mostly arbitrary, which however does not prevent investigators from drawing conclusions from band calculations about reality. This is especially unsatisfactory for the transition metals where the relative positions of the s and d levels are very sensitive to the details of the potential. A detailed analysis of the effect of α on band-structure would be inappropriate here. Several calculations of this type have been made [110-124], but, as we shall see in Sec. 4.1, the dependence of band levels on potential is interwoven with their dependence on the k -coordinate for which the levels are computed. In a way, the band levels are "pushed away" from the nearest empty lattice levels, the positions of which vary from point to point in the Brillouin zone. The real sensitivity of an energy spectrum to the potential cannot therefore be easily estimated from these data.

In order to separate out the effect of the potential, we should consider the α dependence of the atomic levels rather than the band ones. The reader is reminded that even though the X_α atomic levels $E_i^{X_\alpha}$ do not coincide with the Hartree-Fock E_i^{HF} , there should still, as (3.16) implies, be a correlation between them (in the Hartree-Fock method, by the Koopmans theorem, $I_i = E_i^{\text{HF}}$).

Since no such calculations have been reported, we carried out a number of self-consistent X_α -calculations for the Cr atom using different values of α , both with and without Latter's correction. Chromium is a typical transition metal whose valence-shell configuration, $3d^5 4s^1$, is well established. The results of the calculation are

plotted in Fig. 3.1 where, for comparison, the corresponding Hartree-Fock levels [125] are also shown. It is worth discussing these curves in some detail.

First, it will be realized that spin polarization is ignored, so the d level is not split into sublevels and is ten-fold degenerate. A comparison of the s and d levels shows that both the Hartree-Fock and X_α methods produce a "hole" in the spectrum: the s electron, instead of occupying a vacant place on the lower d level, is promoted to the

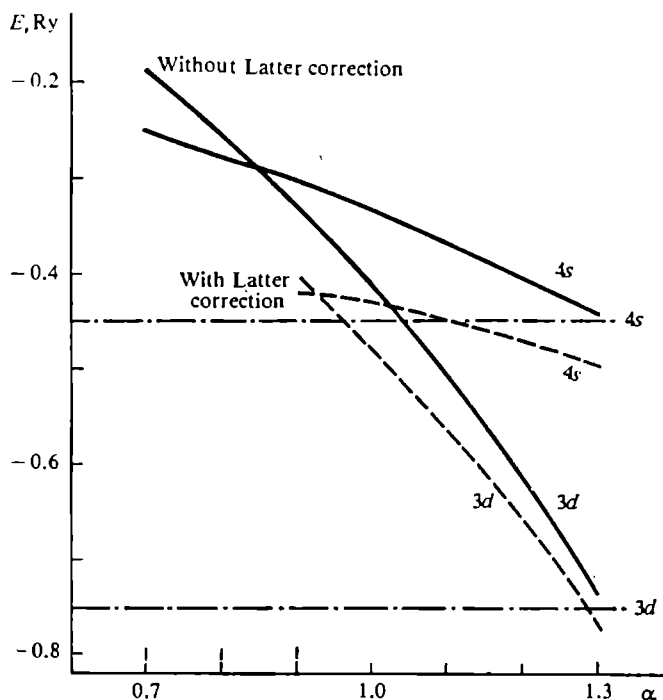


Fig. 3.1. Sensitivity of the $3d$ and $4s$ valency levels in Cr to the exchange parameter α . The Hartree-Fock energy levels are shown by the dash-dot lines.

higher s level. The reason why this looks rather odd is that usually we deal with local potentials that do not need self-consistency (that is, do not depend on their own wave functions). In such potentials, the one-electron levels are occupied in the order of increasing energy. It may be argued that a spectrum has no holes if the potential is such that orbital relaxation may be neglected in electron transitions.

If we assumed the Cr atom has a $3d^6 4s^0$ configuration thereby transferring the s electron down to the lower d level, the Coulomb repulsion would raise this level and the total energy would increase instead of decrease. It thus turns out that, even though the vacant d level is *below* the s level, the s -to- d electron transition results in an *excited* rather than a ground state. The $3d^6 s^0$ configuration is therefore an excitation configuration.

A transition from a $d^{n-x}s^x$ to $d^{n-x+1}s^{x-1}$ configuration thus corresponds to an excitation of the atom. The reason for this is that as the number of inner-region (or d) electrons increases the nucleus becomes dramatically less attractive, the increase in the exchange potential being insufficient to compensate for the Coulomb repulsion. In terms of electrostatics, this means that the nucleus's Coulomb potential becomes more screened when the inner region contains more electrons. Since the attractive force of the potential decreases in this region, the orbitals become less tightly bound: they rise to become more diffuse. Since the d orbitals are more sensitive to the inner-region potential, they clearly will be shifted more markedly than the s orbitals.

We conclude that, for an excitation configuration, the d levels (in a crystal, d bands) will be shifted up relative to the s levels (s bands). This effect has indeed been observed [126].

An analogous phenomenon takes place in other transition metals: their one-electron spectra contain holes. In a crystal, the relaxation of the Bloch wave functions is negligible since there are very many electrons and the change in the state of one does not affect others. [87, 89]. Hence the filled part of a crystal spectrum (below the Fermi level) contains no holes. Sometimes vacant states above the Fermi level are also referred to as band holes.

Another interesting point is that the atomic levels differ in their sensitivity to the value of α , the d levels depending more on α than do the s levels. It is tempting (and customary) to ascribe this to some specific influence the exchange potential has on the d electrons, and having done so move on.

Some insight into the nature of this influence (which undoubtedly exists because all magnetic phenomena are due to the exchange interaction) is provided by Fig. 3.2 where the $3d$ - and $4s$ -electron densities are plotted for the vanadium atom [116]. The Wigner-Seitz sphere radius R_a and the Bohr radius a_0 (alias the radius of a hydrogen atom, 0.53 Å) are also shown. It can be seen that the valence s electrons are mainly kept at the periphery of an atom (s region) while the d electrons occupy the inner (d) region. Even in an isolated atom, the d density at $r = R_a$ is comparable with the s density. For comparison, we also show self-consistent computed partial densities for a crystal [116]. It may be seen that in this case s and d densities are displaced outwards. Moreover, there is some p density in a crystal in contrast to an atom where there is none. The reason for this is that the p phase shifts are nonzero (cf. Fig. 2.3).

The $4s$ -electron density is highest in the outer regions of an atom, while that of the $3d$ electrons is highest in the interior. It should be noted that this correlates with the difference between the pseudopotentials of the $4s$ and $3d$ electrons.

To see this, recall that a chromium atom has core s states (which follows, by the way, from the occurrence of oscillations in ρ_{4s}). For the $4s$ electrons we can introduce a pseudopotential by "cutting off" the core region of the potential. They will then be acted on only by the outer region of the atom's potential, that is, the behavior of $4s$ electrons is again determined by the details of the outer region of

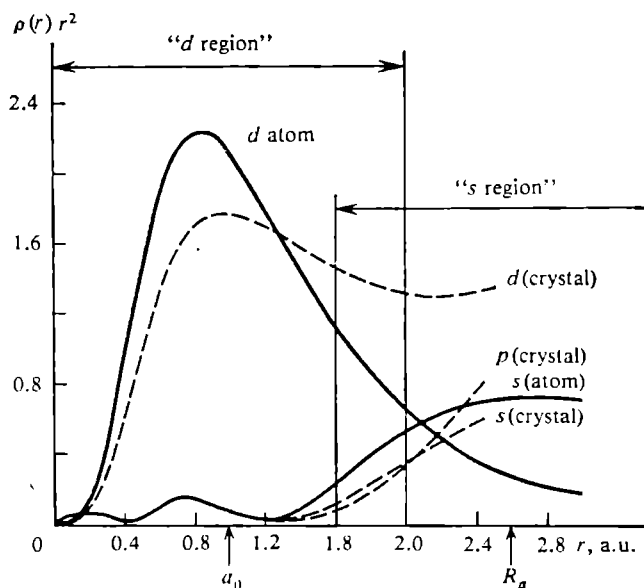


Fig. 3.2. Self-consistent partial electron densities in vanadium for a free atom (bold lines) and crystal (dashed lines). The data are from [116].

the atom. In fact, we came to this conclusion in the framework of scattering theory, which led us in Sec. 2.2 to the concept of pseudopotential.

There are no core states for $3d$ electrons and hence no pseudopotential can be introduced. These electrons are acted upon by the whole of the atomic potential. Since the main feature of this potential is its Coulomb singularity at $r \rightarrow 0$, it follows that for the d electrons it is the inner part of the atom which is important. This conclusion is based, once again, only on the concepts of pseudopotential theory.

Let us now return to the X_α exchange potential to see why it is d electrons which experience the specific influence of the exchange potential. The exchange potential (3.12) is strong where the electron density is large. The larger the electron density, the stronger is the exchange-potential attraction. Hence the density is pulled into the high-potential region and this, in turn, causes a further increase in the exchange potential. This density self-contraction continues until the attraction is compensated for by Coulomb repulsion.

A change in α most strongly affects the attraction in the high-density (i.e., inner) region and only slightly affects the attraction

in the low-density (outer) region. Therefore, as α increases, the d functions are pulled in more strongly than are the s functions, which results in the d level being more depressed than the s level. This is what we see in Fig. 3.1.

Since in the X_α method the Coulomb and exchange self-action terms do not cancel, it follows that the density contraction in the X_α method must be stronger than it is using Hartree-Fock approach. As a result, the X_α atomic wave functions must be more "shrunk" than the Hartree-Fock ones or, in other words, the electrons in the X_α method are more localized. This should be borne in mind when constructing a crystal potential from atomic X_α functions: they must be made somewhat "blurred". This may be accomplished (see below) by considering an excitation configuration and thus including more diffuse wave functions (it is not necessary to transfer the whole of the s electron to the d level).

Concerning this shrinking of X_α functions, it should be remembered that according to the calculations in [87] the agreement between the X_α and Hartree-Fock functions is better for $\alpha < 1$, i.e., with smaller X_α exchange potentials.

Increasing α makes the outer region less important (because of the density self-contraction) and thereby reduces the effect of Latter's correction (see Fig. 3.1).

Figure 3.1 shows the results up to $\alpha = 1.3$. It may be seen that for this α , the X_α levels (without Latter's correction) are in good agreement with the Hartree-Fock levels. The reason for this particular choice is that at $\alpha = 1.3$ the exchange potential (3.8) corresponds to the bottom of the free-electron band, i.e., at $k = 0$.

To see this, note that by (3.7)

$$F(k=0) = 1,$$

$$\bar{F}_{\text{Sl}} = \frac{4\pi}{(4\pi/3)k_F^3} \int_0^{k_F} F(k) k^2 dk = \frac{3}{4}, \quad F(k=0) = \frac{4}{3} \bar{F}_{\text{Sl}},$$

that is, the exchange at the bottom of the band is 4/3 times the Slater exchange. By the definition of the X_α approximation, Eq. (3.11), this leads to a new value $\alpha_{k=0}$:

$$\alpha_{k=0} = 4/3.$$

It will be remembered that it was, in fact, the same argument that led us to the quantity $\alpha_{k=k_F}$ for the Gaspar-Kohn-Sham exchange:

$$F(k=k_F) = 1/2, \quad \bar{F}_{\text{Sl}} = 3/4, \quad F(k=k_F) = (2/3) \bar{F}_{\text{Sl}},$$

that is, the Fermi-level exchange is weaker than the Slater's one by a factor of 2/3:

$$\alpha_{k=k_F} = 2/3.$$

The question of why the X_α levels coincide with the Hartree-Fock ones at $\alpha_{h=0}$ is beyond the scope of this section. We note, however, that the condition $k = 0$, which corresponds to a band bottom in the statistical approximation, corresponds thereby to the lowest and most favorable level.

3.1.6. The positions of the levels across a d period. According to (3.12), an increase in α is equivalent, in a way, to an increase in the

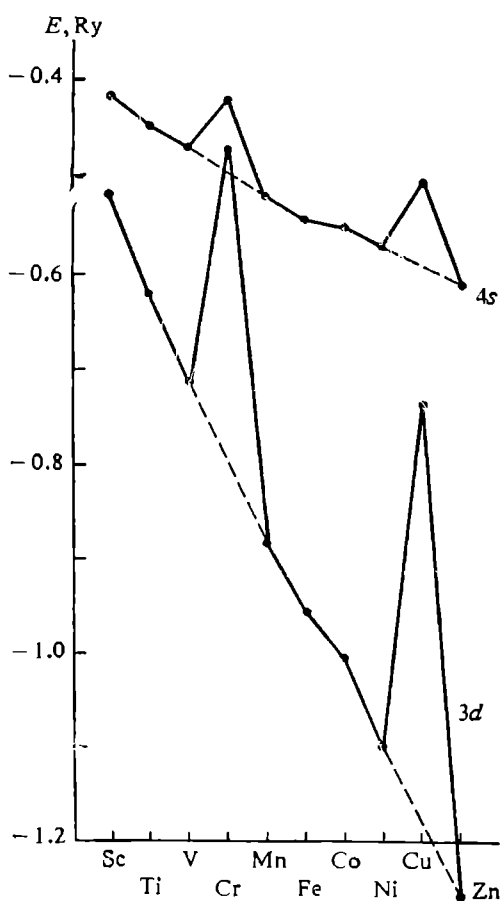


Fig. 3.3. $3d$ and $4s$ free-atom levels along the d period, computed for $\alpha = 1$ using the Latter correction [101].

electron density, which is predominantly due to d electrons. Figure 3.1 may therefore be considered as a model for describing how the valence levels move from one element to another across the periodic table. As the atomic number increases, so does the attractive force of the atom's nucleus. This is not compensated for by the increasing Coulomb repulsion of the valence electrons and so the total attraction increases. As a result, the orbitals are, so to speak, pulled into the interior of the atom, the d orbitals relatively more so because the s electrons are screened from the nuclear charge by the increasing number of d electrons "below" them.

Figure 3.1 thus illustrates the difference in the sensitivity of s and d levels to the change in the atomic number.

Figure 3.3 shows s and d levels computed using the self-consistent X_α method [98] for $\alpha = 1$ and Latter's correction (the Hartree-Fock levels vary across a period in very much the same fashion).

It should be noted that in all elements a vacant d level is below an occupied s level, that is, there is no level inversion as in Fig. 3.1. It is clear that the s and d electrons differ in the way they depend on the atomic number, as we "predicted" on general grounds they should. Towards the end of a period, the d level is virtually inside the ion core. In this case, the energy gap between the s and d levels

is so wide that having accepted an extra electron from the s shell, the d level cannot rise high enough to make the transfer energetically unfavorable. It is for this reason that at the end of a period the atomic d holes become occupied.

For all the elements except chromium and copper, the configuration is assumed to be $d^{n-2}s^2$, n being the number of the series. With chromium and copper (the configuration is $d^{n-1}s^1$), we can see how the occupation of one d hole affects the position of the levels: as the nucleus is screened more, its attraction reduces, and the levels rise.

To summarize, although our topic in this section was mainly the X_α approximation, all our conclusions as to the effect of the exchange interaction on the energy structure of atoms (and crystals) are independent of the approximation. The same is true of the sensitivity of s and d electrons to various regions in the potential. It may be said *a priori*, for example, that on forming a crystal it is the s electron wave functions that will change most because clearly the atomic potential will be altered most in the outer region. At the same time, the d -electron wave functions will remain very atom-like. Hence, even though the d electrons will be disturbed in the crystal formation process, they cannot be put on the same footing as the s electrons. In going from $3d$ to $4d$ and further to $5d$ metals, the core will acquire bound d states which will make the d orbitals more diffuse and less dependent on the inner region, i.e., they will become more s -like and hence a d pseudopotential will become possible. It then follows that a pseudopotential theory with s and d electrons treated equally would be more suitable for the heavy d metals (note, though, that relativistic corrections may be important there).

It should be remarked that attempts to improve further the X_α method continue [127-137].

3.2. Dielectric screening

We shall in the next few sections discuss the modification of the atomic potential due to the formation of a crystal.

3.2.1. The concept of a pseudoatom. We saw in Sec. 2.2 that when a scatterer (atom or ion) is placed in a free-electron gas, the electron density around it is changed. The total displaced charge is equal to the charge of the scatterer Z which is to say that the introduced potential is screened by the electron gas.

In a real crystal, the electrons screening a potential are not free ones. In the pseudopotential theory we have to ignore this difference because otherwise the problem of constructing a screened pseudopotential would be too hard to solve. In band-structure calculations using secular equations, the (crystal) potential-constructing pro-

cedure takes into account the atom-like nature of the wave functions of the screening electrons (see Sec. 3.4). In both models the original potential (placed in the crystal) and the charge that screens it may be considered as a single whole, i.e., as a solid-state analog of the atomic potential. This entity (the original potential plus the screening charge) is called a pseudoatom*, whether the potential being screened is a true or a pseudopotential.

A pseudoatom differs from a real one, first of all, in its large-distance behavior. In a true atom the density decreases exponentially with r , the exponent depending solely on the atomic energy levels. In a pseudoatom the density falls off like $r^{-3} \cos(2k_F r)$ (see Sec. 2.2), which is much more slowly and depends, through k_F , on the characteristics of the crystal.

Let then V^{ion} be the original potential (say, that of a certain ion) and V^{scr} the screening potential of the electrons. The crystal potential V^{cr} (the one due to the pseudoatom) is the sum of these:

$$V^{\text{cr}} = V^{\text{ion}} + V^{\text{scr}} \quad (3.17)$$

This total potential acts on the electrons and in turn requires screening. The resultant new potential also requires screening, and so on *ad infinitum*. It will be understood, however, that at each successive "iteration" the screening has a progressively smaller effect on the potential until the potential becomes self-consistent (i.e., such that, were it introduced as the original potential, the crystal would have no effect on it).

3.2.2. Dielectric operator. We want to know whether a self-consistent crystal potential can be found in a general form without invoking a painstaking iterative process.

We need to express V^{scr} in terms of the final result of screening V^{cr} . We denote the density of the screening electrons as ρ^{scr} and, for simplicity, we will use operator notation.

At every iteration

$$V^{\text{scr}} = \hat{A} \rho^{\text{scr}}, \quad (3.18)$$

where \hat{A} is an operator. This equation expresses the obvious fact that a screening potential arises from the nonuniformity of the electron-gas density. On the other hand, this departure from the mean is caused by the total crystal potential V^{cr} . In a general form this

* It would be more proper to call it a "quasi-atom" because first there would be no unnecessary associations with the pseudopotential, and second an individual atom within a solid is not a well-defined notion. "Pseudoatom", however, is the generally accepted term.

may be written

$$\rho^{\text{scr}} = \hat{B}V^{\text{cr}} \quad (3.19)$$

where the operator \hat{B} is to be found later.

The screening potential can thus be expressed in terms of the result of its action:

$$V^{\text{scr}} = \hat{A}\hat{B}V^{\text{cr}}. \quad (3.20)$$

We are now in a position to subject the solution to a self-consistency condition (it should be emphasized that thus far this has not been done). We suppose, namely, that the iterative process has been carried through to self-consistency, i.e., V^{cr} (that produces the screening charge) coincides with the crystal potential given by the sum of the original potential and the corresponding screening potential. We may then consider that V^{cr} in (3.17) coincides with its counterpart in (3.20). Finally, from (3.17)-(3.20) we get

$$V^{\text{cr}} = V^{\text{ion}} + \hat{A}\hat{B}V^{\text{cr}}. \quad (3.21)$$

Note that the crystal potential is thus recursively defined. Another option we might choose for constructing V^{scr} is to employ a model. We shall meet this approach in Sec. 3.3 and we shall see there that it is more versatile than the present scheme because the mathematical complexities of the self-consistent screening method make simplifications unavoidable.

Let us introduce the operators

$$\hat{\epsilon} = 1 - \hat{A}\hat{B} \quad \text{and} \quad \hat{\epsilon}^{-1} = (1 - \hat{A}\hat{B})^{-1}. \quad (3.22)$$

Obviously,

$$\hat{\epsilon}V^{\text{cr}} = V^{\text{ion}} \quad \text{and} \quad V^{\text{cr}} = \hat{\epsilon}^{-1}V^{\text{ion}}. \quad (3.23)$$

The operator $\hat{\epsilon}$ is called the dielectric operator and equations (3.17)-(3.23) form a basis for what is known as the dielectric formalism. They are applicable to both potentials and pseudopotentials since there are no restrictions on the strength of the original potential V^{ion} . However, the computational difficulties encountered in dealing with $\hat{\epsilon}$ necessitate small-parameter expansions and, accordingly, the use of a pseudopotential. The dielectric potential formalism is only used in pseudopotential theory while in band-structure calculations* other methods for constructing crystal potentials are employed. We compare these approaches in Sec. 3.4.

* Based on methods stemming from scattering theory such as the APW and KKR approaches.

3.2.3. The dielectric function $\epsilon(\mathbf{q})$. Let us now discuss some concrete approximations. We shall use the matrix representation of operators. The matrices of the operators V^{ion} and V^{cr} are formed from the potential formfactors. From (3.22) we get

$$\sum_{\mathbf{q}'} \langle \mathbf{k} + \mathbf{q} | \hat{\epsilon} | \mathbf{q}' \rangle \langle \mathbf{q}' | V^{\text{cr}} | \mathbf{k} \rangle = \langle \mathbf{k} + \mathbf{q} | V^{\text{ion}} | \mathbf{k} \rangle.$$

In the general case the matrix ϵ is nondiagonal. To set up a self-consistent potential V^{cr} , we must find the inverse dielectric matrix, which is a rather difficult problem because as we shall see later the operator B is nonlinear in V^{cr} . At present, the matrix ϵ is inverted approximately [138-140].

In pseudopotential theory the simple assumption that the matrix ϵ is diagonal is made. If nondiagonal ϵ -elements are in some way taken into account, one speaks of "nondiagonal" screening. With diagonal screening, then, we get the dielectric function $\epsilon(\mathbf{k}, \mathbf{q})$:

$$\langle \mathbf{k} + \mathbf{q} | \hat{\epsilon} | \mathbf{q}' \rangle = \epsilon(\mathbf{k}, \mathbf{q}) \delta_{\mathbf{k}+\mathbf{q}, \mathbf{q}'}. \quad (3.24)$$

From (3.23) and (3.24) we now obtain the basic formula in the theory of dielectric screening:

$$\langle \mathbf{k} + \mathbf{q} | V^{\text{cr}} | \mathbf{k} \rangle = \frac{\langle \mathbf{k} + \mathbf{q} | V^{\text{ion}} | \mathbf{k} \rangle}{\epsilon(\mathbf{k}, \mathbf{q})}. \quad (3.25)$$

Conceptually, this formula is close to those used in electrostatics where to determine a field in a medium its "vacuum" value is to be divided by the dielectric permittivity of the medium. The dielectric function $\epsilon(q=0)$ is in fact the dielectric permittivity. For metals, $\epsilon(q=0) = \infty$ which means that external fields are completely screened.

We now turn to the evaluation of the matrices A and B . In differential form (and the CGS unit system) the Poisson equation (3.18) has the form

$$\nabla^2 V^{\text{scr}}(\mathbf{r}) = -4\pi e^2 \rho^{\text{scr}}(\mathbf{r}). \quad (3.26)$$

Fourier-analyzing the potential and density, we have

$$V^{\text{scr}}(\mathbf{q}) = \frac{4\pi e^2}{q^2} \rho^{\text{scr}}(\mathbf{q}), \quad (3.27)$$

$$\langle \mathbf{k} + \mathbf{q} | \hat{A} | \mathbf{q}' \rangle = \frac{4\pi e^2}{q^2} \delta_{\mathbf{k}+\mathbf{q}, \mathbf{q}'}. \quad (3.28)$$

To evaluate \hat{B} , ρ^{scr} should be determined in terms of the perturbation potential V^{cr} . To do this, we write down the first-order wave function $\Psi_{\mathbf{k}}^{\text{cr}}$, construct the crystal density (with spin taken into

account):

$$\rho^{cr}(\mathbf{r}) = 2 \sum_{\mathbf{k}} |\Psi_{\mathbf{k}}^{cr}(\mathbf{r})|^2 \quad (3.29)$$

and subtract the original density from ρ^{cr} to obtain ρ^{scr} .

Thus,

$$\begin{aligned} \Psi_{\mathbf{k}}(\mathbf{r}) &= |\mathbf{k}\rangle - \sum_{\mathbf{q} \neq 0} \frac{\langle \mathbf{k} + \mathbf{q} | V^{cr} | \mathbf{k} \rangle}{\epsilon_{\mathbf{q}} - k^2} |\mathbf{k} + \mathbf{q}\rangle, \\ \rho^{cr}(\mathbf{r}) &= \rho^0(\mathbf{r}) - \frac{2}{(2\pi)^3} \int_{h \leq h_F} \sum_{\mathbf{q} \neq 0} \left[\frac{\langle \mathbf{k} + \mathbf{q} | V^{cr} | \mathbf{k} \rangle}{\epsilon_{\mathbf{q}} - k^2} e^{i\mathbf{q}\mathbf{r}} \right. \\ &\quad \left. + \frac{\langle \mathbf{k} | V^{cr} | \mathbf{k} + \mathbf{q} \rangle}{\epsilon_{\mathbf{q}} - k^2} e^{-i\mathbf{q}\mathbf{r}} \right] d^3k. \end{aligned} \quad (3.30)$$

In fact we derived this expression in the section on scattering theory (Sec. 2.4). It can be obtained by combining Eq. (2.112) for the wave function with the Born approximation (2.120). The \mathbf{q} sums in (3.30) will then arise from using Green's function (2.122) rather than from first-order perturbation theory.

Bearing (3.25) in mind, we should go over to reciprocal space. The sums over \mathbf{q} will then vanish:

$$\begin{aligned} \rho^{cr}(\mathbf{q}) &= \rho_0(\mathbf{q}) - \frac{2}{(2\pi)^3} \int_{h \leq h_F} \frac{\langle \mathbf{k} + \mathbf{q} | V^{cr} | \mathbf{k} \rangle}{\epsilon_{\mathbf{q}} - k^2} d^3k \\ &\quad - \frac{2}{(2\pi)^3} \int_{h \leq h_F} \frac{\langle \mathbf{k} | V^{cr} | \mathbf{k} - \mathbf{q} \rangle}{\epsilon_{\mathbf{q}} - k^2} d^3k. \end{aligned}$$

The "summation" in the integral is over all \mathbf{k} ; the third term remains unchanged on changing the sign of \mathbf{k} and becomes Hermitian-conjugate of the second term. For Hermitian potentials these terms will be equal to each other giving

$$\rho^{scr}(\mathbf{q}) = -\frac{4}{(2\pi)^3} \int_{h \leq h_F} \frac{\langle \mathbf{k} + \mathbf{q} | V^{cr} | \mathbf{k} \rangle}{\epsilon_{\mathbf{q}} - k^2} d^3k. \quad (3.31)$$

We have thus succeeded in expressing ρ^{scr} in the desired form given by (3.19). If the formfactor depends on \mathbf{k} , the integration can actually be performed only if the dependence is known. Note that not only is \hat{B} nonlinear in V^{cr} (due to perturbation theory) but, for nonlocal potentials, it is also an integral operator.

For a local potential, (3.31) simplifies since $\langle \mathbf{k} + \mathbf{q} | V^{cr} | \mathbf{k} \rangle = V^{cr}(\mathbf{q})$ and $V^{cr}(\mathbf{q})$ may be taken out of the k -integral. We shall then be left with the Lindhard function we met in the Introduction,

and Eq. (3.31) takes the form

$$\rho^{\text{scr}}(\mathbf{q}) = \frac{Z}{\Omega} V^{\text{cr}}(\mathbf{q}) \chi(\mathbf{q}). \quad (3.32)$$

Finally, we get

$$\epsilon(q) = 1 - \frac{4\pi Z e^2}{\Omega q^2} \chi\left(\frac{q}{2k_F}\right), \quad (3.33)$$

where

$$\chi(x) = -\frac{1}{2} \left(\frac{2}{3} E_F^0\right)^{-1} \left[1 + \frac{1-x^2}{2x} \ln \left| \frac{1+x}{1-x} \right| \right]. \quad (3.34)$$

The function (3.33) is called Lindhard's dielectric permittivity [141, 3] although it was Bardeen who first derived it [142]. It is also referred to as the Hartree function because the underlying assumption in constructing it is that the emergence of a scattering density results in a purely Coulomb potential V^{scr} . What actually happens (and must be taken into account) is that a change in the electron density alters the exchange potential of the electron gas. The change in the correlation potential should also be allowed for.

The relevant theory, however, is beyond the scope of this book and we shall only reproduce its main results (for details, the reader is referred to [73, 17, 143, 144]).

The inclusion of an exchange-correlation potential leads to replacement of $A(q)$ by $A(q)p(q)$ with $p(q)$ depending on the particular model of the potential (the corresponding dielectric function is designated by an asterisk, that is, Eq. (3.25) involves ϵ^*) and we get

$$\epsilon^*(q) = 1 - \frac{4\pi Z e^2}{\Omega q^2} p(q) \chi\left(\frac{q}{2k_F}\right). \quad (3.35)$$

It is customary to use $p(q)$ in the form suggested by Hubbard [145, 146], although quite a number of other formulas are also available [147-158] (for a brief review, see [17, 159]). A recent analysis [158] indicated that the treatment of the correlation in [150] is very valuable.

There are only few investigations [160-166] about how the computed properties of crystals depend on the specific model of many-electron effects.

Note that since $V^{\text{cr}}(q) = V^{\text{ion}}(q)/\epsilon^*(q)$, the function $\alpha(q)$ defined in (1.39) by the ratio $V^{\text{ion}}(q)/V^{\text{cr}}(q)$, in dielectric formalism becomes $\epsilon^*(q)$. Were the screening introduced in another way, $\chi(q)$ would again enter Eqs. (1.39)-(1.41), but $\epsilon^*(q)$ would not.

3.2.4. The q dependence of the dielectric function. Let us now investigate how ϵ depends on q . For small q ,

$$\chi(q)|_{q \rightarrow 0} = -\left(\frac{2}{3} E_F^0\right)^{-1}, \quad (3.36)$$

and $\epsilon(q)$ diverges as q^{-2} .

At $q = 2k_F$ χ is finite, but $d\chi/dq$ has a logarithmic singularity. Although this latter is very weak and hardly even visible on an $\epsilon(q)$ plot, it is nevertheless essential for some crystal properties, such as the Kohn singularities in phonon spectra ([3, 73, 89]).

As $q \rightarrow \infty$

$$\chi(q)|_{q \rightarrow \infty} \rightarrow -2/q^2, \quad (3.37)$$

and $\epsilon(q)$ tends to unity, i.e., at large q ($q \gg 2k_F$) there is no difference between $V^{\text{cr}}(q)$ and $V^{\text{ion}}(q)$.

We see that $\epsilon(q)$ is a monotonic function which does not change sign. Screening is important at small q . After a Fourier transformation to real space, small q corresponds to large r , i.e., screening removes the long-range nature of the Coulomb potential.

If a purely Coulomb potential (1.26) is placed in a free-electron gas, screening theory gives

$$\langle \mathbf{k} + \mathbf{q} | V^{\text{cr}} | \mathbf{k} \rangle = -\frac{4\pi Ze^2}{\Omega(q^2 + \alpha^2(q))}, \quad (3.38)$$

where (3.33) and (3.34) have been used and

$$\alpha^2(q) = -4\pi Ze^2 \chi(q)/\Omega > 0. \quad (3.39)$$

Equation (3.38) is simply a generalization of (1.25). If α is independent of q , we get the Thomas-Fermi approximation and the screened Coulomb potential is described by (1.24), i.e., it no longer is a long-range one of the type $1/r$.

The logarithmic singularity in $\epsilon(q)$ gives rise to (spatial) oscillations of the screening charge. This may be seen by taking the Fourier transform of (3.25):

$$V^{\text{cr}}(\mathbf{r}) = \Omega \int \frac{\langle \mathbf{k} + \mathbf{q} | V^{\text{ion}} | \mathbf{k} \rangle}{\epsilon(q)} e^{-i\mathbf{q}\mathbf{r}} d^3q. \quad (3.40)$$

Changing to spherical coordinates and integrating twice by parts [73, 89] yields second derivatives of $\epsilon(q)$ in (3.40). All the other functions depend on q only weakly and can be taken out of the integral. At the limit of $r \rightarrow \infty$ we find

$$V^{\text{cr}}(\mathbf{r}) \rightarrow \frac{3Ze^2}{k_F} \frac{V^{\text{ion}}(q=2k_F)}{\epsilon^2(q=2k_F)} \frac{\cos(2k_F r)}{(2k_F r)^3}, \quad (3.41)$$

that is, the potential and charge density behave, in fact, in the same way they do in scattering theory (Sec. 2.2, Eq. (2.94)).

The oscillations have the same origin in both approaches, viz. the discontinuity in the electron energy distribution at the Fermi level. In scattering theory, this discontinuity appears in a direct way, whereas with dielectric formalism, it comes about as a singularity in $\epsilon(q)$ at $q = 2k_F$, which then manifests itself in the Fourier transform of (3.40).

It would be wrong to argue that at large distances from an ion, only oscillations of the type (3.41) will be present. It may be shown [167] that a rapid decrease of $\epsilon(q)$ with q (even with the $q = 2k_F$ singularity ignored) also leads to oscillations in V^{cr} with r , but these will be modulated by an exponential rather than by r^{-3} , that is, the use of (3.37) gives rise to oscillations in the tail of the Yukawa potential (1.24).

If the potential V^{cr} has a resonance state with an energy E_d , the electron energy distribution drastically changes in this vicinity. In real space, we should expect then that the charge density and V^{cr} have extra oscillations, similar to those in (3.41), but with k_F replaced by $\sqrt{E_d}$. This result is due to Rennert [168].

It follows from Eqs. (3.41) and (1.41) that the indirect interatomic interaction potential $\Phi_{bs}(t)$ has Friedel oscillations. If there are resonance states, Rennert oscillations will also be associated with this potential. When calculating the properties of crystals, Rennert oscillations should be taken into account in constructing the pseudopotential because they do not arise in a standard derivation of $\epsilon^*(q)$.

Rennert oscillations can be incorporated in a *model* approach by adding to $\epsilon^*(q)$ a term having a logarithmic singularity at $q = 2\sqrt{E_d}$, E_d being a d -resonance energy.

The same result may be obtained *more rigorously* by evaluating the dielectric function $\epsilon^*(q)$ as a matrix element [143] of the "system's response to a perturbation" between wave functions that incorporate d -electron effects. Such a procedure was suggested in [169, 170] with wave functions taken from unhybridized s bands (i.e., from the NFE model) and d bands (i.e., from the LCAO model). As a result, in addition to the ss and dd interaction terms, an sd contribution to $\epsilon^*(q)$ appeared and the d electrons in narrow d bands may be strongly localized, their response to a perturbation weak and the dd interaction in ϵ^* negligible. We are thus left with two terms in ϵ^* , one corresponding to the usual s -electron screening and the other to the screening by d electrons. The d -screening has a logarithmic singularity at $q = 2k_F$ and leads therefore to Rennert's oscillations.

This formalism was developed in [171-176] and it turned out that in the noble metals, the off-diagonal correction terms in ϵ_{sd} are small as compared with the diagonal terms [172]. This is very important since there is no *a priori* reason to believe that the diagonal approximation is applicable to the transition metals.

The role of screening is extremely important. A pure unscreened Coulomb potential always produces bound states and the perturbation expansion will therefore be always divergent. This is easily shown for a pseudopotential of the type (2.100) (with $V \propto -r^{-1}$) by using the Bargmann criterion (2.109). Furthermore, a pseudopotential with a long-range Coulomb tail cannot, strictly speaking, be factored as shown in (1.21). The reason is that the sum of these contributions diverges and termwise integration (only possible for absolutely convergent series) becomes illegitimate. This difficulty was pointed out in [177]. These singularities may be avoided by assuming some "background" screening leading to a short-range potential [177-182].

The formulas for linear dielectric screening are thus only true for relatively weak pseudopotentials which produce small perturbations.

As a measure of the disturbance caused by a pseudopotential, we can take the single-ion screened pseudopotential averaged over the cell volume Ω_0 . It is clear from Eq. (1.23) that this is simply the long-wavelength limit of the formfactor. To evaluate this limit, it suffices to let q go to zero in Eq. (3.25). Using Eqs. (3.33) and (3.36) we find for the pseudopotential of a screened ion W^{cr} that

$$\lim_{q \rightarrow 0} \langle \mathbf{k} + \mathbf{q} | W^{\text{cr}} | \mathbf{k} \rangle = -\frac{2}{3} E_F^0. \quad (3.42)$$

Here care has been taken of the fact that since the ion pseudopotential $W^{\text{ion}}(r)$ behaves at $r \rightarrow \infty$ like $-Ze^2/r$, its formfactor $W^{\text{ion}}(q)$ at small q is $-4\pi Ze^2/(\Omega_0 q^2)$ (cf. (1.26)).

We thus see that whatever the initial ion pseudopotential the crystal pseudopotential as given by linear screening theory (LST) will have the same mean value, namely, $-(2/3)E_F^0$. The properties of an ion pseudopotential are thus taken into account in the screening process and its "identity" is more or less lost. This is the reason why many pseudopotentials, each leading to the same result, are possible.

3.2.5. Possible pseudoatom potentials. Let us see, qualitatively, which screened pseudopotentials correspond to which ion pseudopotentials. To do this, we must go over from the formfactor of the crystal potential (3.25) to coordinate space. The explicit form of $\epsilon(q)$, (3.33) is too complicated to use in analytical calculations and so it must be replaced by model functions.

It will be realized that what we are now concerned with is not the behavior of the potential at infinity but rather at intermediate distances where Friedel oscillations do not yet appear. We can therefore take a model function $\epsilon(q)$ without a logarithmic singularity.

Let it be the Thomas-Fermi approximation (cf. (3.38)):

$$\epsilon(q) = 1 + \frac{3}{2} \frac{4\pi Ze^2}{\Omega q^2 E_F^0}. \quad (3.43)$$

The factor 3/2 in the second term is introduced following [183, 184] to secure the correct long-wavelength limit (3.42).

We may choose the form of (2.100) suggested by scattering theory as the ion pseudopotential. This is a square well of depth A (i.e., $V = -A$) at $r < R$ and a Coulomb attraction potential ($V = -Ze^2/r$) at $r > R$, R being a model radius. Two characteristic values for the well depth are $A = 0$ and $A = Ze^2/R$ (when there is no potential jump at $r = R$).

A few words about terminology are also appropriate. The model pseudopotential we are dealing with is known in the literature as the Heine-Abarenkov potential [3, 13, 17]. Its special cases are the Ashcroft ($A = 0$) and Shaw ($A = Ze^2/R$) pseudopotentials. These potentials are local, but there are many nonlocal potentials with A and R depending on the orbital quantum number l .

We return now to constructing a pseudoatom potential (recall that the pseudoatom is a combination of the original and screening potentials). Our aim is to see how the shape of a pseudoatom potential depends on the assumed well depth. With this knowledge we shall be able to analyze all the possible forms of pseudoatom that can arise in dielectric screening theory.

First we evaluate the formfactor of our model pseudopotential

$$W^{\text{ion}}(q) = -\frac{4\pi}{\Omega_0} \frac{q(Ze^2 - AR) \cos qR + A \sin qR}{q^3} \quad (3.44)$$

Substituting (3.44) and (3.43) into (3.25) and passing to coordinate space, we obtain the screened pseudopotential W^{cr} (which is a crystal single-site potential alias a pseudoatom potential):

$$W^{\text{cr}}(r) = -\text{const} \frac{R}{r} \begin{cases} [A(1+b) - A_S] e^{-d} \sinh(ar), & r < R, \\ [A_S \cosh d + A(b \sinh d - \cosh d)] e^{-ar}, & r > R, \end{cases} \quad (3.45)$$

where

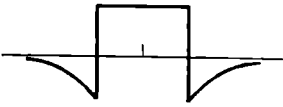
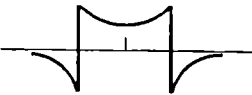


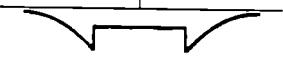
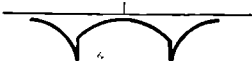
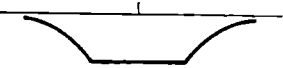
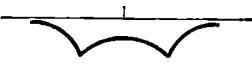
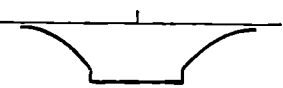
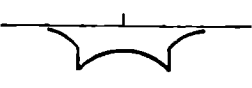

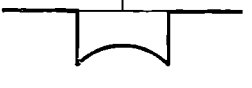
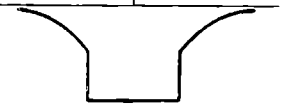

$$a^2 = \frac{6\pi Ze^2}{\Omega_0 E_F^0}, \quad d = aR, \quad b = \frac{1}{d}, \quad (3.46)$$

and

$$A_S = \frac{Ze^2}{R} \quad (3.47)$$

is the well depth for the Shaw pseudopotential.

Table 3.1. Ion and pseudoatom potentials as functions of the model depth

No.	A	Unscreened pseudopotential (ion)	Screened pseudopotential (pseudoatom)
1	$-\infty < A < A_{EA}$		
2	$A = A_{EA}$		
3	$A_{EA} < A < A_S$		
4	$A = A_S$		
5	$A_S < A < A_{NA}$		
6	$A = A_{NA}$		
7	$A_{NA} < A < \infty$		

It can easily be seen that $W^{\text{cr}}(r)$, taken as a function of A , involves two more characteristic values of well depth:

$$A_{EA} = A_S(1+b)^{-1}, \quad (3.48)$$

$$A_{NA} = A_S(1-b \tanh d)^{-1}. \quad (3.49)$$

If $A = A_S$, neither the pseudoatom nor the initial Shaw potential have jumps at $r=R$ (Table 3.1, No. 4). With $A = A_{EA}$, $W^{\text{cr}}(r)$ is

identically zero (see No. 2). By analogy with the term "empty core potential" sometimes applied to the Ashcroft potential, we have introduced here the "empty atom (EA) potential". Note the similarity between the pseudoatom with A_{EA} and the pseudoatom of the phase function method, cf. (2.99).

If $A = A_{NA}$, the function $W^{cr}(r)$ is zero for $r > R$, i.e., the ion potential is completely screened (see Table 3.1, No. 6). Outer electrons are neither attracted nor repelled by this pseudopotential for electroneutrality is already achieved within the sphere of radius R . This case we denote as the "neutral atom" (NA).

As A goes from minus infinity to plus infinity, the square well changes from being infinitely repulsive to infinitely attractive and the pseudoatom changes its form as shown in Table 3.1. If $A < A_{EA}$, then for $r < R$ the pseudoatom has a repulsive core, the size of which gradually increases in magnitude with A (Table 3.1, No. 1). For $A > A_{NA}$, the repulsion arises in the outside region and increases with A (No. 7).

It should be pointed out that although there are no Friedel oscillations in our model, actual (not Thomas-Fermi) screening does produce such oscillations in the "tail" of every pseudoatom.

The above qualitative argument (due to Shaw [184]) is supported by some quantitative data. For example, Meyer and Young [185] did a direct numerical calculation of an Ashcroft pseudopotential based on Thomas-Fermi screening. In the same article, the pseudopotential was screened with a dielectric function taken in the Hartree approximation and then the corresponding pseudoatom potential was calculated. The results agreed both with each other and with our qualitative discussion (Table 3.1). Rasolt et al. [186] numerically computed Hartree-screened local pseudopotentials for two values of A ; the form of the resulting pseudoatom is in accordance with Table 3.1 (Nos. 3, 5). It is worth mentioning that these calculations exhibited no Friedel oscillations in the pseudoatom because the distances considered were too short.

We thus have used the Thomas-Fermi model for the dielectric screening of a model pseudopotential. This is not the only application the model has in solid-state theory. When applied to a crystal, the Thomas-Fermi method in its classical formulation* fails to minimize the total energy with respect to the lattice parameter. The situation, however, is saved by including exchange effects [187, 188]. This scheme is known as the Thomas-Fermi-Dirac-Weizsacker (TFDW) method and has been used in a number of crystal studies.

* The term "Thomas-Fermi method" is generally used in the context of solving the Thomas-Fermi equation. In Eqs. (3.43)-(3.49) a different approach is taken.

In [189], for example, the TFDW method was combined with pseudopotential theory and the Wigner-Seitz radii for the first 55 elements of the Periodic Table were calculated. In the majority of cases, the agreement with experiment was within 5%, even for the transition metals. When applied to nonmetals (such as Si and Ge) the method led to large errors, as might be expected. On the whole, however, the agreement was quite satisfactory. The method was later applied to alloys [190, 191] and semiconductors [192]. The Thomas-Fermi method thus turns out to be a rather reliable tool for calculating pseudoatom potentials.

3.2.6. Interatomic interaction potential. To demonstrate the applications of dielectric screening theory further, we employ the Thomas-Fermi method for an analysis of the interatomic interaction potential (1.43) in the framework of the pseudopotential theory. We consider the simplest pseudopotential possible, namely the Coulomb potential ($-Ze^2/r$) with a formfactor (1.26) (this is in fact a Heine-Abarenkov type potential with $R = 0$). To incorporate screening, we use the Thomas-Fermi model (3.43). Some precautions should be taken though because, as remarked earlier, this model requires the inclusion of an exchange potential. Moreover, the function $\varepsilon(q)$ should be assumed to fall off faster than q^{-2} . Let us introduce into (3.43) an "average" correction due to purely Coulomb effects C and one for purely exchange-correlation effects X . We denote $p^2 = a^2 C^2$ and $g^2 = a^2 X^2$. The dielectric function $\varepsilon(q)$ without exchange is $\varepsilon = 1 + p^2/q^2$ and with both exchange and correlation effects it is $\varepsilon^* = 1 + g^2/q^2$. The function $\chi(q)$ is simply $-\Omega a^2/8\pi e^2$; the quantity a^2 is given by Eq. (3.46).

The interatomic interaction potential has the form of (1.43) [17]:

$$\Phi(r) = \frac{Z^2 e^2}{r} + \frac{2\Omega}{(2\pi)^3} \int [W^{\text{cr}}(q)]^2 \chi(q) \varepsilon^*(q) e^{i\mathbf{q}\mathbf{r}} d^3q.$$

For the pseudopotential and screening chosen, the integral can be evaluated analytically, giving

$$\Phi(r) = \frac{Z^2 e^2}{X^2 r} [X^2 - 1 + e^{-gr}]. \quad (3.50)$$

This potential has no oscillations since we have used the Thomas-Fermi function rather than Lindhard's.

Our next concern is to find out under what circumstances $\Phi(r)$ may have a minimum corresponding to the equilibrium interatomic separation in a crystal. The condition for the existence of a minimum is obtained by differentiating (3.50) with respect to r :

$$(1 + gr)\exp(-gr) = 1 - X^2. \quad (3.51)$$

The left-hand side of (3.51) is a positive function smoothly decreasing with r ; at $r = 0$ its value is unity. Hence, whether or not this

crystal model is capable of giving an equilibrium separation depends on the right-hand side of Eq. (3.51).

The quantity X^2 is, by the way it was introduced, an average of the function $p(q)$ involved in (3.35). Whatever model is assumed, this function monotonically decreases from 1 to 0.5 or even lower [17]. We may therefore assume that

$$X^2 < 1. \quad (3.52)$$

Consequently, if the exchange correction is included, the right-hand side of (3.51) is always less than unity and (3.51) is always solvable. If exchange effects are ignored, i.e., $X = 1$, there is no attraction between the atoms and no crystal forms, as is the case in the ordinary Thomas-Fermi model or in the Hartree model [193].

Interestingly, even as simple a model as this makes it possible to characterize each element by its own "effective exchange". Furthermore, there may be then a quantitative agreement with experiment for each element, namely, the distance obtained by (3.51) coincides with the radius of the crystal first coordination sphere.

Taking into account that $1 - X^2 > 0$, Eq. (3.50) may be rewritten as

$$\Phi(r) = B \frac{\exp(-gr)}{r} - A \frac{1}{r} \quad (3.53)$$

with A and B positive. In this form, the interatomic interaction potential corresponds to the Born-Mayer potential, which is frequently employed in interpreting interatomic forces. In a sense, then, we have justified the Born-Mayer potential in terms of pseudopotential theory.

Note that the coefficients A and B in (3.53) have very much the same meaning they have in the theory of Born-Mayer potentials. A feature common to both approaches is that both the repulsion and the attraction are in (3.53) due to electron-electron interaction. There is a major difference, though. In the Born-Mayer theory repulsion at small distances is due to exchange interactions arising between atomic cores brought too close together. In pseudopotential theory, we see that this repulsion arises instead from the Coulomb term while the exchange is responsible for the stability of the crystal. If exchange is not allowed, no minimum will appear.

Certainly the above argument on the role of exchange in the stability of crystal structures can only be given a qualitative significance. It does indicate, however, that the exchange-correlation interaction may be very important in crystal studies.

3.2.7. The screening potential and the convergence of series. It is appropriate here to raise an interesting point. We have used the

Coulomb potential, whose feature is the presence of bound states. If the potential is screened, bound states may disappear because of the additional Coulomb repulsion produced by the screening. The screened potential (pseudoatom) has the form

$$W^{\text{cr}}(r) = -\frac{Ze^2}{r} \exp(-gr).$$

The Bargmann integral (2.109) for the potential is

$$B_1 = \frac{Ze^2}{g^2} = \frac{Ze^2}{a^2 X^2}.$$

A screened crystal potential will have no bound states if $B_1 < 1$, i.e., $X^2 > Ze^2/a^2$. To estimate X^2 , we evaluate the quantity Ze^2/a^2 making use of (3.46). We then find that for copper, for example, one should take $X^2 > 1.53$, for caesium $X^2 > 3.04$, for molybdenum $X^2 > 5.53$, all the figures disagreeing with condition (3.52).

It thus turns out that the screened pseudopotential we used has a *bound state*. But then this is a paradox for, on the one hand, this pseudopotential allowed some reasonable conclusions about the stability of crystals and, on the other, as proved in Sec. 2.4, a perturbation series diverges for a potential having bound states. A possible answer is that the divergence only becomes critical when there are an infinite number of terms in the perturbation expansion. In other words, the divergence of an infinite perturbation series does not necessarily exclude the calculation of crystal properties because, in practice, the series is always truncated. (In Sec. 4.2.2, we shall discuss the use of the secular equation in OPW band-structure calculations. Strictly speaking, this equation is not applicable if the wave function is expanded over an infinite basis set. Nevertheless, the OPW method is workable, though not very accurate.)

Another possible answer is as follows. We saw in Sec. 2.4. that a perturbation theory series diverges for any isolated potential screened by the dielectric formalism. This being the way in which all pseudopotentials are screened, must we reject pseudopotential theory as a whole, ignoring thereby all its successes? Certainly not. The paradox is resolved, strange as it may seem, by the fact that the crystal actually contains an infinite number of such "bad" potentials. Their combined effect is to lower the total potential; the bound states then fall into the conduction band and are "destroyed" because the motion of a "bound" electron becomes infinite.

To put it another way, there are an infinite number of ways in which the potential of a crystal as produced by all the pseudoatoms in the crystal may be decomposed into single-site contributions. Naturally, we can divide this potential into potentials with bound states. But perhaps we can build it up from identical single-site potentials none of which have bound states? Needless to say, the

convergence of the series may not depend on our choice of the way the potential is divided. It is important to realize that the perturbation theory convergence is determined by the *total* crystal pseudopotential (rather than the single-site ones).

One feature of screening is worth noticing. Depending on the "strength" (i.e., on the well depth) of the initial model pseudopotential, the screened pseudopotential acquires a repulsive region either inside the well (a finite region) or outside it (an infinite region). By the Bargmann criterion (2.111), it is only the attraction region which should be considered and we observe that depending on the value of A the pseudoatom may or may not produce a bound state. As one might expect, the convergence of the perturbation series is determined by the well depth. On the other hand, the convergence criterion (2.118) requires that both the repulsive and attractive regions of the pseudoatom be considered and this may lead to entirely different results. Using the simple analytical form (3.45) we can easily evaluate the first moment of the pseudoatom (Sec. 2.4.1) and then, by letting it go to zero and applying Pendry's criterion (2.135), we can obtain a new optimized pseudopotential.

3.2.8. Screening in alloys. The dielectric formalism is particularly convenient when studying disordered systems. In this case, all the information about the arrangement of atoms is contained in the structure factor $S(\mathbf{q})$. Each ion is screened independently of its neighbors, i.e. all single-site potentials are identical.

In reality, a screened single-site potential must depend on its position in a disordered crystal, but the linear dielectric formalism ignores this dependence.

A similar situation occurs when pseudopotential theory is applied to alloys. A crystal total pseudopotential may be written

$$W^{\text{cr}}(q) = S(q) \frac{c_A W_A^{\text{ion}}(q) + c_B W_B^{\text{ion}}(q)}{\epsilon^{\text{all}}(q)} \quad (3.54)$$

where W_A^{ion} and W_B^{ion} are the ion pseudopotentials of components A and B , respectively, and c_A , c_B are their concentrations. The function ϵ^{all} is determined from the equation $Z^{\text{all}} = c_A Z_A + c_B Z_B$.

Strictly speaking, the pseudopotential (3.54) does not allow separation of the contributions of each component, however conveniently its terms may seem to be grouped. This form of screened pseudopotential results from the earlier assumption of linearity of screening. To see this, consider the screening pseudopotential (3.20), $V^{\text{scr}} = \hat{A} \hat{B} W^{\text{cr}}$, where \hat{B} is a "perturbation theory" operator. Had we used higher-order perturbation theory, V^{scr} would not be linear in the pseudopotentials of the components and, consequently, it

would be impossible to separate out the screening for each component.

In the linear case this separation can be done and we write

$$W_{A,B}^{\text{cr}}(\mathbf{q}) = W_{A,B}^{\text{ion}}(\mathbf{q})/\epsilon^{\text{all}}(q). \quad (3.55)$$

This means that if dielectric screening theory is applied to alloys, the pseudopotential of each component is screened regardless of whether or not the crystal is capable of supplying enough electrons for the screening.

We saw in Sec. 3.1 that, provided it is energetically favorable, an isolated atom may accept more electrons than the charge of the nucleus would seem to permit. An analogous phenomenon may occur in dielectric screening theory when applied to alloys. It may happen that in a crystal containing an impurity B (whose valency Z_B is greater than the host valency Z_A) the average electron density of the crystal will be higher than it would have been without B , and the lower-valency component will thus be charged negatively. But, as far as metals are concerned, we know that lower valencies correspond to the alkali and alkali-earth atoms and we must conclude that these behave like acceptors of electrons, in contradiction to elementary chemistry which regards them as electron donors.

In single-element crystals, such phenomena do not occur because the average charge per unit cell corresponds to the ion valency. In pure metals, as we shall see in Sec. 3.5, the total number of accepted electrons is indeed equal to the valency.

It should be expected that screening will be described most accurately in alloys made up of components with equal valencies. The difference between the chemistries of the atoms will be brought out by the formula (3.32): the deeper the initial pseudopotential, the greater must be the screening density, in approximate correspondence to the charge distribution in the alloy. Why approximate? Because the second component will also pull electrons to itself in competition with the first. This will result in the interatomic density being distributed in some "compromise" way (an analog of the covalent bond), whereas in the dielectric formalism this region will necessarily be depleted of electrons. It is interesting to note that in calculations of short-range-order parameters (Sec. 7.3) [194] it is for components with close valencies that the best results are obtained.

3.3. The self-consistency of pseudopotential and additive screening

3.3.1. The problem of self-consistent potential. In the previous section, the theory of self-consistent (dielectric) potential screening was discussed. The theory is not self-consistent however. To prove

this we return to the dielectric screening problem for a "single-site" potential.

Formula (3.25) should be considered as related to the total crystal potential \mathcal{V}^{cr} made up of single-site contributions. Using the factorization (1.21) it can be shown that (3.25) holds equally well for each individual single-site potential. This means that the formfactors of the individual ionic potentials are screened independently. But so too are then the potentials themselves because Fourier transformation (to real space) is linear. The only effect neighboring ions have on a given ion is that all the ions contribute their Z electrons to a homogeneous electron gas. Each ion then seizes from this "store" however many electrons it needs, irrespective of what is happening to a neighbor.

The total crystal density will, of course, be a sum of the single-site densities since the Friedel "tails" of the individual pseudoatoms overlap:

$$\rho^{\text{cr}}(\mathbf{r}) = \sum_{\mathbf{v}} \rho(\mathbf{r} - \mathbf{t}_{\mathbf{v}}). \quad (3.56)$$

Thus there is an additional (earlier disregarded) density and this enhances the screening of the ion.

Qualitatively, the same follows from the addition formula for the potentials: the "tail" of each pseudoatomic potential will reach inner parts of neighboring pseudoatoms thereby changing their potentials, in contradiction to the dielectric model which assumes the potential is self-consistent. But is there really a contradiction?

It was stated at the end of the previous section that there are an infinite number of ways in which the total crystal potential can be decomposed into single-site contributions. It is clear that, in principle, this potential may be represented as a sum of *nonoverlapping* potentials; the summation will not change the single-site potentials (or pseudoatoms).

Are the potentials of these pseudoatoms self-consistent? On the one hand, such a pseudoatom remains unchanged when placed in a crystal, so that the answer would seem to be "yes". But on the other hand, each ion is screened by a homogeneous gas, and so the answer seems to be "no", for having introduced nonoverlapping potentials we have placed, as it were, artificial barriers at the boundaries of the pseudoatoms and made the interpenetration of the electron densities impossible. In a homogeneous gas, we would not think of boundaries around an atom and the density of such a pseudoatom should therefore be "blurred"; it is too "compact" an entity as far as the boundary conditions for such a gas are concerned.

It must always be borne in mind therefore that self-consistency implies subjection to some boundary conditions. A potential may be self-consistent for one boundary condition and may be not for

another. However evident, this point is frequently overlooked when discussing self-consistent potentials.

We thus conclude that a potential screened using the dielectric formalism is self-consistent for an homogeneous electron gas and is not so for a crystal. This, of course, has nothing to do with the dielectric screening formalism itself but rather follows from the assumed linearity in the perturbation potential (3.31).

3.3.2. Additive screening. The problem of self-consistent screening may be approached by a different method.

In the dielectric method, the self-consistency of screening is required from the start (the screening density is expressed in terms of the final result) and then various approximations (or models) are invoked. We can reverse the procedure by first simplifying our equations (i.e., choosing a model) and next requiring self-consistency. This approach is advantageous in that it is more sensible (and easier) to improve on a well understood (chosen) model than to destroy the exact picture by using approximations that are sometimes hardly interpretable.

We shall call this procedure the “additive screening” method since in Eq. (3.17) for the screened potential W^{cr} , the initial and screening potentials are additive.

What is the difference then between additive and dielectric screening? In both theories the crystal potential W^{cr} is written as a sum of the initial (V^{init}) and screening (V^{scr}) potentials. By (3.18), V^{scr} is then expressed in terms of the screening density ρ^{scr} . In both cases we demand that the result be self-consistent, i.e., ρ^{scr} must be expressed in terms of W^{cr} using (3.19). Introducing $\hat{C} = \hat{A}\hat{B}$, we obtain an integral equation for W^{cr} that is valid for both approaches:

$$W^{\text{cr}} = V^{\text{init}} + V^{\text{scr}}, \quad (3.57)$$

$$W^{\text{cr}} = V^{\text{init}} + \hat{C}W^{\text{cr}}. \quad (3.58)$$

In the dielectric formalism, we solve (3.58) exactly by writing the solution in the form

$$W^{\text{cr}} = (1 - \hat{C})^{-1}V^{\text{init}}. \quad (3.59)$$

We then simplify the operator $(1 - \hat{C})^{-1}$ by assuming it to be diagonal, considering some terms as a small perturbation, etc. In the first approximation, solution (3.59), thus far “exact”, may be written as a power-series in \hat{C} ,

$$W_{(1)}^{\text{cr}} = V^{\text{init}} + \hat{C}V^{\text{init}}, \quad (3.60)$$

where V^{init} is the zeroth approximation for W^{cr} .

In the additive screening theory, the integral equation (3.58) for the (exact) self-consistent potential is solved iteratively,

$$W_{(n)}^{\text{cr}} = V^{\text{init}} + \hat{C}W_{(n-1)}^{\text{cr}}, \quad (3.61)$$

where $W_{(n)}^{\text{cr}}$ is the crystal potential at the n th iteration. The crystal potential before the first iteration (at the zeroth stage) is V^{init} . In the first approximation, then, the *additive* screening theory gives

$$W_{(1)}^{\text{cr}} = V^{\text{init}} + \hat{C}V^{\text{init}}, \quad (3.62)$$

which is the first approximation given by the *dielectric* screening scheme, Eq. (3.60). (We shall encounter this situation later, when comparing the dielectric and additive screening mechanisms as applied to an "electrically neutral" pseudoatom.)

At higher approximations, the formulas yielded by the two theories differ. With additive screening, the N th iteration gives the N th order perturbation theory term for the nonscreened potential (cf. (2.113) and (2.147)):

$$W_{(N)}^{\text{cr}} = V^{\text{init}} + \hat{C}V^{\text{init}} + \hat{C}V^{\text{init}}\hat{C}V^{\text{init}} + \dots + (\hat{C}V^{\text{init}})^N. \quad (3.63)$$

For the N th term in the expansion (3.59) the result is different:

$$W_{(N)}^{\text{cr}} = V^{\text{init}} + \hat{C}V^{\text{init}} + \hat{C}\hat{C}V^{\text{init}} + \dots + (\hat{C})^N V^{\text{init}}. \quad (3.64)$$

The difference between these expressions arises presumably from the fact that the \hat{C} operator is nonlinear and accordingly depends on the potential it acts upon. Therefore in (3.64) the operator \hat{C} , in view of (3.58), is determined by the *final* self-consistent crystal potential W^{cr} , whereas in each i th term of (3.63) it is determined by the crystal potential resulting from the i th *iteration*.

Whatever the case may be, it is clear that calculating a self-consistent potential is equivalent to summing a perturbation theory series either like (3.63) or like (3.64). Hence the purely academic problem of perturbation theory convergence is closely related to the very practical question of the convergence of iterative procedures involved in constructing self-consistent crystal potentials.

Note also that the extension of dielectric screening theory beyond the linear approximation, or "nonlinear screening", requires including higher terms in the W^{cr} -dependence of ρ^{scr} , i.e., the nonlinearity of the operators \hat{B} and \hat{C} . On the other hand, the question of whether self-consistent linear dielectric screening is equivalent to its nonlinear version has not yet been investigated. We can only be certain that self-consistency lies beyond linear screening.

A comparison of (3.63) and (3.64) indicates that in additive screening the convergence may be either faster or slower than with dielec-

tric screening. The additive scheme is however more convenient because the real-space treatment makes functional dependences much more transparent. It is therefore much easier to choose screening models closer to the self-consistent result*.

3.3.3. Self-consistency and electroneutrality. The next question to be addressed is the possible forms such self-consistent potentials may take.

The number of electrons within a Wigner-Seitz cell must be equal to the charge Z of its ion. (All Wigner-Seitz cells are identical and were one of them charged, so would be all the others, which, by assumption, is not the case.) The electroneutrality of a Wigner-Seitz cell is thus a consequence of the translational invariance of a neutral crystal.

Further, since electroneutrality secures the complete compensation of charge, the region outside a Wigner-Seitz cell must have neither an attractive nor a repulsive potential. Consequently, a single-site crystal pseudoatom obeying the "crystalline" conditions for potential self-consistency, should be "of finite range":

$$W^{\text{cr}}(\mathbf{r})|_{|\mathbf{r}| > |\mathbf{R}_{\text{WS}}|} = 0, \quad (3.65)$$

where \mathbf{R}_{WS} is a vector at the boundary of the Wigner-Seitz cell. This formula excludes Friedel oscillations, which is wrong for a single scatterer placed in an electron gas, but is correct for an infinite set of scatterers (a crystal) where all the Friedel "tails" are identical and must be summed up.

When single-site potentials obeying (3.65) are combined to form a crystal potential (which is the sum of them), the potentials of neighboring sites no longer affect each other. A potential that obeys (3.65) is thus more "self-consistent" than one that disobeys it. Expression (3.65) may therefore be considered as an optimization criterion for the potential or, more generally, pseudopotential.

In practice, the surface of a Wigner-Seitz cell is too complicated a geometry for this criterion to be reasonably applied. To get around this obstacle it is customary to replace the polyhedral Wigner-Seitz cell by a Wigner-Seitz sphere of the same volume (which is the atomic volume Ω_0 or the volume per atom). Denoting the radius of the sphere as R_a , we rewrite (3.65) in a spherically-symmetric form:

$$W^{\text{cr}}(\mathbf{r})|_{|\mathbf{r}| > R_a} = 0. \quad (3.66)$$

* In band theory, the construction of an additively screened self-consistent potential takes a great deal of computational effort. First, the secular equation must be solved for $E(\mathbf{k})$. Then the electronic wave functions are found. These are used to calculate the crystal potential (the input potential for the next iteration), and the procedure is repeated. The construction of V^{init} ("starting" potential) is described in Sec. 3.4.

It should be remarked that spherically-symmetric pseudoatoms of radius R_a will overlap. To avoid this, R_a should be set equal to the MT-radius, which is half the nearest-neighbor distance (the MT potential was introduced in Sec. 2.2). But then all the charge Z will concentrate in a volume smaller than the Wigner-Seitz sphere, which is *a priori* a more restrictive condition than (3.65). Indeed, the MT-sphere is the one inscribed in the Wigner-Seitz cell and there is no reason to assume that all of the charge is pulled into the sphere. Perhaps R_a should be considered as a model radius, but this possibility has not yet been investigated. We thus assume the model radius of (3.66) equals the atomic radius R_a defined as the radius of the atomic sphere of volume Ω_0 (the Wigner-Seitz sphere).

Note that (3.65) in fact contains two conditions. The first (and stronger) one may be applied as a condition for screening: it requires that the potential be of finite range (incidentally, this requirement automatically removes the divergence in the long-wavelength limit of the formfactor).

The second condition, the electroneutrality of the Wigner-Seitz cell, is complementary to the first.

3.3.4. Comparison of screening models. It would be desirable to compare dielectric and additive approaches to the potential screening problem. We restrict ourselves to potentials satisfying the optimization criterion (3.66). This will make it easier to estimate the reliability of our conclusions.

Starting from dielectric screening, how can we construct a pseudoatom that obeys criterion (3.66)? The only way to do this is to go from the formfactor of the screened potential (3.25) to its prototype and then to fit the potential parameters so that condition (3.36) is fulfilled. Clearly, the Friedel oscillations make this infeasible because within the dielectric screening approach the "tails" of pseudoatoms will necessarily interpenetrate.

Help comes from the problem we solved back in Sec. 3.2.5 while discussing screening in the Thomas-Fermi approximation. In this approximation there are no Friedel oscillations, so that a disadvantage from the dielectric screening point of view (for a potential embedded into an electron gas) becomes an advantage for a potential within a "community of its likes".

Thus, by choosing $R_a = (3\Omega_0/4\pi)^{1/3}$ and using the results of Sec. 3.2.5 for Thomas-Fermi screening, we obtain from Eq. (3.49) a condition for determining the well depth for a Heine-Abarenkov type pseudopotential. From the dielectric formalism point of view, this potential will be an optimized one.

The next step is to set up an optimized pseudopotential within the additive screening approach. We reason that to retain consistency with the dielectric formalism, we may assume the screening electron

gas to be initially distributed over all space. This means that each Wigner-Seitz cell must contain exactly Z electrons. In coordinate space, their distribution density is Z/Ω_0 . We may calculate the corresponding Coulomb potential and then to add it to the original pseudopotential (3.44), the same we used in the dielectric screening. In this case we obtain an additively screened pseudopotential.

By electrostatics we then easily obtain for the screening (repulsive) potential

$$V^{\text{scr}}(r) = \begin{cases} \frac{Ze^2}{2R_a} \left[3 - \left(\frac{r}{R_a} \right)^2 \right], & r \leq R_a, \\ + \frac{Ze^2}{r}, & r \geq R_a. \end{cases} \quad (3.67)$$

It can easily be seen that while at small r the behavior of the crystal pseudopotential is the same for both screening models ($a - br^2$), at large r the agreement breaks down. This might have been expected because the mathematical formalism we are using is different.

To compare the pseudopotentials numerically, the well depth \tilde{A} of an additively screened pseudopotential should be chosen so that the long-wavelength limit of its formfactor be the same as with the dielectric screening. The two pseudopotentials will then have the same mean value and ranges but will differ in the well depths; it is this difference that will allow us to distinguish between the two screening models.

Let us then evaluate using (3.67) the formfactor of the potential screened

$$\begin{aligned} W^{\text{cr}}(q) &= W^{\text{ion}}(q) + V^{\text{scr}}(q) \\ &= -3A_S \frac{\cos qR_a}{(qR_a)^2} - 3 \left[\tilde{A} - \frac{3A_S}{(qR_a)^2} \right] \frac{j_1(qR_a)}{qR_a}. \end{aligned} \quad (3.68)$$

At the limit $q \rightarrow 0$ we obtain a relationship between the well depth and the long-wavelength limit of the formfactor:

$$W^{\text{cr}}(0) = 1.2A_S - \tilde{A}. \quad (3.69)$$

Setting $W^{\text{cr}}(0) = -(2/3)E_F^0$, we find the required relationship:

$$\tilde{A} = 1.2A_S + \frac{2}{3} E_F^0. \quad (3.70)$$

As it must, this (optimized) well depth differs substantially from that given by dielectric screening theory, Eq. (3.49). This makes the results of calculations by (3.70)* all the more significant. The

* Lack of space prevents us from quoting the numbers. If needed, they can be easily reproduced by the reader.

parameter A is invariably larger than A_{NA} but the difference is at most 3% and the agreement between the two theories is better for transition than for nontransition metals.

There are three conclusions to be drawn from this. First, the simplification of the dielectric operator makes it hardly sensible to speak of self-consistent dielectric screening. For in the additive formalism, assuming a uniform screening density and thereby neglecting the effect of the crystal potential, we obtained the same result as given by the dielectric formalism which does incorporate this effect in Eq. (3.32).

Second, the simplest additive screening method, while not inferior in accuracy, may prove more versatile than the dielectric, since it is an easy matter to replace the uniform screening density by a nonuniform one (provided the integral for the screening potential is calculable).

Finally, the agreement between the two screening methods as applied to a potential optimized with respect to the electroneutrality of the Wigner-Seitz cell suggests that this criterion may be regarded as internally consistent and potentially useful.

In addition to incorporating the nonuniformity of the electron gas, the additive screening method seems to have another major advantage over the dielectric screening method. Using the X_α method or a similar technique we can explicitly introduce the exchange interaction, including that between the core and valence electrons.

The reader should be reminded that in the dielectric screening method, the exchange interaction is also taken into account but in a different way. The exchange interaction between the core electrons is included as part of the definition of the ion's model parameters, the interaction between the valence electrons is incorporated in $\epsilon^*(q)$, while the core-valence exchange cannot be considered in a consistent way because the corresponding expression may not be included in the interaction potential between free valence electrons that determine $\epsilon^*(q)$.

Although the additive screening method is frequently combined with the MT approximation in band calculations based on secular equations (the method has then some similarity to the LCAO method), its philosophy goes beyond this approximation. In the following section we shall discuss the way additively screened potentials are derived for the widely used augmented plane wave (APW) and Korringa-Kohn-Rostoker (KKR) band calculation methods. A comparison with the dielectric screening will also be made.

In pseudopotential theory this method, whatever its advantages, has not been widely used, although one feature of it has been applied in a number of papers. This is the possibility of self-consistent (iterative) calculations in which each iteration gives, by (3.32), a screen-

ing density which is then transformed into coordinate space. Using Poisson's formula we determine from this density the screening potential and using the X_α approximation we find the exchange potential. Having added these two contributions to the initial ion pseudopotential, we evaluate the formfactor of the screened pseudopotential, and the iteration process is repeated to self-consistency.

Calculations of this kind have been performed for model pseudopotentials on semiconductors [195-200], transition metals [201-207], semiconductor surfaces [200, 208-219], and transition-metal surfaces [205, 220].

3.4. Muffin-tin potential

3.4.1. MT approximation. This approximation was introduced in 1937 by Slater [221] in a paper on the augmented plane wave (APW) method. His idea was to make the functions involved in the scattering theory more tractable.

The essence of the approximation is the introduction of a sphere (MT or Slater's) such that inside it the potential is spherically symmetric and outside zero. It is implicit that MT spheres do not overlap, that is, the MT radius is no greater than half the nearest-neighbor distance, d_{nn} .

In this section the MT approximation is to a certain degree justified. We compare it with the dielectric screening formalism and discuss their relative strengths and shortcomings.

Thus, in terms of Sec. 3.3, the principal idea of the MT approximation is the use of nonoverlapping single-site potentials.

Suppose the crystal is monatomic. We assume the total initial potential is the sum of the atomic (or ionic) potentials, as in Eq. (3.56) for the electron density:

$$\mathcal{V}^{\text{init}}(\mathbf{r}) = \sum_{\mathbf{v}} \mathcal{V}^{\text{at}}(\mathbf{r} - \mathbf{t}_{\mathbf{v}}). \quad (3.71)$$

Then in the directions to the first nearest neighbors, the quantity $\mathcal{V}^{\text{init}}(d_{nn}/2)$ will be smaller (the potential lower) than in the directions to the second nearest neighbors. The "anisotropy" in the nearest-neighbor distances thus gives rise to the anisotropy in crystal potential.

But, as we saw in Sec. 3.3, any potential, when placed in a crystal, causes a redistribution of electrons in it. Clearly, so will potential (3.71). In this case the electrons will "flow" into the regions of lower potential, i.e., in the directions of lower values of $\mathcal{V}^{\text{init}}$. To put it another way, the electron distribution will become anisotropic.

But this anisotropy will lead to an anisotropy in the screening potential: the regions of minimum $\mathcal{V}^{\text{init}}$ will have maximum values of \mathcal{V}^{scr} . The screening (or rather the self-consistency of screening)

will thus result in smoothing off the anisotropy of the crystalline potential. Note that this effect must be more pronounced for elements whose electrons are less tightly bound to their atoms, that is, for simple metals.

The space distribution of self-consistent screened potential \mathcal{V}^{cr} may be thought of as consisting of nearly flat regions between the atoms (where the extrema of $\mathcal{V}^{\text{init}}$ and \mathcal{V}^{scr} cancel each other) and nearly spherical regions inside atoms, where the screening cannot compete with the atomic potential and \mathcal{V}^{cr} resembles the free-atom potential. Consequently, the self-consistent \mathcal{V}^{cr} may indeed be subdivided into a sum of single-site nonoverlapping contributions from Wigner-Seitz cell potentials V^{WS} :

$$\mathcal{V}^{\text{cr}}(\mathbf{r}) = \sum_{\mathbf{v}} V^{\text{WS}}(\mathbf{r} - \mathbf{t}_{\mathbf{v}}), \quad (3.72)$$

where

$$V^{\text{WS}}(\mathbf{r}) = \begin{cases} V^{\text{WS}}(|\mathbf{r}|), & 0 < |\mathbf{r}| < R_{\text{MT}}, \\ V_0 & R_{\text{MT}} < |\mathbf{r}| < R_{\text{WS}}, \\ 0, & R_{\text{WS}} < |\mathbf{r}| < \infty. \end{cases} \quad (3.73)$$

Here R_{MT} must be less than or (as it is customarily chosen) equal to half the nearest-neighbor distance, $d_{\text{nn}}/2$. R_{WS} is a vector on the boundary of the polyhedral Wigner-Seitz cell. The shape of V^{WS}

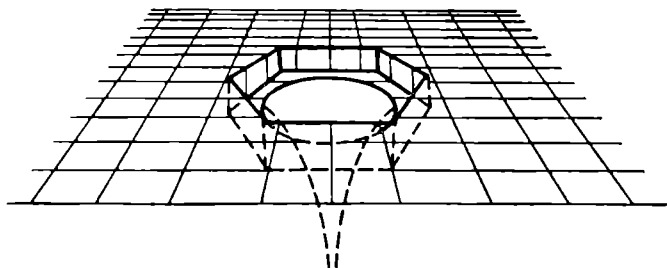


Fig. 3.4. Potential of an isolated Wigner-Seitz cell (in two dimensions).

(3.73) is shown in Fig. 3.4. The MT plateau and the spherically symmetrical (or, in this case, cylindrically symmetrical) potential can be seen in the centre of the cell, both depressed by V_0 relative to the vacuum zero. Above the plane the motion is infinite. The energy bands of the crystal lie below the vacuum zero, as illustrated in Fig. 2.5.

That $V(\mathbf{r})$ outside a Wigner-Seitz cell is zero follows from the requirement that these potentials do not overlap. On forming a crystal, the Wigner-Seitz polyhedra will tessellate and there will be no potential barriers between neighboring cells for electrons whose energies are between the vacuum and the MT zeroes. As a result,

the electrons are permitted to move unhindered throughout the crystal like "free" electrons. In this model, it is only the MT potentials which are significant.

Consider now the Schrödinger equation with potential (3.73):

$$(-\nabla^2 + V^{\text{WS}}(\mathbf{r}) - E) \Psi(\mathbf{r}) = 0, \quad (3.74)$$

where E is measured from the vacuum zero. The energy levels of the crystal lie at $E < 0$. We introduce a new variable

$$E_{\text{MT}} = E - V_0. \quad (3.75)$$

This quantity is measured from the MT plateau and is positive for energies above it. Note that $V_0 < 0$. Equation (3.74) may be rewritten as

$$(-\nabla^2 + V^{\text{WS}}(\mathbf{r}) - V_0 - E_{\text{MT}}) \Psi(\mathbf{r}) = 0.$$

It can be seen that, by shifting the energy zero, we can introduce a new MT potential V_{MT} defined as

$$V_{\text{MT}}(\mathbf{r}) = V^{\text{WS}}(\mathbf{r}) - V_0.$$

When an infinite crystal is being formed, we saw that the specific value of the potential outside the cell is immaterial, which enables us to write

$$V_{\text{MT}}(\mathbf{r}) = \begin{cases} V_{\text{MT}}(|\mathbf{r}|), & 0 < |\mathbf{r}| < R_{\text{MT}}, \\ 0, & R_{\text{MT}} < |\mathbf{r}| < \infty. \end{cases} \quad (3.76)$$

A shift by V_0 could be applied to a crystal-potential made up of V^{WS} potentials. The energy zero would then lie on the MT plateau and (3.76) for the MT potential would become self-evident.

Equation (3.76) for a single-site potential is closely related to the condition for the potential optimization based on electroneutrality (Eq. 3.65). Equation (3.73) corresponds to this condition exactly. An MT potential thus reflects the electroneutrality of the Wigner-Seitz cell and, furthermore, incorporates self-consistency in that a self-consistent potential is less anisotropic than a nonself-consistent one. An MT potential is thus not as far-fetched as might at first seem.

3.4.2. Construction of an MT potential. With a model potential chosen, we now turn to the potential construction proper (for additive screening, for dielectric, the MT potential was discussed in Secs. 3.2 and 3.3).

Since, the MT potential is associated with screening by electrons, we obviously must add together the electron density "tails" of all of the initial atomic potentials (it will be assumed that even a non-self-consistent calculation yields the exact value of ρ^{cr} rather than

a mere sum of atomic densities):

$$\rho^{\text{cr}}(\mathbf{r}) = \sum_{\mathbf{v}} \rho^{\text{at}}(\mathbf{r} - \mathbf{t}_{\mathbf{v}}). \quad (3.77)$$

The above expression has the same anisotropy as Eq. (3.71). Let us average (3.77) over all directions of the vector \mathbf{r} . This will be equivalent to resettling electrons from high-density to low-density regions, or to creating a more uniform electron density which, as we saw earlier, is reminiscent of self-consistency. We obtain

$$\rho^{\text{cr}}(|\mathbf{r}|) = \frac{1}{4\pi} \sum_{\mathbf{v}} \int \rho^{\text{at}}(\mathbf{r} - \mathbf{t}_{\mathbf{v}}) \sin \Theta d\Theta d\varphi. \quad (3.78)$$

The integral here can only be taken numerically. The usual technique for doing this is to re-expand a function centered on one site

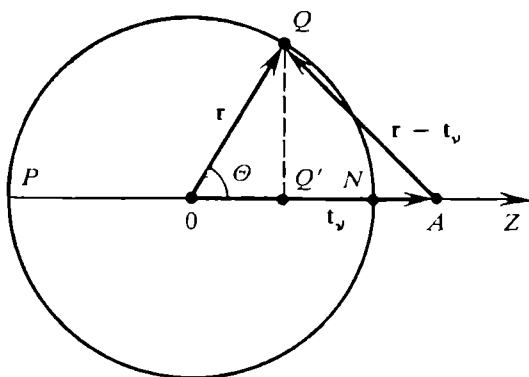


Fig. 3.5. Vector \mathbf{r} forms an angle Θ with the vector from the atom at point O to that at point A . As Θ is varied from 0 to π , the projection of AQ (or the segment AQ') changes from AN to AP .

in terms of functions centered on another. This scheme is due to Löwdin [12] and is usually referred to as Löwdin's α -expansion. Since Mattheiss [222] was the first to apply this scheme to crystals, the following procedure of constructing a crystal MT potential is often called the Mattheiss method (for detailed reviews, see [223, 224]).

Since the final results may seem somewhat doubtful, it is worthwhile to outline here the main features of Löwdin's α -technique.

Consider the density re-expansion from the v th to the zeroth site. Let the z direction be chosen along the axis of the two sites, as shown in Fig. 3.5. Since the problem is cylindrically symmetrical, the integration over φ will simply yield 2π . In integrating over Θ (from 0 to 2π) the z -projection of the vector $AQ = \mathbf{r} - \mathbf{t}_{\mathbf{v}}$ will change from $AN = |\mathbf{t}_{\mathbf{v}}| - |\mathbf{r}|$ to $AP = |\mathbf{t}_{\mathbf{v}}| + |\mathbf{r}|$. Since $\cos \Theta = z/r$ and $\sin \Theta d\Theta = -dz/r = -dz/|\mathbf{r}|$, a Θ -averaging relative to the zeroth center is equivalent to z -averaging from $|\mathbf{t}_{\mathbf{v}}| - |\mathbf{r}|$ to $|\mathbf{t}_{\mathbf{v}}| + |\mathbf{r}|$. After the necessary substitutions we obtain

$$\rho^{\text{cr}}(|\mathbf{r}|) = \rho^{\text{at}}(\mathbf{r}) + \frac{1}{2r} \sum_{\mathbf{v} \neq 0} \frac{1}{t_{\mathbf{v}}} \int_{t_{\mathbf{v}} - r}^{t_{\mathbf{v}} + r} \rho(r_1) r_1 dr_1. \quad (3.79)$$

The first term here corresponds to the initial density of the central atom and the second term to the screening density.

Given the crystal density ρ^{cr} , the Coulomb potential is determined from the Poisson equation. The solution may conveniently be written as

$$V^{\text{Coul}}(r) = -\frac{Ze^2}{r} + \frac{4\pi e^2}{r} \int_0^r \rho(r_1) r_1^2 dr_1 + 4\pi e^2 \int_r^{R_{\alpha}} \rho(r_1) r_1 dr_1, \quad (3.80)$$

the sum of integrals resulting from the multipole expansion of $(\mathbf{r} - \mathbf{r}_1)^{-1}$ involved in the integral of the type (3.4).

The exchange potential is evaluated by Slater's formula (3.12):

$$V^{\text{ex}}(r) = -\frac{3}{\pi} \alpha (3\pi^2 \rho(r))^{1/3}. \quad (3.81)$$

Some workers [129-131] multiply V^{ex} by the function F of Eq. (3.8), thereby incorporating correlation effects [225-229] and taking into account the dependence of the exchange potential on the electron state it acts upon. Other attempts to introduce dependence on the state of the electron may be found in [230-235].

The shape of the potential at $r < R_{\text{MT}}$ is thus known. Next we should determine the quantity V_0 .

From the way it was introduced, V_0 is the *potential* averaged over the region between the MT sphere (where $r \leq R_{\text{MT}}$) and the boundaries of the Wigner-Seitz cell. This is exactly the way it is usually evaluated [223, 224, 345, 346].

Another option is to apply the criterion for the electroneutrality of the Wigner-Seitz cell by averaging the *density* over the volume [236]. The charge inside the MT sphere is simply

$$Q_{\text{MT}} = 4\pi \int_0^{R_{\text{MT}}} \rho^{\text{cr}}(r) r^2 dr. \quad (3.82)$$

The charge outside the MT sphere is then given by the difference between Z , which is the total number of electrons, and Q_{MT} , so that the charge density outside the MT sphere is

$$\rho^{\text{out}} = (Z - Q_{\text{MT}})/(\Omega_0 - \Omega_{\text{MT}}). \quad (3.83)$$

With this approach, the MT approximation is applied to the density rather than to the potential. The important point is that in contrast to the additive screening scheme, which uses a homogeneous screening charge (Sec. 3.3), the density in question is the total one rather than the screening density alone. A spherically symmetrical crystal density automatically brings about a spherically symmetrical crystal potential in accordance with the self-consistent potential being nearer to the spherical symmetry than the initial one.

The MT approximation for the density leads automatically to the MT form of the exchange potential; the MT shift due to the exchange is readily evaluated by using (3.81) and (3.83), under the assumption that (3.81) holds for all r . The expression for the Coulomb MT shift (due to the Coulomb potential) is rather cumbersome but, in principle, straightforward [236-238].

Other methods for evaluating V_0 are discussed in [222, 223, 239-243].

As the foregoing argument suggests, a specific value of V_0 may be found from some model assumptions about the MT potential, whether or not these are optimization criteria of the type (3.55). V_0 should therefore be considered an optimization parameter (see Sec 3.4.4). This means that the conduction band bottom need not coincide with the MT zero. Even in the NFE model (Chapter 1) we saw that the use of perturbation theory resulted in lowering the bottom of the nearly-free-electron band relative to the energy zero (or, in that model, the vacuum zero). The conduction band may be either wholly above the MT plateau or partially below, in which latter case Eq. (3.75) will yield negative energies.

3.4.3. Limitations of the MT model. The strengths of the MT model are (as often happens) its weaknesses. The finite-range nature of the MT potential results in a potential jump at the boundary of the MT sphere, which means by the Poisson theorem that there is a charge on this boundary [244] with a surface density

$$\sigma = \frac{1}{4\pi} \left. \frac{dV_{\text{MT}}}{dr} \right|_{r=R_{\text{MT}}}. \quad (3.84)$$

The existence of a surface charge follows very clearly from the MT approximation for density which has a jump at the MT boundary. It is this jump which forms the surface charge. The effect cannot be given any physical significance and is simply an artifact of this potential constructing model.

It may be said that we have subdivided the screening density into two contributions, one of which is "smeared" within the MT sphere (no uniformity is assumed for the density) and the other is on the MT boundary. Perhaps we would be better off if the latter were also smeared throughout the sphere—if in no better way, then uniformly. Although computationally this would not be difficult to carry through, such a model has not been tried.

Although the subject of our discussion has been the modeling of a self-consistent potential with an appropriate MT form, we note that there is actually no self-consistency, and this not only from a numerical point of view (here the lack of self-consistency is obvious if no special iterative procedures are employed). The point is that the MT model is intrinsically inconsistent. (Recall that it is gener-

ally used in APW and KKR band calculations.) The reason is that the consistency between the MT potential and the MT density is *impossible in principle* until the latter is zero at $r > R_{\text{MT}}$. This can easily be seen from Poisson's equation, according to which the screening density is proportional to the Laplacian of the screening potential. If the potential is constant, the density equals zero rather than the ρ^{out} of (3.83). If the screening density is a (non-zero) constant, the screening potential is different from a constant and by the Poisson equation (cf. (3.67)) we obtain

$$V_{\text{out}}^{\text{scr}} = \frac{\rho^{\text{out}}}{6r} [-2R_{\text{MT}}^3 + 3rR_a^2 - r^3]. \quad (3.85)$$

It follows that even if ρ ($r > R_{\text{MT}}$) is independent of r , $V_{\text{out}}^{\text{scr}}$ does depend on the coordinate, i.e., because of the MT approach to the density, the single-site potential V_{MT} must also be coordinate-dependent in the region between the MT sphere and the boundary of the Wigner-Seitz cell. But this is inconsistent with the MT form (3.76) usually employed in calculations. (The reader will be reminded that the "self-consistency requirement" underlying the MT approximation implies a Θ -independent, and not an r -independent, potential.)

3.4.4. Atomic sphere approximation. We have ascertained that the presence of the MT plateau makes a potential curve a poor approximation. But is it not possible to do away with the plateau while retaining the finite-range nature of the single-site potential? Clearly we are again obliged (as we were in pseudopotential theory) to optimize the crystal potential. What then may the optimization parameter for the MT model be?

To answer this question, consider the potential of an isolated Wigner-Seitz cell, (3.73). We see that V_0 , the MT shift whose magnitude is to be chosen from some considerations, is just the parameter we need. The quantity V_0 is determined from the requirement that the electroneutrality of a cell, by analogy with the electroneutrality of the atom, is preserved.

The potential shown in Fig. 3.6 by the bold line is for a *pseudoatom* of the MT model. The MT plateau in the pseudoatom replaces the true behavior of the potential at $R_a > r > R_{\text{MT}}$. If we reconstruct this curve, then at $r = R_a$ the potential will have a jump as $U_0 = V(R_a) \neq V_0$. The physical meaning of the jump is transparent. In the absence of the jump ($U_0 = 0$) there would be too few electrons in the cell because the potential $V^{\text{ws}} - U_0$ would not be deep enough. The pseudoatomic electronic levels would thus be positive, and the electrons therefore free to move throughout space and leave the cell. To "retrieve" them, we have to lower the potential (in this case, as a single rigid whole) thereby localizing electrons inside. To

prevent this new charge density from destroying the "old" potential, these electrons must be distributed so as to make the resulting screening potential the same square well we added to lower the initial potential. Clearly, the only distribution to satisfy this requirement is one that yields a surface charge, q.e.d.

Now, however, the single-site potential is no longer isotropic because $U_0(R_a)$ takes on different values in different directions. The

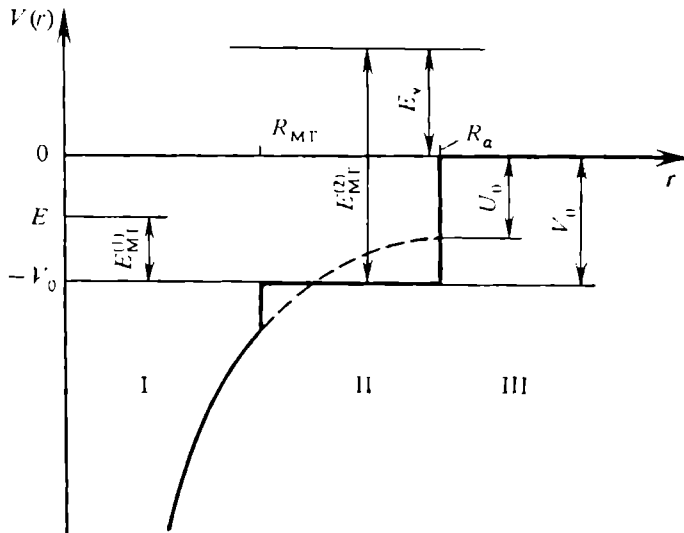


Fig. 3.6. The potential of an MT pseudoatom. In the atomic-sphere model (Secs. 3.4.4 and 4.5.3) the potential extends to R_a (dashed line).

departure of the Wigner-Seitz cell from a sphere should therefore be neglected. Replacing the true cell with a Wigner-Seitz sphere is known as the atomic sphere (AS) approximation:

$$V_{AS}(r) = \begin{cases} V(|r|), & r < R_a, \\ 0, & r > R_a. \end{cases} \quad (3.86)$$

Although this approximation was suggested by Anderson [245, 246] from a somewhat different position, his parameters have very nearly the same meaning as ours.

The crystal potential is the sum of atomic sphere potentials (3.86). In this case the single-site potentials overlap, which is undesirable. However, in dielectric screening theory we did not bother about this overlap either for ordinary pseudoatoms, where it was very much stronger than in this case or in Thomas-Fermi MT pseudoatoms, where it was of the same magnitude.

The AS model not only preserves the electroneutrality of the Wigner-Seitz cell (sphere) (which means a fulfilment of the optimization criterion (3.65)), it also ensures consistency between the density

and potential (which means intrinsic self-consistency of the model). It should be noted that the AS model is different from the sometimes used model of overlapping MT spheres, in this the MT plateau is also present but the overlap results from large MT radii.

In the AS approximation the quantity U_0 plays the role of a new "MT shift" and may be chosen more or less arbitrarily. In Sec. 5.2 we shall analyze the extent of this arbitrariness and discuss some aspects of the AS approximation as used in band theory.

The AS model is an attempt to strengthen the MT approximation at its weakest point, the plateau. There have been other attempts because a model of spherically symmetrical potential is too convenient to be easily given up.

3.4.5. Improvement of the MT approximation. The first attempts were made long ago [247, 248]; any improvement involves some amendments both inside the MT sphere and outside it. In the latter case, the MT plateau is no longer a true flat plateau but rather a warped surface, hence the term "warped MT" [249]. Since it is the plateau where the MT model is most vulnerable, the introduction of potentials with warped plateaux is often the only measure used for improving the model. (Such potentials are called warped MT potentials [247, 250] or more generally, non-MT (NMT) potentials.)

But is the removal of the plateau sufficient? We saw in Sec. 3.1 that the d electrons are most affected by the inner (rather than outer) region of potential. This means that in the transition metals the band structure must be very sensitive to the actual potential inside the MT sphere and a warped MT plateau may therefore prove an insufficient measure.

A large number of completely NMT calculations have been carried out for both nontransition [251-253] and transition metals (Fe in [254-256], V and Cr in [257]).

The transition-metal calculations indicate the importance of NMT corrections. On the other hand, a semi-empirical Fermi-surface study for Mo and W has shown that the inclusion of deviations from the MT form improves the agreement with experiment.

At present a considerable effort is being spent to eliminate the shortcomings of the MT model itself [259-261] (also see [261] for references). But even if such an NMT potential is constructed, the resulting Schrödinger equation would be difficult to solve. This topic is discussed in a number of works. In [262] and [263], for example, Williams and Morgan extend the phase function method to include nonspherical potentials. A number of workers [264-270] employ the idea [271] of replacing l and m , the orbital quantum numbers for a spherical scatterer, by new quantum numbers in whose representation the phase shift matrix is again diagonal. (Since the orbital momentum for a nonspherical scatterer is no longer

an integral of motion, the phase shift matrix cannot be diagonal in the l representation.) All these methods, however, are too complicated to be popular.

In spite of all this work, the effect of a departure from the MT model is still an open, and sometimes controversial, question. In [272], for example, the significance of NMT corrections was investigated for the typical transition metals Rb (completely empty d band), Nb (half-filled) and Pd (completely filled d band). The effect of the corrections on band structure was found to be all but negligible, with level shifts of only 0.002-0.01 Ry, with larger figures for Nb, as might have been expected. Shortly afterwards, however, relativistic calculations of the Nb band structure and Fermi surface [273] proved to be very sensitive to NMT corrections. It should be noted that the potential-constructing procedure adopted in [273] is different from that in [272]. The greatest NMT-related differences occur at the Fermi surface where an NMT potential gives rise to new (previously absent) electronic orbitals which should be observable in experiment.

The discrepancy between the two works is perhaps less significant than it may seem. In a metal like Nb where the Fermi level lies in the middle of a dense d band, small variations in the dispersion laws produce (or eliminate) intersections of some of $E(\mathbf{k})$ branches with the Fermi level. This will result, as found in [273]*, in the appearance (or disappearance) of Fermi-surface "pockets".

Errors introduced by the MT approximation are larger in loose structures in which even a self-consistent density is not isotropic. This may be illustrated by a Fermi-surface calculation for tin [275], where the introduction of a warped plateau reduced, by nearly threefold, both the rms and maximum errors in reproducing the Fermi surface.

A Fermi surface is thus expected to be very sensitive to corrections for the departure of a potential from the MT form. Unfortunately, this is difficult to verify (e.g., by the de Haas-van Alphen effect) because the shape of the surface is also sensitive to many other effects. The electron-phonon interaction, for example, while little affecting the dispersion law $E(\mathbf{k})$ within the Fermi sphere, greatly influences the behavior of the Fermi-surface electrons [276, 277]. (Which suggests, conversely, the importance of NMT corrections in calculating electron-phonon effects.)

3.4.6. Effect of α on band structure. The shape of the Fermi surface also depends on other parameters of the potential, for example, on the α in the exchange potential (3.81). An increase in α raises the

* Self-consistency greatly reduces the difference between MT and NMT results [274].

potential in the inner region of the scatterer. In an isolated atom this results in lowering s and (more markedly) d levels. Consequently, in an isolated MT potential an increase in α will lower the d resonance relative to the MT zero while simultaneously sharpening it. This means, in turn, that the d -type band will be brought down relative to the s band (and sharpened at the same time). The result will not only be a modification of the band pattern but of the Fermi surface as well much like with NMT correction for nonsphericity.

The α -dependence of the scattering characteristics of the MT-potential is a very useful (if somewhat unusual) model for describing the behavior of an atom during a crystal formation. It is worthwhile therefore to discuss the effect of α in some detail.

Table 3.2 shows the position of the s -band bottom (E_{Γ_1}), the energy of the d resonance (E_d), the width of the d resonance (Γ) and the

Table 3.2. Effect of α on characteristic band levels [278]

<div style="display: inline-block; transform: rotate(-45deg);"> E α </div>	Fe ($3d^6 4s^2$); Ry		Cu ($3d^{10} 4s^1$); Ry	
	2/3	1.0	2/3	1.0
E_{Γ_1}	0.182	0.094	0.093	-0.012
E_d	1.200	0.461	1.469	0.451
$\Gamma(E_d)$	0.213	0.022	0.269	0.017
$E_d - E_{\Gamma_1}$	1.018	0.367	1.376	0.463

“height” of the d resonance above the s -band bottom ($E_d - E_{\Gamma_1}$) as calculated in [278] for Fe and Cu for different α -values. The MT potential was constructed by the Mattheiss procedure from wave functions calculated by the X_α method with the Latter correction and $\alpha = 1$ [101].

As expected (see Sec. 3.1), the s and d energies are lowered and the width of the d resonance is reduced as α is increased.

Note that from general considerations the d electrons in Cu must be more localized than those in Fe and hence more sensitive to changes in the inner-region potential (and thereby in α). Table 3.2 shows that indeed all the Cu parameters vary more rapidly with α than those of Fe. But since the d resonance in Cu is more α -sensitive than that in Fe, a decrease in α may result in the Cu resonance being higher (and hence wider). Paradoxically, the d electrons in Cu may prove to be less localized than those in Fe! Table 3.2 shows that this is indeed the case at $\alpha = 2/3$ when $E_d^{\text{Cu}} > E_d^{\text{Fe}}$ and $\Gamma^{\text{Cu}} > \Gamma^{\text{Fe}}$, that is, the d band in Cu is wider than that in Fe. This is of course unacceptable.

3.4.7. The quasi-excited atom model. Admittedly some fundamental mistake must have been overlooked in our apparently flawless argument.

This mistake may have nothing to do with the variation of α (see Sec. 3.1) and the finger can only be pointed at the assumption concerning the orbital configuration. Is it actually justified? Suppose an atom in the crystal is not in the ground state but in an excited one. For iron this means a transfer of an s electron to the d orbital.

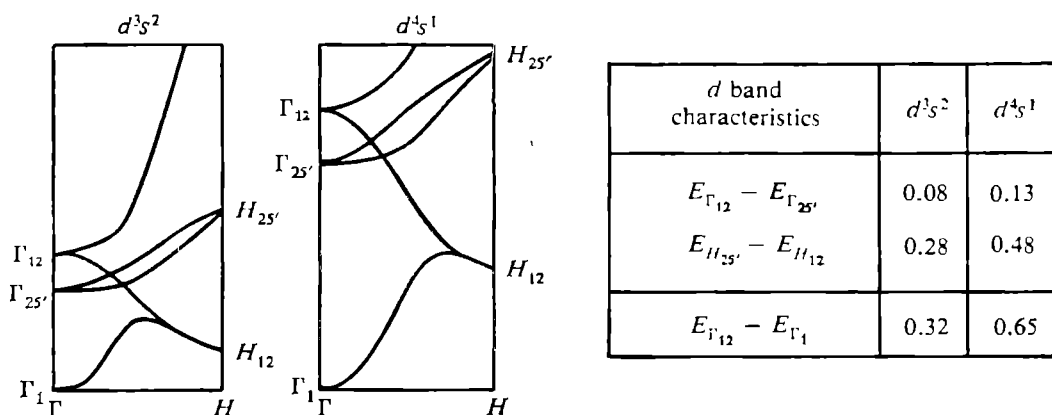


Fig. 3.7. The effect of configuration on the dispersion law of the V atom, non-self-consistent calculation. The assumed ground-state configurations is d^3s^2 .

The nucleus will thus be screened better (see Sec. 3.1), the atomic levels will rise and the d resonance will be higher in energy than it is in the ground-state case. The d -electron wave functions will then become more diffuse or, equivalently, the d electrons will somewhat delocalize.

For copper the excitation assumption implies an electron transfer from a d to the s orbital. This will lead to the d shell contracting and the d resonance lowering and narrowing.

The dependence of band structure on the assumed configuration has been reported. Figure 3.7 shows the band structure of V calculated in [240] for two configurations (the ground one is $3d^34s^2$). The energy is measured from the bottom of the s band (point Γ_1) so that visible only are the rise in the d band relative to the s band and its broadening in accordance with the above argument (the filling of d holes raises the d levels in energy).

The excited atom model thus seems to be able to resolve the paradox of the wrong d -band widths because in Fe it makes the d band wider and in Cu narrower. The trouble is that the model appears to be even more absurd than the initial dependence of scattering characteristics. Nevertheless, it is easily justifiable.

On placing an atom into a crystal, it will be penetrated by the electron densities of neighboring atoms. The screening in the inner

parts of it will then become stronger than it was in the free atom and, naturally, all the atomic levels will be raised. Since no mechanism is there to compensate for the rise, the total energy must increase, which is unfavorable. To remedy this, the atoms should rearrange their valence shells which means a transition from the ground to any other (or, to use the accepted term, excited) level. Thus an atom in a crystal must indeed be in an excited state, the excitation coming from the screening potential V^{scr} which is created by the electron-density "tails" of the neighboring atoms.

It has been known for some time that the best agreement with experiment is shown by dispersion laws obtained by the following model [279-281]. In calculating the crystal density by (3.56), the wave functions are taken from a free-atom excited configuration while the occupancy of the electron shells is assumed to be that of the ground-state configuration. (This is reminiscent of the transition state discussed in Sec. 3.2.) For example, the single-site density for an atom in the ground-state configuration $3d^{n-2}4s^2$ is

$$\begin{aligned}\rho(r) &= (n-2)\rho_{3d}^{\text{at}}(\text{conf. } 3d^{n-1}4s^1) + 2\rho_{4s}^{\text{at}}(\text{conf. } 3d^{n-1}4s^1) \\ &= (n-1)\rho_{3d}^{\text{at}}(\text{conf. } 3d^{n-1}4s^1) + \rho_{4s}^{\text{at}}(\text{conf. } 3d^{n-1}4s^1) \\ &\quad + \rho_{4s}^{\text{at}}(\text{conf. } 3d^{n-1}4s^1) - \rho_{3d}^{\text{at}}(\text{conf. } 3d^{n-1}4s^1).\end{aligned}$$

As a result, we have

$$\rho(r) = \rho^{\text{at}}(\text{conf. } 3d^{n-1}4s^1) + [\rho_{4s}^{\text{at}} - \rho_{3d}^{\text{at}}]_{\text{for conf. } 3d^{n-1}4s^1} \quad (3.87)$$

The density of an atom in a quasi-excited state is thus that of the atom in an excited state plus the addition $\rho_{4s}^{\text{at}} - \rho_{3d}^{\text{at}}$ which on the one hand leads to an additional depletion of electrons in the inner region (ρ_{3d}^{at} is subtracted) and on the other to the enrichment of the outer region (ρ_{4s}^{at} is added). It will be noticed that this redistribution is complementary to the one arising in the density of the excited state in (3.87) relative to the ground state density. It can be easily verified that for the ground configuration $3d^{n-1}4s^1$ the effect will be somewhat different, namely, the outer region will be depleted.

When such quasi-excited atoms are brought together to form a crystal, the "enriched" densities of neighboring atoms will penetrate the inner region of a given atom compensating for the (associated with the model) deficiency of electrons. If the inner region is not depleted in the model, an excess of electrons will be produced. We thus conclude that forming a crystal from excited atoms (as proposed in [279, 280] without any physical justification) we obtain more self-consistency than with ground-state atoms.

However successful the initial choice for the crystal potential is, it is clear that the subsequent self-consistency procedure will alter the charge distribution: the charge inside the MT sphere will either

increase or decrease depending on whether the effect of neighboring densities was underestimated or overestimated. An example to illustrate this is provided by our calculations (in cooperation with G. M. Zhidomirov, O. T. Malyuchkov and I. S. Shpotin) for small transition-metal clusters. We employed the SCF- X_α -SW method [87, 283] which is a cluster-oriented KKR scheme [284, 26]. The initial superposition of densities was calculated in the usual manner, that is, the excitation of the atoms was neglected.

The model of excited atoms predicts that after the first iteration the charge of the MT sphere will be markedly larger or smaller (depending on the metal) than that produced by the superposed ground-state densities. In the course of a self-consistency procedure, the charge slowly returns to the initial (superpositional) value while the cluster's energy levels move away from their nonself-consistent positions. After the self-consistency procedure, the charge of the MT sphere is always greater than that given by the density superposition. This nonmonotonic behavior of the charge inside the MT sphere should be kept in mind when comparing the results for a given screening potential model with those for a nonself-consistent calculation. As our estimates indicate, the superpositional MT-sphere charges are closer to the self-consistent values than are the charges resulting from the first iteration*. It should be emphasized that the charge we are talking of is an integral characteristic. A partial analysis (with respect to the orbital quantum numbers) shows considerable differences in the details of the charge distribution (cf. Fig. 3.2).

The same effect may be taken into account in a somewhat different manner, viz. by first orthogonalizing the atomic wave functions with respect to each other. This scheme was proposed by Löwdin [12] and used in [286, 287] for calculating a crystal potential. In this approach one actually constructs the Wannier functions, that is, the approximate electronic wave functions are found prior to the band calculation.

To sum up, when a crystal is formed, the effect of excitation leads to d functions becoming either more diffuse or more shrunk, depending on whether the atom has its d shell unfilled or, respectively, filled.

Interestingly, the excited-atom model is even capable of explaining effects that have little or nothing to do with ordinary band theory. One example concerns the way transition metals catalyze heterogeneous reactions. It is known [288] that copper sometimes acts as a metal with an unfilled d shell. This cannot be given a regular explanation but it is easily interpreted in the excitation scheme because the excitation of an atom is only possible when accompanied by a partial depopulation of the d shell.

* An analogous effect is reported in [285] for V, Cr, Nb, and Mo.

3.4.8. Additive screening in the MT model. We saw that the excitation of an atom is related to its being screened in the crystal. We will focus now on the mechanism by which the additive screening in the above cellular model is determined.

The electron density in a crystal $\rho(r)$ consists of two contributions: the atomic density $\rho^{\text{at}}(r)$ (alias the free-atom density) and the screening density $\Delta\rho(r)$ which is made up of the density "tails" from neighboring atoms. A crystal density is usually calculated

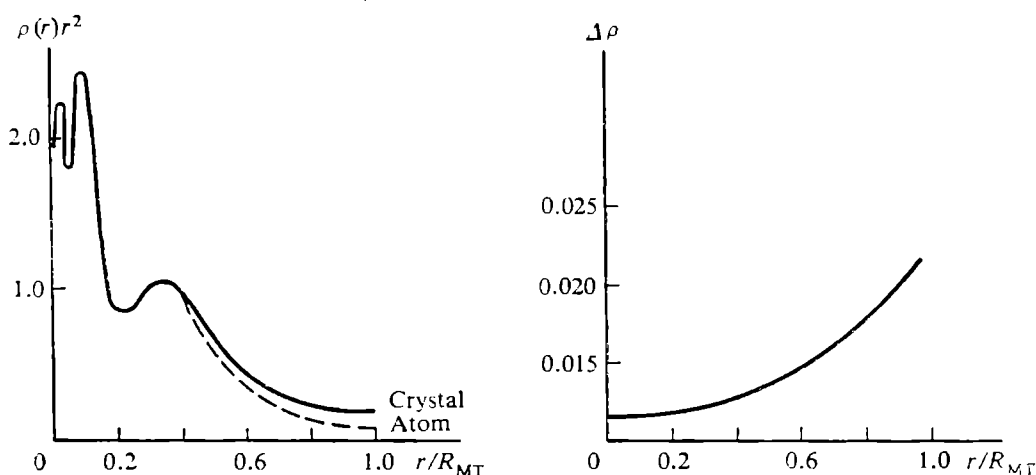


Fig. 3.8. Electron density for the d^4s^2 chromium atom, non-self-consistent calculation [281]. Left—a free atom (dashed line) and an atom in the crystal after the superposition of neighboring atomic densities (bold line). Right—the contribution from the neighboring atoms.

from self-consistent atomic wave functions. This means that in computing the atomic density contribution, $\rho^{\text{at}}(r)$, the perturbation expansion is carried to all orders (cf. Secs. 3.1 and 3.3) instead of being truncated after the first-order term as in the dielectric screening case. (We mean not the core electrons but those valence electrons that are concentrated within the Wigner-Seitz cell.)

The screening MT density $\Delta\rho$ also contains information about the valence shell configuration and is therefore a more suitable approximation for screening than the uniform electron background in the dielectric screening theory. Fig. 3.8 shows these contributions to the density [281]. The contribution from neighboring atoms $\Delta\rho(r)$ increases with r . In the outer region, near $r = R_{MT}$, it is greater than $\rho^{\text{at}}(r)$, which means that it is indeed "screening". Can we expect that if $\Delta\rho(r)$ is replaced by a uniform distribution (as for (3.67)) the two screening theories will be equivalent in this respect?

The answer is negative because given additive MT screening the uniform background is only formed by an external addition to the density rather than by the whole of it, as is the case in the dielectric formalism. The "internal" contribution to the electron density

is obtained self-consistently and the d -electron density remains atom-like which fact is ignored in pseudopotential dielectric screening. The electron-gas density from the rest of the atoms contained within the Wigner-Seitz sphere is relatively low. To calculate it, the atomic density $\rho^{\text{at}}(r)$ should be integrated from R_a to infinity; this gives the electronic charge outside the free-atom atomic sphere:

$$Z_a = 4\pi \int_{R_a}^{\infty} \rho^{\text{at}}(r) r^2 dr.$$

This integral can be calculated not only for the total density but also for its partial components; this will give the number of s , p and d electrons outside the free-atom Wigner-Seitz sphere.

This sort of calculation presents no difficulties. Assuming a program of the type described in [101], we estimate the computer time needed for each element to be no more than 5 to 10 minutes on an IBM-360/40 (or similar) machine. Results of this kind (for Hartree-Fock densities) are given for $3d$ and $4d$ transition metals in [289]. In both cases the d charge outside the atomic sphere decreases along a period but since the number of atomic electrons increases with atomic number, the total outside d charge reaches a maximum in the middle of the period, decreasing again to the end of it. The percentage of this charge ranges from 0.14 (Sc) to 0.60 (Mo). For the s electrons the range is only from 0.60 to 0.75. The total charge outside the atomic sphere is minimum in the noble metals (0.85) and maximum in the middle of the $4d$ period (1.35).

These data indicate that even though d electrons do contribute to the "free" electron gas in a crystal, they cannot be regarded as completely free. The d electron density is, in a way, frozen inside the cell and is mainly influenced there by its own atom.

Additive MT screening thus automatically takes into account that d electrons are neither localized nor actually free. Furthermore, since the atomic radius is determined by the crystal structure and so is the summation in (3.78) it turns out that a single-site MT potential depends on the arrangement of atoms whereas in the dielectric screening this dependence is lost. The MT model is thus closer to reality. It is interesting that a potential optimized within the dielectric formalism with respect to the electroneutrality of the Wigner-Seitz cell (see back to Secs. 3.2.5 and 3.3.4) also depends on the environment, namely, through the atomic radius. A nonoptimized pseudopotential has no such dependence.

The above comparison between the dielectric and additive screening mechanisms may prove helpful for improving the pseudopotential screening theory. Firstly, it is clear that a pseudopotential may be greatly improved if in optimizing it the crystalline environment is taken into account. Secondly, it is clear that transition-metal d

electrons may not be considered as completely free and some effective valency should be introduced to account for their being partially frozen. Perhaps the best choice for this valency would be the number of the s electrons plus the number of the d electrons that happen to be outside the atomic sphere. This effective valency can be used both in calculating the ionic pseudopotentials and in their subsequent screening with the dielectric function $\epsilon(q)$ in which the effective valency is involved.

3.4.9. Screening in alloys. Let us now compare the dielectric and additive screening mechanisms as applied to the theory of alloys.

For simplicity, we consider a stoichiometrically ordered alloy of two components A and B each with different electronegativities \mathcal{E} . Let $\mathcal{E}_A > \mathcal{E}_B$. The levels in the A atom are thus lower than those in the B atom, which means that the A wave functions are relatively more compact and the atom itself is smaller. The B atom is thus more "metallic" and one would expect a charge flow from the B to the A atoms.

In the dielectric formalism atoms are screened independently of each other by formula (3.32) and, as we saw in Sec. 3.3, charge may even flow, paradoxically, from a non-metallic atom to metallic one.

This may not happen with additive screening. In a pure crystal made up of atoms of one sort, say B , all the charge that has been outside the atomic sphere of the atom B "is given back" to it by its neighbors. In an alloy, each B atom is at least partially surrounded by A atoms, whose wave functions are more localized than those of B . Therefore the charge will only partially "return" to the B atom. As a result, a Wigner-Seitz cell containing a B atom will be depleted of electronic charge and the A atoms will receive more electronic density than they "gave away". We thus observe a "flow" of charge from metal to nonmetal.

It thus follows from the way the MT scheme was introduced that it is capable of accounting for the differences in the screening of chemically different atoms. The flow of charge is included automatically (even without self-consistency) and simply follows from the superposition of densities. The self-consistency process causes an additional redistribution of charge and the picture becomes more complicated than for pure components. As our calculations reveal, the charge is redistributed not only in the MT spheres of the components but also in the intersphere region which suggests that the model of charge flow between the A and B "atoms" is oversimplified and three regions instead of two (A and B) must actually be considered. Of course, the MT model of superposed densities also takes this into account to a first approximation.

Unfortunately, the MT model for an alloy has a number of serious disadvantages. Because of the different chemistries of the compo-

nents, the alloy's crystal potential may be rather anisotropic; this possibility is artificially excluded out of the MT model. Moreover, the MT radii of the components are chosen very arbitrarily.

Note that in the *dielectric* formalism some potential anisotropy is taken into account through the structure factor $S(\mathbf{q})$. It would be desirable to combine the advantages of the MT model (the direct summation of atomic densities) with the anisotropy of the crystal potential. This problem was considered in [290] but it would carry us too far afield to discuss it.

3.5. Average value of the screened potential

3.5.1. The long-wavelength limit of the formfactor. Depending on the screening mechanism adopted we may come to different screened potentials and we would like to be able to compare them. One way of doing this is by using the average value of the screened potential:

$$\overline{W} = \frac{1}{\Omega_0} \int W(\mathbf{r}) d^3r. \quad (3.88)$$

In this expression the integration is over all space but the normalization factor is taken to be Ω_0 , the volume per atom (the volume of the crystal being too large a quantity to be meaningfully used).

If the potential is screened by way of the dielectric formalism, there is no need to calculate W in coordinate space to find \overline{W} . This may be seen by noting that the long-wavelength limit for the formfactor of a screened potential coincides with \overline{W} :

$$W(q \rightarrow 0) \equiv \frac{1}{\Omega_0} \lim_{q \rightarrow 0} \int W(\mathbf{r}) e^{i\mathbf{q}\mathbf{r}} d^3r = \overline{W}. \quad (3.89)$$

Therefore the theory of linear dielectric screening predicts (by 3.42) and (3.89)) equal average values for all potentials:

$$\overline{W}^{\text{cr}} = \lim_{q \rightarrow 0} \frac{W^{\text{ion}}(\mathbf{q})}{\epsilon(q)} = -\frac{2}{3} E_F^0. \quad (3.90)$$

Since other screening mechanisms are also possible, the above expression needs generalizing. We do this by rewriting the formfactor of a local screened potential in the form

$$W^{\text{cr}}(\mathbf{q}) = \frac{1}{\Omega_0} \int e^{-i(\mathbf{k}+\mathbf{q})\mathbf{r}} W^{\text{cr}}(\mathbf{r}) e^{i\mathbf{k}\mathbf{r}} d^3r.$$

The following argument applies equally well to a nonlocal pseudopotential although its average value and the long-wavelength limit of the formfactor will be related to each other in a more complicated

way. Making use of (2.32), it can be shown that

$$\langle \mathbf{k} + \mathbf{q} | W^{\text{cr}} | \mathbf{k} \rangle = \frac{1}{\Omega_0} \sum_L \int_0^\infty h_L(\mathbf{k} + \mathbf{q}, r) h_L(\mathbf{k}, r) W^{\text{cr}}(r) r^2 dr.$$

In the Fermi-sphere approximation $|\mathbf{k} + \mathbf{q}| = |\mathbf{k}| = k_F$. Using (2.153), we obtain

$$\langle \mathbf{k} + \mathbf{q} | W^{\text{cr}} | \mathbf{k} \rangle = -\frac{4\pi}{\Omega_0} \frac{1}{k_F} \sum_l (2l+1) \tan \eta_l^{\text{B}}(k_F) P_l(\cos \theta_{\mathbf{k}, \mathbf{k}+\mathbf{q}}). \quad (3.91)$$

In the small- q limit we have

$$\langle \mathbf{k} | W | \mathbf{k} \rangle = -\frac{4\pi}{\Omega_0} \frac{1}{k_F} \sum_l (2l+1) \tan \eta_l^{\text{B}}(k_F).$$

It is easy to prove the identity

$$\frac{1}{\Omega_0} = \frac{(E_F^0)^{3/2}}{3\pi^2 Z}.$$

Using the smallness of the phase and the definition of the Friedel sum, (2.91), we arrive at the following generalization of (3.90):

$$\lim_{q \rightarrow 0} \langle \mathbf{k} + \mathbf{q} | W^{\text{cr}} | \mathbf{k} \rangle = -\frac{2}{3} E_F^0 \frac{\mathcal{F}}{Z}. \quad (3.92)$$

3.5.2. Linear-screened potential. For Eqs. (3.90) and (3.92) to be consistent, it is necessary that a linearly screened potential (LSP) obey the equation:

$$\mathcal{F}^{\text{LSP}} = Z. \quad (3.93)$$

In other words, the Friedel sum for a crystal potential given by the linear (dielectric) screening method is equal to the ion valency. This is consistent with the NFE model: an isolated ion, stripped of its Z valence electrons and immersed in an electron gas retrieves its electrons from the gas.

The first-order perturbation theory result for a crystal Fermi energy is

$$E_F^{\text{cr}} = k_F^2 + \langle \mathbf{k} | W^{\text{cr}} | \mathbf{k} \rangle = E_F^0 \left(1 - \frac{2}{3} \frac{\mathcal{F}}{Z} \right). \quad (3.94)$$

From (3.93) and (3.94) we obtain in the LSP model [291, 292]:

$$E_F^{\text{cr}} = \frac{1}{3} E_F^0. \quad (3.95)$$

This result is easy to interpret: the free electron band is brought down as a whole by the amount equal to the average value of the crystal

potential (Fig. 3.9a). For a nonlocal pseudopotential, the (downward) shift by the long-wavelength value of the formfactor.

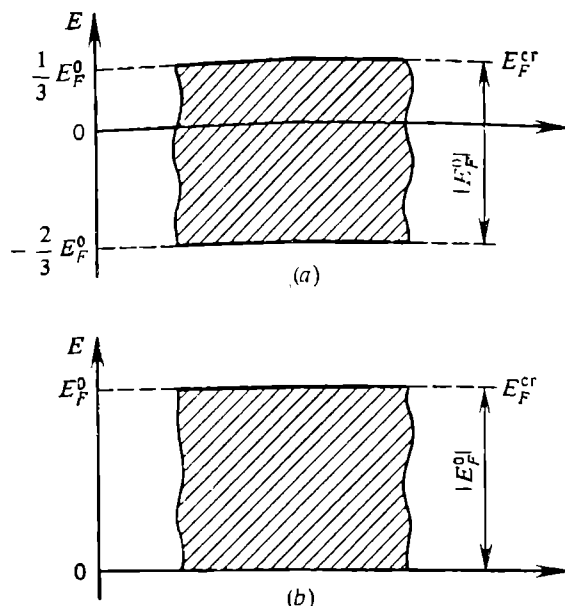


Fig. 3.9. The shift of an NFE band by the average value of the crystal potential—(a) linear screening potential, (b) minimum perturbation potential.

The LSP model is thus described by Eqs. (3.90), (3.93) and (3.95); the total number of electrons scattered by this potential is Z .

3.5.3. Minimum perturbation potential. If the valency of an ion immersed in an electron gas is $Z^* < Z$, it is intuitively clear that the perturbation caused by the ion will be weaker than that caused by an ion with valency Z . This may be seen from Eq. (3.92). Since the Friedel sum is Z^* , the ratio \mathcal{F}/Z is less than unity, i.e., the magnitude of the average value of the screened pseudopotential is less.

It is clear that the minimum perturbation will come from a pseudopotential with a zero Friedel sum

$$\mathcal{F}(E_F^{cr}) = 0, \quad (3.96)$$

i.e., with the zero average crystal potential. From (3.92) and (3.96) it follows that

$$\lim_{q \rightarrow 0} \langle \mathbf{k} + \mathbf{q} | W^{cr} | \mathbf{k} \rangle = 0. \quad (3.97)$$

In this case the Fermi energy of the crystal equals that of the free electron gas (see Fig. 3.9b):

$$E_F^{\text{cr}} = E_F^0. \quad (3.98)$$

The physical meaning of such a pseudopotential is simple: the entity we have placed in the electron gas is a neutral atom and not an ion. The neutral atom already has all the electrons needed to screen the nucleus and so will not borrow them from its surroundings.

For scattering on this potential the phase shifts may be either negative or positive, that is, electrons may either be repelled or attracted by it. The total number of electrons displaced by the potential is, by (3.96), zero which means that, on the average the potential described by (3.96)-(3.98) does not cause a perturbation in the electron gas. Hence its name, the minimum perturbation potential (MPP) [291-293].

Note that in the dielectric screening scheme there can be no MPP for a Heine-Abarenkov type pseudopotential (see Sec. 3.2). The reason is that at small q the dielectric function behaves like q^{-2} so that (3.97) can only be satisfied if the formfactor of a non-screened potential decreases as $q^{-(2+\delta)}$, δ being positive. But, as can easily be seen from (3.44), for a Heine-Abarenkov pseudopotential $\delta = 0$, that is, in dielectric screening theory any such potential is always a linearly screened one.

In the *additive* scheme, an MPP is even possible for a Heine-Abarenkov pseudopotential. For example, by screening this latter with (3.67), we obtain from (3.69) that the well depth of the pseudopotential optimized "to the minimum perturbation" is

$$\tilde{A}_{\text{MP}} = \frac{6}{5} A_S. \quad (3.99)$$

A pseudoatom corresponding to such a pseudopotential will be an MT and MP potential simultaneously.

As pointed out earlier, an MT potential is not by any means a minimum perturbation one. An MPP is a scatterer that has all the "necessary" electrons, i.e. has a zero Friedel sum. There is no requirement that all these electrons be concentrated in the Wigner-Seitz cell. In contrast to the electron density of the MT potential, the MPP electron density may extend to infinity because of its Friedel oscillations, which are absent, by definition, both in the MT potential itself and the charge density around it.

A word should be said about the convergence of the perturbation theory series. For a pseudopotential having no bound states, we saw in Sec. 2.4 that by (2.118) the convergence depends on the average value of the pseudopotential. It is clear that an MPP will ensure better perturbation series convergence than will an LSP. It is possible that optimization to minimum perturbation is stronger than that to

electroneutrality. The additive screening theory must then have certain advantages over dielectric screening. Formula (3.99) is a special case of such an optimized pseudopotential.

Certainly, the minimum perturbation criterion is not the final word in the analysis of perturbation theory convergence. We saw in Sec. 3.2 that in this analysis the possibility should be taken into account that the crystal potential made up of single-site potentials may be weaker than each of the single-site potentials taken alone. It would be wrong, therefore, to argue that from the viewpoint of convergence an LSP will always be inferior to an MPP.

3.5.4. Friedel sums. The next question to be discussed is the meaning of a Friedel sum.

The Friedel sum for a given potential may be viewed as a condition determining the Fermi energy of a crystal in which the potential will act as an ion having a given valency Z' . To see this, let us demand that the number of electrons needed for screening the ion (i.e., the Friedel sum \mathcal{F}) be Z' :

$$\mathcal{F}(E_F^{\text{cr}}) = Z'. \quad (3.100)$$

The scattering phase shifts for a given potential and the corresponding Friedel sums should be calculated for different energies, starting from $E = 0$ and then moving to increasingly higher energies. The energy satisfying (3.100) will be the desired Fermi energy.

Let us invert the problem. An ion of valency Z is placed in a crystal whose Fermi energy E_F^{cr} is characteristic of another valency. What is the Friedel sum?

We transform Eq. (3.94) to

$$\mathcal{F}(E_F^{\text{cr}}) = -\frac{Z}{2/3 E_F^0} (E_F^{\text{cr}} - E_F^0). \quad (3.101)$$

From Eqs. (3.101), (3.93) and (3.96) it follows that a given value of E_F^{cr} specifies a potential-screening model. If $E_F^{\text{cr}} = E_F^0$, Eq. (3.101) gives $\mathcal{F}(E_F^{\text{cr}}) = 0$, that is, the potentials in the crystal have been chosen in such a way that their average values are zero. If $E_F^{\text{cr}} = (1/3) E_F^0$, then $\mathcal{F}(E_F^{\text{cr}}) = Z$ showing that the average values satisfy the rules of linear dielectric screening.

It follows that specifying the Fermi energy of the crystal fixes the position of the free-electron band bottom relative to the vacuum zero: the lower E_F^{cr} , the deeper the band bottom (cf. Fig. 3.9). But this position is determined by the average value of the crystal potential, which determines the background, as it were, against which all the scattering processes evolve. Depending on the properties of the background, the pseudopotential may appear as either an ion

of valency Z or a neutral atom. It makes no sense to ask for the value of the Friedel sum unless the characteristics of the background are known.

We thus come to the extremely important concept, namely, the effective medium surrounding the scatterer.

In the theory of dielectric linear screening, the effective medium is simply a Sommerfeld gas. In the construction of an MPP (i.e., in the additive screening scheme) characteristics of the effective-medium have already been optimized somehow. In Secs. 4.4 and 5.2 we shall see how an effective medium may be introduced in band-structure calculations. The concept of effective medium is employed in the coherent potential approximation in the theory of alloys. The scattering properties of a pseudopotential depend on the properties of the effective medium. When choosing a pseudopotential it is necessary to take account of the effective medium it will be placed in.

Expression (3.101) can also be derived in a somewhat different manner. The Friedel sum represents the number of electrons withdrawn, as it were, by the scatterer from the stream of *free* electrons. Let Z be the number of electrons (per unit volume) in a crystal without the scatterer and Z^{cr} be the effective number of free electrons after the scatterer has been introduced. Assuming the equipotential surfaces in the crystal are spherical, we can write

$$Z = \frac{\Omega_0}{3\pi^2} (E_F^0)^{3/2}, \quad Z^{\text{cr}} = \frac{\Omega_0}{3\pi^2} (E_F^{\text{cr}})^{3/2}$$

which gives

$$\mathcal{F} (E_F^{\text{cr}}) = Z (1 - (E_F^{\text{cr}}/E_F^0)^{3/2}). \quad (3.102)$$

This expression is due to Lee [294]. It shows that at $E_F^{\text{cr}} = E_F^0$, $\mathcal{F} = 0$ as in the linear formula (3.101) so that for an MPP the two approaches agree with each other. With an LSP, however, they do not: by (3.102), $\mathcal{F} = Z$ only for $E_F^{\text{cr}} = 0$ and not for $E_F^{\text{cr}} = (1/3) E_F^0$. If, formally, we assume \mathcal{F}/Z to be small, then

$$E_F^{\text{cr}} = E_F^0 \left(1 - \frac{\mathcal{F}}{Z} \right)^{2/3} \approx E_F^0 \left(1 - \frac{2}{3} \frac{\mathcal{F}}{Z} \right),$$

which leads to Eq. (3.101) [294]. Which of (3.101) or (3.102) is more correct may only be shown by an experiment (note though that a direct comparison is impossible). The choice may be essential if the formulae are considered as optimization criteria.

3.5.5. Charge flow in alloys. We can apply Eq. (3.92) to the study of charge flow in alloys. From (3.92) we have

$$\bar{W}^{\text{all}} = - \frac{2}{3} E_F^{0,\text{all}} \frac{\mathcal{F}^{\text{all}}}{\bar{Z}}, \quad (3.103)$$

where \bar{Z} and $E_F^{0,\text{all}}$ are given by (3.60) and (3.61) respectively.

Using the smallness of Born approximation scattering phases, the Friedel sum may be rewritten as follows:

$$\begin{aligned}\mathcal{F}^{\text{all}} &\approx \frac{2}{\pi} \sum_l (2l+1) \tan \eta_l^{\text{B}} \\ &= -k_F^{\text{all}} \frac{2}{\pi} \sum_l (2l+1) \int W^{\text{all}}(r) j_l^2(k_F^{\text{all}} r) r^2 dr \\ &= c_A \mathcal{F}_A^{\text{all}} + c_B \mathcal{F}_B^{\text{all}}.\end{aligned}\quad (3.104)$$

Here we have introduced Friedel sums for the screened alloy pseudopotentials:

$$\begin{aligned}\mathcal{F}_{A(B)}^{\text{all}} &= \frac{2}{\pi} \sum_l (2l+1) \eta_l^{A(B), \text{all}}, \\ \tan \eta_l^{A(B), \text{all}} &= -k_F^{\text{all}} \int W_{A(B)}^{\text{all}}(r) j_l^2(k_F^{\text{all}} r) r^2 dr.\end{aligned}\quad (3.105)$$

The above Friedel sums differ from those of the pure components in that the dielectric function used for screening the pseudopotential $W_{A(B)}^{\text{all}}$ in (3.105) is that of the alloy rather than that of a pure component. It may be said that $\mathcal{F}_A^{\text{all}}$ ($\mathcal{F}_B^{\text{all}}$) correspond to the charge possessed by the A (B) pseudoatom in the alloy. Thus, the charge flow is given by

$$\Delta Q = \mathcal{F}_A^{\text{all}} - \mathcal{F}_B^{\text{all}}. \quad (3.106)$$

By the same argument,

$$\overline{W_{A(B)}^{\text{all}}} = -\frac{2}{3} E_F^{0, \text{all}} \frac{\mathcal{F}_{A(B)}^{\text{all}}}{\overline{Z}}. \quad (3.107)$$

Multiplying (3.107) by c_A (c_B) and adding the results together we come to Eq. (3.103), which means that Eqs. (3.103)-(3.107) are consistent with each other. Using Eqs. (3.106) and (3.107) we find the difference between the average values of the screened crystal pseudopotentials:

$$\overline{W_A^{\text{all}}} - \overline{W_B^{\text{all}}} = -\frac{2}{3} \overline{E_F^{0, \text{all}}} \frac{\Delta Q}{\overline{Z}}. \quad (3.108)$$

We have thus proved a theorem relating the difference between the average values of a crystal pseudopotential to the magnitude of the charge flow.

When applied to screen an impurity potential in the atom's sphere model (3.108) indicates that the potential is shifted as a whole by

$$\Delta U_0 = \frac{2}{3} \left(\frac{9\pi}{4} \right)^{2/3} \frac{\Delta Q}{R_a^2 \overline{Z}^{1/3}}. \quad (3.109)$$

The result would be different had we distributed the charge ΔQ uniformly over the surface of a sphere of radius R_a and then applied the Gauss theorem.

The impurity potential shift as a means to include screening has been used in order to calculate the physical properties of aluminium and copper [295-300] with low impurity concentrations. In these investigations the MT potential of the impurity was shifted up or down until the Friedel sum computed for the MT sphere coincided with the valency difference between the host and impurity atoms. It was assumed both that the impurity atoms must retrieve their valence electrons and that all the electrons would be contained in the MT sphere, that is, there would be no electrons between the surfaces of the MT and the atomic spheres. Nevertheless, the results turned out to be in good qualitative (and often quantitative) agreement with experiment, and this even for transition metal impurities. A possible explanation is that the requirement for the Friedel sum to correspond to valency is a very strong optimization condition for an impurity potential. To a certain degree, formulae (3.108) and (3.109) are a justification for the above procedure of shifting the impurity potential as a whole.

Note that although the above optimization to the Wigner-Seitz cell "non-neutrality" has emerged within pseudopotential theory, it is not actually used in pseudopotential alloy calculations.

Theory of pseudopotential formfactors

4.1. Nonlocality, the energy dependence of formfactors and perturbation theory

The topic of this section is the dependence of formfactors on two main variables, the energy E and the momentum transfer vector \mathbf{q} . These are not entirely separable in this context and must therefore be considered together.

4.1.1. \mathbf{q} -Dependence of formfactor. A pseudopotential $W(\mathbf{r})$ is usually called nonlocal if its formfactor $\langle \mathbf{k}' | W | \mathbf{k} \rangle$ depends both on the vector difference $\mathbf{k}' - \mathbf{k}$ (i.e., on the momentum transfer vector $\mathbf{q} = \mathbf{k}' - \mathbf{k}$) and on the vector \mathbf{k} itself. Nonlocality arises when the pseudopotential, unlike the original crystal potential $V(\mathbf{r})$, is not a multiplication operator. In other words, a pseudopotential is nonlocal if it does not commute with $\exp(i\mathbf{k}\mathbf{r})$.

This may be seen by noting that for a local pseudopotential W

$$\begin{aligned} \langle \mathbf{k}' | W | \mathbf{k} \rangle &\equiv \frac{1}{\Omega_0} \int e^{-i\mathbf{k}'\mathbf{r}} W(\mathbf{r}) e^{i\mathbf{k}\mathbf{r}} d^3r \\ &\equiv \frac{1}{\Omega_0} \int W(\mathbf{r}) e^{-i(\mathbf{k}' - \mathbf{k})\mathbf{r}} d^3r \equiv W(\mathbf{k}' - \mathbf{k}). \end{aligned} \quad (4.1)$$

For a spherically symmetrical pseudopotential, the formfactor depends solely on $|\mathbf{k}' - \mathbf{k}|$ and not on the angles between the vector $\mathbf{k}' - \mathbf{k}$ and the coordinate axes.

For a nonlocal pseudopotential involving, for example, projection operators, we have

$$\begin{aligned} &\langle \mathbf{k}' | \sum_l W_l(\mathbf{r}) \hat{P}_l | \mathbf{k} \rangle \\ &\equiv \frac{4\pi}{\Omega_0} \int e^{-i\mathbf{k}'\mathbf{r}} \sum_l W_l(\mathbf{r}) j_l(kr) Y_L(\mathbf{k}) Y_L(\mathbf{r}) d^3r \\ &= \frac{4\pi}{\Omega_0} \sum_l (2l+1) \left[\int_0^\infty j_l(k'r) W_l(r) j_l(kr) r^2 dr \right] P_l(\cos \Theta_{\mathbf{k}, \mathbf{k}'}). \end{aligned} \quad (4.2)$$

This formfactor depends on both the vectors \mathbf{k} and \mathbf{k}' . It can be shown from Eq. (2.34) that the formfactor also depends on $\mathbf{q} = \mathbf{k}' - \mathbf{k}$

and \mathbf{k} . Either way, there are two vectors the formfactor depends on.

A nonlocal formfactor is extremely inconvenient to work with because for any given pair of \mathbf{k} and \mathbf{q} the functions that must be calculated are rather complicated. To avoid this, the formfactor's dependence on \mathbf{k} and \mathbf{q} is usually simplified. To see the meaning of these simplifications it is worthwhile examining the dependence $W(\mathbf{q})$.

Consider the scattering-theory simple-metal formfactor (2.172). Since $V(\mathbf{r})$ is a multiplication operator, the first term is local. The \mathbf{q} -dependence in the second term is determined by the factors $\langle \mathbf{k} + \mathbf{q} | \alpha \rangle$, which require the explicit form of core orbitals ϕ_α to be evaluated. Taking Slater orbitals [14]

$$\phi_\alpha = N_\alpha \exp(-ar) \quad (4.3)$$

and employing the same device used to evaluate (1.25) we have

$$\begin{aligned} \langle \mathbf{k} + \mathbf{q} | \alpha \rangle &= \frac{N_\alpha}{\Omega_0} \int e^{-i(\mathbf{k}+\mathbf{q})\mathbf{r}} e^{-ar} d^3r \\ &= \frac{2\pi N_\alpha}{\Omega_0} \int_0^\infty \int_{-1}^1 e^{-ar} e^{-i|\mathbf{k}+\mathbf{q}||\mathbf{r}|\cos\Theta} r^2 dr d(\cos\Theta) \\ &= -8\pi a N_\alpha \Omega_0^{-1} [(\mathbf{k} + \mathbf{q})^2 + a^2]^{-2}. \end{aligned} \quad (4.4)$$

Thus the second term in (2.172) falls off as q^{-4} whereas the original-potential formfactor does not decrease faster than q^{-2} . Then, the simple-metal formfactor as a whole falls off like q^{-2} .

Turning now to the formfactor of a transition metal, (2.170), we observe that its \mathbf{q} dependence comes through the factors $\langle \mathbf{k} + \mathbf{q} | V | \alpha \rangle$. These can be estimated by assuming that $V(\mathbf{r})$ is a purely Coulomb potential. By (1.25) we find

$$\begin{aligned} \langle \mathbf{k} + \mathbf{q} | V | \alpha \rangle &= -\frac{Ze^2 N_\alpha}{\Omega_0} \int e^{-i(\mathbf{k}+\mathbf{q})\mathbf{r}} \frac{1}{r} e^{-ar} d^3r \\ &= -4\pi Ze^2 N_\alpha \Omega_0^{-1} [(\mathbf{k} + \mathbf{q})^2 + a^2]^{-1}, \end{aligned} \quad (4.5)$$

that is, the "compensatory" addition to the potential (the second term in (2.170)) decreases as q^{-2} and hence slower than that for the simple metals. As a whole, however, the transition metal formfactor decreases like q^{-2} , that is, exactly like its simple-metal counterpart.

We can see from (4.4) and (4.5) how the formfactor depends on $\Theta_{\mathbf{k},\mathbf{k}'}$, the angle between \mathbf{k} and $\mathbf{k}' = \mathbf{k} + \mathbf{q}$ (see Fig. 4.1).

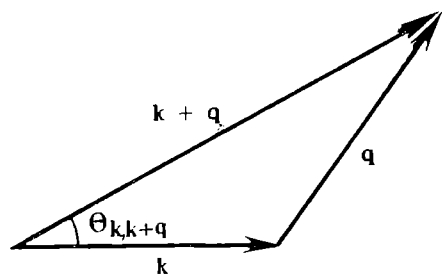
Consider the two limiting cases $\Theta_{\mathbf{k},\mathbf{k}'} = 0$ and $\Theta_{\mathbf{k},\mathbf{k}'} = \pi$ for forward and backward scattering respectively. It can be seen that while for forward scattering the quantity $[(\mathbf{k} + \mathbf{q})^2 + a^2]^{-1}$ decreases monotonically with $|\mathbf{q}|$, for backward scattering it has a maximum at

$\mathbf{q} = -\mathbf{k}$, i.e., it first increases with $|\mathbf{q}|$. It follows that in the backward scattering case the second terms in (2.170) and (2.172) increase with $|\mathbf{q}|$, so that at small $|\mathbf{q}|$ the compensation of the original potential is better than it is for forward scattering. The point \mathbf{q}_0 where the terms in (2.170) and (2.172) cancel out, is determined by

$$\langle \mathbf{k} + \mathbf{q}_0 | W | \mathbf{k} \rangle = 0. \quad (4.6)$$

It is clear that for backward scattering \mathbf{q}_0 is nearer to the origin than it is for forward scattering. The backward scattering formfactor may thus be thought of as being closer to the origin

Fig. 4.1. Relative positions of the vectors \mathbf{k} , \mathbf{q} , and $\mathbf{k} + \mathbf{q}$.



than the forward scattering formfactor (see Fig. 4.2).

Note that when calculating the band-structure energy (1.36) the backward scattering formfactor is more important than the forward

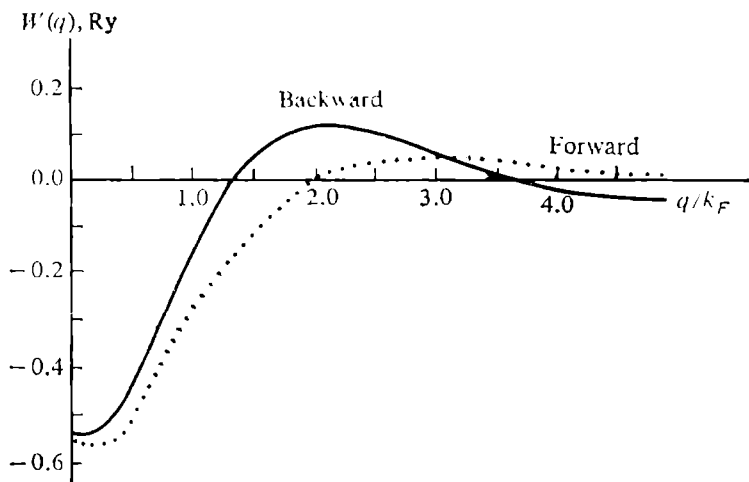


Fig. 4.2. Forward- and backward-scattering formfactors of Al. From Harrison [73].

scattering one. The reason is that the relevant second order perturbation theory denominators in (1.31) are small for backward scattering. In particular, the Bragg reflection condition corresponds to backward scattering, which means that singularities in (1.31) occur at momenta given by $q = -2k_F$. The specific value the formfactor assumes at a Brillouin zone face (i.e., the value of the backward scattering formfactor) determines the applicability of the Rayleigh-Schrödinger expansion (see Chapter 1), the magnitude of the cohesion energy, and whether the crystal will be a metal or a dielectric.

The forward scattering formfactor is also important, and is used, for example, when the total scattering cross-section for a given atom is determined by the optics theorem [7, 39].

Since a rigorous local formfactor is impossible to obtain, artificial methods must be employed to eliminate the non-locality. For example, a quasi-local formfactor can be approximated for backward

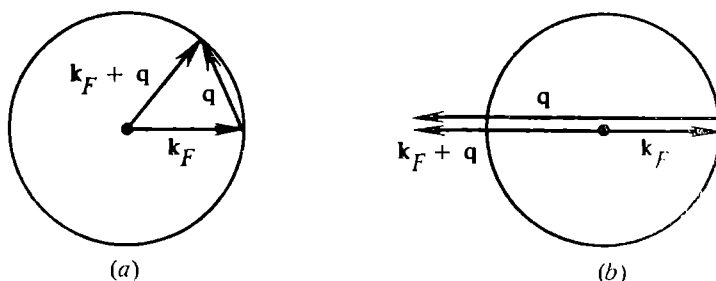


Fig. 4.3. Illustration to the Fermi-sphere approximation.

scattering or for some other (than π) empirically chosen scattering angle. This approximation is rarely seen, however. The most widely used is the following one [13, 73, 17].

It is assumed that the Fermi-energy electrons play the dominant role in a crystal. Accordingly, the wave vector \mathbf{k} in the formfactor is taken to be \mathbf{k}_F . It is further assumed that at small $|\mathbf{q}|$ the magnitude of the wave vector is conserved in a scattering process and it is only the direction of the vector $\mathbf{k}' = \mathbf{k} + \mathbf{q}$ that changes (\mathbf{k}' , as it were, “turns away” from \mathbf{k} , see Fig. 4.3a). When \mathbf{k}' is antiparallel to the original vector \mathbf{k} , there is no word of further “turning away” and what the vector \mathbf{k}' is left to do is to increase its magnitude at a fixed scattering angle. Clearly we are dealing here with backward scattering (Fig. 4.3b).

Mathematically, this approximation may be written as

$$\begin{aligned} q \leq 2k_F: |\mathbf{k}_F + \mathbf{q}| &= |\mathbf{k}_F|, \quad \cos \Theta_{\mathbf{k}, \mathbf{k}+\mathbf{q}} = 1 - 0.5 (q/k_F)^2, \\ q \geq 2k_F: |\mathbf{k}_F + \mathbf{q}| &= |q| - |\mathbf{k}_F|, \quad \cos \Theta_{\mathbf{k}, \mathbf{k}+\mathbf{q}} = -1. \end{aligned} \quad (4.7)$$

This scheme, usually called the “Fermi sphere” or quasi-local approximation, can be applied to any formfactor.

4.1.2. The linear E -dependence of the formfactor. We now turn our attention to how the formfactor depends on energy.

We saw in Chapter 2 that a pseudopotential that replaces a true potential is energy-dependent. This, of course, causes some difficulty when calculating the total energy by (1.36). To obtain this quantity we must add together the energies of all the occupied states. This is easily done if the energies are related analytically to the quantum numbers of their respective states or, in other words, if the explicit

form of the dispersion law $E(\mathbf{k})$ is known. If, however, the pseudopotential formfactor is energy-dependent, expression (1.31) becomes a nonlinear equation for E , the explicit form of the dispersion law is lost and the right-hand side of (1.31) cannot be integrated over \mathbf{k} .

A similar difficulty was encountered in Chapter 1 in the discussion of the NFE model. We saw there that a more correct expression for the dispersion law is given by (1.30) with energy-dependent denominators. Now it turns out that the numerators are energy-dependent too!

It can be seen from (2.170) and (2.171) for the scattering theory formfactor that the formfactor may depend on energy either linearly or it may have poles. Since a zero in the denominator in (2.170) is also a pole singularity, it is appropriate that the singularities in (1.30) be considered together.

We start with simple metals and hence with formfactors linear in energy. In a simple metal the Fermi surface does not touch a Brillouin zone face, so there is no fear of singularities at $\mathbf{k}_F^2 = \epsilon_n$ and the Rayleigh-Schrödinger perturbation theory is applicable.

It is worthwhile noting here that in the case of simple metals the following way of reasoning is possible [73]. Energy E enters the formfactor in combination with large quantities E_α , which are of the order of tens of rydbergs, whereas in the conduction band E is typically no more than half a rydberg. But then even a rough approximation for $E(\mathbf{k})$ will do because against the background of E_α it will not introduce any perceptible error. Let us discuss the validity of this argument.

Consider the second term in (2.172). The following transformation is identical (cf. (2.162)):

$$\begin{aligned} E_\alpha \langle \alpha | \mathbf{k} \rangle &= \langle \alpha | E_\alpha | \mathbf{k} \rangle = \langle \mathbf{k} | -\nabla^2 + V(\mathbf{r}) | \alpha \rangle^* \\ &= \langle \alpha | -\nabla^2 + V(\mathbf{r}) | \mathbf{k} \rangle = k^2 \langle \alpha | \mathbf{k} \rangle + \langle \alpha | V | \mathbf{k} \rangle. \end{aligned} \quad (4.8)$$

When substituted in (2.172) this yields

$$\begin{aligned} \langle \mathbf{k} + \mathbf{q} | W | \mathbf{k} \rangle &= \langle \mathbf{k} + \mathbf{q} | V | \mathbf{k} \rangle \\ &- \sum_{\alpha} [(\mathbf{k}^2 - E) \langle \mathbf{k} + \mathbf{q} | \alpha \rangle \langle \alpha | \mathbf{k} \rangle + \langle \mathbf{k} + \mathbf{q} | \alpha \rangle \langle \alpha | V | \mathbf{k} \rangle]. \end{aligned} \quad (4.9)$$

Within the ion core (i.e., for $r < R_c$, here R_c is the core radius) the wave functions Φ_α form a complete set. Hence

$$\sum_{\alpha} \Phi_{\alpha}(\mathbf{r}) \Phi_{\alpha}^*(\mathbf{r}') = \delta(\mathbf{r} - \mathbf{r}') \Theta(R_c - r) \Theta(R_c - r'),$$

where $\Theta(R_c - r)$ is the Heaviside step function (1 for $r < R_c$ and 0 for $r > R_c$), which takes care of the fact that for $r > R_c$ the core functions vanish.

As a result, we get (noting that $1 - \Theta(x) = \Theta(-x)$)

$$\langle \mathbf{k} + \mathbf{q} | W | \mathbf{k} \rangle = \langle \mathbf{k} + \mathbf{q} | V | (\mathbf{r}) \Theta(r - R_c) | \mathbf{k} \rangle - \frac{4\pi R_c^2}{\Omega_0} (\mathbf{k}^2 - E) \frac{j_1(qR_c)}{q}. \quad (4.10)$$

The formfactor thus contains two contributions: (i) the integral of the potential over the outside region (where the potential is relatively low) and (ii) the oscillatory addition term whose amplitude is determined by the departure of E from \mathbf{k}^2 (rather than from E_α). The quantities E and \mathbf{k}^2 are of the same order of magnitude and small errors in the energy are therefore not as harmless as might at first seem.

Note that the first term in (4.10) corresponds to the potential with the core region removed.

It follows from (2.29) that at large q the second term in (4.10) falls off like q^{-2} .

Note also that the formfactor (4.10) is nearly local at least in the sense that it does not depend on the direction of the vector \mathbf{k} (the energy dependence still remains). Let us assume a first-order dispersion law

$$E^{(1)}(\mathbf{k}) = \mathbf{k}^2 + \langle \mathbf{k} | W | \mathbf{k} \rangle \quad (4.11)$$

with the same pseudopotential as used in (4.10). Substituting (4.11) in (4.10) we find after a little manipulation that

$$\langle \mathbf{k} + \mathbf{q} | W | \mathbf{k} \rangle = \frac{\langle \mathbf{k} + \mathbf{q} | V(r) \Theta(r - R_c) | \mathbf{k} \rangle}{1 - \frac{4\pi R_c^2}{\Omega_0} \frac{j_1(qR_c)}{q}}. \quad (4.12)$$

We have derived a Hermitian local *energy-independent* formfactor and all our problems thus seem to have been rigorously solved. Or have they?

Not entirely, because we made a very important approximation, namely, that the core wave functions are well localized. This is true for simple metals but it is not true, for example, for the noble metals where even free-atom d electron wave functions are poorly localized (equation (2.172) does not apply at all to the transition metals). A direct calculation (see Sec. 3.4.8) shows that the d electrons are not localized in the core region, so much so that some 2 to 2.5% of the atomic d electrons (that is, 0.2-0.25 of an electron) lie even outside a Wigner-Seitz sphere drawn around a noble metal atom. The localization boundary for the d electrons is thus very blurred. This suggests that we need two core radii for the noble metals, one for the ordinary core and the other for the d electron core. We might then hope to obtain a local energy-independent pseu-

dopotential of the type (4.12) for these metals. Local model pseudopotentials have indeed been constructed for the noble metals.

Were the original potential taken (in the spirit of the NFE model) in a purely Coulomb form, i.e., $-Ze^2/r$ (Z being the valency), equation (4.12) would describe a one-parameter model pseudopotential that ought to be called a modified Ashcroft pseudopotential* because its formfactor is

$$\langle \mathbf{k} + \mathbf{q} | W | \mathbf{k} \rangle = -\frac{4\pi Ze^2}{\Omega_0 q^2} \frac{\cos(qR_c)}{1 - \frac{4\pi R_c^2}{\Omega_0} \frac{j_1(qR_c)}{q}}. \quad (4.13)$$

Were the energy dependence of the formfactor approximated by a zeroth (instead of a first) order of perturbation theory, the second term in (4.10) would go to zero and the denominator in (4.13) would be unity. The formfactor would thus become a simpler function of q and (4.13) would represent the formfactor of the ordinary Ashcroft pseudopotential.

This simple example thus demonstrates that modeling the E dependence of the formfactor may modify its dependence on \mathbf{q} . This modification would be most significant for small \mathbf{q} , which are very important in the study of disordered systems.

We have thus considered the modeling of the formfactor's energy dependence. Note that with simple metals there is no need to eliminate this energy dependence, provided it is linear and the dispersion law is accurate to second order. This may be seen by noting that the formfactor (2.172) can be rewritten as

$$W(\mathbf{q}) = a(\mathbf{q}) + Eb(\mathbf{q}), \quad (4.14)$$

where the functions a and b are E -independent. Substituting (4.14) in (1.31) yields a quadratic equation for E , whose solution is

$$E_{\pm} = \frac{-1 + b(0) - B}{2C} \pm \frac{1}{2C} \sqrt{(1 - b(0) + B)^2 + 4C(k^2 + a(0) - A)}, \quad (4.15)$$

where

$$A = \sum_n \frac{|a(g_n)|^2}{\epsilon_n - k^2}, \quad B = \sum_n \frac{a(g_n) b^*(g_n) + \text{compl. conjugate}}{\epsilon_n - k^2},$$

$$C = \sum_n \frac{|b(g_n)|^2}{\epsilon_n - k^2}. \quad (4.16)$$

The integration of (4.15) over \mathbf{k} is only slightly more complicated computationally than integrating the original expression (1.31), while the accuracy may be greatly improved.

* The ordinary Ashcroft pseudopotential is discussed in Sec. 3.2.5. Its formfactor is obtained from (3.44) by setting $A = 0$.

Equation (4.15) has the same form as the solution for the two-band model discussed in Chapter 1 (Eq. (1.14)). However, while in that model the dispersion-law "splitting" occurred about the "average level" $(\mathbf{k}^2 + (\mathbf{k} + \mathbf{g}_n)^2)/2$, in the present case the \mathbf{k}^2 term is under a radical and the average level is $(-1 + b(0) - B)/(2C)$. In this expression, it is impossible to separate out a parabolic \mathbf{k} dependence which is characteristic of the nearly free electron model.

Equation (4.15) is now reminiscent of the dispersion law splitting that occurs in the LCAO model (devised for narrow bands). The inclusion of the formfactor's energy dependence thus makes an NFE model look like an LCAO model and the stronger the dependence, the more so. In the limiting case of a resonant E dependence, narrow bands of the LCAO type will appear.

The effect of the formfactor's energy dependence on the band width may also be seen from (2.172). It follows from (4.4) and (4.5) that the sum of the orthogonalization coefficients must be positive, that is, relative to the attractive potential, the term $\sum_{\alpha} E_{\alpha} \langle \mathbf{k} + \mathbf{q} | \alpha \rangle \times \langle \alpha | \mathbf{k} \rangle$ is compensatory in that if added to the original potential's formfactor it decreases this latter. If E is approximated by its maximum possible value, the crystal's Fermi energy E_F^{cr} , it is clear that there will be too much compensation and so the formfactor will be underestimated. In the NFE model reducing the perturbation makes the allowed bands wider while increasing it (i.e., using energies lower than E_F^{cr}) narrows the bands, as we would expect.

To sum up, an energy-independent formfactor (in the "Fermi surface" approximation) must lead to wider bands than those generated with an energy-dependent formfactor with different contributions for different conduction band states.

4.1.3. The "repelled" solutions. The next topic to be discussed is singular energy dependence. We start from the zero denominators of second-order perturbation theory. We rewrite (1.30) to read

$$E = E^{(1)}(\mathbf{k}) - \sum_n \frac{B_n}{\varepsilon_n - E}, \quad (4.17)$$

where $E^{(1)}$ is defined by (4.11) and

$$B_n = |\langle \mathbf{k} + \mathbf{g}_n | W | \mathbf{k} \rangle|^2.$$

We designate the (as yet) unknown solution of (4.17) as E_x . Suppose E_x is near ε_m , then the dominant term in (4.17) is the one with $n = m$ and so we have

$$E_{\pm} = \frac{E^{(1)} + \varepsilon_m \pm \sqrt{(\varepsilon_m - E^{(1)})^2 + 4B_m}}{2}. \quad (4.18)$$

If the pseudopotential is such that $E^{(1)} = \varepsilon_m$, then $E_{\pm} = \varepsilon_m \pm |B_m|$ showing that we meet again the effect of removing degeneracy discussed in the Introduction, Section 5, in terms of the two-band secular equation. Equation (4.17) corresponds to many-band model, every n th term in (4.17) gives a correction term to E_x thus preventing it from coinciding with ε_n .

It may be said that perturbation theory pole singularities tend to repel the solutions from the energies corresponding to the poles.

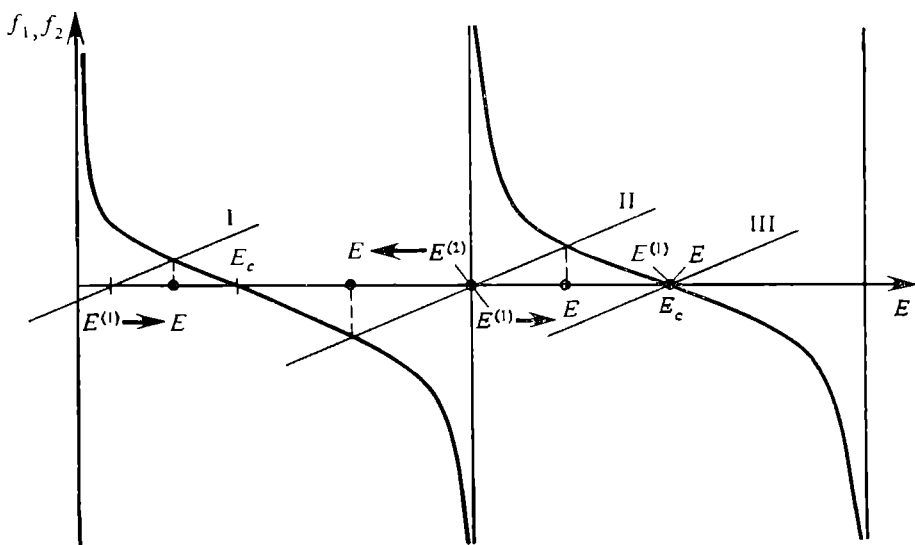


Fig. 4.4. The repulsion effect (cf. Eq. (4.17)).

Denoting $f_1(E) = \sum_n B_n (E - \varepsilon_n)^{-1}$ and $f_2(E) = E - E^{(1)}$, Eq. (4.17) may be rewritten as $f_1(E) = f_2(E)$. This equation is graphically solved in Fig. 4.4. The band solutions for E are given by the intersections of the curves $f_1(E)$ and $f_2(E)$ and are marked by points. Three different initial approximations are shown. (They are not chosen arbitrarily but correspond to different potentials and different points of \mathbf{k} space.) The arrows show how much the band solutions have been repelled from the corresponding first approximation value $E^{(1)}$.

The repulsion effect becomes stronger as the corresponding matrix element increases, and tends to put E_x halfway between the poles corresponding to the energies ε_m and ε_{m+1} . The nearer $E^{(1)}$ is to a particular ε_m , the further the solution is repelled from it, the same being true of the next value ε_{m+1} . Only when $E^{(1)}$ lies halfway between two poles are the effects of ε_m and ε_{m+1} balanced (and $E^{(1)}$ is then a good approximation of E_x). If $E^{(1)}$ coincides with E_c , as defined by $f_1(E_c) = 0$, then there is no repulsion and the band solution coincides with $E^{(1)}$.

We have thus established that electronic energy levels in a crystal are repelled from empty lattice levels.

The band spectra of a series of metals having the same lattice type but different valencies Z (and hence different pseudopotentials) should be similar because the levels of the low- Z metals will be pushed down to the values characteristic of large Z , and the levels of large- Z metals are pushed up to the values characteristic of low Z . The effect of Z is thus "averaged" (as illustrated in Fig. 4.4).

Note that this similarity may also be predicted from group-theoretical considerations.

The repulsion effect explains why band levels at different points of the Brillouin zone have different sensitivities to small variations in the potential. It follows from Fig. 4.4 (see Fig. 4.5) that if $E^{(1)}$ is equidistant between two empty-lattice levels, changing off-diagonal pseudopotential matrix elements will have little effect on the levels whereas for an E_x close to an ϵ_m a similar change will shift the level significantly. To put it another way, the solution is repelled from levels neighboring ϵ_n to levels E_c . When $E^{(1)}$ coincides with E_c , the solution E_x is weakly dependent on changes in the potential. The positions of E_c are different at different points of \mathbf{k} space. Therefore a change in the potential at some points will bring the energy levels down, while it will force them up at others, and in some places the changes will have no effect on the levels. The repulsion effect also explains, for example, why energy levels at different points have different sensitivities to the exchange parameter α , the interatomic distance, the temperature, or impurity concentration.

We thus see that some levels in a band structure are potential-sensitive and some are not and that the positions of these latter are largely determined by the lattice type. We can in principle predict for a given metal, at which \mathbf{k} points the levels will be more sensitive to the potential. This sort of information is very important when analyzing the errors that may occur in fitting a pseudopotential to

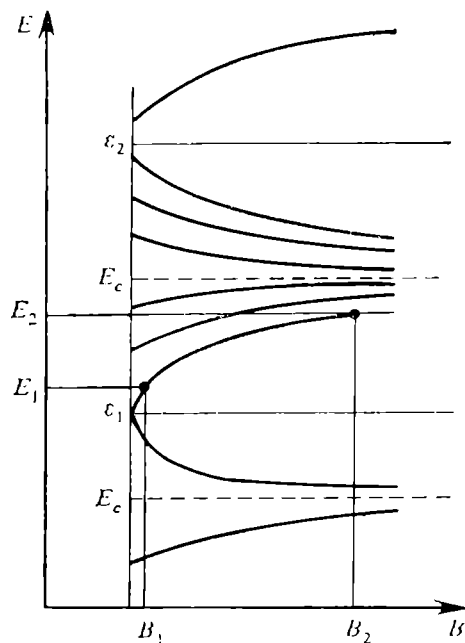


Fig. 4.5. The sensitivity of band solutions E to the change in potential depends on the position of $E^{(1)}$ relative to the energies E_c and the empty-lattice dispersion laws.

experimental band-structure data. If, for example, the fitting involves the energy of an insensitive level, the error may be quite considerable.

Certainly, the repulsion effect is simply a convenient way to illustrate the nature of band-structure formation processes in crystals. Regrettably, such a rearrangement of energy spectrum is ignored in Rayleigh-Schrödinger perturbation theory.

Level repulsion also takes place when there is a quasi-bound state that produces a singularity in the formfactor (2.170), as is the case for the transition metals. The difference is that an interaction with a quasi-bound level is a first-order perturbation theory effect, whereas an interaction with an empty-lattice level is a second-order one.

Moreover, since a quasi-bound state produces a single pole, all of the band states will be repelled from this pole. The repulsion will not be compensated for, for the simple reason that there is nowhere for the compensation to come from.

The important topic which will be always of relevance in handling energy-dependent pseudopotentials is the sign of the energy derivative of the formfactor

$$\frac{d}{dE} \langle \mathbf{k} + \mathbf{q} | W | \mathbf{k} \rangle = - \sum_{\alpha} \frac{\langle \mathbf{k} + \mathbf{q} | V | \alpha \rangle \langle \alpha | V | \mathbf{k} \rangle}{(E_{\alpha} - E)^2} . \quad (4.19)$$

If q tends to zero, the numerator is positive, that is, the right-hand side of (4.19) is negative:

$$\frac{d}{dE} \langle \mathbf{k} + \mathbf{q} | W | \mathbf{k} \rangle < 0. \quad (4.20)$$

If q increases, inequality (4.20) remains true up to very large q values. For a Coulomb potential, it is not violated at all (see (4.5)).

The sign of the derivative, however academic the topic might seem, is of principal importance in pseudopotential theory.

From the scattering theory point of view, the positive numerator in (4.17) corresponds to a positive resonance width for a quasi-bound level or, in the context of Eq. (2.77), to the decay state (when an electron leaves the atom to enter the free-electron pool) [301].

On the other hand, a positive resonance width (negative energy derivative) means that after introducing a quasi-bound level into a continuum, the level will make the continuum levels move apart as shown in Fig. 4.6.* For a negative resonance width (positive ener-

* The figure shows schematically the interaction (hybridization) between the quasi-bound level ε_d and the free electron band k^2 . This interaction can be described by a two-band model (see the Introduction, subsection 5) and results in a complicated dispersion law.

The same scheme explains the interaction between s and d bands in the transition metals. In this case we have a dispersion law $\varepsilon_d(k)$ instead of the level ε_d and the spectrum has no gap similar to that shown in Fig. 4.6.

gy derivative) the continuum levels will merge to the resonance energy. This difference can be most easily seen from (4.18), which in this case takes the form

$$E_{\pm} = \frac{k^2 + E_{\alpha} \pm \sqrt{(k^2 - E_{\alpha})^2 + 4B_{\alpha}}}{2},$$

where B_{α} is the resonance width.

If B_{α} is positive, $|E_+ - E_-| = \sqrt{(k^2 - E_{\alpha})^2 + 4B_{\alpha}} > |k^2 - E_{\alpha}|$ and the continuum levels are pushed apart. For negative B_{α} , $|E_+ - E_-| < |k^2 - E_{\alpha}|$ and the levels converge. In the range $E_{\alpha} - 2\sqrt{|B_{\alpha}|} < k^2 < E_{\alpha} + 2\sqrt{|B_{\alpha}|}$, the energy E_x acquires a complex addition term for negative resonance width, which means that the corresponding states are described by damped functions and are therefore unstable. From the scattering theory point of view a *negative* resonance width corresponds to a trap state, for which an electron is *localized* on the atom. In the NFE model, the binding of atoms into a crystal is due to the delocalization of electrons; their localization on the atoms is tantamount to the collapse of the crystal.

The use of a resonance pseudopotential with a positive energy derivative (negative resonance width) may thus lead to an entirely wrong description of the band structure and hence all the crystal's properties will be incorrectly modeled. It is for this reason that when studying formfactors in the next two sections we shall always be concerned with their energy dependence.

It should be noted that the parameters of the model pseudopotentials currently in use are also energy-dependent. This dependence is described by a resonance formula with a negative resonance width but because of the "Fermi sphere" approximation with $E = E_F$, nothing goes wrong. The sin of fixing the energy thus saves us from a much more serious error.

On the other hand, it is clear that the $E = E_F$ approximation as it stands is only valid for simple metals. For the transition metals, model pseudopotential theory faces a rather awkward choice: the

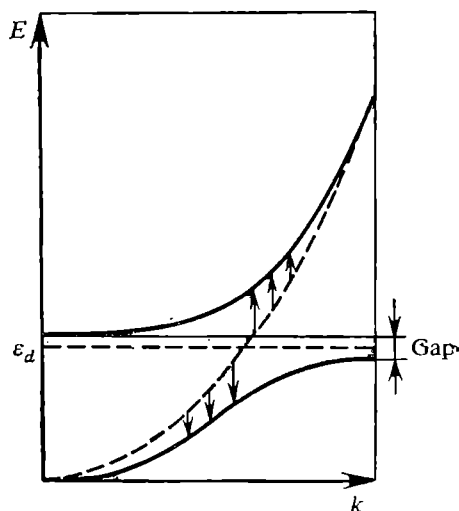


Fig. 4.6. The ε_d level (horizontal dashed line) interacts with the free-electron band (parabolic dashed line) to form the dispersion law shown by the bold line.

“Fermi surface” scheme can neither be used nor, less still, abandoned! In this connection, the reader should refer to [302] for a pseudopotential renormalization procedure which alters the position of a singularity and thus reduces the effect of the “troublesome” energy dependence.

4.2. The OPW formfactor

We now turn to constructing the OPW formfactor, which arises, as the name implies, within the orthogonalized plane wave (OPW) method. First, a brief historical review. In fact, the pseudopotential idea could have been introduced in its present-day form as far back as 1940 when the OPW method was proposed as a tool for band theory studies [303]. This however was done by Phillips and Kleinman only in 1959 [304]. It became clear fairly soon that the OPW pseudopotential method was not useful for the transition metals. In 1965 Ziman [70] modified the Korringa-Kohn-Rostoker (KKR) method which is the Green’s function method adapted for band structure calculations, and in 1967 Heine [305] employed this modification (the KKRZ method) to construct the model Hamiltonian (see Sec. 5.1). Some time later Hubbard [81, 306, 307] discussed the basic principles underlying the model Hamiltonian approach within the scattering theory framework. In 1969 Harrison [308] introduced the transition-metal pseudopotential. That his work is conceptually close to Hubbard’s is only natural if we remember (see Chapter 2) that pseudopotential theory is a special case of scattering theory.

4.2.1. OPW pseudopotential. The construction of an OPW pseudopotential is discussed below following the argument in Harrison’s paper [308] on transition metals, the simple-metal result will then emerge as a special case.

We saw that the transition metals are characterized by having quasi-discrete states. In formfactor language, see Eq. (2.170), this means that the sum over α has contributions from both bound and quasi-bound states, either contribution introducing its own energy dependence. When constructing an OPW pseudopotential, it is necessary that the set of trial functions should contain both types of state.

The function $\Psi_{\mathbf{k}}$ must then be written as

$$\Psi_{\mathbf{k}} = \sum_n B_n |\mathbf{k} + \mathbf{g}_n\rangle + \sum_{\alpha} A_{\alpha} |\alpha\rangle + \sum_d C_d |d\rangle, \quad (4.21)$$

where the first term corresponds to the ordinary NFE plane-wave expansion and the second and third terms describe the interaction with, respectively, the core states $|\alpha\rangle$ and quasi-stationary d states $|d\rangle$.

To actually perform the expansion, the explicit form of these functions is needed. The core orbitals $|\alpha\rangle$ can be represented by free-atom core functions. The crystal potential will move the corresponding levels (the core shift) but leave the wave functions themselves unaltered. In principle, the computational accuracy may be improved by taking these functions in Bloch LCAO combinations. This is the approach actually employed in OPW band calculations using a secular determinant (see [309, 310]).

Throughout the following, $|\alpha\rangle$'s are assumed to be the eigenfunctions of the crystal Hamiltonian because on forming the crystal the core region remains unaltered. The implication is that the core functions of neighboring atoms must not overlap.

As for the $|d\rangle$ functions, we may choose the atomic d orbitals to model them but, since transition-metal d electrons are delocalized (d bands exist), these functions cannot be considered to be eigenfunctions of the crystal Hamiltonian because the potential affecting the d electrons differs from the atomic potential. To take this difference into account, we suppose that the crystal potential V^{cr} may be related to the atomic potential by

$$V^{\text{cr}}(r) = V^{\text{at}}(r) - \delta V. \quad (4.22)$$

It is clear that the effect of the crystal Hamiltonian on the d states may always be written

$$(-\nabla^2 + V^{\text{cr}}(r))|d\rangle = (\epsilon_d - \Delta)|d\rangle, \quad (4.23)$$

where we have separated out an r -independent parameter ϵ_d and introduced an operator Δ . Note that thus far the partition into ϵ_d and Δ is quite arbitrary.

Operating on (4.23) by the function $\langle d|$ (on the left) and using (4.22) gives

$$\epsilon_d = E_d^{\text{at}} - \langle d|\delta V|d\rangle + \langle d|\Delta|d\rangle, \quad (4.24)$$

where E_d^{at} is the atomic d level. For the core states $|\alpha\rangle$ the operator Δ is, by definition, zero and they satisfy (4.24) with d replaced by α . It is then clear, incidentally, that although the atomic core states remain unchanged on forming a crystal, the core levels are displaced, which fact should be taken into account.

We assume that the crystal potential is spherically symmetric in the localization region of the d functions, i.e., d functions with different magnetic quantum numbers do not hybridize, or mathematically (cf. Sec. 2.2)

$$\langle d' | -\nabla^2 + V^{\text{cr}} | d \rangle = \epsilon_d \delta_{d'd}. \quad (4.25)$$

Clearly, $\langle d' | d \rangle = \delta_{d'd}$. From (4.23) we have

$$\langle d' | \Delta | d \rangle = 0.$$

Now we turn to the pseudopotential itself. By analogy with (1.18) we introduce a new function φ , often referred to as the "pseudowave" function. The true wave function Ψ is given by (4.21) while φ is given by the first term in (4.21). We have

$$\varphi = \sum_n B_n |\mathbf{k} + \mathbf{g}_n\rangle. \quad (4.26)$$

Substituting (4.21) in the Schrödinger equation gives

$$\begin{aligned} (-\nabla^2 + V^{\text{cr}})\varphi + \sum_{\alpha} A_{\alpha}(E_{\alpha} - E)|\alpha\rangle \\ + \sum_d C_d(\varepsilon_d - E)|d\rangle - \sum_d C_d \Delta |d\rangle = E\varphi. \end{aligned} \quad (4.27)$$

To evaluate the coefficients A_{α} we multiply (4.27) by $\langle\alpha|$ to obtain

$$E_{\alpha}\langle\alpha|\varphi\rangle + A_{\alpha}(E_{\alpha} - E) - \sum_d C_d\langle\alpha|\Delta|d\rangle = E\langle\alpha|\varphi\rangle,$$

where the Hermiticity of the Hamiltonian and the strong localization of $|\alpha\rangle$ have been used in the first term.

In [308] the operator Δ was assumed to be constant in the ion core region. This is of course an approximation on the shape of the screening potential, but it considerably simplifies the formalism and is quite in the spirit of the MT scheme (see Secs. 3.4 and 3.5). The resulting expression for A_{α} is of the type (2.155):

$$A_{\alpha} = -\langle\alpha|\varphi\rangle. \quad (4.28)$$

In order to evaluate C_d we multiply (4.27) by $\langle d|$. The calculation of the first term requires the assumption of strong d -orbital localization, otherwise a boundary correction term will appear, similar to that occurring in B_{α} in (2.171). This assumption also implies that the d functions of neighboring atoms do not overlap, i.e., the d bands are only formed by the perturbation potential δV acting through the operator Δ . The result is

$$C_d = -\langle d|\varphi\rangle + \frac{\langle d|\Delta|\varphi\rangle}{\varepsilon_d - E}. \quad (4.29)$$

It will be seen that (4.29) corresponds to (2.166) in that both have the same resonant form and the same envelope functions for the perturbation potential matrix elements. This similarity is not removed by the first term in (4.29).

As a result, Eq. (4.27) becomes

$$(-\nabla^2 + \hat{W} + \hat{\mathfrak{B}}_t - E)\varphi = 0, \quad (4.30)$$

where we have introduced the simple-metal pseudopotential \hat{W} and the transition-metal resonance addition \mathfrak{R}_t which are

$$\hat{W} = V^{\text{cr}} - \sum_{\alpha} (E_{\alpha} - E) |\alpha\rangle \langle \alpha| - \sum_d (\varepsilon_d - E) |d\rangle \langle d| + \sum_d (|d\rangle \langle d| \Delta) + \sum_d \Delta |d\rangle \langle d|, \quad (4.31)$$

$$\mathfrak{R}_t = - \sum_d \frac{\Delta |d\rangle \langle d| \Delta}{\varepsilon_d - E}. \quad (4.32)$$

Note that (4.32) coincides with the second term in (2.169).

Consequently, we arrive at expressions for the formfactor of a simple metal (where $\Delta = 0$) and for the resonance part (cf. (2.170) and (2.172)):

$$\begin{aligned} \langle \mathbf{k} + \mathbf{q} | W^{\text{OPW}} | \mathbf{k} \rangle \\ = \langle \mathbf{k} + \mathbf{q} | V^{\text{cr}} | \mathbf{k} \rangle - \sum_{\alpha} (E_{\alpha} - E) \langle \mathbf{k} + \mathbf{q} | \alpha \rangle \langle \alpha | \mathbf{k} \rangle, \end{aligned} \quad (4.33)$$

$$\langle \mathbf{k} + \mathbf{q} | \mathfrak{R}_t | \mathbf{k} \rangle = - \sum_d \frac{\langle \mathbf{k} + \mathbf{q} | \Delta | d \rangle \langle d | \Delta | \mathbf{k} \rangle}{\varepsilon_d - E}. \quad (4.34)$$

Since (4.34) contains a matrix element between the functions $|\mathbf{k}\rangle$ and $|d\rangle$, the term \mathfrak{R}_t is often called the hybridization potential [308, 89]. It should be remembered when constructing the formfactor that \mathfrak{R}_t , like the original ion potential, will act as a scatterer of electrons and its screening must therefore be taken into account.

The pseudopotential (4.33) and (4.34) can be used to calculate the total energy of a nontransition metal whose resonance energy ε_d is far outside the filled part of the conduction band (otherwise the perturbation expansion diverges). Treating \mathfrak{R}_t as a hybridization potential allows us to speak of a hybridization energy. It follows from the discussion of scattering in Chapter 2 that the "hybridization" should be interpreted as the interaction of a quasi-bound d level with the continuum of levels. This is just what this term usually means in the theory of transition metals, i.e., the interaction between a wide nearly-free-electron band and a narrow atom-like one. In terms of the LCAO model, the wide band similar to those in nontransition metals is essentially due to s levels while the narrow band arises from the d levels. The interaction between such two bands may therefore be somewhat loosely termed sd hybridization. The same follows from the scattering theory approach: at low energies the scattering mainly affects (cf. (2.89)) the s component of the incoming wave, that is, the quasi-bound d level is indeed mainly hybridized with s electrons.

Apart from Harrison's paper [308] there are a number of other related works, in particular those by Moriarty [311-316, 181, 182] on

heavy alkali and noble metals. All of them, however, also treat the d orbitals as a separate group, an approach which automatically brings about the resonance form of \mathfrak{B}_t and so leaves one within the Harrison scheme. It is worth mentioning here Ball's idea of an initial background screening of an ion pseudopotential [177] which was employed in [181, 182, 316].

The energy dependence of the OPW formfactor is the same as that of the scattering theory formfactor and does not threaten level merging (see Sec. 4.1.3). Needless to say, the resonance form of the formfactor is an obstacle when using perturbation theory, but as d states are, by assumption, outside the energy region of interest, no convergence problems will arise (the quantity \mathfrak{B}_t is small because the energy denominator is large).

Strictly speaking, the OPW formfactor (4.33), (4.34) has been set up for the noble metals and there is no reason to believe that had we succeeded in constructing a transition-metal formfactor (which is questionable), it would also be of resonance form. In the above case, however, the resonance in the formfactor is actually brought about by quasi-bound states, as is the resonance in the scattering theory formfactor (2.170). Since this also applies to the transition metals, we would suggest that the transition metal OPW formfactor also has a resonance.

That this is indeed true can be proved in a strikingly simple manner, without an intricate analysis like that for Eq. (4.34). The proof involves the secular equation of the crystal band-structure problem (see Chapter 1).

4.2.2. Secular equation and hybridization. The OPW pseudopotential construction was based on the expansion (4.24) of the wave function Ψ in terms of plane waves and atomic orbitals. Since the expansion coefficients for the orbitals were determined from certain additional conditions prior to the calculation, the orbitals were "underprivileged" with respect to the plane waves and, strictly speaking, were not trial functions at all.

Clearly, in order to improve the mathematics the atomic orbitals should be treated on equal footing with the plane waves and their expansion coefficients should be determined by the same computational procedure. The extension of the class of trial functions always improves the accuracy of the method [37, 317].

Let us then take the wave function to be

$$\Psi = \sum_{\mathbf{k}} B_{\mathbf{k}} |\mathbf{k}\rangle + \sum_{\alpha} A_{\alpha} |\alpha\rangle \quad (4.35)$$

in which expression there is no sense in isolating the d orbitals beforehand into a special group: they are included in the sum over α . To unify our notation, the plane waves are labeled by the vectors \mathbf{k} themselves, rather than by the reciprocal lattice vectors \mathbf{g}_n .

We proceed by following the argument of Introduction, Section 5. Inserting (4.35) into the Schrödinger equation gives

$$(H - E) \left[\sum_{\mathbf{k}} B_{\mathbf{k}} |\mathbf{k}\rangle + \sum_{\alpha} A_{\alpha} |\alpha\rangle \right] = 0. \quad (4.36)$$

By multiplying (4.36) by $\langle \mathbf{k}' |$, integrating over \mathbf{r} and using the notation

$$H_{ab} = \langle a | H | b \rangle, \quad S_{ab} = \langle a | b \rangle,$$

where $a, b = \{\mathbf{k}\}, \{\alpha\}$, we get

$$\sum_{\mathbf{k}} (H - ES)_{\mathbf{k}'\mathbf{k}} B_{\mathbf{k}} + \sum_{\alpha} (H - ES)_{\mathbf{k}'\alpha} A_{\alpha} = 0. \quad (4.37a)$$

If we then multiply (4.36) by $\langle \alpha' |$ and integrate over \mathbf{r} we get

$$\sum_{\mathbf{k}} (H - ES)_{\alpha'\mathbf{k}} B_{\mathbf{k}} + \sum_{\alpha} (H - ES)_{\alpha'\alpha} A_{\alpha} = 0. \quad (4.37b)$$

Expression (4.37a) may be written for the $N_{\mathbf{k}}^{\alpha}$ functions $|\mathbf{k}\rangle$, and (4.37b) for the N_{α} functions $|\alpha\rangle$. The total number of equations is equal to the number of unknown coefficients. Equations (4.37a) and (4.37b) thus provide an homogeneous system for the coefficients $\{B_{\mathbf{k}}\}$ and $\{A_{\alpha}\}$. In symbolic form, the system is

$$\begin{pmatrix} (H - ES)_{\mathbf{k}'\mathbf{k}} & (H - ES)_{\mathbf{k}'\alpha} \\ (H - ES)_{\alpha'\mathbf{k}} & (H - ES)_{\alpha'\alpha} \end{pmatrix} \begin{pmatrix} B_{\mathbf{k}} \\ A_{\alpha} \end{pmatrix} = 0. \quad (4.38)$$

The system has nonzero solutions if

$$\det \begin{pmatrix} (H - ES)_{\mathbf{k}'\mathbf{k}} & (H - ES)_{\mathbf{k}'\alpha} \\ (H - ES)_{\alpha'\mathbf{k}} & (H - ES)_{\alpha'\alpha} \end{pmatrix} = 0. \quad (4.39)$$

The upper left-hand block in (4.39) describes a band formed in terms of the NFE model, whereas the lower right block, a band in terms of the LCAO model. The off-diagonal blocks describe the hybridization of the two models (or the hybridization of the bands).

Thus the band structure resulting from Eq. (4.39) contains bands of two types (the wide NFE and narrow LCAO) hybridized with each other. In particular, this model is consistent with the generally accepted view that the band structure of a transition metal is made up of wide s bands hybridized with narrow d bands.

Next we consider the construction of pseudopotential *formfactors* using the secular equation (4.39).

In the absence of hybridization we would obtain an ordinary equation of the plane wave method,

$$\det |(H - ES)_{\mathbf{k}'\mathbf{k}}| = \det |(\epsilon_n - E) \delta_{nn'} + \langle \mathbf{k} + \mathbf{g}_{n'} | W | \mathbf{k} + \mathbf{g}_n \rangle| = 0,$$

where $\langle \mathbf{k} + \mathbf{g}_{n'} | W | \mathbf{k} + \mathbf{g}_n \rangle$ plays the role of a formfactor.

The effect of hybridization on the wide NFE band may be estimated by subjecting (4.39) to Löwdin's folding procedure (see Introduction, Section 8). The result will be

$$\det |(\varepsilon_{\mathbf{k}} - E) S_{\mathbf{k}'\mathbf{k}} + \langle \mathbf{k}' | V | \mathbf{k} \rangle + F_{\mathbf{k}'\mathbf{k}}(E)| = 0, \quad (4.40)$$

where

$$F_{\mathbf{k}'\mathbf{k}}(E) = - \sum_{\alpha'\alpha} (H - ES)_{\mathbf{k}'\alpha} [(H - ES)^{-1}]_{\alpha\alpha'} (H - ES)_{\alpha'\mathbf{k}}. \quad (4.41)$$

The functions $|\mathbf{k}\rangle$ are assumed to be mutually orthogonal as are the functions $|\alpha\rangle$:

$$S_{\mathbf{k}'\mathbf{k}} = \delta_{\mathbf{k}'\mathbf{k}}, \quad S_{\alpha'\alpha} = \delta_{\alpha'\alpha}.$$

Assuming the LCAO band to lie well below the conduction band, the functions $|\alpha\rangle$ may be considered to be core states, i.e., the eigenfunctions of the crystal Hamiltonian:

$$H_{\alpha'\alpha} = \langle \alpha' | H | \alpha \rangle = E_{\alpha} \delta_{\alpha'\alpha}, \quad (4.42)$$

$$H_{\mathbf{k}\alpha} = \langle \mathbf{k} | H | \alpha \rangle = \sum_{\beta} \langle \mathbf{k} | \beta \rangle \langle \beta | H | \alpha \rangle = E_{\alpha} S_{\mathbf{k}\alpha} \quad (4.43)$$

and we obtain

$$\begin{aligned} F_{\mathbf{k}'\mathbf{k}}(E) &= - \sum_{\alpha'\alpha} \frac{(E_{\alpha} - E) S_{\mathbf{k}'\alpha} \delta_{\alpha\alpha'} (E_{\alpha'} - E) S_{\alpha'\mathbf{k}}}{E_{\alpha} - E} \\ &= - \sum_{\alpha} (E_{\alpha} - E) \langle \mathbf{k}' | \alpha \rangle \langle \alpha | \mathbf{k} \rangle, \end{aligned} \quad (4.44)$$

that is, the folding gives rise, as a result of the inclusion of the core orbitals, to a compensatory term in the simple-metal OPW formfactor.

If the LCAO band is close to the conduction band, the $|\alpha\rangle$ functions are no longer Hamiltonian eigenfunctions, that is, (4.42) is nondiagonal and (4.43) should be replaced by

$$H_{\mathbf{k}\alpha} = \sum_{\beta} S_{\mathbf{k}\beta} H_{\beta\alpha}.$$

As a result, the factors in the numerator and denominator of (4.41) do not cancel and we obtain [318] the same resonance-type energy dependence as that in (4.34):

$$F_{\mathbf{k}'\mathbf{k}}(E) = - \sum_{\alpha} \frac{(H - ES)_{\mathbf{k}'\alpha} (H - ES)_{\alpha\mathbf{k}}}{H_{\alpha\alpha} - E}. \quad (4.45)$$

The energy dependence of the formfactor thus arises from the interaction with atom-like orbitals (the atomic orbitals that have survived the transition to solid state).

The above argument may be reversed. Given a certain energy-dependent formfactor, we can write in terms of it the matrix elements of the secular equation and then "unfold" the equation into an expression of the type (4.39), thus coming to the coexistence of wide and narrow bands. This explains why taking into account the energy dependence of formfactors (see Sec. 4.1) brings about some features of the LCAO model.

An important by-product of the analysis of Eqs. (4.44) and (4.45) is that it becomes clear why the parameters of the pseudopotential in the secular equation can be fitted by small-size matrices. The energy dependence of the pseudopotential formfactor is such that neglecting the matrix elements with large reciprocal vectors is equivalent to including them, by (4.44), into the formfactors of smaller matrices. In other words, the "neglected" terms are actually included in the pseudopotential's parameters. This means that pseudopotentials fitted for calculating band structures from small-size matrices will almost certainly be inadequate for determining other crystal properties whose calculation does not involve convolution.

It is clear, on the other hand, that treating a pseudopotential's parameters as adjustable, it is possible even with a small matrix to obtain a band structure in a narrow energy range (for example, to map the Fermi surface).

The simultaneous expansion of the wave function in terms of $|\mathbf{k}\rangle$ and $|\alpha\rangle$ was first suggested in [319, 320] in the context of interpolation schemes. The Hamiltonian matrix elements were treated as adjustable parameters. If they are *calculated*, then the band-calculation scheme is called the mixed basis method [321-325]. Equations (4.35) through (4.45) are borrowed from [318].

Strictly speaking, the expansions in (4.21) and (4.35) are illegitimate since a basis made up of plane waves and atomic orbitals is "overcomplete" (a plane wave basis being complete in itself). As a result, the trial functions are linearly dependent and some of the rows of the secular determinant (4.39) are combinations of some others. This, of course, makes the determinant zero. It should be emphasized [13, 326] that this conclusion is independent of the values of the energy E and wave vector \mathbf{k} .

We demonstrated earlier that the OPW pseudopotential method arises from the secular equation (4.39). Now that we see this equation is "wrong", is there any justification at all for the use of the pseudopotential method?

The linear dependence of trial functions only become significant for large matrices, say, 1000×1000 or more. But even before that the poor convergence of the OPW method manifests itself. The solution (i.e., the energy level) must approach a certain limit as the matrix size increases. In the OPW method, even a relatively small matrix provides a good approximation to the correct value (as

given, for example, by another band theory method). As the matrices grow larger, the solutions start oscillating about this value. The OPW method thus seems to be of little help in improving the accuracy of the eigenvalues [326-329]*.

Even though the OPW determinant fails to provide sufficiently accurate solutions, it does not vanish as might have been expected. What saves the situation is that we can never get an infinitely large determinant, for which the overcompleteness of the basis would be important. To put it another way, the actual basis set we deal with (be it a plane-wave or OPW basis) is always truncated, with no linear dependence between the functions.

The practical conclusion to be drawn from the above is that if carried through from first principles, the OPW pseudopotential method cannot be expected to be very accurate. In band-structure calculations the accuracy of the method is at most 0.01 Ry [327, 328] and it is unlikely to be higher for other crystal properties. Needless to say, the use of appropriate experimental data for improving the parameters of OPW formfactors will be always profitable.

We shall see in Sec. 5.1 that the OPW method is not alone in having the property of overcompleteness. Even the Green's function method uses an expression of the type of (4.35) and is therefore also overcomplete.

Attempts have been made to eliminate the overcompleteness of the OPW scheme. The way this is usually done is to ignore plane waves with large wave vectors (which in practice cannot anyway be included in the expansion of Ψ). This removes the overcompleteness of the OPW basis and makes OPWs orthogonalizable [333-336] (the orthogonalization of each plane wave to core states prevents the plane waves from being mutually orthogonal). We can thus obtain an energy-independent OPW pseudopotential [337-339] (and this even for transition metals [340, 341]).

4.2.3. Energy-independent formfactors. In Sec. 4.1.2 we actually considered a method for constructing an energy-independent simple-metal OPW formfactor using a model dispersion law (see (4.11)). The use of the OPW secular method makes it possible to do away with this energy approximation. To see this, we transform the OPW matrix element to the form

$$\begin{aligned} (\varepsilon_{\mathbf{k}} - E) \delta_{\mathbf{k}'\mathbf{k}} + V_{\mathbf{k}'\mathbf{k}} - \sum_{\alpha} (E_{\alpha} - E) \langle \mathbf{k}' | \alpha \rangle \langle \alpha | \mathbf{k} \rangle \\ = (\varepsilon_{\mathbf{k}} - E) \left[\delta_{\mathbf{k}'\mathbf{k}} - \sum_{\alpha} \langle \mathbf{k}' | \alpha \rangle \langle \alpha | \mathbf{k} \rangle \right] + V_{\mathbf{k}'\mathbf{k}} \\ - \sum_{\alpha} (E_{\alpha} - \varepsilon_{\mathbf{k}}) \langle \mathbf{k}' | \alpha \rangle \langle \alpha | \mathbf{k} \rangle. \end{aligned}$$

* Among other things, the solution is sensitive to the choice of core level energies [75, 330-332] which in a real crystal differ from those of the free-atom ones [73, 75, 330] (this can be observed experimentally [76-78]).

Introducing a pseudopotential \tilde{W}

$$\langle \mathbf{k}' | \tilde{W} | \mathbf{k} \rangle = \langle \mathbf{k}' | V | \mathbf{k} \rangle - \sum_{\alpha} (E_{\alpha} - \epsilon_{\mathbf{k}}) \langle \mathbf{k}' | \alpha \rangle \langle \alpha | \mathbf{k} \rangle,$$

and a matrix $Q_{\mathbf{k}'\mathbf{k}}$ formed by the overlap of individual OPWs

$$\begin{aligned} Q_{\mathbf{k}'\mathbf{k}} &= [\langle \mathbf{k}' | - \sum_{\alpha'} \langle \mathbf{k}' | \alpha' \rangle \langle \alpha' |] [| \mathbf{k} \rangle - \sum_{\alpha} | \alpha \rangle \langle \alpha | \mathbf{k} \rangle] \\ &= \delta_{\mathbf{k}'\mathbf{k}} - \sum_{\alpha} \langle \mathbf{k}' | \alpha \rangle \langle \alpha | \mathbf{k} \rangle, \end{aligned}$$

we get the secular equation to read

$$\det |(\epsilon_{\mathbf{k}} - E) Q_{\mathbf{k}'\mathbf{k}} + \langle \mathbf{k}' | \tilde{W} | \mathbf{k} \rangle| = 0. \quad (4.46)$$

Since the matrices we are dealing with are finite in size, the determinant of the matrix Q is different from zero. The matrix Q may be taken out and since it is energy-independent, the zeros of the determinant (4.46) will be given by

$$\det |(\epsilon_{\mathbf{k}} - E) \delta_{\mathbf{k}'\mathbf{k}} + \sum_{\mathbf{k}''} (Q^{-1})_{\mathbf{k}'\mathbf{k}''} \langle \mathbf{k}'' | \tilde{W} | \mathbf{k} \rangle| = 0.$$

It follows from this expression that the formfactor can be represented by the matrix element

$$\langle \mathbf{k}' | W | \mathbf{k} \rangle = \sum_{\mathbf{k}''} (Q^{-1})_{\mathbf{k}'\mathbf{k}''} \langle \mathbf{k}'' | \tilde{W} | \mathbf{k} \rangle. \quad (4.47)$$

This formfactor does not depend on energy. Unlike equation (4.12), the transformation leading to (4.47) is exact.

We will not discuss here the advantages or disadvantages of Eq. (4.47). Our purpose has been to demonstrate that the problem of an energy-independent OPW formfactor seems to be solvable in principle.

It should be stressed that the fundamental difference between the simple-metal and transition-metal OPW formfactors arises from the fact that atomic d orbitals are not eigenstates of the crystal Hamiltonian. The d electrons cannot therefore be considered to be either bound or free. Treating them as a separate group (in scattering language these are quasi-bound electrons) brings about a resonance-type energy dependence of the formfactor (see (4.34) and (4.45)).

4.2.4. Depletion hole. An important feature of any pseudopotential constructing procedure is the "orthogonalization (or depletion) hole".

The effect is essentially simple. Replacing the true wave function by a model necessarily alters the charge in the region where the two functions differ. The electroneutrality condition may thus be violated, which cannot be tolerated. But then, having constructed a cer-

tain pseudopotential, we are obliged to evaluate the corresponding variation in charge Z_{dpl} (the depletion hole) and somehow take this charge into account. The way this is done is as follows.

Let the true function Ψ and model function ϕ coincide outside a model region of radius R_M (which need not be the same as the core radius R_c but is simply a certain length). Then the total variation in charge due to the replacement of Ψ by ϕ is given by

$$Z_{\text{dpl}} = \sum_{\mathbf{k} \leq k_F} \int_{\Omega_M} [|\Psi|^2 - |\phi|^2] d^3r. \quad (4.48)$$

The Schrödinger equations for Ψ and ϕ are

$$(-\nabla^2 + V(\mathbf{r}) - E) \Psi(\mathbf{r}, E) = 0, \quad (4.49)$$

$$(-\nabla^2 + W(\mathbf{r}, E) - E) \phi(\mathbf{r}, E) = 0. \quad (4.50)$$

We now proceed along the lines used in Sec. 2.2 for deriving the Friedel sum rule. Namely, we write down (4.49) for an energy E_1 and multiply it by $\Psi^*(E_2)$. Next we write down (4.49) for E_2 , make it complex conjugate and multiply by $\Psi(E_1)$. We then subtract one equation from the other and assume that E_1 is close to E_2 , which allows a Taylor expansion for all functions of E_2 . The resulting expression for $|\Psi(E)|^2$ will then contain no potential. The same procedure, when applied to (4.50), will lead to an expression for $|\phi(E)|^2$ involving an energy derivative of the pseudopotential (which has also been expanded).

By substituting the expressions for $|\Psi|^2$ and $|\phi|^2$ in (4.48), using Green's theorem and taking into account that on the surface of the integration sphere the functions Ψ and ϕ , by assumption, coincide, we find the charge of the depletion hole [342]

$$Z_{\text{dpl}} = - \sum_{\mathbf{k} \leq k_F} \int \phi_{\mathbf{k}}^*(\mathbf{r}) \frac{\partial W}{\partial E} \phi_{\mathbf{k}}(\mathbf{r}) d^3r. \quad (4.51)$$

It may be worthwhile before proceeding further to discuss this expression. At first glance it seems to be at odds with our earlier assumption that the replacement of the true wave function by a model wave function necessarily gives rise to a depletion hole. According to (4.51) this may only be true for an energy-dependent pseudopotential. Had we constructed an energy-independent pseudopotential, Eq. (4.51) tells us there would be no such a hole.

Strange as it may seem, this is indeed the case. Consider the starting formula (4.48). What it actually gives is the difference between two normalization integrals, one for the true function and the other for the model function. As (4.48) suggests, a depletion hole arises when the model function is not normalized. It follows from (4.51) that if the depletion hole is different from zero, the pseudopotential

is energy-dependent. The lack of normalization of the model function thus brings about an energy dependence of the pseudopotential.

The derivation of the energy-independent OPW formfactor (4.47) was based on the separation of the Q matrix in the OPW normalization integrals and the subsequent "normalization" of the formfactor. Since there is a connection between the way the pseudopotential depends on energy and the lack of normalization in the model functions, clearly an additional orthogonalization between the OPWs and their normalization may lead to an energy-independent pseudopotential, a subject for further study.

We now proceed with our discussion of (4.51). This expression, is reminiscent of the Friedel sum, which appears as an integral over all states of the sum of time delays also defined through energy derivatives, viz. $\tau_l = \partial \eta_l / \partial E$. (Note that in scattering theory the states are labelled with their energies rather than with the wave vectors as in (4.51)).

The energy dependence of the depletion charge is similar to the energy dependence of the model potential radius involved in the phase function method. We saw in Sec. 2.4 that the radius of the region which can be cut off from the scattering potential depends on energy. But then so is the amount of the "cut-off" charge.

Note that (4.48) involves the wave functions of an electron in a crystal rather than trial functions. Accordingly, (4.51) involves a "crystal" model function rather than a trial ($|\mathbf{k}\rangle$ -type) function. However, an order-of-magnitude analysis in [342] indicates that (4.51) may be rewritten as

$$Z_{\text{dpl}} = - \sum_{\mathbf{k} \leq \mathbf{k}_F} \langle \mathbf{k} | \frac{\partial W}{\partial E} | \mathbf{k} \rangle. \quad (4.52)$$

The Z_{dpl} for the OPW formfactor is

$$Z_{\text{dpl}} = - \sum_{\mathbf{k} \leq \mathbf{k}_F} \left(\sum_{\alpha} \langle \mathbf{k} | \alpha \rangle \langle \alpha | \mathbf{k} \rangle \right) + \sum_{\mathbf{k} \leq \mathbf{k}_F} \left(\sum_{\beta} \frac{\langle \mathbf{k} | V | \beta \rangle \langle \beta | V | \mathbf{k} \rangle}{(E_{\beta} - E)^2} \right). \quad (4.53)$$

Here the first term is the depletion charge for simple metals and the second is the one for transition metals. A new "strange effect" to be seen from (4.53) is that in a transition metal the depletion hole may prove to be smaller than that in a simple metal. Thus far the difficulties we encountered in simple metals were invariably more pronounced in transition metals.

The paradox is easily resolved by noting that the resonance-producing quasi-bound state is localized in the vicinity of the core (it would be wrong to say "inside" since for d electrons the core boundary is blurred, see Sec. 3.4.8). Hence a conduction electron whose energy coincides with the energy of this state can penetrate deeper into the core than an electron with a different energy. The "resonant"

electrons thus reduce the charge deficit produced in the core by the pseudopotential construction process, in this particular case by orthogonalization (the depletion charge is frequently called the orthogonalization hole). With model pseudopotentials it turns out that the depletion hole is indeed small for the transition metals (within 10% of the valency) whereas for the noble metals it is much greater, ranging from 11% for Cd through 16% for Cu to 32% for Au [349].

In both OPW and model pseudopotential calculations the depletion charge is always taken into account. The way it is usually done is by replacing the valency Z , wherever it occurs, by the effective valency Z^* [73, 17, 344] which is

$$Z^* = Z + Z_{\text{dpl}} = Z(1 + \alpha). \quad (4.54)$$

(Certainly, the Fermi energy and wave vector are determined for the true valency Z .)

To conclude this section, we note that the construction procedure for the OPW formfactor, Eqs. (4.40) to (4.45), must also apply to the LCAO model. We might have considered the effect of a wide s band on a narrow d band and obtained the secular equation

$$\det |H_{\alpha'\alpha} - ES_{\alpha'\alpha} + F_{\alpha'\alpha}(E)| = 0,$$

where

$$F_{\alpha'\alpha} = - \sum_{\mathbf{k}'\mathbf{k}} (H - ES)_{\alpha'\mathbf{k}} [(H - ES)^{-1}]_{\mathbf{k}\mathbf{k}'} (H - ES)_{\mathbf{k}'\alpha}.$$

We would thus have considered the formation of bands from "atomic-levels" $H_{\alpha\alpha}$ with the additional perturbation (pseudopotential) coming from the interaction of a given "atomic" level (through the continuum) with other "atomic" levels.

It follows that the hybridization between wide and narrow bands broadens the narrow band, the reason being the increased perturbation.

In broad terms, then, the pseudopotential method is not restricted to the OPW formalism but can equally well be developed in the LCAO scheme. It may be said that both "limiting cases", the nearly-free-electron (NFE) and nearly-localized-electron model (we called it the LCAO), may be formally united in one secular equation (4.39). The possibility of changing from one model to the other cannot be claimed to have been proved here because we incorporated it ourselves when expanding the wave function Ψ in terms of the mixed basis (4.35).

It will be shown in Sec. 5.1 that a rigorous scattering-theory treatment justifies expansion (4.35) although the models the secular equation generates in the limit of no interaction will be neither the sim-

ple free-electron models (as in the NRE approach) nor the simple atomic-electron models (as in the LCAO approach) but modifications of them, viz., the empty lattice and individual cell models.

4.3. Phase-shift formfactors

4.3.1. Terminology. In Sec. 2.3.3 we introduced the scattering-theory pseudopotential by using the formula (2.56) for \mathcal{R}_l and phase shift η_l . Clearly any pseudopotential defined in terms of $\lambda_l(E)$ can be rewritten in terms of phase shifts using Eq. (2.67). We shall therefore call this a "phase-shift" (PS) pseudopotential. Its formfactor is defined in the usual way as the pseudopotential matrix element between plane waves $|\mathbf{k}\rangle$ and $|\mathbf{k} + \mathbf{q}\rangle$.

We shall see in Sec. 5.1 that the formfactors of the scattering-theory pseudopotential (2.105) coincide with the matrix elements of the secular determinant in the reciprocal lattice representation that arises from the Green's function method. This secular equation is known as the secular equation of the Korringa-Kohn-Rostoker method in the Ziman representation (KKRZ). We shall now call the formfactor of pseudopotential (2.105) the KKRZ formfactor*.

Another secular equation written in the reciprocal-space representation is that of the augmented-plane-wave (APW) method [221]. It will not be discussed here in as much detail as the Green function method but will be sometimes referred to. Conceptually, it is intermediate between the OPW and KKRZ methods. Augmented plane waves (or the trial functions of the APW method) are set up in the same way as are orthogonalized plane waves (the OPW trial functions). Both are plane waves far from a scatterer. The difference is in the way the effect of the scatterer is described. In the OPW method, a plane wave is orthogonalized to the scatterer's core states ($E < 0$) whereas in the APW method it is matched with a function describing the scattering, i.e., with the exact solution for $E > 0$. With the KKRZ trial functions, things are more complicated and a more detailed analysis is needed (postponed until Sec. 5.1).

Since the OPW method employs scattering theory, the matrix elements of the OPW secular determinant are expressible in terms of phase shifts. Therefore the phase-shift formfactors will be discussed with those of the augmented-plane-wave method.

4.3.2. KKRZ and APW formfactors. To find a KKRZ formfactor we evaluate the matrix element between plane waves for pseudopoten-

* Traditionally, the names of computational methods are chosen to reflect the approach used (e.g., the OPW, LCAO, Green's function methods). The name "the KKRZ method" is however generally accepted.

tial (2.105):

$$\begin{aligned}
 \langle \mathbf{k} + \mathbf{q} | W^{\text{KKRZ}} | \mathbf{k} \rangle &= \langle \mathbf{k} + \mathbf{q} | \sum_{lm} (\lambda_l - \beta_l) \delta(\mathbf{r} - R) \hat{P}_{lm} | \mathbf{k} \rangle \\
 &= \frac{1}{V_{\Omega_0}} \sum_L (\lambda_L - \beta_L) \int e^{-i(\mathbf{k} + \mathbf{q})\mathbf{r}} \delta(r - R) h_L(\mathbf{k}, |\mathbf{r}|) Y_L(\mathbf{r}) d^3r \\
 &= \sum_L T_L^{\text{KKRZ}}(E) S_L(\mathbf{k}, \mathbf{k} + \mathbf{q}), \quad (4.55)
 \end{aligned}$$

where

$$\bar{T}_l^{\text{KKRZ}}(E) = \lambda_l(E) - \beta_l(E), \quad (4.56)$$

$$S_L = R^2 h_L(\mathbf{k}, R) h_L^*(\mathbf{k} + \mathbf{q}, R). \quad (4.57)$$

The function h_L is defined by (2.33); λ_L is the logarithmic derivative for the radial wave function \mathcal{R}_L and is defined by (2.66).

An APW formfactor is more difficult to obtain so we shall only reproduce the final result (for more detail of the APW method see [13, 223, 345, 346]):

$$\begin{aligned}
 \langle \mathbf{k} + \mathbf{q} | W^{\text{APW}} | \mathbf{k} \rangle \\
 = \frac{4\pi R^2}{\Omega_0} (E - \mathbf{k}(\mathbf{k} + \mathbf{q})) \frac{j_1(qR)}{q} + \sum_L T_L^{\text{APW}} S_L(\mathbf{k}, \mathbf{k} + \mathbf{q}), \quad (4.58)
 \end{aligned}$$

where S_L is defined by (4.57), and

$$T_L^{\text{APW}}(E) = \lambda_L(E). \quad (4.59)$$

The important point about Eqs. (4.55) and (4.58) is that the energy-dependent and energy-independent contributions, T_L and S_L , are separated out to form a product. A function of several variables which is transformable into the sum of the products of functions of one variable, is said to be separable. For example, Green's function (2.9) depends on \mathbf{r} and \mathbf{r}' and is a separable function of these variables. For a spherically symmetrical scatterer, the wave function is also separable with respect to the magnitude and angles of the vector \mathbf{r} (see (2.26)).

The APW formfactor has a nonseparable term, the first one in (4.58). This term is independent of the potential and the reason it appears is that the plane wave $\exp(i\mathbf{q}\mathbf{r})$ has been integrated over a sphere of radius R , the range of the crystal potential, rather than over the Wigner-Seitz cell (the integral would then be $\delta_{\mathbf{q},0}$). Note that the KKRZ and APW methods employ finite-ranged potentials (MT potentials), as follows from definitions (4.56) and (4.59) in which there is a logarithmic derivative over the sphere. The introduction of pseudopotential (2.105) was only possible because we had assumed the potential to be of finite range. Had the potential extended beyond

this (muffin-tin) sphere, we would have been obliged to divide it into two regions, one inside and the other outside the sphere; the inside potential could be replaced by a pseudopotential of the type (2.105) and we would obtain a separable term like that in (4.55) while the outside potential (corrections to the MT form, cf. Sec. 3.4) would give nonseparable terms (which are the Fourier transforms of the potential).

The separability of the KKRZ formfactor is not limited by the energy-dependent functions being separable from energy-independent ones. Separated also are the potential and structure contributions to the formfactor (this is to be distinguished from the matrix element factorization we met in Chapter 1). The function S_L only depends on the crystal type, the lattice parameter, and the range of the potential (which is related to the interatomic separation) and is therefore determined uniquely by the crystal structure. The function T_l is in fact only determined by the crystal potential's characteristics.

There is a major difference between the two phase-shift formfactors. The KKRZ formfactor contains the difference between the logarithmic derivatives for the motion with and without scattering, whereas the APW formfactor only involves the derivative for motion with scattering. This means that in the empty lattice model the KKRZ formfactor is automatically zero because

$$\lambda_l |_{\text{no scattering}} = \mathcal{J}_l(E), \quad T_l^{\text{KKRZ}}(E) \equiv 0$$

The APW empty lattice formfactor is different from zero

$$\begin{aligned} \langle \mathbf{k} + \mathbf{q} | W^{\text{APW}} | \mathbf{k} \rangle |_{\text{no scattering}} \\ = \frac{4\pi R^2}{\Omega_0} (E - \mathbf{k}(\mathbf{k} + \mathbf{q})) \frac{j_1(qR)}{q} + \sum_L \mathcal{J}_l(E) S_L(\mathbf{k}, \mathbf{k} + \mathbf{q}). \end{aligned}$$

It follows that the KKRZ formfactor can be expressed in terms of the APW formfactor:

$$\begin{aligned} \langle \mathbf{k} + \mathbf{q} | W^{\text{KKRZ}} | \mathbf{k} \rangle &= \langle \mathbf{k} + \mathbf{q} | W^{\text{APW}} | \mathbf{k} \rangle_{\text{scattering present}} \\ &\quad - \langle \mathbf{k} + \mathbf{q} | W^{\text{APW}} | \mathbf{k} \rangle |_{\text{no scattering}}. \end{aligned} \quad (4.60)$$

The APW formfactor can be converted into a form very similar to the KKRZ formfactor. Using an equation from [223]

$$\begin{aligned} \mathbf{k}(\mathbf{k} + \mathbf{q}) \frac{j_1(qR)}{q} &= k^2 \frac{j_1(qR)}{q} \\ &\quad + \frac{\Omega_0}{4\pi} \sum_L \left(\frac{d}{dR} h_L(\mathbf{k}, R) \right) h_L(\mathbf{k} + \mathbf{q}, R) \end{aligned} \quad (4.61)$$

we obtain

$$\langle \mathbf{k} + \mathbf{q} | W^{\text{APW}} | \mathbf{k} \rangle = \frac{4\pi R^2}{\Omega_0} (E - k^2) \frac{j_1(qR)}{q} + \sum_L \tilde{T}_l(E, k^2) S_l(\mathbf{k}, \mathbf{k} + \mathbf{q}) \quad (4.62)$$

where we have generalized (4.56) to

$$\tilde{T}_l(E, E_1) = \lambda_l(E) - \mathcal{J}_l(E_1). \quad (4.63)$$

In the Fermi-sphere approximation $E = E_F^0$ and $\mathbf{k} = \mathbf{k}_F^0$ so that the nonseparable term disappears (incidentally it no longer depends on the angle between \mathbf{k} and $\mathbf{k} + \mathbf{q}$ in (4.62) as it did in (4.58)), and the APW formfactor is identical to the KKRZ formfactor.

Anticipating a further result, we note that the KKRZ formfactor has a singularity both at $\mathcal{R}_l = 0$ and at $j_l = 0$. Although this circumstance affords nearly energy-independent formfactor for simple metals, the way transition-metal formfactors depend on energy becomes more complicated.

With the APW formfactor no such difficulties arise for the transition metals. In the simple-metal case, the departure of $E(\mathbf{k})$ from k^2 is small and the quantity \tilde{T}_l is a weak function of energy for the same reasons KKRZ formfactor is. Moreover, since the functions λ_l and \mathcal{J}_l in (4.63) behave very much alike, they compensate for each other's energy dependence to some extent.

The APW formfactor is thus in no way inferior to its KKRZ counterpart, especially for the transition metals where, as experience shows [346], the singularities in $\mathcal{J}_l(E)$ greatly affect the convergence of the KKRZ secular equation (the same is true for the heavy alkali metals [347]).

For this reason, the KKRZ method is used very rarely in band calculations on metals, and preference is given to the APW and KKR methods and a modification of the latter, the model Hamiltonian method. In Sec. 5.2 we shall investigate why scattering theory suffers this failure in the consistent pseudopotential construction. We shall find that the theory actually provides a certain class of pseudopotentials which includes the KKRZ pseudopotential but this latter is sometimes not quite satisfactory. It is possible to set up a pseudopotential having the same functional form as the KKRZ one, but with a "better" energy dependence (see also Sec. 4.4).

Unfortunately, the KKRZ formfactor is the only one of this formfactor class to have been studied. In the following, therefore, we shall restrict ourselves to the KKRZ pseudopotential, whose specific features will be easily distinguished from those "generic" to the class.

In the KKRZ formfactor (4.55), the sum over l may, in view of (4.56) and (2.89), contain only a few terms ($l_{\max} \approx 3$) since at higher l the scattering is small and therefore $\lambda_l(E) \approx \gamma_l(E)$. With the APW method, the analogous sums (4.58) and (4.62) should contain enough terms to secure convergence, which increases somewhat the required computer time.

On the whole, the APW method has proved to be a workable scheme for band calculations for metals and alloys [10, 223, 345, 346, 348], although, in terms of scattering theory, it is less justifiable than the KKRZ method.

4.3.3. The formfactor's q -dependence. Let us investigate how the PS formfactor depends on q . In the APW formfactor, we know that the nonseparable term decreases (see (4.58) and (2.29)) as $1/q$, i.e., the APW formfactor as a whole falls off no faster than $1/q$ whereas the OPW formfactor decreases like $1/q^2$.

The KKRZ formfactor has no nonseparable term, but it is easy to see that its q dependence is determined by the spherical Bessel functions (entering S_L) whose asymptotic value is such (see (2.29)) that the overall behavior is again $1/q$. It thus follows that phase-shift formfactors decrease more slowly with q than do the OPW formfactors or the scattering-theory formfactors (2.161), (4.5), which are based on orthogonalized plane waves.

Let us separate out explicitly the q -dependence of the PS formfactor. This was impossible in the OPW case. By applying (2.34) to the factor $h_L(\mathbf{k} + \mathbf{q})$ in S_L and using, for simplicity, real harmonics we obtain

$$\sum_L T_L S_L(\mathbf{k}, \mathbf{k} + \mathbf{q}) = \frac{4\pi R^2}{\Omega_0} \sum_L F_L(E, \mathbf{k}) j_l(qR) y_L(\mathbf{q}), \quad (4.64)$$

where

$$F_L(E, \mathbf{k}) = 4\pi \sum_{L'L''} C_{L'L''}^L T_{L'} j_{L'}(kR) j_{L''}(kR) y_{L'}(\mathbf{k}) y_{L''}(\mathbf{k}). \quad (4.65)$$

The Gaunt coefficients can be shown to obey the following sum rule:

$$\sum_{mm'} C_{LL_1}^{L'} C_{LL_2}^{L'} = \frac{\delta_{L_1 L_2}}{\sqrt{4\pi}} \sqrt{\frac{(2l+1)(2l'+1)}{2l_1+1}} C_{l_0, l'_0}^{l_0}, \quad (4.66)$$

which when substituted in (4.65) gives a factorized expression

$$F_L(E, \mathbf{k}) = f_l(E, |\mathbf{k}|) y_L(\mathbf{k}),$$

where

$$f_l(E, |\mathbf{k}|) = \sqrt{4\pi(2l+1)} \times \sum_{l'l''} \sqrt{(2l'+1)(2l''+1)} C_{l'_0, l''_0}^{l_0} j_{l'}(kR) j_{l''}(kR) T_{l'}(E). \quad (4.67)$$

The PS formfactor is thus reduced to the form

$$\sum_L T_l S_L(\mathbf{k}, \mathbf{k} + \mathbf{q}) = \frac{4\pi R^2}{\Omega_0} \sum_L f_l(E, k) j_l(qR) y_L(\mathbf{q}) y_L(\mathbf{k}), \quad (4.68)$$

which is convenient in that the angles of the vectors \mathbf{k} and \mathbf{q} enter on equal footing.

In Sec. 4.1.2 we introduced the quasi-local Fermi surface approximation. The purpose of doing this was to treat a nonlocal formfactor as a local one. Our reasoning was that for $q > 2k_F$ the forward-scattering formfactor is of more importance. We may reason, however, in a different manner. In the evaluation of the band structure energy in (4.40) the summation goes over all vectors \mathbf{q} , i.e., all directions of the vector \mathbf{q} are included. The immediate idea is that we can do without the Fermi surface approximation by averaging the formfactor over these directions instead. This will give us another quasi-local expression. Or perhaps we might reason the other way round, namely: if computational difficulties arise from the dependence of the formfactor on the angles of the vector \mathbf{k} , why not average over the angles? It follows from (4.68) for the PS formfactor that the two averaging processes are equivalent and the form of the averaged formfactor will be the same for both cases.

Averaging (4.68) over the angles (of, for example, the vector \mathbf{q}) gives

$$\begin{aligned} \langle \mathbf{k} + \mathbf{q} | \sum_L T_l S_L | \mathbf{k} \rangle &\equiv \frac{1}{4\pi} \int \langle \mathbf{k} + \mathbf{q} | \sum_L T_l S_L | \mathbf{k} \rangle d\Omega_{\mathbf{q}} \\ &= \frac{R^2}{\Omega_0} \sum_L f_l(E, k) j_l(qR) y_L(\mathbf{k}) \sqrt{4\pi} \int y_{00}(\mathbf{q}) y_L(\mathbf{q}) d\Omega_{\mathbf{q}} \\ &= \frac{R^2}{\Omega_0} f_0(E, k) j_0(qR). \end{aligned} \quad (4.69)$$

The zero index on f_l greatly simplifies the calculations because

$$C_{l'0, l'0}^{l0} = \int y_{l0} y_{l'0} y_{l'0} d\Omega |_{l=0} = \frac{1}{\sqrt{4\pi}} \delta_{l'l'}.$$

Then

$$f_0 = \sum_l (2l+1) T_l(E) j_l^2(kR). \quad (4.70)$$

We have thus arrived at an exceptionally simple form for the formfactor (4.69).

The model formfactor of Veljković and Slavić [349] has the same form as (4.69). The reason for introducing it is that its q dependence is the simplest possible. It is amazing that this model formfactor turned out to be obtainable within the framework of the scattering theory.

Let us now find the pseudopotential corresponding to the averaged phase-shift formfactor (4.69). It can be readily verified that

$$\frac{R^2}{\Omega_0} f_0 j_0(qR) = \frac{1}{\Omega_0} \int e^{-i(\mathbf{k}+\mathbf{q})\mathbf{r}} f_0 \delta(\mathbf{r}-\mathbf{R}) e^{i\mathbf{k}\mathbf{r}} d^3r.$$

Therefore the pseudopotential in question is the following local one:

$$W(\mathbf{r}) = f_0 \delta(\mathbf{r}-\mathbf{R}). \quad (4.71)$$

4.3.4. Formfactor's E dependence. The next question to discuss is how the PS formfactor depends on energy. We shall start with the KKRZ method because its formfactor is better justified from the scattering theory point of view. A knowledge of its energy dependence may then shed light on the energy dependence of other formfactors. In particular, we shall learn where singularities may be expected when the undoubtedly more convenient energy-independent model potentials are applied to transition metals.

We saw in Sec. 2.4 that scattering theory in the Born approximation is equivalent to using perturbation theory in pseudopotential calculations. Therefore the study of a formfactor's energy dependence is best started from a discussion of Born scattering.

The Born approximation is applicable when the scattering phase is small. In the zeroth approximation, the phase shift is found by replacing the wave function with a plane wave; in the first approximation a singular solution must be "admixed" through a zeroth-order phase shift:

$$\mathcal{R}_l^B = j_l(\kappa r) - \tan \eta_l^B n_l(\kappa r). \quad (4.72)$$

The expression for the logarithmic derivative λ_l^B is readily obtained by expressing λ_l in terms of $\tan \eta_l$ by (2.67) and then dividing the numerator by the denominator, i.e.,

$$\lambda_l^B(E) \simeq \frac{j'_l}{j_l} - \frac{\tan \eta_l}{\kappa R^2 j_l^2} \left[1 + \frac{n_l}{j_l} \tan \eta_l + \left(\frac{n_l}{j_l} \tan \eta_l \right)^2 + \dots \right]. \quad (4.73)$$

The ratio j_l/n_l in (4.73) is, by (2.73), the tangent of the scattering phase for a perfectly hard sphere, $\tan \beta_l$. It can be seen that (4.73) converges if

$$|\tan \eta_l| \ll |\tan \beta_l| \quad (4.74)$$

which, by the argument that followed equation (2.107), is the condition for weak scattering (the scattering by potential is much weaker than that by a perfectly hard sphere).

It may be said that expression (4.74) is a new convergence criterion, with respect to the Bargmann one (Sec. 2.4), for the perturbation expansion. It was actually (4.74) that we used when deriving (2.153) from (2.56).

In the first approximation, then, the depth of the scattering theory "pseudopotential" (or, what for this particular case is the same, the KKRZ pseudopotential) is

$$\lambda_l^B - \gamma_l = - \frac{\tan \eta_l}{\kappa R^2 j_l^2(\kappa R)}, \quad (4.75)$$

that is, the Born approximation is equivalent to the replacement of the phase η_l^* in (2.106) by η_l .

We now turn to the energy dependence of a Born approximation pseudopotential. The energy behavior of the phase shifts (see Sec. 2.4) indicates that small phases are equivalent to low energies and (2.153) may be written in the form

$$\tan \eta_l^B \approx a_l \kappa^{2l+1}. \quad (4.76)$$

This formula may also be obtained directly from the definition of the Born approximation phase, (2.153), using the asymptotic behavior of the Bessel functions given by (2.28) and valid over an extended energy range.

Substituting (4.75) and (4.76) in (4.73) yields

$$\begin{aligned} T_l^B \equiv \lambda_l^B - \gamma_l = - [(2l+1)!!]^2 \frac{a_l}{R^{2l+2}} \left[1 - \frac{2l+1}{R^{2l+1}} a_l \right. \\ \left. + \left(\frac{2l+1}{R^{2l+1}} a_l \right)^2 - \dots \right]. \end{aligned} \quad (4.77)$$

It can be seen that a pseudopotential in the Born approximation does not depend on energy. This is extremely important for in fact it provides the basis for the theory of energy-independent model pseudopotentials (at least for simple metals, when scattering is small).

A departure from the Born approximation can be represented in the form of a power series in E :

$$\tan \eta_l(E) = a_l \kappa^{2l+1} + b_l \kappa^{2l+3} + \dots, \quad (4.78)$$

$$T_l^B(E) = A_l + B_l E + \dots \quad (4.79)$$

We saw in Sec. 2.2 that the transition metals are characterized by having bound states and this results in $\tan \eta_l$ going to infinity. The singularity in $\tan \eta_l(E)$ is related to that in $\lambda_l(E)$ (by (2.83)). The Born approximation thus fails for the transition metals because the KKRZ pseudopotential depends on energy resonantly. Formally, in the transition-metal case we should replace (4.79) by

$$\begin{aligned} \lambda_l(E) &= \alpha_l + \beta_l E + \frac{\gamma_l}{E - \epsilon_l}, \\ T_l(E) &= A_l + B_l E + \frac{D_l}{E - \epsilon_l}. \end{aligned} \quad (4.80)$$

Figure 4.7 shows λ_l and j_l as functions of E for Mg [350a] and Zr [350b], and in Fig. 4.8 the logarithmic derivatives $T_l(E) = \lambda_l - j_l$ are plotted for a number of transition metals [346].

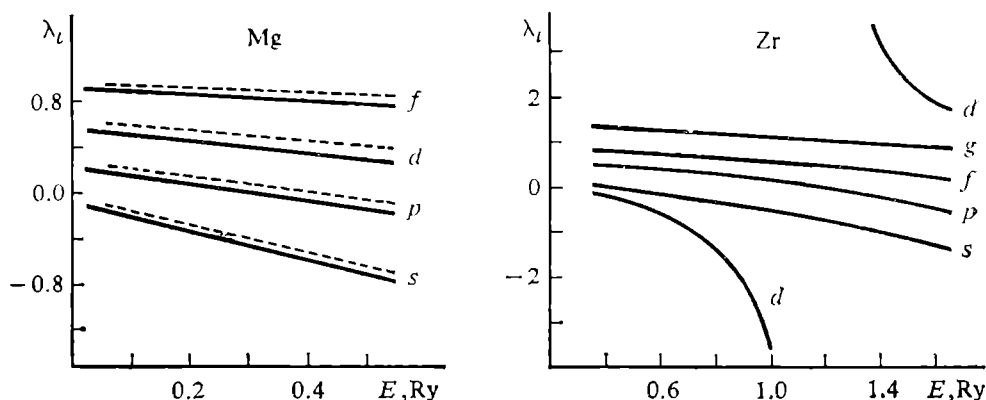


Fig. 4.7. Bold lines are logarithmic derivatives for typical simple (Mg) and transition (Zr) metals. Data are from [350]. Dashed lines are the free-electron logarithmic derivatives, j_l . Note the difference in scale along the ordinate axes.

It can be seen that for Mg the Born condition $T_l(E) \approx \text{const}$ is satisfied rather well, while for the other metals the energy dependence of the pseudopotential is appreciable. This is exactly what should be expected because Mg is one of the simple metals for which* the usefulness of the energy-independent pseudopotentials is beyond any doubt [17, 159]. The logarithmic derivatives shown in Figs. 4.7 and 4.8 were computed in [346, 350] using crystal potentials whose construction was described in Sec. 3.4.

4.3.5. KKRZ and OPW formfactors. We are now able to compare the KKRZ and OPW formfactors.

We note first that the OPW formfactor has a \mathbf{q} -dependent separable term similar to that in the KKRZ formfactor. The former, however, falls off more rapidly with q . The reason for this is that in the OPW formfactor the direct-space integration of spherical Bessel functions (which are plane wave components) brings about an additional factor of $1/q$; the appearance of this factor is illustrated by the integration of the $\exp(i\mathbf{q}\mathbf{r})$ term in the Fourier transform of the square well of radius R :

$$\int e^{i\mathbf{q}\mathbf{r}} d^3r = 4\pi \int \frac{\sin qr}{qr} r^2 dr \xrightarrow{q \rightarrow \infty} 4\pi R \frac{\cos qR}{q^2}.$$

* Similar curves are obtained in [350a] for Be. Our computer calculations for the alkali metals give the same results. The situation is more complicated for the transition metals.

In the KKRZ formfactor, this integration is not actually carried out (because of the δ function), and this is why it decreases more slowly than the OPW formfactor. The slow decrease of the KKRZ formfactor with q is thus not fortuitous, rather it follows from the fundamental properties of the scattering theory pseudopotential (2.105).

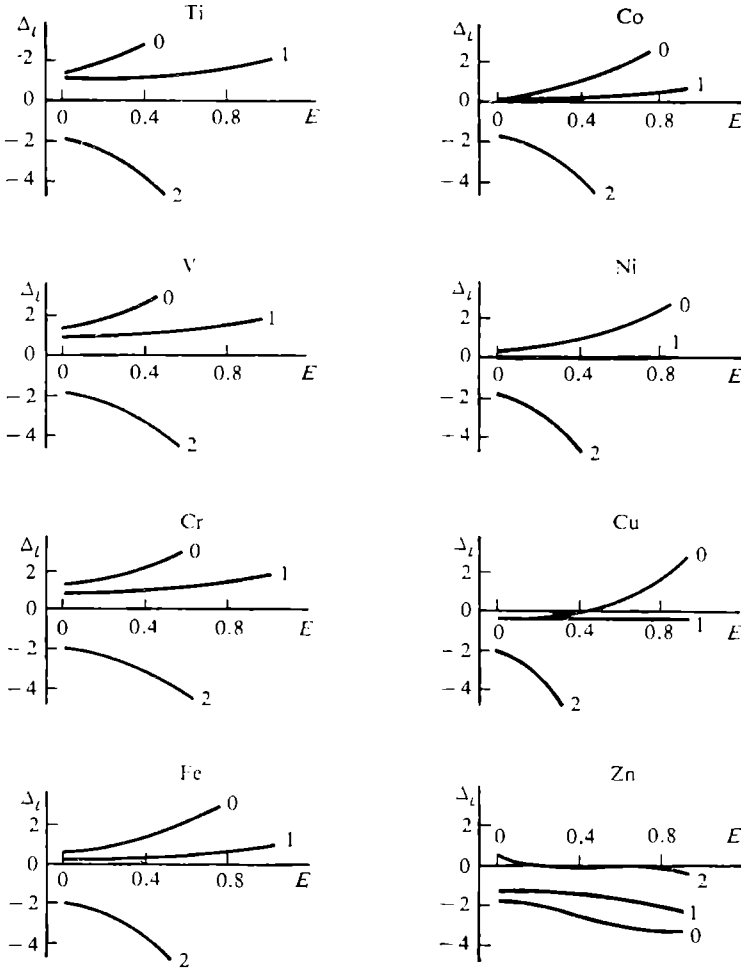


Fig. 4.8. Difference logarithmic derivatives $\Delta_l = R^2 (\lambda_l - \mathcal{J}_l)$ in transition metals. E is measured in Ry, Δ_l in arbitrary units.

It should be recalled, before comparing the energy dependences, that in Sec. 4.1. we discussed the relation between the E and \mathbf{q} dependences of the formfactor and noted that a correctly introduced E dependence may affect the \mathbf{q} dependence. Since the PS and OPW formfactors have different \mathbf{q} dependences, it follows that the E dependences may not be transferable from one type of formfactor to another. It is therefore all the more interesting that the basic features of the energy dependence (which are in fact responsible for the

form of the dispersion law, see Sec. 4.1) are the same for both type of formfactors.

For a transition metal, the OPW formfactor is strongly energy-dependent as are the scattering theory formfactor (2.170), KKRZ (4.55), and APW (4.58) formfactors. For the OPW formfactor (which is the sum of (4.31) and (4.32)) we have in the vicinity of a resonance:

$$\begin{aligned} \frac{d}{dE} \langle \mathbf{k} + \mathbf{q} | W^{\text{APW}} | \mathbf{k} \rangle &\simeq \frac{d}{dE} \langle \mathbf{k} + \mathbf{q} | \mathfrak{R}_t | \mathbf{k} \rangle \\ &= - \sum_d \frac{\dots}{(\varepsilon_d - E)^2} < 0, \end{aligned} \quad (4.81)$$

and similarly for (2.170).

For the KKRZ formfactor, in view of (4.80),

$$\frac{d}{dE} \langle \mathbf{k} + \mathbf{q} | W^{\text{KKRZ}} | \mathbf{k} \rangle < 0. \quad (4.82)$$

The energy dependence of a formfactor in the vicinity of a resonance is thus the same for all the models. This means that some features of the pseudopotential formfactor are independent of the computational method we adopt (cf. Sec. 2.5).

There is a subtlety in the formfactor energy dependence of a simple (nontransition) metal. We can argue [73] that all E_α in such a metal lie deep down and that variations in E on the right-hand side of (2.172) and (4.31) are small as compared with E_α . This means, by (2.60), that a simple metal's OPW formfactor is weakly energy-dependent which is consistent with the Born approximation form (4.77) of the KKRZ formfactor. When scattering is small, the latter formfactor is virtually energy-independent. If the energy dependence is weak but noticeable, we obtain the following from (2.172) and (4.31):

$$\frac{d}{dE} \langle \mathbf{k} + \mathbf{q} | W^{\text{OPW}} | \mathbf{k} \rangle > 0. \quad (4.83)$$

Using the general result that b_l in (4.78) is negative (this can easily be seen by considering the next-order terms in the asymptotic form of Bessel functions) we see from Eqs. (4.75) and (4.78) for the KKRZ formfactor that B_l in (4.79) is positive:

$$\frac{d}{dE} \langle \mathbf{k} + \mathbf{q} | W^{\text{KKRZ}} | \mathbf{k} \rangle > 0, \quad (4.84)$$

which is consistent with (4.83) but disagrees with (4.82). What is the physical (or rather mathematical) meaning of this disagreement? There are two kinds of singularities in the KKRZ formfactor, namely, those associated with the zeroes of \mathcal{R}_l at $E = \varepsilon_l$, and those occurring at $E = E_l^f$ and related to the zeroes of $j_l(R\sqrt{E})$. The position of E_l^f depends on the quantity R which is related to the lattice parameter. When the lattice parameter is large, so is R , and since

$R\sqrt{E_l^f} = \text{const}$, E_l^f is shifted downward in energy. Since T_l in (4.55) has a minus in front of \mathcal{J}_l it follows that the energy dependences of λ_l and \mathcal{J}_l compete with each other and the sign of dT_l/dE depends on "which singularity is nearer". For crystals with large interatomic separations, the dominant singularity is the one in \mathcal{J}_l , which leads to (4.84). When the lattice parameter gets smaller, the energy dependences of $\lambda_{l(=0)}$ and $\mathcal{J}_{l(=0)}$ compensate for each other, the \mathcal{J}_l singularity shifts toward higher energies and the resonance in $\lambda_{l(=2)}$ predominates. In the alkali and alkali-earth metals the lattice parameter is large, the formfactors are virtually independent of E and conventional pseudopotential theory is quite applicable. In the transition metals, the lattice parameter is smaller and a resonance pseudopotential is required.

It follows from the foregoing that a pseudopotential may be thought of as consisting of two contributions (in the KKRZ method, λ_l and \mathcal{J}_l) one of which is determined by the interatomic separation and the other by the electronic structure of the initial atom. For simple metals, the dominant role is played by the "lattice" pseudopotential, while individual features of the specific substance only enter as small perturbations. This means that a *new* pseudopotential theory is conceivable in which these parameters (which are responsible for chemical bonds in a solid) would be explicitly used. One aspect of this approach is the possible optimization of the pseudopotential by considering environmental effects (see discussion in Secs. 3.3 and 3.4).

4.3.6. Andersen's radii. The important question to be discussed is the dependence of the formfactor on the range of the crystal potential, R .

It follows from Eq. (2.104) for the scattering theory pseudopotential (2.105) that for each l we choose, it has its own value of R . The question is: what criteria should be applied?

Analysis of the R dependence of the PS formfactor requires a knowledge of the dependence of T_l on R . Let us define the function $\lambda_l(E)$ for all r by defining $\lambda_l(E, r)$ to be

$$\lambda_l(E, r) = \frac{1}{\mathcal{R}_l(E, r)} \frac{d}{dr} \mathcal{R}_l(E, r).$$

The Schrödinger equation (2.25) then will read

$$\frac{d\lambda_l}{dr} = - \left(\lambda_l + \frac{1}{r} \right)^2 - E + V(r) + \frac{l(l+1)}{r^2}. \quad (4.85)$$

λ_l is now a function of two variables, E and r . We examine the effect of the E dependence on the r dependence.

It can be easily seen that the derivation of (2.71) in Sec. 2.2 could in fact be carried out for a sphere of any radius R . It then follows

from (2.71) that for any r

$$\frac{d}{dE} \lambda_l(E, r) < 0. \quad (4.86)$$

If r is sufficiently large and the centripetal potential term is smaller than the other terms on the right-hand side of (4.85) we get

$$\frac{d}{dr} \lambda_l(E, r) < 0. \quad (4.87)$$

The r dependence of λ_l is thus similar to its E dependence and the function $\lambda_l(r)$ has singularities, whose positions we shall denote by R_s^l . It can be readily seen that R_s^l depends on energy, i.e., the radial and energy dependences of the function $\lambda_l(E, r)$ and thus of the PS formfactor are related to each other.

By (4.86), for any r a small increment in energy gives rise to a small decrease in the value of $\lambda_l(E)$. Had it happened that $R_s^l(E + \Delta E) > R_s^l(E)$, it may be shown graphically that (4.86) would inevitably have been violated. It follows from this that $R_s^l(E + \Delta E) < R_s^l(E)$. Since instead of the $R_s^l(E)$ dependence we can consider the $\varepsilon_l(r)$ dependence, any value of r will have its own singularity energy ε_l . Let us take an r and two energies $E_<$ and $E_>$ such that

$$E_< < \varepsilon_l(r) < E_>.$$

Since for $E_<$ the function λ_l is negative and for $E_>$ positive (both values are close to the singularity but lie on different sides of it) we come to a formal contradiction with (4.86):

$$\lambda_l(E_>) > \lambda_l(E_<), \quad (4.88)$$

which is immediately resolved, however, by noting that the limit may not actually be taken: as $E_< \rightarrow E_>$ the function λ_l is discontinuous.

By (4.85),

$$\left| \frac{d\lambda_l}{dr} \right|_{E=E_>} > \left| \frac{d\lambda_l}{dr} \right|_{E=E_<},$$

and the two functions, $\lambda_l(E_>)$ and $\lambda_l(E_<)$ should intersect at some point R_A^l . This gives rise to the important equation

$$\lambda_l(E_>, R_A^l) = \lambda_l(E_<, R_A^l). \quad (4.89)$$

Like (4.88), expression (4.89) does not contradict (4.86) simply because it is not differentiable with respect to E .

The positions of the points R_A^l are related to the positions of R_s^l .

It is clear that the values of R_A^l will be different for each l . Each pseudopotential component can thus be "optimized" in the sense of energy independence but, of course, only over a limited energy range and only approximately. This may be seen from the fact that the

functions $\lambda_l(r)$ only intersect at energies lying on different sides of a singularity in λ_l . Although the quantity R_A^l will depend on energy, the dependence will be weaker than that in the function $\lambda_l(E)$.

The existence of the MT radii R_A^l was first noticed by Andersen [351] when he was doing a direct recalculation of empirically determined energy dependence of the λ_l into their dependence on the MT radius. Some idea as to why and when these points of "energy independence" occur is given by the argument leading to (4.89).

Although we were actually concerned with T_l^{APW} , the argument may be equally well applied to T_l^{KKRZ} .

Because of the way they were introduced, the Andersen radii R_A^l are related to the dimension Ω_M of the region in which the model and true wave functions lead to equal normalization integrals in expression (4.48) for the depletion hole charge. It can be seen that if the radius R_A^l is such that the l th component of a phase-shift pseudopotential is energy-independent, then the depletion charge corresponding to it by (4.52) must be close to zero, that is, R_A^l is the radius of the region Ω_M .

Rather unexpectedly, we thus observe once again that physically equivalent concepts occur under different names in different theoretical models.

To end our discussion of the r dependence of T_l , we note that the singularities of $\lambda_l(r)$ will be seen as inflexion points on a plot of the $\eta_l(r)$ function. It turns out then that the r 's for which $\tan \eta_l(r)$ goes to infinity alternate with the r 's for which $\lambda_l(r) = 0$. These two families of points cannot coincide which means that the energies E_l and ε_l also cannot coincide, a result obtained from (2.83) on entirely different grounds.

Optimization of logarithmic derivatives to "energy independence" by using (4.89) and choosing R_A^l will affect, first of all, the relationship between different S_L because they are multiplied by T_l . This will modify the \mathbf{q} dependence of the PS formfactor and of each of the functions S_L (because changing R affects the argument $(|\mathbf{k} + \mathbf{q}|R)$ of the spherical Bessel functions). We ascertain once again that the energy dependence of the formfactor is related to its \mathbf{q} dependence.

4.3.7. The formfactor's long-wavelength limit. The optimization of the PS pseudopotential is closely related to the long wavelength limit of its formfactor.

Consider the KKRZ formfactor (4.55). By letting q tend to zero we find that its long wavelength limit is f_0 (4.70). Making use of (4.55) and (2.106) and assuming the phase shifts to be sufficiently small we obtain

$$T_l^{\text{KKRZ}} = -\frac{\tan \eta_l^2(E)}{\kappa R^2 j_l^2(\kappa R)} \simeq -\frac{\eta_l(E)}{\kappa R^2 j_l^2(\kappa R)}. \quad (4.90)$$

In the Fermi sphere approximation we set $k = k_F$ and replace the energy in the denominator of (4.90) by the free-electron Fermi energy. This gives [352]

$$\langle \mathbf{k} | W^{\text{KKRZ}} | \mathbf{k} \rangle \simeq - \sum_L \frac{R^2 \hbar_L^2(\mathbf{k}_F) \eta_L(E_F^{\text{cr}})}{\sqrt{E_F^0} R^2 j_L^2(k_F R)}.$$

Using Eqs. (2.33) and (3.91) gives [352]:

$$\begin{aligned} \langle k | W^{\text{KKRZ}} | k \rangle &\simeq - \frac{4\pi}{\Omega_0} \frac{1}{\sqrt{E_F^0}} \sum_l (2l+1) \eta_l(E_F^{\text{cr}}) \\ &= - \frac{2}{3} E_F^0 \frac{\mathcal{F}(E_F^{\text{cr}})}{Z}. \end{aligned} \quad (4.91)$$

We have thus succeeded, with some reservations, in reducing the PS formfactor to the general form of pseudopotential theory, i.e. Eq. (3.92). It follows that the formfactor can be optimized both to "linear screening" (by equating the long wavelength limit to $-(2/3) E_F^0$) and to "minimum perturbation" (by equating it to zero). It is clear, on the other hand, that the Friedel sum in (4.91) is due to approximations and that in strict terms there is no relationship between the sum and the long wavelength limit of the PS pseudopotential formfactor.

How then should a PS formfactor be numerically optimized and what should the optimization criterion be?

The simplest way to change the magnitude of a potential is by moving it uniformly along the energy axis (essentially, varying the MT jump or MT shift, see Sec. 3.4). A check can be made either by a direct calculation of the Friedel sum from the phase shifts (taking the Fermi energy in the first order perturbation theory approximation, (3.102)) or by the magnitude of the long wavelength limit of the formfactor.

No first-principles calculations of phase-shift formfactors, not to mention their optimization, have been published. The matrix elements $\langle \mathbf{k} + \mathbf{g}_n | W^{\text{KKRZ}} | \mathbf{k} + \mathbf{g}_n \rangle$ and $\langle \mathbf{k} + \mathbf{g}_n | W^{\text{APW}} | \mathbf{k} + \mathbf{g}_n \rangle$ are, of course, relevant in every band-structure calculation, but are never represented as formfactors. Therefore we will not discuss this question now.

If the local PS formfactor (4.69) is considered to be a model one with parameters R and $A = R^2 f_0 / \Omega$, then expression (4.95) serves as a definition for the parameter A :

$$A = - \frac{2}{3} E_F^0 \frac{\mathcal{F}(E_F^{\text{cr}})}{Z}. \quad (4.92)$$

We now wish to verify whether or not the theory of the long wavelength limit is internally consistent. We shall evaluate the Friedel sum $\mathcal{F}_?$ for the local PS pseudopotential (4.71) to see whether it

coincides with the one in (4.92). This Friedel sum we shall denote $\mathcal{F}_1(E_F^{\text{cr}})$. Of necessity, we shall use the Born approximation and replace the phase by its tangent. Using (2.38) we obtain

$$\begin{aligned}\mathcal{F}_2(E_F^{\text{cr}}) &= \frac{2}{\pi} \sum_l (2l+1) \eta_l^B \simeq \frac{2}{\pi} \sum_l (2l+1) \tan \eta_l^B \\ &= \frac{2k_F}{\pi} \sum_l (2l+1) \int_0^\infty j_l^2(r \sqrt{E_F^{\text{cr}}}) f_0 \delta(r-R) r^2 dr \\ &= -\frac{2k_F}{\pi} f_0 R^2 \sum_l (2l+1) j_l^2(r \sqrt{E_F^{\text{cr}}}) = -\frac{2k_F}{\pi} \Omega A. \quad (4.93)\end{aligned}$$

Making use of (4.92) we then obtain the required relationship:

$$\mathcal{F}_2(E_F^{\text{cr}}) = -\frac{2k_F}{\pi} \Omega A = \mathcal{F}_1(E_F^{\text{cr}}).$$

Thus, whatever the model radius or specific optimization procedure, the local PS pseudopotential (4.71) has a correct Friedel sum. The only difference from more rigorous nonlocal pseudopotentials is that (4.71) cannot be optimized to a minimum perturbation because its formfactor would then be identically zero for all q .

Something should be said about the long wavelength limit of the APW formfactor. Using the same approximations that led to (4.90) we can write

$$\lambda_l = \mathcal{J}_l - \frac{\tan \eta_l^z}{\kappa R^2 j_l^2} \simeq \mathcal{J}_l(E_F^0) - \frac{\eta_l(E_F^{\text{cr}})}{R^2 j_l^2(k_F R) \sqrt{E_F^0}}. \quad (4.94)$$

Substituting (4.94) in (4.58), setting $k = k_F$ and using (4.61) in the form

$$\sum_l (2l+1) \left(\frac{d}{dR} j_l(k_i R) \right) j_l(k_j R) P_l(\cos \Theta_{\mathbf{k}_i \mathbf{k}_j}) = (\mathbf{k}_i^2 - \mathbf{k}_i \mathbf{k}_j), \quad (4.95)$$

we find

$$\begin{aligned}\langle \mathbf{k} | W^{\text{APW}} | \mathbf{k} \rangle &= -\frac{4\pi R^3}{3\Omega_0} (E_F^0 - E_F) \\ &\quad + \frac{4\pi R^2}{\Omega_0} \sum_l (2l+1) \frac{d j_l(k_F R)}{dR} j_l(k_F R) + \langle \mathbf{k} | W^{\text{KKRZ}} | \mathbf{k} \rangle \\ &= -\frac{\Omega_{\text{MT}}}{\Omega_0} (E_F^0 - E_F) + \langle \mathbf{k} | W^{\text{KKRZ}} | \mathbf{k} \rangle \\ &= -\frac{\Omega_{\text{MT}}}{\Omega_0} (E_F^0 - E_F) - \frac{2}{3} E_F^0 \frac{\mathcal{F}(E_F^{\text{cr}})}{Z}. \quad (4.96)\end{aligned}$$

Since, by (3.109), $\mathcal{F}(E_F) \propto (E_F^0 - E_F)$, we thus see from (4.91) and (4.96) that both PS formfactors are linear in the Fermi energy E_F .

This has been verified experimentally by employing the APW and KKRZ secular equations to reproduce observed Fermi surface cross sections using E_F^{cr} and the phase shifts as adjustable parameters. For each (assumed) E_F^{cr} value it proved possible [294, 353–360, 291, 292] to reconstruct the Fermi surface by an appropriate choice of phase shifts. This work yielded experimentally determined functions $\eta_l(E_F)$ (not to be confused with $\eta_l(E)$ since at any given value $E \neq E_F$ the surface of constant energy differs in shape from the Fermi surface). Long wavelength limit formfactors were calculated from these functions and they were indeed quasi-linear in E_F [292]. We shall discuss this in more detail at the end of the next section.

4.4. Effective medium and pseudopotential formfactors

4.4.1. Effective medium as an energy zero. We saw in Sec. 3.5 that the perturbation a potential introduces into a crystal is determined by the properties of the effective medium that models the environment of the potential. Depending on these properties the potential may disturb the electron gas strongly or weakly and accordingly we will be dealing with a strong or weak pseudopotential.

In other words, the optimization of a potential is related to that of the effective medium. For example, raising the MT potential (inside the MT sphere) by V_0 is equivalent to lowering the effective medium around it (outside the sphere) by V_0 . The relationship between the effective medium and the way the pseudopotential is optimized has not so far been investigated. The effective medium concept is used extensively in the theory of alloys (for modeling a metal-solvent [361–366]) and it should be noted that even a pure (monatomic) metal is an “alloy” in the sense that an array of perturbing potentials (impurity atoms as it were) has been introduced as it were into a uniform electron gas (metal-solvent).

We see that a variation in the effective medium “displaces” the average potential around an MT sphere. This means that we can shift the energy zero *outside* the MT sphere while leaving it unchanged *inside*. Needless to say, some precautions must be taken to retain a correct description of the scattering processes.

Let the wave function outside the MT potential (free electrons, as it were) be characterized by an energy F while the wave function inside (a scattered state) by an energy E . Then the difference between these two energies determines the properties of the effective medium.

The description of a scattering process requires that the “outer” function smoothly join to the inner function at the edge of the potential. Clearly, such a composite function will depend on two energies. The scattering phase shift will also depend on two energies, F

and E . We thus face the problem of developing a scattering theory “outside a surface of constant energy”, with the initial and final states having different energies.

Note that the matching procedure for wave functions with different energies is not entirely new. In the augmented-plane-wave (APW) method the trial function “inside” the potential is a superposition of the radial solutions associated with energy E , while “outside” the potential it is a plane wave of wave vector \mathbf{k} , with no conditions on the relationship between E and \mathbf{k} . (Note, though, that in this case the functions are only matched with respect to the amplitude.) This procedure is known not to prevent the APW method from being one of the most successful band structure schemes [13, 345, 223]. In a sense, an explanation for this success is the exceptional flexibility of the APW trial functions. This enables independent variations of the energy E and wave vector \mathbf{k} .

It should be expected that the scattering theory “outside the surface of constant energy” will provide more versatile pseudopotentials than are those currently in use.

4.4.2. Phase shifts “outside the surface of constant energy”. We introduce a wave function $\Phi_l(F, E)$ such that an ordinary solution of the radial equation on the constant-energy surface $\mathcal{R}_l(E)$ will be given by

$$\mathcal{R}_l(E) = \int \Phi_l(F, E) \delta(F - E) dE \equiv \Phi_l(E, E). \quad (4.97)$$

We demand that Φ_l should solve an integral equation of the type (2.4):

$$\Phi_l(F, E) = j_l(fr) + \int G_l(F, r, r_1) V(r_1) \Phi_l(F, E, r_1) r_1^2 dr_1 \quad (4.98)$$

where $f = \sqrt{F}$ and the Green function is defined for “free” electrons, i.e., for those on the MT plateau (the effective medium):

$$G_l(F, r, r_1) = f j_l(fr_<) n_l(fr_>).$$

This choice of Green’s function makes (4.98) satisfy the Schrödinger equation for the free motion of energy F (for all r). Equation (4.98) determines how Φ_l depends on F while its E dependence may thus far be as we please.

Requiring that the function Φ_l inside the muffin sphere satisfy the Schrödinger equation for the energy E :

$$\left(-\nabla_r^2 + V(r) + \frac{l(l+1)}{r^2} - E \right) \Phi_l(F, E) = 0, \quad (4.99)$$

we find for $r < R$

$$\Phi_l(F, E) = \mathcal{R}_l(E). \quad (4.100)$$

For $r > R$ the function Φ_l is determined by (4.93).

By using Eqs. (4.98) and (4.100) we find the scattering phase outside the constant energy surface (cf. (2.56)), i.e.

$$\tan \eta_l(F, E) = -f \int_0^R j_l(fr) V(r) \mathcal{R}_l(E, r) r^2 dr, \quad (4.101)$$

which reduces the function Φ_l for $r > R$ to a form similar to (2.57):

$$\Phi_l(F, E) = j_l(fr) - n_l(fr) \tan \eta_l(F, E). \quad (4.102)$$

Equation (4.101) is a matrix element for the interaction potential V taken between the eigenstate corresponding to V , $\mathcal{R}_l(E)$, and the free-electron solution $j_l(r\sqrt{F})$. Since $\eta_l(F, E) \neq \eta_l(E, F)$, the order of the arguments is important. In the following the first argument will always be taken to be the energy of the "incoming" wave (i.e., that occurring in $j_l(r\sqrt{F})$), the second will be taken to be the energy of the scattered wave (involved in $\mathcal{R}_l(E)$).

Since at $r < R$ the function \mathcal{R}_l coincides with the Φ_l which is smoothly defined for all r , we require that the Φ_l defined outside the MT sphere should smoothly join to the solution defined inside. This means that Φ_l should be continuous at $r = R$ in both amplitude and derivative. For the logarithmic derivative $\lambda_l(E)$ defined by (2.66) we obtain

$$\tan \eta_l(F, E) = \frac{j'_l(fr) - j_l(fr) \lambda_l(E)}{n'_l(fr) - n_l(fr) \lambda_l(E)} \Big|_{r=R}. \quad (4.103)$$

and this is a generalization of the usual expression (2.67) for scattering "on a constant energy surface". Equation (2.67) can be retrieved by setting $F = E$.

4.4.3. The KKRZ formfactor and the effective medium. To see how the choice of effective medium influences the KKRZ formfactor, consider scattering from the potential of the Wigner-Seitz cell (3.73) (see Fig. 3.6). There are two natural zeroes for this potential from which to measure the energy, namely, the MT plateau (the energy E_{MT}) and the vacuum zero (the energy E_v). There are three characteristic regions in the problem, namely, $0 < r < R_{\text{MT}}$ (region I), $R_{\text{MT}} < r < R_a$ (region II), and $R_a < r < \infty$ (region III).

It may be argued that if in region III an electron has an energy E_v , its energy in region II is

$$E_{\text{MT}} = E_v + V_0. \quad (4.104)$$

In region I there is no potential plateau and the electron may have either of the energies, E_v or E_{MT} .

To see how the scattering theory formulae are modified when E_{MT} is replaced by E_v , we introduce an MT potential

$$V_{\text{MT}}(r) = V^{\text{WS}}(r) - V_0 \quad (4.105)$$

into region *I*.

The Schrödinger equation in this region takes the form

$$\left(-\nabla_r^2 + V_{\text{MT}}(r) + \frac{l(l+1)}{r^2} - E_{\text{MT}} \right) \mathcal{R}_l^{\text{MT}}(E_{\text{MT}}) = 0. \quad (4.106)$$

Shifting the energy zero, substituting (4.104) in (4.106) and using (4.105) we find

$$\left(-\nabla_r^2 + V^{\text{WS}}(r) + \frac{l(l+1)}{r^2} - E_v \right) \mathcal{R}_l^{\text{MT}}(E_{\text{MT}}) = 0 \quad (4.107)$$

which is simultaneously an equation for $\mathcal{R}_l^{\text{WS}}$, so that

$$\mathcal{R}_l^{\text{WS}}(E_v) = \mathcal{R}_l^{\text{MT}}(E_{\text{MT}}). \quad (4.108)$$

Consider now region *III*. Obviously, the solution is

$$\mathcal{R}_l^{\text{WZ}}(E_v) = A_l [j_l(r\sqrt{E_v}) - n_l(r\sqrt{E_v}) \tan \eta_l^{\text{WS}}(E_v)]. \quad (4.109)$$

Difficulties come from region *II* because here the solution has to be matched with the solutions for regions *I* and *III*. The task is simplified by using the atomic sphere (AS) approximation (see Sec. 3.4.4) which (i) replaces the polyhedral Wigner-Seitz cell by an equivalent (Wigner-Seitz) sphere, and (ii) extends the MT sphere to the boundary of the Wigner-Seitz sphere (3.86).

In this approximation region *II* disappears and the solutions of regions *I* and *III* smoothly match at R_a . For the scattering from the Wigner-Seitz sphere we have (dropping the index on R_a)

$$\tan \eta_l^{\text{WS}}(E_v) = \frac{j'_l(R\sqrt{E_v}) - j_l(R\sqrt{E_v}) \lambda_l^{\text{WS}}(E_v)}{n'_l(R\sqrt{E_v}) - n_l(R\sqrt{E_v}) \lambda_l^{\text{WS}}(E_v)}. \quad (4.110)$$

This, in view of (4.108), can be rewritten as

$$\tan \eta_l^{\text{WS}}(E_v) = \frac{j'_l(R\sqrt{E_v}) - j_l(R\sqrt{E_v}) \lambda_l^{\text{MT}}(E_{\text{MT}})}{n'_l(R\sqrt{E_v}) - n_l(R\sqrt{E_v}) \lambda_l^{\text{MT}}(E_{\text{MT}})} \quad (4.111)$$

which, in fact, describes the MT-potential outside the constant energy surface:

$$\tan \eta_l^{\text{WS}}(E_v) \equiv \tan \eta_l^{\text{MT}}(E_v, E_{\text{MT}}). \quad (4.112)$$

The AS approximation thus automatically leads to a scattering theory valid outside the constant energy surfaces of MT potentials.

Having developed the mathematical formalism, we are now ready to investigate its physical meaning.

The definition of the MT potential does not involve V_0 explicitly. It follows from Sec. 3.4 that the purpose of introducing this quantity is to "hold" electrons within the Wigner-Seitz cell and it has therefore the meaning of the average kinetic energy of the electrons contained in the cell. This means that V_0 is the average effective-medium potential involved in the pseudopotential optimization procedure in Sec. 3.5.

The Lloyd pseudopotential may be easily generalized to include scattering outside the constant energy surface or, what is the same, to include the influence of the effective medium on the properties of the scatterer. By the same argument used in (2.103)-(2.105), we find from (4.101) an analog of (4.63)

$$T_l^{\text{KKRZ}}(E_{\text{MT}}, E_v) = (\mathcal{V}_l^{\text{MT}}(E_{\text{MT}}) - \mathcal{J}_l(E_v))_{R_l} = \tilde{T}_l(E_{\text{MT}}, E_v). \quad (4.113)$$

The formfactor of this pseudopotential is evaluated as before

$$\langle \mathbf{k} + \mathbf{q} | W^{\text{KKRZ}}(E_{\text{MT}}, E_v) | = \sum_L \tilde{T}_l(E_{\text{MT}}, E_v) S_L(\mathbf{k}, \mathbf{k} + \mathbf{q}, R_a) \quad (4.114)$$

giving the generalized KKRZ formfactor mentioned in Sec. 4.3.

We next consider how this generalized KKRZ pseudopotential depends on the properties of the effective medium.

The simplest approximation possible would be to give up optimization, neglect totally the effective medium, and when constructing the MT potential ignore the effect of all the other MT potentials in the crystal lattice on the given one. It may be said that in this approach no attention is paid to the electroneutrality of the Wigner-Seitz cell.

We thus assume that the potential is embedded in the electron gas. The result we are supposed to obtain is $\mathcal{F} = Z$, that is, neglecting the effective medium is actually equivalent, in terms of Sec. 3.5, to optimizing the potential or in other words we must obtain the linear screening potential (LSP). Since, by assumption, $V_0 = 0$, Eq. (4.104) implies that $E_v = E_{\text{MT}}$ and we are led to a conventional KKRZ formfactor.

A more elegant approach is to choose V_0 as the average value of the electron kinetic energy. The \mathcal{J}_l involved in the KKRZ formfactor then depends on energy much less strongly.

Certainly, the most bizarre (although, as will be shown in Sec. 5.2, a strict) approach is to use an energy-dependent effective medium:

$$V_0 = E_{\text{MT}}. \quad (4.115)$$

It then follows from (4.104) and (4.115) that the energy of the "incident" electrons is zero, $E_v = 0$. In this case the energy dependence

of the KKRZ formfactor is determined by the function λ_l alone:

$$T_l^{\text{KKRZ}}(E, 0) = \left(\lambda_l^{\text{MT}}(E) - \frac{l}{R} \right)_{R_a}. \quad (4.116)$$

It will be noted that like any other pseudopotential, the one in (4.113) affects the gas of the free electrons it scatters. The energy of a scattered electron is equal, in the AS model, to the energy of region III (see Fig. 3.6), which is E_v . Consequently, the Schrödinger equation for the pseudopotential (4.113) takes the form

$$(-\nabla^2 + W^{\text{KKRZ}}(E_{\text{MT}}, E_v) - E_v) \Psi(E_{\text{MT}}) = 0,$$

and the perturbation expansion (1.30) will be

$$E_v = k^2 + \langle \mathbf{k} | W^{\text{KKRZ}}(E_{\text{MT}}, E_v) | \mathbf{k} \rangle - \sum_{\mathbf{q} \neq 0} \frac{|\langle \mathbf{k} + \mathbf{q} | W^{\text{KKRZ}}(E_{\text{MT}}, E_v) | \mathbf{k} \rangle|^2}{(\mathbf{k} + \mathbf{q})^2 - E_v}. \quad (4.117)$$

The dispersion laws are nevertheless determined by the dependence $E_{\text{MT}}(\mathbf{k})$, that is, (4.117) must be solved for E_{MT} rather than E_v . This is proved rigorously in Sec. 5.2.

Note that in the AS approach the unseparable term in the APW formfactor (4.58) or (4.62) must vanish. This may be seen by writing

$$\frac{4\pi}{\Omega_0} R_a^2 \frac{j_1(qR_a)}{q} = \frac{1}{\Omega_0} \int_{\text{over Wigner-Seitz sphere}} e^{i\mathbf{q}\cdot\mathbf{r}} d^3r = \frac{1}{\Omega_0} \int_{\text{over Wigner-Seitz cell}} e^{i\mathbf{q}\cdot\mathbf{r}} d^3r = \delta_{\mathbf{q}, 0}.$$

To get the third expression from the second we took into account that in the AS model the Wigner-Seitz sphere coincides with the Wigner-Seitz cell, and to get the fourth from the third we took into account that plane waves in an infinite crystal are normalized to the Wigner-Seitz cell. Thus the only term to survive in the APW formfactor is the separable one corresponding to the scattering "outside the surface of constant energy".

Let us return to the KKRZ formfactor (4.114). By choosing the parameter V_0 in the form

$$V_0 = E_{\text{MT}} - k^2 \quad (4.118)$$

we obtain from (4.104)

$$E_v = k^2 \quad (4.119)$$

and, as can be seen from (4.113), (4.114) and (4.62), this choice of the effective medium changes the KKRZ formfactor into the APW formfactor.

Different V_0 yield different Friedel sums, that is, different optimizations of the KKRZ formfactors.

4.4.4. Experimental data. Suppose we are given the reverse problem, namely, that of fitting pseudopotential parameters to experimental data. In this case, we specify the value of E_F^{cr} (rather than V_0) in order to reproduce the Fermi surface shape. Hence we specify the characteristics of the effective medium and impose consciously or unconsciously some conditions on the pseudopotential. The result is (as was mentioned in Sec. 4.3.7) that for any given E_F^{cr} the PS formfactor has a special set of parameters [291-294, 353-360]. These may be either phase shifts η_l or logarithmic derivatives λ_l . The dependence $\eta_l(E_F^{\text{cr}})$ is illustrated in Fig. 4.9 where the Friedel sum is plotted as a function of E_F^{cr} . It can be seen that theory and experiment are in reasonable agreement.

The Friedel sum \mathcal{F} is related to the long wavelength formfactor limit as approximated by (4.91). Comparing (3.101) and (4.91)

shows that increasing E_F^{cr} increases the numerical value of the long wavelength limit of the formfactor. It follows that determining the

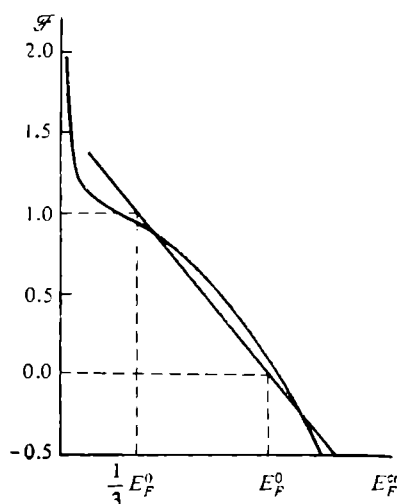


Fig. 4.9. Friedel sum plotted as a function of the assumed Fermi energy of the crystal. Bold line for an APW fit to experimental Fermi-surface data for Cu[357]. Thin line for first-order perturbation theory calculation, Eq. (3.101).

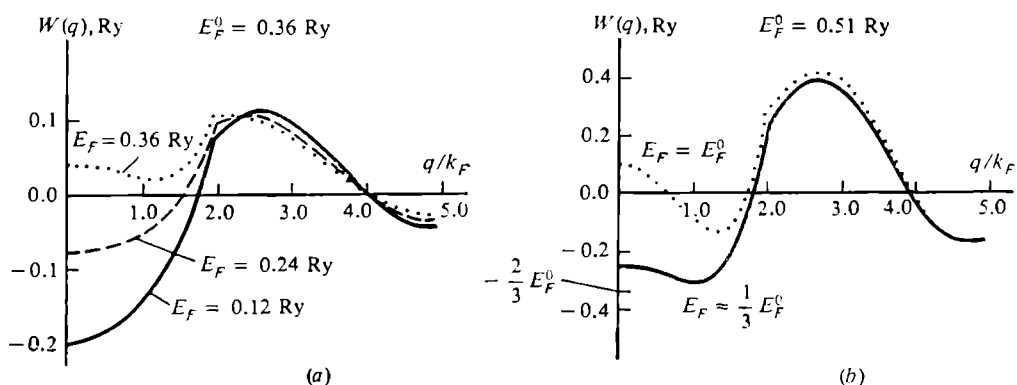


Fig. 4.10. APW formfactors from fitting the experimental Fermi-surface data on (a) Li and (b) Cu [294, 353, 354].

dependence of $\langle \mathbf{k} | W^{\text{KKRZ}} | \mathbf{k} \rangle$ on E_F^{cr} and comparing the result with our prediction gives some insight into how adequate our approxima-

tions are. Figure 4.10 shows the APW formfactors for Li and Cu that were obtained in [234, 353, 354] by fitting experimental data. The curves are shown for different values of the assumed Fermi energy E_F^{cr} and thereby for different sets of parameters. Large values of E_F^{cr} correspond to small Friedel sums, i.e., to a small number of screening electrons relative to the “given” pseudopotential depth. It can be seen that as E_F^{cr} increases the PS formfactor is bound sooner or later to acquire a downward bend, otherwise the curve would simply miss the experimental points. At $q = 0$ the PS formfactor depends on E_F^{cr} much more strongly than elsewhere. In PS formfactors, increasing E_F^{cr} implies, by (3.101), a decrease in \mathcal{F} and hence fewer screening electrons at fixed (experimental) values of $W(q_n)$. In other words, if the screening becomes insufficient the PS formfactor is bent downward. If the density of screening electrons is insufficient to secure the electroneutrality of the Wigner-Seitz cell, a characteristic downward bend may also be expected in a model potential formfactor.

Note that were we interested in the influence of the effective medium on first-principles APW or KKRZ formfactors, we should displace the MT potential as a whole rather than just E^{cr} . This may be seen from the fact that as E_F^{cr} rises from $(1/3) E_F^0$ to E_F^0 , the average potential decreases, that is, rises relative to the MT plateau. This, as may be seen from (3.94) and (3.101), is equivalent to a change in the MT shift. In a first approximation, raising the MT potential by ΔV is equivalent to taking $\lambda_l(E)$ at energy $E - \Delta V$ and not at E . Since $d\lambda_l/dE$ is negative, λ_l will increase. It follows that the observed function $\lambda_l(E_F^{\text{cr}})$ is increasing because the computed $\lambda_l(E)$ is decreasing.

We have confirmed this dependence of the PS formfactor on the MT shift in computer calculations.

Chapter 5

Pseudism and the secular equations of band theory

5.1. The Green's function (or KKR) method

5.1.1. The KKRZ secular equation. The scattering theory pseudopotential introduced in Sec. 2.3 replaces the true potential in the evaluation of formfactors. It is also suitable for band structure calculations.

To see this, recall that the electronic wave function which satisfies the Bloch boundary condition (1.2) may be expanded in plane waves:

$$\Psi = \frac{1}{\sqrt{\Omega_0}} \sum_n B_n e^{i(\mathbf{k} + \mathbf{g}_n)\mathbf{r}}. \quad (5.1)$$

Using the secular equation technique described in the Introduction, subsection 5, and taking the Lloyd pseudopotential (2.105) as a perturbation, we arrive after using (4.55)-(4.57) at a system of homogeneous equations for the coefficients B_n :

$$\sum_{n'} \left[(\epsilon_n - E) \delta_{nn'} + \sum_L T_L^{\text{KKRZ}} S_L(\mathbf{k} + \mathbf{g}_n, \mathbf{k} + \mathbf{g}_{n'}) \right] B_{n'} = 0. \quad (5.2)$$

This system only yields nontrivial solutions if its determinant vanishes:

$$f(E, \mathbf{k}) \equiv \det \left| (\epsilon_n - E) \delta_{nn'} + \sum_L T_L(E) S_L(\mathbf{k} + \mathbf{g}_n, \mathbf{k} + \mathbf{g}_{n'}) \right| = 0. \quad (5.3)$$

Equation (5.3) holds for any wave vector \mathbf{k} ; at low energies of the order of 1 Ry there are usually several values of E_i that satisfy (5.3) for a given \mathbf{k} (it is only these values which give rise to nonzero B_n). The set of E_i corresponding to a given \mathbf{k} is called the energy structure for the given point in \mathbf{k} space; the $E_i(\mathbf{k})$ dependence is known as the i th dispersion law (or the i th band). The set of dispersion laws gives the band structure of the crystal. Equations of the type (5.3) which appear as the solubility condition for a homogeneous system are called secular equations.

Equation (5.2) was first derived by Ziman in his paper [70] on the multiple scattering of electrons by MT potentials forming a crystal lattice. It may be obtained [70] by transforming the secular equation of the band theory method of Korringa [367] and Kohn and Rostoker [368] developed on the basis of the Green's function method (see be-

low). The secular equation (5.3) is therefore often called the Korringa-Kohn-Rostoker-Ziman (KKRZ) secular equation.

Note the simplicity of the procedure we used to derive the KKRZ secular equation. We started by considering scattering from an isolated MT potential. We then chose an appropriate pseudopotential, expanded the desired wave function in functions which incorporate the crystal periodicity, and arrived at equation (5.2) for the expansion coefficients.

Let us consider the properties of the KKRZ secular equation. First of all, it satisfies the empty lattice criterion: for vanishingly shallow potentials we have $\lambda_l(E) = \mathcal{J}_l(E)$, so that T_l^{KKRZ} is identically zero and (5.6) reduces to the secular equation (1.27):

$$\det |(\varepsilon_n - E) \delta_{nn'}| = 0. \quad (5.4)$$

Clearly, solutions of (5.4) are empty lattice dispersion laws. Since the KKRZ matrix elements are energy-dependent, it is impossible to determine E_i by the usual technique of matrix eigenvalues (the matrix depends on the eigenvalues to be found). Equation (5.3) is therefore solved as follows.

Considering the determinant of (5.3) to be a function of energy, it is evaluated for a sequence of energies, and then the roots of the function (that is, its intersections with the energy axis) are found. These roots are the energy levels required.

In transition metal calculations we must be confident that the Fermi level in question will fall within the energy range chosen: the position of the level can only be determined using the density of states, which is itself obtained from the band structure calculation. However, the KKRZ method turns out to be unsatisfactory for energies well above the Fermi level. The problem is that the KKRZ matrix elements involve the function $\mathcal{J}_l(E) \propto j_l^{-1}(\kappa R)$, that is the KKRZ pseudopotential is singular for energies obeying the condition

$$j_l(R\sqrt{E_l}) = 0. \quad (5.5)$$

Even though these resonances exist in pseudopotential energy dependences, they are totally unphysical and are therefore called "spurious poles". The spurious pole nearest the Fermi energy will be for $l = 0$ (the lowest pole possible) for which $E_0^f = (\pi/R)^2$, R being the muffin-tin radius. For an FCC lattice, $E_0^f/E_F^0 = 8\pi^2 (12\pi^2 Z)^{-2/3}$, thus showing that a spurious pole will indeed be observable near the Fermi level, especially in metals with large valencies Z . The occurrence of singularities in the KKRZ matrix elements indicates that they are not small, even for large reciprocal lattice vectors. This means that in the determinant (5.3) large vectors \mathbf{g}_n must be included and the dimensionality of the secular equation becomes too large for the problem to be tractable.

In this case a singularity in the secular equation matrix elements is said to violate the convergence over the reciprocal lattice vectors. Furthermore, a singularity of the type (5.5) gives rise to a resonance of negative width and hence (see Sec. 4.1.3) to the unphysical (or as yet unaccounted for) effect of the merging of band solutions to this resonance level, possibly with the appearance of complex $E_i(\mathbf{k})$ values which indicate the finiteness of the electron lifetime in a given state. The occurrence of such states means that the electron must leave the crystal in the same manner as it leaves a (single) MT scatterer with a quasi-bound state (Sections 2.2, 2.3). This, however, is prohibited by our earlier assumption of the crystal's infiniteness: the electron simply has nowhere to go. It is for this reason that we consider the poles to be spurious.

Spurious poles only arise in the KKRZ method; in the OPW or APW schemes they do not. Furthermore, if a secular matrix is large enough, the poles have no effect on the band solutions, so the APW and KKRZ band structures are virtually indistinguishable [346, 347]. The same is true of the KKR method (see below): these band structure methods yield quantitatively close results.* We may conclude that spurious poles, while affecting the computational procedure, do not alter the final result.

5.1.2. The KKR secular equation. The difficulties of the KKRZ method can be circumvented by using the KKR secular method. This was first done by Ziman [70] with the help of a unitary transformation. We will resort to a similar transformation which is a non-unitary and therefore a simpler one.

Let us substitute an explicit expression for S_L , Eq. (4.57), into (5.2). Summing over n' , we obtain

$$(\varepsilon_n - E) B_n + \sum_L R^2 T_l h_L(n) \sum_{n'} h_L(n') B_{n'} = 0, \quad (5.6)$$

where n in the argument of h_L is a shorthand for $\mathbf{k} + \mathbf{g}_n$. Introducing coefficients C_L defined by

$$-\frac{1}{R^2 T_l} C_L + \sum_n h_L(n) B_n = 0, \quad (5.7)$$

and combining (5.6) and (5.7) we find

$$(\varepsilon_n - E) B_n + \sum_L h_L(n) C_L = 0, \quad (5.8)$$

which when substituted in (5.7), gives

$$\sum_{L'} \left[-\frac{\delta_{LL'}}{R^2 T_l(E)} - \sum_n \frac{h_L(n) h_{L'}(n)}{\varepsilon_n - E} \right] C_{L'} = 0.$$

* For the same potentials, see [369].

We have thus arrived at a system of homogeneous equations for the coefficients C_L . The system will have nonzero solutions if its determinant is zero. Introducing

$$G_{LL'}(\mathbf{k}, E) = \sum_n \frac{h_L(n) h_{L'}(n)}{\varepsilon_n - E} \quad (5.9)$$

we obtain the secular equation

$$\det \left| G_{LL'}(\mathbf{k}, E) - \frac{\delta_{LL'}}{R^2 (\lambda_l(E) - \mathcal{J}_l(E))} \right| = 0 \quad (5.10)$$

which is the KKR secular equation (or rather it can be made so after a little algebra).

We consider first the matrix $G_{LL'}$. Clearly, $G_{LL'}(\mathbf{k}, E)$ is generated from a function $G(\mathbf{r}, \mathbf{r}')$:

$$G(\mathbf{r}, \mathbf{r}') = \sum_{LL'} G_{LL'}(\mathbf{k}, E) Y_L(\mathbf{r}) Y_{L'}(\mathbf{r}'). \quad (5.11)$$

Substituting (5.9) in (5.11) yields

$$G(\mathbf{r}, \mathbf{r}') = -\frac{1}{\Omega_0} \sum_n \frac{e^{i(\mathbf{k} + \mathbf{g}_n)\mathbf{r}} e^{-i(\mathbf{k} + \mathbf{g}_n)\mathbf{r}'}}{\varepsilon_n - E}. \quad (5.12)$$

Since ε_n are the "eigenvalues" and $\Omega_0^{-1/2} \exp[i(\mathbf{k} + \mathbf{g}_n)\mathbf{r}]$ are the eigenfunctions of the empty lattice model, it follows by definition (2.9) that $G(\mathbf{r} - \mathbf{r}')$ of (5.12) is the empty lattice Green's function. The involvement of this latter in the KKR secular equation is the reason why the KKR approach is frequently called the Green's function method.

5.1.3. Structure constants. The Green's function (5.12) may be represented in a somewhat different form. We can rewrite (5.12) as

$$G(\mathbf{r}, \mathbf{r}') \equiv -\frac{1}{\Omega_0} \sum_n \int \delta(\mathbf{k} + \mathbf{g}_n - \mathbf{q}) \frac{e^{i\mathbf{q}(\mathbf{r} - \mathbf{r}')}}{q^2 - E} d^3q$$

where the integration is over all reciprocal space. Representing the δ -function as

$$\delta(\mathbf{k} + \mathbf{g}_n - \mathbf{q}) \equiv \frac{1}{(2\pi)^3} \int e^{i(\mathbf{k} + \mathbf{g}_n - \mathbf{q})\mathbf{r}_1} d^3r_1$$

where the integration extends throughout the crystal, we have

$$G(\mathbf{r}, \mathbf{r}') = -\frac{1}{(2\pi)^3 \Omega_0} \int \int e^{i(\mathbf{k} - \mathbf{q})\mathbf{r}_1} \left[\sum_n e^{i\mathbf{g}_n\mathbf{r}_1} \right] \frac{e^{i\mathbf{q}(\mathbf{r} - \mathbf{r}')}}{q^2 - E} d^3q d^3r_1.$$

The sum over n is zero for an arbitrary \mathbf{r}_1 and goes to infinity each time when $\mathbf{r}_1 = \mathbf{t}_v$ (cf. the structure factor (1.22)). Taking into account

the plane wave normalization, we have

$$\frac{1}{\Omega_0} \sum_n e^{i\mathbf{g}_n \cdot \mathbf{r}_1} = \sum_v \delta(\mathbf{r}_1 - \mathbf{t}_v)$$

giving

$$G(\mathbf{r}, \mathbf{r}') = -\frac{1}{(2\pi)^3} \sum_v e^{i\mathbf{k}\mathbf{t}_v} \int \frac{e^{i\mathbf{q}(\mathbf{r}-\mathbf{r}'-\mathbf{t}_v)}}{\mathbf{q}^2 - E} d^3q. \quad (5.13)$$

A similar integral was encountered in expression (2.11) for the free-electron Green's function G_0 :

$$-\frac{1}{(2\pi)^3} \int \frac{e^{i\mathbf{q}\mathbf{x}}}{\mathbf{q}^2 - E} d^3q = G_0(|\mathbf{x}|) = -\frac{1}{4\pi} \frac{e^{i\sqrt{E}\mathbf{x}}}{|\mathbf{x}|}. \quad (5.14)$$

Substituting (5.14) into (5.13) yields

$$G(\mathbf{r}, \mathbf{r}') = \sum_v G_0(|\mathbf{r} - \mathbf{r}' - \mathbf{t}_v|) e^{i\mathbf{k}\mathbf{t}_v}. \quad (5.15)$$

The empty-lattice electron Green's function $G(\mathbf{r}, \mathbf{r}')$ is thus a Bloch combination of free-electron Green's functions centered on various lattice sites. This is reminiscent of the combination of atomic orbitals used in the LCAO method, Eq. (1.15). The empty lattice Green's function is periodic throughout the crystal, as is any function which satisfies the Bloch boundary condition (1.2).

Making use of expansion (2.36), the matrix elements $G_{LL'}$ can be rewritten as

$$G_{LL'}(|\mathbf{r}|, |\mathbf{r}'|, E, \mathbf{k}) = A_{LL'}(E, \mathbf{k}) j_l(r_{<}) j_{l'}(r_{>}) + \kappa \delta_{LL'} j_l(r_{<}) n_l(r_{>}), \quad (5.16)$$

where $A_{LL'}$ is defined by the identity:

$$A_{LL'} = \frac{1}{j_l(\kappa r_{<})} G_{LL'} \frac{1}{j_{l'}(\kappa r_{>})} - \kappa \delta_{LL'} \frac{n_l(\kappa r_{>})}{j_l(\kappa r_{>})}. \quad (5.17)$$

Thus there are two forms for $A_{LL'}$. The first one follows from (5.9) and (5.17):

$$A_{LL'} = -\frac{1}{j_l j_{l'}} \sum_n \frac{h_L(n) h_{L'}(n)}{\epsilon_n - E} - \kappa \delta_{LL'} \frac{n_l}{j_l}. \quad (5.18)$$

The second form can be obtained using (5.15), (5.14), and (2.34)-(2.36):

$$A_{LL'} = 4\pi \sum_{L''} C_{LL''}^{L'} D_{L''}(E, \mathbf{k}), \quad (5.19)$$

where $C_{LL''}^{L'}$ are the Gaunt coefficients (2.21) and

$$D_L(E, \mathbf{k}) = \kappa \sum_{v \neq 0} e^{i\mathbf{k}\mathbf{t}_v} [n_l(\kappa t_v) - i j_l(\kappa t_v)] Y_L(\mathbf{t}_v) - \frac{i\kappa \delta_{L,0}}{\sqrt{4\pi}}. \quad (5.20)$$

More complicated but more rapidly converging expansions for D_L have been derived in [368, 370-372].

5.1.4. Properties of the KKR secular equation. Substituting (5.16) in (5.10) and using the identity (2.106) gives the KKR secular equation in the form it is generally used:

$$\det |A_{LL'}(E, \mathbf{k}) + \sqrt{E} \delta_{LL'} \cot \eta_l(E)| = 0. \quad (5.21)$$

A point to note about this form is the appearance of the phase shift η_l for MT potential scattering. (The partition (5.16) of the Green's function that gives rise to $A_{LL'}$ is related to some subtleties of the Green function formalism which have to do with singularities the Green's function may have at $r = r'$.) The coefficients $A_{LL'}$ can be shown to be independent of the choice of r and r' . This can easily be seen from expression (5.20) which does not involve r and r' explicitly. The Green's function (5.9) has thus been divided into regular and irregular (at $r = r'$) parts, one of which is $A_{LL'} j_l j_{l'}$ (all the spatial dependence being included in the $j_l j_{l'}$ product) and the other is $\kappa j_l n_l$. It is easy to see that at $r = r'$ the derivative of the regular part is continuous, whereas that of the irregular part is discontinuous (because of the linear independence between $j_n(x)$ and $n_l(x)$). The irregular part was combined with the second term in the secular equation matrix element (5.10) and, since this term has no singularities at $r = r'$, the $r = r' = R$ limit can be taken in either term of the matrix element. As a result, the secular equation (5.21) involves the range of the potential R instead of r, r' and $\cot \eta_l$ is evaluated at $r = R$.

Now what is remarkable about the KKR secular equation?

First of all, the structure and potential parts are separated which is reminiscent of the factorized matrix elements of the pseudopotential method. The matrix elements $A_{LL'}$ depend on the wave vector \mathbf{k} , the energy E , the lattice type, and lattice parameter a , but do not depend on the crystal potential; they are called therefore structure constants.

Let us consider the dependence of the structure constants on the lattice parameter. It is appropriate to introduce variables and functions that are independent of the specific value of a (we designate them by waved letters):

$$\tilde{\mathbf{k}} = \frac{a}{a_0} \mathbf{k}; \quad \tilde{\mathbf{g}}_n = \frac{a}{a_0} \mathbf{g}_n; \quad \tilde{\epsilon}_n = \left(\frac{a}{a_0}\right)^2 \epsilon_n; \quad \tilde{E} = \left(\frac{a}{a_0}\right)^2 E \quad (5.22)$$

where a_0 is the Bohr (or any other fixed) radius.

Let us substitute (5.22) into (2.33). Since R is the MT (or atomic) radius, we have $R \propto a$; $|\mathbf{k} + \mathbf{g}_n| R$ is therefore independent of a . Since $h_L(n)$ involves Ω_0 we obtain

$$\tilde{h}_n(n) = (a/a_0)^{3/2} h_L(n). \quad (5.23)$$

Substituting (5.22) and (5.23) in (5.21) gives

$$A_{LL'} = (a_0/a) \tilde{A}_{LL'}, \quad (5.24)$$

$$\det \left| \tilde{A}_{LL'}(\tilde{E}, \tilde{\mathbf{k}}) + \sqrt{V} \tilde{E} \delta_{LL'} \cot \eta_l(E) \right| = 0, \quad (5.25)$$

where $\tilde{A}_{LL'}$ is independent of the specific lattice parameter. Given the structure constants for one substance, it is a simple matter to find them for a substance with different lattice parameter (for the same lattice symmetry).

In practice, instead of the structure constants $\tilde{A}_{LL'}$ we evaluate the coefficients \tilde{D}_L of (5.19), which are less in number. The structure constants are rather inconvenient in being dependent on energy; this makes it necessary to tabulate them with a very small energy spacing. For this reason tables of the KKR structure constants [373, 374] are only available for a limited number of points in the Brillouin zone, namely, for those lying on high symmetry axes.

The l convergence of the KKR secular equation (5.21) is exceptionally rapid: the first few orbital numbers are sufficient to get steady solutions. In practice, l_{\max} is taken to be 2 which means that only s , p and d components are included in the Lloyd pseudopotential. This is connected with inequality (2.89). Because of this rapid convergence, the number of coefficients D_L nowhere exceeds 25 in \mathbf{k} space, whatever the energy. The explanation is that the Gaunt coefficients $C_{LL'}^{L''}$ vanish for $l'' > l + l'$, i.e., the maximum orbital number l''_{\max} in (5.19) is 4 (if $l_{\max} = l'_{\max} = 2$) and the total number of terms in this equation is $(l''_{\max} + 1)^2$. Some of the other properties of the Gaunt coefficients reduce the necessary number of D_L still further.

The way dispersion laws are determined in the KKR method is similar to that used in the KKRZ scheme: the determinant is evaluated over a certain energy range and then the energies that make it zero are determined. The energy dependence of the structure constants makes this procedure rather difficult because it is very nonlinear in energy; it has singularities when $E = \epsilon_n$. We saw, however, that the band solutions are pushed away from the empty lattice dispersion laws (Sec. 4.1.3). In computer calculations, some measures must therefore be taken to get around these singularities.

5.1.5. Features of the energy band structure. The KKR secular equation in the form (5.21) yields information as to the energy band structure. In a transition metal, we know that the tangent of the phase shift has a resonance in energy (see (2.80)). The simplest way to write this down is to neglect nonresonant scattering with phase η_l^0 :

$$\tan \eta_{l=2} = \frac{\Gamma(E_d)}{E_d - E} \equiv \frac{\tilde{\Gamma}}{\tilde{E}_d - \tilde{E}}$$

where E_d and Γ are, respectively, the energy and width of the quasi-bound state. For the d band we have a 5×5 secular equation (neglecting for the moment ds and dp hybridization):

$$\det |(E_d - E) \delta_{mm'} + \sum_{\nu \neq 0} I_{mm'}(\mathbf{t}_\nu) e^{i\mathbf{k}\mathbf{t}_\nu}| = 0, \quad (5.26)$$

where we have used (5.19) and introduced

$$I_{mm'}(\mathbf{t}_\nu) = \Gamma \sum_{L''} C_{2m, 2m'}^{L''}(n_{l'}(\kappa \mathbf{t}_\nu) - ij_{l'}(\kappa \mathbf{t}_\nu)) Y_{L''}(\mathbf{t}_\nu). \quad (5.27)$$

It can be seen that (5.26) has a typical form of an LCAO secular equation. E_d plays the role of an initial atomic level that splits into a narrow band, while $I_{mm'}$ corresponds to a two-center overlap integral responsible for the finite band width. An interesting fact following from symmetry considerations [375, 378] is that $I_{mm'}$ is a sum of the LCAO-type contributions known as the $dd\sigma$, $dd\pi$ and $dd\delta$ integrals [379, 37].

The width Γ of the resonant level determines the magnitude of the overlap integral $I_{mm'}$ and hence the width of the d band. The larger Γ is, the wider the d band. Since $\Gamma(E) \propto E^{l+1/2}$ we obtain in view of (5.22)

$$\Gamma(E_d) \propto E_d^{5/2} \propto a^{-5}. \quad (5.28)$$

Since the position of a quasi-bound level in a solid is determined by the position of the corresponding bound level in the atom, Γ depends on the metal's position in the periodic table in the same manner as the atomic level does. The variation in atomic level was illustrated in Fig. 3.3. We may conclude that d bands get lower in energy and narrower along a period. The exception is middle-period metals: their d^3s^1 atomic configuration leads to a rise in the atomic level and hence to a broadening of the d band. This is illustrated in Fig. 5.1.

The KKR secular equation (5.25) suggests, to a first approximation, that metals having the same crystal lattice have similar band structures: the differences may be ascribed to the difference in interatomic separations. In higher approximations the difference in crystal potential should be taken into account. Figure 5.1 illustrates this conclusion too.

Some conclusions can be drawn from secular equation (5.25) as to the way the band structure depends on pressure when a crystal is uniformly compressed. It can be seen from (5.22) that the positions of all the energy levels change as a^{-2} ($E \propto \tilde{E}a^{-2}$). To a first approximation, the d band width increases with uniform compression as the inverse square of the lattice parameter; in the next approximation, by (5.28), it is proportional to the inverse fifth power. A numerical experiment [380] supports the a^{-5} dependence, first pointed out in

{305] from somewhat different considerations. It is also clear that pressure will raise all the levels in the crystal and so will increase its total energy, which is unfavorable. It follows that increasing pressure increases the probability for the system to change to another crystal type, whose energy levels will be arranged in such a way as to lower the total energy.

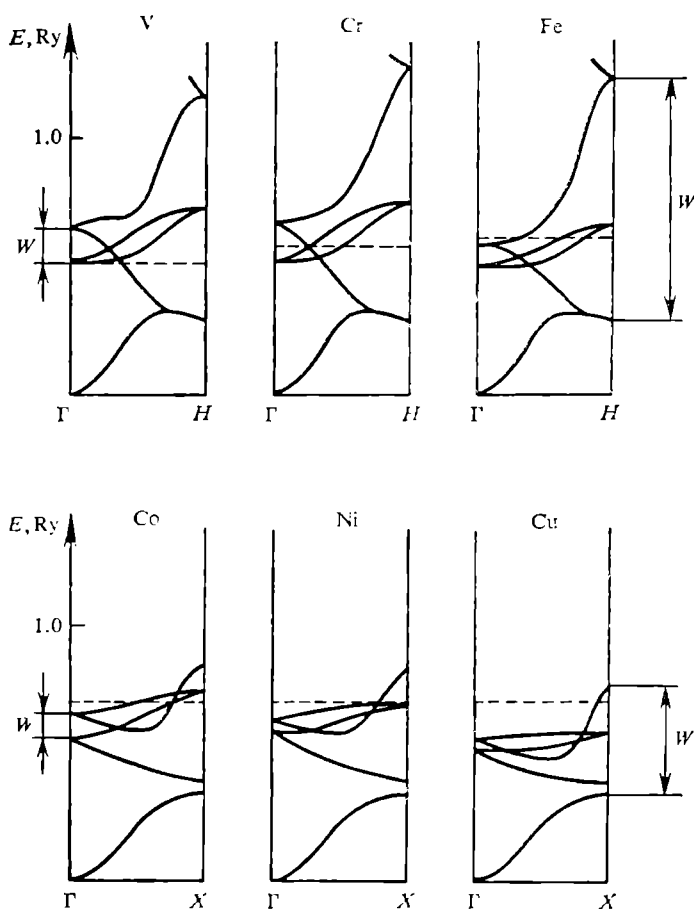


Fig. 5.1. The band structure of BCC (above) and FCC (below) transition metals. W is the band width.

Band theory formalism has thus allowed us, without going into mathematical detail, to draw very general conclusions concerning the physics of crystals. A similar situation was encountered in Sec. 2.3 in the discussion of the periodic table in terms of pseudism. The KKR approach is a natural generalization of the scattering-theory pseudo-potential method to the case of an infinite number of scatterers.

It would therefore be interesting to derive the KKR secular equation by the same method we used for obtaining the phase shifts for a single scatterer, namely, by using integral equation (2.4).

5.1.6. Green's function formalism. As is the case with an isolated potential, an electronic wave function in a crystal may be written as a superposition of the radial solutions \mathcal{R}_l of Schrödinger's equation. The effect of the other scatterers (which are identical to the given one) should be taken into account by subjecting the wave function to appropriate boundary conditions. What is appealing about the Green's function representation (2.4) is that, provided the Green's function has been evaluated for the particular boundary conditions, these are then directly incorporated into the equation.

The Green's function formalism we discuss below is simple to use and may be applied to any infinite system of scatterers. The use of expression (5.16) allows us to consider both ordered and disordered crystals, the periodicity of the lattice not being invoked. It will be understood that the only model assumption we make in this section is that the potential is finite in range. The KKR technique is simply a development of the scattering theory formalism outlined in Sec. 2.1.

The important point to note is that in an infinite crystal there is no incident wave: the crystal fills the whole space and there is nowhere a (formerly free) electron might come from. The immediate implication is that Eq. (2.4) does not contain a solution ϕ of the homogeneous equation; its absence is dictated by the boundary conditions.

The integral equation for Ψ thus takes the form

$$\Psi(\mathbf{r}) = \int G(\mathbf{r}, \mathbf{r}_1) V(\mathbf{r}_1) \Psi(\mathbf{r}_1) d^3r_1, \quad (5.29)$$

where V is the single-site potential and G is the "empty crystal" Green's function, $G = \sum_{\mathbf{v}} G_0(\mathbf{r} - \mathbf{r}_1 - \mathbf{t}_{\mathbf{v}})$.

On the other hand, as already mentioned, Ψ is made up of solutions of the radial Schrödinger equation (the weights of this superposition have to be determined from (5.29)):

$$\Psi(\mathbf{r}) = \sum_L C_L \mathcal{R}_l(r) Y_L(\mathbf{r}). \quad (5.30)$$

Substituting (5.11) and (5.30) into (5.29), we find after integrating over the angles that

$$C_L \mathcal{R}_l(r) = \sum_{L'} C_{L'} \int_0^R G_{LL'}(r, r_1) V(r_1) \mathcal{R}_{L'}(r_1) r_1^2 dr_1. \quad (5.31)$$

We shall assume r to be somewhat larger than the range of the potential R . Then the integration over r_1 in (5.31) does not change the form of $G_{LL'}$ as a function of $r_<$ or $r_>$ (because $r_1 \leq R \leq r$).

Let us consider the integral in (5.31). Making use of the radial equation we write $V \mathcal{R}_l$ as a differential operator and then take the

integral by parts:

$$C_L \mathcal{R}_L = \sum_{L'} \left\{ r_1^2 \left[G_{LL'} \frac{\partial}{\partial r_1} \mathcal{R}_{L'}(r_1) - \mathcal{R}_{L'}(r_1) \frac{\partial}{\partial r_1} G_{LL'} \right]_0^R + \int_0^R \mathcal{R}_{L'}(r_1) \left[\frac{1}{r_1^2} \frac{\partial}{\partial r_1} r_1^2 \frac{\partial}{\partial r_1} - \frac{l(l+1)}{r_1^2} + E \right] G_{LL'} r_1^2 dr_1 \right\} C_{L'}. \quad (5.32)$$

Substituting (5.16) into (5.32) we find the integral to be $\delta_{LL'} \mathcal{R}_l(r=R)$. This means that since in the $r \rightarrow r_1 \rightarrow R$ limit $\mathcal{R}_l(r)$ smoothly joins to $\mathcal{R}_l(R)$, we obtain a system of linear homogeneous equations for the unknown quantities C_L (at $r_1 = 0$ the Wronskian in (5.32) is zero):

$$\sum_{L'} \left[G_{LL'}(r, r_1) \frac{\partial}{\partial r_1} \mathcal{R}_{L'}(r_1) - \mathcal{R}_{L'}(r) \frac{\partial}{\partial r_1} G_{LL'}(r, r_1) \right] C_{L'} = 0. \quad (5.33)$$

By substituting (5.16) into (5.33) and collecting like terms we find

$$\sum_{L'} \{ A_{LL'} j_l(j_{L'} \mathcal{R}_{L'} - j_{L'} \mathcal{R}_{L'}) + \sqrt{E} \delta_{LL'} j_l(n_{L'} \mathcal{R}_{L'} - n_{L'} \mathcal{R}_{L'}) \} C_{L'} = 0.$$

If we introduce a new coefficient a_L , viz.

$$a_L = \left(j_l(\kappa R) \frac{\partial}{\partial r} \mathcal{R}_l(E, r) - \mathcal{R}_l(E, R) \frac{\partial}{\partial r} j_l(\kappa R) \right)_{r=R} C_L \quad (5.34)$$

and take j_l out of the summation, we retrieve the earlier derived form:

$$\sum_{L'} (A_{LL'}(E, \mathbf{k}) + \sqrt{E} \delta_{LL'} \cot \eta_l(E)) a_{L'} = 0. \quad (5.35)$$

The condition for the existence of nonzero coefficients a_L is the KKR secular equation (5.24). The coefficients C_L determined from (5.34) and (5.35) must coincide with C_L found from (5.7) because they are solutions of the same system of linear homogeneous equations.

We thus see that scattering theory makes it possible to change from a "wave vector" representation (of the NFE type) to a representation of "orbital numbers" of a single-site potential (the LCAO type). This being so, can we conceive of a model which would be *opposite* to the empty lattice or the NFE model?

5.1.7. Solitary cell model. If in the LCAO scheme the lattice parameter tends to infinity, we get the limiting case of free atoms. In the KKR (or Green's function) method we have imposed a specific boundary condition, the absence of any incoming wave. Thus an isolated scatterer cannot be a limiting case much as in the NFE model the limiting case is not a simple plane wave $|\mathbf{k}\rangle$ with a dispersion

\mathbf{k}^2 , but rather a set of plane waves $|\mathbf{k} + \mathbf{g}_n\rangle$ with dispersions $(\mathbf{k} + \mathbf{g}_n)^2$.

So let us consider the KKR secular equation and take the limit as the lattice parameter tends to infinity keeping the range of the potential R constant. The resulting model clearly will be an infinite number of infinitely separated Wigner-Seitz cells. We shall call it the solitary cell model. This is not to be confused with the isolated cell model of Sec. 3.4 in which the boundary conditions were taken to be those of free electrons. Here we retain the Bloch boundary conditions, i.e., the Born-Karman conditions.

What then are the dispersions of a solitary cell model?

Consider the KKR secular equation (5.10). An increase in a for constant R means that $|\mathbf{k} + \mathbf{g}_n| R \propto a^{-1}$ and tends to zero, i.e., $j_l(|\mathbf{k} + \mathbf{g}_n| R) \rightarrow \delta_{L,0}$ and, by (2.33) and (5.9),

$$G_{LL'} \xrightarrow{a \rightarrow \infty} \frac{(4\pi)^2}{\Omega_0} \sum_n \frac{\delta_{L,0} \delta_{L',0}}{E} \left(\frac{1}{\sqrt{4\pi}} \right)^2 \propto a^{-3} \xrightarrow{a \rightarrow \infty} 0 \quad (5.36)$$

which, combined with (5.10) gives the secular equation for the solitary cell model:

$$\det \left| \frac{\delta_{LL'}}{\lambda_l(E) - \mathcal{J}_l(E)} \right| = 0. \quad (5.37)$$

As might be expected, the orbital momentum is the motion integral in this model and (5.37) contains $\delta_{LL'}$, that is, as is the case in a free atom, there is no mixing of different orbital numbers. For any given l there are an infinite number of solutions arising when

$$(\lambda_l(E) - \mathcal{J}_l(E))^{-1} = 0. \quad (5.38)$$

Equation (5.38) is fulfilled whenever E equals the energy of a singularity of λ_l or \mathcal{J}_l , that is, there are two sorts of solution of the solitary cell model,

$$E = \varepsilon_l, \quad E = E_l^f, \quad (5.39)$$

where E_l^f is defined by (5.5) and ε_l is the energy of the singularity of the logarithmic derivative λ_l related, by (2.83), to the energy E_l of a quasi-bound state.

It may be said that stretching the crystal narrows the energy bands and as $a \rightarrow \infty$ they "merge" into the ε_l level. These, like $E(k)$, are stationary (their lifetimes are infinite) and are found from the solitary-cell eigenvalue problem, but with the boundary conditions being taken for the crystal rather than for the atom. These levels may thus arise for both negative and positive E_{MT} . As is the case with atomic levels, they are also separated by forbidden gaps; they cannot be considered as states located within a continuum of "free-electron" levels because these latter have all merged into the levels of the solitary cell.

Substituting the parametrization (4.80) into (5.37) we obtain* a typical eigenvalue problem similar to the empty-lattice secular equation (5.4):

$$\det | (\varepsilon_l - E) \delta_{LL'} | = 0. \quad (5.40)$$

We may conclude that scattering theory described the crystal in terms of a model which is intermediate between the empty lattice and solitary cell models. Depending on what features are the most distinctive in the band structure of a crystal, it should be approached by either the NFE or LCAO method.

5.1.8. A model Hamiltonian for the KKR secular equation. It is natural to ask whether the models are convertible. The answer is definitely yes. Consider Eqs. (5.8) and (5.7) as a system of equations for the unknown quantities B_n and C_L . In matrix form we have

$$\begin{pmatrix} (\varepsilon_n - E) \delta_{nn'} & h_{L'n} \\ h_{Ln'} & -\frac{\delta_{LL'}}{R^2 T_l} \end{pmatrix} \begin{pmatrix} B_n \\ C_L \end{pmatrix} = 0. \quad (5.41)$$

Using (4.80) we obtain the secular equation

$$\det \begin{pmatrix} (\varepsilon_n - E) \delta_{nn'} & \sqrt{\gamma_l} h_{L'n} \\ \sqrt{\gamma_l} h_{Ln'} & (\varepsilon_l - E) \delta_{LL'} \end{pmatrix} = 0 \quad (5.42)$$

which is valid for E close to ε_l . The upper left-hand diagonal block corresponds to the empty lattice model, and the lower right-hand one corresponds to the solitary cell model. The two off-diagonal blocks describe their hybridization.

For an infinitely sharp λ_l resonance, the resonance width γ_l and thereby the hybridization elements in (5.42) are zero, which turns the crystal band structure into a set of empty lattice dispersions combined with the E_l' levels and the solitary cell levels. A finite resonance width implies "interaction" between the two models.

Equation (5.42) leads to a widely used transition-metal band-structure model [70, 73, 3] which is a combination of a wide NFE-type $E = k^2$ band with the narrow d level ($E = \varepsilon_{l=2}$) typical of the LCAO model. This gives rise to a 2×2 determinant. A solution of the arising equation is illustrated in Fig. 4.6.

Of course, even in such a simple model as this, we must account for the five-fold degeneracy of the d level. The resulting determinant will then be 6×6 and the secular equation may be interpreted in the following way. The perturbation introduced by the free-electron band (that is, continuum levels) splits the five-fold degenerate ε_d

* Near $E \simeq \varepsilon_l$ the quantity \mathcal{Y}_l is small compared with λ_l and may be neglected leaving only the singular term, $\lambda_l - \mathcal{Y}_l \propto (E - \varepsilon_l)^{-1}$.

level into levels that start interacting with each other through the continuum, thus giving rise to an LCAO band. This is precisely the effect we encountered in the LCAO model: the change in boundary conditions relative to those occurring in the atom (that is, the appearance of a continuum) was equivalent there to a perturbation that "smeared out" a level into a band.

If the resonance in λ_l is unimportant for orbital numbers other than two, it is sensible to retain such terms in the NFE block rather than including them into the LCAO-type block. This will result in a typical NFE pseudopotential and in the loss of diagonality in this block, that is, empty lattice dispersion laws will hybridize in the same way they do in *s*- and *p*-band metals. The infinite dimensionality of the determinant (resulting from the plane-wave expansion) may be reduced by means of the Löwdin convolution procedure as discussed in the Introduction. This will bring about correction terms similar to the KKR structure constants $A_{LL'}$ (compare the expression (5.9) for $G_{LL'}$ with the second-order term in (4.31)). Substituting these corrections in the form of lattice sums (as done in (5.26)) we will see that in this case the KKR method involves the interaction of a typically narrow LCAO band with a typically wide NFE band describable in terms of the pseudopotential method.

A procedure of this kind was first proposed by Heine [305], and was later developed by Hubbard [81, 306, 307], Jacobs [375, 381, 382] and Pettifor [376, 383-385]. It greatly simplifies the (nonlinear) KKR secular equation by reducing it to an eigenvalue problem. Along the same lines, Koelling [386] treated the APW method.

Although the parametrization (4.80) clearly reduces the accuracy of solutions, Heine-Hubbard's "model Hamiltonian" method (of which there are a number of varieties) is quite a reliable tool [387-391] for both qualitative and semiquantitative band studies. The model Hamiltonian method may be said to transform the singularity in the pseudopotential formfactor in such a way as to give rise to a resonance level explicitly. This procedure is the reverse to the one leading, through Eqs. (4.35)-(4.45), to the Harrison pseudopotential (4.32).

5.1.9. The overcompleteness of a basis. There is a great similarity between (5.41) and (4.38). Since Eq. (5.41) is entirely equivalent to the initial problem in both the KKRZ and KKR methods, it turns out that in the Green's function method the wave function at $r = R$ is expanded in terms of plane waves and $\mathcal{R}_l Y_l$ functions simultaneously:

$$\Psi(\mathbf{r}) = \sum_n B_n |\mathbf{k} + \mathbf{g}_n\rangle + \sum_L C_L \mathcal{R}_l(r) Y_L(\mathbf{r}) \quad (5.43)$$

(here we have rewritten the vector-column representation of (5.41)).

It should be recalled now that a basis which is complete for *all space* will be overcomplete for a Fourier transformation into a (finite) subspace. But the introduction of the pseudopotential was in fact equivalent to replacing a part of space by a "black box" whose actual properties were irrelevant, provided the true scattering picture was not distorted. This means that the wave function inside the box is expanded in terms of functions other than plane waves. This leads to this part of space being disregarded in a Fourier analysis. But then a plane-wave expansion is always performed in pseudopotential theory in a certain (coordinate) *subspace* and hence all pseudopotential methods must be overcomplete.

The KKR method has for a long time not been considered to be overcomplete [13]. The treatment above shows, however, that this is not the case. Using the theory of model Hamiltonians [70, 305, 81, 307] we have arrived at a generalized secular equation (5.41) and we have shown thereby that since it comes from scattering theory, the KKR method is bound to include an overcomplete basis expansion. This is clearly illustrated by formula (5.43) in which the original plane-wave basis is complemented by a superposition of $\mathcal{R}_l Y_l$ -type solutions. We thus conclude that all pseudopotential band-theory methods are overcomplete and, importantly, the KKR method is closely related to the others.

In the next section we discuss in more detail the pseudism of secular equations. We show that what makes the KKR method overcomplete is the introduction of scattering phase shifts (which is equivalent, because of modulo- π indeterminacy, to using pseudopotentials).

5.1.10. Lattice of perfectly hard spheres. In conclusion it should be noted that when $E = \varepsilon_l$, a solitary cell scatters the same way a perfectly hard sphere does (cf. (2.73), (2.74)). We saw in Sec. 2.4 that in pseudopotential theory a perfectly hard sphere is the strongest possible perturbation. Suppose we are able to calculate the band structure of a crystal whose lattice-site MT-potentials are represented by hard spheres. For strong scattering we shall then be able to derive pseudopotential-type expressions using as a small perturbation parameter the departure of the true potential from that of a perfectly hard sphere (this, of course, in the sense of scattering and not in the sense of their difference in coordinate space).

The band structure of such a "crystal" is easily found with KKR method. For a perfectly hard sphere, the logarithmic derivative λ_l is infinite for any energy,

$$T_l(E) |_{\text{perfectly hard sphere}} = \infty \quad (5.44)$$

which, when substituted into (5.10), gives the secular equation

$$\det |G_{LL}(E, \mathbf{k})| = 0. \quad (5.45)$$

This scheme varies from the empty lattice model in a somewhat different way than does the solitary cell model: the interatomic separation is taken to be that of the real crystal while the single-site potentials, instead of being infinitely shallow, are assumed to be infinitely deep (high). Unlike the empty lattice model, the dispersion laws are determined by energies satisfying (5.45)—by the Green's function zeroes, as it were—rather than by the Green's function poles (located at $E = \varepsilon_n$). These are characteristic energy levels for the crystal structure which are related to the singularities in λ_l , that is, to the energies of the quasi-bound states produced by the potential. We might even suggest that there is a direct relationship between these energies and the crystal structure because it is only the structure that determines the Green's function in (5.45). This has not yet been verified.

Note also that in the first (diagonal) approximation the solutions of (5.45) coincide with the energies of the potential-insensitive points of the Brillouin zone (see Sec. 4.1). This supports our idea that certain "structure-sensitive" energies are important when forming a band picture.

5.2. Pseudopotential secular equations *

5.2.1. Boundary conditions on the wave function. Let us return to the Schrödinger equation for an isolated scatterer described by the potential $V(r)$. This equation can be solved for any energy if the wave function is not subject to boundary conditions. If it is, the equation is only solvable for certain energy values, the set of which forms what is called the spectrum of the problem.

We saw in the previous section that boundary conditions can be incorporated in the problem by writing the Schrödinger equation in an integral form and using an appropriate Green's function. The method we present in this section is more flexible and includes the Green's function formalism as a special case. Moreover, it gives us better insight into the meaning of band-theory pseudopotentials.

Instead of imposing boundary conditions on the wave function Ψ itself we may require that they be satisfied by trial functions φ_n . Clearly, a linear combination of such functions will also satisfy these conditions. The requirement that the wave function Ψ be expandable in terms of φ_n is therefore equivalent to imposing relevant boundary conditions on Ψ .

In fact, we are already familiar with this procedure. In the NFE or LCAO models we expanded the required wave function in appro-

* The authors are grateful to Professors V. L. Bonch-Bruевич and I. V. Abarenkov for fruitful criticism of the first version of the theory discussed in this section.

appropriate trial functions, substituted the expansion into the Schrödinger equation and obtained a secular equation by demanding that this wave function should be a solution.

We may take a different approach. We may express Ψ in terms of solutions of the Schrödinger equation for an arbitrary energy and then make this expression smoothly join to an expansion in trial functions obeying the boundary conditions. Clearly this will also be equivalent to imposing boundary conditions on the wave function.

5.2.2. Matching wave functions. Consider an infinite lattice of identical MT scatterers. The wave function scattered by the zeroth site is (cf. (5.30))

$$\Psi_{\text{out}}(\mathbf{r}) = \sum_L C_L \mathcal{R}_L(r, E) Y_L(\mathbf{r}). \quad (5.46)$$

We require that the wave incident on a given MT sphere should be a superposition of waves scattered by all the other spheres, viz.,

$$\Psi_{\text{inc}}(\mathbf{r}) = \sum_{t \neq 0} C_L^t \mathcal{R}_L(|\mathbf{r} - \mathbf{t}|, E) Y_L(\mathbf{r} - \mathbf{t}), \quad (5.47)$$

where t 's indicate the positions of sites and \mathcal{R}_L is the solution of the radial Schrödinger equation for the l th site.

If we now require that the wave scattered by the zeroth site smoothly join to the incident wave at the boundary of the MT sphere, we obtain the condition (for $r = R$)

$$\begin{aligned} \Psi_{\text{out}} &= \Psi_{\text{inc}}, \\ \frac{d}{dr} \Psi_{\text{out}} &= \frac{d}{dr} \Psi_{\text{inc}}, \end{aligned} \quad (5.48)$$

which must be transformed to the multiple-scattering-theory secular equation for determining the energy spectrum and wave functions of the problem. The procedure is as follows.

We start by writing (5.47) for a point \mathbf{r} on the MT plateau. Note that (5.46) and (5.47) are defined in this region (as is (5.48)) while inside the MT sphere (5.47) is not defined. We may rewrite (5.47) by adding and subtracting the scattered wave (5.46). This yields

$$\Psi_{\text{inc}} = \sum_t \sum_L C_L^t \mathcal{R}_L(|\mathbf{r} - \mathbf{t}|) Y_L(\mathbf{r} - \mathbf{t}) - \Psi_{\text{out}}(\mathbf{r}), \quad (5.49)$$

where the first term is the one-electron wave function of the crystal $\Psi(\mathbf{r})$, so that

$$\Psi_{\text{inc}}(\mathbf{r}) = \Psi(\mathbf{r}) - \Psi_{\text{out}}(\mathbf{r}), \quad (5.50)$$

which when rewritten as

$$\Psi(\mathbf{r}) = \Psi_{\text{inc}}(\mathbf{r}) + \Psi_{\text{out}}(\mathbf{r})$$

expresses the obvious fact that the wave on the MT plateau is a superposition of waves coming from all the scatterers.

Setting $r = R_+$ and substituting (5.50) into (5.48) yields

$$\begin{aligned} \Psi_{\text{out}}(R_-) &= \Psi(R_+) - \Psi_{\text{out}}(R_+), \\ \frac{d}{dr} \Psi_{\text{out}} \Big|_{r=R_-} &= \frac{d}{dr} (\Psi(r) - \Psi_{\text{out}}(r)) \Big|_{r=R_+}. \end{aligned} \quad (5.51)$$

Since Ψ is a Bloch function, that is, $\Psi = e^{i\mathbf{k}\mathbf{r}} u_{\mathbf{k}}(\mathbf{r})$ where $U_{\mathbf{k}}(\mathbf{r})$ is periodic over the direct lattice, it follows that at each point of the lattice we may expand Ψ over the reciprocal lattice:

$$\Psi(\mathbf{r}) = \frac{1}{\sqrt{\Omega}} \sum_n B_n e^{i(\mathbf{k} + \mathbf{g}_n) \cdot \mathbf{r}}, \quad (5.52)$$

where Ω is the unit cell volume. Substituting (5.46) and (5.52) into (5.51), using the plane wave expansion (2.32) and multiplying by $Y_L(\mathbf{r})$ on both sides, we find after integrating over all \mathbf{r} directions

$$\begin{aligned} C_L(\mathcal{R}_l(R_-) + \mathcal{R}_l(R_+)) &= \sum_n B_n h_L(n, R_+), \\ C_L \left(\frac{d}{dr} \mathcal{R}_l \Big|_{r=R_-} + \frac{d}{dr} \mathcal{R}_l \Big|_{r=R_+} \right) &= \sum_n B_n \frac{d}{dr} h_L(n, R_+). \end{aligned} \quad (5.53)$$

By a simple scattering-theory argument the function \mathcal{R}_l is continuous at $r = R$, so we may take the limit $R_- \rightarrow R_+$ in the left-hand sides of (5.53) assuming R_+ kept fixed. It will be understood that the two radii are not interchangeable in this context because R_+ has appeared in the right-hand side of (5.53) from (5.49), in which Ψ_{inc} is only meaningful outside an MT sphere. Finally,

$$2C_L \mathcal{R}_l = \sum_n B_n h_L(n, R), \quad (5.54a)$$

$$2C_L \mathcal{R}_l' = \sum_n B_n h_L'(n, R), \quad (5.54b)$$

where obvious notations have been dropped and (d/dr) replaced by the prime. Dividing (5.54a) by (5.54b) and collecting like terms yields

$$\sum_n (h_L'(n) - h_L(n) \lambda_l) B_n = 0, \quad (5.55)$$

where λ_l is the logarithmic derivative familiar from scattering theory and all functions are taken at $r = R$, that is, on the edge of the MT potential. This system of equations provides, in principle, the energy spectrum of the problem but is not acceptable from the computational point of view. Incidentally, the system satisfies the empty-lattice criterion in that, for an infinitely shallow MT potential, the function \mathcal{R}_l tends to $j_l(r\sqrt{E})$ and if $E = \varepsilon_n$ for a certain n , then the determinant of the system vanishes thus providing a condition from which the energy spectrum is determined.

What makes the system (5.55) impractical is that its equations are written in a mixed representation, i.e., the matrix elements are labeled by the quantum numbers n and L . It would be desirable to transform the system (5.54) in such a way as to obtain matrix elements labeled by identical quantum numbers, for example, by L and L' in the orbital momentum representation. Clearly we would achieve this goal if we were able to express the coefficients B_n in terms of C_L . There are difficulties, however, which arise from the matrix $h_L(n)$ not being reversible.

5.2.3. The coefficients B_n in terms of C_L . Let us define coefficients a_L such that

$$B_n = \frac{1}{\varepsilon_n - F} \sum_L h_L(n, \mathbf{r}') a_L, \quad (5.56)$$

where \mathbf{r}' is different from \mathbf{r} , $\varepsilon_n = (\mathbf{k} + \mathbf{g}_n)^2$, and F is a certain energy. The idea is that a relation between the a_L and C_L must be easier to find out than that between the B_n and C_L .

Substituting (5.56) into (5.54) and defining (for any \mathbf{r}, \mathbf{r}')

$$\Gamma_{LL'}(r, r') = \sum_n \frac{h_L(n, r) h_{L'}(n, r')}{\varepsilon_n - F} \quad (5.57)$$

equations (5.54) become

$$2C_L \mathcal{R}_I = \sum_{L'} \Gamma_{LL'} a_{L'}, \quad (5.58a)$$

$$2C_L \mathcal{R}'_I = \sum_{L'} \left(\frac{d}{dr} \Gamma_{LL'} \right)_{r=R} a_{L'}, \quad (5.58b)$$

where $r = R_+$ while \mathbf{r}' is so far arbitrary.

The matrix $\Gamma_{LL'}$ is easily recognized as the orbital-momentum representation of an empty-lattice Green's function for an electron of energy F . It should be noted that F need not coincide with E in (5.46) and in (5.47). The energy E identifies the state we are considering whereas F enters our discussion through equation (5.56), which thus far only expresses our belief in there being certain a_L 's which make (5.56) true. The existence of the a_L will be proved if a relation between a_L and C_L is found. If this proof turns out to be independent of F , then the a_L exist independently of F , and (5.56) holds for any F , including $F \neq E$.

In order to carry out the proof, let us first find the Wronskian of the $\Gamma_{LL'}$ matrix. We start with defining a function corresponding to $\Gamma_{LL'}$ matrix,

$$\Gamma(\mathbf{r}, \mathbf{r}') = \sum_{LL'} \Gamma_{LL'}(\mathbf{r}, \mathbf{r}') Y_L(\mathbf{r}) Y_{L'}(\mathbf{r}'),$$

which may be rewritten as

$$\Gamma(\mathbf{r}, \mathbf{r}') = \frac{1}{\Omega} \sum_n \frac{\exp[i(\mathbf{k} + \mathbf{g}_n)(\mathbf{r} - \mathbf{r}')] }{\varepsilon_n - F} \quad (5.59)$$

using (2.32). It will be seen that the last two equations are Eqs. (5.11) and (5.12) in which E is replaced by F . Using (5.16) we write

$$\begin{aligned} \Gamma(\mathbf{r}, \mathbf{r}') = \sum_{LL'} [j_l(fr) A_{LL'}(k, F) j_{l'}(fr') \\ + f\delta_{LL'} j_l(fr_{<}) n_l(fr_{>})] Y_L(\mathbf{r}) Y_{L'}(\mathbf{r}'), \end{aligned} \quad (5.60)$$

where $f = +\sqrt{F}$, and $r_{<}$ ($r_{>}$) is the smallest (largest) of the radii \mathbf{r} , \mathbf{r}' . Note that the matrix $A_{LL'}$ does not depend on vectors \mathbf{r} and \mathbf{r}' . From (5.59) and (5.60) we find

$$\Gamma_{LL'} = j_l(fr) A_{LL'} j_{l'}(fr') + f\delta_{LL'} j_l(fr_{<}) n_l(fr_{>}). \quad (5.61)$$

Assuming $r > r'$, which means that $r_{>} = r$ and $r_{<} = r'$, we differentiate (5.61) with respect to r to obtain

$$\frac{d}{dr} \Gamma_{LL'} = j'_l A_{LL'} j_{l'} + f\delta_{LL'} j_l(fr') n'_l(fr). \quad (5.62)$$

We now multiply (5.61) by $j'_l(fr)$, (5.62) by $j_l(fr)$, and subtract one from the other. This yields

$$\begin{aligned} j'_l(fr) \Gamma_{LL'} - j_l(fr) \frac{d}{dr} \Gamma_{LL'} \\ = 0 \cdot A_{LL'} j_{l'} + f\delta_{LL'} j_l(fr') [n_l(fr) j'_l(fr) - n'_l(fr) j_l(fr)]. \end{aligned}$$

Using theorems on the Wronskians of the Bessel and Neumann functions we find a theorem on the Wronskian of the empty-lattice Green's function, viz.

$$j_l(fr) \frac{d}{dr} \Gamma_{LL'} - \Gamma_{LL'} \frac{d}{dr} j_l(fr) = \frac{1}{r^2} \delta_{LL'} j_l(r'f) \text{ for } r > r', \quad (5.63a)$$

$$j_l(fr) \frac{d}{dr} \Gamma_{LL'} - \Gamma_{LL'} \frac{d}{dr} j_l(fr) = 0 \text{ for } r < r'. \quad (5.63b)$$

We are now in the position to find a relation between a_L and C_L . Let us multiply (5.58a) by $j'_l(fR)$, (5.58b) by $j_l(fR)$ and assume $r' < R$. Subtracting one equation from the other and using (5.63) we obtain

$$2C_L(j_l \mathcal{R}_l - j'_l \mathcal{R}_l) = \sum_{L'} \frac{1}{R^2} \delta_{LL'} j'_l(fr') a_L \quad (5.64)$$

from which the required relation is

$$a_L = \frac{2R^2}{j_l(fr')} \left[j_l(fr) \frac{d}{dr} \mathcal{J}_l(E, r) \Big|_{r=R} - \frac{d}{dr} j_l(fr) \Big|_{r=R} \mathcal{R}_l(E, R) \right] C_L \quad (5.65)$$

showing that the a_L coefficients do exist and are defined for any F .

5.2.4. Derivation of the secular equation. Denoting the term in the square brackets as $[j_l, \mathcal{R}_l]$ we write

$$a_L = \frac{2R^2}{j_l(fr')} [j_l, \mathcal{R}_l] C_L. \quad (5.66)$$

Using (5.61) and (5.66) we find from (5.58a)

$$j_l \sum_{L'} j_{L'} a_{L'} \left(A_{LL'}(k, F) + \delta_{LL'} f \frac{[n_l, \mathcal{R}_l]}{[j_l, \mathcal{R}_l]} \right) = 0, \quad (5.67)$$

where (2.30) was used for functions of fr . The condition for there-existing nontrivial solutions of (5.67) is the required secular equation

$$\det | A_{LL'}(F, \mathbf{k}) + \sqrt{F} \delta_{LL'} \cot \eta_l(F, E) | = 0, \quad (5.68)$$

where ($y = fR$),

$$A_{LL'}(F, \mathbf{k}) = \frac{-1}{j_l(y) j_{L'}(y)} \sum_n \frac{h_{L'}^{(n)} h_L^{(n)}}{\varepsilon_n - F} - f \delta_{LL'} \frac{n_l(h)}{j_l(y)}, \quad (5.69)$$

$$\cot \eta_l(F, E) = (j'_l(y) - \lambda_l j_l(y))^{-1} (n'_l(y) - \lambda_l(E) n_l(y)). \quad (5.70)$$

5.2.5. Pseudism in the secular equation. We have thus arrived at phase shifts defined outside the isoenergetic surface. Although similar to phase shifts discussed in Sec. 4.5.2, these shifts are of entirely different origin. In Sec. 4.5.2 they resulted from the atomic sphere approximation whereas in the present formalism they appear as a manifestation of the "structural" pseudopotential and are related to the arbitrariness inherent in the transformation (5.56) (or the arbitrariness in the choice of the coefficients a_L).

In the atomic sphere approximation (Sec. 3.4.4) the MT radius was taken to be equal to the Wigner-Seitz radius. This is not necessary in the present context, but the fact that the matching radius is a variational parameter is consistent with the atomic sphere model (Sec. 4.5.3).

With the simplest possible choice for the variational parameter F ,

$$F = 0, \quad (5.71)$$

we obtain a simple secular equation

$$\det \left| R^2 \sum_n \frac{h_L(n) h_{L'}(n)}{\epsilon_n} + \frac{\delta_{LL'}}{\lambda_l(E) - l/R} \right| = 0 \quad (5.72)$$

known as the LCMTO or LMTO secular equation (from the method of the linear combination of MT orbitals [392-397]) and first obtained by Anderson [245] in the atomic sphere approximation for $R = R_a$.

It is worthwhile discussing here the physical meaning of the KKR secular equation (5.68). Introducing, formally,

$$\varphi_{LL'} = -\arctan \left[\frac{1}{f} A_{LL'}(F, k) \right] \quad (5.73)$$

(5.68) takes the form

$$\det |\cot \varphi_{LL'} - \delta_{LL'} \cot \eta_l| = 0. \quad (5.74)$$

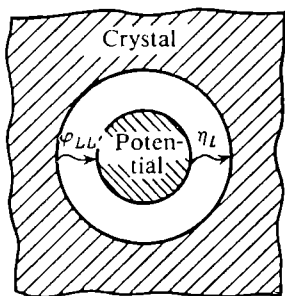


Fig. 5.2. Schematic illustration of a scattering process as described in terms of pseudopotential secular equations. The MT "black box" is surrounded by a "black box" representing the rest of the crystal.

This equation allows a simple interpretation (see Fig. 5.2). The effective medium around a given MT potential (a crystal lattice in our case) is considered as a scatterer. Since the phase shift matrix $\varphi_{LL'}$ is nondiagonal, the scatterer is nonspherical. The MT potential in this case turns out

to be a spherically symmetric scatterer. The requirement that the electron scattered by one of the two scatterers should be effectively ignored by the other scatterer (the requirement for the coincidence of phase shifts, Eq. (5.74)) secures the stationary motion of the electron throughout the crystal.

In other words, the MT potential "black box" is surrounded by the "black box" of the lattice pseudopotential. If the phase shifts are equal on their "interface", the electron moves freely between the two. It is this steady-state condition which determines (by (5.74)) the band solution $E(\mathbf{k})$. Note that according to Eq. (5.74) the phase shifts must only coincide modulo π .

In the context of the discussion of Sec. 3.5 it may be said that the variational parameter F (a property of the lattice pseudopotential in (5.69)) and the average potential outside the MT sphere (a property of the effective medium, see Sec. 4.5) are related similarly to (4.104):

$$F = E - V_0 \quad (5.75)$$

where E is measured from the MT zero, i.e., E is E_{MT} .

It is against the background of this effective medium that scattering processes evolve. A different V_0 corresponds to a different "background" space. The nearer the properties of the space to those of the MT potential, the smaller is the phase shift due to the MT potential, i.e., the weaker the MT pseudopotential.

Using equations (5.6)-(5.10) and (5.16)-(5.24), the KKR-type secular equation (5.68) can be transformed to a KKRZ-type one giving the generalization of the KKRZ method (see (4.113), (4.63)):

$$\det | (\varepsilon_n - F) \delta_{nn'} + \sum_L \tilde{T}_l(E, F) S_L(\mathbf{k} + \mathbf{g}_n, \mathbf{k} + \mathbf{g}_{n'}) | = 0. \quad (5.76)$$

This equation should be solved for E . Applying the Löwdin convolution procedure to (5.76) we obtain (4.117).

It is interesting to note that the wave-vector representation can also be derived from the exact secular equation (5.55). To show this we first perform the summation in (5.55) with a weighting factor $h_L(n')$ to obtain

$$\sum_{n'} (\alpha_{nn'} - \beta_{nn'}) B_{n'} = 0, \quad (5.77)$$

where

$$\beta_{nn'} = \sum_{LL'} h_L(n) \lambda_l \delta_{LL'} h_{L'}(n') = \frac{1}{R^2} \sum_L \lambda_l(E) S_L(n, n'), \quad (5.78)$$

with S_L defined by (4.57) (as in (5.76)) and

$$\alpha_{nn'} = \sum_L h_L(n) h'_L(n'). \quad (5.79)$$

Using Eqs. (5.77)-(5.79) we finally arrive at the secular equation in the wave vector representation:

$$\det | \sum_L \tilde{T}_l(E, \varepsilon_n) S_L(\mathbf{k} + \mathbf{g}_n, \mathbf{k} + \mathbf{g}_{n'}) | = 0. \quad (5.80)$$

This equation is reminiscent of the APW secular equation ((4.19) combined with (4.62)) which may be rewritten as

$$\det \left| (\varepsilon_n - E) \left(\delta_{nn'} - \frac{4\pi R^2}{\Omega_0} \frac{j_1(|\mathbf{g}_n - \mathbf{g}_{n'}| R)}{|\mathbf{g}_n - \mathbf{g}_{n'}|} \right) + \sum_L \tilde{T}_l(E, \varepsilon_n) S_L(n, n') \right| = 0, \quad (5.81)$$

where R is the range of the potential, Ω_0 the volume of the Wigner-Seitz cell, and \tilde{T}_l is given by (4.113) outside the isoenergetic surface (as in (5.76)).

In the atomic sphere approximation we know that

$$\frac{4\pi R^2}{\Omega_0} \frac{j_1(|\mathbf{g}_n - \mathbf{g}_{n'}| R)}{|\mathbf{g}_n - \mathbf{g}_{n'}|} \rightarrow \delta_{n,n'}$$

(see Sec. 4.5.3, Eq. (4.118)). The only remaining term in the APW secular equation (5.81) is then the last one and (5.81) coincides with (5.80). It is also clear that if F is formally set equal to ε_n in the KKRZ-type secular equation (5.79), then all the three secular equations will be the same. It should be noted that within the APW method, the secular equation (5.80) can only be obtained in the atomic sphere approximation, that is, by approximating the *potential*; within the generalized KKRZ method using a specially chosen X matrix, (5.80) is obtained, as it were*, by the choice of the *variational parameter* F ; and finally, we have seen that (5.80) can be derived *exactly* (Eqs. (5.77)-(5.80)). This is reminiscent of the Austin-Heine-Sham theorem (Sec. 2.4.3) according to which there are more than one pseudopotentials by which one and the same scatterer may be described.

To summarize, the APW and KKRZ(KKR) methods devised for band structure studies employ different pseudopotentials; different trial functions imply different "lattice" pseudopotentials, i.e., different effective mediums. It is for this reason that, even though the methods converge differently, the band structures they lead to are the same.

* The explicit form of $\Gamma_{LL'}$ (5.57) and the Green's function formalism as a whole (which led to (5.68)) do not allow us to perform the transformation for $F = \varepsilon_n$. The similarity is therefore only formal.

Part 2

The use of pseudopotential theory for crystal-structure calculations

Chapter 6

Formalism of crystal-structure energy calculations

6.1. Basic assumptions

The total energy of pure metals and binary alloys has been a subject of many pseudopotential studies and general formulae for calculating it have been obtained by many investigators even though the underlying assumptions are essentially the same. A crystal is represented as a system of N periodically arranged positive ions (of one or two species) immersed in an electron gas. For the (more general) case of an alloy, the density of the gas is $\rho_0 = \bar{Z}/\bar{\Omega}$, where $\bar{\Omega}$ is the average atomic volume of the alloy and $\bar{Z} = (1 - c) Z_A + c Z_B$ is the average atomic valency, Z_A , Z_B being the valencies of the A and B components and $(1 - c)$ and c their respective atomic concentrations. For a pure crystal of, say, A atoms, c is zero and $\rho_0 = Z_A/\Omega_A$, as it must.

The total energy of a crystal may be regarded as the sum of two contributions, one of which depends only on the volume, and the other, formally, only on the structure. The former, U_0 , includes terms which are independent of the atomic distribution, namely, the kinetic energy of free electrons, the exchange-correlation energy, etc. [17, 73]. The structure-dependent energy is the sum of the electrostatic energy U_{es} and the band energy U_{bs} . An expression for U_0 may be found elsewhere [17, 73]; the derivation of U_{es} and U_{bs} is given in this chapter.

6.2. Band structure energy of pure metals and binary alloys

The first calculations of an alloy's band energy were attempted in [398] for a nonlocal and in [399] for local potential. The latter case is easier to handle and will be discussed first. The discussion is mainly based on [400-404].

We showed in the Introduction that second-order perturbation theory approximates the band energy to*

$$U_{\text{bs}} = \frac{\bar{\Omega}}{8\pi} \sum_{\mathbf{q}}' q^2 |\mathcal{W}_{\text{cr}}^b(\mathbf{q})|^2 \frac{1 - \epsilon(\mathbf{q})}{\epsilon^*(\mathbf{q})}, \quad (6.1)$$

where $\mathcal{W}_{\text{cr}}^b(\mathbf{q})$ is the formfactor of the crystal pseudopotential. In order to obtain U_{bs} explicitly, the crystal pseudopotential must be expressed either in terms of the ion pseudopotentials or their formfactors. Recall that $\mathcal{W}_{\text{cr}}^b(\mathbf{r})$ and its Fourier transform are related by

$$\mathcal{W}_{\text{cr}}^b(\mathbf{q}) = \frac{1}{\Omega} \int e^{-i(\mathbf{k}+\mathbf{q})\cdot\mathbf{r}} \mathcal{W}_{\text{cr}}^b(\mathbf{r}) e^{i\mathbf{k}\cdot\mathbf{r}} d\mathbf{r}. \quad (6.2)$$

Next we represent $\mathcal{W}_{\text{cr}}^b(\mathbf{r})$ in terms of ion pseudopotentials

$$\mathcal{W}_{\text{cr}}^b(\mathbf{r}) = \frac{1}{N} \sum_{\nu\mu} W_{\nu\mu}^b(\mathbf{r} - \mathbf{t}_{\nu\mu}), \quad (6.3)$$

where ν labels the lattice site and μ indicates the species of the ion.

In the following treatment, we shall assume the ions of a crystal to occupy all (and only) the lattice sites. In a real problem, this perfect order may be violated by thermal vibrations, lattice defects, or the difference between the atomic radii of the components. These effects can, in principle, be included and will be discussed later.

We shall consider, for generality, the case of an alloy; pure-metal expressions will be obtained in the limit of zero impurity concentration.

Let the quantity c_ν be unity or zero depending on whether the ν th site is occupied by a B or, respectively, an A atom**. $\mathcal{W}_{\text{cr}}^b(\mathbf{r})$ then takes the form

$$\mathcal{W}_{\text{cr}}^b(\mathbf{r}) = \frac{1}{N} \sum_{\nu} \{(1 - c_\nu) W_A^b(\mathbf{r} - \mathbf{t}_\nu) + c_\nu W_B^b(\mathbf{r} - \mathbf{t}_\nu)\}. \quad (6.4)$$

Obviously, the summation in (6.4) is over all ν . Substituting (6.4) into (6.2) we obtain

$$\mathcal{W}_{\text{cr}}^b(\mathbf{q}) = \frac{1}{N} \sum_{\nu} \{(1 - c_\nu) W_A^b(\mathbf{q}) e^{-i\mathbf{q}\cdot\mathbf{t}_\nu} + c_\nu W_B^b(\mathbf{q}) e^{-i\mathbf{q}\cdot\mathbf{t}_\nu}\}. \quad (6.5)$$

In this expression, we can separate out the average value $\overline{\mathcal{W}_{\text{cr}}^b}(\mathbf{q})$ by adding and subtracting, at each site, the averaged Fourier trans-

* Throughout this part of the book, the pseudopotential of an (unscreened) ion is labeled with the superscript b for bare.

** It would be more proper to speak of ions. Traditionally, however, lattice sites are said to be occupied by atoms.

form of the alloy atomic pseudopotential. We have

$$\mathcal{W}_{\text{cr}}^b(\mathbf{q}) = \frac{1}{N} \sum_{\mathbf{v}} \overline{W^b}(\mathbf{q}) e^{-i\mathbf{q}\mathbf{t}_{\mathbf{v}}} + \frac{1}{N} \sum_{\mathbf{v}} (c_{\mathbf{v}} - c) \Delta W^b(\mathbf{q}) e^{-i\mathbf{q}\mathbf{t}_{\mathbf{v}}}. \quad (6.6)$$

Here

$$\overline{W^b}(\mathbf{q}) = c W_B^b(\mathbf{q}) + (1 - c) W_A^b(\mathbf{q}), \quad (6.7)$$

$$\Delta W^b(\mathbf{q}) = W_B^b(\mathbf{q}) - W_A^b(\mathbf{q}). \quad (6.8)$$

Since $\overline{W^b}(\mathbf{q})$ and $\Delta W^b(\mathbf{q})$ are independent of \mathbf{v} , they can each be taken out of its respective sum. The remaining expressions will be denoted

$$\frac{1}{N} \sum_{\mathbf{v}} e^{-i\mathbf{q}\mathbf{t}_{\mathbf{v}}} = S(\mathbf{q}),$$

$$\frac{1}{N} \sum_{\mathbf{v}} (c_{\mathbf{v}} - c) e^{-i\mathbf{q}\mathbf{t}_{\mathbf{v}}} = C(\mathbf{q}). \quad (6.9)$$

In our case of a perfectly periodic infinite lattice,

$$S(\mathbf{q}) = \delta_{\mathbf{q}, \mathbf{g}_n}, \quad (6.10)$$

where \mathbf{g}_n is any (n th) reciprocal lattice vector. At the same time

$$C(\mathbf{q} = \mathbf{g}_n) = \frac{1}{N} \sum_{\mathbf{v}} (c_{\mathbf{v}} - c) e^{-i\mathbf{g}_n \mathbf{t}_{\mathbf{v}}} \equiv 0 \quad (6.11)$$

so that

$$S(\mathbf{q}) C(\mathbf{q}) \equiv 0. \quad (6.12)$$

As a result,

$$|\mathcal{W}_{\text{cr}}^b(\mathbf{q})|^2 = S(\mathbf{q}) S^*(\mathbf{q}) |\overline{W^b}(\mathbf{q})|^2 + C(\mathbf{q}) C^*(\mathbf{q}) |\Delta W^b(\mathbf{q})|^2 \quad (6.13)$$

which, when substituted in (6.1), yields

$$U_{\text{bs}} = \frac{\overline{\Omega}}{8\pi} \sum_{\mathbf{q}}' q^2 \frac{1 - \varepsilon(\mathbf{q})}{\varepsilon^*(\mathbf{q})} [S(\mathbf{q}) S^*(\mathbf{q}) |\overline{W^b}(\mathbf{q})|^2 + C(\mathbf{q}) C^*(\mathbf{q}) |\Delta W^b(\mathbf{q})|^2]. \quad (6.14)$$

Of the two terms in (6.14), the first one is proportional to the squared average formfactor of the alloy atoms (in a pure crystal, to the squared formfactor of the constituent atom); the second term is only meaningful for alloys. The first term may be written

$$\begin{aligned} U_{\text{bs}}^{(1)} &= \frac{\overline{\Omega}}{8\pi} \sum_{\mathbf{q}}' q^2 \frac{1 - \varepsilon(\mathbf{q})}{\varepsilon^*(\mathbf{q})} |\overline{W^b}(\mathbf{q})|^2 \delta_{\mathbf{q}, \mathbf{g}_n} \\ &= \frac{\overline{\Omega}}{8\pi} \sum_n' g_n^2 \frac{1 - \varepsilon(\mathbf{g}_n)}{\varepsilon^*(\mathbf{g}_n)} |\overline{W^b}(\mathbf{g}_n)|^2. \end{aligned} \quad (6.15)$$

It is thus reduced to a sum over reciprocal lattice vectors (except $\mathbf{g}_n = 0$) and is therefore only determined by the (discrete) values the functions $\varepsilon(\mathbf{q})$, $\varepsilon^*(\mathbf{q})$ and $W(\mathbf{q})$ take on at $\mathbf{q} = \mathbf{g}_n$. If the energy of an alloy depends on this term alone, then when an alloy is being considered instead of a pure crystal it is enough to replace Ω and $W(\mathbf{q})$ by $\bar{\Omega}$ and $\bar{W}(\mathbf{q})$ respectively. It should however be remembered that the differences in interatomic separation and average valency between pure crystals and alloys may alter the screening functions and formfactors of the constituent atoms. To take account of this, the formfactor of an alloy atom, $W_\mu(\mathbf{q})$, is often expressed in terms of the formfactor of the pure-metal ion, $W_\mu^{\text{met}}(\mathbf{q})$,

$$W_\mu(\mathbf{q}) = \frac{\Omega^{(\mu)} \varepsilon_\mu(\mathbf{q})}{\bar{\Omega} \bar{\varepsilon}(\mathbf{q})} W_\mu^{\text{met}}(\mathbf{q}), \quad (6.16)$$

where $\Omega^{(\mu)}$ and $\varepsilon_\mu(\mathbf{q})$ are respectively the specific atomic volume and the dielectric permittivity of an atom of the μ species as a pure component. There is no entire agreement, however, as to the value of this approach as many workers consider (6.16) to be oversimplified.

The next question to be examined is the crystal-structure stability from the point of view of the function $U_{\text{bs}}^{(1)}$. It is convenient to re-write this function as

$$U_{\text{bs}}^{(1)} = \sum_n' |\bar{W}^b(\mathbf{g}_n)|^2 \frac{\chi(\mathbf{g}_n)}{\varepsilon^*(\mathbf{g}_n)} = \sum_n' \Phi_{\text{bs}}(\mathbf{g}_n). \quad (6.17)$$

The quantity $\Phi_{\text{bs}}(\mathbf{g}_n)$ is called the (band structure) characteristic function.

It follows from (6.17) that a crystal structure is the more stable the larger the magnitude of $\Phi_{\text{bs}}(\mathbf{g}_n)$ at the points corresponding to the vectors \mathbf{g}_n of the structure (recall that $\Phi_{\text{bs}}(\mathbf{q}) < 0$ because $\chi(\mathbf{q}) < 0$). The stability of a given structure thus depends on the properties of the function $\Phi_{\text{bs}}(\mathbf{g}_n)$.

The behavior of this function as a whole is determined by the \mathbf{q} -dependences of the functions it is composed of. In this section we will therefore discuss the behavior of the dielectric permeability $\varepsilon(\mathbf{q})$, the Lindhard function $\chi(\mathbf{q})$, and a typical pseudopotential $W(\mathbf{q})$ and its absolute square.

We first consider the function $\chi(q)$. In Fig. 6.1 we plot this function, as given by the Fermi-sphere approximation,

$$\chi(q) = -\frac{3}{8} \frac{Z}{E_F} \left[1 + \frac{1-\eta^2}{2\eta} \ln \left| \frac{1+\eta}{1-\eta} \right| \right], \quad (6.18)$$

where $\eta = q/2k_F$. It can be seen that $\chi(q)$ is everywhere negative and its absolute magnitude is a maximum at $q = 0$, and $\chi(0) = (-3/8) Z/E_F$. The function changes fastest in the vicinity of $q = 2k_F$, where the term containing $(1 - \eta) \ln |1 - \eta|$ gives rise

to a relatively weak singularity of the type $0 \times \ln 0$. The singularity becomes more pronounced in the derivatives: it is of the type $\ln 0$ in the first and 0^{-1} in the second derivative. For q larger than $2k_F$, $|\chi(q)|$ becomes small and so does $\Phi_{bs}(q)$.

The dielectric permittivity $\epsilon(q)$ is everywhere positive (Fig. 6.2), diverges at $q \rightarrow 0$ as q^{-2} and rapidly approaches unity with increasing q . Its singularity at $q \simeq 2k_F$ is similar to that in $\chi(q)$.

The behavior of $\epsilon(q)$ is very similar to that of $\epsilon^*(q)$, the only difference being that the factor $f(q)$ [146] makes $\epsilon^*(q)$ approach unity more rapidly with increasing q . All in all, because of the rapid decrease of $|\chi(q)/\epsilon^*(q)|$ with q , we see that U_{bs} is dominated by $\Phi_{bs}(q)$ for q not appreciably exceeding $2k_F$. We must, however, add

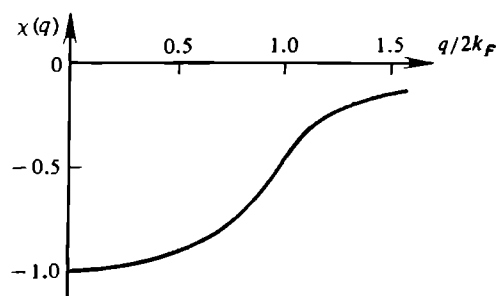
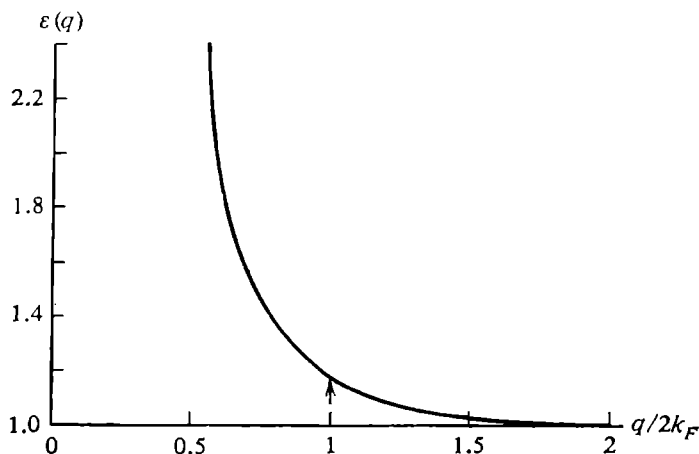


Fig. 6.1. Lindhard function.

Fig. 6.2. Dielectric permittivity as a function of q .

a note of caution: the $\Phi_{bs}(q)$ for $q > 2k_F$ cannot be neglected until after a careful analysis of the convergence properties of U_{bs} ; otherwise the resulting value of U_{bs} may be totally incorrect.

The next function to be examined is $W(q)$. We have shown that in principle a local screened pseudopotential tends to $-(2/3)E_F^0$ as $q \rightarrow 0$. The magnitude of $W(q)$ increases with q , passes through zero at $q \simeq 0.8 \times 2k_F$ (usually denoted as q_0), reaches a maximum at $q \simeq 1.2 \times 2k_F$, and then decreases to zero. For some types of pseudopotential formfactor, oscillations may occur at relatively large q .

They are usually eliminated by the damping factor $D(q) = \exp(-0.03 (q/2k_F)^4)$ [405].

It can be seen from (6.17) that the values of \mathbf{q} which determine the $|W(\mathbf{q})|^2$ in the band structure energy correspond to reciprocal lattice vectors for which $S(q)$ is different from zero. Hence as far as stability of a crystal structure is concerned, we are mainly interested in $|W(\mathbf{g}_n)|^2$ for the first few reciprocal lattice vectors of the structure under study.

It will be convenient in the following to choose unit length for \mathbf{q} to be $2\pi/R_a$, R_a being the radius of the Wigner-Seitz sphere. In this scale, the BCC, FCC and HCP structures have the same value of $2k_F$, namely, $(9Z/4\pi^2)^{1/3}$, Z being the ionic charge. This means that for $Z = 1, 2, 3, 4$ the quantity $2k_F$ is, respectively, 0.611, 0.770, 0.881 and 0.970. The lengths of the first reciprocal lattice vectors are in this scale (i) 0.696 and 0.895 for the BCC vectors (110) and (200); (ii) 0.677, 0.782, and 1.105, for the FCC vectors (111), (200) and (220); (iii) 0.638, 0.677, 0.722 and 0.930 for the HCP vectors (100), (002), (011), and (102).

Comparing these lengths with $2k_F$ shows that for the above close-packed structures, they are in the range between 1 and $3k_F$. The point $q_0 (\simeq 1.6k_F)$ also falls within this range. In pure crystals, the low \mathbf{q} region (where the singularity in $\epsilon(q)$ occurs) does not contain the \mathbf{g}_n vectors and therefore has little effect on stability.

There are a number of factors which may affect quantitative results. These are the properties of the pseudopotentials and their formfactors, the manner in which s - d hybridization is included (in the transition, noble, alkali earth and other metals), exchange-correlation effects, etc. The way in which the particular result has been obtained will be described in some detail in future discussions of the energetics of a specific material.

Now that we have obtained some insight into the behavior of the characteristic function as a whole, we are ready to discuss the main factors which determine the structural stability of pure crystals. We begin with an analysis of the function's behavior in \mathbf{q} space. In doing so we use aluminum as an example because it was one of the first materials to have been studied by the pseudopotential method. In Fig. 6.3 we plot the function $\Phi_{bs}(q)$ for Al together with the values of $|\mathbf{g}_n|$ which correspond to the BCC, FCC and HCP structures.

Since the values of $\Phi_{bs}(q)$ for $q \simeq q_0$ contribute very little to U_{bs} , the first vectors in the BCC and FCC structures are of little importance, as are the first two in the HCP structure. As for the rest the largest contribution to $\Phi_{bs}(q)$ comes from the (200) vector of the FCC structure, which makes this the most stable structure for aluminum, in full agreement with experiment. We thus see that, to predict qualitatively the structural stability of pure crystals, the

relative positions of q_0 and the first few reciprocal lattice vectors must be studied for the major crystal structures. A structure will not arise if its first vectors are close to q_0 . It will have a certain amount of stability if at least some of the corresponding reciprocal lattice vectors are lower in magnitude than $2k_F$, because for $q > 2k_F$ the quantity $|\chi(q)/\epsilon^*(q)|$ is relatively small.

A general formulation of this rule might be: structures for which there are a large number of reciprocal lattice vectors whose magnitudes are less than $2k_F$ and at the same time are sufficiently different

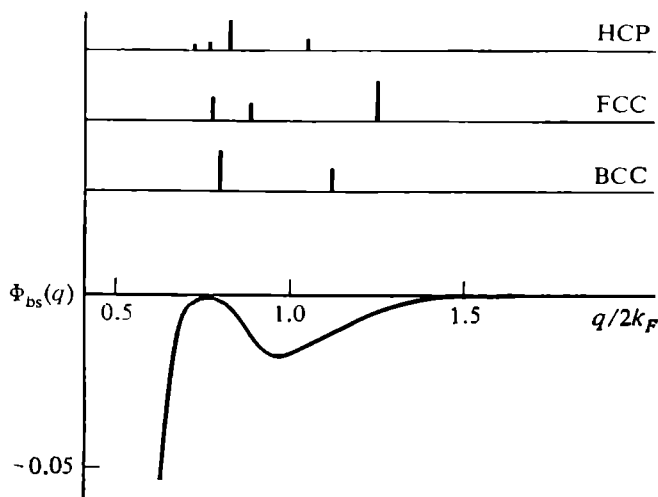


Fig. 6.3. Characteristic function $\Phi_{bs}(q)$ for Al.

from q_0 are stable. The rule is confirmed by a great many examples and even holds for the distorted crystal structures that gallium and mercury adopt.

The rule explains the stability of the structures certain pure metals and semiconductors adopt and may be useful for preliminary analysis of relevant data. It will be realized, however, that a complete explanation of stability would require a total energy calculation including the electrostatic interaction and the contribution from the characteristic function for many reciprocal vectors. To illustrate this we again take aluminum as an example.

The band, electrostatic, and total energies of aluminum were calculated in [154]. The band energy was calculated by summing over more than a hundred reciprocal lattice vectors. Table 6.1 presents these band, electrostatic, and total energies in units of $Z^2/2R_A$.

It can be seen that, judging by the electrostatic energy alone, the most stable structure is BCC, while the least stable are the hexagonal structures whose axial c/a ratios differ from the ideal value, which is 1.633. If only band energy is considered for only the BCC, FCC and HCP ($c/a = 1.633$) structures then BCC has the lowest stability

and FCC the highest (this also follows from the relative positions of g_n and q_0 in these structures). It should be noted that these structures differ more in band energy than in electrostatic energy, so that it is in fact the band energy contribution that determines the sequence of structures in terms of total energy.

Table 6.1. The parameters α_{es} , α_{bs} , α_{total} for Al

Structure	c/a	$-\alpha_{es}^*$	$-\alpha_{bs}$	$-\alpha_{total}$
BCC	1	1.79186	0.01247	1.80433
FCC	1	1.79172 **	0.01414	1.80585
Hexagonal	1.5	1.78998	0.01489	1.80487
Hexagonal	1.6	1.79156	0.01395	1.80551
HCP	1.633	1.79168	0.01390	1.80558
Hexagonal	1.7	1.79129	0.01420	1.80553
Hexagonal	1.8	1.78909	0.01583	1.80492
Hexagonal	1.9	1.78497	0.01874	1.80370

* Note that α_{es} is the same for all materials having the same structure as that assumed for Al.

** The latest data is 1.79175.

It would be wrong, however, to deduce from this that the electrostatic energy is not important for stability. Calculations show that, from the energy band point of view, the hexagonal structure, whose axial c/a ratio is far from ideal, is most favored. The departure of a hexagonal structure from close packing leads to an increase in U_{es} , which compensates for the band structure effects in such a way that the total energy turns out to be lowest for FCC (which is indeed observed).

This shows, incidentally, that $\Phi_{bs}(g_n)$ for a few first g_n are insufficient for a stability analysis, and U_{bs} for a large number of g_n must be added.

Thus the minimum total energy, or the stability condition for a particular crystal structure, comes as a result of an interplay between the band and electrostatic contributions, and generally no single factor may be claimed to uniquely determine the actual structure. There are however factors which may be considered to be responsible, to some degree, for certain properties of a crystal structure. For example, the electrostatic energy contribution secures the formation of close-packed structures, and the choice of the most stable of these is determined by the band energy (and, in particular, by the rule that the $|g_n|$ must be less than $2k_F$ and lie away from q_0).

The occurrence of distorted structures in metals cannot be caused by the electrostatic contribution, but is related to the behavior of the characteristic function and is, as a rule, due to q_0 being close to the positions of \mathbf{g}_n in close-packed structures. The behavior of the characteristic function is determined, in this context, by the form of pseudopotential.

It is worthwhile discussing how the structure is affected by the structure-independent contribution to the total energy. This might sound paradoxical considering our statement at the beginning of this chapter that this contribution is only determined by the free electron gas and has no effect on the arrangement of the atoms. Actually, the statement was only partially true because it is the structure-independent contribution which is responsible for most (90%) of the interatomic separations in a crystal, the structure-dependent contribution to the total energy controlling the remaining 10%. The energy U_0 thus approximately determines the interatomic separation in a metal of a given valency and hence the geometry of the \mathbf{g}_n vectors of the various possible crystal structures. Depending on their positions relative to q_0 (which depends on the behavior of the form-factor of the pseudopotential, which is determined, in turn, by the electron-ion and electron-electron interactions), a specific structure is preferred. Thus the structure-dependent contribution determines the arrangement of atoms at approximately constant volume. It is important to realize that the division of the energy into the structure-dependent and structure-independent parts is to some extent arbitrary.

Thus far we have discussed the behavior of the energy contributions in reciprocal \mathbf{q} space. Any function, however, may be described in both reciprocal and direct spaces, and it is of interest to repeat our analysis for a direct-space representation of the energy.

The corresponding expressions for the band and total energies may be found by using the potentials of indirect and total interatomic interaction, respectively $\Phi_{bs}(\mathbf{r})$ and $\Phi(\mathbf{r})$. These were defined in the Introduction as

$$\begin{aligned}\Phi_{bs}(\mathbf{r}) &:= \frac{2\Omega}{(2\pi)^3} \int \Phi_{bs}(\mathbf{q}) e^{i\mathbf{q}\cdot\mathbf{r}} d\mathbf{q}, \\ \Phi(\mathbf{r}) &= \frac{(Ze)^2}{r} + \Phi_{bs}(\mathbf{r}).\end{aligned}\tag{6.19}$$

The band energy may be expressed as

$$U_{bs} = \frac{1}{2N} \sum_j \sum_{j'} \Phi_{bs}(|\mathbf{r}|).\tag{6.20}$$

At large r , the function $\Phi_{bs}(r)$ describes an attractive Coulomb potential. This can be understood by remembering that at small q ,

$\Phi_{bs}(q) \propto q^{-2}$ and that the Fourier transform to real space for functions of this type behaves as r^{-1} at large distances.

An interesting feature of $\Phi_{bs}(r)$ and $\Phi(r)$ is their nonmonotonic oscillatory behavior with increasing r ; at large r they take the form of Friedel oscillations of the type $(k_F r)^{-3} \cos 2k_F r$. These originate [89] from the strong singularities of the type $(1 - \eta)^{-1}$ occurring at $q \simeq 2k_F$ in the second derivative of the characteristic function.

The function $\Phi(r)$ also oscillates at moderate r 's but the oscillations are generally determined both by singularities in $\epsilon(q)$ and by the behavior of the pseudopotential formfactors. In this region, the

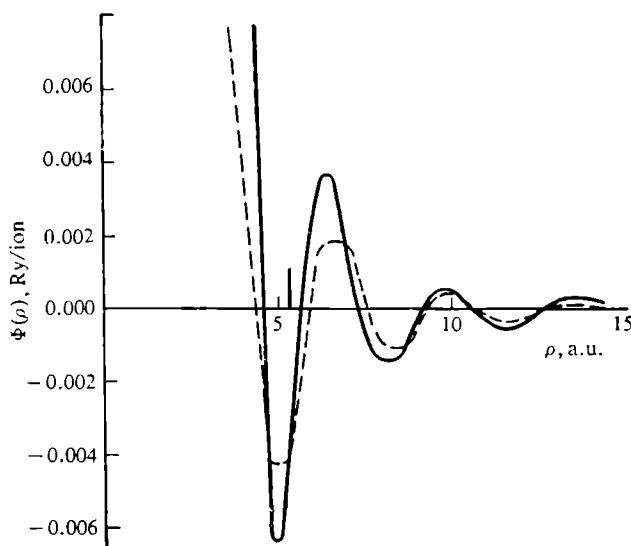


Fig. 6.4. Interatomic potential $\Phi(r)$ for Al. Bold line—pseudopotential calculation, dashed line—asymptotic approximation.

position of the first minimum of $\Phi(r)$ which, in principle, must be related to the nearest-neighbor distance of the crystal is of interest. Figure 6.4 shows the $\Phi(r)$ for aluminum calculated for the first few coordination spheres. It can be seen that the position of the minimum does indeed correspond to the nearest-neighbor distance.

The reader is reminded, however, that the interatomic separation is determined by both the structure-dependent contribution to the total energy and the structure-independent contribution. The function $\Phi(r)$ has been obtained from the former and should therefore be corrected by a term related to the latter. As this will include a rather strong interatomic interaction, the separation may be shifted by the correction from a minimum of the potential to its maximum, which is related to the structure and thereby to atomic redistributions. The energy of the crystal may then be reduced and because some of the atoms will be closer together and some farther apart, the "ideal" structure will in fact be distorted. This is indeed the mechanism re-

sponsible for the distortions in the crystal structures of gallium and mercury.

The topic of stability may thus be approached equally in terms of direct and reciprocal space. From the purely mathematical viewpoint, the direct approach is less convenient because a great many terms each of which oscillates with the number of coordination sphere, must be summed. The direct space is however often better suited for a qualitative analysis and yields more insight into the physics of the results.

Although these arguments are widely used for the stability analysis of crystal structures, the theory is being developed in several ways, e.g. improvements in the exchange and correlation corrections, and searches for more effective pseudopotentials to include nonlocality, *d* and *f* resonances, and *sd* hybridization [3].

We wish now to address another topic of general importance, namely, the crucial relationship between the Fermi sphere and the Brillouin zone boundary. When these touch we have

$$2k_F = g_n, \quad (6.21)$$

and the denominator of the second-order energy term goes to zero. According to Jones [406, 9], the resulting singularity in $\epsilon(q)$ minimizes U_{bs} and is therefore the reason for the phase transitions which occur at the (critical) electron concentrations satisfying (6.21); the electron concentrations are governed by the Hume-Rothery rules.

The second-order perturbation theory result for the dispersion $E(\mathbf{k})$ is

$$E(\mathbf{k}) = \frac{1}{2} \mathbf{k}^2 + \langle \mathbf{k} | W | \mathbf{k} \rangle + \sum_n' \frac{|\langle \mathbf{k} + \mathbf{g}_n | W | \mathbf{k} \rangle|^2}{\frac{1}{2} (\mathbf{k}^2 - |\mathbf{k} + \mathbf{g}_n|^2)}. \quad (6.22)$$

It can be seen from Fig. 6.5 that $E(\mathbf{k})$ as given by (6.22) has a singularity in the neighborhood of the energy gap. In a two-wave model, the exact expression for $E(\mathbf{k})$ is found near the Brillouin zone boundary from the secular equation

$$\begin{vmatrix} \frac{1}{2} \mathbf{k}^2 - E(\mathbf{k}) & W_{\mathbf{g}_n} \\ W_{\mathbf{g}_n} & \frac{1}{2} |\mathbf{k} + \mathbf{g}_n|^2 - E(\mathbf{k}) \end{vmatrix} = 0 \quad (6.23)$$

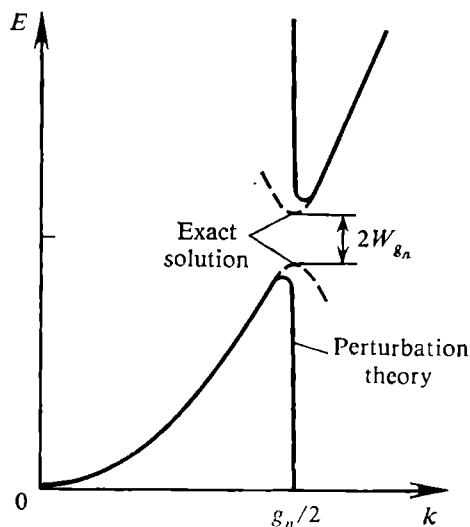


Fig. 6.5. Dispersion law $E(\mathbf{k})$.

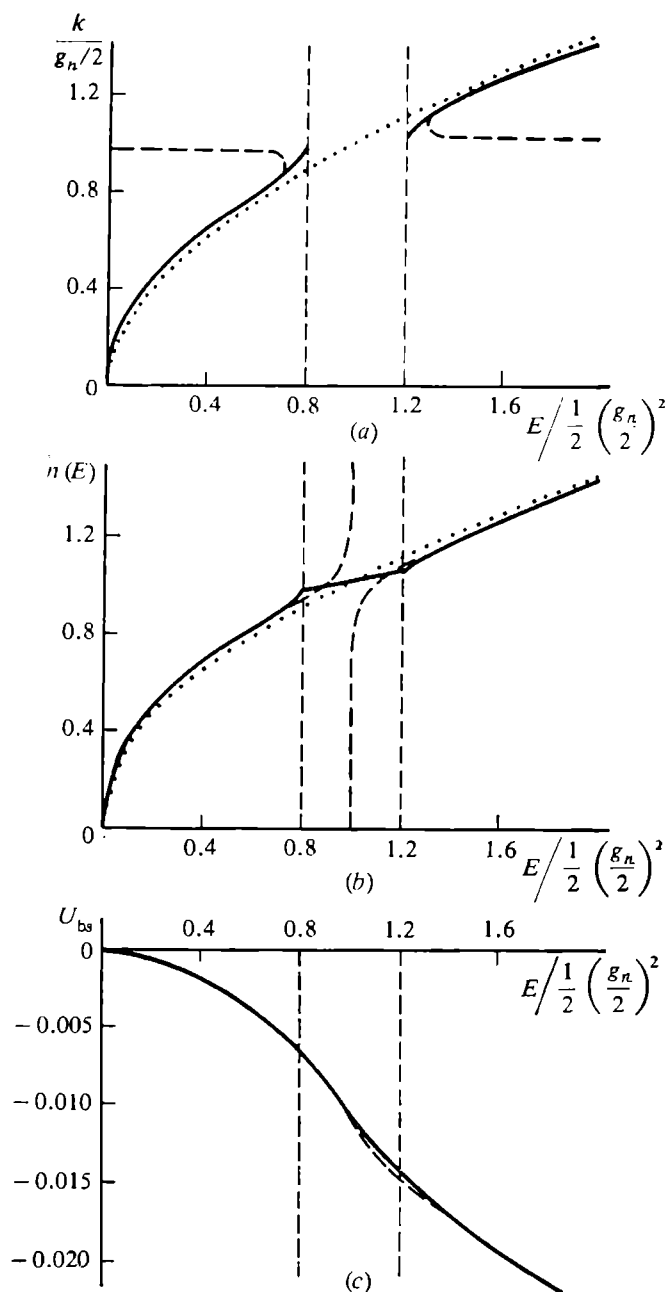


Fig. 6.6. (a) Dispersion law, (b) density of states, (c) the departure U_{bs} of the total energy from the free-electron value near the Brillouin zone boundary. Bold lines—exact solution, dashed lines—second-order perturbation theory, dotted lines—free-electron gas. The vertical lines correspond to the condition $g_n = 2k_F$.

and its explicit form is

$$E(\mathbf{k}) = \frac{1}{4} \left\{ \mathbf{k}^2 + |\mathbf{k} + \mathbf{g}_n|^2 \pm \left[\frac{1}{2} \mathbf{k}^2 - \frac{1}{2} |\mathbf{k} + \mathbf{g}_n|^2 + 4W_{\mathbf{g}_n}^2 \right]^{1/2} \right\}, \quad (6.24)$$

where $W_{\mathbf{g}_n} \equiv \langle \mathbf{k} + \mathbf{g}_n | W | \mathbf{k} \rangle$. Figure 6.5 also shows $E(\mathbf{k})$ as given by (6.24). Comparing (6.22) and (6.24) indicates that the second-order approximation for $E(\mathbf{k})$ is unsatisfactory near the Brillouin zone boundary.

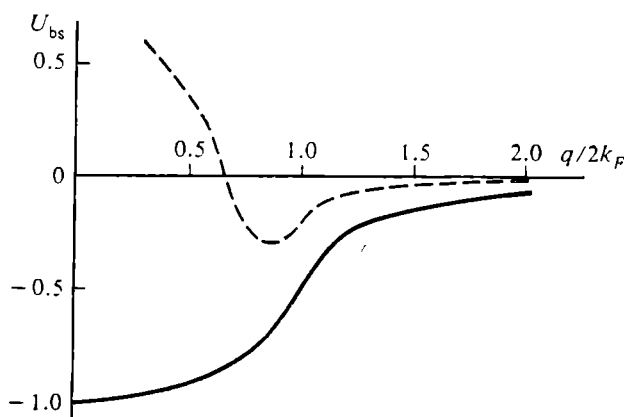


Fig. 6.7. U_{bs} plotted as a function of $q/2k_F$ for a single Brillouin zone face. The summation is over the entire Fermi sphere (bold line) and over the cone of solid angle $4\pi/N$ (dash line).

The density of states in a metal and the corresponding total energy (per ion) have been exactly calculated in [407]. These formulae are too cumbersome to reproduce, but Figure 6.6 shows $E(\mathbf{k})$, $n(E)$, and U_{bs} calculated both from these formulae and from second-order perturbation theory, Eq. (6.22). Although $E(\mathbf{k})$ and $n(E)$ differ substantially in these two cases, the two U_{bs} plots as functions of the number of electrons only slightly differ and in neither case is there a minimum at $g_n \simeq 2k_F$. The results of [407] are significant for a number of reasons.

First, they disprove Jones's idea [406] that band energy minima occur at points where the Fermi sphere (surface) touches the boundary of the Brillouin zone; his interpretation of the Hume-Rothery rules is therefore devalued. According to [407], Jones's results can be explained by the way he treated the summations in the total-energy calculations; namely, instead of summing over the entire Fermi surface, Jones only considered a cone of solid angle $4\pi/N_p$, N_p being the number of equivalent faces of the Brillouin zone. As a result, the energy-gap effect was largely ignored (see Fig. 6.7).

Second, it was predicted that the total energy varies rapidly around $g_n \simeq 2k_F$ due to the square-root-type van Hove singularities in the density-of-state function; these lead to discontinuities in the third and higher derivatives:

$$\left. \frac{d^3 U_{bs}}{dZ^3} \right|_{E_F} = - \frac{1}{n(E_F)^3} \left(\frac{dn(E)}{dE} \right)_{E_F}. \quad (6.25)$$

These variations may reduce the structural stability of a phase for which g_n happens to be equal to $2k_F$. However, since U_{bs} decreases

very smoothly with Z , no strict criterion may be suggested by which the stability range of a particular crystal structure can be found. It should be remarked though that a transition is most likely at $g_n \simeq 2k_F$, where U_{bs} varies somewhat more rapidly than elsewhere [419].

Finally, it turns out that the band-structure energy may in many cases be calculated by combining second-order perturbation theory, Eq. (6.22), with the Fermi sphere approximation. According to [407] the reason for this is that the relevant summations are over

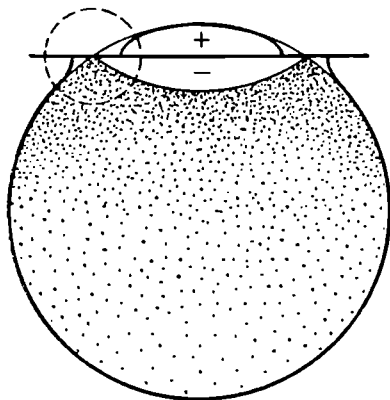


Fig. 6.8. The regions contributing to the total energy. The “+” and “-” regions cancel out.

occupied states lying both below and above the energy gap. Since $E(\mathbf{k})$ in either region are symmetric in \mathbf{k} , the corresponding contributions essentially cancel each other out and the resulting error turns out to be very small. This is clearly illustrated in Fig. 6.8.

Sometimes, however, the interpretation of an experiment depends on U_{bs} difference (for different phases) rather than on the U_{bs} values themselves. In this case, even a small discrepancy between the exact and second-order results may prove crucial, which is indeed the case [276, 408, 409] so that higher-order terms are needed. It would be interesting of course to study the higher-order contributions in a manner similar to that of [407]. It also seems necessary to investigate if the above conclusions retain their validity for nonlocal OPW calculations.

Thus far we have only been concerned with the $U_{bs}^{(1)}$ term, so, strictly speaking, our considerations are only valid for a stability analysis of pure crystals. Nevertheless, the energetics of alloys have also been treated in this manner, especially in the earlier papers. This approach is called in this context the virtual (or average) crystal approximation. A more correct total energy calculation must certain-

ly include the term $U_{bs}^{(2)}$ which is

$$U_{bs}^{(2)} = \frac{\bar{\Omega}}{8\pi} \sum_{\mathbf{q}} \mathbf{q}^2 \frac{1 - \varepsilon(\mathbf{q})}{\varepsilon^*(\mathbf{q})} C(\mathbf{q}) C^*(\mathbf{q}) |\Delta W^b(\mathbf{q})|^2. \quad (6.26)$$

The difference between the Fourier transforms of the potentials of the components must generally be less than their average value (for the same \mathbf{q}). This appears to be a sufficient argument for neglecting $U_{bs}^{(2)}$. But it is not. The $U_{bs}^{(1)}$ term is a sum over the \mathbf{q} 's which are equal to the reciprocal lattice vectors. The summation in (6.26) is over the continuum of \mathbf{q} values including the relatively small ones for which the formfactors $W_A^b(\mathbf{q})$, $W_B^b(\mathbf{q})$ may be considerably larger than $W_A^b(\mathbf{g}_n)$, $W_B^b(\mathbf{g}_n)$. Hence the difference between the pseudopotential formfactors of the components may be comparable with (and perhaps even larger than) the average formfactor. Neglecting the second contribution in (6.14) thus becomes very questionable.

We will obtain various explicit expressions for (i) complete disorder, (ii) complete order, and (iii) short-range order depending on the manner in which atoms of different species are distributed over lattice sites.

In the first case we deal with a disordered alloy, by which we mean, here and in the following, that it has no long-range order. Thus its atoms are distributed over the sites either completely at random or with some degree of short-range order. For such an alloy we have, by (6.9),

$$C(\mathbf{q}) C^*(\mathbf{q}) = \frac{1}{N^2} \sum_{\mathbf{v}} \sum_{\mathbf{v}'} \langle (c_{\mathbf{v}} - c)(c_{\mathbf{v}'} - c) \rangle e^{-i\mathbf{q} \cdot (\mathbf{t}_{\mathbf{v}} - \mathbf{t}_{\mathbf{v}'})}. \quad (6.27)$$

Since $c_{\mathbf{v}} = 1$ only if the \mathbf{v} th site is occupied by a B atom,

$$c_{\mathbf{v}} c_{\mathbf{v}'} = c P_{\mathbf{v}\mathbf{v}'}^{BB}, \quad (6.28)$$

where $P_{\mathbf{v}\mathbf{v}'}^{BB}$ is the probability of finding the \mathbf{v} th and \mathbf{v}' th sites simultaneously occupied by B atoms. Substituting (6.28) into (6.27) and denoting $\mathbf{t}_{\mathbf{v}} - \mathbf{t}_{\mathbf{v}'} = \rho_i$, we obtain

$$|C(\mathbf{q})|^2 = \frac{1}{N} \sum_i (c P_i^{BB} - c^2) e^{-i\mathbf{q} \cdot \rho_i}. \quad (6.29)$$

In arriving at this result we utilized the fact that $P_{\mathbf{v}\mathbf{v}'}^{BB}$ decreases rapidly with ρ_i ; the double sum is therefore replaced by a single one and hence the factor $1/N$.

Using the total probability theorem

$$P_i^{BB} + P_i^{BA} = 1 \quad (6.30)$$

and introducing a short-range order parameter [411]

$$\alpha_i = 1 - \frac{P_i^{BA}}{1-c}, \quad (6.34)$$

we find

$$|C(\mathbf{q})|^2 = \frac{c(1-c)}{N} \sum_{\rho_i} \alpha(\rho_i) e^{-i\mathbf{q}\cdot\mathbf{e}_i}, \quad (6.32)$$

the summation running over all ρ_i . Thus, for a crystal with short-range order we have

$$U_{\text{bs}}^{(2)} = \frac{\bar{\Omega}}{8\pi N} \sum_{\mathbf{e}_i} \sum_{\mathbf{q}}' \mathbf{q}^2 \frac{1-\varepsilon(\mathbf{q})}{\varepsilon^*(\mathbf{q})} |\Delta W^b(\mathbf{q})|^2 c(1-c) \alpha(\rho_i) e^{-i\mathbf{q}\cdot\mathbf{e}_i}. \quad (6.33)$$

If $\alpha(\rho_i)$ does not depend on the orientation of ρ_i , we may convert the summation to an integral and then average over all angles between \mathbf{q} and ρ_i to obtain

$$U_{\text{bs}}^{(2)} = c(1-c) \sum_i C_i \alpha_i V_{\text{bs}}(\rho_i). \quad (6.34)$$

Here C_i is the coordination number of the i th coordination sphere and $V_{\text{bs}}(\rho_i)$ is given by

$$V_{\text{bs}}(\rho_i) = \frac{\bar{\Omega}}{\pi^2} \int d\mathbf{q} q^2 \mathcal{F}_{\text{p,bs}}(q) \frac{\sin q\rho_i}{q\rho_i} \quad (6.35)$$

where

$$\mathcal{F}_{\text{p,bs}}(q) = \frac{\bar{\Omega}}{8\pi} |\Delta W^b(q)|^2 q^2 \frac{1-\varepsilon(q)}{\varepsilon^*(q)}. \quad (6.36)$$

In the case of no short-range order (the atoms of both species are distributed completely at random over the lattice sites), all the α_i 's are zero except for α_0 , which is unity. The second band-energy term (which involves formfactor differences of the two components) may then be written in the \mathbf{q} -sum representation as

$$U_{\text{bs, chaotic}}^{(2)} = \frac{\bar{\Omega}}{8\pi} \sum_{\mathbf{q}}' \mathbf{q}^2 \frac{1-\varepsilon(\mathbf{q})}{\varepsilon^*(\mathbf{q})} \left\{ \frac{c}{N} (1-c) |\Delta W^b(\mathbf{q})|^2 \right\}. \quad (6.37)$$

The band energy of a completely disordered alloy thus takes the form

$$U_{\text{bs, chaotic}} = \frac{\bar{\Omega}}{8\pi} \sum_{\mathbf{q}}' \frac{1-\varepsilon(\mathbf{q})}{\varepsilon^*(\mathbf{q})} \mathbf{q}^2 \left\{ |\overline{W^b}(\mathbf{q})|^2 \delta_{\mathbf{q}, \mathbf{g}_n} + \frac{c(1-c)}{N} |\Delta W^b(\mathbf{q})|^2 \right\}. \quad (6.38)$$

Allowing for short-range order we find instead

$$U_{\text{bs,sh}} = \frac{\bar{\Omega}}{8\pi} \sum_{\mathbf{q}}' \mathbf{q}^2 \frac{1-\varepsilon(\mathbf{q})}{\varepsilon^*(\mathbf{q})} \left\{ |\overline{W^b}(\mathbf{q})|^2 \delta_{\mathbf{q},\mathbf{g}_n} + \frac{c(1-c)}{N} \sum_{\rho_i} \alpha(\rho_i) |\Delta W^b(\mathbf{q})|^2 e^{-i\mathbf{q}\cdot\boldsymbol{\rho}_i} \right\}. \quad (6.39)$$

Thus in the absence of long-range order, the energy characteristics of a crystal will be estimated either by (6.38) or (6.39), depending on whether it has short-range order or not. Although short-range order is ubiquitous [412] and, indeed, alloys without it are the exception, most theoretical studies have until now been based on (6.38). This was due to a now out-of-date underestimate of the short-range effects and to a lack of an adequate theory which would allow us to incorporate them correctly into the pseudopotential calculations. Note also the extra numerical difficulties arising from the inclusion of these effects.

We now wish to obtain the U_{bs} for an alloy with long-range order. The above discussion suggests that the task is actually to find the $\mathcal{W}_{\text{cr}}^b(\mathbf{r})$ for this case. If the atoms of an alloy are arranged in a completely ordered manner, a summation over a crystal is conveniently subdivided into (i) sums over the sites \mathbf{v} of the unit cell and (ii) sums over the centers j of the unit cells. We would then have

$$\mathcal{W}_{\text{cr}}^b(\mathbf{r}) = \frac{1}{N} \sum_j \sum_{\mathbf{v}} \{(1-c_{\mathbf{v}j}) W_A^b(\mathbf{r}-\mathbf{t}_{\mathbf{v}j}) + c_{\mathbf{v}j} W_B^b(\mathbf{r}-\mathbf{t}_{\mathbf{v}j})\} \quad (6.40)$$

or, in the \mathbf{q} -space representation

$$\mathcal{W}_{\text{cr}}^b(\mathbf{q}) = \frac{1}{N} \sum_j \sum_{\mathbf{v}} \{(1-c_{\mathbf{v}j}) W_A^b(\mathbf{q}) e^{-i\mathbf{q}\cdot\mathbf{t}_{\mathbf{v}j}} + c_{\mathbf{v}j} W_B^b(\mathbf{q}) e^{-i\mathbf{q}\cdot\mathbf{t}_{\mathbf{v}j}}\}. \quad (6.41)$$

Since all unit cells are by definition identical, the factor $e^{-i\mathbf{q}\cdot\mathbf{t}_j}$ may be taken out of the sum ($\mathbf{t}_{\mathbf{v}j} = \mathbf{t}_{\mathbf{v}} + \mathbf{t}_j$) giving

$$\mathcal{W}_{\text{cr}}^b(\mathbf{q}) = \frac{1}{N} \left\{ \sum_{\mathbf{v}} e^{-i\mathbf{q}\cdot\mathbf{t}_{\mathbf{v}}} \right\} \sum_{\mathbf{v}} [(1-c_{\mathbf{v}}) W_A^b(\mathbf{q}) e^{-i\mathbf{q}\cdot\mathbf{t}_{\mathbf{v}}} + c_{\mathbf{v}} W_B^b(\mathbf{q}) e^{-i\mathbf{q}\cdot\mathbf{t}_{\mathbf{v}}}] \quad (6.42)$$

The first sum here is clearly

$$\frac{1}{N'} \sum_j e^{-i\mathbf{q}\cdot\mathbf{t}_j} = \delta_{\mathbf{q},\mathbf{g}_n}, \quad (6.43)$$

where N' is the number of unit cells in the crystal. This actually means that (6.43) is equivalent to (6.9), except that instead of sum-

ming over the atoms the sum is over the centers of (the) unit cells. The v -summation yields the "pseudopotential" structure amplitude of the unit cell, which is identical in form to an analogous quantity involved in X-ray studies. In the present case, however, it is electron "rays" that are scattered and the role of X-ray atomic factors is taken by the pseudopotential formfactors.

Thus, for crystals having a Cu_3Au -type cubic cell we obtain

$$W_c^b(\mathbf{q}) = \frac{1}{n'} \{ W_B^b(\mathbf{q}) + W_A^b(\mathbf{q}) [e^{-\pi i (H_1 + H_2)} + e^{-\pi i (H_2 + H_3)} + e^{-\pi i (H_3 + H_1)}] \}, \quad (6.44)$$

where n' is the number of atoms in the unit cell.

For reciprocal lattice sites with equal-parity vector components H_1, H_2, H_3 (the basic reciprocal-lattice vectors $\mathbf{g}_{n,f}$ are associated with these) we have

$$W_c^b(\mathbf{q}) = \frac{1}{4} \{ W_B^b(\mathbf{q}) + 3W_A^b(\mathbf{q}) \} = \overline{W^b}(\mathbf{q}). \quad (6.45)$$

For sites whose H_1, H_2, H_3 components are different in parity (the superstructure reciprocal vectors $\mathbf{g}_{n,ss}$ are associated with these) we have

$$W_c^b(\mathbf{q}) = \frac{1}{4} \{ W_B^b(\mathbf{q}) - W_A^b(\mathbf{q}) \} = \frac{1}{4} \Delta W^b(\mathbf{q}). \quad (6.46)$$

As a result, the pseudopotential formfactor for such a crystal will be (per ion)

$$\mathcal{W}_{\text{cr}}^b(\mathbf{q}) = \begin{cases} \overline{W^b}(\mathbf{q}) & \text{for equal-parity } H_1, H_2, H_3, \\ \frac{1}{4} \Delta W^b(\mathbf{q}) & \text{for unequal-parity } H_1, H_2, H_3. \end{cases} \quad (6.47)$$

Similarly, for CuZn -type cubic crystals, we find

$$\mathcal{W}_{\text{cr}}^b(\mathbf{q}) = \begin{cases} \overline{W^b}(\mathbf{q}) & \text{for } H_1 + H_2 + H_3 = 2n, \\ \frac{1}{2} \Delta W^b(\mathbf{q}) & \text{for } H_1 + H_2 + H_3 = 2n + 1. \end{cases} \quad (6.48)$$

It should be noted that in a disordered state the Cu_3Au -type superstructures change into FCC structures and the CuZn -type into BCC structures.

Similar expressions can be obtained for other superstructures. Although the argument that led to these results is somewhat different from that at the beginning of this section, it is easy to show that equations like (6.45) may equally well be derived from (6.27).

Thus the band-structure energy of ordered CuZn-type alloys has the form

$$U_{bs} = \frac{\bar{\Omega}}{8\pi} \sum_{n,f} g_{n,f}^2 \frac{1 - \varepsilon(g_{n,f})}{\varepsilon^*(g_{n,f})} |\overline{W^b}(g_{n,f})|^2 + \frac{\bar{\Omega}}{8\pi} \sum_{n,ss} g_{n,ss}^2 \frac{1 - \varepsilon(g_{n,ss})}{\varepsilon^*(g_{n,ss})} \frac{|\Delta W^b(g_{n,ss})|^2}{4}. \quad (6.49)$$

It is now clear that analogous expressions can be derived for an ordered alloy of any other type. In our discussion below of specific alloys, some of these expressions will also be required for partially ordered alloys.

It is worth emphasizing once more that the formulae for the absolute square of the electron transition matrix element (between states $|\mathbf{k}\rangle$ and $|\mathbf{k} + \mathbf{q}\rangle$) are analogous to the formulae for the intensity of X-ray (neutron or electron) scattering. The latter formulae may therefore sometimes be used to obtain the absolute square of the pseudopotential formfactor for various types of order (including partially long-range order, which we have not, for the lack of space, discussed). It should be remembered, however, that the \mathbf{q} dependence of the pseudopotential formfactor is entirely different, so that numerical estimates may not be sensibly transferred from X-ray (neutron or electron) scattering.

To conclude this section, note that, strictly speaking, our results are only justified for simple metals, either pure or in alloys. With the noble metals, the additional hybridization potential [308] makes a total-energy pseudopotential calculation much more difficult (for details, see [313, 430-432]). The interesting point concerning the noble and transition metals is that both the interatomic potentials of pure metals and the ordering potentials of their alloys not only exhibit Friedel-type oscillations but also contain terms with cosines of $2\sqrt{E_d}$ instead of cosines of $2k_F$ [433].

6.3. Electrostatic energy

Following the pattern of the previous section, we start with derivations of general expressions, and then we apply them first to pure crystals and then to alloys, first completely disordered, and then with short-range and long-range order.

The electrostatic energy of a pure metal may be calculated by applying the Ewald procedure [413, 414] to a system of charges distributed in a uniform compensatory field. In [415] this method was extended to include alloys. Our discussion will closely follow the argument in [404].

Let the sites of a crystal lattice be occupied (randomly or with some degree of short-range or long-range order) by positive point charges Z_A^* and Z_B^* , whose concentrations are, respectively, $1 - c$ and c . This array is embedded in a uniformly distributed negative charge of density $\bar{Z}^*/\bar{\Omega} = [(1 - c) Z_A^* + c Z_B^*] [(1 - c) \Omega_A + c \Omega_B]^{-1}$. Clearly, this choice of charge density makes the crystal electrically neutral as a whole. The charge density produced by the positive point charges at a point r is

$$\rho(r) = \sum_v \{ (1 - c_v) Z_A^*(r - t_v) + c_v Z_B^*(r - t_v) \}. \quad (6.50)$$

Here the functions $Z_A^*(r - t_v)$ and $Z_B^*(r - t_v)$ are delta-like (we are dealing with point charges), so that to do the summation each point charge should be given a (positive or negative) Gaussian "cap". We first evaluate the potential φ_1 produced by the combined action of the total uniform negative charge and of all the "positive" Gaussian caps, $\Delta\rho_1$. This latter term is

$$\Delta\rho_1 = \sum_v \{ (1 - c_v) Z_A^* e^{-\eta |r - t_v|^2} + c_v Z_B^* e^{-\eta |r - t_v|^2} \} \left(\frac{\eta}{\pi} \right)^{3/2}. \quad (6.51)$$

Taking the Fourier transform of $\Delta\rho_1$, adding the Fourier transform of the uniform charge, and solving Poisson's equation yield the potential due to the total charge:

$$\varphi_1(r) = \frac{4\pi}{\Omega} \sum_q' \frac{e^{-q^2/4\eta}}{q^2} e^{iqr} \sum_v \{ (1 - c_v) Z_A^* + c_v Z_B^* \} e^{-iqt_v}. \quad (6.52)$$

The potential φ_2 , which arises from the positive point charges and negative Gaussian caps (these exactly cancel the positive caps) is also obtained by integrating Poisson's equation. The result may be represented as

$$\varphi_2(r) = \sum_v \{ (1 - c_v) Z_A^* + c_v Z_B^* \} \frac{1 - \text{erf}[\sqrt{\eta} |r - t_v|]}{|r - t_v|}. \quad (6.53)$$

Since the Gaussian caps have no physical meaning, the total potential $\varphi = \varphi_1 + \varphi_2$ must be independent of η . The sum of the positive and negative Gaussian caps is zero, which makes it possible to choose the constant of integration as $-\pi \bar{Z}^* (\eta \bar{\Omega})^{-1}$.

From electrodynamics the total energy of a charge distributed in the field $\varphi(r)$ is known to be

$$U_{\text{es}} = \frac{1}{2} \int \rho(r) \varphi(r) dr. \quad (6.54)$$

By evaluating $\varphi(\mathbf{r})$, substituting the result into (6.50), and making some transformations we find (per ion)

$$\begin{aligned}
 U_{\text{es}} = & \frac{1}{2} \left\{ \frac{4\pi}{\Omega} \sum_{\mathbf{q}}' \frac{1}{q^2} \exp\left(-\frac{q^2}{4\eta}\right) [(\bar{Z}^*)^2 |S(\mathbf{q})|^2 \right. \\
 & + (Z_A^* - Z_B^*)^2 |C(\mathbf{q})|^2] + \frac{1}{N} \sum_{\substack{\mathbf{v} \\ \mathbf{v} \neq \mathbf{v}'}} \sum_{\mathbf{v}'} [(\bar{Z}^*)^2 \\
 & + (c_{\mathbf{v}} - c) \bar{Z}^* (Z_A^* - Z_B^*) + (c_{\mathbf{v}'} - c) \bar{Z}^* (Z_A^* - Z_B^*) \\
 & + (c_{\mathbf{v}'} - c)(c_{\mathbf{v}} - c)(Z_A^* - Z_B^*)^2] \frac{1 - \text{erf}(\sqrt{\eta} |t_{\mathbf{v}} - t_{\mathbf{v}'}|)}{|t_{\mathbf{v}} - t_{\mathbf{v}'}|} \\
 & \left. - \frac{\pi}{\eta\Omega} (\bar{Z}^*)^2 - 2 \sqrt{\frac{\eta}{\pi}} \bar{Z}^{*2} \right\}. \quad (6.55)
 \end{aligned}$$

This may be rewritten as

$$\begin{aligned}
 U_{\text{es}} = & \frac{\bar{Z}^{*2}}{2} \left\{ \frac{4\pi}{\Omega} \sum_{\mathbf{q}}' \frac{1}{q^2} \exp\left(-\frac{q^2}{4\eta}\right) |S(\mathbf{q})|^2 \right. \\
 & + \frac{1}{N} \sum_{\mathbf{v}, \mathbf{v}' \neq \mathbf{v}} \left[\frac{1 - \text{erf}(\sqrt{\eta} |t_{\mathbf{v}} - t_{\mathbf{v}'}|)}{|t_{\mathbf{v}} - t_{\mathbf{v}'}|} - \frac{\pi}{\eta\Omega} - 2 \sqrt{\frac{\eta}{\pi}} \right] \Big\} \\
 & + \frac{(Z_A^* - Z_B^*)^2}{2} \left\{ \frac{4\pi}{\Omega} \sum_{\mathbf{q}}' \frac{1}{q^2} \exp\left(-\frac{q^2}{4\eta}\right) |C(\mathbf{q})|^2 \right. \\
 & + \frac{1}{N} c(1-c) \sum_{\mathbf{v}, \mathbf{v}' \neq \mathbf{v}} (c_{\mathbf{v}} c_{\mathbf{v}'} - c^2) \frac{1 - \text{erf}(\sqrt{\eta} |t_{\mathbf{v}} - t_{\mathbf{v}'}|)}{|t_{\mathbf{v}} - t_{\mathbf{v}'}|} \\
 & \left. - 2 \sqrt{\frac{\eta}{\pi}} c(1-c) \right\}, \quad (6.56)
 \end{aligned}$$

where the first term in curly brackets represents the contribution from the "average" crystal and the second is that from the charge fluctuations.

By an appropriate choice of the Ewald parameter η , the \mathbf{v} and \mathbf{v}' sums can be made small and the electrostatic energy of the alloy takes the form

$$\begin{aligned}
 U_{\text{es}} = & \frac{(\bar{Z}^*)^2}{2} \left\{ \frac{4\pi}{\Omega} \sum_{\mathbf{q}}' \frac{1}{q^2} \exp\left(-\frac{q^2}{4\eta}\right) |S(\mathbf{q})|^2 - \frac{\pi}{\eta\Omega} - 2 \sqrt{\frac{\eta}{\pi}} \right\} \\
 & + \frac{(Z_A^* - Z_B^*)^2}{2} \left\{ \frac{4\pi}{\Omega} \sum_{\mathbf{q}}' \frac{1}{q^2} \exp\left(-\frac{q^2}{4\eta}\right) |C(\mathbf{q})|^2 - 2 \sqrt{\frac{\eta}{\pi}} c(1-c) \right\}. \quad (6.57)
 \end{aligned}$$

The pure-metal case is obtained from (6.57) by setting $c=0$. We have

$$U_{\text{es}} = \frac{1}{2} Z^{*2} \left\{ \frac{4\pi}{\bar{\Omega}} \sum_{\mathbf{q}}' \frac{1}{q^2} e^{-q^2/4\eta} |S(\mathbf{q})|^2 - \frac{\pi}{\eta\bar{\Omega}} - 2 \sqrt{\frac{\eta}{\pi}} \right\}. \quad (6.58)$$

The term in the curly brackets here is usually denoted as α_{es}/R_a ; its values for various structures are listed in Table. 6.1. It can be seen that the electrostatic energy favors the compactness of structure: it is greater in hexagonal structures other than the HCP and increases from close-packed cubic FCC and BCC structures to the simple cubic ($\alpha_{\text{es}} = -1.76012$) and the diamond-type ($\alpha_{\text{es}} = -1.67100$). The BCC structure should be the most favored by this criterion: its higher stability with respect to FCC and HCP is due to the effect of second nearest neighbors.

The electrostatic energy of alloys will be evaluated using the $|S(\mathbf{q})|^2$ and $|C(\mathbf{q})|^2$ obtained earlier. By substituting them into (6.57) we find

(i) for a completely ordered alloy

$$U_{\text{es,ord}} = \frac{\bar{Z}^{*2}}{2} \left\{ \frac{4\pi}{\bar{\Omega}} \sum_{n,f}' \frac{1}{g_{n,f}^2} \exp\left(-\frac{g_{n,f}^2}{4\eta}\right) |S(g_{n,f})|^2 - \frac{\pi}{\eta\bar{\Omega}} \right. \\ \left. - 2 \sqrt{\frac{\eta}{\pi}} \right\} + \frac{(Z_A^* - Z_B^*)^2}{2} \left\{ \frac{4\pi}{\bar{\Omega}} \sum_{n,ss}' \frac{1}{g_{n,ss}^2} \exp\left(-\frac{g_{n,ss}^2}{4\eta}\right) |C(g_{n,ss})|^2 \right. \\ \left. - 2c(1-c) \sqrt{\frac{\eta}{\pi}} \right\}. \quad (6.59)$$

(ii) for an alloy with short-range order

$$U_{\text{es,sh.-r}} = \frac{1}{2} \bar{Z}^{*2} \left\{ \frac{4\pi}{\bar{\Omega}} \sum_{n,f}' \frac{1}{g_{n,f}^2} \exp\left(-\frac{g_{n,f}^2}{4\eta}\right) \right. \\ \times |S(g_{n,f})|^2 - \frac{\pi}{\eta\bar{\Omega}} - 2 \sqrt{\frac{\eta}{\pi}} \left\{ \right. \\ \left. + \frac{(Z_A^* - Z_B^*)^2}{2} \left\{ \frac{4\pi}{N\bar{\Omega}} \sum_{\mathbf{q}}' \frac{1}{q^2} \exp\left(-\frac{q^2}{4\eta}\right) \right. \right. \\ \left. \times \sum_{\mathbf{q}} c(1-c) \alpha(\rho_i) e^{-q\rho_i} - 2c(1-c) \sqrt{\frac{\eta}{\pi}} \right\} \right\}. \quad (6.60)$$

(iii) for a completely disordered alloy

$$\begin{aligned}
 U_{\text{es, chaotic}} &= \frac{1}{2} \overline{Z}^{*2} \left\{ \frac{4\pi}{\Omega} \sum'_{n,f} \frac{1}{g_{n,f}^2} \exp \left(-\frac{g_{n,f}^2}{4\eta} \right) |S(g_{n,f})|^2 - \frac{\pi}{\eta\Omega} - 2 \sqrt{\frac{\eta}{\pi}} \right. \\
 &+ \left. \frac{(Z_A^* - Z_B^*)^2}{2} \left\{ \frac{4\pi}{N\Omega} \sum_q \frac{1}{q^2} \exp \left(-\frac{q^2}{4\eta} \right) c(1-c) - 2c(1-c) \sqrt{\frac{\eta}{\pi}} \right\} \right\}. \quad (6.61)
 \end{aligned}$$

It has been shown [415] that the second sum here is zero.

6.4. The total internal energy of an alloy: second-order perturbation theory and the locality approximation

The configurational part of the total internal energy (i.e., the sum of the band and electrostatic contributions) determines a structure's stability at low temperatures (in principle, at the absolute zero if zero-point energy is ignored). We did not think it appropriate to discuss here the mechanical destabilization of lattice due to shear effects (for more details see [416-417]).

Expressions for the configurational part of the internal energy are given below (i) for crystals with long-range order, (ii) for crystals without long-range but with short-range order and (iii) for a completely disordered alloy.

6.4.1. An alloy with perfect long-range order. From (6.26), (6.49) and (6.59), the configurational part of the total energy is

$$\begin{aligned}
 U_{\text{conf}} &= \frac{1}{2} \left\{ \overline{Z}^{*2} \left[\frac{4\pi}{\Omega} \sum'_{n,f} \frac{1}{g_{n,f}^2} \exp \left(-\frac{g_{n,f}^2}{4\eta} \right) |S(g_{n,f})|^2 - \frac{\pi}{\eta\Omega} \right. \right. \\
 &- 2 \sqrt{\frac{\eta}{\pi}} \left. \right] + \frac{\overline{\Omega}}{4\pi} \sum'_{n,f} g_{n,f}^2 \frac{1 - \varepsilon(g_{n,f})}{\varepsilon^*(g_{n,f})} |S(g_{n,f})|^2 |\overline{W}^b(g_{n,f})|^2 \left. \right\} \\
 &+ \frac{1}{2} \left\{ (Z_A^* - Z_B^*)^2 \left[\frac{4\pi}{\Omega} \sum_{n,ss} \frac{1}{g_{n,ss}^2} \exp \left(-\frac{g_{n,ss}^2}{4\eta} \right) |C(g_{n,ss})|^2 \right. \right. \\
 &- 2c(1-c) \sqrt{\frac{\eta}{\pi}} \left. \right] + \frac{\overline{\Omega}}{4\pi} \sum_{n,ss} g_{n,ss}^2 \frac{1 - \varepsilon(g_{n,ss})}{\varepsilon^*(g_{n,ss})} |C(g_{n,ss})|^2 \\
 &\left. \left. \times |\Delta W^b(g_{n,ss})|^2 \right\}. \quad (6.62)
 \end{aligned}$$

The first term in the curly brackets represents the contribution due to the average crystal; the second is due to fluctuations. The essential point to note is that, unlike the pure-crystal case, terms with relatively small wave vectors are important in (6.62) and the fluctuation contribution may happen to be sizeable. It is for this reason that ordered alloys received a great deal of attention even in the earliest works on the electronic theory of metallic alloys.

The above expressions may be helpful for studying the stability of ordered alloys. They may be used, for example, for obtaining the thermodynamic potentials of neighboring phases (with the subsequent determination of the points where these potentials are equal) or for calculating the configurational energies of different phases. An interesting study would be to combine alloy pseudopotential statistical-dynamical theory with the method of statistical concentration waves.

As is discussed in [401] the type of the ordering that occurs below a certain ("ordering") temperature T_c is controlled by the symmetry of the Fourier transform of the ordering potential. The ordering temperature and the depth of the minimum of the Fourier transform are related by

$$T_c = -(1-c)cW(g_{n,ss}) \quad (6.63)$$

so that when determining T_c and the type of ordering, or when finding the existence range of an ordered phase we need not calculate the total energy of the alloy; it is enough to find the Fourier transform of the ordering energy in the vicinity of its minimum. Certainly, the position of the minimum has also to be calculated. In other words, we must calculate the reciprocal-space distribution for the Fourier transform of the ordering potential, locate minima, determine their symmetry and depth, and this may yield enough information for finding the stable ordered phases, their types, existence ranges, transition temperatures, etc.

The following method for obtaining the ordering potential's Fourier transform is taken from [401]. We begin with an analysis of the band energy (cf. (6.26)) as given by

$$U_{bs}^{(2)} = \frac{\bar{\Omega}}{8\pi} \sum_{\mathbf{q}}' q^2 \frac{1-\varepsilon(\mathbf{q})}{\varepsilon^*(\mathbf{q})} |\Delta W^b(\mathbf{q})|^2 |C(\mathbf{q})|^2. \quad (6.64)$$

It is known that an arbitrary wave vector \mathbf{q} may be represented as a sum of the closest reciprocal lattice vector \mathbf{g}_n plus the difference between the \mathbf{q} and \mathbf{g}_n :

$$\mathbf{q} = \mathbf{g}_n + \Delta\mathbf{q}. \quad (6.65)$$

The \mathbf{q} summation in (6.26) may then be divided into the sum over $\Delta\mathbf{q}$ within the first Brillouin zone and the sum over the reciprocal

lattice vectors \mathbf{g}_n :

$$U_{bs}^{(2)} = \frac{\bar{\Omega}}{8\pi} \sum_{\Delta\mathbf{q}}' \sum_n' |\mathbf{g}_n + \Delta\mathbf{q}|^2 |\Delta W^b(\mathbf{g}_n + \Delta\mathbf{q})|^2 \\ \times \frac{1 - \varepsilon(\mathbf{g}_n + \Delta\mathbf{q})}{\varepsilon^*(\mathbf{g}_n + \Delta\mathbf{q})} |C(\mathbf{g}_n + \Delta\mathbf{q})|^2. \quad (6.66)$$

The function $|C(\mathbf{q})|^2$ possesses translational symmetry so that

$$|C(\mathbf{q})|^2 = |C(\Delta\mathbf{q})|^2, \quad (6.67)$$

Denoting the reciprocal lattice sum in (6.66) as

$$V_{bs}(\Delta\mathbf{q}) = \frac{\bar{\Omega}_0}{4\pi} \left\{ \sum_n |\mathbf{g}_n + \Delta\mathbf{q}|^2 |\Delta W^b(\mathbf{g}_n + \Delta\mathbf{q})|^2 \frac{1 - \varepsilon(\mathbf{g}_n + \Delta\mathbf{q})}{\varepsilon^*(\mathbf{g}_n + \Delta\mathbf{q})} \right. \\ \left. - \frac{1}{N} \sum_{\mathbf{q}} |\Delta W^b(\mathbf{q})|^2 \mathbf{q}^2 \frac{1 - \varepsilon(\mathbf{q})}{\varepsilon^*(\mathbf{q})} \right\}, \quad (6.68)$$

where the last sum results from dropping the primes in the first, the fluctuational contribution to the band energy takes the form

$$U_{bs}^{(2)} = \frac{1}{2} \sum_{\Delta\mathbf{q}} V_{bs}(\Delta\mathbf{q}) |C(\Delta\mathbf{q})|^2 \quad (6.69)$$

Clearly, $V_{bs}(\Delta\mathbf{q})$ is the Fourier transform for the band contribution to the ordering potential (in the first Brillouin zone).

The electrostatic contribution to the total energy should be treated in a similar manner. The starting point this time is (6.57). By the same argument as used for the band energy we find

$$U_{es}^{(2)} = \frac{1}{2} (Z_A^* - Z_B^*)^2 \left\{ \frac{4\pi}{\bar{\Omega}} \sum_{\Delta\mathbf{q}}' \sum_n' \frac{1}{\mathbf{q}^2} \exp\left(-\frac{\mathbf{q}^2}{4\eta}\right) |C(\mathbf{q})|^2 \right. \\ \left. - 2c(1-c) \sqrt{\frac{\eta}{\pi}} \right\} = \frac{1}{2} \sum_{\Delta\mathbf{q}} |C(\Delta\mathbf{q})|^2 V_{es}(\Delta\mathbf{q}), \quad (6.70)$$

where the Fourier component $V_{es}(\Delta\mathbf{q})$ of the electrostatic energy is given by

$$V_{es}(\Delta\mathbf{q}) = \frac{4\pi}{\bar{\Omega}} \left\{ \sum_n \frac{(\Delta Z^*)^2}{|\mathbf{g}_n + \Delta\mathbf{q}|^2} \exp\left(-\frac{|\mathbf{g}_n + \Delta\mathbf{q}|^2}{4\eta}\right) \right. \\ \left. - \frac{1}{N} \sum_{\mathbf{q}} \frac{(\Delta Z^*)^2}{\mathbf{q}^2} \exp\left(-\frac{\mathbf{q}^2}{4\eta}\right) \right\}. \quad (6.71)$$

The total configurational energy takes the form

$$U^{(2)} = \frac{1}{2} \sum_{\Delta\mathbf{q}} |C(\Delta\mathbf{q})|^2 V(\Delta\mathbf{q}), \quad (6.72)$$

where

$$V(\Delta \mathbf{q}) = V_{bs}(\Delta \mathbf{q}) + V_{cs}(\Delta \mathbf{q}) \quad (6.73)$$

is the Fourier component for the ordering potential. By calculating $V(\Delta \mathbf{q})$ for the most important points (directions) within the first Brillouin zone (or, if necessary, over the whole of it), it is always possible to locate the minima of $V(\Delta \mathbf{q})$ and to evaluate them for vectors which correspond to superstructural sites of the reciprocal lattice. We note that the ordering potential itself

$$V(\rho_i) = V_{AA}(\rho_i) + V_{BB}(\rho_i) - 2V_{AB}(\rho_i) \quad (6.74)$$

will take the form

$$V(\rho_i) = \frac{2}{N} \sum_{\mathbf{q}}' \mathcal{F}_p(\mathbf{q}) e^{i\mathbf{q}\rho_i} \quad (6.75)$$

or

$$V(\rho_i) = \frac{\bar{\Omega}}{\pi^2} \int dq q^2 \mathcal{F}_p(q) \frac{\sin q\rho_i}{q\rho_i}, \quad (6.76)$$

where

$$\begin{aligned} \mathcal{F}_p(q) = & \frac{\bar{\Omega}}{8\pi} |\Delta W^b(q)|^2 q^2 \frac{1-\epsilon(q)}{\epsilon^*(q)} \\ & + \frac{2\pi}{\bar{\Omega}} (\Delta Z^*)^2 \frac{1}{q^2} \exp\left(-\frac{q^2}{4\eta}\right) = \mathcal{F}_{bs}(q) + \mathcal{F}_{es}(q). \end{aligned} \quad (6.77)$$

It is an easy matter to show that $V(\rho_i)$ may be written as

$$\begin{aligned} V(\rho_i) = & \frac{\bar{\Omega}}{\pi^2} \int dq q^2 \frac{\sin q\rho_i}{q\rho_i} \left\{ \frac{\bar{\Omega}}{8\pi} q^2 \frac{1-\epsilon(q)}{\epsilon^*(q)} |W_B^b(q)|^2 \right. \\ & + \frac{2\pi}{q^2} Z_B^{*2} \exp\left(-\frac{q^2}{4\eta}\right) \left. \right\} - \frac{2\bar{\Omega}}{\pi^2} \int dq q^2 \frac{\sin q\rho_i}{q\rho_i} \left\{ \frac{\bar{\Omega}}{8\pi} q^2 \frac{1-\epsilon(q)}{\epsilon^*(q)} W_A^b(q) \right. \\ & \times W_B^b(q) + \frac{2\pi}{q^2} Z_A^* Z_B^* \exp\left(-\frac{q^2}{4\eta}\right) \left. \right\} \\ & + \frac{\bar{\Omega}}{\pi^2} \int dq q^2 \frac{\sin q\rho_i}{q\rho_i} \left\{ \frac{\bar{\Omega}}{8\pi} q^2 \frac{1-\epsilon(q)}{\epsilon^*(q)} |W_A^b(q)|^2 \right. \\ & \left. + \frac{2\pi}{q^2} Z_A^{*2} \exp\left(-\frac{q^2}{4\eta}\right) \right\}. \end{aligned} \quad (6.78)$$

Each integral in (6.78) corresponds to the total effective interatomic potential and depends on the interatomic separation in a quasi-oscillatory manner. For nontransition metals, the behavior of these potentials corresponds to Friedel oscillations. Clearly, the sum of these integrals (i.e., the ordering potential) will behave in a similar manner.

Expressions like (6.73) have also been derived for alloys with complex structure (see [419, 420]).

6.4.2. Alloys with short-range order. Using (6.33) and (6.60), the configurational energy of such alloys may be written as

$$\begin{aligned}
 U_{\text{conf.sh.-r.}} = & \frac{1}{2} \left\{ \overline{Z}^{*2} \left[\frac{4\pi}{\Omega} \sum'_{n,f} \frac{1}{g_{n,f}^2} \exp \left(-\frac{g_{n,f}^2}{4\eta} \right) |S(g_{n,f})|^2 - \frac{\pi}{\eta\Omega} \right. \right. \\
 & \left. \left. - 2 \sqrt{\frac{\eta}{\pi}} \right] + \frac{\overline{\Omega}}{4\pi} \sum'_{n,f} g_{n,f}^2 \frac{1-\varepsilon(g_{n,f})}{\varepsilon^*(g_{n,f})} |S(g_{n,f})|^2 |\overline{W^b(g_{n,f})}|^2 \right\} \\
 & + \frac{1}{2} \left\{ \Delta Z^{*2} \left[\frac{4\pi}{\Omega} \sum'_{\mathbf{q}} \frac{1}{q^2} \exp \left(-\frac{q^2}{4\eta} \right) |C(\mathbf{q})|^2 - 2c(1-c) \sqrt{\frac{\eta}{\pi}} \right] \right. \\
 & \left. + \frac{\overline{\Omega}}{4\pi} \sum'_{\mathbf{q}} q^2 \frac{1-\varepsilon(\mathbf{q})}{\varepsilon^*(\mathbf{q})} |C(\mathbf{q})|^2 |\Delta W^b(\mathbf{q})|^2 \right\}. \quad (6.79)
 \end{aligned}$$

The first part of this expression again corresponds to the average crystal; if the short-range order leaves the average atomic separation unchanged, this term will have no effect on the formation of short-range order. The effect of the interatomic separation and average-crystal energy on short-range order was first discussed in [403].

The second term in (6.79) represents the alloy energy associated with short-range order. If $\alpha(\rho_i)$ is independent of the orientation of ρ_i , it may be conveniently written as

$$U_{\text{conf.sh.-r.}} = c(1-c) \sum_i C_i \alpha_i V(\rho_i), \quad (6.80)$$

where $V(\rho_i)$ is given by (6.76).

It should be noted that to use these results requires a knowledge not only of the ordering potentials (and this for as many coordination spheres as possible) but also of the short-range-order parameters themselves. For this reason, these results are in fact unsuitable for predicting short-range-order and may only be helpful when estimating it in the (very rare) situations when independent considerations indicate that one of the spheres will predominate.

A somewhat different and more promising way to employ these expressions was suggested in [404, 421-423]. Since the equilibrium short-range order corresponds to the minimum of the free energy (more generally, of a thermodynamic potential), it follows that to get the equilibrium short-range-order parameters we must evaluate the free energy (using the above expressions for the configurational energy) and then minimize it with respect to the parameters. Assuming the latter to be independent we obtain

$$\frac{\alpha_1}{(1-\alpha_1)^2} = c(1-c) \left\{ \exp \left(-\frac{V(\rho_i)}{k_B T} \right) - 1 \right\}. \quad (6.81)$$

This formula gives the short-range-order parameter for the first coordination sphere, provided it contributes more heavily than

the other spheres. Although this approach is still used in interpreting experimental data [412] it is not strict enough. It is more consistent to obtain the $V(\rho_i)$ from (6.75)-(6.76) and then to improve them using the statistical theory of short-range-order. This gives [418, 424]:

$$\alpha(\rho_i) = \int \frac{e^{-iq\mathbf{e}_i} d\mathbf{q}}{1 + \frac{c(1-c)}{k_B T} \sum_{\rho \neq 0} V(\rho_i) e^{iq\mathbf{e}_i}}. \quad (6.82)$$

It can be seen from this that this method involves the summation over the unit cell of reciprocal space. Accordingly, $U_{\text{conf.sh-r.}}$ and $\alpha(\rho_i)$ will contain small q terms whose contribution to the band and electrostatic energies will require a careful analysis.

6.4.3. Totally random alloys. The configurational energy may be found from (6.79) or earlier expressions to be

$$\begin{aligned} U_{\text{conf.,chaotic}} &= \frac{1}{2} \left\{ \overline{Z^{*2}} \left[\frac{4\pi}{\overline{\Omega}} \sum'_{n,f} \frac{1}{g_{n,f}^2} \exp\left(-\frac{g_{n,f}^2}{4\eta}\right) |S(g_{n,f})|^2 \right. \right. \\ &\quad \left. \left. - \frac{\pi}{\eta\Omega} - 2\sqrt{\frac{\eta}{\pi}} \right] + \frac{\overline{\Omega}}{4\pi} \sum'_{n,f} \frac{1-\varepsilon(g_{n,f})}{\varepsilon^*(g_{n,f})} |S(g_{n,f})|^2 |\overline{W^b(g_{n,f})}|^2 \right\} \\ &\quad + \frac{1}{2} \left\{ \frac{\overline{\Omega}}{4\pi N} c(1-c) \sum'_{\mathbf{q}} \mathbf{q}^2 \frac{1-\varepsilon(\mathbf{q})}{\varepsilon^*(\mathbf{q})} |\Delta W^b(\mathbf{q})|^2 \right\}. \quad (6.83) \end{aligned}$$

Both the average crystal and the fluctuational contributions may be important. The fluctuations are important because at small \mathbf{q} the pseudopotential matrix elements are large. When calculating the configurational energy for a disordered alloy, either with or without short-range order, it is always necessary to verify the correctness of the fluctuation term.

6.5. Higher-order perturbation analysis

Important contributions to pseudopotential alloy theory came from [409] and [410], which examined alloys with long-range order and short-range order, respectively. In [410], an inclusion of higher-order perturbation terms was attempted. Since second-order perturbation theory corresponds to pairwise interaction, this is equivalent to an incorporation of multi-ion effects. According to Krasko and Makhnovetsky's argument [409], a second-order approximation is only sufficient if

$$W(\mathbf{q})/E_F \ll 1. \quad (6.84)$$

The appearance of an ordered phase gives rise to superstructural reflexes of the reciprocal lattice in the region of relatively small \mathbf{q} where the pseudopotential formfactors (and their differences) need not be small. It has been estimated that, typically,

$$\left(\frac{W(\mathbf{g}_{n,ss})}{E_F} \right)^2 \propto \left| \frac{W(\mathbf{g}_{n,f})}{E_F} \right| \quad (6.85)$$

Consequently, while the average formfactor of components may be calculated to the second order for the smallest $\mathbf{g}_{n,f}$ the difference formfactor which corresponds to the superstructure site $\mathbf{g}_{n,ss}$ requires the inclusion of the third and fourth orders (i.e., the three- and four-particle interactions). Working along the lines of [425], Krasko and Makhnovetsky [409] were able to show that the inclusion of the third and fourth order terms is in fact equivalent to the replacement of the ordinary potential by an effective \mathbf{k} -dependent one,

$$\begin{aligned} \tilde{W}(\mathbf{g}_n, \mathbf{k}) = & W(\mathbf{g}_n) + \sum'_{n \neq n'} \frac{W(\mathbf{g}_{n'}) W(\mathbf{g}_{n'} - \mathbf{g}_n)}{E_{\mathbf{k}} - E_{\mathbf{k} + \mathbf{g}_n}^0} \\ & + \sum'_{n \neq n'} \sum'_{n'' \neq n} \frac{W(\mathbf{g}_{n''}) W(\mathbf{g}_{n''} - \mathbf{g}_{n'}) W(\mathbf{g}_{n'} - \mathbf{g}_n)}{(E_{\mathbf{k}} - E_{\mathbf{k} + \mathbf{g}_n}^0) (E_{\mathbf{k}} - E_{\mathbf{k} + \mathbf{g}_n}^0)}, \end{aligned} \quad (6.86)$$

where \mathbf{g}_n are sites (both structural and superstructural) for which (6.84) is not satisfied, and $E_{\mathbf{k}}^0$ is the free-electron energy. Krasko and Makhnovetsky point out that to go beyond the third order requires consideration of the nonsphericity of the Fermi surface and they suggest a way of doing this. After transforming to the effective pseudopotential $\tilde{W}(\mathbf{g}_n, \mathbf{k})$ the energy $E_{\mathbf{k}}$ takes the form

$$E_{\mathbf{k}} = E_{\mathbf{k}}^0 + \sum'_n \frac{W(\mathbf{g}_n) \tilde{W}(\mathbf{g}_n, \mathbf{k})}{E_{\mathbf{k}} - E_{\mathbf{k} + \mathbf{g}_n}^0}. \quad (6.87)$$

The total band energy of an ordered alloy may be written as

$$U_{bs} = U_{bs}^{(2)} + \sum'_{n,f} \Delta U_{bs}(\mathbf{g}_{n,f}) + \sum'_{n,ss} \Delta U_{bs}(\mathbf{g}_{n,ss}), \quad (6.88)$$

where $U_{bs}^{(2)}$ is the second-order band energy (earlier, U_{bs}) and $\Delta U_{bs}(\mathbf{g}_{n,f})$ and $\Delta U_{bs}(\mathbf{g}_{n,ss})$ are the third- and fourth-order corrections due to the structural and superstructural sites for which (6.84) fails. The pairwise contribution to the crystal energy is regarded in [409] as the "metallic" part of the cohesion energy; this is a sum of the band and electrostatic contributions:

$$U_{\text{met}} = U_{\text{es}} + U_{bs}^{(2)}. \quad (6.89)$$

The higher-order corrections characterize the covalent part of the cohesion energy. The application of this theory (in combination with the statistical theory of [401]) to the analysis of phase stability required the Fourier transform of the ordering potential $V(\rho)$ for a number of characteristic points in the first Brillouin zone. This is a sum of "metallic" and "covalent" parts

$$V(\mathbf{g}_n, ss) = V^{\text{met}}(\mathbf{g}_n, ss) + V^{\text{cov}}(\mathbf{g}_n, ss) \quad (6.90)$$

where $V^{\text{met}}(\mathbf{g}_n, ss)$ describes the pairwise interaction, discussed above,

$$V^{\text{cov}}(\mathbf{k}) = \frac{\bar{\Omega}}{4\pi} \sum_{n_1} \frac{\overline{W^b}(\mathbf{g}_{n_1})}{\varepsilon(\mathbf{g}_{n_1})} \left\{ \sum_{n_2} \Phi(\mathbf{g}_{n_1}, \mathbf{k} + \mathbf{g}_{n_2}) - \frac{1}{N} \sum_{\mathbf{q}} \Phi(\mathbf{g}_{n_1}, \mathbf{q}) \right\} \quad (6.91)$$

(the last sum in the curly bracket arises because the $V^{\text{cov}}(R=0)$ term was dropped in the configurational energy) and

$$\begin{aligned} \Phi(\mathbf{q}_1, \mathbf{q}_2) = & \frac{\Delta W^b(\mathbf{q}_2) \Delta W^b(\mathbf{q}_2 - \mathbf{q}_1)}{\varepsilon(\mathbf{q}_2) \varepsilon(\mathbf{q}_2 - \mathbf{q}_1)} \{ \mathbf{q}_1^2 [\varepsilon(\mathbf{q}_1) - 1] [2\varepsilon(\mathbf{q}_1) + 1] I(\mathbf{q}_2) \\ & + \mathbf{q}_2^2 [\varepsilon(\mathbf{q}_2) - 1] [2\varepsilon(\mathbf{q}_2) + 1] [I(\mathbf{q}_1) + I(\mathbf{q}_2 - \mathbf{q}_1)] \}, \end{aligned} \quad (6.92)$$

where

$$\begin{aligned} I(\mathbf{k}, \mathbf{g}_n) &= (E_{\mathbf{k}}^0 - E_{\mathbf{k}+\mathbf{g}_n}^0)^{-1}, \\ I(\mathbf{k}, \mathbf{g}_{n'}, \mathbf{g}_{n''}) &= (E_{\mathbf{k}}^0 - E_{\mathbf{k}+\mathbf{g}_{n'}}^0)^{-1} (E_{\mathbf{k}}^0 - E_{\mathbf{k}+\mathbf{g}_{n''}}^0)^{-1}. \end{aligned} \quad (6.93)$$

The third-order short-range-order energy was evaluated in [410, 426] using the formalism developed in [276]. The total energy of a crystal in n th-order perturbation theory may be written [276] as

$$U = U^{(0)} + U^{(1)} + U_{\text{bs}}^{(2)} + \dots + U_{\text{bs}}^{(n)} \quad (6.94)$$

For the third order,

$$\begin{aligned} U_{\text{bs}}^{(3)} = & \bar{\Omega} \sum_{\mathbf{q}_1, \mathbf{q}_2, \mathbf{q}_3} \frac{W_{\mathbf{q}_1}^b W_{\mathbf{q}_2}^b W_{\mathbf{q}_3}^b}{\varepsilon^*(\mathbf{q}_1) \varepsilon^*(\mathbf{q}_2) \varepsilon^*(\mathbf{q}_3)} \\ & \times \Lambda^{(3)}(\mathbf{q}_1, \mathbf{q}_2, \mathbf{q}_3) S(\mathbf{q}_1) S(\mathbf{q}_2) S(\mathbf{q}_3) \Delta(\mathbf{q}_1 + \mathbf{q}_2 + \mathbf{q}_3). \end{aligned} \quad (6.95)$$

Here $\Delta(\mathbf{q}_1 + \mathbf{q}_2 + \mathbf{q}_3)$ secures the conservation of momentum and $\Lambda^3(\mathbf{q}_1, \mathbf{q}_2, \mathbf{q}_3)$ is the irreducible three-pole for a circular diagram with three external-field "tails". For the present case

$$\Delta(\mathbf{q}_1 + \mathbf{q}_2 + \mathbf{q}_3) = \begin{cases} 1 & \text{for } \mathbf{q}_1 + \mathbf{q}_2 + \mathbf{q}_3 = 0, \\ 0 & \text{for } \mathbf{q}_1 + \mathbf{q}_2 + \mathbf{q}_3 \neq 0, \end{cases} \quad (6.96)$$

and

$$\begin{aligned} \Lambda^3(\mathbf{q}, \mathbf{q} + \mathbf{g}_n, \mathbf{g}_n) = & \frac{2}{3} \frac{(m^*)^2}{\pi} [q^2 g_n^2 - (\mathbf{q} \mathbf{g}_n)^2]^{-1/2} \\ & \times \left\{ \frac{\mathbf{q} \mathbf{g}_n + g_n^2}{g_n |\mathbf{q} + \mathbf{g}_n|} \ln \left| \frac{2k_F + q}{2k_F - q} \right| - \frac{\mathbf{q} \mathbf{g}_n}{q g_n} \ln \left| \frac{2k_F + |\mathbf{q} + \mathbf{g}_n|}{2k_F - |\mathbf{q} + \mathbf{g}_n|} \right| \right. \\ & \left. + \frac{q^2 + \mathbf{q} \mathbf{g}_n}{q |\mathbf{q} + \mathbf{g}_n|} \ln \left| \frac{2k_F + q}{2k_F - q} \right| - D \left[\ln \frac{1 - DA}{1 + DA}, \quad q_R > k_F \right. \right. \\ & \left. \left. - 2 \arctan DA, \quad q_R < k_F \right] \right\}, \quad (6.97) \end{aligned}$$

where m^* is the effective mass,

$$\begin{aligned} D = & \sqrt{\left(\frac{k_F}{q_R}\right)^2 - 1}, \quad q_R = \frac{1}{2} \frac{q g_n |\mathbf{q} + \mathbf{g}_n|}{\sqrt{q^2 g_n^2 - (\mathbf{q} \mathbf{g}_n)^2}}, \\ A = & \frac{q g_n |\mathbf{q} + \mathbf{g}_n|}{(2k_F)^2 \left[1 - \frac{1}{2} \frac{q^2 + g_n^2 + |\mathbf{q} + \mathbf{g}_n|^2}{(2k_F)^2} \right]}, \quad \pi \geq \arctan DA \geq 0. \end{aligned}$$

Using the crystal potential as given by (6.5) and (6.6) and taking the Fourier transform of the set of occupation numbers c_v , the third-order band-structure energy is

$$\begin{aligned} U_{bs}^{(3)} = & \bar{\Omega} \sum_{\mathbf{q}_1, \mathbf{q}_2, \mathbf{q}_3} \frac{\Lambda^{(3)}(\mathbf{q}_1, \mathbf{q}_2, \mathbf{q}_3)}{\varepsilon^*(\mathbf{q}_1) \varepsilon^*(\mathbf{q}_2) \varepsilon^*(\mathbf{q}_3)} \\ & \times \{ \bar{W}^b(\mathbf{q}_1) \bar{W}^b(\mathbf{q}_2) \bar{W}^b(\mathbf{q}_3) S(\mathbf{q}_1) S(\mathbf{q}_2) S(\mathbf{q}_3) \\ & + 3 \bar{W}^b(\mathbf{q}_1) \bar{W}^b(\mathbf{q}_2) \Delta W^b(\mathbf{q}_3) S(\mathbf{q}_1) S(\mathbf{q}_2) C(\mathbf{q}_3) \\ & + 3 \Delta W^b(\mathbf{q}_1) \Delta W^b(\mathbf{q}_2) \bar{W}^b(\mathbf{q}_3) C(\mathbf{q}_1) C(\mathbf{q}_2) S(\mathbf{q}_3) \\ & + \Delta W^b(\mathbf{q}_1) \Delta W^b(\mathbf{q}_2) \Delta W^b(\mathbf{q}_3) C(\mathbf{q}_1) C(\mathbf{q}_2) C(\mathbf{q}_3) \} \Delta(\mathbf{q}_1 + \mathbf{q}_2 + \mathbf{q}_3) \quad (6.98) \end{aligned}$$

where the "difference" and the average crystal terms are separated.

It can be shown that the first term in the curly brackets corresponds to the average crystal contribution and gives only a small addition to it.

The second term is proportional to $S(\mathbf{q}_1) S(\mathbf{q}_2) C(\mathbf{q}_3)$ and is zero for the following reason. If $\Delta(\mathbf{q}_1 + \mathbf{q}_2 + \mathbf{q}_3) = 1$, then $\mathbf{q}_1 + \mathbf{q}_2 + \mathbf{q}_3 = 0$ and since \mathbf{q}_1 and \mathbf{q}_2 are reciprocal lattice vectors, so too is \mathbf{q}_3 , and $S(\mathbf{q}_1) S(\mathbf{q}_2) C(\mathbf{q}_3)$ will therefore vanish because $C(\mathbf{q}_3 = \mathbf{g}_n) = 0$. If $\mathbf{q}_1 + \mathbf{q}_2 + \mathbf{q}_3 \neq 0$ then $\Delta(\mathbf{q}_1 + \mathbf{q}_2 + \mathbf{q}_3) = 0$ so that the second term in (6.98) is again zero.

The third term in (6.98) corresponds to the double scattering of electrons on ion pairs and must add something to the pairwise interaction energy.

The last term is proportional to triple correlations in solid alloys; since the probability of such correlations is very small this term should be negligible.

As a result, the short-range-order contribution to the energy of a solid solution will be (to third order)

$$\begin{aligned}
 U_{\text{bs, sn.-r.}} = & \frac{1}{N} c (1-c) \sum_{\rho_i} \alpha(\rho_i) e^{-i\mathbf{q}\rho_i} \sum'_{\mathbf{q}} \left\{ |\Delta W^b(\mathbf{q})|^2 \frac{\chi(\mathbf{q})}{\epsilon^*(\mathbf{q})} \right. \\
 & + \frac{2\pi}{\Omega} \frac{\Delta Z^{*2}}{q^2} \exp\left(-\frac{q^2}{4\eta}\right) + 3\bar{\Omega} \Delta W^b(\mathbf{q}) \\
 & \times \left[\sum'_n \Delta W^b(\mathbf{q} + \mathbf{g}_n) W(\mathbf{g}_n) \frac{\Lambda^3(\mathbf{q}_1, \mathbf{q} + \mathbf{g}_n, \mathbf{g}_n)}{\epsilon^*(\mathbf{q}) \epsilon^*(\mathbf{q} + \mathbf{g}_n) \epsilon^*(\mathbf{g}_n)} \right] \Big\}, \quad (6.99)
 \end{aligned}$$

the ordering potential including, and the electrostatic contribution takes the form

$$\begin{aligned}
 V(\rho_i) = & \frac{\bar{\Omega}}{\pi^2} \int \left[\frac{2\pi \Delta Z^{*2} \exp\left(-\frac{q^2}{4\eta}\right)}{\bar{\Omega} q^2} \right. \\
 & \left. + \frac{\bar{\Omega}}{8\pi} q^2 \frac{1 - \epsilon(q)}{\epsilon^*(q)} |\Delta W^b(q)|^2 + T(q) \right] \frac{\sin q\rho_i}{q\rho_i} q^2 dq, \quad (6.100)
 \end{aligned}$$

where

$$\begin{aligned}
 T(q) = & 3\bar{\Omega} \frac{\Delta W^b(q)}{\epsilon^*(q)} \sum'_n \frac{W^b(\mathbf{g}_n)}{\epsilon^*(\mathbf{g}_n)} \frac{\Delta W^b(|\mathbf{q} + \mathbf{g}_n|)}{\epsilon^*(|\mathbf{q} + \mathbf{g}_n|)} \\
 & \times \Lambda^{(3)}[q, |\mathbf{q} + \mathbf{g}_n|, \mathbf{g}_n], \quad (6.101)
 \end{aligned}$$

the summation running over the entire reciprocal lattice except for the vector $\mathbf{g}_n = 0$. It can be seen that the third-order term gives rise to the term $T(\mathbf{q})$ which may affect the ordering potential. The third-order contribution may thus influence both the ordering energy and the short-range-order contribution to the alloy energy.

6.6. OPW nonlocal alloy theory

The above results were obtained using local model potentials. It would be desirable to rederive them using true pseudopotentials, based on the orthogonalized plane wave approximation (the OPW or first-principle pseudopotential).

Pseudopotential alloy theory was pioneered by Hayes *et al.* [398] who formulated the OPW nonlocal alloy theory and calculated the ordering parameters of Li-Mg alloys. It is only natural, however, that most of the papers which followed were based on local model potentials, as these make numerical work easier and simplify the

interpretation of results. These studies yielded a number of useful results some of which were outlined above. Quantitatively the agreement with experiment was not entirely satisfactory and the most natural way to remedy this was, of course, to question the assumption of locality. This gave rise to extensive work on nonlocal OPW pseudopotentials and their application to alloys. An important contribution came from Hafner [427] and [428]; and the following discussion of OPW alloy theory is based, in fact, on [428]. The starting point of the theory is the standard Schrödinger equation with a potential

$$Y(\mathbf{r}) = \sum_{j(A)} Y_A(\mathbf{r} - \mathbf{r}_j) + \sum_{j(B)} Y_B(\mathbf{r} - \mathbf{r}_j) \quad (6.102)$$

which is to be determined self-consistently later.

For both types of core state, the orthogonalized plane wave of quasi-momentum \mathbf{k} ($OPW_{\mathbf{k}}$) has the form

$$\begin{aligned} |OPW_{\mathbf{k}}\rangle = & \mathbf{k} - \sum_{j(A)} \sum_t |\mathbf{r}_j, At\rangle \langle \mathbf{r}_j, At|\mathbf{k}\rangle \\ & - \sum_{j(B)} \sum_s |\mathbf{r}_j, Bs\rangle \langle \mathbf{r}_j, Bs|\mathbf{k}\rangle = (1 - P_A - P_B)|\mathbf{k}\rangle, \end{aligned} \quad (6.103)$$

where \mathbf{k} is related to the normalized plane wave, P_A and P_B are projection operators and the bra- and ket-vectors represent ion-core states centered on the \mathbf{r}_j sites,

$$\langle \mathbf{r}|\mathbf{r}_j, At\rangle = \Psi_t^A(\mathbf{r} - \mathbf{r}_j), \quad \langle \mathbf{r}|\mathbf{r}_j, Bs\rangle = \Psi_s^B(\mathbf{r} - \mathbf{r}_j). \quad (6.104)$$

By expressing the wave function $\Psi_{\mathbf{k}}$ in terms of the generalized OPW (6.103) we have

$$|\Psi_{\mathbf{k}}\rangle = \sum_{\mathbf{q}} a_{\mathbf{k}}(\mathbf{q}) |OPW_{\mathbf{k}+\mathbf{q}}\rangle = (1 - P_A - P_B) \Phi_{\mathbf{k}}, \quad (6.105)$$

where

$$\Phi_{\mathbf{k}} \equiv \sum_{\mathbf{q}} a_{\mathbf{k}}(\mathbf{q}) |\mathbf{k} + \mathbf{q}\rangle \quad (6.106)$$

is a pseudowave function. By substituting the above relationships into the Schrödinger equation, we find

$$(T + \mathcal{W})|\Phi_{\mathbf{k}}\rangle = E_{\mathbf{k}}|\Phi_{\mathbf{k}}\rangle, \quad (6.107)$$

where the pseudopotential \mathcal{W} is given by

$$\mathcal{W} = Y(\mathbf{r}) + (E_{\mathbf{k}} - H)(P_A + P_B). \quad (6.108)$$

By applying the Hamiltonian $H = T + Y$ to the core states we obtain the Phillips-Kleinman pseudopotential generalized to the case

of an alloy,

$$\mathcal{W} = Y(\mathbf{r}) + \sum_{j(A)} \sum_t (E_{\mathbf{k}} - E_t^A) |\mathbf{r}_j, At\rangle \langle \mathbf{r}_j, At| \\ + \sum_{j(B)} \sum_s (E_{\mathbf{k}} - E_s^B) |\mathbf{r}_j, Bs\rangle \langle \mathbf{r}_j, Bs|. \quad (6.109)$$

By generalizing the optimization procedure of [74] for an alloy and linearizing the equation we find

$$\mathcal{W} = (1 - P_A - P_B) Y + \frac{\langle \mathbf{k} | (1 - P_A - P_B) Y | \mathbf{k} \rangle}{\langle \mathbf{k} | (1 - P_A - P_B) | \mathbf{k} \rangle} (P_A + P_B). \quad (6.110)$$

Applying the operator $Y = H - T$ to the projection operators yields the alloy generalization of the optimized Harrison pseudopotential:

$$\mathcal{W}|\mathbf{k}\rangle = Y|\mathbf{k}\rangle + \sum_{j(A)} \sum_t (k^2 + \langle \mathbf{k} | \mathcal{W} | \mathbf{k} \rangle - E_t^A) |\mathbf{r}_j, At\rangle \langle \mathbf{r}_j, At| \mathbf{k}\rangle \\ + \sum_{j(B)} \sum_s (k^2 + \langle \mathbf{k} | \mathcal{W} | \mathbf{k} \rangle - E_s^B) |\mathbf{r}_j, Bs\rangle \langle \mathbf{r}_j, Bs| \mathbf{k}\rangle. \quad (6.111)$$

We are now in a position to evaluate the diagonal and off-diagonal matrix elements of the pseudopotential; they may be expressed in terms of single-ion pseudopotentials. By making use of partial structure factors, the matrix elements may be written as

(i) off-diagonal:

$$\langle \mathbf{k} + \mathbf{q} | \mathcal{W} | \mathbf{k} \rangle = S_A(\mathbf{q}) \langle \mathbf{k} + \mathbf{q} | W_A | \mathbf{k} \rangle + S_B(\mathbf{q}) \langle \mathbf{k} + \mathbf{q} | W_B | \mathbf{k} \rangle, \quad (6.112)$$

where

$$\langle \mathbf{k} + \mathbf{q} | W_A | \mathbf{k} \rangle = Y_A(\mathbf{q}) + \sum_t (k^2 + \langle \mathbf{k} | \mathcal{W} | \mathbf{k} \rangle - E_t^A) \langle \mathbf{k} + \mathbf{q} | 0, At \rangle \langle 0, At | \mathbf{k} \rangle, \\ \langle \mathbf{k} + \mathbf{q} | W_B | \mathbf{k} \rangle = Y_B(\mathbf{q}) + \sum_s (k^2 + \langle \mathbf{k} | \mathcal{W} | \mathbf{k} \rangle - E_s^B) \langle \mathbf{k} + \mathbf{q} | 0, Bs \rangle \langle 0, Bs | \mathbf{k} \rangle. \quad (6.113)$$

(ii) diagonal:

$$\langle \mathbf{k} | \mathcal{W} | \mathbf{k} \rangle = (1 - c) \langle \mathbf{k} | W_A | \mathbf{k} \rangle + c \langle \mathbf{k} | W_B | \mathbf{k} \rangle, \quad (6.114)$$

where

$$\langle \mathbf{k} | W_A | \mathbf{k} \rangle = Y_A(0) + (1 - \langle \mathbf{k} | P | \mathbf{k} \rangle)^{-1} \\ \times \sum_t (k^2 + \bar{Y} - E_t^A) |\langle 0, At | \mathbf{k} \rangle|^2, \quad (6.115) \\ \langle \mathbf{k} | W_B | \mathbf{k} \rangle = Y_B(0) + (1 - \langle \mathbf{k} | P | \mathbf{k} \rangle)^{-1} \\ \times \sum_s (k^2 + \bar{Y} - E_s^B) |\langle 0, Bs | \mathbf{k} \rangle|^2,$$

where we have used the notation

$$\begin{aligned}\bar{Y} &= (1-c) Y_A(0) + c Y_B(0), \\ \langle \mathbf{k} | P | \mathbf{k} \rangle &= (1-c) \sum_t |\langle \mathbf{k} | 0, At \rangle|^2 + c \sum_s |\langle \mathbf{k} | 0, Bs \rangle|^2.\end{aligned}\quad (6.116)$$

The important qualitative conclusion to be drawn from these results is as follows [428]. Since the optimized formfactor of either component depends on the other component, it differs from the pure-component formfactor and this difference cannot be reduced to a mere change in the specific atomic volume or in the density of valence electrons.

Since the self-consistent crystal potential is unknown, we start with electron-ion potentials which are substituted into the above formulae in place of W_A (W_B). This is followed by a linear screening procedure using a uniform electron gas of density $\rho = \bar{Z}\bar{\Omega}^{-1}$ (the atomic volume $\bar{\Omega}$ should be found from a thermodynamic stability condition). As a result, the matrix element of the self-consistent potential takes the form

$$\langle \mathbf{k} + \mathbf{q} | W_{A,B} | \mathbf{k} \rangle = \langle \mathbf{k} + \mathbf{q} | W_{A,B}^b | \mathbf{k} \rangle + W_{A,B}^{\text{scr}}(\mathbf{q}), \quad (6.117)$$

where

$$W_{A,B}^{\text{scr}}(\mathbf{q}) = \frac{4 [1 - f(q)]}{\varepsilon^*(q) \pi^2 q^2} \int_{|\mathbf{k}| < k_F} \frac{\langle \mathbf{k} + \mathbf{q} | W_{A,B}^b | \mathbf{k} \rangle}{k^2 - |\mathbf{k} + \mathbf{q}|^2} d\mathbf{k}, \quad (6.118)$$

$$\varepsilon^*(q) = 1 + [1 - f(q)] [\varepsilon(q) - 1]. \quad (6.119)$$

Here the function $f(q)$ takes into account the exchange and correlation corrections (in [428] these are given in the form obtained in [429]). The electron-ion potential used in [428] is evaluated by the X_α method, as was the case for pure metals. The important features of this process are the following.

First, only one free parameter is employed to describe many-electron effects. Second, the normalized OPW density is made up of a constant term $\Omega^{-1} (1 - \langle \mathbf{k} | P | \mathbf{k} \rangle)^{-1}$, and site-centered localized terms

$$N^{-1} \langle \mathbf{k} | P_A | \mathbf{k} \rangle (1 - \langle \mathbf{k} | P | \mathbf{k} \rangle)^{-1} \quad \text{and} \quad N^{-1} \langle \mathbf{k} | P_B | \mathbf{k} \rangle (1 - \langle \mathbf{k} | P | \mathbf{k} \rangle)^{-1}$$

which describe orthogonalization holes. Taken together with ion charges they give effective valencies

$$Z_{A(B)}^* = Z_{A(B)} + \frac{1}{N} \sum_{|\mathbf{k}| < k_F} \frac{\langle \mathbf{k} | P_{A(B)} | \mathbf{k} \rangle}{1 - \langle \mathbf{k} | P | \mathbf{k} \rangle} \quad (6.120)$$

different from the valencies of pure metals. Third, the theory makes it possible to evaluate the energy eigenvalues of the ion-core

electrons:

$$\bar{Y} - E_{t(s)}^{A(B)} = -\frac{18}{5} \left(\frac{\bar{Z}^*}{r_0} \right) + \bar{Y}^b + \bar{Y}^{\text{ex}} + Y_{A(B)}^{\text{OPW}} - \varepsilon_{t(s)}^{A(B)}. \quad (6.121)$$

There \bar{Y}^b and \bar{Y}^{ex} are the averaged (at $q = 0$) matrix elements of the Coulomb potential (for conduction and core electrons) and the exchange potential respectively; $\varepsilon_{t(s)}^{A(B)}$ are the ion eigenvalues, Y^{OPW} is the orthogonalization hole. It should be stressed that these relations are only true for completely disordered alloys; otherwise the effect of nearest neighbors on the core states must be considered.

The pseudopotentials obtained were used for evaluating the total energy which, as in the local case, contains the free-electron, band and electrostatic contributions. The free-electron energy is

$$\begin{aligned} U_0 = & \frac{3}{5} \bar{Z} k_F^2 + Z U_{\text{xc}} + \bar{Z}^* (\bar{Y}^b + \bar{Y}^{\text{ex}}) \\ & + \frac{1-c}{N} \sum_{|\mathbf{k}| < k_F} \sum_t \left(k^2 + |\varepsilon_t^A| - \frac{1}{2} Y_A^{\text{OPW}} \right) \frac{|\langle \mathbf{k} | 0, A t \rangle|^2}{1 - \langle \mathbf{k} | P | \mathbf{k} \rangle} \\ & + \frac{c}{N} \sum_{|\mathbf{k}| < k_F} \sum_s \left(k^2 + \varepsilon_s^B - \frac{1}{2} Y_B^{\text{OPW}} \right) \frac{|\langle \mathbf{k} | 0, B s \rangle|^2}{1 - \langle \mathbf{k} | P | \mathbf{k} \rangle}, \quad (6.122) \end{aligned}$$

and for the band energy we have

$$U_{\text{bs}} = \sum_{\mathbf{q}}' |S(\mathbf{q})|^2 \bar{\mathcal{F}}(\mathbf{q}) + \sum_{\mathbf{q}}' |C(\mathbf{q})|^2 \Delta \mathcal{F}(\mathbf{q}), \quad (6.123)$$

where

$$\bar{\mathcal{F}}(\mathbf{q}) = \frac{2\Omega}{(2\pi)^3} \int_{|\mathbf{k}| < k_F} \frac{|\langle \mathbf{k} + \mathbf{q} | \bar{W} | \mathbf{k} \rangle|^2}{k^2 - |\mathbf{k} + \mathbf{q}|^2} d\mathbf{k} - \frac{q^2}{16\pi} \frac{|\bar{W}^{\text{scr}}(\mathbf{q})|^2}{1 - f(\mathbf{q})}, \quad (6.124)$$

$$\Delta \mathcal{F}(\mathbf{q}) = \frac{2\Omega}{(2\pi)^3} \int_{|\mathbf{k}| < k_F} \frac{|\langle \mathbf{k} + \mathbf{q} | \Delta W | \mathbf{k} \rangle|^2}{k^2 - |\mathbf{k} + \mathbf{q}|^2} d\mathbf{k} - \frac{q^2}{16\pi} \frac{|\Delta W^{\text{scr}}(\mathbf{q})|^2}{1 - f(\mathbf{q})}. \quad (6.125)$$

It is worth noting that (6.123) is similar to the corresponding local-potential results. Eqs. (6.123) and (6.125) differ from the analogous local-theory expressions in that the local potential is replaced by a nonlocal one. It follows from (6.124) that for a completely disordered alloy

$$\Delta U_{\text{bs}} = \frac{\bar{\Omega}}{(2\pi)^3} c(1-c) \int \Delta \mathcal{F}(\mathbf{q}) d\mathbf{q}. \quad (6.126)$$

The relations derived in this section are particularly valuable in that they are rigorous and may therefore form a basis for more consistent and fundamental studies. It should also be noted that the obvious possibility of changing to local theory expressions (merely by replacing nonlocal by local potentials) justifies the earlier efforts in the field.

Pseudopotential theory of alloys. Structure stability application

7.1. Phase boundaries in terms of pseudopotential theory

There are two major questions which an alloy stability theory must answer, namely, which phases can exist in a given alloy and when. One of the earliest attempts to attack this subject in terms of pseudopotential theory was undertaken by Stroud and Ashcroft [434]. As no reasonable theory can do without an explanation of the Hume-Rothery rules (see Chapter 6), it was on this point that they focused their attention.

The internal configurational energy is represented in [434] in the usual way as the sum of the electrostatic and band contributions. The former is written (in ryd per electron) as

$$U_{\text{es}} = \frac{1}{2N\bar{Z}} \sum_{v \neq v'} \frac{2\langle Z_v Z_{v'} \rangle}{|\mathbf{t}_v - \mathbf{t}_{v'}|}, \quad (7.1)$$

where the brackets denote an average over all possible configurations of the A and B ions. As these are assumed to be distributed at complete random, we get $\langle Z_v Z_{v'} \rangle = \bar{Z}^2$, and in the Fourier representation we have

$$U_{\text{es}} = \frac{1}{2} \sum_{\mathbf{q}} \frac{8\pi\bar{Z}}{q^2} \{N|S'(\mathbf{q})|^2 \delta_{\mathbf{q}, \mathbf{g}_n} - 1\}, \quad (7.2)$$

where $S'(\mathbf{q})$ is the Röntgen structure factor divided by the number of atoms in the unit cell.

The band energy term was written as

$$U_{\text{bs}} = \sum_n \frac{g_n^2}{8\pi\bar{Z}} |\overline{W^b(\mathbf{q})}|^2 |S'(\mathbf{g}_n)|^2 \left[\frac{1}{\varepsilon(\mathbf{q})} - 1 \right]. \quad (7.3)$$

From (7.2) and (7.3), the relative energies of the FCC, BCC and the ideal c/a ratio HCP structures of the alloy systems Cu-Al, Li-Mg and Cu-Zn were calculated using the pseudopotentials $W^b = 8\pi Z/g_1^2$ and $W^b = (8\pi Z/g_1^2) \cos g_1 r_c$ (where r_c is the core radius and is fitted to experimental data). There are a number of approximations which are made in the above expressions and which were quite natural when the study was made. The virtual crystal approximation is used both in (7.2) and (7.3); there is no Ewald exponential in the sum over \mathbf{q} in (7.2); and the exchange-correlation corrections

are omitted in (7.3). Even so, interesting qualitative results were obtained.

The major result is clearly illustrated in Fig. 7.1. As the radius of the Fermi sphere becomes equal to half a reciprocal lattice vector, the energy of the corresponding structure decreases sharply relative to the other two. In other words, a fall in the energy of a crystal structure occurs when the Fermi sphere touches the Brillouin zone's face. The effect was observed in transitions between various pairs

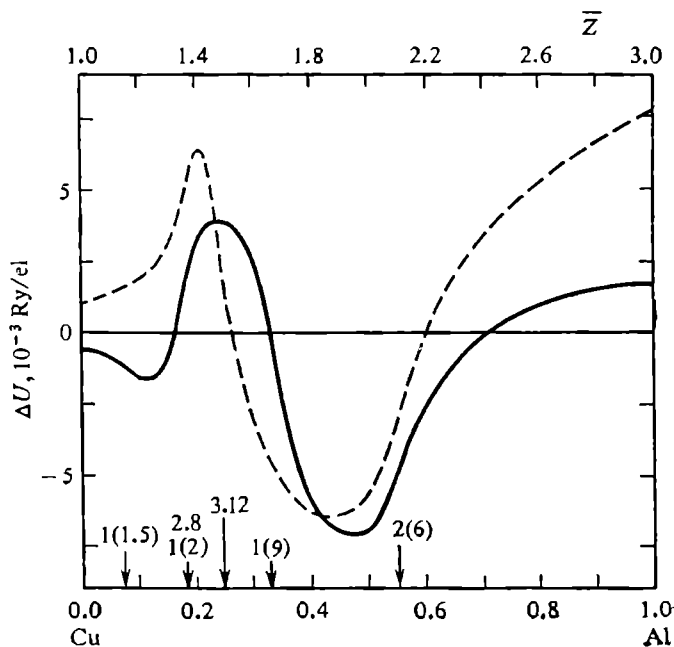


Fig. 7.1. Energy differences between the HCP and FCC structures (bold line), and BCC and FCC structures (dashed line) for the Cu-Al alloys. The arrows indicate the g_n for the HCP (1), FCC (2), and BCC (3) phases. Figures in parentheses are structure weights.

of phases and could not therefore be dismissed as fortuitous. The reason for this effect is, presumably, the discontinuity occurring in the third derivative of the energy with respect to electron concentration at $g_n \simeq 2k_F$. This discontinuity causes a precipitous drop in the energy of the corresponding phase and hence changes the sign of the energy difference between the phases. For elaboration of these views see [419].

Hence, when the Fermi sphere comes in contact with the face of the first Brillouin zone, a phase transition takes place. Though this observation is an agreement with earlier views, the underlying reason for the effect is somewhat different from the one assumed earlier to be the case because U_{bs} has no minimum at $g_n \simeq 2k_F$. Although the sums involved in total energy calculations were carried in [434]

over about 160 reciprocal lattice vectors, it is interesting that each sum is dominated by a vector which corresponds to the contact between the Brillouin zone and the Fermi sphere. It should be noted that although Stroud and Ashcroft were rather successful in explaining the Hume-Rothery rules, their mathematical formalism is not entirely rigorous.

Interestingly, Stroud and Ashcroft's conclusions were supported by Kogachi and Matsuo who published their results [435] at about

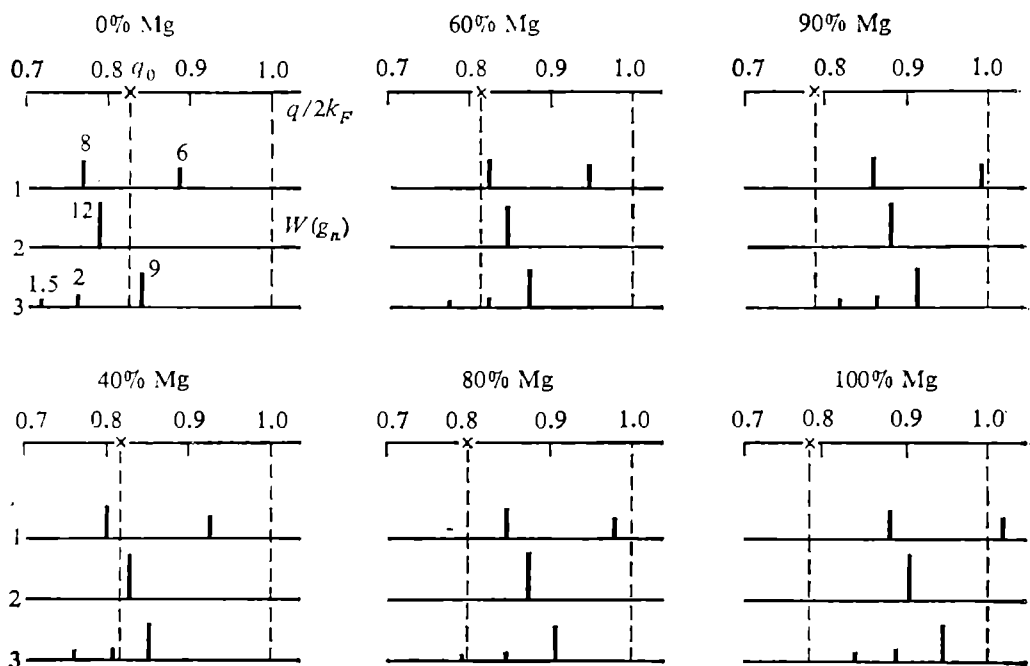


Fig. 7.2. Positions for the q_0 and g_n for the FCC (1), BCC (2), and HCP (3) phases of the In-Mg alloys.

the same time. In the latter pseudopotential alloy theory was applied to an investigation of the phase boundaries and structure stability of the alloy systems In-Mg and Al-Mg. Since all the three elements are not transition metals it might be expected from the start that the results of [435] should be more accurate than those of [434], in which the alloys studied were mainly noble-metal ones. Kogachi and Matsuo, however, not only dropped the fluctuational term but also neglected the difference between the electrostatic energies of neighboring phases (assuming the phases to be simple). In both [434] and [435] the band energy does not include exchange-correlation corrections in the dielectric permeability. Thus in [435] a binary alloy was in fact treated as a pure metal, the only "binary" effect being a change of \bar{Z} and $\bar{\Omega}$ with composition. As a result, the quantitative

analysis more or less reduced to a determination of the relative positions of q_0 and the first reciprocal lattice vectors.

Figures 7.2 and 7.3 illustrate the positions of q_0 , $2k_F$ and the structural sites of the FCC, BCC and HCP structures (with their weights) for the alloy systems In-Mg and Al-Mg. It can be seen for the In-Mg system that in the absence of Mg, q_0 turns out to be close to the structural sites of close-packed structures, which explains the tetragonally distorted structure of In. When Mg is introduced the

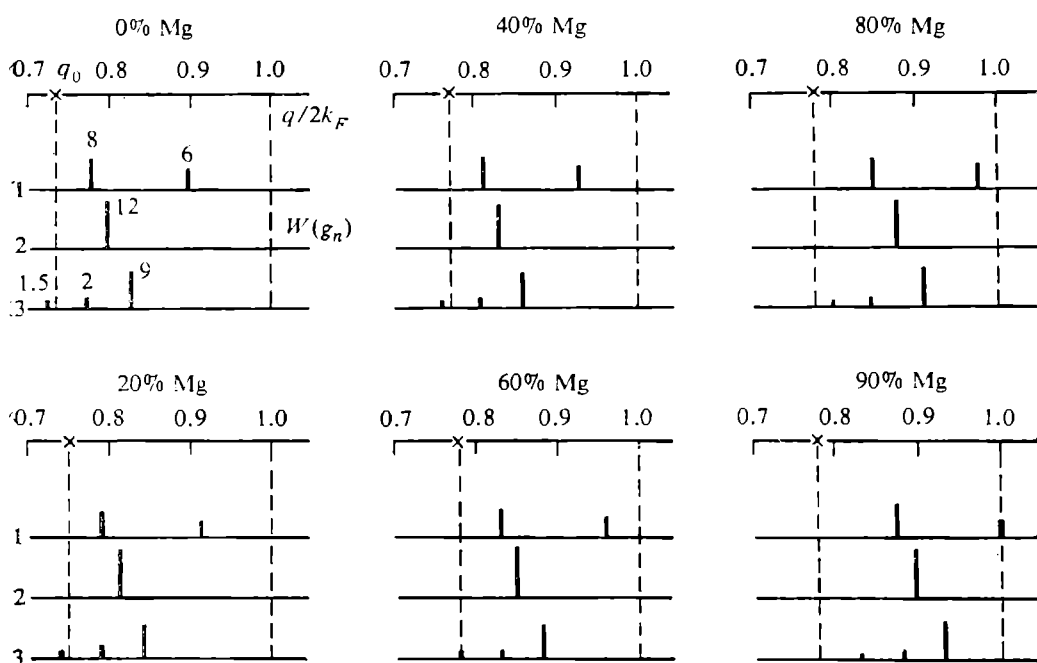


Fig. 7.3. Positions of the q_0 and g_n for the FCC (1), BCC (2), and HCP (3) phases of the Al-Mg alloys.

value of q_0 falls to lower q 's whereas the reciprocal lattice sites are raised to higher ones. As a result, the degree of tetragonality decreases with Mg concentration and at a certain composition the appearance of the FCC structure becomes possible. At about 80-90 at. %Mg, the (200) site of the FCC structure moves into the region $q > 2k_F$ thus giving rise to an HCP structure which is also typical of pure Mg.

For the Al-Mg system, the situation differs in that even for low concentrations of Mg, the values of g_n are greater than q_0 in all the major structures. Accordingly, the low Mg concentration favors one of the close-packed structures, namely FCC, while HCP is only favored from 90 at. % Mg, at which $g_{(200)}$ become greater than $2k_F$.

The predicted behavior of phase transition correlates rather well with what is actually observed in these systems, though the complex structures are not describable in terms of the above theory.

The condition $g_n = 2k_F$ is thus the key factor to determine phase boundaries in this work [435]. Another important factor when determining phase structure and phase transition points is the position of g_n in relation to q_0 .

7.2. Ordered phases, their structures, and existence conditions

With the notable exception of the very first paper [398], all early pseudopotential calculations on ordered phases were performed to second order in local pseudopotential. Even with this restriction, the results obtained were important enough to encourage further application of pseudopotential theory to the study of ordered alloys, intermediate phases, etc. [399, 436-438].

It was usually assumed that the atomic volumes and valencies of the components were the same and exchange-correlation effects were neglected. Given these approximations, the band energy was written in the form

$$U_{bs} = \frac{1}{N^2} \sum_n |S(g_n)|^2 |\overline{W}(g_n)|^2 \varepsilon(g_n) \chi(g_n) + \frac{1}{N^2} \sum_{\mathbf{q}} \Phi_a(\mathbf{q}) |cS_A(\mathbf{q}) - (1-c)S_B(\mathbf{q})|^2, \quad (7.4)$$

where

$$S_A(\mathbf{q}) = \sum_{\mathbf{v}(A)} \exp[-i\mathbf{q}\mathbf{t}_{\mathbf{v}(A)}], \quad S_B(\mathbf{q}) = \sum_{\mathbf{v}(B)} \exp[-i\mathbf{q}\mathbf{t}_{\mathbf{v}(B)}]$$

are partial structure factors, and $\Phi_a(\mathbf{q}) = |\Delta W(\mathbf{q})|^2 \varepsilon(\mathbf{q}) \chi(\mathbf{q})$ is the characteristic function of alloying.

The first sum in (7.4) represents the energy of the average crystal and is associated with the arrangement of crystal lattice sites; the second term depends on the way the atoms of different sorts are distributed over the sites. For a completely random alloy, for example, the second sum is

$$U_{bs, \text{rand}} = \frac{1}{N} c(1-c) \sum_{\mathbf{q}} \Phi_a(\mathbf{q}). \quad (7.5)$$

The effect of alloying is determined by the difference between the energy U_{bs} as given by (7.4) and the averaged energy of the pure components,

$$\Delta = U_{bs, \text{all}} - cU_{bs}^B - (1-c)U_{bs}^A. \quad (7.6)$$

Explicitly,

$$\begin{aligned}\Delta &= N^{-2} \sum_{\mathbf{q}} \Phi_a(\mathbf{q}) |cS_A - (1-c)S_B|^2 \\ &\quad + N^{-2} \sum_n' |S(\mathbf{g}_n)|^2 \varepsilon(\mathbf{g}_n) \chi(\mathbf{g}_n) [|\overline{W}(\mathbf{g}_n)|^2 \\ &\quad - (1-c)^2 |W_A(\mathbf{g}_n)|^2 - c^2 |W_B(\mathbf{g}_n)|^2] \\ &= U_a - N^{-2} c(1-c) \sum_n' |S(\mathbf{g}_n)|^2 |\Delta W(\mathbf{g}_n)|^2 \varepsilon(\mathbf{g}_n) \chi(\mathbf{g}_n). \quad (7.7)\end{aligned}$$

Here the first term is the energy of ordering and the second is the amount by which the energy of the average crystal changes on alloying. For a disordered alloy,

$$\Delta = \frac{1}{N} c(1-c) \left\{ \sum_{\mathbf{q}} \Phi_a(\mathbf{q}) - \frac{1}{N} \sum_n' \Phi_a(\mathbf{g}_n) \right\}. \quad (7.8)$$

Figure 7.4 shows the characteristic alloying function $\Phi_a(\mathbf{q})$ for the Hg-Mg alloy. The positions of the (structural and superstructural)

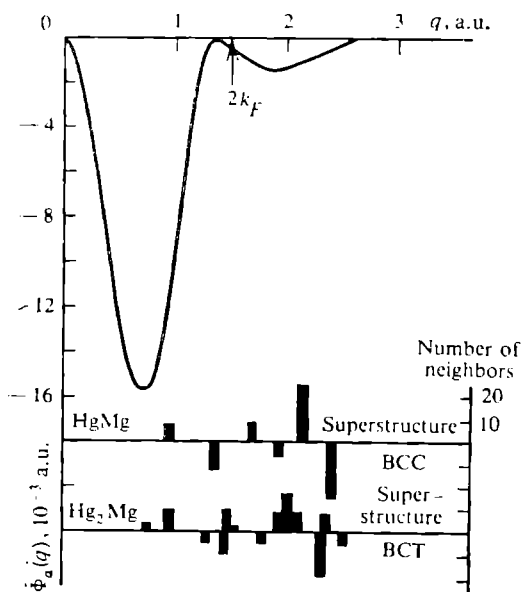


Fig. 7.4. Characteristic alloying function $\Phi_a(\mathbf{q})$ for the Hg-Mg alloys. Below—structural and superstructural sites of the BCC and BCT structures.

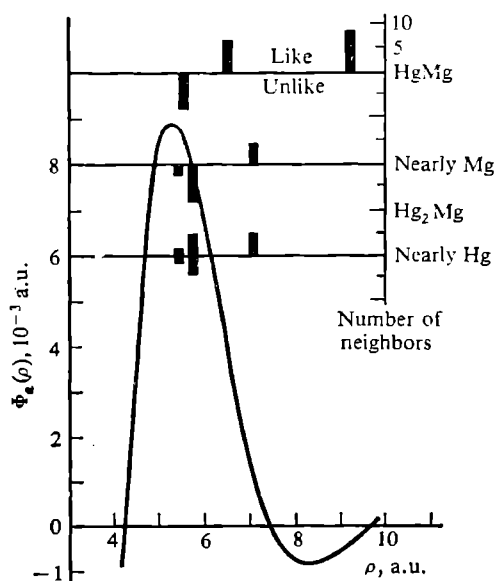


Fig. 7.5. Alloying potential $\Phi_a(\rho)$ for the Hg-Mg alloy.

reciprocal lattice sites and their respective weights are also shown. It can be seen that large magnitudes of $\Phi_a(\mathbf{q})$ correspond to the positions of superstructural sites. This leads to an increase in the ordering energy as a whole.

The configurational energy of an alloy may also be written in terms of the pairwise alloying potential

$$\Phi_a(\rho) = \frac{(Z_A - Z_B)^2}{4\rho} + \frac{2\bar{\Omega}}{(2\pi)^3} \int |\Delta W(\mathbf{q})|^2 \varepsilon(\mathbf{q}) \chi(\mathbf{q}) \exp(i\mathbf{q}\rho) d\mathbf{q}, \quad (7.9)$$

ρ being the interatomic separation.

Figure 7.5 shows the pairwise alloying potential $\Phi_a(\rho)$ for HgMg, together with the number of like and unlike neighbors for the ordered structures HgMg and Hg_2Mg_2 . It can be seen that the maximum in $\Phi_a(\rho)$ falls in the region of ρ for which the number of unlike neighbors is increased on alloying. Clearly, this correlation between the maxima of $\Phi_a(\rho)$ and interatomic separation makes the total energy decrease with ordering and is therefore a mechanism for the appearance of order.

A comparative analysis of the ordering energy was carried out by Inglesfield in his work on the (equiatomic) CdMg, HgMg and CdHg systems [437]. In calculating the matrix elements $W(q)$ he used a spherically symmetric square-well pseudopotential of depth A and width R_m . The depth A was chosen so that the magnitude of the minimum in $\Phi_a(q)$ was equal to that found from a model potential calculation [405]. The parameter R_m was taken to be the same ($R_m = 2.6$ a.u.) for all the systems. In this approximation, the value of Δ turned out to be proportional to A^2 while A itself was proportional to the difference in the Pauling electronegativities of the components. This has led Inglesfield [437] to the conclusion that the alloying and ordering effects are determined by A^2 , that is, by electronegativity differences between the components (provided, of course, that the alloy is essentially metallic).

The ordering energy of the phases studied was found, for HgMg, CdMg, and CdHg, respectively, to be 3.8×10^{-3} , 0.8×10^{-3} , and 0.5×10^{-3} a.u. per ion. In the HgMg system the ordering energy turned out to appreciably exceed the thermal energy at the melting temperature, indicating that an ordered state persists up to the melting point in this particular alloy. In CdMg the computed ordering energy was found to be in fair agreement with the experimental ordering temperature. A comparison of results for CdMg and CdHg suggested that at about 300 K the CdHg system should go through an order-disorder phase transition. As a phase transition is indeed observed in this system at 260 K, it was reasonable to argue that it should be of the order-disorder type.

In his structural analysis of ordered phases [438] Inglesfield pointed out that for spherically symmetric square wells the alloy energy may be written as

$$U = \bar{U} + A^2 \Delta_m, \quad (7.10)$$

where \bar{U} is the weighted average energy of pure components and $\Delta_m = \Delta/A^2$.

If A^2 is very small, clearly the total energy will be determined by the energy of the pure components and the alloy structure will be very nearly that of the constituents: if A^2 is large, Inglesfield suggests, the resulting compound must be ionic.

In the same series of papers [394, 436-438] there is an interesting attempt to estimate the range of existence of an ordered phase. This was done by considering the change in the ordering energy when $N\delta$ atoms of species A were replaced by the same number of B atoms arbitrarily distributed over the sites originally occupied by the A atoms. The energy difference for an ordered phase having $(1/2 + \delta)N$ of the B atoms and $1/2N$ atoms of the same sort is

$$U_{a, \text{ord}+\delta} - U_{a, \text{ord}} = 4\delta [U_{a, \text{disord}} - U_{a, \text{ord}}]. \quad (7.11)$$

Consequently,

$$\frac{dU}{dc} = U_B - U_A \pm 4 [U_{a, \text{disord}} - U_{a, \text{ord}}]. \quad (7.12)$$

It follows from this that the higher the ordering energy, the stronger the singularity in dU/dc at $c \simeq 1/2$ and hence the narrower the range of existence of the ordered phase.

In [439-441], the above theory was extended to include (ordered) alloys with components of different valencies.

The ordered phases considered in [439] consist of components whose ions have different charges and radii. The formulae for calculating the energy of the phases are basically similar to those given in the previous chapter. There are some differences though.

For example, the band energy is written in [439] for an alloy with short-range and long-range order. This, in fact, is formula (6.39) in which the short-range order parameter α (ρ_i) is replaced by

$$\varphi(\rho_m) = \alpha(\rho_m) + \frac{\xi_\alpha \xi_\beta}{c(1-c)} \eta^2 \sigma(\rho_m), \quad (7.13)$$

where $\alpha(\rho_m)$ is the short-range-order parameter and the second term describes the way atoms of different sorts are distributed over the α and β sublattices in the presence of long-range order of amount η (the atoms A and B are assumed to be distributed arbitrarily over the sites of either sublattice); ξ_α and ξ_β are the concentrations of the α and β sites; σ_m is a geometry factor determined by the structure of the ordered alloy.

For the superstructure $\mathcal{L}1_0$,

$$\sigma(\rho_m) = e^{2\pi i m_3}, \quad (7.14)$$

for $\mathcal{L}1_2$ and $\mathcal{L}2_0$,

$$\sigma(\rho_m) = \frac{1}{3} (e^{2\pi i m_1} + e^{2\pi i m_2} + e^{2\pi i m_3}). \quad (7.15)$$

In both expressions m_1 , m_2 and m_3 are integers or half-integers. If there is short-range order and some amount of long-range order in these structures, (6.33) takes the form

$$\Delta U_{bs}^{(2)} = \frac{\bar{\Omega}}{8\pi N} \sum_{\mathbf{q}}' \mathbf{q}^2 \frac{1-\varepsilon(\mathbf{q})}{\varepsilon^*(\mathbf{q})} |\Delta W^b(\mathbf{q})|^2 \\ \times \left\{ \xi_\alpha \xi_\beta \eta^2 \delta_{\mathbf{q}, \mathbf{g}_{n,ss}} + c(1-c) \sum_i C_i \alpha_i \frac{\sin q\rho_i}{q\rho_i} \right\}. \quad (7.16)$$

It should be kept in mind that instead of introducing the usual weight functions, Katada *et al.* [440] sets $\sigma_{\mathbf{q}, \mathbf{g}_{n,ss}} = 1/3$ for $\mathbf{q} = \mathbf{g}_{n,ss}$ in the superstructure $\mathcal{L}1_2$. It is also worth noting that, by definition, $\varphi(0) = 1$ and $\sigma(0) = 1$ so that $\alpha_0 = 1 - (\xi_\alpha \xi_\beta \eta^2 / c(1-c))$.

The electrostatic energy is written in [440] as

$$U_{es} = N^{-2} \sum_{\mathbf{q}} \frac{2\pi}{\Omega q^2} \left\{ \sum_{\mathbf{v}} \sum_{\mathbf{v}'} Z(\mathbf{t}_{\mathbf{v}}) Z(\mathbf{t}_{\mathbf{v}'}) \exp(-i\mathbf{q} \cdot \mathbf{t}_{\mathbf{v}} - \mathbf{t}_{\mathbf{v}'}) \right. \\ \left. - \sum_{\mathbf{v}} |Z(\mathbf{t}_{\mathbf{v}})|^2 \right\}, \quad (7.17)$$

where $Z(\mathbf{t}_{\mathbf{v}})$ is the charge at point $\mathbf{t}_{\mathbf{v}}$. By isolating the energy of the average crystal we find

$$U_{es} = \bar{U}_{es} + \Delta U_{es} = \sum_{\mathbf{q}}' \mathcal{F}_{es}(\mathbf{q}) \left\{ \delta_{\mathbf{q}, \mathbf{g}_{n,ss}} - \frac{1}{N} \right\} \\ + \sum_{\mathbf{q}}' \mathcal{G}_{es}(\mathbf{q}) \left\{ \xi_\alpha \xi_\beta \eta^2 \delta_{\mathbf{q}, \mathbf{g}_{n,ss}} + \frac{1}{N} c(1-c) \sum_i C_i \alpha_i \frac{\sin q\rho_i}{q\rho_i} - \frac{c(1-c)}{N} \right\}, \quad (7.18)$$

where

$$\mathcal{F}_{es}(\mathbf{q}) = \frac{2\pi}{\Omega} \frac{(\bar{Z})^2}{q^2} \quad \text{and} \quad \mathcal{G}_{es}(\mathbf{q}) = \frac{2\pi}{\Omega} \frac{\Delta Z^2}{q^2}. \quad (7.19)$$

Thus, if we assume the volume to be constant (which is not always the case), the energy associated with the appearance of long-range order may be represented as

$$U_{ord} = \Delta U_{es} + \Delta U_{bs} = \xi_\alpha \xi_\beta \eta_{\max}^2 \sum_{\mathbf{q}}' [\mathcal{G}_{bs}(\mathbf{q}) \\ + \mathcal{G}_{es}(\mathbf{q})] \left\{ \delta_{\mathbf{q}, \mathbf{g}_{n,ss}} - \frac{1}{N} \right\}. \quad (7.20)$$

Katada *et al.* point out that ΔU_{es} is always negative and favors order in the arrangement of the atoms. At the same time, ΔU_{bs} is chiefly

determined by the behavior of $\mathcal{G}_{bs}(\mathbf{q})$ at \mathbf{q} 's smaller than the first zero of the function ($\mathcal{G}_{bs}(\mathbf{q}) \leq 0$ in this region).

In alloys for which $Z_A = Z_B$, an ordered state may only occur if ΔU_{bs} is negative because $\Delta U_{es} = 0$ in this case. If, however, $Z_A \neq Z_B$, the value of U_{ord} may also be positive, provided that the positive contribution, ΔU_{bs} , outweighs the negative one, ΔU_{es} . Even though the above expressions were derived by neglecting the Ewald term and the exchange correlation effects, they can reasonably be used for numerical estimates of the energies of ordered phases.

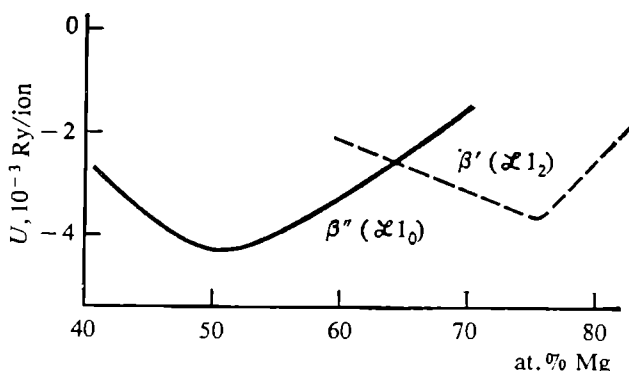


Fig. 7.6. The energies of the β' - and β'' -phases as functions of composition (the In-Mg alloy).

Numerical results for In-Mg alloys are shown in Fig. 7.6 for the region where the ordered phases of InMg ($\mathcal{L}1_0$) and InMg₃ ($\mathcal{L}1_2$) exist. The calculations were carried out with an optimized potential taken from [154]; the sum $\frac{1}{N} \sum_{\mathbf{q}} \mathcal{G}_{bs}(\mathbf{q})$ was replaced by an integral.

The results show that the ordered phase of the $\mathcal{L}1_0$ -type structure is stable in the range 40-65 at.% Mg, that of the $\mathcal{L}1_2$ -type in the range 65-80 at.% Mg. In both cases the energy minimum corresponds to the stoichiometric compositions.

If a completely ordered state is considered and the Gorskii-Bragg-Williams entropy contribution is assumed, then the transition temperature T_c for the In-Mg alloy will be $T_c = -U_{ord} (k_B \ln 2)^{-1}$ and for In-Mg₃ $T_c = -U_{ord} [k_B (2 \ln 2 - 0.75 \ln 3)]^{-1}$. The computed temperatures will be, respectively, 1000 K and 1200 K whereas the observed ones are 600 K and 620 K. This discrepancy, Kogachi argues, cannot be due to a poorly chosen potential because a potential taken from [405] only increased the predicted temperature by another 10%. This argument is not, of course, entirely satisfactory, but the true reason for the discrepancy remains unclear.

In [440], the above theory was developed to include alloys with more than one atom in the unit cell. Specifically, HCP alloys were investigated. The expressions for the band and electrostatic energies

were found to be

$$\bar{U}_{bs} = \sum'_{\mathbf{q}} \mathcal{F}_{bs}(\mathbf{q}) \sigma_n,$$

$$\Delta U_{bs} = \sum'_{\mathbf{q}} \mathcal{G}_{bs}(\mathbf{q}) \left\{ \xi_\alpha \xi_\beta \eta^2 \sigma' + \frac{c(1-c)}{N} \sum_i C_i \alpha_i \frac{\sin q \rho_i}{q \rho_i} \right\}, \quad (7.21)$$

and

$$\bar{U}_{es} = \sum'_{\mathbf{q}} \mathcal{F}_{es}(\mathbf{q}) \left\{ \sigma_n - \frac{1}{N} \right\},$$

$$\Delta U_{es} = \sum'_{\mathbf{q}} \mathcal{G}_{es}(\mathbf{q}) \left\{ \xi_\alpha \xi_\beta \eta^2 \sigma' - \frac{c(1-c)}{N} + \frac{c(1-c)}{N} \sum_i C_i \alpha_i \frac{\sin q \rho_i}{q \rho_i} \right\}, \quad (7.22)$$

where

$$\sigma_n = \frac{1}{2} \left\{ 1 + \frac{1}{2} [\gamma(\mathbf{q}) + \gamma^*(\mathbf{q})] \right\} \delta(\mathbf{q}, \mathbf{g}_n), \quad (7.23)$$

$$\gamma(\mathbf{q}) = \exp \left[-i\mathbf{q} \left(\frac{2}{3} \mathbf{a}_1 + \frac{1}{3} \mathbf{a}_2 + \frac{1}{2} \mathbf{a}_3 \right) \right]. \quad (7.24)$$

The exact form of σ' depends on the type of the superstructure. For example, for $\mathcal{B}19$

$$\sigma' = \frac{1}{2} \left\{ 1 + \frac{1}{2} [\gamma(\mathbf{q}) + \gamma^*(\mathbf{q})] \right\} \delta\left(\mathbf{q}, \mathbf{g}_n + \frac{\mathbf{a}_1^*}{2}\right) = \sigma_n^{(1)}, \quad (7.25)$$

for the superstructure \mathcal{DO}_{19}

$$\sigma' = \frac{1}{3} (\sigma'_n + \sigma_s^{(2)} + \sigma_s^{(1,2)}), \quad (7.26)$$

$$\sigma_s^{(2)} = \frac{1}{2} \left\{ 1 - \frac{1}{2} [\gamma(\mathbf{q}) + \gamma^*(\mathbf{q})] \right\} \delta\left(\mathbf{q}, \mathbf{g}_n + \frac{\mathbf{a}_2^*}{2}\right), \quad (7.27)$$

$$\sigma_s^{(1,2)} = \frac{1}{2} \left\{ 1 - \frac{1}{2} [\gamma(\mathbf{q}) + \gamma^*(\mathbf{q})] \right\} \delta\left(\mathbf{q}, \mathbf{g}_n + \frac{\mathbf{a}_1^* + \mathbf{a}_2^*}{2}\right). \quad (7.28)$$

The ordering energy calculations for the Cd-Mg system are very interesting. For the compositions CdMg_3 and Cd_3Mg the ordering energies were found to favor the \mathcal{DO}_{19} structure, and to favor $\mathcal{B}19$ for CdMg . These are indeed the structures observed in experiment. The phase stability boundaries calculated for these structures were also found to be in agreement with experiment. It is interesting to note that for the equiatomic CdMg system the results [440] are to within 20% of those in [437].

Since ordering phenomena are characteristic of noble-metal alloys, it was natural to apply pseudopotential theory to this case. Alloys based on Ag, Au, Mg and Al were studied by Kogachi [441] using the pseudopotentials proposed in [313]. These potentials, however, contain additional repulsion terms due to the overlap of d states, so some corrections had to be introduced into the theory.

With a repulsion potential, the structure-dependent term of the total energy has the form

$$U = U_{bs} + U_{es} + U_{rp}, \quad (7.29)$$

where the repulsion energy U_{rp} may be written for the BCC and FCC structures as

$$U_{rp} = \frac{1}{2N} \sum_i \sum_{j \neq i} \{ P_A(t_i) P_A(t_j) W_{AA}(|t_i - t_j|) \\ + P_B(t_i) P_B(t_j) W_{BB}(|t_i - t_j|) - [P_A(t_i) P_B(t_j) \\ + P_B(t_i) P_A(t_j)] W_{AB}(|t_i - t_j|) \}. \quad (7.30)$$

Here the fluctuational and average crystal terms are easily separated. By combining them with known results for the band and electrostatic energies we find the energies of a completely disordered and an ordered crystal:

$$U_{chaot} = \sum_{\mathbf{q}}' \{ \mathcal{F}_{bs}(\mathbf{q}) \delta_{\mathbf{q}, \mathbf{g}_{n,f}} + \mathcal{F}_{es}(\mathbf{q}) \} \left[\delta_{\mathbf{q}, \mathbf{g}_{n,f}} - \frac{1}{N} \right] \\ + \sum_i \frac{1}{2} C_i \bar{W}(\rho_i), \quad (7.31)$$

$$U_{ord} = U_{chaot} + \xi_\alpha \xi_\beta \eta_{\max}^2 \sum_{\mathbf{q}}' [\mathcal{G}_{bs}(\mathbf{q}) + \mathcal{G}_{es}(\mathbf{q})] \left[\delta_{\mathbf{q}, \mathbf{g}_{n,ss}} - \frac{1}{N} \right] \\ + \sum_i \frac{C_i \alpha_{i \max}}{2} \Delta W(\rho_i). \quad (7.32)$$

Here $\alpha_{i \max}$ are the limiting values of the short-range order parameters for the i th coordination sphere; $W_{AA}(\rho_i)$, $W_{BB}(\rho_i)$ and $W_{AB}(\rho_i)$ are the repulsion potentials for, respectively, AA , BB and AB pairs (separated by ρ_i); and $\Delta W(\rho_i) = W_{AA} + W_{BB} - 2W_{AB}$, $\bar{W} = (1 - c)^2 W_{AA} + c^2 W_{AB} + 2c(1 - c) W_{AB}$. It was assumed in calculating the repulsion potential that it remains unchanged on alloying, operates only between noble metal atoms, and is only substantial for the first four coordination spheres.

Pure Mg and pure Al were predicted to be stable in, respectively, the HCP and FCC structures which are actually observed in these metals. When either Ag or Au is added, then at a certain concentration of a minor component, the Ag-Mg or Au-Mg system becomes BCC and the Ag-Al system becomes HCP and so on. If, however, the concentration of the noble metal is increased further, the computed (energetically favorable) structures depart from those observed, which is consistent with [313]. Thus, although the pseudopotential in [313]

is not good enough to predict the favorable structures in pure metals or noble metal-rich alloys, it is still useful for moderate noble metal concentrations.

For ordered phases, only the energy calculations on the Ag-Mg system proved to be successful. It was found in this case that for $\mathcal{L}2_0$ -alloys in the β' phase, an ordered state is possible when the positive contribution from the band energy is outweighed by the negative contribution from the repulsion and electrostatic terms.

It is pointed out in [441] that the perseverance of an ordered phase up to the melting temperature cannot be explained unless the repulsion energy is taken into account. Even if it is, however, the results for the Au-Mg system disagree with experiment. The prevalence of the positive band-energy contribution makes the ordering energy positive and thereby precludes the existence of an ordered phase in this system.

As was mentioned in Chapter 6, a promising and conceptually different way of using pseudopotentials in alloy theory in general and in ordering problems in particular is to invoke the statistical thermodynamic theory of atomic ordering. It is worthwhile here to discuss some of the applications of this approach. In [402] it was employed in a stability analysis of an ordered phase in an equiatomic Ca-Ba alloy. A model potential used in the calculations was taken from [442].

In the disordered phase, the lowest energy was found in the actually observed BCC structure. The next step was to calculate the function $V(\Delta\mathbf{q})$ in the [100], [110], and [111] directions. This particular choice of directions was suggested by a statistical thermodynamical analysis, which showed that for the BCC structure the possible stars of superstructural wave vectors have minima of $V(\mathbf{g}_{n,ss})$ at the (100) or (111) points (CsCl-type superstructure), at the $(1/2, 1/2, 1/2)$ point (NaTl-type superstructure), and at the $(1/2, 1/2, 0)$ point (their superstructure is similar to that arising in implantation phases).

The numerical results represented in Fig. 7.7 predict for the Ca-Ba system a CsCl-type superstructure and T_c (as derived from the value of $V(\mathbf{g}_{n,ss})$) of about 890 K. Experimentally the order-disorder transition occurs at about 400 K in this system and the superstructure is rather of the NaTl type.

We may thus conclude that the approach suggested in [401, 402] can also be used to interpret experimental data. The appeal of the approach is its insensitivity to low- \mathbf{q} "discontinuities". We noted earlier that the low- \mathbf{q} behavior of formfactors may substantially limit, sometimes perhaps prohibitively, the applicability of pseudopotentials to alloy theory. It should be noted, however, that the value of [402] is greatly reduced because only the model potential from [442] was considered.

The theory proposed in [401, 402] was elaborated in [420, 443-447] for the case of complex-structure alloys and was then applied to calculations of some alloy properties that are associated with the total energy. The first problem was to find the equilibrium lattice parameters and energetically favorable superstructures for Cd-Mg alloys. The model potential of [442] was used, its parameters being determined by setting to zero the potential formfactor and the derivatives of the energy with respect to the volume and to the axial c/a

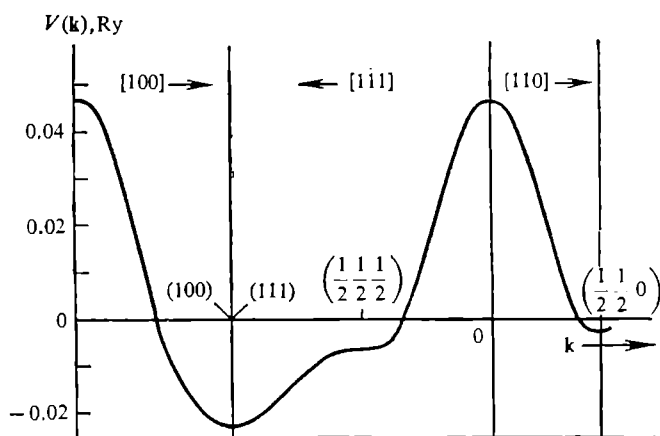


Fig. 7.7. The Fourier transform of the alloying potential of the Ca-Ba alloy against vector k along the [100], [111], and [110] directions in the first Brillouin zone.

ratio. Consequently, there were three equations for the two parameters to be fitted so that it was possible to obtain the equilibrium value of c/a by considering it as the third parameter. The exchange correlation corrections were taken from [448].

The total energy calculations for the pure metals Mg, Cd, and Zn indicate, in agreement with experiment, that all three must be HCP. The computed equilibrium volumes were also close to those measured. As for the c/a ratio, however, a satisfactory result was only obtained for Mg. For Cd and Zn the computed values turned out, as occurs in most papers, to be lower than the experimental ones (1.63 instead of 1.85-1.89). Calculations of mixing energy showed that it is negative for all compositions, in accordance with the observed unlimited solubility of the components of the Mg-Cd system. An energetically favored phase, however, could only be calculated for the equiatomic alloy.

Various applications of the above theory may be found in subsequent papers in this series (see [447] for a review). For example, the configurational energy was calculated by Fuks, Zhorovkov, and Panin [442] for the disordered solid solutions Mg-Zn, Cd-Zn, Ba-Cd, and Cd-Mg. That the concentration dependence of the mixing energy

is in most cases nonparabolic is an extremely important result showing that the widely accepted model of regular solutions is rather inaccurate. In the first three systems the mixing energy was found to be positive, which suggests the existence of a low-temperature dissociation of these alloys (which is indeed observed).

It is pointed out that generally each term of the total energy contributes to the mixing energy, and it is therefore impossible to form a criterion for predicting the sign of ΔU . Although this conclusion is somewhat at variance with [434, 435] it should be born in mind that in these two papers the availability of a criterion was only verified for a very limited material and remains therefore open to question.

Another interesting conclusion to be found in these papers is that the energy parameters may change both during alloying and during ordering, if for no other reason than because of changes in specific atomic volume. Fuks, Zhorovkov, and Panin also confirmed the result obtained in [436, 437] that a rise in ΔU narrows the existence range of intermediate phases. The demonstration of the possibility of calculating the mixing and ordering energies, and the equilibrium volume of an alloy has general importance [420, 443-447].

It is worthwhile noticing here that the authors of [443-447] are quite right in emphasizing the difference between the mixing energy and the ordering energy. They define the former as the energy difference between the alloy and its components and the latter as that between the ordered and disordered phases. It is pointed out in [447] that ΔU_{mix} and ΔU_{ord} may even differ in sign. In Table 7.1 we list the results of [447] for the mixing and ordering energies and for the equilibrium volume of the Mg-Zn system at normal conditions and at a pressure of 5×10^{10} Pa.

Table 7.1. Equilibrium volume, mixing energy and ordering energy for the β 19 superstructure of Mg-Zn (upper row [for no pressure, lower row for 5×10^{10} Pa)

c_{Mg}	0	0.1	0.3	0.5	0.7	0.9	1.0
Ω (a.u)	101.9 74.9	107.4 77.8	118.4 83.6	129.3 89.1	140.0 94.4	150.0 99.5	156.0 102.0
ΔU_{mix} (10^{-3} Ry)	— —	3.12 2.71	6.61 6.30	7.23 7.10	5.61 5.53	2.32 2.21	— —
$-\Delta U_{\text{ord}}$ (10^{-3} Ry)	— —	0.21 0.28	1.63 2.41	3.96 6.35	1.25 2.17	0.12 0.22	— —

It can be seen from the table that the ordering energy and the mixing energy differ in sign and that uniform compression increases the magnitude of the former while decreasing that of the latter. The implication is that systems of this kind may show ordering at high pressures.

We may conclude that the papers we have just reviewed demonstrate the usefulness of the pseudopotential method for the theory of metallic alloys or, more specifically, the usefulness of local pseudopotentials as treated in second-order perturbation theory.

It is of interest, in this connection, to mention an application of higher order perturbation theory to a structure stability analysis of the binary intermetallic systems LiAl, LiTl and NaTl [471]. A second-order total energy calculation predicted (see Table 7.2) that LiAl and LiTl should be stable in the $\mathcal{B}2$ superstructure while NaTl must exist in a two-phase state (note parenthetically that when the exchange correlation effects are neglected, NaTl will also crystallize in the $\mathcal{B}2$ structure). Experiment shows, however, that LiTl is stable in the $\mathcal{B}2$ structure while LiAl and NaTl are stable in $\mathcal{B}32$. So a second-order approximation is only satisfactory for the Li-Tl system.

Table 7.2. Total configurational energies of LiAl, LiTl, and NaTl, second- and third-order perturbation theory results

Structure	\mathcal{B}^2			\mathcal{B}^{32}		
	$U_{bs}^{(2)}$	$U_{bs}^{(cov)}$	$U_{bs}^{(2)} + U_{bs}^{(cov)}$	$U_{bs}^{(2)}$	$U_{bs}^{(cov)}$	$U_{bs}^{(2)} + U_{bs}^{(cov)}$
LiAl	-0.0027	-0.0013	-0.0040	0.0004	-0.0049	-0.0045
NaTl	-0.0013	-0.0079	-0.0092	-0.0011	-0.0108	-0.0119
LiTl	-0.0048	-0.0017	-0.0065	-0.0003	-0.0029	-0.0032

A third-order approximation, as Table 7.2 shows, yields a far better agreement with experiment. True, the computed "ordering" temperatures differ substantially from those observed, but as a whole, there is no doubt that including the higher orders improves the results.

7.3. Short-range order problems

There is almost always some degree of short-range order in solid solutions, the nature of which is determined, in each particular case, by the way the atoms of the different species interact with each other. It would be desirable to be able to predict the sign and

the type* of the order from the properties of the components.

The problem is not only of purely academic importance because short-range order greatly influences [412] the thermal, mechanical, electrical and other physical properties of alloys. In particular, short-range order causes the anomalies in electrical resistance and some other properties found when annealing hardened and deformed alloys (the *K*-effect). Short-range order as opposed to long-range order may occur in alloys of any composition and is very often necessary in order to explain the changes in physical properties during processing.

The early works on the electron theory of short-range order either employed the free-electron model [412, 449] or, when using the pseudopotential method, only the internal energy was analyzed [398, 399, 339-441]. Some short-range order effects were qualitatively interpreted in this way.

In further works on short-range order [404, 421-423] the minimizing of the free energy was combined with the use of Eqs. (6.79)-(6.81) which yielded the parameter α_1 from the charges and pseudopotentials of the ions of pure components. Other refinements in [422, 423] and subsequently were (i) the inclusion of the Ewald correction term in the electrostatic energy; (ii) the calculation of $V(\rho)$ for the sum of the band and electrostatic energies rather than separately for each of them; this approach reducing errors due to low- q discontinuities; (iii) an analysis of the exchange-correlation corrections [164]; and (iv) an analysis of the computational procedure [458].

Since short-range order is found in many noble-metal and transition-metal alloys, it was with these alloys that the above papers were mainly concerned. Calculations were performed using the Animalu pseudopotential [405, 456] (for transition metals, [443, 455]), which has been defined and whose formfactors have been found [456] for a large number of elements. One reason for this restriction to this pseudopotential was to make the interpretation and comparison of results easier.

The first objective of this series of papers [423, 450] was to check the predicting ability of the theory using as an example three alloys of the pentavalent metals V, Nb, and Ta. Experimental data on short-range order were only available for the systems Nb-Ta and V-Nb and it was known that despite their similar electronic structures the two alloys differed in the sign of the parameter α_1 . There had been no explanation for this fact and hence no reasonable guess could be made at the possible sign of α_1 in V-Ta. The calculation

* The sign of short-range order is that of α_1 or, in case $\alpha_1 = 0$, of α_2 ; the type is determined by the spectra of the parameters α_i , their ratios, and the alternation of their signs.

yielded the correct sign for α_1 in V-Nb and Nb-Ta (negative and positive, respectively) and predicted a negative sign for V-Ta. This prediction was later confirmed by experiment [450].

This investigation was followed by the calculation of α_1 for more than forty other systems [451-454] for which the pseudopotentials and the (experimental) signs of the short-range order parameter α_1 were available. The important aspects of these results are as follows.

It was shown that, in accordance with qualitative arguments about the asymptotic behavior of $V(\rho)$, it is quasi-oscillatory for all the

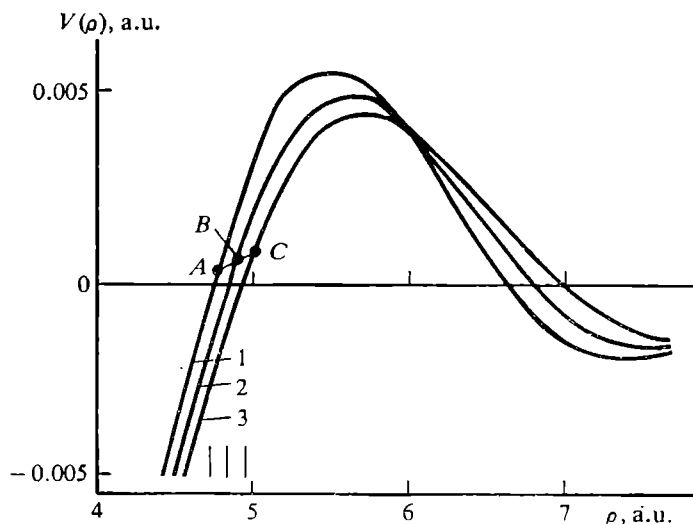


Fig. 7.8. The ordering potential of the Ni-Pt alloys against the interatomic separation. The curves 1, 2, and 3 correspond to 11, 31, and 50 at. % Pt, respectively. Vertical lines mark ρ_1 values for each alloy, and A, B and C are the corresponding values of $V(\rho_1)$.

systems studied. This is clearly illustrated in Fig. 7.8 for the Ni-Pt system. These oscillations are not purely Friedel ones [430, 168].

It can be seen that the specific value of $V(\rho)$ is dependent on composition even though its general behavior is not.

If we look at $V(\rho_1)$ for the three curves (ρ_1 being the radius of the first coordination sphere) we see that $V(\rho_1)$ increases with Pt content, at least from 11 to 50 at. % Pt. This behavior agrees reasonably well with experiment [459] thus disproving the earlier conclusion of statistical thermodynamical alloy theory that the ordering potential is only determined by the nature of the components and is independent of their concentrations.

The above results also show that any change in structure, if accompanied by a change in interatomic separation, may affect the short-range order. Obviously, $V(\rho)$ and $\alpha(\rho)$ are the most sensitive to separation where small values of $V(\rho)$ are combined with large derivatives $dV/d\rho$.

The factors that may affect short-range order via interatomic separation are temperature, pressure, and defect-producing treatments, whether thermal, mechanical, or due to radiation. The direction in which the order changes depends on the sign of the derivative $dV/d\rho$ and the value of $V(\rho)$ itself near ρ_1 .

Since plastic deformation, defects, or radiation treatment may increase the separations in some regions of the crystal and decrease it in others, the ordering potential may vary throughout the crystal, thus giving rise to non-uniform short-range order (local order, [412]). This allows a pseudopotential interpretation of some experimental data [412, 460-467]. For example, the systems Ni-Pt [459], Cu-Al [460] and Cu-Au [461] have $V(\rho)$ that varies with temperature (in copper-containing systems the effect can be measured directly at the investigation temperature).

It was pointed out in [467] that besides kinetic factors, non-uniform short-range order may also result from differences between ordering potentials in the vicinity of defects. This may be ascribed in the present context to features of the indirect interaction via the conduction electron gas. Unfortunately, the agreement with experiment is as yet far from being satisfactory, even in qualitative terms. As far as the parameter α_1 is concerned, the predicted sign turns out to be correct in only two out of three systems studied. The agreement with experiment is better if the alloy components have the same valency. Therefore the sign of α_1 for a given system may only be predicted in terms of probability. Curiously enough, there is no agreement with experiment for alloys composed of noble metals alone or in alloys of transition or noble metals with aluminum. Considering the nature of these elements, one reason for this may be the inadequacy of Animalu pseudopotentials. It should be noted, however, that there are more successful calculations than when the free-electron approach of [468, 469] is used.

In all papers cited, the α_1 parameter was calculated using pseudopotential theory. In [470] the short-range order parameters of the alloys Ni-Fe and Ni-Pt were calculated for the first three coordination spheres from the combined formulae (6.76), (6.77) and (6.82). Using second-order perturbation theory, the computed parameters α_1 - α_3 had the right signs (except for the cases when their experimental values were within the measurement accuracy), but the values themselves were rather unrealistic as was the case when evaluating α_1 alone. The agreement was improved, though, by using a third-order approximation.

The second- and third-order results are summarized in Table 7.3 for α_1 and in Table 7.4 for α_1 , α_2 , and α_3 .

For most of the alloys the inclusion of the third order improved the agreement between theory and experiment. For the Ti-Zr system, for example, it provided the right sign of α_1 . For Cu-Au, Ag-Au and

Table 7.3. Parameter α_1 . Second- and third-order results and experiment

Alloy	$\alpha_1^{(2)}$	$\alpha_1^{(3)}$	α_1^{exp}
Al-Zn (10 at. % Zn)	0.04	0.04	0.08
Mg-In (10 at. % In)	-0.04	-0.08	-0.08
Ni-Pt (31 at. % Pt)	-0.03	-0.11	-0.135
Ni-Pt (11 at. % Pt)	-0.002	-0.032	-0.013
Ni-Fe (25 at. % Fe)	-0.040	-0.055	-0.098
Co-Pt (50 at. % Pt)	-0.06	-0.18	-0.14
Ni-Pt (50 at. % Pt)	-0.04	-0.16	-0.18
Cu-Au (50 at. % Au)	0.28	0.15	-0.16
Ag-Au (20 at. % Au)	0.16	0.07	-0.17
Ti-Zr (50 at. % Zr)	-0.26	0.24	0.05
Zr-Hf (50 at. % Hf)	0.027	0.030	0.04
Ti-Hf (50 at. % Hf)	-0.43	-0.12	0.02

Table 7.4. Parameters α_1 , α_2 , and α_3 for Ni-Fe and Ni-Pt alloys (second- and third-order results)

Alloy	$\alpha_1^{(2)}$	$\alpha_2^{(2)}$	$\alpha_3^{(2)}$	$\alpha_1^{(3)}$	$\alpha_2^{(3)}$
Ni-Fe (25 at. % Fe)	-0.035	0.017	0.004	-0.050	0.020
Ni-Pt (11 at. % Pt)	0.003	0.018	0.015	-0.033	0.019
Ni-Pt (31 at. % Pt)	-0.017	0.031	0.034	-0.128	0.080
Ni-Pt (50 at. % Pt)	-0.042	0.035	0.033	-0.239	0.196

Alloy	$\alpha_2^{(3)}$	α_1^{exp}	α_2^{exp}	α_2^{exp}	
Ni-Fe (25 at. % Fe)	0.009	-0.098	0.116	—	
Ni-Pt (11 at. % Pt)	0.011	-0.013	0.06	0.02	
Ni-Pt (31 at. % Pt)	0.044	-0.13	0.11	0.06	
Ni-Pt (50 at. % Pt)	0.086	-0.18	0.31	-0.01	

Ti-Hf, even though the sign of $\alpha_1^{(2)}$ was incorrect, its magnitude was moved in the right direction. There is an improvement for Mg-In, Ni-Pt, and Co-Pt too.

Table 7.4 [470] shows that third-order calculations also represented an improvement for the order parameter of the higher coordination spheres.

Although the above results thus demonstrate the usefulness of the third-order corrections, there is every reason to believe that for some alloys at least, especially for those composed of polyvalent elements, other factors will be found to improve the theory. To begin with, the large magnitude of the third-order corrections seems to necessitate the inclusion of the fourth and probably even higher-order corrections. On the other hand, obtaining more adequate pseudopotentials and finding the real shape of the Fermi surface are becoming more essential. The role of these factors in the theory of short-range order is discussed in [432, 449, 472-475, 500].

7.4. Crystal structure stability in the OPW approach

In order to obtain phase stability boundaries, the total energy as found in Sec. 6.6 should be substituted in the thermodynamic potential $H = U + p\Omega - TS$. OPW calculations of crystal structure stability were performed by Hafner for disordered alloys of the Li-Mg system [428] and for solid solutions and complex-structure compounds [476].

Hafner [477] started by calculating the characteristic functions $\overline{\mathcal{F}}$ and $\Delta\mathcal{F}$, and the specific volume, and from these obtained the concentration dependences of the internal energy (for the FCC, BCC and HCP structures), the equilibrium atomic radius, cohesion energy, isothermic elasticity modulus and the equation of state. The calculations were performed throughout the entire range of concentrations in steps of 10%. The elasticity modulus and equation of state were obtained by a technique similar to that used in [477] for pure metals.

Comparing his results with experiment shows that the computed atomic radii are correct to within 2 or 3% for pure Li and pure Mg. In solid solutions they depart substantially from Vegard's rule, which agrees with the experimental departure in sign (toward the lower values) but is by a factor of two larger. It is interesting that at concentrations for which $2k_F$ is a reciprocal lattice vector an inflection-type singularity was observed in [477] as well as in [478]. The higher-pressure form of the equation of state also agrees with experiment both for the pure elements Li and Mg and for their alloys. The predicted elasticity moduli are correct to within 25%. Of considerable interest is the calculation of the equilibrium crystal structures.

Figure 7.9 is reproduced from [428] to show the energy differences of the FCC and HCP structures relative to the BCC structure. The arrows mark the concentrations for which the Fermi sphere comes in contact with the Brillouin (Jones) zone boundary. It can be seen that for Li-rich or Mg-rich solid solutions, the preferred phase is

HCP, for 35-80 at. % Mg it is BCC and for 15-35 at. % Mg it is FCC. With the exception of the FCC phase, which only exists in a metastable state, the existence ranges predicted are close to those observed. Phase-to-phase transition regions (corresponding to sharp changes in energy differences) are close to Fermi-sphere/Brillouin-zone-boundary contacts. The reason for the energy changes at these points is, as we have already discussed, the steep slope of the screening function.

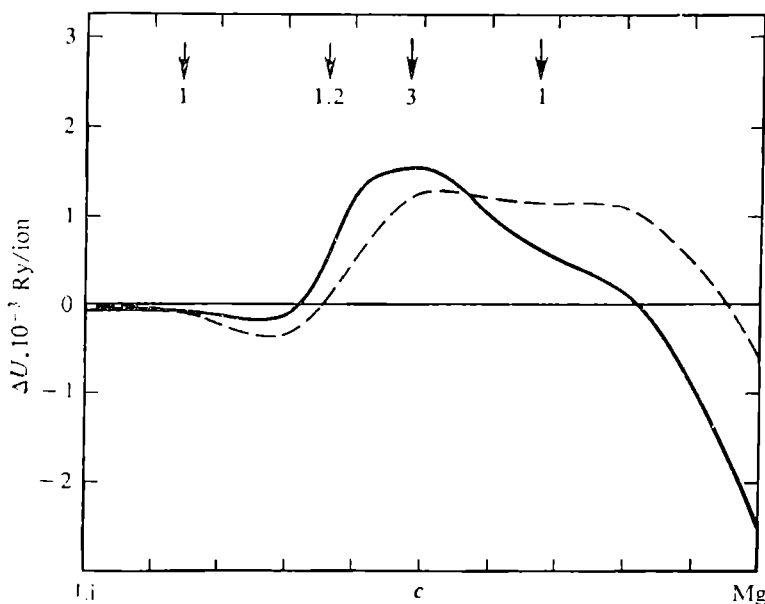


Fig. 7.9. HCP/BCC (bold line) and FCC/BCC (dashed line) energy differences. The concentrations marked by the arrows are those for which the Fermi surface touches the Brillouin-zone face (1—HCP, 2—FCC, 3—BCC).

Figure 7.10 shows the concentration dependence of enthalpy, $\Delta H(c) = U_{\text{Li-Mg}}(c) - (1-c)U_{\text{Li}} - cU_{\text{Mg}}$ for a number of phases [428]. It can be seen in the region from 8 to 53 at. % Mg that the ΔH versus c curve is convex, which indicates that the mixture of BCC and HCP phase has a lower enthalpy than each one of them taken alone. Accordingly, the FCC phase cannot be stable in this concentration region even though its energy is the lowest. Under some circumstances, however, it is because of the lower energy that a metastable FCC phase may occur. The results of the calculations are in fairly good agreement with experiment and so provide good evidence for the adequacy of the theory. Hafner seems to be quite justified therefore in his conclusion that, given a reasonable choice for the pseudopotential, second-order calculations may be reliable.

The next paper of the series was concerned with the formation enthalpies of alkali intermetallic compounds with stoichiometry AB_2 , A_6B_7 and A_4B_3 and the structure classified in [479, 480]

and their solid solutions. To gain more insight into the binding mechanisms in these systems, the coordination numbers of atoms were varied. The comparison of the band and electrostatic contributions, which required the determination of the effective interatomic potentials between the A-A, B-B and A-B pairs was basic to the study.

For the solid solutions Li-K, Na-Cs, Na-Rb, Li-Na, Na-K, K-Rb, Rb-Cs, and K-Cs it was found that the predicted mixing enthalpies

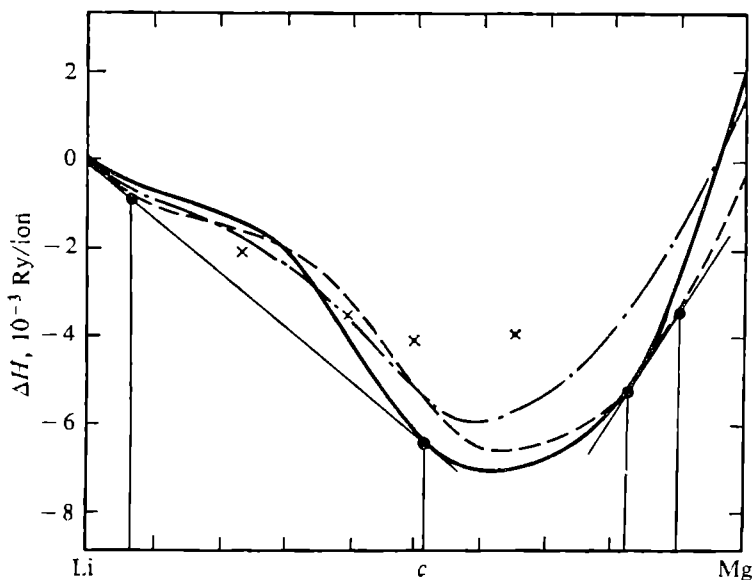


Fig. 7.10. Formation heats of the BCC (bold line), HCP (dash line), and FCC (dash-dot line) phases of Li-Mg alloys as functions of composition. Common tangents show the existence ranges of the phases. Crosses show the experimental enthalpies of the liquid alloys.

are consistent with the Hume-Rothery rule, which limits the mutual solubility of components with atomic dimensions differing by more than 15%. Furthermore, low entropy (that is, almost perfect) solid solutions very closely follow the Vegard rule in their concentration/lattice-period dependence. In particular, this is true of K-Rb, Rb-Cs, and to some extent K-Cs.

The complex-structure phase calculations in [477] were the first of the kind and as such are of interest. We will limit our discussion to the results for three Laves phases AB_2 , namely, the cubic $\mathcal{C}15$ (like $MgCu_2$), hexagonal $\mathcal{C}14$ (like $MgZn_2$) and multilayer $\mathcal{C}36$ (like $MgNi_2$). Electrostatically, the most favored of these is the cubic phase. If, however, the band energy is also considered, then, in accordance with experiment, the hexagonal structure becomes stable. The reason is that the relatively shorter reciprocal lattice vectors make the characteristic function of this structure larger than that

of the competing structures. It is interesting that the greatest contribution comes from the interaction of like neighbors (AA, BB), whereas the AB-type interaction is about the same for all the structures. Note also that in this paper the parameters of, say, the AA interaction, turned out to depend on the second component (B).

Other properties were calculated, such as the formation enthalpy, the coordinates of the atoms, and the equilibrium values of the parameters a , c and c/a . These results together with the corresponding experimental values are summarized in Table 7.5. We can see a fairly good agreement between theory and experiment.

Table 7.5. Equilibrium values a , c , c/a of atomic coordinates x and z , and formation enthalpy ΔH . Theoretical and experimental results for the Na_2K and K_2Cs intermetallic compounds [477].

Phase characteristics	Na_2K		K_2Cs	
	theoretical	experimental	theoretical	experimental
a (10^{-10} m)	7.62	7.50	9.56	9.07
c (10^{-10} m)	12.79	12.31	16.26	14.76
c/a	1.68	1.62	1.70	1.63
x (fractions of a period)	0.0635	0.0625	0.064	0.0625
z (fractions of a period)	-0.1675	-0.1667	-0.167	-0.1667
ΔH (J g^{-1} atom^{-1})	-522	-605	-751	< 0

Figures 7.11 and 7.12 show the potentials of interaction between various pairs of atoms as calculated in [477]. It is easy to see that in the Laves structures of K_2Cs and Na_2K the minima of these potentials are in better agreement with the measured separations R than they are in the solid solutions Na-K and K-Cs. It was pointed out in [477] that the same situation occurs in other structures, for example in K_7Rb_6 , K_7Cs_6 , and Rb_7Cs_6 .

The reader may have noticed an inconsistency in our discussion. In Sec. 7.2 it was argued, with the reference to [409, 471], that a reliable calculation requires third- or even fourth-order perturbation theory. In the present section we found it permissible to work only to the second order. However, there is no contradiction because the potentials employed in [409, 471] and [428, 477] were different. If, on the other hand, we assume the potential is good, it is not yet clear whether second-order perturbation theory will always do or whether in some cases it will not.

Whatever may be the case, the OPW theory has proved very successful in stability studies, even for complex structures like the Laves phases. This, undoubtedly, will encourage further applications

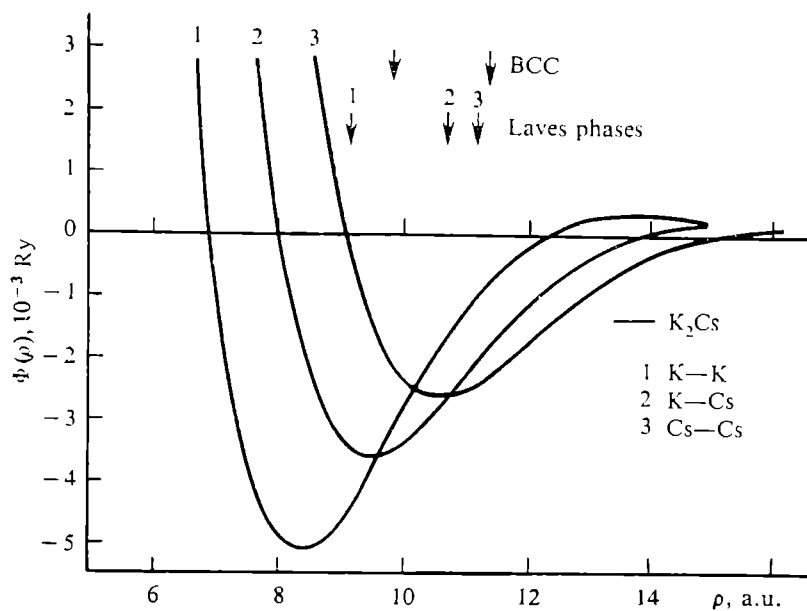


Fig. 7.11. Interatomic potential for the K_2Cs alloys. The arrows indicate R^* values for solid solutions and for Laves phases.

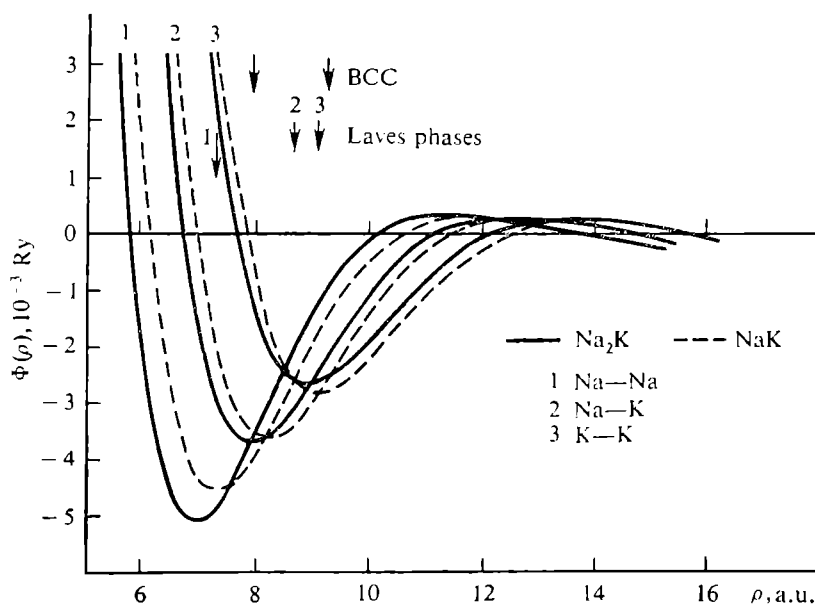


Fig. 7.12. Interatomic potential for the NaK alloys. The arrows indicate R^* values for solid solutions and for Laves phases.

of the theory. It is perhaps worth noticing that apart from the differences we have mentioned, this present section has an important point in common with Sec. 7.2. Namely, a good agreement with experiment is obtained through the use of nonlocal potentials, whether the nonlocality is inherent or arises from the use of higher-order perturbation theory. This finding implies, of course, the importance and necessity of nonlocal potentials. However, local approximation is numerically much more convenient to use and must not be abandoned at present.

Chapter 8

Pseudopotential theory and imperfections in crystals

8.1. Introductory remarks

The single- and two-component crystals we studied in the preceding chapters were very idealized in that their constituent atoms were assumed to be fixed in the positions characteristic of a perfect lattice. There are two kinds of imperfections in a real crystal. Dynamic imperfections are the displacements of the atoms as a result (or rather manifestation) of thermal motion. Static imperfections include vacancies, interstitial atoms, dislocations, stacking faults, etc. Impurities are also ordinarily classified as static imperfections; this in fact limits perfect crystals to single-component ones. The disturbing effect of an impurity is two-fold in nature. First, it substitutes a host atom at the atom's site; this effect was already considered in the two preceding chapters. Second, an impurity displaces neighboring host atoms from their equilibrium positions.

In this chapter we are concerned with the effect of imperfections on the crystal energy as calculated in pseudopotential theory. This, however, is too vast a subject to be covered fully in a single chapter. Moreover, some aspects of the problem have been discussed by Heine *et al.* [17] and Harrison [73]. Our task here is only to outline the principles and to show a few examples of their application.

8.2. Crystal lattice vibrations

Remember that the crystal energy is the sum of the structure-independent term U_0 plus the structure-dependent term, which is in turn the sum of the band-structure energy U_{bs} and electrostatic energy U_{es} . Thus far we have considered the crystal energy at the limit of no thermal vibration. Our purpose in this section is to lift this restriction. It should be noted that in doing so we remain within the framework of the adiabatic or Born-Oppenheimer approximation. We will start our discussion with the band-structure contribution U_{bs} .

First, we must rewrite the formfactor $\mathcal{H}_{cr}^b(\mathbf{q})$ of the crystal pseudopotential. For the sake of simplicity, we use the local approximation and we assume there is only one atom in the unit cell of the crystal.

We have

$$\mathcal{W}_{\text{cr}}^b(\mathbf{q}) = \frac{1}{\Omega} \int e^{-i(\mathbf{k}+\mathbf{q})\mathbf{r}} \mathcal{W}_{\text{cr}}^b(\mathbf{r}) e^{i\mathbf{k}\mathbf{r}} d\mathbf{r}, \quad (8.1)$$

where

$$\mathcal{W}_{\text{cr}}^b(\mathbf{r}) = \frac{1}{N} \sum_{\mathbf{v}} W^b(\mathbf{r} - \mathbf{t}_{\mathbf{v}} - \mathbf{u}_{\mathbf{v}}), \quad (8.2)$$

$\mathbf{u}_{\mathbf{v}}$ being the displacement of the \mathbf{v} -site atom from its equilibrium position. Substituting (8.2) into (8.1) gives

$$\mathcal{W}_{\text{cr}}^b(\mathbf{q}) = \frac{1}{N} \sum_{\mathbf{v}} W^b(\mathbf{q}) e^{-i\mathbf{q}(\mathbf{t}_{\mathbf{v}} + \mathbf{u}_{\mathbf{v}})}. \quad (8.3)$$

If we assume the atomic displacements are small, it is legitimate to expand the exponential in terms of displacements and retain the quadratic terms,

$$\mathcal{W}_{\text{cr}}^b(\mathbf{q}) = \frac{1}{N} \sum_{\mathbf{v}} W^b(\mathbf{q}) e^{-i\mathbf{q}\mathbf{t}_{\mathbf{v}}} \left\{ 1 - i\mathbf{q}\mathbf{u}_{\mathbf{v}} - \frac{1}{2} (\mathbf{q}\mathbf{u}_{\mathbf{v}})^2 + \dots \right\}. \quad (8.4)$$

The quantity we shall actually need in the following is

$$|\mathcal{W}_{\text{cr}}^b(\mathbf{q})|^2 = \frac{|W^b(\mathbf{q})|^2}{N^2} \sum_{\mathbf{v}\mathbf{v}'} e^{-i\mathbf{q}(\mathbf{t}_{\mathbf{v}} - \mathbf{t}_{\mathbf{v}'})} \left\{ 1 - i\mathbf{q}(\mathbf{u}_{\mathbf{v}} - \mathbf{u}_{\mathbf{v}'}) - \frac{1}{2} [\mathbf{q}(\mathbf{u}_{\mathbf{v}} - \mathbf{u}_{\mathbf{v}'})]^2 + \dots \right\}. \quad (8.5)$$

Since the average value of $\mathbf{u}_{\mathbf{v}}$ is zero, we may write

$$|\mathcal{W}_{\text{cr}}^b(\mathbf{q})|^2 = \frac{|W^b(\mathbf{q})|^2}{N^2} \sum_{\mathbf{v}\mathbf{v}'} e^{-i\mathbf{q}(\mathbf{t}_{\mathbf{v}} - \mathbf{t}_{\mathbf{v}'})} \left\{ 1 - \frac{1}{2} [\mathbf{q}(\mathbf{u}_{\mathbf{v}} - \mathbf{u}_{\mathbf{v}'})]^2 \right\}. \quad (8.6)$$

It is now convenient to transform to normal modes, which means that instead of the system of vibrating atoms, we shall be dealing with a set of waves (modes). The amplitudes of these are called normal (model) coordinates and we shall see later that they depend on the wave vector. We have

$$\mathbf{u}_{\mathbf{v}} = \sum_{\mathbf{Q}=1}^N \sum_{j=1}^3 2a_{\mathbf{Q}} \mathbf{e}_{\mathbf{Q}} \cos(\omega_{\mathbf{Q}j}t - \mathbf{Q}_j\mathbf{t}_{\mathbf{v}} - \delta_{\mathbf{Q}j}), \quad (8.7)$$

where $2a_{\mathbf{Q}j}$ is the amplitude of a wave having the wave vector \mathbf{Q} and polarization j ; $\mathbf{e}_{\mathbf{Q}j}$ is the unit vector for the direction in which the atom is moved by the wave (for longitudinal vibrations, $\mathbf{e}_{\mathbf{Q}j} \parallel \mathbf{Q}$; for transversal, $\mathbf{e}_{\mathbf{Q}j} \perp \mathbf{Q}$); and $\delta_{\mathbf{Q}j}$ is the phase of the wave.

When evaluating $(\mathbf{u}_v - \mathbf{u}_{v'})^2$, we encounter terms of the form

$$\cos^2(\omega_{Q_j}t - Q_j t_v - \delta_{Q_j}), \quad \cos^2(\omega_{Q_{j'}}t - Q_{j'} t_{v'} - \delta_{Q_{j'}})$$

and

$$2 \cos(\omega_{Q_j}t - Q_j t_v - \delta_{Q_j}) \cos(\omega_{Q_{j'}}t - Q_{j'} t_{v'} - \delta_{Q_{j'}})$$

The quantity $(\mathbf{u}_v - \mathbf{u}_{v'})^2$ is the superposition of a large number of waves and can be easily estimated by averaging each of its constituent terms.

The average value of cosine squared is 1/2 while for the product of cosines the result depends on whether the pairs Q, j and Q', j' are equal or different. In the latter case, the corresponding waves are independent and the average of the product will be zero. If $Q = Q'$ and $j = j'$,

$$\begin{aligned} & \overline{2 \cos(\omega_{Q_j}t - Q_j t_v - \delta_{Q_j}) \cos(\omega_{Q_j}t - Q_j t_{v'} - \delta_{Q_j})} \\ &= \overline{\cos[2\omega_{Q_j}t - Q_j(t_v + t_{v'}) - 2\delta_{Q_j}] + \cos Q_j(t_v - t_{v'})}, \end{aligned} \quad (8.8)$$

where the last term is of course time-independent.

Thus

$$[\mathbf{q}(\mathbf{u}_v - \mathbf{u}_{v'})]^2 = 4|\mathbf{q}a_{Q_j}e_{Q_j}|^2 [1 - \cos Q_j(t_v - t_{v'})]. \quad (8.9)$$

The same result can be derived more rigorously, but we shall not do so here. Substituting (8.9) into (8.6) we find

$$\begin{aligned} |\mathcal{W}_{\text{cr}}^b(\mathbf{q})|^2 &= \frac{1}{N^2} |W^b(\mathbf{q})|^2 \sum_{vv'} e^{-i\mathbf{q}(t_v - t_{v'})} \\ &\times \left\{ 1 - \sum_Q \sum_j 2|\mathbf{q}e_{Q_j}a_{Q_j}|^2 [1 - \cos Q_j(t_v - t_{v'})] \right\}. \end{aligned} \quad (8.10)$$

It is easy to see that $|\mathcal{W}_{\text{cr}}^b(\mathbf{q})|^2$ consists of two terms. One,

$$|\mathcal{W}_{\text{cr}}^b(\mathbf{q})|_{\text{st}}^2 = \frac{1}{N^2} |W^b(\mathbf{q})|^2 \sum_{vv'} e^{-i\mathbf{q}(t_v - t_{v'})}, \quad (8.11)$$

corresponds to the case of a stationary crystal which we have. The effect of thermal motion is described by the second term which is

$$\begin{aligned} |\mathcal{W}_{\text{cr}}^b(\mathbf{q})|_{\text{dyn}}^2 &= \frac{1}{N^2} |W^b(\mathbf{q})|^2 \sum_{vv'} e^{-i\mathbf{q}(t_v - t_{v'})} \\ &\times \left\{ \sum_Q \sum_j 2|\mathbf{q}e_{Q_j}a_{Q_j}|^2 [\cos Q_j(t_v - t_{v'}) - 1] \right\}. \end{aligned} \quad (8.12)$$

Writing the cosine as a half sum of exponentials of imaginary arguments $\pm i\mathbf{Q}_j(t_v - t_{v'})$ we obtain

$$\begin{aligned}
 |\mathcal{W}_{\text{cr}}^b(\mathbf{q})|_{\text{dyn}}^2 &= \frac{1}{N^2} |W^b(\mathbf{q})|^2 \sum_{\mathbf{Q}} \sum_j |\mathbf{q}, \mathbf{e}_{\mathbf{Q}_j} a_{\mathbf{Q}_j}|^2 \\
 &\times \sum_{\mathbf{v}\mathbf{v}'} \{e^{-i(\mathbf{q}-\mathbf{Q}_j)(t_v-t_{v'})} + e^{-i(\mathbf{q}+\mathbf{Q}_j)(t_v-t_{v'})} - 2e^{-i\mathbf{q}(t_v-t_{v'})}\} \\
 &= |W^b(\mathbf{q})|^2 \sum_{\mathbf{Q}} \sum_j \sum_n \{\delta_{\mathbf{q}, \mathbf{Q}_j+\mathbf{g}_n} |(g_n + \mathbf{Q}_j) \mathbf{e}_{\mathbf{Q}_j} a_{\mathbf{Q}_j}|^2 \\
 &+ \delta_{\mathbf{q}, \mathbf{g}_n-\mathbf{Q}_j} |(g_n - \mathbf{Q}_j) \mathbf{e}_{\mathbf{Q}_j} a_{\mathbf{Q}_j}|^2 - 2\delta_{\mathbf{q}, \mathbf{g}_n} |g_n \mathbf{e}_{\mathbf{Q}_j} a_{\mathbf{Q}_j}|^2\}. \quad (8.13)
 \end{aligned}$$

When substituted into (6.4) this gives the \mathbf{Q} wave contribution to the vibrational band structure energy,

$$\begin{aligned}
 \delta U_{\text{bs}}(\mathbf{Q}) &= \frac{\Omega}{8\pi} \sum_n \sum_j \{|(g_n + \mathbf{Q}_j) \mathbf{e}_{\mathbf{Q}_j} a_{\mathbf{Q}_j}|^2 \Phi(g_n + \mathbf{Q}_j) \\
 &+ |(g_n - \mathbf{Q}_j) \mathbf{e}_{\mathbf{Q}_j} a_{\mathbf{Q}_j}|^2 \Phi(g_n - \mathbf{Q}_j)\} - \frac{\Omega}{4\pi} \sum_n' \sum_j |g_n \mathbf{e}_{\mathbf{Q}_j} a_{\mathbf{Q}_j}|^2 \Phi(g_n). \quad (8.14)
 \end{aligned}$$

The total change in band energy clearly will be obtained by summing $\delta U_{\text{bs}}(\mathbf{Q})$ over all \mathbf{Q} . In order to carry out the summation, it is of course necessary to know the way the amplitudes $a_{\mathbf{Q}_j}$ depend on the wave vector and polarization vector.

The effect of thermal motion on the electrostatic energy can be found in a similar fashion. We first find the total electrostatic energy and then exclude the terms corresponding to the stationary lattice. For the simple case we are considering (one atom in a unit cell), it is easy to verify that the contribution from the \mathbf{Q} wave is

$$\begin{aligned}
 \delta U_{\text{es}}(\mathbf{Q}) &= 2\pi Z^{*2} \sum_n \sum_j \left\{ \frac{|(g_n + \mathbf{Q}_j) \mathbf{e}_{\mathbf{Q}_j} a_{\mathbf{Q}_j}|^2}{|g_n + \mathbf{Q}_j|^2} e^{-\frac{(g_n + \mathbf{Q}_j)^2}{4\eta}} \right. \\
 &\quad \left. + \frac{|(g_n - \mathbf{Q}_j) \mathbf{e}_{\mathbf{Q}_j} a_{\mathbf{Q}_j}|^2}{|g_n - \mathbf{Q}_j|^2} e^{-\frac{(g_n - \mathbf{Q}_j)^2}{4\eta}} \right\} \\
 &\quad - 4\pi Z^{*2} \sum_n' \sum_j \frac{|g_n \mathbf{e}_{\mathbf{Q}_j} a_{\mathbf{Q}_j}|^2}{g_n^2} e^{-\frac{g_n^2}{4\eta}}. \quad (8.15)
 \end{aligned}$$

It should be remembered that in both (8.14) and (8.15), the $g_n = 0$ contributions are dropped in the last terms. Clearly, by summing (8.14) and (8.15) we obtain the total \mathbf{Q} -wave contribution to the configurational part of the crystal energy.

We have thus demonstrated that, in principle, pseudopotential theory might well be used for determining the way thermal motion affects the crystal energy. In practice, the above expressions require a knowledge of the wave amplitude, which makes their direct use rather difficult.

They can be used in a somewhat indirect way, however. Combining pseudopotential theory with crystal lattice dynamics reveals that the quantities $\delta U_{\text{bs}}(\mathbf{Q}) + \delta U_{\text{es}}(\mathbf{Q})$ may be quite useful in calculating phonon (or vibration) spectra, which can be measured quite reliably by modern techniques. It is therefore worthwhile to outline here the basic principles of lattice dynamics.

The potential energy of a crystal may always be represented as a power series in atomic displacements.

$$V = V_0 + \sum_{\nu l j} \mathbf{u}_{\nu l}^j \left[\frac{\partial V}{\partial \mathbf{u}_{\nu l}^j} \right]_0 + \frac{1}{2} \sum_{\nu \nu', l l', j j'} \mathbf{u}_{\nu l}^j \mathbf{u}_{\nu' l'}^{j'} \left[\frac{\partial^2 V}{\partial \mathbf{u}_{\nu l}^j \partial \mathbf{u}_{\nu' l'}^{j'}} \right]_0 + \dots, \quad (8.16)$$

where ν and l are the indices of, respectively, an atom and cell, j is the component of the displacement vector, and the subscript 0 corresponds to the state of equilibrium. The ground-state potential energy, V_0 , can be always set to zero and thereby made a reference point. Since the potential energy has a minimum at $\mathbf{u}_{\nu l}^j = 0$, it follows that $[\partial V / \partial \mathbf{u}_{\nu l}^j]_0 = 0$. The only remaining term in (8.16) is quadratic in displacements and describes the harmonic vibrations of the lattice atoms. This is the term which corresponds to δU above.

The kinetic energy of the lattice is

$$E_{\text{kin}} = \sum_{\nu l j} \frac{1}{2} M_{\nu} |\dot{\mathbf{u}}_{\nu l}^j|^2, \quad (8.17)$$

where M_{ν} is the mass of the ν th atom. Since the sum of the kinetic and potential energies is constant, it follows that

$$M_{\nu} \ddot{\mathbf{u}}_{\nu l}^j = - \sum_{\nu' l' j'} \left[\frac{\partial^2 V}{\partial \mathbf{u}_{\nu l}^j \partial \mathbf{u}_{\nu' l'}^{j'}} \right]_0 \mathbf{u}_{\nu' l'}^{j'}. \quad (8.18)$$

This equation holds for each j -component of the displacement vector of each ν th atom in each l th elementary cell. Equation (8.18) is therefore a system of a huge number of coupled differential equations and there is no hope of solving it directly.

By classical mechanics, the quantities

$$G_{\nu \nu', l l'}^{j j'} = \left[\frac{\partial^2 V}{\partial \mathbf{u}_{\nu l}^j \partial \mathbf{u}_{\nu' l'}^{j'}} \right]_0 \quad (8.19)$$

are the components of the force tensor. Since all the crystal cells are identical, the G tensor does not depend on the values of l and l' but rather on their difference h . We thus have

$$G_{vv',ll'}^{jj'} = G_{vv'}^{jj'}(h) \quad (8.20)$$

which, when substituted into (8.18), gives

$$M_v \ddot{\mathbf{u}}_{vl}^j = - \sum_{v', h, j'} G_{vv'}^{jj'}(h) \mathbf{u}_{v', l+h}^{j'}. \quad (8.21)$$

This expression is invariant under translation and hence satisfies the Bloch theorem,

$$\mathbf{u}_{vl}^j(t) = e^{i\mathbf{Q}l} \mathbf{u}_{v0}^j(t). \quad (8.22)$$

Substituting this into (8.21) gives

$$M_v \ddot{\mathbf{u}}_{v0}^j e^{i\mathbf{Q}l} = - \sum_{v', j'} \left\{ \sum_h G_{vv'}^{jj'}(h) e^{i\mathbf{Q}h} \right\} \mathbf{u}_{v', 0}^{j'} e^{i\mathbf{Q}l}. \quad (8.23)$$

The expression within the curly brackets is the Fourier transform of the force tensor G . Taking $e^{i\mathbf{Q}l}$ out of the sum and canceling it, we find

$$M_v \ddot{\mathbf{u}}_{v0}^j = - \sum_{v', j'} G_{vv'}^{jj'}(\mathbf{Q}) \mathbf{u}_{v0}^{j'}, \quad (8.24)$$

where $G_{vv'}^{jj'}(\mathbf{Q})$ is the Fourier transform for $\partial^2 V / \partial \mathbf{u}_{vl}^j \partial \mathbf{u}_{v'l'}^{j'}$. Since the $G_{vv'}^{jj'}$ are functions of \mathbf{Q} , so too are the amplitudes of the thermal (elastic) waves and we may write

$$\mathbf{u}_{v0}^j = \mathbf{u}_{v\mathbf{Q}}^j. \quad (8.25)$$

It follows from the theory of oscillations that (8.24) may be transformed to

$$\sum_{v', j'} \{ G_{vv'}^{jj'}(\mathbf{Q}) - \omega^2 M_v \delta_{vv'} \delta_{jj'} \} \mathbf{u}_{v'\mathbf{Q}}^{j'} = 0, \quad (8.26)$$

which is a (homogeneous) system of equations for the amplitude $\mathbf{u}_{v\mathbf{Q}}^{j'}$. This system can only have nontrivial solutions if the determinant of its coefficients is zero, which is the condition from which the frequency spectrum $\omega(\mathbf{Q})$ can be obtained. But, as can be seen from the above argument, the sum $\delta U_{bs}(\mathbf{Q}) + \delta U_{es}(\mathbf{Q})$ coincides with the quadratic term in (8.16) and therefore, the amplitude coefficients may be found by evaluating the \mathbf{Q} -wave contribution to the change of the band and electrostatic energies.

The number of equations in (8.26) is given by the number of possible polarization directions (3) times the number of atoms in the unit cell. As this product is a factor N smaller than the number of equations in (8.18) (N being the number of cells in the crystal), the solution

of (8.26) becomes quite feasible. Strictly speaking, this system ought to be solved for all possible Q values (of which there are N). In practice, it is enough to do this for a reasonable number of them, the solutions for the others being found by interpolation. As compared with (8.18), this approach requires far less numerical work.

It follows from the above discussion that the dynamic matrix (8.26) may be found using pseudopotential theory. The calculation of its determinants then gives the phonon spectra of the crystal. These calculations are interesting in a number of respects. First, comparing the calculated and measured phonon spectra makes it possible to check the reliability of the pseudopotentials used and, if need be, to correct (fit) them. Second, the calculations provide information about the role electron-electron and electron-ion interactions play in constructing pseudopotentials.

On the other hand, it sometimes proves possible, by comparing computed and measured spectra, to explain phonon characteristics which are responsible for atomic properties.

Finally, pseudopotential calculations of the phonon contribution to the free energy (or, for finite pressures, to the thermodynamic potential) provide a necessary basis for solving fundamental solid-state problems such as the calculation of phonon effects in electrical conductivity, the calculation of thermoelectric and galvanometric effects, and the compilation of phase diagrams.

One application of pseudopotential theory to phonon studies is given in a paper by Animalu [455]. Using his own model potential [343] for the transition metals, Animalu calculated the phonon spectra of some $3d$, $4d$, and $5d$ pure metals. As there is only one atom in the unit cell of a pure metal, the matrix in (8.26) will be (3×3) . For the major axes of a cubic crystal we have

$$\sum_{j'} [M\omega^2\delta_{jj'} - G^{jj'}(Q)] e_{\mathbf{q}j} = 0, \quad (8.27)$$

where $G^{jj'}$ is the dynamics matrix, which in this case may be written as

$$G^{jj'} = G_{\text{es}}^{jj'} + G_{\text{BM}}^{jj'} + G_{\text{bs}}^{jj'}. \quad (8.28)$$

Here the first term describes the electrostatic energy, the second the Born-Mayer repulsion potential, and the third the band structure energy. For the vibration frequencies we have, accordingly,

$$\omega^2 = \omega_{\text{es}}^2 + \omega_{\text{BM}}^2 - \omega_{\text{bs}}^2, \quad (8.29)$$

where $\omega_{\text{es}}^2 = G_{\text{es}} M^{-1}$ and so on.

In actual calculations, the electrostatic contribution was written in a conventional form and the Born-Mayer term was dropped in view of the small size of the ions involved. The band-structure

term was written as

$$[\omega_{bs}^2(\mathbf{Q})]^{jj'} = \frac{4\pi Z^2}{M\Omega} \left\{ \sum_n \frac{(\mathbf{Q} + \mathbf{g}_n)^{(j)} (\mathbf{Q} + \mathbf{g}_n)^{(j')}}{|\mathbf{Q} + \mathbf{g}_n|^2} \Phi(\mathbf{Q} + \mathbf{g}_n) - \sum'_{n \neq 0} \frac{\mathbf{g}_n^j \mathbf{g}_n^{j'}}{|\mathbf{g}_n|^2} \Phi(\mathbf{g}_n) \right\}. \quad (8.30)$$

where

$$\Phi(\mathbf{q}) = \left[\frac{4\pi Z (1 + \alpha_{\text{eff}})}{\Omega q^2} \right]^{-2} |W^b(\mathbf{q})|^2 \frac{\epsilon(\mathbf{q}) - 1}{\epsilon(\mathbf{q}) [1 - f(\mathbf{q})]}. \quad (8.31)$$

The results for FCC metals were found to agree reasonably well with experimental data on phonon spectra, at least for longitudinal waves (see Fig. 8.1). The agreement was less satisfactory for BCC metals.

This, Animalu felt, might be the result of the local approximation. A more sophisticated phonon-dispersion calculation was attempted by Oli and Animalu [481] for the typical BCC transition metal V

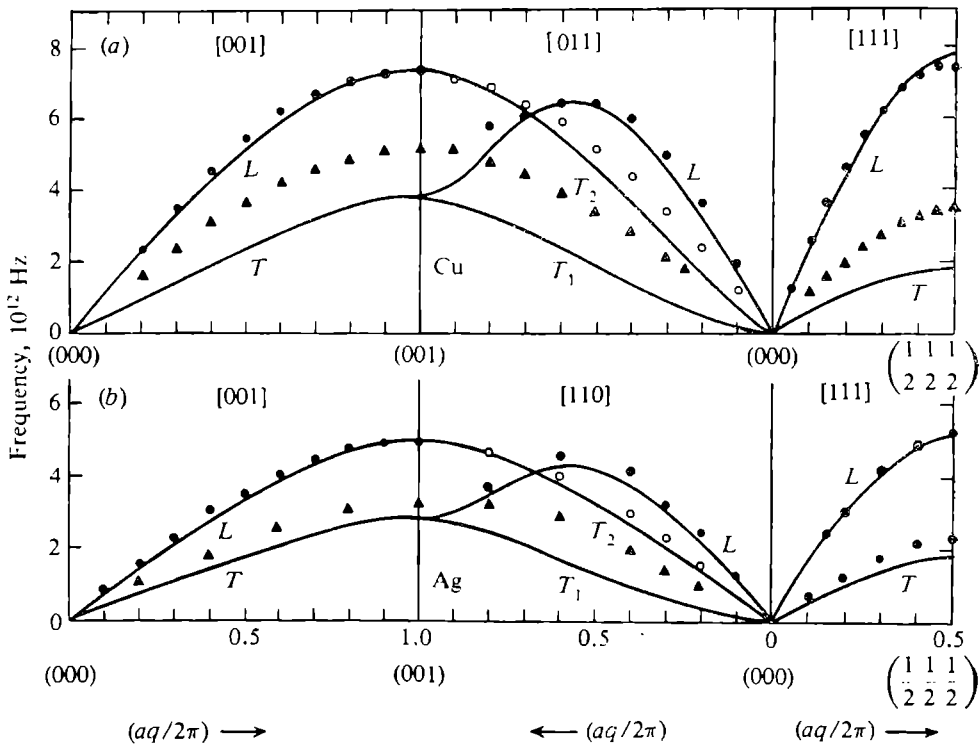


Fig. 8.1. Phonon spectra of (a) Cu and (b) Ag as derived from the Animalu potential [343]. The longitudinal branch is marked by L , the transversal branches by T_1 and T_2 , their respective experimental values are shown by the full circles, empty circles and triangles.

They included nonlocal effects and the Born-Mayer repulsion and, when calculating the dielectric permittivity, they determined the *sd* hybridization using the resonance model of Animalu's metal potential.

The resulting $\omega(\mathbf{Q})$ curves are plotted in Fig. 8.2. In the [100] direction, it can be seen that both local and nonlocal calculations agree well with experiment. In the [111] and [110] directions, the predicted longitudinal frequencies are rather too high and in the [110] direction the transverse frequencies are too low. That nonlocality allows better results for longitudinal waves may be a valuable hint, Oli and Animalu argue, towards an explanation of the nature of soft modes. The use of a nonlocal resonance potential also improved the results for Cu [302, 482] (see Fig. 8.3).

We thus see that a comparison of calculated and measured spectra is indeed a good check on new potentials (see [73] for an extensive discussion on the subject). It should be noted, however, that phonon data alone may be insufficient for fitting, and information about other properties may be necessary [483].

So far we have mainly discussed phonon-spectrum calculations as a tool for testing pseudopotentials. They are also important for determining some of material properties.

In [484] Animalu calculated the phonon spectra of the alkali-earth metals Ca, Sr and Ba and used them as a basis for the electron theory of phase transitions in these metals. At any finite temperature, the competing phases must have equal thermodynamic potentials (or free energies in the absence of pressure) for a transition to occur. Apart from the purely configurational contributions derived in the previous chapter for the stationary crystal, the phonon contributions to the internal energy and entropy may be of importance. The former is finite even at absolute zero, viz,

$$U_{\text{ph}} = \frac{1}{2} \sum_{\mathbf{q}j} \hbar \omega_{\mathbf{q}j}. \quad (8.32)$$

At finite temperatures, the phonon contribution to entropy is

$$S_{\text{ph}} = -k_{\text{B}} \sum_{\mathbf{q}j} \ln \left[1 - \exp \left(-\frac{\hbar \omega_{\mathbf{q}j}}{k_{\text{B}} T} \right) \right] + \sum_{\mathbf{q}j} \frac{\hbar \omega_{\mathbf{q}j}}{T} \left[\exp \left(\frac{\hbar \omega_{\mathbf{q}j}}{k_{\text{B}} T} \right) - 1 \right]^{-1}, \quad (8.33)$$

and that of the free energy is

$$F_{\text{ph}} = k_{\text{B}} T \sum_{\mathbf{q}j} \ln \left[2 \sinh \frac{\hbar \omega_{\mathbf{q}j}}{2 k_{\text{B}} T} \right]. \quad (8.34)$$

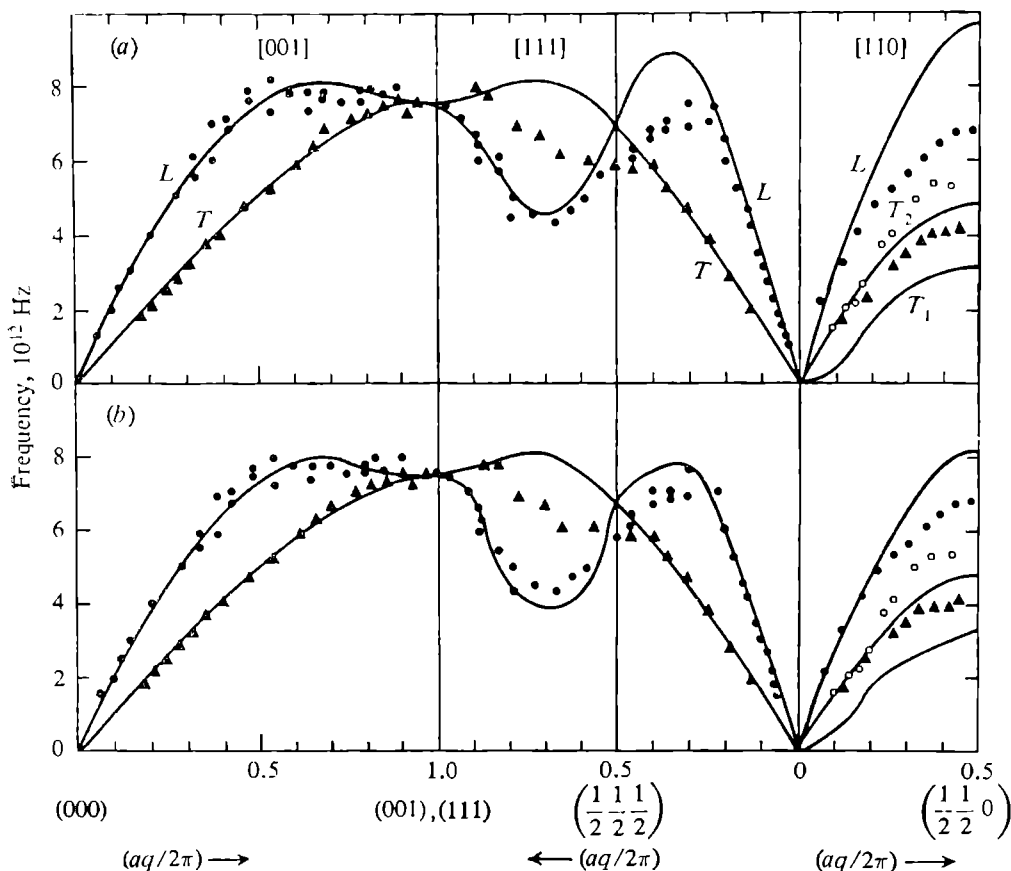


Fig. 8.2. Vanadium phonon spectra calculated by Oli and Animalu [481] from (a) a local pseudopotential and (b) a nonlocal pseudopotential. Bold lines—calculation. L , T_1 , and T_2 denote the longitudinal and two transversal branches, the respective experimental values are shown by full circles, empty circles, and triangles.

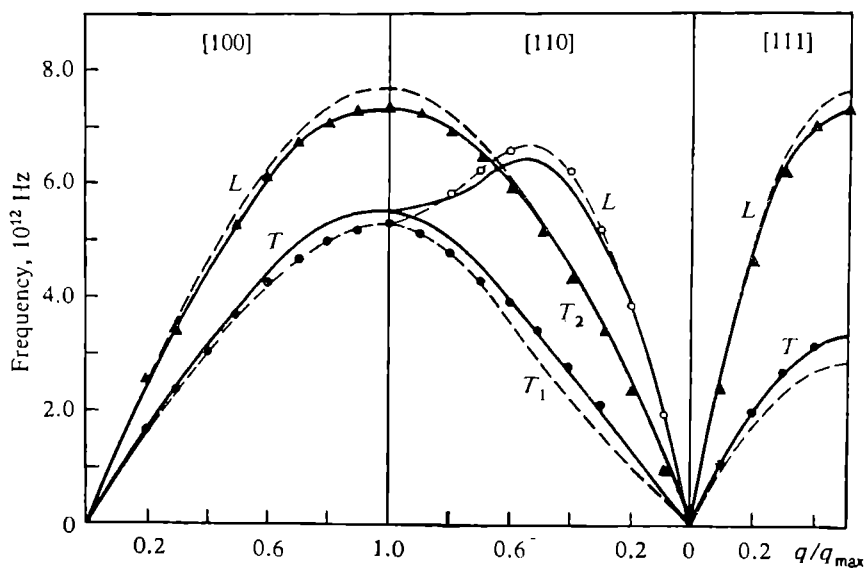


Fig. 8.3. Cuprum phonon spectra calculated by Dagens [302] in local approximation (dash lines) and with nonlocal effects (bold lines). Other notations are as in Fig. 8.2.

Using these formulae Animalu found the phonon frequencies (taking into account the band and electrostatic contributions) and obtained the phonon part of the free energy (F_{ph}). He then calculated the internal energy $U = U_0 + U_{\text{es}} + U_{\text{bs}}$ and the thermodynamic potential

$$G(p, T) = U + F_{\text{ph}} + p\Omega. \quad (8.35)$$

The resulting phase diagram for Sr is shown in Fig. 8.4 together with the experimental phase diagram. The agreement is rather good considering the time of the study (note that virtually no fitting was

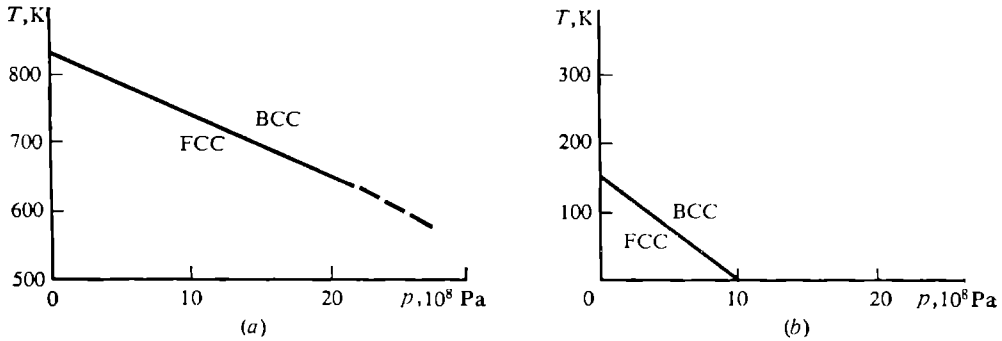


Fig. 8.4. Phase diagram for Sr: (a) experiment, (b) theory.

carried out for the potential). Physically, the reason for the FCC-BCC transition is that the phonon spectrum of the BCC lattice contains a low-frequency transverse branch which markedly increases the phonon part of entropy at elevated temperatures. For Ba, too, the results are satisfactory, at least qualitatively, whereas calculations for Ca show rather poor agreement with experiment, presumably because of d -band effects.

The role of thermal vibrations in the theory is not limited to the results we have cited.

Regrouping the terms between $|\mathcal{W}_{\text{cr}}^b(\mathbf{q})|_{\text{st}}^2$ and $|\mathcal{W}_{\text{cr}}^b(\mathbf{q})|_{\text{dyn}}^2$ it can be shown that

$$\begin{aligned} |\mathcal{W}_{\text{cr}}^b(\mathbf{q})|^2 = & \frac{1}{N^2} |W^b(\mathbf{q})|^2 \sum_{\mathbf{v}\mathbf{v}'}' e^{-i\mathbf{q}(\mathbf{t}_{\mathbf{v}} - \mathbf{t}_{\mathbf{v}'})} \left\{ 1 - 2 \sum_{\mathbf{Q}, j} |\mathbf{q}\mathbf{e}_{\mathbf{Q}j} a_{\mathbf{Q}j}|^2 \right\} \\ & + \frac{1}{N^2} |W^b(\mathbf{q})|^2 \sum_{\mathbf{v}\mathbf{v}'\mathbf{Q}j} 2 |\mathbf{q}\mathbf{e}_{\mathbf{Q}j} a_{\mathbf{Q}j}|^2 e^{-i\mathbf{q}(\mathbf{t}_{\mathbf{v}} - \mathbf{t}_{\mathbf{v}'})} \cos[\mathbf{Q}j(\mathbf{t}_{\mathbf{v}} - \mathbf{t}_{\mathbf{v}'})]. \end{aligned} \quad (8.36)$$

This expression has an analog in the theory of diffraction on a vibrating crystal lattice [3, 485]. It is easy to see, that the term in the curly brackets in (8.36) corresponds to the Debye-Waller factor

e^{-2M} where

$$2M = 2 \sum_{\mathbf{Q}_j} | \mathbf{q} \mathbf{e}_{\mathbf{Q}_j} a_{\mathbf{Q}_j} |^2. \quad (8.37)$$

In X-ray analysis, this factor is known to damp down the X-ray maxima, thus reflecting the physical fact that the peripheral electron density of the atoms is "smeared out" by their thermal motion. In pseudopotential theory we have, by the same token,

$$| W_T^b(\mathbf{q}) |^2 = | W_0^b(\mathbf{q}) |^2 e^{-2M}, \quad (8.38)$$

where $W_0^b(\mathbf{q})$ and $W_T^b(\mathbf{q})$ are the matrix elements at, respectively, zero and finite temperatures. The reader is referred to [3, 485] for a detailed discussion of the factor M . A few points worth mentioning here are as follows.

At high temperatures ($T \gg \Theta$) we have, in the Debye approximation,

$$M = \frac{3}{2} \frac{\hbar^2 g_n^2 T}{M_{\text{at}} k_B \Theta^2}, \quad (8.39)$$

where M_{at} is the mass of an atom and Θ the Debye temperature which is usually between 100 and 600 K. In typical metals and semiconductors, the room temperature value of $2M$ is about $(4-8) \times 10^{-2}$ for the shortest \mathbf{g}_n . Note that $2M$ is very sensitive to the magnitude of the reciprocal lattice vector (as \mathbf{g}_n^2). Raising the temperature increases M both explicitly, through the factor T , and implicitly, through the Debye temperature Θ , which decreases with temperature. The low temperature expression for M is rather involved, but it is greatly simplified in the zero-temperature limit:

$$M \propto \frac{3}{8} \frac{\hbar^2 g_n^2}{M_{\text{at}} k_B \Theta}. \quad (8.40)$$

As this is only one fourth the Debye temperature M value, it follows that, in principle, a pseudopotential formfactor should always be corrected by a Debye factor of the form (8.38). Even though the correction may be small, its possible effect must always be estimated.

This result is very significant, for pseudopotential formfactors are essential in determining important properties of crystals such as the band structure and the temperature dependence of band gaps. It is worth mentioning, in this connection, a paper by Altshuller *et al.* [486] on the band structure of ionic-covalent compounds. By computing energy levels at a number of high-symmetry points, Altshuller and coworkers were able to calculate: (i) the band-gap temperature dependence of Si, Ge, GaAs, InSb, and GaSb, (ii) the p - T diagram for Si, InSb, and CdTe; and (iii) the Ge-Si phase diagram. The effect of temperature was taken into account by multiplying the pseudopotential formfactors by a Debye-Waller factor,

the effect of pressure was allowed for by varying the lattice parameters.

Altshuller and coworkers concluded that the stability boundaries of semiconducting compounds could be found by determining where their indirect band-gaps have disappeared. For the compounds studied, the estimates obtained by this criterion agreed reasonably well with experiment.

To sum up, phonon effects are readily incorporated into the pseudopotential theory of crystals and greatly extend its potentialities in determining major material properties.

8.3. Static imperfections

These are (i) the substitution of one atomic species for another, (ii) the disappearance of an atom at one place and its appearance at another, and (iii) the displacement of atoms around a distortion site. A common assumption is that atomic cores remain undisturbed in a distorted crystal. This means that static imperfections could be regarded as "frozen" atomic vibrations which may be treated adiabatically (taking into account, of course, changes in interatomic separation, average charge density, etc.). But then the effect of imperfections on the crystal energy may be reduced to a change in the structure factor, and the energetics of an imperfect crystal would reduce more or less to that for an alloy or vibrating crystal. An illustration of this is a single-component crystal containing substitutional point defects.

Starting, once again, with the band structure energy, we first calculate the matrix element $\mathcal{W}_{\text{cr}}^b(\mathbf{q})$ taking into account the displacement of ions about the defects and the change in the formfactors at the defect sites. Consider a crystal with Nc randomly distributed defects (c being the defect concentration). We have

$$\mathcal{W}_{\text{cr. d}}^b(\mathbf{r}) = \frac{1}{N} \sum_{\mathbf{v}} \{ (1 - c_{\mathbf{v}}) W_{\text{m}}^b(\mathbf{r} - \mathbf{t}_{\mathbf{v}} - \mathbf{u}_{\mathbf{v}}) + c_{\mathbf{v}} W_{\text{d}}^b(\mathbf{r} - \mathbf{t}_{\mathbf{v}} - \mathbf{u}_{\mathbf{v}}) \}, \quad (8.41)$$

where the $c_{\mathbf{v}}$ are the operators defined in Chapter 6, and $W_{\text{m}}^b(\mathbf{r} - \mathbf{t}_{\mathbf{v}} - \mathbf{u}_{\mathbf{v}})$ and $W_{\text{d}}^b(\mathbf{r} - \mathbf{t}_{\mathbf{v}} - \mathbf{u}_{\mathbf{v}})$ are, respectively, the host-atom and defect pseudopotentials at the point $\mathbf{t}_{\mathbf{v}} + \mathbf{u}_{\mathbf{v}}$. Taking the Fourier transform we obtain

$$\mathcal{W}_{\text{cr. d}}^b(\mathbf{q}) = \frac{1}{N} \sum_{\mathbf{v}} \{ (1 - c_{\mathbf{v}}) W_{\text{m}}^b(\mathbf{q}) e^{-i\mathbf{q}(\mathbf{t}_{\mathbf{v}} + \mathbf{u}_{\mathbf{v}})} + c_{\mathbf{v}} W_{\text{d}}^b(\mathbf{q}) e^{-i\mathbf{q}(\mathbf{t}_{\mathbf{v}} + \mathbf{u}_{\mathbf{v}})} \}. \quad (8.42)$$

Let us now consider the energy change caused by Nc vacancies which do not displace their neighboring atoms (note that we are dealing

with a single-component crystal). We introduce the matrix elements for the "average" and "difference" ions in the crystal

$$\overline{W^b}(\mathbf{q}) = (1-c) W_m^b(\mathbf{q}) + 0, \quad \Delta W^b(\mathbf{q}) = 0 - W_m^b(\mathbf{q}). \quad (8.43)$$

Using (6.5)-(6.13) we obtain in this approximation

$$|\mathcal{W}_{\text{cr. d}}^b(\mathbf{q})|^2 = (1-c)^2 |W_m^b(\mathbf{q})|^2 \delta_{\mathbf{q}, \mathbf{g}_n} + \frac{c(1-c)}{N} |W_m^b(\mathbf{q})|^2, \quad (8.44)$$

and for the band structure energy,

$$U_{\text{bs, d}} = \frac{\Omega_0}{8\pi} \sum_n' g_n^2 (1-c)^2 \frac{1-\varepsilon(\mathbf{g}_n)}{\varepsilon^*(\mathbf{g}_n)} |W_m^b(\mathbf{g}_n)|^2 \\ + \frac{\Omega_0 c(1-c)}{8\pi N} \sum_q'' q^2 \frac{1-\varepsilon(\mathbf{q})}{\varepsilon^*(\mathbf{q})} |W_m^b(\mathbf{q})|^2, \quad (8.45)$$

where in the first and second sums, respectively, the terms with $\mathbf{g}_n = 0$ and $\mathbf{q} = \mathbf{g}_n$ must be dropped.

Because of the low defect concentration ($c \leq 10^{-3}$) it is not too crude to assume that the lattice period remains unchanged in the presence of defects, and we may write

$$U_{\text{bs, d}} - U_{\text{bs, perf}} = \frac{\Omega_0}{8\pi} \sum_n' (-2c + c^2) g_n^2 \frac{1-\varepsilon(\mathbf{g}_n)}{\varepsilon^*(\mathbf{g}_n)} |W_m^b(\mathbf{g}_n)|^2 \\ + \frac{\Omega_0 c(1-c)}{8\pi N} \sum_q'' q^2 \frac{1-\varepsilon(\mathbf{q})}{\varepsilon^*(\mathbf{q})} |W_m^b(\mathbf{q})|^2. \quad (8.46)$$

Since the number of terms in the second sum is N times that in the first, the two sums must be of the same order of magnitude. Furthermore, since the sums are opposite in sign, the sign of $U_{\text{bs, d}} - U_{\text{bs, perf}}$ may only be determined by an actual calculation for a specific model. Needless to say, the calculation should include the change in the average atomic volume and related parameters.

There is another interesting point about equation (8.46). In its first terms, the wave vectors of the initial and final electron states are allowed to differ by a reciprocal *lattice* vector, in the second term they may differ by *any* reciprocal vector. Hence the first term, which differs from its perfect-crystal counterpart by a constant factor $(-2c + c^2)$ will not contribute to electrical conductivity, thermo-emf, or other transport properties, and the residual resistance of an imperfect crystal will be determined by the second term alone. It has been shown [17] that the electrical resistivity of some

materials is qualitatively described by the formula

$$\rho = 3\pi m \frac{\Omega_0 N}{8E_F} \int_0^2 |s(\mathbf{q})|^2 |W(\mathbf{q})|^2 x^3 dx, \quad (8.47)$$

where $x = q/2k_F$.

Our next step is to include atomic displacements. The point of departure will be equation (8.42), in which the displacement \mathbf{u}_v may be expressed as a sum of contributions from all the defects,

$$\mathbf{u}_v = \sum_{v'} c_{v'} \mathbf{A}_{v-v'}, \quad (8.48)$$

where the displacement function $\mathbf{A}_{v-v'}$ depends on the distance between the displaced atom (at the v th site) and the disturbing defect (at the v' th site). Since (8.48) is the convolution of the functions $c(\mathbf{r})$ and $\mathbf{A}(\mathbf{r})$, it is convenient here to take their Fourier transforms. The Fourier transform of a convolution of two functions is the product of their Fourier transforms, hence

$$\mathbf{U}_Q = C_Q \mathbf{A}_Q. \quad (8.49)$$

Here C_Q is found from (6.9) and the coefficients \mathbf{A}_Q are obtained [418] from the equilibrium condition with respect to displacements. Treating a crystal as an isotropic elastic continuum,

$$\mathbf{A}_Q = \frac{1+\sigma}{3(1-\sigma)} \frac{1}{V} \frac{dV}{dc} \frac{Q}{Q^2}, \quad (8.50)$$

where σ is Poisson's modulus and $(1/V)(dV/dc)$ describes the dependence of the specific volume of the crystal on defect concentration. The expressions for \mathbf{A}_Q become more complicated in anisotropic elastic crystals and still more so in microscopic theory. For the [100] direction in an FCC lattice,

$$\mathbf{A}_Q = \frac{1}{2} d (c_{11} + 2c_{12}) c_{11}^{-1} \frac{1}{V} \frac{dV}{dc} \left(\cot \frac{Qd}{4} \right) Q, \quad (8.51)$$

where c_{11} and c_{12} are the elasticity moduli, and d is the lattice parameter.

A knowledge of the \mathbf{A}_Q makes it possible to determine the displacement of an ion as a function of the distance to the defect (impurity atom), viz.

$$\mathbf{u}_v(\mathbf{r}) = \frac{1}{N} \sum_Q \mathbf{A}_Q \sin Q\mathbf{r}. \quad (8.52)$$

The mean square of static displacement is

$$\overline{u_v^2} = \sum_Q \overline{|c_Q|^2} A_Q^2. \quad (8.53)$$

For a random distribution of defects,

$$\overline{u_v^2} = \frac{3}{4\pi^2} c (1-c) d^2 M^0, \quad (8.54)$$

where $M^0 = b (1/V)^2 (dV/dc)^2$. If only nearest-neighbor interactions are included and noncentral forces are considered (the Born-Begbie approximation, [487]), the value of b is about 0.25-0.45 in typical metals Ag, Al, Ni and the like.

We consider next the contribution from atomic displacements to the square of the modulus of the matrix element, $|\mathcal{H}_{cr,d}^b(\mathbf{q})|^2$. By analogy with the effects of thermal vibration, we expect the result to contain two parts. The first one may be written as

$$|\mathcal{H}_{cr,d}^{b(1)}(\mathbf{q})|^2 = |W^b(\mathbf{q})|^2 e^{-2M_{st}} \delta_{\mathbf{q}, \mathbf{g}'_n}, \quad (8.55)$$

where $M_{st} = (1/2) (\overline{\mathbf{q}\mathbf{u}_v})^2$ and the \mathbf{g}'_n are the reciprocal lattice vectors for a crystal distorted by defects.

The band-structure energy associated with this part of the matrix element is

$$U_{bs,d}^{(1)} = \frac{\Omega'_0}{8\pi} \sum_n (g_n^{(1)})^2 \frac{1-\varepsilon(\mathbf{g}'_n)}{\varepsilon^*(\mathbf{g}'_n)} |W^b(\mathbf{g}'_n)|^2 e^{-2M_{st}} \delta_{\mathbf{q}, \mathbf{g}'_n}. \quad (8.56)$$

It can be seen from (8.55) and (8.56) that if crystal defects displace atoms from their perfect positions, the interaction of the electron gas with the defects alters the electron-transition matrix elements. If Ω'_0 is little affected by defects, the absolute magnitude of $U_{bs}^{(1)}$ will be less than that in a perfect crystal. Since U_{bs} is negative the atomic displacements will have, through $U_{bs,d}$, a somewhat destabilizing effect on the lattice. It is implied, of course, that, in an actual calculation, the electrostatic contribution is also included. This will be achieved if, in (8.56), we replace

$$\frac{\Omega'_0}{8\pi} (g_n')^2 \frac{1-\varepsilon(\mathbf{g}'_n)}{\varepsilon^*(\mathbf{g}'_n)} |W^b(\mathbf{g}'_n)|^2 \quad \text{by} \quad \frac{2\pi}{\Omega'_0 (g_n')^2} Z^{*2} e^{-\frac{(g_n')^2}{4\eta}}. \quad (8.57)$$

The second part of the square of the modulus of the matrix element is given by

$$|\mathcal{H}_{cr,d}^{b(2)}(\mathbf{q})|^2 = \frac{c(1-c)}{2N} |W^b(\mathbf{q})|^2 \{ |\mathbf{A}_Q(\mathbf{g}_n + \mathbf{Q})|^2 \delta_{\mathbf{q}, \mathbf{g}_n + \mathbf{Q}} \\ + |\mathbf{A}_Q(\mathbf{g}_n - \mathbf{Q})|^2 \delta_{\mathbf{q}, \mathbf{g}_n - \mathbf{Q}} \}. \quad (8.58)$$

By substituting this into the formulae for the band structure energy, we find the change in this energy, the sign of which will coincide with that of U_{bs} . Therefore, both the magnitude and sign of the total energy change can only be determined by rigorous calculation. (Note that (8.58) should be complemented by the electrostatic energy; this is achieved by the substitution defined in (8.57).)

The value of the internal energy may be used for calculating the free energy. By minimizing this energy it is possible, in principle, to find the equilibrium concentration of defects.

In the above discussion, the \mathbf{A}_Q coefficients were assumed to have been calculated either for the case of isotropic elastic continuum or in the Born-Begbie approximation. Pseudopotential theory offers new possibilities by allowing the calculation of interatomic potentials at any distance from a defect.

Using the formalism developed in [418, 488] the α -component of the displacement of a host ion may be written as

$$\mathbf{u}_\alpha(\mathbf{t}_v) = -i \frac{\Omega_0}{(2\pi)^3} \int d\mathbf{q} \sum_{\beta=1}^3 g_{\alpha\beta} \times \left\{ \sum_n (\mathbf{q}_\beta + \mathbf{g}_{n\beta}) \cdot \bar{\mathcal{F}}(\mathbf{q} + \mathbf{g}_n) \right\} e^{-i\mathbf{q}(\mathbf{t}_v - \mathbf{T}_{v'})}. \quad (8.59)$$

Here \mathbf{t}_v is the position of the ion in question, $\mathbf{T}_{v'}$ is the position of a defect, the integration is over the Brillouin zone and

$$g_{\alpha\beta}(\mathbf{q}) = D^{-1}(\mathbf{q})_{\alpha\beta} = \sum_{\lambda=1}^3 \frac{e_\alpha^*(\mathbf{q}, \lambda) e_\beta(\mathbf{q}, \lambda)}{M\omega_{\mathbf{q}, \lambda}^2} \quad (8.60)$$

is the Fourier transform of the lattice Green's function [489], where D is the dynamics matrix, M the mass of a host atom and $\mathbf{e}(\mathbf{q}, \lambda)$ the polarization vector with a polarization index λ . The quantity

$$\bar{\mathcal{F}}(\mathbf{t}_v) = \frac{1}{N} \sum_{\mathbf{k}} \mathbf{k} \cdot \bar{\mathcal{F}}(\mathbf{k}) e^{i\mathbf{k}(\mathbf{t}_v - \mathbf{T}_{v'})} \quad (8.61)$$

is the Fourier component of the force exerted by the impurity atom upon the host atom located at the site \mathbf{t}_v .

The above expressions may be derived using the harmonic approximation for the total energy of the matrix-impurity system,

$$U = U(\Omega_0) + \frac{1}{N} \sum_v \bar{\mathcal{F}}(\mathbf{t}_v) \cdot \mathbf{u}_v + \frac{1}{2N} \sum_{v\alpha v'\alpha'} D_{v\alpha v'\alpha'} \mathbf{u}_{\alpha v} \cdot \mathbf{u}_{\alpha' v'}, \quad (8.62)$$

where $U(\Omega_0)$ is the energy of the crystal with periodically regular atoms and

$$D_{v\alpha v'\alpha'} = \frac{1}{N} \sum_{\mathbf{q}} D(\mathbf{q}) e^{-i\mathbf{q}(\mathbf{t}_v - \mathbf{t}_{v'})} \quad (8.63)$$

is the site representation for the dynamics matrix of the pure crystal.

We have seen, on the other hand, that the total energy of an alloy may be expanded as

$$U = U_{\text{es}} + U_0(\Omega_0) + U^{(1)}(\Omega_0) + U^{(2)} + U^{(3)} + \dots \quad (8.64)$$

Here again the terms U_{es} , $U^{(2)}$ and $U^{(3)}$ are structure-dependent. Their form was discussed above. For example,

$$U^{(2)} = \frac{\Omega_0}{8\pi} \sum_{\mathbf{q}}' \mathbf{q}^2 |f(\mathbf{q})|^2 \frac{1 - \varepsilon(\mathbf{q})}{\varepsilon(\mathbf{q})}, \quad (8.65)$$

where

$$f(\mathbf{q}) = \frac{1}{N} W_{\text{m}}(\mathbf{q}) \sum_{\mathbf{v}} e^{i\mathbf{q}\mathbf{r}_{\mathbf{v}}} + \frac{1}{N} \Delta W(\mathbf{q}) e^{i\mathbf{q}\mathbf{T}_{\mathbf{v}}}, \quad (8.66)$$

and $\Delta W(\mathbf{q}) = W_{\text{d}}(\mathbf{q}) - W_{\text{m}}(\mathbf{q})$. By setting $\mathbf{r}_{\mathbf{v}} = \mathbf{t}_{\mathbf{v}} + \mathbf{u}_{\mathbf{v}}$, expanding (8.66) in powers of $\mathbf{u}_{\mathbf{v}}$ and substituting in (8.62), we find $\mathcal{F}(\mathbf{t}_{\mathbf{v}})$ and $D_{\mathbf{v}\alpha\mathbf{v}'\alpha'}$. In second-order perturbation theory [490], we have

$$\mathcal{F}^{(2)}(\mathbf{k}) = -W_{\text{m}}(\mathbf{k}) \Delta W(\mathbf{k}) \Omega_0 \frac{k^2}{4\pi} [1 - \varepsilon^{-1}(\mathbf{k})]. \quad (8.67)$$

In principle, third-order corrections can also be obtained. Using the above relations Solt and Zhernov [491] calculated atomic displacements for dissolved atoms and, in an asymptotic approximation, for diluted alkali alloys. The displacements were found to be very anisotropic and the asymptotic approximation was found to be valid from the eighth or tenth coordination sphere.

Thus far we have been discussing the pseudopotential approach to static substitutional defects. The distorting effect of interstitial atoms may be considered in the same spirit [492].

In this case, the band structure energy is calculated using (6.1) and (6.2) with the crystal pseudopotential in the form

$$\mathcal{W}_{\text{cr.d}}(\mathbf{r}) = \sum_{\mathbf{v}} [W_{\text{m}}(\mathbf{r} - \mathbf{t}_{\mathbf{v}} - \mathbf{u}_{\mathbf{v}}) + c_{\mathbf{v}} W_{\text{d}}(\mathbf{r} - \mathbf{t}_{\mathbf{v}} - \boldsymbol{\alpha})], \quad (8.68)$$

where the vector $\boldsymbol{\alpha}$ characterizes the position of the sites of the z-lattice of the interstitials relative to the matrix sites. In the Fourier representation we then find, to the first order in atomic displacement,

$$W(\mathbf{q}) = W_{\text{m}}(\mathbf{q}) \left[S(\mathbf{q}) - i \sum_{\mathbf{Q}_j} \mathbf{U}_{\mathbf{Q}_j}(\mathbf{q} \mathbf{e}_j(\mathbf{Q})) S(\mathbf{q} + \mathbf{Q}) \right] + W_{\text{d}}(\mathbf{q}) \sum_{\mathbf{Q}} C_{\mathbf{Q}} S(\mathbf{q} + \mathbf{Q}) e^{-i\mathbf{q}\boldsymbol{\alpha}}, \quad (8.69)$$

where the \mathbf{Q} summation is over the Brillouin zone and the j summation over the polarization directions, as determined by the vectors $\mathbf{e}_j(\mathbf{Q})$.

Substituting (8.69) into (6.1) yields the band structure energy, in which the electron scattering term (arising from impurity and deformation potentials) is given by

$$U_{\text{bs,d}} = \sum_{\mathbf{q}, \mathbf{Q}, \boldsymbol{\kappa}} \Phi_{\text{bs,d}}(\mathbf{q}) S(\mathbf{q} + \boldsymbol{\kappa}) \{ -i(\mathbf{q} \mathbf{U}_{\mathbf{Q}}) c_{\boldsymbol{\kappa}}^* e^{-i\mathbf{q}\boldsymbol{\alpha}} + \text{c.c.} \}, \quad (8.70)$$

where

$$\Phi_{bs, d} = W_d W_m \chi(\mathbf{q}) \varepsilon(\mathbf{q}).$$

Transforming the complex-conjugate term, we obtain

$$U_{bs, d} = -2i \sum_{\mathbf{Q}, n} \Phi_{bs, d}(|\mathbf{g}_n + \mathbf{Q}|) ((\mathbf{g}_n + \mathbf{Q}) \mathbf{U}_{-\mathbf{Q}}) C_{\mathbf{Q}} e^{-i(\mathbf{g}_n + \mathbf{Q})\alpha}, \quad (8.71)$$

where we have taken advantage of the fact that the structure factor is only nonzero if its argument is a reciprocal lattice vector. The electrostatic contribution can be found from (8.71) by replacing $\Phi_{bs, d}$ by $2\pi Z_m Z_d / \Omega q^2$ where Z_m and Z_d are the valencies of, respectively, the host and impurity atoms. The renormalization of the screened impurity formfactor,

$$W_d(\mathbf{q}) \rightarrow \tilde{W}_d(\mathbf{q}) = W_d(\mathbf{q}) \frac{\varepsilon_d(\mathbf{q}) \Omega_d}{\varepsilon(\mathbf{q}) \Omega} \quad (8.72)$$

secures the low- \mathbf{q} convergence of the Fourier transform of the total effective interatomic potential. The deformation effects of impurity atoms will then be described by the term

$$U_d = -2i \sum_{\mathbf{Q}, n} \Phi_d(|\mathbf{g}_n + \mathbf{Q}|) ((\mathbf{g}_n + \mathbf{Q}) \mathbf{U}_{-\mathbf{Q}}) C_{\mathbf{Q}} e^{-i(\mathbf{g}_n + \mathbf{Q})\alpha}, \quad (8.73)$$

where

$$\Phi_d = \Phi_{es, d} + \Phi_{bs, d} (W_d \rightarrow \tilde{W}_d).$$

Comparing this with the corresponding phenomenological result [401] yields a relation between the quasi-elastic force $\mathcal{F}_{\mathbf{Q}}$ and the microscopic parameters of the system,

$$\mathcal{F}_{\mathbf{Q}} = -i \sum_n (\mathbf{g}_n + \mathbf{Q}) \Phi_d(|\mathbf{g}_n + \mathbf{Q}|) e^{-i(\mathbf{g}_n + \mathbf{Q})\alpha}. \quad (8.74)$$

The effective deformation potential $V_{\mathbf{Q}}$ is then given (omitting a constant factor) by

$$V_{\mathbf{Q}} = - \sum_{j=1}^3 \frac{|\mathbf{e}_j(\mathbf{Q}) \mathcal{F}_{\mathbf{Q}}|^2}{m \omega_j^2(\mathbf{Q})}, \quad (8.75)$$

where m is the mass of the atom and $\omega_j(\mathbf{Q})$ the phonon frequencies of the host matrix.

Belen'kii [492] used (8.74) and (8.75) to calculate the quasi-elastic force and effective interaction potential for the case of carbon and phosphorus interstitials in α -iron. The formfactors for Fe, C and P were taken from [343] and the exchange-correlation effects were treated in the Hubbard-Sham approximation.

The calculated quasi-elastic force was more anisotropic than that observed (the predicted z -component was much larger

than the x - and y -component). This discrepancy might be due to the strong electrostatic repulsion which exists between impurity atoms and their nearest host neighbors on the z -axis (note that $\alpha = (0, 0, a/2)$). The other possible reasons are the formation of impurity-matrix covalent bonds or underestimation of the screening of impurity atoms. To include these effects, however, requires higher-order perturbation theory.

It was found that phosphorus V_Q curves were always below those for carbon. The V_Q behavior in the vicinity of the $(0\ 1/2\ 1/2)$ superstructural site reveals that the phosphorus solution has a somewhat stronger tendency to form a metastable ordered phase. A similarity between the pseudopotentials of phosphorus and nitrogen enabled Belen'kii to consider his result as consistent with experiment.

Belen'kii concluded that even though his pseudopotential calculations were too simplistic to be quantitatively reliable, they were quite useful for qualitative estimates.

To sum up, pseudopotential theory is now being extensively applied in defect-related problems. These include the role of defects in the formation of real crystal structure, the formation energy of defects, and the stability of defects and their influence on the physical properties of solids. Note that the types of defect treatable by pseudopotential theory are by no means limited to those considered in this book. Other results obtained by the pseudopotential method may be found in [17, 73, 493-499].

At present, the pseudopotential theory of real crystals may be considered one of the more important fields of solid-state theory.

Principles of pseudopotential calculations of the properties of metals

9.1. General

Basically, there are three types of physical properties which can be calculated by the pseudopotential method. The first type demands the value of the total crystal energy or some of its components, the stability of a crystal lattice being the best known example. Calculations of this type have been the subject of many papers and are reviewed in [500-503] which makes it unnecessary to discuss them here.

The second type involves the properties associated with the way a solid responds to external influences (including heat). These properties are therefore determined by coordinate derivatives of the total energy rather than by its magnitude. The phonon spectra discussed in the previous chapter are one example of this kind of property. In this chapter, we will discuss elasticity, Grüneisen's constants, the equations of state, etc.

The third type of properties involves electron transport effects and are determined by the matrix elements for the electron transitions between energy states. We will consider disordered systems such as liquid and amorphous metals and alloys, and disordered crystalline alloys to illustrate the main idea underlying the calculation of these properties. We have emphasized the principles and the citations and information are neither exhaustive nor complete.

9.2. Calculation of the atomic properties of crystalline metals and alloys

The physical properties of both perfect and imperfect crystals may be associated either with the total energy of the crystal or with the matrix elements for the electron transitions. In the former case we may deal with either the energy itself or with its coordinate or deformation derivatives. When dealing with matrix elements the square of the modulus of the matrix element is often involved. In what may be considered a canonical way of using pseudopotentials, the first step in calculating a physical property is to write an expression for it in terms of the total energy, the total energy derivatives, and the matrix elements. A calculation is then carried out by sub

stituting those quantities found by the pseudopotential method for the specific problem. It is this method that will mainly be followed in this chapter.

Pseudopotential calculations of the elastic properties of crystals have been performed in quite a number of papers (see [500-512, 276, 482]). Elastic properties are determined by the derivatives of the total crystal energy with respect to the parameters of deformation. The parameters are defined by

$$\eta_{ij} = \frac{1}{2} \left(\sum_i \frac{\partial x'_i}{\partial x_i} \frac{\partial x'_i}{\partial x_j} - \delta_{ij} \right), \quad i, \quad 1, 2, 3, \quad (9.1)$$

where i and j indices are usually replaced by J indices according to Focht's rule ($11 \rightarrow 1$, $22 \rightarrow 2$, $33 \rightarrow 3$, $23 \rightarrow 4$, $31 \rightarrow 5$, and $12 \rightarrow 6$). The second-order elasticity coefficients in this notation become

$$c_{JJ} = \frac{1}{\Omega} \left(-\frac{\partial^2 U}{\partial \eta_J \partial \eta_J} \right)_{\{\eta=0\}}. \quad (9.2)$$

In order to describe a transition from a nondeformed state to a deformed one, it is customary to employ the deformation parameters ε_i , γ_i , and ν defined by the relations

$$\begin{aligned} x' &= x(1 + \varepsilon_1), & x' &= x + \gamma_1 y, & x' &= \nu^{1/3} x; \\ y' &= y(1 + \varepsilon_1)^{-1}, & y' &= y, & y' &= \nu^{1/3} y; \\ z' &= z, & z' &= z, & z' &= \nu^{1/3} z; \end{aligned} \quad (9.3)$$

which relate the coordinates of particles in a nondeformed crystal to those in a deformed one. The parameters $\gamma_{i \neq 1}$ and $\varepsilon_{i \neq 1}$ may be defined in a similar fashion. In terms of these parameters the second-order elasticity coefficients take the form

$$\begin{aligned} \frac{\partial^2 U_{\text{total}}}{\partial \nu^2} &= \frac{1}{3} (c_{11} + 2c_{12}) = B, \\ \frac{\partial^2 U_{\text{total}}}{\partial \gamma_1^2} &= c_{44}, \\ \frac{1}{4} \frac{\partial^2 U_{\text{total}}}{\partial \varepsilon_1^2} &= \frac{1}{2} (c_{11} - c_{12}) = c'. \end{aligned} \quad (9.4)$$

The first of these coefficients is known as the bulk modulus and the others are shear moduli.

The total energy of a crystal which has a volume V and is made up of N ions of valency Z (so that the free-electron-gas density is $n_0 = zN/V = 3/(4\pi r_s)^3$ and the volume of the Wigner-Seitz cell is $V/N = 4\pi R_a^3/3 = \Omega$) is

$$U_{\text{total}} = U_0 + U_1 + U_{\text{hs}} + U_{\text{es}}. \quad (9.5)$$

The first term on the right is the energy of a free electron gas, which is the sum of the kinetic, exchange, and correlation energies. Its va-

value per atom is

$$U_0 = Z \left(\frac{2.21}{r_s^2} - \frac{0.91}{r_s} - 0.115 + 0.031 \ln r_s \right). \quad (9.6)$$

The second, third, and fourth terms are, respectively, the average energy of electron-ion interaction

$$U_1 = \lim_{q \rightarrow 0} \frac{Z}{\Omega} \left[\frac{8\pi Z}{q^2} + W_{\text{cr}}^b(q) \right] = \beta n_0, \quad (9.7)$$

the band structure energy

$$U_{\text{bs}} = \sum_{\mathbf{q}}' |S(\mathbf{q})|^2 |W^b(\mathbf{q})|^2 \chi(q) \varepsilon^*(q) = \sum_{\mathbf{q}}' \Phi_{\text{bs}}(\mathbf{q}), \quad (9.8)$$

and the electrostatic energy

$$U_{\text{es}} = -\alpha Z^2 / 2R_a. \quad (9.9)$$

α in (9.9) is Madelung's constant, and $\varepsilon^*(q)$ in (9.8) is the dielectric permittivity containing corrections for exchange and correlation. The function $\varepsilon^*(q)$, the dielectric susceptibility $\chi(q)$, and the function $f(\mathbf{q})$, which describes the exchange and correlation corrections, are related by (see also Secs. 3.2, 6.2, and 6.3)

$$\varepsilon^*(q) = 1 - \frac{16\pi}{\Omega q^2} [1 - f(q)] \chi(q). \quad (9.10)$$

Since U_0 and U_1 only depend on volume and do not depend directly on structure, they are often combined together to give what is called the volume-dependent contribution to the total energy. A third-order perturbation theory correction U_3 may also be included when calculating physical properties [506, 508, 509].

The average energy of electron-ion interaction U_1 is defined differently by different workers. Apart from directly calculating the long-wavelength limit of β , this quantity may be found [507, 511] by setting the derivative

$$\frac{\partial U_{\text{total}}}{\partial r_s} = -P \quad (9.11)$$

equal to zero in the absence of external pressure. To find the elasticity coefficients, the derivatives of the total energy with respect to deformation parameters must be found. The expressions for some of these derivatives are reproduced below from the paper by Suzuki *et al.* [504]. The first and second derivatives of the characteristic band structure function $\Phi_{\text{bs}}(\eta, r_s)$ with respect to v are of the form

$$\begin{aligned} \frac{\partial \Phi(\eta, r_s)}{\partial v} &= \frac{1}{3} r_s \frac{\partial \Phi(\eta, r_s)}{\partial r_s}, \\ \frac{\partial^2 \Phi(\eta, r_s)}{\partial v^2} &= \frac{1}{9} r_s^2 \frac{\partial^2 \Phi(\eta, r_s)}{\partial r_s^2} - \frac{2}{9} r_s \frac{\partial \Phi(\eta, r_s)}{\partial r_s}, \end{aligned} \quad (9.12)$$

where $\eta = q/2k_F$.

The derivatives with respect to the shear parameters γ_i and ε_i have the form

$$\frac{\partial^2 \Phi(\eta, r_s)}{\partial \gamma_i^2} = \frac{\partial^2 \Phi(\eta, r_s)}{\partial \eta^2} \left(\frac{\partial \eta}{\partial \gamma_i} \right)^2 + \frac{\partial \Phi(\eta, r_s)}{\partial \eta} \frac{\partial^2 \eta}{\partial \gamma_i^2}. \quad (9.13)$$

In order to obtain the derivatives of η with respect to γ_1 and ε_1 it should be taken into account that deformation changes the translational vectors of both the direct and reciprocal lattices. For the BCC lattice we have

$$\begin{aligned} \frac{\partial \eta}{\partial \gamma_1} &= - \left(\frac{\pi}{6} \right)^{1/3} \frac{m_1 m_2}{(m_1^2 + m_2^2 + m_3^2)^{1/2}}, \\ \frac{\partial \eta}{\partial \varepsilon_1} &= - \left(\frac{\pi}{6} \right)^{1/3} \frac{m_1^2 - m_2^2}{(m_1^2 + m_2^2 + m_3^2)^{1/2}} \\ \frac{\partial^2 \eta}{\partial \gamma_1^2} &= \left(\frac{\pi}{6} \right)^{1/3} \left[- \frac{m_1^2 m_2^2}{(m_1^2 + m_2^2 + m_3^2)^{3/2}} + \frac{m_1^2}{(m_1^2 + m_2^2 + m_3^2)^{1/2}} \right] \\ \frac{\partial^2 \eta}{\partial \varepsilon_1^2} &= \left(\frac{\pi}{6} \right)^{1/3} \left[- \frac{m_1^2 m_2^2}{(m_1^2 + m_2^2 + m_3^2)^{3/2}} + \frac{3m_1^2 + m_2^2}{(m_1^2 + m_2^2 + m_3^2)^{1/2}} \right], \end{aligned} \quad (9.14)$$

where the integers m_1 , m_2 and m_3 are the components of reciprocal lattice sites.

Using (9.14) the second derivatives of the characteristic function with respect to γ_1 and ε_1 are found to be

$$\begin{aligned} \frac{\partial^2 \Phi(\eta, r_s)}{\partial \gamma_1^2} &= \frac{\partial^2 \Phi(\eta, r_s)}{\partial \eta^2} \left(\frac{\pi}{6} \right)^{2/3} \frac{m_1^2 m_2^2}{m_1^2 + m_2^2 + m_3^2} + \frac{\partial \Phi(\eta, r_s)}{\partial \eta} \left(\frac{\pi}{6} \right)^{1/3} \\ &\quad \times \left\{ - \frac{m_1^2 m_2^2}{(m_1^2 + m_2^2 + m_3^2)^{3/2}} + \frac{m_1^2}{(m_1^2 + m_2^2 + m_3^2)^{1/2}} \right\}, \end{aligned} \quad (9.15)$$

$$\begin{aligned} \frac{\partial^2 \Phi(\eta, r_s)}{\partial \varepsilon_1^2} &= \frac{\partial^2 \Phi(\eta, r_s)}{\partial \eta^2} \left(\frac{\pi}{6} \right)^{2/3} \frac{(m_1^2 - m_2^2)^2}{m_1^2 + m_2^2 + m_3^2} \\ &\quad + \frac{\partial \Phi(\eta, r_s)}{\partial \eta} \left(\frac{\pi}{6} \right)^{1/3} \left\{ - \frac{(m_1^2 - m_2^2)^2}{(m_1^2 + m_2^2 + m_3^2)^{3/2}} + \frac{3m_1^2 + m_2^2}{(m_1^2 + m_2^2 + m_3^2)^{1/2}} \right\}. \end{aligned}$$

The derivatives of other components of the total energy were also obtained in [504] but the corresponding expressions are too cumbersome to reproduce here.

From these results, the elasticity coefficients for a number of the alkali and other metals have been calculated. In [505, 506] the coefficients c_{11} , c_{12} and c_{44} were calculated for Al and Na, and from them the parameters B , c' and c_{44} were found. Benckert used an Ashcroft model potential (with a damping factor) whose parameters were fitted to experimental Fermi-surface data.

Table 9.1 shows the (computed) contributions to the total energy (U_3 is the third-order correction) and to the elasticity coefficients. The sums of the contributions are also shown and can be compared with the corresponding experimental results.

Table 9.1. Contributions to total energy (Ry/at) and elasticity coefficients (10^{10} N/m²) for Al and Na [508]

	Al					Na				
	U	$\partial U / \partial r_s$	B	c'	c_{44}	U	$\partial U / \partial r_s$	B	c'	c_{44}
U_0	-0.054	-0.817	14.71	—	—	-0.163	-0.006	0.263	—	—
U_{es}	-5.417	2.624	32.02	1.66	14.90	-0.456	0.116	-1.171	0.072	0.537
U_1	1.473	-2.141	39.20	—	—	0.163	-0.124	1.858	—	—
U_{bs}	-0.121	0.440	-18.62	1.44	-10.86	-0.010	0.017	-0.343	-0.007	0.055
U_3	0.016	-0.106	5.89	-1.05	-1.08	0.001	-0.003	0.059	-0.009	-0.027
U_{total}	-4.103	0	9.16	2.05	2.96	0.405	0	0.666	0.056	0.565
U_{exp}	-4.142	—	7.95	2.61	3.17	-0.459	—	0.76	0.073	0.62

Although the computed and experimental values can be seen to agree fairly well, it turns out [506] that the agreement depends significantly on the choice of potential, the third-order contributions being the most sensitive ones.

Shimada [507] employed a three-parameter model pseudopotential having a continuous logarithmic derivative. The parameters of the pseudopotential were fitted to equilibrium conditions. It can be seen from Table 9.2 that the values of B and c' computed in [507] agree well with the experimental data. There are at least three general conclusions to be drawn from the above results.

Table 9.2. Elasticity constants c' and B for Li, Na, K, Rb, Cs, Al, Pb (theory [507] and experiment)

Element	c' (10^{11} dyn/cm ²)		B (10^{11} dyn/cm ²)	
	theoretical	experimental	theoretical	experimental
Li	0.117	0.117	1.335	1.365
Na	0.0761	0.075	0.737	0.775
K	0.0376	0.0377	0.363	0.366
Rb	0.0279	0.0287	0.281	0.291
Cs	0.0218	0.0205	0.216	0.219
Al	1.306	2.619	7.944	7.938
Pb	0.647	0.506	4.887	4.879

The experimental values are obtained for each element by averaging the data from Table 3 of [507].

First, it may be argued that second-order elasticity constants can be calculated rather accurately for pure metals by fitting pseudopotential parameters both from atomic properties (equilibrium conditions) and from electronic characteristics (the shape of the Fermi surface, etc.). The pseudopotentials thus obtained may then be used to calculate the other parameters of pure metals. Second, these results may provide a basis for calculating the elastic properties of alloys. And finally, comparing computed and experimental elastic parameters may help bring out the factors which determine the elastic properties of crystals.

These conclusions may be said to have been confirmed. In their work on pure metals, Khanna and Sharma [512] fitted the model pseudopotential of [513] to Fermi surface data in order to calculate the cohesion energy, compressibility, electrical resistivity due to single vacancies, third-order elasticity constants, and the superconductivity transition temperature. Some of their results are given

in Table 9.3, which actually consists of two parts. In columns 1 through 7 the computed values are compared with the experimental results and it can be seen that pseudopotentials fitted for one property may indeed be useful for determining another. For the theoretical values given in the last two columns, no experimental data are as yet available, but judging from the good results in the previous columns, the predictions can be expected to be realistic.

Table 9.3. Pseudopotential results and experimental values for some physical properties [512]

Element	Cohesion energy (Ry/el)		Compressibility (K/K ⁰)			T _c K	(μΩ/at.%)	C _{III} ⁽¹⁰¹¹⁾ dyn/cm ²
	theoreti- cal	experi- mental	theoreti- cal	experi- mental	theoreti- cal			
Li	-0.550	-0.551	1.65	2.0	0.014	0.08	0.49	—
Na	-0.470	-0.460	1.30	1.5	0.0071	—	1.01	-6.82
K	-0.396	-0.390	1.08	1.0	0.0071	—	1.58	-4.99
Rb	-0.371	-0.366	0.90	0.82	—	—	—	—
Al	—	—	—	—	2.0	1.196	0.57	—
Pb	—	—	—	—	6.5	7.23	0.98	—

Vaks *et al.* [483, 510] used the method of adjusting pseudopotential parameters to calculate various properties of the alkali metals such as elasticity moduli, phonon spectra, equations of state, dielectric permittivity, and the effect of third-order perturbation theory corrections. They thoroughly compared their results with experimental data and the reliability of the results was carefully checked against the various factors in the calculation. It is pointed out that the condition

$$\frac{\partial U_{\text{total}}}{\partial r_s} = 0 \quad (9.11a)$$

is crucial for a correct description of the static properties of metals in that it fixes the constant β and hence determines the quantity U_1 (see Eq. (9.7)), which greatly contributes to all the atomic properties as Table 9.1 shows. Another important point is that using their fitting procedure the experimental dielectric permittivity was fitted best if the exchange-correlation corrections were taken in the form proposed in [514, 429]. It was also found that the third-order contribution may be significantly reduced by redefining the pseudopoten-

tial parameters, the important implication being that a large third-order contribution may simply be due to a "bad" pseudopotential. A comparison of computed results with experiment showed that the local pseudopotential of [483, 510] is not only useful for Na but also for K and Rb, even though the *d*-band in these two metals is rather close to the Fermi level. For Li and Cs, however, the computed values of the cohesion energy and the derivatives of the elasticity moduli disagreed significantly with experimental results, although the phonon spectra, equations of state, and the moduli themselves were reproduced correctly. Pseudopotential calculations may thus be very helpful in predicting physical properties although comparison with experiment is always needed to determine the reliability of results. It should also be kept in mind that the accuracy of the results may vary from element to element if for no other reason than because the core states contribute differently to different elements of the same group. The optimization schemes may also differ. In [510] the volume dependences of some properties of alkali metals and the equations of state for a wide range of pressures were calculated. It is shown that in the well-studied pressure range of $p < 50$ kbar, the results for Li, Na, and K are in good agreement with experiment and the uniform compression data on Na and K were even reproduced for pressures as high as 400 kbar. It should be expected therefore that pseudopotential calculations may be helpful at high pressures, design pressure gauges being a possible application.

There are other approaches to pseudopotential calculations of elastic characteristics. Brovman and Kagan [508, 509, 276] used the relations which exist between the elasticity properties (the moduli and sound velocities) and the dynamic matrix responsible for the phonon spectrum of the crystal. In cubic crystals, for example, the propagation velocities for the longitudinal and transversal waves in the [100] symmetry direction are, respectively,

$$v_l = (c_{11}/\rho)^{1/2} \quad \text{and} \quad v_{t[100]} = (c_{44}/\rho)^{1/2}, \quad (9.16)$$

where ρ is the density of the crystal.

The shear modulus $c' = (1/2)(c_{11} - c_{12})$ is directly related to the propagation velocity of the transversal wave in the [100] direction:

$$v_{t,[110]} = [(c_{11} - c_{12})/2\rho]^{1/2} \quad (9.17)$$

(atoms are displaced along $[\bar{1}10]$).

Since the velocities are, in turn, the frequency-to-wave vector ratios of the corresponding vibrations, clearly a pseudopotential calculation of phonon frequencies makes it possible to find elasticity moduli. We refer the reader to [276] for more detail and only repro-

duce here the results, which are

$$c_{11} = \frac{\varphi(0)}{\Omega_0} + \frac{1}{\Omega_0} \sum_{n \neq 0} \left[\varphi(\mathbf{g}_n) + 2g_{nx} \frac{\partial \varphi(\mathbf{g}_n)}{\partial g_{nx}} + \frac{1}{2} g_{nx}^2 \frac{\partial^2 \varphi(\mathbf{g}_n)}{\partial g_{nx}^2} \right] \\ + \frac{1}{\Omega_0} \sum_{n \neq 0} \left[2n_0 \frac{\partial \varphi(\mathbf{g}_n)}{\partial n_0} + \frac{1}{3} g_n^{(\alpha)} \frac{\partial^2 \varphi(\mathbf{g}_n)}{\partial g_n^\alpha \partial n_0} + \frac{1}{2} n_0^2 \frac{\partial^2 \varphi(\mathbf{g}_n)}{\partial n_0^2} \right], \\ c_{44} = \frac{1}{2\Omega_0} \sum_{n \neq 0} g_{nx}^2 \frac{\partial^2 \varphi(\mathbf{g}_n)}{\partial g_{ny}^2}, \quad (9.18)$$

$$c' = \frac{1}{2\Omega_0} \sum_{n \neq 0} \left[g_{nx}^2 \frac{\partial^2 \varphi(\mathbf{g}_n)}{\partial g_{nx}^2} + g_{ny}^2 \frac{\partial^2 \varphi(\mathbf{g}_n)}{\partial g_{ny}^2} - 2g_{nx}g_{ny} \frac{\partial^2 \varphi(\mathbf{g}_n)}{\partial g_{nx} \partial g_{ny}} \right]$$

where

$$\varphi(\mathbf{q}) = \frac{4\pi Z^2 e^2}{q^2 \Omega_0} - \frac{\Omega_0}{4\pi e^2} \frac{|W^b(\mathbf{q})|^2 [\varepsilon(q) - 1] q^2}{\varepsilon(q)}.$$

It is worthwhile discussing the relationship between the dynamic moduli as defined from the sound velocity and the static moduli. It was shown in [509] that the inclusion of multi-ion interaction should make these moduli equal. That this is indeed the case was confirmed by a comparison of results obtained by both methods.

Thus far we have been concerned with the "ground-state" properties of a crystal. The dependence of these on external parameters such as temperature and pressure may also be determined by the pseudopotential method. Portnoi *et al.* [501], for example, calculated Grüneisen's constant γ , which characterizes the changes in phonon frequencies ν_i caused by variations in volume V

$$\gamma = - \frac{d \ln \nu_i}{d \ln V}. \quad (9.19)$$

Apart from the constant itself (in fact, the constant's average over the frequencies is usually computed), its frequency dependence has been calculated [515-517]. In order to determine the (average) value of Grüneisen's parameter, it is convenient to write

$$\gamma = - \frac{1}{2} \frac{\partial \ln \bar{\nu}^2}{\partial \ln V}, \quad (9.20)$$

where $\bar{\nu}^2$ is the second moment of the frequency spectrum. Since $\bar{\nu}^2$ is related [518] to the coordinate derivative of the interatomic potential V_p we find for the pairwise central interaction

$$\gamma = - \frac{1}{6} \frac{\sum_i C_i \left[-\frac{2}{R} V_p'(R) + 2V_p''(R) + R V_p'''(R) \right]_{R=R_i}}{\sum_i C_i \left[\frac{2}{R} V_p'(R) + V_p''(R) \right]_{R=R_i}}, \quad (9.21)$$

where C_i is the coordination number for the i th coordination sphere of radius R_i , and V'_p , V''_p , and V'''_p are the derivatives of the interatomic potential.

In Table 9.4 the γ as computed in [519] are given with their experimental values.

Table 9.4. The values of γ for the alkali metals

γ	Na	K	Rb	Cs
theoretical	1.015	1.024	1.102	1.086
experimental	0.94	1.159	1.28	1.28

In view of the strong frequency dependence of Grüneisen parameters [517] the agreement between theory and experiment is reasonably good.

A knowledge of γ enables Senoo *et al.* [520] to relate pressure to volume by using the Mee-Grüneisen equation in the Debye approximation [521]

$$p = - \left(\frac{\partial U_{\text{total}}}{\partial V} \right)_T + \gamma \frac{k_B T}{\Omega} \sum_i \left(\frac{h \nu_i}{k_B T} \right) \frac{e^{-\frac{h \nu_i}{k_B T}}}{\left(1 - e^{-\frac{h \nu_i}{k_B T}} \right)} \quad (9.22)$$

and solving (9.11) for the absolute zero temperature. A Heine-Abarenkov model potential was chosen from the condition that the equilibrium values of lattice constant as found for (absolute) zero temperature and zero pressure should correspond to the experimental values. The volume-pressure dependence in the range from zero to 100 kbar was found rather accurately for Al, Si, Ge, and four alkali metals (Na, K, Rb and Cs). Calcium alone gave poor agreement.

It was pointed out in Chapter 8 that the pseudopotential method is applicable to real crystals. Soma [522] employed the method to estimate the energy of vacancy formation and to demonstrate the (rather substantial) dependence of this energy on relaxation [522, 523]. Du Charmé and Weaire [497] used the principles discussed by Harrison [73] to calculate the self-diffusion activation energy. They found that the activation energy is the sum of the vacancy-formation energy [73] plus the energy of vacancy migration. This latter may be found when calculating U_{es} and U_{bs} by taking into account that diffusing atoms migrate via saddle points located between lattice sites. The computed self-diffusion activation energy for Al was close to the measured value but it was very overestimated for Li, Na,

and K, implying that the migration of single vacancies is the mechanism for self-diffusion in Al alone and that in the alkali metals they studied it is not. The same scheme may be used for calculating the energy of formation of vacancy pores produced, for example, in irradiated metals [498].

9.3. Transport properties of noncrystalline metals and alloys

An important application of pseudopotentials is the calculating of the transport properties of disordered materials such as liquid or amorphous metals and alloys. The topic was first considered in [524-527] in which the expressions for electrical resistivity, thermoelectric emf, etc. were derived using pseudopotential formfactors for both liquid [524-526] and amorphous [527] metals. In the more general approach developed in [528] for liquid metals and extended in [529] for amorphous metals, T -matrix formfactors were used. This approach is particularly well suited for transition metals because it poses no problems in constructing a pseudopotential when d electrons are present, which belong neither to core nor to outer shells. Both methods are widely in use and will be discussed below.

Basically, there are two approaches to the transport properties of disordered materials, one based on the nearly-free-electron picture and the other on the tight-binding approximation. We will only be concerned with the first approach. The second approach usually involves either the average T -matrix approximation (ATA) or the coherent potential approximation (CPA) and is far beyond the confines of pseudopotential theory. The reader is referred to [530-533] for more details.

The physical properties of noncrystalline materials are sometimes studied in parallel with those of disordered crystal alloys [534]. A feature of such alloys is their compositional (chemical) short-range order [412], as opposed to the topological short-range order specific of noncrystalline systems. Note, though, that compositional short-range order is also possible in noncrystalline alloys [535, 536].

The method discussed here assumes the model of a gas of conduction electrons which interact with and are scattered by irregularly placed metal ions. As an external electric field drives the electron through the disordered medium, the scattering determines the electrical resistance, which can be calculated using perturbation theory or more general methods. This is in fact an extension of the Drude-Lorentz-Sommerfeld model, for which conductivity in the relaxation-time approximation is given by [537]

$$\sigma = \frac{1}{3} e^2 v_F^2 \tau N(E_F). \quad (9.23)$$

Here e is the electron charge, v_F is the velocity of electrons at the Fermi level, $N(E_F)$ the density of electronic states on the Fermi surface, and the relaxation time τ is defined by

$$\tau^{-1} = \int (1 - \cos \vartheta) Q(\vartheta) d\Omega, \quad (9.24)$$

where ϑ is the scattering angle, Ω is the solid angle and $Q(\vartheta)$ is the probability for scattering through the angle ϑ determined by

$$Q(\vartheta) = \frac{2\pi}{\hbar} |\langle \mathbf{k} | U | \mathbf{k}' \rangle|^2 \frac{1}{2} N(E_F) / 4\pi, \quad (9.25)$$

where $\langle \mathbf{k} | U | \mathbf{k}' \rangle$ is the matrix element for the transition of an electron from a state \mathbf{k}' to a state \mathbf{k} caused by the potential $U(\mathbf{r})$. The factor $1/2$ indicates that the electron spin is not affected by scattering. The potential $U(\mathbf{r})$ is the superposition of ionic potentials,

$$U(\mathbf{r}) = \sum_i U(\mathbf{r} - \mathbf{r}_i), \quad (9.26)$$

where the \mathbf{r}_i indicate the positions of the (irregularly arranged) ions.

In the local approximation, the matrix element $\langle \mathbf{k} | U | \mathbf{k}' \rangle$ may be considered as the Fourier transform of the potential $U(\mathbf{r})$

$$\langle \mathbf{k} | U | \mathbf{k}' \rangle = \frac{1}{V} \int U(\mathbf{r}) \exp[i(\mathbf{k} - \mathbf{k}') \cdot \mathbf{r}] d\mathbf{r} = U(\mathbf{q}) \sum_i e^{i\mathbf{q} \cdot \mathbf{r}_i}, \quad (9.27)$$

where a normalization to volume is assumed and $\mathbf{q} = \mathbf{k} - \mathbf{k}'$ is the scattering vector.

We invoke the diffraction model of neutron and X-ray scattering [485] to write

$$|\langle \mathbf{k} | U | \mathbf{k}' \rangle|^2 = \frac{1}{L} |U(\mathbf{q})|^2 a(\mathbf{q}), \quad (9.28)$$

where

$$a(\mathbf{q}) = \frac{1}{L} \left\langle \left| \sum_i e^{i\mathbf{q} \cdot \mathbf{r}_i} \right|^2 \right\rangle \quad (9.29)$$

is the structure factor (or interference function) and can be directly estimated from X-ray or neutron scattering data. L is the number of ions. Substituting (9.24), (9.25), and (9.28) into (9.23) yields

$$\rho_1 = \frac{12\pi}{\hbar e^2} \frac{1}{v_F^2} \frac{1}{L} \int_0^1 |U(q)|^2 a(q) \eta^3 d\eta. \quad (9.30)$$

This shows that the electrical resistivity of liquid metals and of their analogs is determined by the square of the modulus of the pseudopotential formfactor and by the structure factor of the media (this is, of course, for simple metals, to which pseudopotential

theory is applicable). Equation (9.30) is helpful both in evaluating electrical resistivity and in determining its behavior under various conditions. For example, the temperature coefficient of resistivity for constant volume [525] is

$$\frac{1}{\rho_1} \left(\frac{\partial \rho_1}{\partial T} \right)_V = \frac{1}{\rho_1} \left(\frac{\partial \rho_1}{\partial T} \right)_p - \frac{\alpha_p V}{\rho_1} \left(\frac{\partial \rho_1}{\partial V} \right)_T, \quad (9.34)$$

where α_p is the thermal expansion coefficient, and it can be seen that a qualitative argument about the upper integration limit and

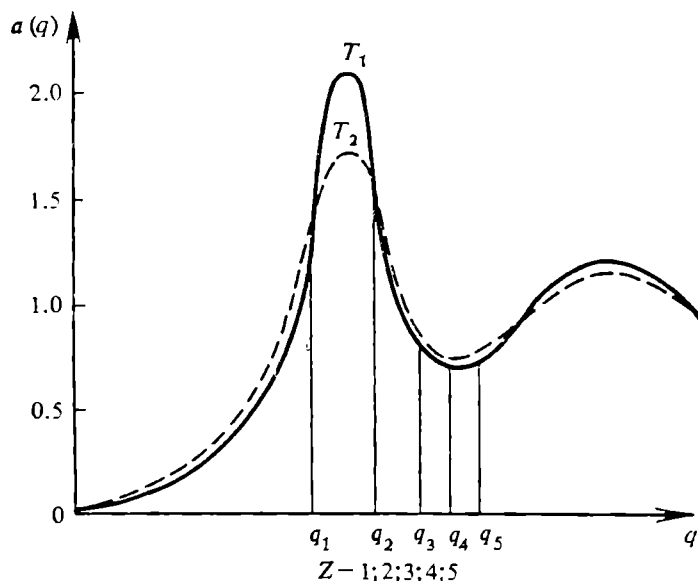


Fig. 9.1. Structure factors of liquid metals for different temperatures ($T_1 < T_2$) as functions of the scattering vector q ($q_i = 2k_F$ for a metal of valency Z_i). From Khar'kov *et al.* [538].

the integrand in (9.30) might be sufficient for predicting the sign of the effect. Figure 9.1, which is taken from [538], demonstrates this for liquid metals of various valencies. The figure shows the approximate behavior of the structure factor for two temperatures ($T_1 < T_2$) and of the product $|U(q)|^2 a(q)$ for T_1 . The position of the upper integration limit in (9.30) ($q = 2k_F$) is also shown. It will be seen that for monovalent metals the upper limit is on the left wing of the structural maximum, while for bivalent and polyvalent metals it is on the right.

The q -dependence of the product $|U(q)|^2 a(q)$ turns out to be nonmonotonic and can be conveniently described in terms of the parameter q_0 , the value of q which makes $|U(q)|^2$ zero (see also [73]). The region $q < q_0$ corresponds to what is known as plasma electrical resistivity ρ_l^{pl} , for which scattering by relatively large

density nonuniformities is relevant; the region $q > q_0$ corresponds to the structural resistance ρ_1^{str} . The total resistivity is the sum of both.

Under the simplifying assumptions

$$U(q) = W(q), \quad \langle |W(q)|^2 \rangle \rightarrow \frac{1}{2} |W(0)|^2 = \frac{1}{2} \left(\frac{2}{3} E_F \right)^2, \\ a(q) \simeq a(0), \quad q_0/2k_F \simeq 0.8 = \eta_0,$$

we obtain

$$\rho_1^{\text{pl}} \simeq \frac{12\pi}{\hbar e^2} \frac{1}{v_F^2} \frac{1}{L} \int_0^{\eta_0} \frac{1}{2} \left(\frac{2}{3} E_F \right)^2 a(0) \eta^3 d\eta \\ = 0.3 \frac{\pi}{\hbar e^2} \frac{a(0)}{L} \frac{E_F^2}{v_F^2}. \quad (9.32)$$

Since according to Ziman [167],

$$a(0) = k_B T / (M s^2), \quad (9.33)$$

where M is the ionic mass and s the velocity of sound, it follows that ρ_1^{pl} increases linearly with T and is inversely proportional to the velocity of sound (which is in turn temperature dependent). This behavior is characteristic of monovalent liquid metals, in which ρ_1^{pl} is the main contribution to the electrical resistivity.

Turning to structural resistivity, we may write

$$\rho_1^{\text{str}} = \frac{12\pi}{\hbar e^2} \frac{1}{v_F^2} \frac{1}{L} \int_{\eta_0}^1 |W(q)|^2 a(q) \eta^3 d\eta. \quad (9.34)$$

It can be seen from this that the temperature dependence of ρ_1^{str} (and hence ρ_1^{total}) for constant volume comes through $a(q)$. A general argument about the structure of disordered materials suggests that disorder should increase with temperature. This means that the maxima of the structure factor will be smeared out so that $a(q)$ will decrease in the peak and increase between the maxima. Simple qualitative considerations like this (see Fig. 9.1) allow us to predict that the derivative $(\partial/\partial T)\rho^{\text{str}}$ must be negative or slightly positive for bivalent metals and very close to zero for polyvalent metals.

We will now extend the above argument to other transport properties and to the transition metals, postponing for a while a quantitative discussion of the structure factor.

We first consider thermo-emf. If we assume that the Fermi surface of conduction electrons is spherical, it is well known [538, 524] that the thermo-emf Q and electrical resistivity are related by

$$Q = - \frac{\pi^2 k_B T}{3e E_F} \left[\frac{\partial \ln \rho(E)}{\partial \ln E} \right]_{E=E_F}. \quad (9.35)$$

This expression holds for any metal or alloy, whether crystalline or not. It can be shown that the dimensionless parameter

$$\xi = - \left[\frac{\partial \ln \rho(E)}{\partial \ln E} \right]_{E=E_F} \quad (9.36)$$

determines the dependence of thermo-emf on microscopic characteristics of the metal so that it is worthwhile investigating this parameter within the nearly-free-electron model. After introducing the cross section for the scattering of an electron by an ion,

$$\sigma_i = \frac{m^2 v^2}{\pi \hbar^4 k_F^4} \int_0^1 a(q) |W(q)|^2 \eta^3 d\eta \quad (9.37)$$

we write

$$\rho = \frac{m v_F}{e^2 Z} \sigma_i. \quad (9.38)$$

Since $v_F = (\hbar k_F)/m = (\hbar/m) \sqrt{(3\pi^2 Z N)/V}$, we have

$$v_F/Z \propto 1/(V E_F) \quad (9.39)$$

giving

$$\rho(E) = A_0 \frac{\sigma(E)}{E}. \quad (9.40)$$

Thus

$$\xi = \left[\frac{\partial \ln E}{\partial \ln E} - \frac{\partial \ln \sigma_i(E)}{\partial \ln E} \right]_{E=E_F} = 1 - r, \quad (9.41)$$

where

$$r = \left[\frac{\partial \ln \sigma_i(E)}{\partial \ln E} \right]_{E=E_F}. \quad (9.42)$$

If σ_i is independent of energy, then $r = 0$ and $\xi = 1$, so that $Q = \pi^2 k_B T / 3e E_F$, and the sign of the thermoelectric effect is determined by the sign of the electric charge, as it normally should in a metal. For $r = 1$ we have $\xi = 0$ and no thermo-emf. For $r > 1$, the thermo-emf has an unusual sign. Ziman and his co-workers [525] expressed r in terms of the structure factor and pseudopotential parameters. According to (9.37), $\sigma_i = \sigma_i(k_F)$, and for the free-electron model we have

$$r = -2 + 2g_0 \text{ and } \xi = 3 - 2g_0, \quad (9.43)$$

where

$$g_0 = \frac{a(2k_F) |W(2k_F)|^2}{\langle a(q) |W(q)|^2 \rangle} \quad (9.44)$$

and

$$\langle a(q) |W(q)|^2 \rangle = \frac{1}{4k_F^4} \int_0^1 a(q) |W(q)|^2 \eta^3 d\eta. \quad (9.45)$$

It can easily be seen that g_0 is non-negative because so are all the quantities which make it up. This parameter is only zero if $W(2k_F) = 0$, i.e., $2k_F = q_0$. For local pseudopotentials $q_0 \simeq 0.8 \times 2k_F$ and so usually $g_0 > 0$ and $\xi < 3$ ($\xi = 3$ when $W(2k_F) = 0$). If $a(2k_F) | W(2k_F) |^2 = \langle a | W |^2 \rangle$, then $g_0 > 1.5$, $r_0 = 0$, $\xi = 1$, and the thermo-emf has a normal sign, as already mentioned. The similar situation occurs if $0 < g_0 < 1.5$. For $g_0 > 1.5$ the quantity ξ is negative, making the sign of thermo-emf unusual. This is possible if the product $a(2k_F) | W(2k_F) |^2$ becomes very large near $q = 2k_F$, which is usually the case when $2k_F$ is close to a maximum of the structure factor $a(q)$. The quantity g_0 is at its largest if a maximum of $|W(q)|^2$ also corresponds to the condition $q \simeq 2k_F$. As the product $a(q) | W(q) |^2$ also enters the expression for electrical resistivity, the resistivity should be high if the thermo-emf is negative. A qualitative argument has thus led us to an important relation between thermo-emf and resistivity.

The transition metals may be treated in a similar fashion, although instead of pseudopotential formfactors, the t -matrix formfactors of muffin-tin potentials are better [528] (see also Sec. 2.5). We have

$$Q(\vartheta) \simeq |\langle \mathbf{k} | t | \mathbf{k}' \rangle|^2 N(E_F), \quad (9.46)$$

where the t operator is defined by

$$t\varphi_{\mathbf{k}} = U\psi_{\mathbf{k}}, \quad (9.47)$$

where $\varphi_{\mathbf{k}}$ and $\psi_{\mathbf{k}}$ are the unperturbed and perturbed functions, respectively. The scattering amplitude is expressed in terms of the formfactor,

$$t(\mathbf{k}, \mathbf{k}') = -\frac{\Omega}{4\pi} \langle \mathbf{k} | t | \mathbf{k}' \rangle, \quad (9.48)$$

and the formfactors $t(\mathbf{k}, \mathbf{k}')$ form the t -matrix. The t operator obeys the integral equation

$$t\varphi_{\mathbf{k}} = U(\varphi_{\mathbf{k}} + G_0 U\psi_{\mathbf{k}}) = U\varphi_{\mathbf{k}} + UG_0 t\varphi_{\mathbf{k}}, \quad (9.47a)$$

where G_0 is the free-particle propagator and U is the true scattering potential for the material under study.

The single-scatterer t -matrix formfactors for energy-conserving transitions are [528]

$$t(\mathbf{k}, \mathbf{k}') = -\frac{2\pi\hbar^3}{m(2mE_F)^{1/2}} \left(\frac{1}{\Omega_0} \right) \sum_l (2l+1) \sin \eta_l(E_F) \\ \times \exp[i\eta_l(E_F)] P_l(\cos \vartheta), \quad (9.49)$$

where l is the orbital quantum number, η_l is the phase shift as derived from the Fermi energy, and P_l , a Legendre polynomial. Substi-

tuting this into (9.23) and changing from σ to ρ we find

$$\rho = \frac{3\pi\Omega_0}{e^2\hbar^2v_F^2} \int_0^1 4\eta^3 a(\mathbf{q}) |t(\mathbf{k}, \mathbf{k}')|^2 d\eta. \quad (9.50)$$

A technique for calculating resistivity by (9.50) is outlined by Dreirach *et al.* [539]. Their results show that the d -components dominate in the transition metals. For nickel, for example, the phase shifts η_0 , η_1 and η_2 are -0.25 , 0.02 , and 2.892 , respectively; for Fe, the figures are -0.479 , -0.071 , and 2.520 . We may then write to a good approximation [528]

$$\rho \simeq \frac{30\pi^3\hbar^3}{me^2\Omega_0k_F^2E_F} \sin^2 \eta_2(E_F) a(2k_F). \quad (9.51)$$

The energy dependence of η_2 is resonant in nature, and if E_0 and Γ denote the position and width of the resonance respectively, we have

$$\tan \eta_2(E) = \Gamma/(E_0 - E). \quad (9.52)$$

In this approximation

$$\rho = \frac{30\pi^3\hbar^3}{me^2\Omega_0k_F^2E_F} a(2k_F) \frac{\Gamma^2}{\Gamma^2 + (E_0 - E_F)^2}. \quad (9.53)$$

The resistivity and thermo-emf calculated by these formulae strongly depend on the relative positions of E_F and E_0 , and if the calculation parameters are appropriately chosen, a reasonably good fit to the experimental data is obtained. For nickel, for example, the experimental values for ρ and Q are $85 \mu\text{ohm}\cdot\text{cm}$ and $-36 \mu\text{V}/\text{grad}$, respectively. The computed values are 227 and -38 for $k_F = 0.851$ a.u., while they are 106 and -33 for $k_F = 0.930$.

Adjustable parameters are also used to calculate the transport properties of nontransition metals. For example, the resistivity of Na computed from an adjusted Ashcroft potential [538] was found to be $9 \mu\text{ohm}\cdot\text{cm}$, which is rather close to the experimental value of $9.6 \mu\text{ohm}\cdot\text{cm}$. Results for the other metals are reviewed in [538, 165, 541]. It should be noted, however, that the good agreement with experiment is only evidence for the promise of pseudopotential theory rather than an indication of its completeness.

We have already mentioned that reliable information about the structure factors is crucial for fitting pseudopotential calculations to experimental data, so the temperature and composition dependence of the structure factor are definitely worth discussing for disordered materials.

The relationship between electrical resistivity and the structure of disordered binary alloys is discussed in much detail by Bhatia and Thornton [542] who obtained the important result that the alloy structure factor may be represented as a sum of two temperature-

dependent terms. The first term is associated with topological short-range order and describes the arrangement of the atoms of an arbitrary species in noncrystalline materials, which may in principle contain any number of components. The second term depends on the compositional short-range order and describes the arrangement of the different species of atoms against the background of the overall arrangement of atoms.

We will first consider the temperature dependence of the structure factor using, as Bhatia and Thornton [542] did, an analogy with neutron and X-ray scattering and employing van Hove's idea [543] of a dynamic structure factor. The structure factor may be written, in general, as the sum

$$S(\mathbf{q}) = S_0(\mathbf{q}) + S_1(\mathbf{q}) + S_2(\mathbf{q}) + \dots, \quad (9.54)$$

where the subscript indicates the number of phonons involved in the scattering process. When there are none, the scattering is elastic and

$$S_0(\mathbf{q}) = a(\mathbf{q}) e^{-2M(\mathbf{q})}, \quad (9.55)$$

where

$$a(\mathbf{q}) = \frac{1}{L} \sum_j \sum_{j'} e^{-i\mathbf{q}(\mathbf{r}_j - \mathbf{r}_{j'})} \quad (9.56)$$

is the interferential function, which is the scattering intensity summed over the average positions of ions; the Debye-Waller temperature factor $e^{-2M(\mathbf{q})}$ describes the reducing effect of thermal motion on the main maximum. The higher terms in (9.54) correspond to one-, two- or multiphonon thermal diffusion scattering. In the simplest case of independent atomic displacements, thermal diffusion scattering is proportional to $(1 - e^{-2M})$.

The first few terms of (9.54) were evaluated in [534, 542, 544] in the Debye approximation. The dynamic structure factor $S(\mathbf{q}, \omega)$ may be represented as

$$S(\mathbf{q}, \omega) = S_0(\mathbf{q}, \omega) + S_1(\mathbf{q}, \omega) + \dots, \quad (9.57)$$

where

$$S_0(\mathbf{q}, \omega) = a(\mathbf{q}) e^{-2M(\mathbf{q})} \delta(\omega), \quad (9.58)$$

$$S_1(\mathbf{q}, \omega) = e^{-2M(\mathbf{q})} \frac{n(-\omega)}{-\omega} \sum_{\varphi} \frac{\hbar q^2}{2M} [a(\mathbf{q} + \varphi) \delta(\omega + \omega_{\varphi}) + a(\mathbf{q} - \varphi) \delta(\omega - \omega_{\varphi})], \quad (9.59)$$

$$a(\mathbf{q} + \varphi) = \frac{1}{L} \sum_j \sum_{j'} \exp[i(\mathbf{q} + \varphi)(\mathbf{r}_j - \mathbf{r}_{j'})], \quad \varphi = (\varphi, i) \quad (9.56a)$$

i and φ are the polarization index and the wave vector of an elastic wave; $x = \hbar\omega/(k_{\mathbf{B}}T)$; and $n(\omega) = (e^x - 1)^{-1}$.

The structure factor of X-ray and neutron scattering,

$$S^x(\mathbf{q}) = \int_{-\infty}^{\infty} S(\mathbf{q}, \omega) d\omega \quad (9.60)$$

and the structure factor of electrical resistance theory,

$$S^p(\mathbf{q}) = \int_{-\infty}^{\infty} S(\mathbf{q}, \omega) x n(x) d\omega \quad (9.61)$$

are clearly the averages over the frequencies of the elastic waves [544]. In the Debye approximation, it can be easily seen that $S_0^x(\mathbf{q}) = S_0^p(\mathbf{q})$ because in this case $\omega \simeq 0$ according to (9.58), and hence we have $\lim_{x \rightarrow 0} x n(x) = x(e^x - 1)^{-1} \simeq 1$. In the same approximation,

$$\begin{aligned} S_1^x(\mathbf{q}) &= \frac{\hbar q^2}{2M} \sum_{\varphi} \frac{1}{\omega_{\varphi}} [a(\mathbf{q} - \varphi)(n_{\varphi} + 1) + a(\mathbf{q} + \varphi)n_{\varphi}] \\ &= \alpha(\mathbf{q}) \int_0^1 \frac{\varphi}{\varphi_D} d\left(\frac{\varphi}{\varphi_D}\right) \left[n(x) + \frac{1}{2}\right] \int \frac{d\Omega}{4\pi} a(\mathbf{q} + \varphi), \quad (9.62) \end{aligned}$$

$$\begin{aligned} S_1^p(\mathbf{q}) &= -\frac{\hbar q^2}{2M} \sum_{\varphi} \frac{\hbar}{k_B T} [a(\mathbf{q} + \varphi) + a(\mathbf{q} - \varphi)] n(x) n(-x) \\ &= \alpha(\mathbf{q}) (\theta/T) \int_0^1 \left(\frac{\varphi}{\varphi_D}\right)^2 d\left(\frac{\varphi}{\varphi_D}\right) n(x) n(-x) \int \frac{d\Omega}{4\pi} a(\mathbf{q} + \varphi), \quad (9.63) \end{aligned}$$

where $x = \hbar \omega_{\varphi}/k_B T = (\hbar \omega_{\varphi}/k_B T)/(\varphi/\varphi_D) = (\theta/T)/(\varphi/\varphi_D)$; φ_D is the wave vector of the elastic wave which corresponds to the radius of the Debye sphere; θ is the Debye temperature; and $\alpha(\mathbf{q}) = 3(\hbar q)^2 (\exp(-2M(\mathbf{q})/Mk_B\theta))$. When $\alpha(\mathbf{q})$ and θ are specified in $S_1^x(\mathbf{q})$ and $S_1^p(\mathbf{q})$, the static structure factors can be evaluated to a required accuracy.

In the high-temperature limit

$$\begin{aligned} S_1^p(\mathbf{q}) &\simeq S_1^x(\mathbf{q}) \simeq \alpha(\mathbf{q}) \frac{T}{\theta} \int_0^1 d\left(\frac{\varphi}{\varphi_D}\right) \int \frac{d\Omega}{4\pi} a(\mathbf{q} + \varphi) \\ &= \alpha(\mathbf{q}) \frac{T}{\theta} A^x(\mathbf{q}), \quad (9.64) \end{aligned}$$

where the second integral averages $a(\mathbf{q})$ over the Debye sphere, which is circumscribed about the vector \mathbf{q} . At high temperatures $A^x(\mathbf{q}) = A^p(\mathbf{q}) \simeq 1$ for any \mathbf{q} . The low-temperature expressions for $A(\mathbf{q})$ [544] are too cumbersome to reproduce. It can be seen from the

expressions for $S_0(\mathbf{q})$ and $S_1(\mathbf{q})$ that $S_0(\mathbf{q})$ decreases with T in proportion to the Debye-Waller factor $e^{-2M(q)}$, whereas $S_1(\mathbf{q})$ increases as the product of the temperature and $e^{-2M(q)}$.

The (multiphonon) static structure factor for electrical resistivity is [545]

$$S^0(\mathbf{q}) = S_0^0(\mathbf{q}) + S_1^0(\mathbf{q}) + \{1 - [1 + 2M(q)] e^{-2M(q)}\}, \quad (9.65)$$

where $S_0^0(\mathbf{q})$ and $S_1^0(\mathbf{q})$ are given above and the last term does not exceed $2M^2(q)$ unless the temperature is very high. For $T < \theta$ we have to a good approximation

$$S^0(\mathbf{q}) = S_0^0(\mathbf{q}) + S_1^0(\mathbf{q}). \quad (9.66)$$

In the low-temperature limit $S_1^0(\mathbf{q}) \propto (T/\theta)^2$.

At arbitrary temperatures, the temperature behavior of the static structure factors is discussed [545] in terms of averaged structure factors

$$A^x(\mathbf{q}) = \int_0^{\varphi_D} \varphi \, d\varphi \left[n(x) + \frac{1}{2} \right] \int \frac{d\Omega}{4\pi} a(|\mathbf{q} + \boldsymbol{\varphi}|) \\ \times \left\{ \int_0^{\varphi_D} \varphi \, d\varphi \left[n(x) + \frac{1}{2} \right] \right\}^{-1} \quad (9.67)$$

and

$$A^0(\mathbf{q}) = \int_0^{\varphi_D} d\varphi \, \varphi^2 n(x) [n(x) + 1] \int \frac{d\Omega}{4\pi} a(|\mathbf{q} + \boldsymbol{\varphi}|) \\ \times \left\{ \int_0^{\varphi_D} d\varphi \, \varphi^2 n(x) [n(x) + 1] \right\}^{-1}. \quad (9.68)$$

If multi-phonon effects are ignored, the static structure factors are

$$S^x(q) = a(q) e^{-2M(q)} + 2M(q) A^x(q) \\ \simeq a(q) e^{-2M(q)} + A^x(q) \{1 - e^{-2M(q)}\} \quad (9.69)$$

and

$$S^0(q) = a(q) e^{-2M(q)} + \alpha(q) \left(\frac{T}{\theta} \right)^2 A^0(q) \gamma_2 \left(\frac{\theta}{T} \right), \quad (9.70)$$

where

$$\gamma_2 \left(\frac{\theta}{T} \right) = \int_0^{\frac{\theta}{T}} dx \, x^2 n(x) [n(x) + 1] \\ = \left(\frac{\theta}{T} \right)^3 \int_0^1 d \left(\frac{\varphi}{\varphi_D} \right) \left(\frac{\varphi}{\varphi_D} \right)^2 n(x) [n(x) + 1] \quad (9.71)$$

and

$$2M(q) = 3 [(\hbar q)^2 / (M k_B \theta)] \left(\frac{T}{\theta} \right)^2 \int_0^{\frac{\theta}{T}} x \left[n(x) + \frac{1}{2} \right] dx. \quad (9.72)$$

As the integrals $\mathcal{J}_2(\theta/T)$ and $M(q)$ are well known in the Debye approximation, the quantities $S_0(q)$, $S_1^x(q)$, and $S_1^p(q)$ may be evaluated as functions of the temperature and scattering vector, and the temperature dependence of resistivity will therefore be determined for various q -to- $2k_F$ ratios. A detailed calculation of this kind was performed by Meisel and Cote [545] who showed that the $A^x(q)$ and $A^p(q)$ curves are Gaussian in nature, both having a maximum at a certain value of $q\sigma$. As the temperature increases, the maxima get closer together and are virtually indistinguishable at about $T \simeq \theta$. Meisel and Cote also calculated the $S^p(T)/S^p(\theta)$ ratio for various $q\sigma$ and showed that the temperature behavior of the ratio varies substantially depending on whether the $q\sigma$ values are near the maximum or far from it. In the former case the ratio varies as T^2 at low temperatures, passes through a maximum at $T \simeq (0.3-0.4)\theta$ and then decreases. In the latter case there is no decrease with increasing temperature. The interpretation of the negative temperature coefficients in amorphous, liquid, and disordered crystalline alloys is undoubtedly an important feature of the diffraction model. Note that while the model is particularly well suited for amorphous metals, other methods may be applied to liquid metals [545] or crystalline disordered alloys. It has been shown, for example, [546] that when heat-treated, a crystalline disordered alloy may become less resistive due to the temperature dependence of the parameters of compositional short-range order.

The pseudopotential theory of resistivity of liquid metals was extended by Faber and Ziman [526] to include alloys of the nontransition metals. For a binary alloy of components α and β with atomic concentrations c_α , c_β and molar volumes V_α , V_β , they found

$$\rho_1 = \frac{12\pi}{\hbar e^2 v_F^2 V} \int_0^1 \overline{|W(q)|^2} \eta^3 d\eta, \quad (9.73)$$

where V is the averaged molar volume, and

$$|W(q)|^2 = N \left\{ \overline{U^2(q)} - \overline{U(q)}^2 \right\} + \sum_{\alpha=1}^2 \sum_{\beta=1}^2 c_\alpha c_\beta U_\alpha(q) U_\beta(q) a_{\alpha\beta}, \quad (9.74)$$

where $W(q)$ is the matrix element of the alloy pseudopotential,

$$U_i(q) = \frac{V_i}{N} W_i(q), \quad (i=1, 2),$$

N is Avogadro's number; $W_\alpha(q)$ and $W_\beta(q)$ the formfactors of the α and β ionic pseudopotentials, and $a_{\alpha\beta}$ the partial structure factor for electron-wave interference from an atomic pair $\alpha\beta$. It is assumed above that the arrangement of unlike atoms is entirely determined by their separation and is independent of other properties of the elements. In this approximation,

$$\overline{U^2(q)} = c_1 U_1^2(q) + c_2 U_2^2(q), \quad (9.75)$$

$$\overline{U(q)} = c_1 U_1(q) + c_2 U_2(q), \quad (9.76)$$

$$\overline{U(q)^2} = c_1^2 U_1^2(q) + 2c_1 c_2 U_1(q) U_2(q) + c_2^2 U_2^2(q). \quad (9.77)$$

By substituting (9.75) and (9.77) into (9.74) we obtain

$$\rho = \frac{mv_F}{e^2 Z} [c_1 \sigma_1 + c_2 \sigma_2 + c_1 c_2 (\sigma_1^0 - 2\sigma_{12}^0 + \sigma_2^0 - \sigma_1 + 2\sigma_{12} - \sigma_2)], \quad (9.78)$$

where $Z = c_1 Z_1 + c_2 Z_2$,

$$\sigma_{ij} = \frac{4m^2}{\pi \hbar^2} \int_0^1 a_{ij}(q) U_i(q) U_j(q) \eta^3 d\eta, \quad (9.79)$$

$$\sigma_{ij}^0 = \frac{4m^2}{\pi \hbar^4} \int_0^1 U_i(q) U_j(q) \eta^3 d\eta, \quad (9.80)$$

and

$$\sigma_{11} = \sigma_1, \quad \sigma_{22} = \sigma_2, \quad \sigma_{11}^0 = \sigma_1^0, \quad \sigma_{22}^0 = \sigma_2^0.$$

Drawing an analogy with solid solutions, Faber and Ziman introduced the idea of a perfect liquid alloy defined by

$$a_{11} = a_{22} = a_{33} = a, \quad V_1 = V_2. \quad (9.81)$$

If we define

$$a_{11} = \frac{\sigma_1}{\sigma_1^0}, \quad \bar{a}_{12} = \frac{\sigma_{12}}{\sigma_{12}^0}, \quad \bar{a}_{22} = \frac{\sigma_2}{\sigma_2^0}, \quad \bar{a}_{11} = \bar{a}_{12} = \bar{a}_{22} = a, \quad (9.82)$$

the resistivity of such an alloy is

$$\rho = \frac{mv_F}{e^2 Z} \left\{ c_1 \sigma_1 + c_2 \sigma_2 + c_1 c_2 (1 - a) \frac{4m^2}{\pi \hbar^4} \int_0^1 [U_1(q) - U_2(q)]^2 \eta^3 d\eta \right\}, \quad (9.83)$$

which may be rewritten as

$$\rho = \rho' + \rho'' \quad (9.84)$$

with

$$\rho' = \frac{mv_F}{e^2} \frac{c_1 \sigma_1 + c_2 \sigma_2}{c_1 Z_1 + c_2 Z_2}, \quad (9.85)$$

and

$$\rho'' = \frac{mv_F c_1 c_2}{e^2 (c_1 Z_1 + c_2 Z_2)} \cdot \frac{4m^2}{\pi \hbar^4} (1-a) \int_0^1 [U_1(q) - U_2(q)]^2 \eta^3 d\eta. \quad (9.86)$$

In polyvalent metals, Faber and Ziman argue that a is close to unity, giving

$$\rho \simeq \rho'. \quad (9.87)$$

For the transition metals, it has been suggested [528] that better results for the resistivity of noncrystalline alloys or disordered crystalline alloys will be obtained by replacing $|W(q)|^2$ by an averaged T -matrix element, for example, in the form

$$\begin{aligned} \langle T_{\text{all}} \rangle^2 = & c_\alpha |t_\alpha|^2 [1 - c_\alpha + c_\alpha a_{\alpha\alpha}(q)] + c_\beta |t_\beta|^2 [1 - c_\beta + c_\beta a_{\beta\beta}(q)] \\ & + c_\alpha c_\beta (t_\alpha^* t_\beta + t_\alpha t_\beta^*) [a_{\beta\beta}(q) - 1], \end{aligned} \quad (9.88)$$

where t_α is the t matrix of the α species.

There is strong evidence that the arrangement of atoms of different kinds is not random both in crystalline [412] and noncrystalline [535, 536, 547, 548] alloys, evidently due to differences in interatomic interactions even between atoms of equal valencies. This led Bhatia and Thornton [542] to introduce new structure factors different from $a_{\alpha\beta}$ and similar to the $|S(\mathbf{q})|^2$ and $|C(\mathbf{q})|^2$ functions we defined in Chapter 6. As in Chapter 6, $|S(\mathbf{q})|^2$ represents the structure of the "average" crystal (i.e., periodic density fluctuations) and $|C(\mathbf{q})|^2$ describes the density fluctuations caused by fluctuations in composition, while the interferential term $S(\mathbf{q})C(\mathbf{q})$ vanishes in a periodic crystal (see Sec. 6.2). The functions introduced by Bhatia and Thornton for a noncrystalline medium are $S_{NN}(q)$, $S_{CC}(q)$, and $S_{NC}(q)$. The first describes the arrangement of sites in a discontinuous network as a whole, the second describes the arrangement of atoms of different species on the sites of the network, and the third is the interferential term. Clearly, $S_{NN}(q)$ corresponds to topological short-range order and $S_{CC}(q)$ to compositional short-range order, and we refer the reader to [535, 536] for the explicit form of these functions. It is worth noting that partial factors like those discussed here are convenient for the calculation of the total energy of noncrystalline alloys [550]. Here we limit ourselves to quoting some of the expressions derived in [539] for resistivity.

It is shown in [549] that if scattering is weak in an alloy the transition of an electron from a state \mathbf{k}' to a state \mathbf{k} may be characterized by the function

$$\Gamma(\mathbf{q}, \omega) = \frac{1}{2\pi L} \int e^{-i\omega t} dt \langle A^*(\mathbf{q}, 0) A(\mathbf{q}, t) \rangle, \quad (9.89)$$

where

$$A(\mathbf{q}, t) = \sum_j W_j(\mathbf{q}) \exp[i\mathbf{q}(\mathbf{R}_j(t))], \quad (9.90)$$

$\hbar\omega = E_{\mathbf{k}} - E_{\mathbf{k}'}$, and $W_j(\mathbf{q})$ is the pseudopotential formfactor for the ion located at \mathbf{R}_j .

For a pure metal

$$\Gamma(\mathbf{q}, \omega) = |W(\mathbf{q})|^2 S(\mathbf{q}, \omega), \quad (9.91)$$

where $S(\mathbf{q}, \omega)$ is the dynamic structure factor of van Hove [543]. Electrical resistivity is given by

$$\rho = \frac{12\pi(m^*)^2}{\hbar^3 e^2 k_F^2} \frac{L}{V} \int_0^1 I_{av}(q) \eta^3 d\eta, \quad (9.92)$$

where $\beta = \hbar/K_B T$, and $I_{av}(q)$ is

$$I(\mathbf{q}) = \int_{-\infty}^{\infty} \frac{\beta\omega}{(e^{\beta\omega} - 1)} \Gamma(\mathbf{q}, \omega) d\omega \quad (9.93)$$

averaged over all directions except the one corresponding to Bragg scattering.

For a binary alloy, we have

$$\begin{aligned} \Gamma(\mathbf{q}, \omega) = & |\bar{W}|^2 S_{NN}(\mathbf{q}, \omega) + |W_1 - W_2|^2 S_{CC}(\mathbf{q}, \omega) \\ & + 2\bar{W}(W_1 - W_2) S_{NC}(\mathbf{q}, \omega) \end{aligned} \quad (9.94)$$

instead of (9.91). Here

$$\begin{aligned} S_{NN}(\mathbf{q}, \omega) &= \frac{1}{2\pi L} \int e^{-i\omega t} dt \langle N^*(\mathbf{q}, 0) N(\mathbf{q}, t) \rangle, \\ S_{CC}(\mathbf{q}, \omega) &= \frac{L}{2\pi} \int e^{-i\omega t} dt \langle C^*(\mathbf{q}, 0) C(\mathbf{q}, t) \rangle, \\ 2S_{NC}(\mathbf{q}, \omega) &= \frac{1}{2\pi} \int e^{-i\omega t} dt \langle N^*(\mathbf{q}, 0) C(\mathbf{q}, t) + C^*(\mathbf{q}, 0) N(\mathbf{q}, t) \rangle, \end{aligned} \quad (9.95)$$

where $N^*(\mathbf{q}, t)$ and $C^*(\mathbf{q}, t)$ are the Fourier transforms of density fluctuations and composition fluctuations, respectively. The functions $S_{NN}(\mathbf{q}, \omega)$, $S_{CC}(\mathbf{q}, \omega)$, and $S_{NC}(\mathbf{q}, \omega)$ are the dynamic structure factors of the alloy. The first corresponds to fluctuations of the average density as a whole, the second corresponds to the composition fluctuations, and the third function is the interference of the first two. Clearly $S_{NN}(\mathbf{q}, \omega)$ is an analog of the dynamic structure factor of a pure metal.

By writing

$$\begin{aligned} S_{NN}(\mathbf{q}) &= \int [\beta\omega/(\epsilon^{\beta\omega} - 1)] S_{NN}(\mathbf{q}, \omega) d\omega, \\ S_{CC}(\mathbf{q}) &= \int [\beta\omega/(\epsilon^{\beta\omega} - 1)] S_{CC}(\mathbf{q}, \omega) d\omega, \\ 2S_{NC}(\mathbf{q}) &= \int [\beta\omega/(\epsilon^{\beta\omega} - 1)] 2S_{NC}(\mathbf{q}, \omega) d\omega, \end{aligned} \quad (9.96)$$

we get

$$\mathcal{J}(\mathbf{q}) = |\bar{W}|^2 S_{NN}(\mathbf{q}) + |W_1 - W_2|^2 S_{CC}(\mathbf{q}) + 2\bar{W}(W_1 - W_2) S_{NC}(\mathbf{q}), \quad (9.97)$$

which is the differential intensity of scattering from a state \mathbf{k}' to a state $\mathbf{k} = \mathbf{k}' + \mathbf{q}$. At high temperatures $\hbar\omega/k_B T \ll 1$, so the factor $\beta\omega/(\epsilon^{\beta\omega} - 1)$ may be replaced by unity, giving

$$\begin{aligned} S_{NN}(\mathbf{q}) &= L^{-1} \langle N^*(\mathbf{q}) N(\mathbf{q}) \rangle, \\ S_{CC}(\mathbf{q}) &= L \langle C^*(\mathbf{q}) C(\mathbf{q}) \rangle, \\ S_{NC}(\mathbf{q}) &= \text{Re} \langle N^*(\mathbf{q}) C(\mathbf{q}) \rangle. \end{aligned} \quad (9.98)$$

The first of these expressions is the high-temperature structure factor for a pure metal or for an alloy; in the latter case $S_{NN}(\mathbf{q})$ is an average over all the species of an atom, viz.,

$$S_{NN}(\mathbf{q}) = \frac{1}{L} \left\langle \sum_m \sum_n e^{i\mathbf{q}(\mathbf{R}_m - \mathbf{R}_n)} \right\rangle - L\delta_{\mathbf{q},0}. \quad (9.99)$$

The other two expressions in (9.98) are only meaningful for alloys.

Bhatia and Thornton [542] also found that the structure factors we are discussing are related to the atom-atom structure factors

$$a_{\alpha\beta} = 1 + \frac{L}{V} \int_0^\infty [\rho_{\alpha\beta} - 1] \frac{\sin qr}{qr} 4\pi r^2 dr, \quad (9.100)$$

where $\rho_{\alpha\beta}(r)$ is the probability of finding an α ion within a unit volume already occupied by a β ion at a distance r from the origin. The probability is normalized to unity at large r . According to [542],

$$\begin{aligned} S_{NN}(q) &= c_1^2 a_{11} + c_2^2 a_{22} + 2c_1 c_2 a_{12}, \\ S_{NC}(q) &= c_1 c_2 [c_1 (a_{11} - a_{22}) - c_2 (a_{22} - a_{12})], \\ S_{CC}(q) &= c_1 c_2 [1 + c_1 c_2 (a_{11} + a_{22} - 2a_{12})] \end{aligned} \quad (9.101)$$

which shows that if the partial structure factors are equal, then

$$S_{NN}(q) = a(q), \quad S_{NC}(q) = 0, \quad \text{and} \quad S_{CC}(q) = c_1 c_2, \quad (9.102)$$

which corresponds to the perfect solution case. It was found that in both the Percus-Yevick and the hard-sphere models the function $S_{CC}(q)$ slightly oscillates about c_1c_2 , $S_{NC}(q)$ oscillates about zero, and $S_{NN}(q)$ is represented by a sequence of bell-shaped functions which get lower and wider with q . The "bells" are not entirely symmetric.

The structure factors like S_{NC} are related to the short-range order parameters of a noncrystalline alloy, which characterize the arrangement of (both like and unlike) atoms in the alloy. This can be seen from the Fourier transforms of the structure factors,

$$\begin{aligned} G_{NN}(r) &= \frac{2}{\pi} \int q [S_{NN}(q) - 1] \sin qr \, dq, \\ G_{NC}(r) &= \frac{2}{\pi} \int q S_{NC}(q) \sin qr \, dq, \\ G_{CC}(r) &= \frac{2}{\pi} \int q \{ [S_{CC}(q) - c_1c_2] / c_1c_2 \} \sin qr \, dq, \end{aligned} \quad (9.103)$$

which are in turn related to the correlation probability functions $g_{NN}(r)$, $g_{NC}(r)$, and $g_{CC}(r)$ for the density and composition fluctuations and to the densities $\rho_{NN}(r)$, $\rho_{NC}(r)$, and $\rho_{CC}(r)$ of these fluctuations. We have

$$\begin{aligned} G_{NN}(r) &= 4\pi r [\rho_{NN}(r) - \rho_0], \\ G_{NC}(r) &= 4\pi r \rho_{NC}(r), \\ G_{CC}(r) &= 4\pi r \rho_{CC}(r). \end{aligned} \quad (9.104)$$

The corresponding coordination numbers are obtained by integrating the fluctuation density functions $\rho_{NN}(r)$, $\rho_{NC}(r)$, and $\rho_{CC}(r)$ over the "bells", viz.,

$$\begin{aligned} z_{NN} &= \int_0^{r_{\max}} 4\pi r^2 \rho_{NN}(r) \, dr, \\ z_{NC} &= \int_0^{r_{\max}} 4\pi r^2 \rho_{NC}(r) \, dr, \\ z_{CC} &= \int_0^{r_{\max}} 4\pi r^2 \rho_{CC}(r) \, dr. \end{aligned} \quad (9.105)$$

Clearly,

$$\rho_i(r) = \sum_j \rho_{ij}(r) \quad (9.106)$$

is the total number of (any kind of) atoms at a distance r from an i th atom. The corresponding coordination numbers are

$$\begin{aligned} z_1 &= z_{NN} + z_{NC}/c_1 = z_{11} + z_{12}, \\ z_2 &= z_{NN} - z_{NC}/c_2 = z_{21} + z_{22}, \end{aligned} \quad (9.107)$$

giving, by (9.104),

$$z_{NN} = c_1 z_1 + c_2 z_2, \quad (9.108)$$

$$z_{NC} = c_1 c_2 (z_1 - z_2), \quad (9.109)$$

$$z_{CC} = c_2 z_1 + c_1 z_2 - \frac{z_{12}}{c_2}, \quad (9.110)$$

where z_{NN} and z_{CC} are the coordination numbers for topological and compositional short-range order respectively. Equation (9.110) may be rewritten as

$$z_{CC} = (c_2 z_1 + c_1 z_2) \left\{ 1 - \frac{z_{12}}{c_2 (c_2 z_1 + c_1 z_2)} \right\} = z_w \alpha_w \quad (9.111)$$

with

$$z_w = c_2 z_1 + c_1 z_2 = z_{NN} + \frac{c_2 - c_1}{c_1 c_2} z_{NC} \quad (9.112)$$

and

$$\alpha_w = 1 - \frac{z_{12}}{z_w c_2}, \quad (9.113)$$

the latter expression also gives the (compositional) short-range order parameter in disordered crystalline alloys [411, 412].

If $z_{NC} = 0$ or $c_1 = c_2$, then $z_w = z_{NN}$ and

$$\alpha_w = 1 - \frac{z_{12}}{c_2 z_{NN}} = \frac{1}{z_{NN}} \int_0^{r_{\text{min}}} 4\pi r^2 \rho_{CC}(r) dr. \quad (9.114)$$

Katsnelson and Safronova [536] used the same approximation to derive a similar expression for binary noncrystalline alloys by considering correlations in arrangements of unlike atoms. The same arguments were used by Katsnelson *et al.* [550] in pseudopotential calculations of the energy of such alloys and in finding the contributions to the energy from topological and compositional short-range order.

We may thus conclude that the electrical resistivity and other transport properties of noncrystalline alloys is determined by the temperature, composition, and interatomic interactions. If there is no dominant component in an alloy, it is sensible to use an average structure factor like S_{NN} as a first approximation and then to correct the result using S_{CC} or S_{NC} -type terms. Although the second step in this program is rarely possible because of the lack of relevant experimental data, encouraging results have been obtained. The

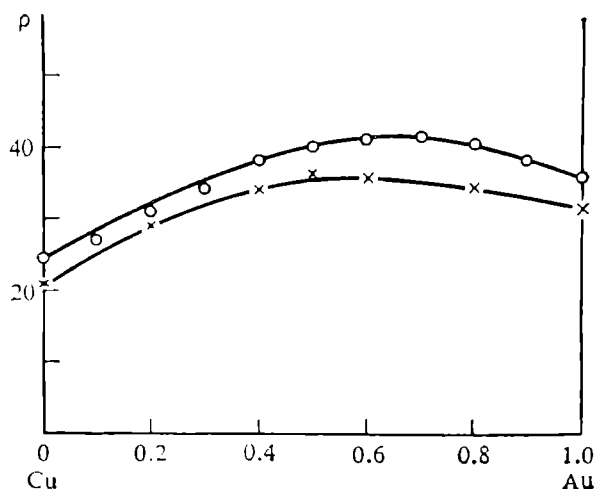


Fig. 9.2. Electrical resistivity of Cu-Au alloys as a function of concentration. Empty circles—theory, crosses—experiment. From Dreirach *et al.* [539].

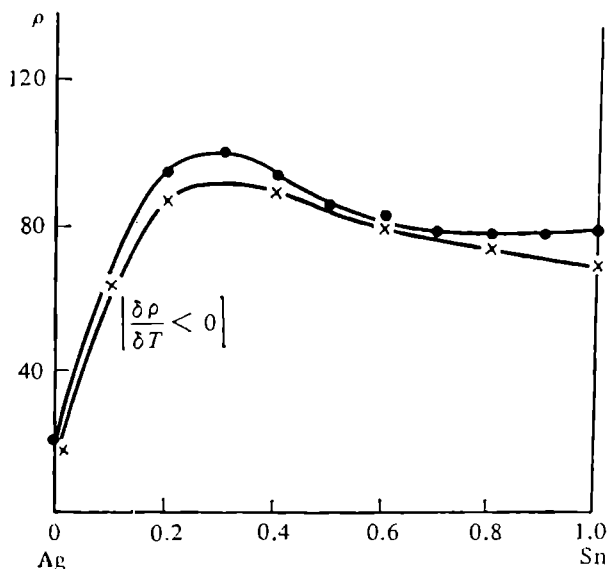


Fig. 9.3. Electrical resistivity of Ag-Sn alloys as a function of concentration. Empty circles—theory, crosses—experiment. From Dreirach *et al.* [539].

concentration dependence of resistivity has been explained for alloys containing elements from different regions of the periodic table. The concentration dependence of $\partial\rho/\partial T$ has been interpreted. A relationship had been found between electrical resistivity and the sign of its temperature coefficient, and finally, the relationship between thermo-emf and anomalies in $\partial\rho/\partial T$ has been explained.

Dreirach *et al.* [539] calculated the electrical resistivity for the liquid alloys Cu-Au, Cu-Sn, Cu-Ge, Ag-Sn, Au-Ni, Ni-Sn, Fe-Ge

and some others. The most interesting data were obtained for noble metal-noble metal alloys (Cu-Au, for example) and for alloys of noble (or transition) metals and polyvalent metals (Cu-Sn, Ag-Sn, Cu-Ge, Fe-Ge). For the first type of alloy no region of negative $\partial\rho/\partial T$ was found (Fig. 9.2), implying that $2k_F$ lies in the region $q < q_{\max}$, q_{\max} being the position of the main structure factor. The computed concentration dependence of resistivity agreed with the experimental data. For the second alloy type (Fig. 9.3), negative $\partial\rho/\partial T$ (and hence thermo-emf anomalies) were found near the maxima of the concentration dependence of ρ and corresponded to intermediate valencies (between 2 and 3). It is noteworthy that the region of $\partial\rho/\partial T < 0$ did not coincide with the position of the resistivity maximum ρ . This means that the temperature dependence of ρ is not only determined by the maximum of the structure factor but also by its wings, where composition short-range order may be important.

Similar results have been found for amorphous alloys (metallic glasses). In the Ni-P system, for example, $\partial\rho/\partial T$ is positive at low content of P (15-20%) and becomes slightly negative at 24-26%, implying a temperature dependence of the structure factor upon the relative positions of $2k_F$ and q_{\max} [545]. Metal-metal amorphous alloys display similar behavior [545, 552] as exemplified by the systems $\text{Zr}_{70}\text{Be}_{30}$, $\text{Zr}_{60}\text{Be}_{40}$, $\text{Zr}_{75}\text{Rh}_{25}$, and $\text{Zr}_{54}\text{Cu}_{46}$, in which the theoretical dependence $S(T)$ agrees well with the experimental curve $\rho(t)$ [552]. Some of the discrepancies could be easily removed by optimizing the calculation parameters and by including more structure details in the calculation. The agreement is more remarkable considering that the low-temperature resistivity ranges from 70 to 300 $\mu\text{ohm}\cdot\text{cm}$ in these alloys. Although these are rather encouraging results, the quantitative description is not as yet entirely satisfactory, especially for very resistive alloys of about 200 $\mu\text{ohm}\cdot\text{cm}$ [545]. There are three main reasons for this.

First, a calculation of resistivity not only requires an accurate knowledge of the q dependence of the structure factor but also of the contributions to the structure factor due to pairs of unlike atoms or fluctuations of various types. This necessitates the same treatment background for samples in which transport properties are studied and for those from which structure data are derived. There are no studies, as far as we know, that fulfil this condition. Since the diffusion halo of the structure factor is narrower in amorphous systems than in liquid systems, calculations for the former necessarily involve more errors and agree worse with experiment [541].

Second, the choice of the shape and parameters of the pseudopotential, the screening functions, and other relevant characteristics remains arbitrary. For example, in diluted crystalline Li-Na alloys the residual resistivity can be changed two- or three-fold by varying

the core radius r_c , exchange-correlation corrections, and the shape of screening function [553]. Indeed, different model potentials are needed for different alloys to fit the experimental data, however similar the electron structures of the alloys might be. Although the use of T matrix may improve the agreement with experiment [503, 528], the results remain sensitive to the details of the calculation scheme.

Finally, the fundamental approximations involved in resistivity calculations may be blamed for discrepancies, the concept of the mean free path being perhaps the most questionable. At resistivities of the order of 150-200 $\mu\text{ohm}\cdot\text{cm}$ the mean free path of the electrons is comparable with the interatomic separation and the nearly-free-electron model becomes inadequate. A more sophisticated theory of transport properties will perhaps remove this difficulty (see, for example, [530-533]). We may be certain, however, that the pseudopotential approach to transport properties will retain its value as a helpful first approximation.

References

1. Kireev P. S., *Physics of Semiconductors*, Vysshaya Shkola, Moscow, 1975 (in Russian).
2. Anselm A. I., *Introduction to the Theory of Semiconductors*, Nauka, Moscow, 1978 (in Russian).
3. Ziman J. M., *Principles of the Theory of Solids*, Cambridge University Press, 1972.
4. Bonch-Bruевич V. L., Kalashnikov S. G., *Physics of Semiconductors*, Nauka, Moscow, 1977 (in Russian).
5. Sommerfeld A., Bethe H., *Electronen Theorie der Metalle, Handbuch der Physik*, Band XXIV, Berlin Verlag von Julius Springer, 1933.
6. Davydov A. S., *Quantum Mechanics*, Nauka, Moscow, 1973 (in Russian).
7. Fock V. A., *Principles of Quantum Mechanics*, Nauka, Moscow, 1976 (in Russian).
8. Kittel C., *Quantum Theory of Solids*, John Wiley and Sons, Inc., New York-London, 1978.
9. Jones H., *The Theory of Brillouin Zones and Electronic States in Crystals*, North-Holland, Amsterdam, 1962.
10. Callaway J., *Energy Band Theory*, Academic Press, New York-London, 1964.
11. Slater J. C., *Quantum Theory of Molecules and Solids*, vol. 2, McGraw-Hill, New York, 1965.
12. Löwdin P. O., *Adv. Phys.* 5, p. 1 (1956).
13. Ziman J. M., in: *Solid State Physics*, vol. 26, Academic Press, New York-London, 1971.
14. Dewar M. J. S., *The Molecular Orbital Theory of Organic Chemistry*, McGraw-Hill, New York, 1969.
15. March N. H., Young W. H., Sampanthar S., *The Many-Body Problem in Quantum Mechanics*, Cambridge University Press, 1967.
16. Brooks H., *Nuovo Cimento*, Suppl., 7, p. 165 (1958).
17. Heine V., Cohen M. L., Weaire D., *Solid State Physics*, vol. 24, Ed. by H. Ehrenreich et al., Academic Press, New York, 1970.
18. Heine V., in: *The Physics of Metals, I, Electrons*, Ed. by Ziman J. M., Cambridge University Press, 1969.
19. Gurskii Z. A., *Ukr. Fiz. Zh.*, 24, p. 466 (1979).
20. Arfken G., *Mathematical Methods for Physicists*, Academic Press, New York, 1967.
21. Schiff L. I., *Quantum Mechanics*, McGraw-Hill, New York-Toronto-London, 1955.
22. McWeeny R., Sutcliffe B. T., *Methods of Molecular Quantum Mechanics*, Academic Press, London-New York, 1969.
23. Messiah A., *Quantum Mechanics*, vol. 1, North-Holland, New York, 1966.
24. Korenev B. G., *Introduction to the Theory of Bessel Functions*, Nauka, Moscow, 1971 (in Russian).
25. Lloyd P., Smith P. V., *Adv. Phys.* 21, p. 69 (1972).
26. Johnson K. H., *Adv. Quant. Chem.* 7, p. 143 (1973).

27. Babikov V. I., *The Phase Function Method in Quantum Mechanics*, Nauka, Moscow, 1976 (in Russian).
28. Calogero F., *Variable Phase Approach to Potential Scattering*, Academic Press, New York, 1967.
29. Demkov Yu. N., *Variational Principles in the Theory of Collisions*, Fizmatgiz, Moscow, 1958 (in Russian).
30. Nesbet R. K., *Computer Phys. Commun.* **17**, p. 163 (1979).
31. Darewych J. W., Sokoloff J., *J. Math. Phys.* **20**, p. 736 (1979).
32. Tietz T., *Nuovo Cimento* **50A**, p. 923 (1967).
33. Bolsterli M., *Phys. Rev. Lett.* **32**, p. 436 (1974).
34. Stern M. S., *J. Comput. Phys.* **25**, p. 56 (1977).
35. Rudge M. R. II., *J. Phys.* **B 10**, p. 2451 (1977).
36. Lee P. A., Beni G., *Phys. Rev.* **B 15**, p. 2862 (1977).
37. Coulson C. A., *Valence*, Oxford University Press, 1961.
38. Sitenko A. G., *Scattering Theory*, Naukova Dumka, Kiev, 1975 (in Russian).
39. Landau L. D., Lifshitz E. M., *Quantum Mechanics*, Pergamon Press, London, 1958.
40. Smirnov V. I., *A Course of Higher Mathematics*, vol. 3, part II, Gostekhnizdat, Moscow, 1958 (in Russian).
41. Levinson N., *Danske Vidensk., Seck. Math.-Fys. Meddr.* **25**, 9 (1949).
42. Newton R. G., *Scattering Theory of Waves and Particles*, McGraw-Hill, New York, 1966.
43. Taylor J. R., *Scattering Theory. The Quantum Theory of Nonrelativistic Collisions*, John Wiley and Sons, Inc., New York-London-Sidney, 1972.
44. Burke P. G., *Potential Scattering in Atomic Physics*, Plenum Press, New York, 1976.
45. Clement D., Schmid E. W., Teufel A. G., *Phys. Lett.* **49B**, p. 308 (1974).
46. Englefield M. J., Shourky H. S. M., *Progr. Theor. Phys.* **52**, p. 1554 (1974).
47. Kermode M. W., *J. Phys.* **A 9**, p. 47 (1976).
48. Newton R. G., *J. Math. Phys.* **18**, p. 1348 (1977).
49. Newton R. G., *J. Math. Phys.* **18**, p. 1582 (1977).
50. Wigner E., *Phys. Rev.* **98**, p. 145 (1955).
51. Baudoing R., *Solid St. Commun.* **9**, p. 1231 (1971).
52. Anderson O. K., *Phys. Rev. B* **2**, p. 883 (1970).
53. Blatt F. J., *Phys. Rev.* **108**, p. 285 (1957).
54. Kohn W., Vosko S. H., *Phys. Rev.* **119**, p. 912 (1960).
55. Alfred L. C. R., van Ostenburg D. O., *Phys. Rev.* **161**, p. 3 (1967).
56. Hurd C. M., Gordon E. M., *J. Phys. Chem. Solids* **29**, p. 2205 (1968).
57. Prakash S., *J. Phys.* **F 8**, p. 1653 (1978).
58. Gshneider K. A., *Solid State Physics*, vol. 16, ed. by Seitz F., Turnbull D., Academic Press, New York, 1964.
59. Regel A. R., Glazov V. M., *The Periodic Law and Physical Properties of Electronic Melts*, Nauka, Moscow, 1978 (in Russian).
60. Kittel C., *Introduction to Solid State Physics*, John Wiley and Sons, Inc., New York-London, 1976.
61. Ubbelohde A. R., *Melting and Crystal Structure*, Clarendon Press, Oxford, 1965.
62. Pendry J. B., *J. Phys.* **C 4**, p. 427 (1971).
63. Rasolt M., Taylor R., *J. Phys.* **F 2**, p. 270 (1972).
64. Rasolt M., Taylor R., *J. Phys.* **F 3**, p. 67 (1973).
65. Friedel J., in: *The Physics of Metals. I. Electrons*, ed. by J. M. Ziman, Cambridge University Press, 1969.
66. Davis J. H., Heine V., *J. Phys.* **C 11**, p. 4957 (1978).
67. Mott N. F., Massey H. S. W., *The Theory of Atomic Collisions*, Clarendon Press, Oxford, 1965.
68. v. Haeringen H., *Nuovo Cimento* **34B**, p. 53 (1976).

69. Lloyd P., *Proc. Phys. Soc.* 86, p. 825 (1965).
70. Ziman J. M., *Proc. Phys. Soc.* 86, p. 337 (1965).
71. Elyutin P. V., Krivchenkov V. D., *Quantum Mechanics*, Nauka, Moscow, 1976 (in Russian).
72. Austin B. J., Heine V., Sham L. J., *Phys. Rev.* 127, p. 276 (1962).
73. Harrison W. A., *Pseudopotentials in the Theory of Metals*, W. A. Benjamin, Inc., New York, 1966.
74. Cohen M., Heine V., *Phys. Rev.* 122, p. 1821 (1961).
75. Lin P. J., Phillips J. C., *Adv. Phys.* 14, p. 257 (1965).
76. Watson R. E., Perlman M. L., Herbst J. F., *Phys. Rev. B* 13, p. 2358 (1976).
77. Shirley D. A., Martin R. L., Kowalczyk S. P., McFeely F. R., Ley L., *Phys. Rev. B* 15, p. 544 (1977).
78. Williams A. R., Lang N. D., *Phys. Rev. Lett.* 40, p. 954 (1978).
79. Pendry J. B., *J. Phys. C* 1, p. 1065 (1968).
80. Krasko G. L., *Phys. St. Sol. B* 60, p. 71 (1973).
81. Hubbard J., *Proc. Phys. Soc.* 92, p. 921 (1967).
82. Kapur P. L., Peierls R. E., *Proc. Roy. Soc. A* 116, p. 277 (1938).
83. Wigner E. P., *Phys. Rev.* 70, p. 15 (1946).
84. Wu T. Y., Ohmura T., *Quantum Theory of Scattering*, Prentice-Hall, New York, 1962.
85. Burke P. G., Robb W. D., *Adv. Atom. Molec. Phys.* 11, p. 143 (1975).
86. Bethe H. A., *Intermediate Quantum Mechanics*, W. A. Benjamin, Inc., New York-Amsterdam, 1964.
87. Slater J. C., *The Self-Consistent Field for Molecules and Solids*, McGraw-Hill, New York-St. Louis-San Francisco, 1974.
88. Koopmans T. A., *Physica* 1, p. 104 (1933).
89. Harrison W. A., *Solid State Theory*, McGraw-Hill, New York-London-Toronto, 1970.
90. Sen K. D., *Phys. Lett.* 69A, p. 85 (1978).
91. Gurvich L. V., Karachevtsev G. V., Kondratyev V. N., Lebedev Yu. A., Medvedev Yu. A., Potapov V. K., Khodeev Yu. S., *Chemical Bond Breaking Energy. Ionization Potentials and Electron Affinity*, Nauka, Moscow, 1974 (in Russian).
92. Cotton F. A., Wilkinson G., *Advanced Inorganic Chemistry*, John Wiley and Sons, Inc., New York-London-Sidney, 1966.
93. Slater J. C., *Phys. Rev.* 81, p. 385 (1951).
94. Gaspar R., *Acta Phys. Hung.* 3, p. 263 (1954).
95. Kohn W., Sham L. I., *Phys. Rev.* 140A, p. 1133 (1965).
96. Slater J. C., Wood J. H., *Intern. J. Quantum Chem.* 4S, p. 3 (1971).
97. Slater J. C., Johnson K. H., *Phys. Rev. B* 5, p. 844 (1972).
98. Herman F., Callaway J., Acton F. S., *Phys. Rev.* 95, p. 371 (1954).
99. Latter R., *Phys. Rev.* 99, p. 510 (1955).
100. Liberman D., Batra J. P., *Multiple Scattering Program Descriptions*, IBM Research Laboratory, San Jose, California, USA, RJ 1224 (N 19467), 1973.
101. Herman F., Skillmann J., *Atomic Structure Calculations*, Englewood Cliffs, New Jersey, 1963.
102. Gopinathan M. S., *J. Phys. B* 12, p. 521 (1979).
103. Wood J. H., *Intern. J. Quant. Chem.* 3S, p. 747 (1970).
104. Kmetko E. A., *Phys. Rev. A* 1, p. 37 (1970).
105. Schwarz K., *Phys. Rev. B* 5, p. 2466 (1972).
106. Schwarz K., *Theor. Chim. Acta* (Berlin), 34, p. 225 (1974).
107. Gopinathan M. S., Whiehead M. A., Bogdanović R. R., *Phys. Rev. A* 14, p. 1 (1976).
108. Lindgren J., Schwarz K., *Phys. Rev. A* 5, p. 542 (1972).
109. Gaspar R., *Acta Phys. Acad. Sci. Hung.* 35, p. 213 (1974).

110. Snow E. C., *Phys. Rev.* **171**, p. 785 (1968).
111. Rudge W. E., *Phys. Rev.* **181**, p. 1033 (1969).
112. Yasui M., Hagashi E., Shimizu M., *J. Phys. Soc. Jap.* **29**, p. 1446 (1970).
113. Borghese F., Denti P., *Nuovo Cimento* **3B**, p. 34 (1971).
114. Ramchdani M. G., *J. Phys.* **F 1**, p. 169 (1971).
115. Boring M., Snow E. C., *Phys. Rev.* **B 5**, p. 1221 (1972).
116. Papaconstantopoulos D. A., Anderson J. R., McCaffrey J. M., *Phys. Rev.* **B 5**, p. 1214 (1972).
117. Neto J. R. P., Ferreira L. G., *J. Phys.* **C 6**, p. 3430 (1973).
118. Jennison D. R., Kunz A. B., *Phys. Rev. Lett.* **39**, p. 418 (1977).
119. Boyer L. L., Papaconstantopoulos D. A., Klein B. M., *Phys. Rev.* **B 15**, p. 3685 (1977).
120. Averill F. W., *Phys. Rev.* **B 6**, p. 3637 (1972).
121. Inoue S. T., Asano S., Yamashita J. J., *Phys. Soc. Jap.* **30**, p. 1546 (1971).
122. Herman F., van Dyke J. P., Ortenburger I. B., *Phys. Rev. Lett.* **22**, p. 807 (1969).
123. Herman F., van Dyke J. P., Ortenburger I. B., *Int. J. Quant. Chem.* **35**, p. 827 (1970).
124. Boring A. M., *Phys. Rev.* **B 3**, p. 3093 (1971).
125. Clementi E., Roetti C., *Atomic Data Nucl. Data Tables* **14**, p. 177 (1974).
126. Mattheiss L. F., *Phys. Rev.* **134A**, p. 970 (1964).
127. Rennert P., *Acta Phys. Acad. Sci. Hung.* **37**, p. 219 (1974).
128. Messmer R. P., *Modern Theoretical Chemistry*, vol. 8, Ed. by Segal G. A., Plenum Press, New York, 1977.
129. Liberman D., *Phys. Rev.* **171**, p. 1 (1968).
130. Leite J. R., Ferreira L. G., Pereira J. R., *Phys. Lett.* **40A**, p. 315 (1972).
131. Dagens L., *Phys. St. Sol.* **B 65**, p. 481 (1974).
132. Talman J. D., Shadwick W. F., *Phys. Rev.* **A 14**, p. 36 (1976).
133. Gopinathan M. S., *Phys. Rev.* **A 15**, p. 2135 (1977).
134. Gazquer J. L., Keller J., *Phys. Rev.* **A 16**, p. 1358 (1977).
135. Wimmer E., *Theoret. Chem. Acta* (Berlin) **51**, p. 339 (1979).
136. Berrondo M., Gosinski O., *Chem. Phys. Lett.* **62**, p. 31 (1979).
137. Berrondo M., Daudey J. P., Gosinski O., *Chem. Phys. Lett.* **62**, p. 34 (1979).
138. Bennett M., Inkson J. C., *J. Phys.* **C 10**, p. 987 (1977).
139. Pasemann L., *Phys. St. Sol.* **B 84**, p. 175 (1977).
140. Viefhues H., Falter C., Ludwig W., Monkenbusch M., Selmke M., Zierau W., *Phys. Lett.* **66A**, p. 404 (1978).
141. Lindhard J., *K. Danske Vidensk. Selsk. Mat.-Fys.* **28**, 8 (1954).
142. Bardeen J., *Phys. Rev.* **52**, p. 688 (1937).
143. Pines D., Noziers P., *The Theory of Quantum Liquids*, W. A. Benjamin, Inc., New York-Amsterdam, 1966.
144. Bonch-Bruевич V. L. (Ed.) *Many-body Quantum Theory*, Inostrannaya Literatura, Moscow, 1959 (in Russian).
145. Hubbard J., *Proc. Roy. Soc.* **A240**, p. 539 (1957).
146. Hubbard J., *Proc. Roy. Soc.* **A243**, p. 336 (1958).
147. Noziers P., Pines D., *Phys. Rev.* **109**, p. 741 (1958).
148. Sham L. J., *Proc. Roy. Soc.* **A283**, p. 3 (1965).
149. Geldart D. J. W., Vosko S. H., *J. Phys. Soc. Jap.* **70**, p. 20 (1965).
150. Geldart D. J. W., Vosko S. H., *Canad. J. Phys.* **44** (1966).
151. Crowel J., Anderson V. E., Ritchie R. H., *Phys. Rev.* **150**, p. 243 (1966).
152. Kleinman L., *Phys. Rev.* **160**, p. 585 (1967); Langreth D. C., *Phys. Rev.* **181**, p. 753 (1969).
153. Ho P. S., *Phys. Rev.* **169**, p. 523 (1968).
154. Shaw R. W., Jr., *J. Phys.* **C 2**, p. 2335 (1969); *J. Phys.* **C 3**, p. 1140 (1970).

155. Singwi K. S., Sjölander A., Tos M. P., Land R. H., *Phys. Rev. B* **1**, p. 1044 (1970); see also erratum in: Vashista P., Singwi K. S., *Phys. Rev. B* **6**, p. 875 (1972).
156. Scheider T., *Physica* **52**, p. 481 (1971).
157. Toigo F., Woodruff T. O., *Phys. Rev. B* **2**, p. 3958 (1970); see also erratum in: Geldart D. J. W., Richard T. G., Rasolt M., *Phys. Rev. B* **5**, p. 2740 (1972).
158. Taylor R., *J. Phys. F* **8**, p. 1699 (1978).
159. Ukhov V. F., Vatolin N. A., Gel'chinskii B. R., Beskachko V. P., Esin O. A., *Interparticle Interaction in Liquid Metals*, Nauka, Moscow, 1979 (in Russian).
160. Morita A., Soma T., Takeda T., *J. Phys. Soc. Jap.* **32**, p. 29 (1972).
161. Benckert S., *Phys. St. Sol. B* **71**, p. K161 (1975).
162. Singh S. P., Marwaha G. L., *Ind. J. Pure Appl. Phys.* **15**, p. 509 (1977).
163. Ball M. A., Islam Md. M., *Phys. St. Sol. B* **87**, p. 145 (1978).
164. Khwaha F. A., Katsnelson A. A., Silonov V. M., *Phys. St. Sol. B* **188**, p. 477 (1978).
165. Sinha N. N., Srivastava P. L., *Phys. St. Sol. B* **90**, p. 369 (1978).
166. Vaks V. G., Kravchuk S. P., Trefilov P. S., *Fiz. Metall. Metalloved.*, **44**, p. 1151 (1977).
167. Ziman J. M., *Adv. Phys.* **13**, p. 89 (1964).
168. Rennert P., *Phys. St. Sol. B* **50**, p. K37 (1972).
169. Prakash S., Joshi S. K., *Phys. Rev. B* **2**, p. 915 (1970).
170. Prakash S., Joshi S. K., *Phys. Rev. B* **4**, p. 1770 (1971).
171. Hanke W., *Phys. Rev. B* **8**, p. 4585 (1973).
172. Singh N., Prakash S., *Phys. Rev. B* **8**, p. 5532 (1973).
173. Singh N., Singh J., Prakash S., *Phys. Rev. B* **12**, p. 1076 (1975).
174. Singh J., Singh N., Prakash S., *Phys. Rev. B* **12**, p. 3166 (1975).
175. Singh N., Singh J., Prakash S., *Phys. Rev. B* **12**, p. 5415 (1975).
176. Singh J., Singh N., Prakash S., *Phys. Lett.* **58A**, p. 59 (1976).
177. Ball M. A., *J. Phys. C* **2**, p. 1248 (1969).
178. Ball M. A., Islam Md. M., *Phil. Mag.* **22**, p. 1227 (1970).
179. Islam Md. M., Ball M. A., *Phil. Mag.* **23**, p. 1329 (1971).
180. Dadens L., *J. Phys. C* **5**, p. 2333 (1972).
181. Moriarty J. A., *Phys. Rev. B* **10**, p. 3075 (1974).
182. Moriarty J. A., *Phys. Rev. B* **16**, p. 2537 (1977).
183. Natapoff M., *Phys. Lett.* **35A**, p. 111 (1971).
184. Shaw R. W. Jr., *Phys. Rev. B* **5**, p. 4742 (1972).
185. Meyer A., Joung W. H., *J. Phys. C Suppl.*, **3**, p. 348 (1970).
186. Rasolt M., Tawil R. A., Taylor R., *Solid St. Commun.* **18**, p. 461 (1976).
187. von Weizacker C. F., *Z. Phys.* **96**, p. 431 (1935).
188. Kirzhnits D. A., *Field Theoretical Methods in Many-Body Systems*, Pergamon Press, Oxford, 1967.
189. Natapoff M., *J. Phys. Chem. Sol.* **37**, p. 59 (1976).
190. Natapoff M., *J. Phys. Chem. Sol.* **36**, p. 53, (1975).
191. Natapoff M., *J. Phys. Chem. Sol.* **39**, p. 1119 (1978).
192. Resta R., *Phys. Rev. B* **16**, p. 2717 (1977).
193. Pines D., *Elementary Excitations in Solids*, W. A. Benjamin, Inc., New York-Asterdam, 1963.
194. Iveronova V. I., Katsnelson A. A., *Izv. Vuzov, Ser. Fiz.*, **8**, p. 40 (1976).
195. Appelbaum J. A., Hamann D. R., *Phys. Rev. B* **8**, p. 1777 (1973).
196. Shindo K., Ohkoshi I., *J. Phys. Soc. Jap.* **42**, p. 1432 (1977).
197. Ohkoshi I., Shindo K., *J. Phys. Soc. Jap.* **43**, p. 1879 (1977).
198. Shindo K., *J. Phys. Soc. Jap.* **45**, p. 699 (1978).
199. Chelikowsky J. R., *Sol. St. Commun.* **22**, p. 351 (1977).
200. Ihm J., Cohen M. L., *Sol. St. Commun.* **29**, p. 711 (1979).

201. Ho K. M., Louie S. G., Chelikowsky J. R., Cohen M. L., *Phys. Rev. B* 15, p. 1755 (1977).
202. Zunger A., Cohen M. L., *Phys. Rev. B* 18, p. 5449 (1978).
203. Zunger A., Cohen M. L., *Phys. Rev. B* 19, p. 568 (1979).
204. Louie S. G., Ho K. M., Cohen M. L., *Phys. Rev. B* 19, p. 1774 (1979).
205. Kerker G. P., Ho K. M., Cohen M. L., *Phys. Rev. B* 18, p. 5473 (1978).
206. Pickett W. E., Ho K. M., Cohen M. L., *Phys. Rev. B* 19, p. 1734 (1979).
207. Ho K. M., Pickett W. E., Cohen M. L., *Phys. Rev. Lett.* 41, p. 580 (1978); *Phys. Rev. B* 19, p. 1751 (1979).
208. Appelbaum J. A., Hamann D. R., *Rev. Mod. Phys.* 48, p. 479 (1976).
209. Appelbaum J. A., Baraff G. A., Hamann D. R., *Phys. Rev. B* 14, p. 588 (1976).
210. Appelbaum J. A., Baraff G. A., Hamann D. R., *Phys. Rev. B* 15, p. 2408 (1977).
211. Schlüter M., Chelikowsky J. R., Louie S. G., Cohen M. L., *Phys. Rev. B* 12, p. 4200 (1975).
212. Chelikowsky J. R., Schlüter M., Louie S. G., Cohen M. L., *Sol. St. Communs.* 17, p. 1103 (1975).
213. Louie S. G., Cohen M. L., *Phys. Rev. B* 13, p. 2461 (1976).
214. Louie S. G., Chelikowsky J. R., Cohen M. L., *J. Vac. Sci. Technol.* 13, p. 790 (1976).
215. Chelikowsky J. R., *Phys. Rev. B* 16, p. 3618 (1977).
216. Pickett W. E., Louie S. G., Cohen M. L., *Phys. Rev. B* 17, p. 815 (1977).
217. Pickett W. E., Cohen M. L., *Phys. Rev. B* 18, p. 939 (1978).
218. Ihm J., Louie S. G., Cohen M. L., *Phys. Rev. B* 17, p. 769 (1978).
219. Kerker G. P., Louie S. G., Cohen M. L., *Phys. Rev. B* 17, p. 706 (1978).
220. Louie S. G., Ho K. M., Chelikowsky J. R., Cohen M. L., *Phys. Rev. B* 15, p. 5627 (1977).
221. Slater J. C., *Phys. Rev.* 51, p. 846 (1937).
222. Mattheiss L. F., *Phys. Rev.* 139A, p. 1893 (1965).
223. Loucks T. L., *Augmented Plane Wave Method*, W. A. Benjamin, Inc., New York, 1967.
224. Papaconstantopoulos D. A., Slaughter W. R., *Computer Phys. Communs.* 7, p. 207 (1974).
225. Rao R. S., Majumdar C. K., Shastry B. S., Singh R. P., *Pramana.* 4, p. 45 (1975).
226. Schöpcue R., Mrosan E., *Phys. Stat. Sol. B* 90, p. K95 (1978).
227. Iyakutti K., Majumdar C. K., Rao R. S., Devanathan V., *J. Phys. F* 6, p. 1639 (1976).
228. Iyakutti K., Asokamani R., Devanathan V., *J. Phys. F* 7, p. 2307 (1977).
229. Asokamani R., Iyakutti K., Rao R. S., Devanathan V., *J. Phys. F* 8, p. 2323 (1978).
230. Asokamani R., Iyakutti K., Devanathan V., *Sol. St. Communs.* 30, p. 385 (1979).
231. Harford R. C., *J. Phys. F* 2, p. 1055 (1972).
232. Altmann S. L., Harford R. C., Blake R. G., *J. Phys. F* 2, p. 1062 (1972).
233. Yasuhara N., Watabe M., *J. Phys. C* 8, p. 4183 (1975).
234. Gunnarsson O., Lundqvist B. I., *Phys. Rev. B* 13, p. 4274 (1976) Erratum in: *Phys. Rev. B* 15, p. 6006 (1977).
235. Mokhracheva L. P., Tskhai V. A., Geld P. V., *Phys. St. Sol. B* 78, p. 465 (1976).
236. Dyakin V. V., Egorov R. V., Schirchkovskii V. P., *Phys. St. Sol. B* 36, p. 447 (1969).
237. Dyakin V. V., Egorov R. F., Kulakova Z. V., Shirokovskii V. P., *Fiz. Metall. Metalloved.*, 32, p. 691 (1971).
238. Wolf G. V., Dyakin V. V., Shirokovskii V. P., *Fiz. Metall. Metalloved.*, 38, p. 949 (1974).

239. Tosi M. P., *Sol. St. Phys.* B 16, p. 1 (1964).
240. Mattheiss L. F., *Phys. Rev.* 133A, p. 1399 (1964).
241. Mattheiss L. F., *Phys. Rev.* 138A, p. 112 (1965).
242. Earn V., Switendick A. C., *Phys. Rev.* 137A, p. 1927 (1965).
243. Snow E. C., Waber J. T., *Phys. Rev.* 157, p. 570 (1967).
244. Grant I. P., Whittehead M. A., *Mol. Phys.* 32, p. 1181 (1976).
245. Anderson O. K., *Sol. St. Commun.* 13, p. 133 (1973).
246. Anderson O. K., Kasowski R. V., *Phys. Rev. B* 4, p. 1064 (1971).
247. Schlosser H., Marcus P. M., *Phys. Rev.* 131, p. 2529 (1963).
248. De Cicco P. D., *Phys. Rev.* 153, p. 931 (1967).
249. Koelling D. D., *Phys. Rev.* 188, p. 1049 (1969).
250. Koelling D. D., Freeman A. J., Mueller F. M., *Phys. Rev. B* 1, p. 1318 (1970).
251. Rudge W. E., *Phys. Rev.* 181, p. 1020 (1969).
252. Rudge W. E., *Phys. Rev.* 181, p. 1024 (1969).
253. Kane E. O., *Phys. Rev. B* 4, p. 1917 (1971).
254. Kleinman L., Shurtleff R., *Phys. Rev.* 188, p. 1111 (1969).
255. Kleinman L., Shurtleff R., *Phys. Rev. B* 4, p. 3284 (1971).
256. Shurtleff R., Kleinman L., *Phys. Rev. B* 3, p. 2418 (1971).
257. Wakoh S., Yamashita J., *J. Phys. Soc. Jap.* 35, p. 1394 (1973).
258. Ketterson J. B., Koelling D. D., Shaw J. C., Windmiller L. R., *Phys. Rev. B* 11, p. 1447 (1975).
259. Evans R., Keller J., *J. Phys. C* 4, p. 3155, (1971).
260. Inoue M., Okazaki M., *J. Phys. Soc. Jap.* 30, p. 1575 (1971).
261. Painter G. S., *Phys. Rev. B* 7, p. 3521 (1973).
262. Williams A. R., Morgan J. v. W., *J. Phys. C* 5, p. L293 (1972).
263. Williams A. R., Morgan J. v. W., *J. Phys. C* 7, p. 37 (1974).
264. John W., Ziesche P., *Phys. St. Sol. B* 47, p. K83 (1971).
265. John W., Lehmann G., Ziesche P., *Phys. St. Sol. B* 53, p. 287 (1972).
266. Ziesche P., *J. Phys. C* 7, p. 1085 (1974).
267. Ziesche P., John W., in: *Electronic Structure of Transition Metals, Their Alloys and Compounds*, Naukova Dumka, Kiev, 1974 (in Russian).
268. Lehmann G., *Phys. St. Sol. B* 70, p. 737 (1975).
269. Dy K. S., *Phys. St. Sol. B* 81, p. K111 (1977).
270. Koelling D. D., Shaw J. C., Windmiller L. R., *Phys. Rev. B* 11, p. 1147 (1975).
271. Demkov Yu. M., Rudakov V. S., *Zh. Exper. Teor. Fiz.*, 59, p. 2035, (1970).
272. Painter G. S., Faulkner J. S., Stocks G. M., *Phys. Rev. B* 9, p. 2448 (1974).
273. Elyashar N., Koelling D. D., *Phys. Rev. B* 13, p. 5362 (1976).
274. Elyashar N., Koelling D. D., *Phys. Rev. B* 15, p. 3620 (1977).
275. Ament M. A. E., de Vroomen A. R., *J. Phys. F* 4, p. 1359 (1974).
276. Brovman E. G., Kagan Yu. M., *Uspekhi Fiz. Nauk*, 112, p. 369 (1974).
277. Elliot M., Ellis T., Springford M., *Phys. Rev. Lett.* 41, p. 709 (1978).
278. Paasch G., Woittenneck H., *Phys. St. Sol. B* 65, p. 493 (1974).
279. Vonsovskii S. V., Egorov R. F., Shirokovskii V. P., in: *Electronic Structure of Transition Metals, Their Alloys and Compounds*, Naukova Dumka, Kiev, 1974 (in Russian).
280. Egorov R. F., Shirokovskii V. P., *Fiz. Metall. Metalloved.*, 40, p. 500, (1975).
281. Ganin G. V., Kuznetsov E. V., Shirokovskii V. P., *Fiz. Metall. Metalloved.*, 41, p. 910 (1976).
282. Shilkova N. A., *Fiz. Metall. Metalloved.*, 43, p. 685 (1977).
283. Rösch N., in: *Electrons in Finite and Infinite Structures*, ed. by Phariseau, P., 1977; Zhidomirov G. M., Yastrebov L. I., in: *Methods of Quantum Chem-*

- istry. Proc. of All-Union Symposium on Quantum Chemistry, Chernogolovka, 1978 (in Russian).
284. Johnson K. H., *J. Chem. Phys.* **45**, p. 3085 (1966); *Intern. J. Quant. Chem.* **18**, p. 367 (1967).
285. Alperovich F. I., Geguzin I. I., Nikolskii A. V., Kochetov V. G., Niki-forov I. Ya., *Izv. Acad. Nauk SSSR, Ser. Fiz.*, **40**, p. 251 (1976).
286. Nazhalov A. I., Egorushkin V. E., Njavro V. F., Popov V. A., Fadin V. P., *Izv. Vuzov, Ser. Fiz.*, **9**, p. 87 (1975).
287. Nazhalov A. I., Popov V. A., Egorushkin V. E., Fadin V. P., in: *Band Structure Calculation Methods and Physical Properties of Crystals*, Naukova Dumka, Kiev, 1977 (in Russian).
288. Landau M. A., in: *Scientific Foundations of Catalyser Selection*, Nauka, Moscow, 1965 (in Russian).
289. Hodges L., Watson R. E., Ehrenreich H., *Phys. Rev.* **B 5**, p. 3953 (1972).
290. Egorushkin V. E., Nazhalov A. I., Fadin V. P., *Izv. Vuzov, Ser. Fiz.*, **9**, p. 22 (1975).
291. Heine V., Lee M. J. G., *Phys. Rev. Lett.* **37**, p. 811 (1971).
292. Lee M. J. G., Heine V., *Phys. Rev.* **B 5**, p. 3839 (1972).
293. Heine V., Shively J. E., *J. Phys.* **C 1**, p. L269 (1971).
294. Lee M. J. G., *Phys. Rev.* **178**, p. 953 (1969).
295. Mrosan E., Lehmann G., Woittenneck H., *Phys. St. Sol.* **B 64**, p. 131 (1974).
296. Mrosan E., Lehmann G., Woittenneck H., *Phys. St. Sol.* **B 64**, p. K1 (1974).
297. Mrosan E., Lehmann G., *Phys. St. Sol.* **B 71**, p. K13 (1975).
298. Mrosan E., Lehmann G., *Phys. St. Sol.* **B 77**, p. 607 (1976).
299. Mrosan E., Lehmann G., *Phys. St. Sol.* **B 77**, p. K161 (1976).
300. Mrosan E., Lehmann G., *Phys. St. Sol.* **B 78**, p. 159 (1976).
301. Baz' A. I., Zel'dovich Ya. B., Perelomov A. M., *Scattering, Reactions, and Decays in Quantum Mechanics*, Nauka, Moscow, 1971 (in Russian).
302. Dagens L., *J. Phys.* **F 6**, p. 1801 (1976).
303. Hering C., *Phys. Rev.* **57**, p. 1169 (1940).
304. Phillips J. C., Kleinman L., *Phys. Rev.* **116**, p. 287 (1959).
305. Heine V., *Phys. Rev.* **157**, p. 673 (1967).
306. Hubbard J., Dalton N. W., *J. Phys.* **C 1**, p. 1637 (1968).
307. Hubbard J., *J. Phys.* **C 2**, p. 1222 (1969).
308. Harrison W. A., *Phys. Rev.* **181**, p. 1036 (1969).
309. Woodruff T. O., *Solid State Physics*, ed. by Seitz P., Turnbull D., Academic Press, New York, **4**, p. 367 (1957).
310. Reser B. I., Shirokovskii V. P., *Fiz. Metall. Metalloved.*, **32**, p. 934 (1971).
311. Moriarty J. A., *Phys. Rev.* **B 1**, p. 1363 (1970).
312. Moriarty J. A., *Phys. Rev.* **B 5**, p. 2060 (1972).
313. Moriarty J. A., *Phys. Rev.* **B 6**, p. 1239 (1972).
314. Moriarty J. A., *Phys. Rev.* **B 6**, p. 4445 (1972).
315. Moriarty J. A., *Phys. Rev.* **B 8**, p. 1338 (1973).
316. Moriarty J. A., *Phys. Rev.* **B 19**, p. 609 (1979).
317. Epstein S. T., *The Variation Method in Quantum Chemistry*, Academic Press, New York-San Francisco-London, 1974.
318. Perdew J. P., Vosko S. H., *Phys. St. Sol.* **B 63**, p. K47 (1974).
319. Hodges L., Ehrenreich H., Lang N. D., *Phys. Rev.* **152**, p. 505 (1966).
320. Mueller F. M., *Phys. Rev.* **153**, p. 659 (1967).
321. Deegan R. A., Twose W. D., *Phys. Rev.* **164**, p. 993 (1967).
322. Kunz A. B., *Phys. Lett.* **27A**, p. 401 (1968).
323. Kunz A. B., *Phys. Rev.* **180**, p. 934, (1969).
324. Euwema R. N., *Phys. Rev.* **B 4**, p. 4332 (1971).
325. Euwema R. N., *Intern. J. Quant. Chem.* **5**, p. 61 (1971).
326. Abarenkov I. V., *Phys. St. Sol.* **B 50**, p. 465 (1972).

327. Euwema R. N., Stukel D. J., *Phys. Rev. B* 1, p. 4670 (1970).
328. Reser B. I., Dyakin V. V., Shirokovski V. P., *Phys. St. Sol. B* 44, p. 425 (1971); Erratum in: *Phys. St. Sol. B* 47, p. 703 (1971); Dyakin V. V., Reser B. I., Shirokovski V. P., *Phys. St. Sol. B* 50, p. 459 (1971).
329. Reser B. I., Dyakin V. V., *Phys. St. Sol. B* 87, p. 41 (1978).
330. Meyer A., Young W. H., *Phys. Rev.* 135A, p. 1363 (1965).
331. Hafner J., *J. Phys. F* 5, p. L150 (1975).
332. Day R. S., Sun F., Cutler P. H., King W. F., *J. Phys. F* 6, p. L137 (1976).
333. Girardeau M. D., *J. Math. Phys.* 12, p. 165 (1971).
334. Juras G. E., Monahan J. E., Shakin C. M., Thaler R. M., *Phys. Rev. B* 5, p. 4000 (1972).
335. Gurskii B. A., Gurskii Z. A., *Ukr. Fiz. Zh.*, 21, p. 1603 (1976).
336. Sakakura A. Y., Brittin W. E., Girardeau M. D., *Phys. Rev. A* 18, p. 2412 (1978).
337. Gurskii B. A., Gurskii Z. A., *Ukr. Fiz. Zh.*, 21, p. 1609 (1976).
338. Gurskii B. A., Gurskii Z. A., *Ukr. Fiz. Zh.*, 23, p. 19 (1978).
339. Gurskii B. A., Gurskii Z. A., *Fiz. Metall. Metalloved.*, 46, p. 903 (1978).
340. Gurskii B. A., Gurskii Z. A., Preprint of the Institute of Theoretical Physics of the Ukrainian Academy of Sciences, ИТФ-76-54P, 1976 (in Russian).
341. Gurskii B. A., Gurskii Z. A., Preprint of the Institute of Theoretical Physics of the Ukrainian Academy of Sciences, ИТФ-77-13P, 1977 (in Russian).
342. Shaw R. W., Harrison W. A., *Phys. Rev.* 163, p. 604 (1967).
343. Animalu A. O. E., *Phys. Rev. B* 8, p. 3542 (1973).
344. Day R. S., Sun F., Cutler P. H., *J. Phys. F* 6, p. L297 (1976).
345. Nemoshkalenko V. V., Aleshin V. G., *Theoretical Foundations of X-ray Emission Spectroscopy*, Naukova Dumka, Kiev, 1974 (in Russian).
346. Mattheiss L. F., Wood J., Switendick A. C., *Methods in Computational Physics*, vol. 8, ed. by B. Alder *et al.*, New York-London, 1968.
347. Lawrence M. J., *J. Phys. C* 4, p. 1737 (1971).
348. Dimmock J. O., *Solid State Physics*, vol. 26, ed. by Seitz F., Turnbull D., Academic Press, New York, 1971.
349. Veljković V., Slavić I., *Phys. Rev. Lett.* 29, p. 105 (1972).
350. (a) Terrell J. H., *Phys. Rev.* 149, p. 526 (1966).
(b) Loucks T. L., *Phys. Rev.* 159, p. 544 (1967).
351. Andersen O. K., *Phys. Rev. Lett.* 27, p. 1211 (1971).
352. Ziman J. M., *Proc. Phys. Soc.* 91, p. 701 (1967).
353. Lee M. J. G., *Phys. Rev.* 187, p. 901 (1969). See discussion in: Cooke J. F., Davis H. L., Wood R. F., *Phys. Rev. Lett.* 25, p. 28 (1970); Lee M. J. G., *Phys. Rev. Lett.* 26, p. 501 (1970).
354. Lee M. J. G., in: *Computational Methods in Band Theory*, ed. by Marcus P. M. *et al.*, Plenum Press, New York, 1971.
355. Devillers M. A. C., de Vroomen A. R., *Sol. St. Commun.* 9, p. 1939 (1971).
356. Devillers M. A. C., *Sol. St. Commun.* 11, p. 395 (1972).
357. Coenen N. J., de Vroomen A. R., *J. Phys. F* 2, p. 487 (1972).
358. Devillers M. A. C., de Vroomen A. R., *J. Phys. F* 4, p. 711 (1974).
359. Devillers M. A. C., Matthey M. M. M. P., de Vroomen A. R., *Phys. St. Sol. B* 63, p. 471 (1974); Matthey M. M. M. P., Devillers M. A. C., de Vroomen A. R., *Phys. St. Sol. B* 63, p. 279 (1974).
360. de Groot D. G., Rijsenbrij D. B. B., van Weeren J. H. P., Lodder A., *Sol. St. Commun.* 19, p. 203 (1976).
361. Soven P., *Phys. Rev.* 156, p. 809 (1967).
362. Soven P., *Phys. Rev.* 178, p. 1136 (1969).
363. Veličky B., Kirkpatrick S., Ehrenreich H., *Phys. Rev.* 175, p. 747 (1968).
364. Bass R., *Phys. Lett.* 46A, p. 189 (1973).

365. Ehrenreich H., Schwartz L. M., *Solid. State Physics*, ed. by Seitz F., Turnbull D., Academic Press, New York, 1976.
366. Gyorffy B. L., Stocks G. M., in: *Electrons in Finite and Infinite Structures*, ed. by Phariseau P., Scheire L., Plenum Press, New York-London, 1977.
367. Korrington J., *Physica* **13**, p. 392 (1947).
368. Kohn W., Rostoker N., *Phys. Rev.* **94**, p. 1111 (1954).
369. Dyakin V. V., Egorov R. F., Kulakova Z. V., Shirokovskii V. P., *Fiz. Metall. Metalloved.*, **30**, p. 1291 (1970).
370. Ham F. S., Segall B., *Phys. Rev.* **124**, p. 1786 (1961).
371. Dyakin V. V., Egorov R. F., Zvezdin V. K., Kulakova Z. V., Shirokovskii V. P., *A Technique for Computing Structure Constants Involved in Green-Function Energy-Band Calculations in Solids*, VINITI, No. 1869-70 Dep., 1970 (in Russian).
372. Nazhalov A. I., Egorushkin V. E., Popov V. A., Fadin V. P., VINITI, No. 2825-74 Dep., 1974 (in Russian).
373. Segall B., Ham F. S., *General Electric Research Laboratory Rep.*, No. 61-RL-2876G, (1961).
374. Dyakin V. V., Egorov R. F., Zvezdin V. K., Kulakova Z. V., Shirokovskii V. P., VINITI, No. 1870-70 Dep., 1970 (in Russian).
375. Jacobs R. L., *J. Phys. C* **1**, p. 492 (1968).
376. Pettifor D. G., *J. Phys. C* **2**, p. 1051 (1969).
377. Hum D. M., Wong K. C., *J. Phys. C* **2**, p. 833 (1969).
378. Moriarty J. M., *J. Phys. F* **5**, p. 873 (1975).
379. Slater J. C., Koster G. F., *Phys. Rev.* **94**, p. 1498 (1954).
380. Deegan R. A., *Phys. Rev.* **171**, p. 659 (1968).
381. Jacobs R. L., *J. Phys. C* **2**, p. 1206 (1969).
382. Jacobs R. L., *J. Phys. C* **1**, p. 1307 (1968).
383. Pettifor D. C., *J. Phys. C* **3**, p. 367 (1970).
384. Pettifor D. C., *Phys. Rev. B* **2**, p. 3031 (1970).
385. Pettifor D. C., *J. Phys. C* **5**, p. 97 (1972).
386. Koelling D. D., *J. Phys. Chem. Solids* **33**, p. 1335 (1972).
387. Kaga H., *Phys. Lett.* **37A**, p. 373 (1971).
388. Donà dello Rose L. F., Radicchio G. M., *Sol. St. Commun.* **14**, p. 869 (1974).
389. Kulikov N. I., *Izv. Vuzov, Ser. Chern. Metallurg.*, **7**, p. 128 (1975).
390. Kulikov N. I., Cand. Thesis, Institute of Steel and Alloys, Moscow, 1976 (in Russian).
391. Kulikov N. I., Borzunov V. N., Zvonkov A. D., *Phys. St. Sol. B* **86**, p. 83 (1978).
392. Andersen O. K., in: *Computational Methods in Band Theory*, ed. by Marcus P. M. et. al., Plenum Press, New York, 1971.
393. Kasowski P. V., Andersen O. K., *Sol. St. Commun.* **11**, p. 799 (1972).
394. Andersen O. K., Wooley R. G., *Molec. Phys.* **26**, p. 905 (1973).
395. Andersen O. K., *Phys. Rev. B* **12**, p. 3060 (1975).
396. Poulsen U. K., Kollár J., Andersen O. K., *J. Phys. F* **6**, p. L241 (1976).
397. Andersen O. K., Jepsen O., *Physica* **91B**, p. 317 (1977).
398. Hayes T. M., Brooks H., Bienenstock A., *Phys. Rev.* **175**, p. 699 (1968).
399. Inglesfield J. K., *J. Phys. C* **1**, p. 1337 (1968).
400. Matysina Z. A., *Fiz. Metall. Metalloved.*, **32**, p. 699 (1971).
401. Khachatryan A. G., *Theory of Phase Transitions and Structure of Solid Solutions*, Nauka, Moscow, 1974 (in Russian).
402. Krasko G. L., Makhnovetskii A. V., *Phys. St. Sol. B* **65**, p. 869 (1974).
403. Katsnelson A. A., Silonov V. M., Khavadzha F. A., *Phys. Stat. Sol. B* **91**, p. 11 (1979).
404. Khavadzha F. A., Silonov V. M., Katsnelson A. A., Khrushchev M.M., *Phys. St. Sol. B* **82**, p. 101 (1977).

405. Animalu A. O. E., Heine V., *Phil. Mag.* **12**, p. 1249 (1965).
406. Jones H., *Proc. Phys. Soc.* (London) **49**, p. 250 (1967).
407. Williams A. R., Weaire D., *J. Phys. C* **3**, p. 387 (1970).
408. Harrison W. A., *Phys. Rev. B* **7**, p. 2408 (1973).
409. Krasko G. L., Makhnovetsky A. V., *Phys. Stat. Sol. B* **66**, p. 349 (1974).
410. Katsnelson A. A., Silonov V. M., Khrushchev M. M., *Fiz. Tv. Tela*, **19**, p. 691 (1977).
411. Cowley J. M., *J. Appl. Phys.* **21**, p. 24 (1950).
412. Iveronova V. I., Katsnelson A. A., *Short-Range Order in Solid Solutions*, Nauka, Moscow, 1977 (in Russian).
413. Ewald P. P., *Ann. Phys.* **64**, p. 253 (1921).
414. Fuchs K., *Proc. Roy. Soc. A* **151**, p. 585 (1935).
415. Krasko G. L., *Pisma Zh. Exper. Teor. Fiz.*, **13**, p. 218 (1974).
416. Cousins C. S., *J. Phys. F* **4**, p. 1 (1974).
417. Tong H. C., Wayman C. M., *Phys. Rev. Lett.* **32**, p. 1185 (1974).
418. Krivoglaz M. A., *Theory of X-Ray and Thermal-Neutron Scattering in Real Crystals*, Nauka, Moscow, 1967 (in Russian).
419. Evans R. et al., *J. Phys. F* **9**, p. 1939 (1979).
420. Zhorovkov M. F., Fuks D. L., Panin V. E., *Phys. Stat. Sol. B* **68**, p. 379, p. 767 (1975).
421. Bagdasaryan R. I., Katsnelson A. A., Silonov V. M., *Kristallografiya*, **22**, p. 191 (1977).
422. Silonov V. M., Khrushchev M. M., Katsnelson A. A., *Fiz. Metall. Metalloved.*, **41**, p. 698 (1976).
423. Khavadzha F. A., Silonov V. M., Katsnelson A. A., *Izv. Vuzov, Ser. Fiz.* **1**, p. 97 (1976).
424. Clapp P. C., Moss S. C., *Phys. Rev.* **142**, p. 418 (1966).
425. Heine V., Jones R., *J. Phys. C* **2**, p. 719 (1969).
426. Katsnelson A. A., Silonov V. M., Khrushchev M. M., *Fiz. Tv. Tela*, **20**, p. 2812 (1978).
427. Hafner J., *Phys. Stat. Sol. B* **57**, p. 101 (1973).
428. Hafner J., *J. Phys. F* **6**, p. 1243 (1976).
429. Vashista P., Singwi K. S., *Phys. Rev. B* **6**, p. 875 (1972).
430. Kozlov E. V., Dementyev V. M., *Izv. Vuzov, Ser. Fiz.*, **8**, p. 21 (1973).
431. Dementyev V. M., Kozlov E. V., in: *Electronic Structure and Physico-Chemical Properties of Transition Metal Alloys and Compounds*, Naukova Dumka, Kiev, 1976 (in Russian).
432. Dementyev V. M., Cand. Thesis, Tomsk University, Tomsk, 1977 (in Russian).
433. Dementyev V. M., Kozlov E. V., *Izv. Vuzov, Ser. Fiz.*, **6**, p. 30 (1974).
434. Stroud D., Ashcroft N. W., *J. Phys. F* **1**, p. 113 (1971).
435. Kogachi M., Matsuo Y., *J. Phys. Chem. Sol.* **32**, p. 2393 (1971).
436. Inglesfield J. E., *J. Phys. C* **2**, p. 1285 (1969).
437. Inglesfield J. E., *J. Phys. C* **2**, p. 1293 (1969).
438. Inglesfield J. E., *Acta Metall.* **17**, p. 1395 (1969).
439. Kogachi M., *J. Phys. Chem. Sol.* **34**, p. 67 (1973).
440. Katada K., Kogachi M., Matsuo Y., *J. Phys. Chem. Sol.* **34**, p. 1703 (1973).
441. Kogachi M., *J. Phys. Chem. Sol.* **35**, p. 109 (1974).
442. Krasko G. L., Gurskii Z. A., *Pisma Zh. Exper. Teor. Fiz.*, **9**, p. 596 (1969).
443. Fuks D. L., Zhorovkov M. F., Panin V. E., *Phys. St. Sol. B* **70**, p. 793 (1975).
444. Fuks D. L., Zhorovkov M. F., Panin V. E., *Phys. St. Sol. B* **71**, p. 87 (1975).
445. Fuks D. L., Zhorovkov M. F., Panin V. E., *Fiz. Metall. Metalloved.*, **39**, p. 384 (1975).

446. Zhorovkov M. F., Fuks D. L., Panin V. E., *Izv. Vuzov, Ser. Fiz.*, 7, p. 80 (1976).
447. Panin V. E., Zhorovkov M. F., Fuks D. L., *Izv. Vuzov, Ser. Fiz.*, 8, p. 22 (1976).
448. Nozieres P., Pines D., *Phys. Rev.* 114, p. 444 (1968).
449. Katsnelson A. A., *Phys. Stat. Sol. B* 52, p. 457 (1972).
450. Khavadzha F. A., Silonov V. M., Katsnelson A. A., *Izv. Vuzov, Ser. Fiz.*, 1, p. 11 (1977).
451. Katsnelson A. A., Silonov V. M., Vasilev G. P., Aksenova O. P., *Izv. Vuzov, Ser. Fiz.*, 4, p. 85 (1978).
452. Khavadzha F. A., Silonov V. H., Koval'chuk A. A., *Izv. Vuzov, Ser. Fiz.*, 12, p. 21 (1976).
453. Safronova L. A., Cand. Thesis, MGU, Moscow, 1977 (in Russian).
454. Katsnelson A. A., Silonov V. M., Khrushchev M. M., Khavadzha F. A., Mekhrabov A. O. O., in: *Atomic Ordering and Alloy Properties*, Tomsk University, Tomsk, 1978 (in Russian).
455. Animalu A.O.E., *Phys. Rev. B* 8, p. 3555 (1973).
456. Silonov V. M., VINITI, Dep. No. 1171-76.
457. Animalu A.O.E., *Proc. Roy. Soc.* 294, p. 376 (1966).
458. Khrushchev M. M., Cand. Thesis, MGU, Moscow, 1980 (in Russian).
459. Katsnelson A. A., *Kristallografiya*, 10, p. 330 (1965).
460. Katsnelson A. A., Sveshnikov S. V., *Izv. Vuzov, Ser. Fiz.*, 7, p. 42 (1975).
461. Bardhean P., Cohen Y. P. *Acta Cryst. A* 32, p. 597 (1976).
462. Iveronova V. I., Katsnelson A. A., *Kristallografiya*, 5, p. 71 (1960).
463. Iveronova V. I., Katsnelson A. A., *Ukr. Fiz. Zh.*, 8, p. 251 (1962).
464. Iveronova V. I., Katsnelson A. A., *Fiz. Metall. Metalloved.*, 19, p. 686 (1965).
465. Kulmanen E. V., Shivrinn O. N., *Izv. Vuzov, Ser. Fiz.*, 5, p. 95 (1968).
466. Averbach B. L., Houska C. R., *J. Appl. Phys.* 30, p. 1525 (1959).
467. Iveronova V. I., Katsnelson A. A., *Fiz. Metall. Metalloved.*, 24, p. 966 (1967).
468. Flinn P. A., *Phys. Rev.* 104, p. 350 (1956).
469. Friedel J., *Adv. Phys.* 3, p. 446 (1954).
470. Katsnelson A. A., Silonov V. M., Khavadzha F. A., *Fiz. Metall. Metalloved.*, 49, p. 51 (1980).
471. Krasko G. L., Makhnovetskii A. V., *Phys. Stat. Sol. B* 80, p. 341 (1977).
472. Krivoglaz M. A., Tju Khao, *Metallofizika*, 24, p. 84 (1968).
473. Blandin A. P., in: *Phase Stability in Metals and Alloys*, ed. by P. S. Rutman et. al., McGraw-Hill, New York-San Francisco-Toronto-London, 1967.
474. Sato H., Toth S. R., *Phys. Rev.* 124, p. 1833 (1961).
475. Dementyev V. M., Kozlov E. V., in: *Calculation Techniques for Energy Structures and Physical Properties of Crystals*, Naukova Dumka, Kiev, 1977 (in Russian).
476. Hafner J., *Phys. Rev. B* 15, p. 617 (1977).
477. Hafner J., *Phys. Stat. Sol. B* 57, p. 427 (1973).
478. Belen'kii A. J., Gurskii Z. A., Krasko G. L., *Fiz. Tv. Tela*, 15, p. 2326 (1974).
479. Frank F. C., Kasper J. C., *Acta Cryst.* 11, p. 184 (1958).
480. Frank F. C., Kasper J. C., *Acta Cryst.* 12, p. 483 (1959).
481. Oli B. A., Animalu O.A.E., *Phys. Rev. B* 13, p. 2398 (1976).
482. Upadhyaya J. C., Dagens L., *J. Phys. F* 8, p. L21 (1978).
483. Vaks V. G., Trefilov A. V., *Fiz. Tv. Tela*, 19, p. 244 (1977).
484. Animalu A.O.E., *Phys. Rev.* 161, p. 445 (1967).
485. Iveronova V. I., Revkevich G. P., *X-Ray Scattering Theory*, MGU, Moscow, 1978 (in Russian).

486. Altshuller A. M., Vekilov Yu. K., Umarov G. P., *Phys. Stat. Sol. B* 69, p. 661 (1975).
487. Begbie G. H., Born M., *Proc. Roy. Soc. A* 188, p. 179 (1947).
488. Kanzaki H., *J. Phys. Chem. Solids* 2, p. 23 (1957).
489. Lifshitz I. M., *Izv. Acad. Nauk SSSR, Ser. Fiz.*, 12, p. 79 (1948).
490. Solt G., *Phys. Rev. B* 18, p. 720 (1978).
491. Solt G., Zhernov A. P., *J. Phys. F* 9, p. 1013 (1979).
492. Belen'kii A. Ya., *Fiz. Metall. Metalloved.*, 44, p. 737 (1977).
493. Hedges C. H., *Phil. Mag.* 15, p. 371 (1967).
494. Dunaev N. M., Zakharova M. I., *Pisma Zh. Exper. Teor. Fiz.*, 20, p. 726 (1974).
495. Katsnelson A. A., Mekhrabov A.O.O., Silonov V. M., *Fiz. Metall. Metalloved.*, 42, p. 278 (1976).
496. Katsnelson A. A., Mekhrabov A.O.O., Silonov V. M., *Fiz. Metall. Metalloved.*, 45, p. 33 (1978).
497. Du Charmé A. P., Weaire H. F., *Sol. St. Comm.* 9, p. 741 (1971).
498. Sacchetti F., *Cryst. Latt. Def.* 7, p. 1 (1977).
499. Chen L. J., Falicov L. M., *Phil. Mag.* 29, p. 1 (1974).
500. Katsnelson A. A., Yastrebov L. I., *Pseudopotential Theory of Crystal Structures*, MGU, Moscow, 1981 (in Russian).
501. Portnoi K. I., Bogdanov V. I., Fuks D. L., *Phase Stability and Phase Interaction Calculation*, Metallurgiya, Moscow, 1981 (in Russian).
502. Panin V. E., Khon Yu. A., Naumov I. I., et al., *Alloy Phase Theory*, Nauka, Novosibirsk, 1984 (in Russian).
503. *Ergebnisse in der Elektronen Theorie der Metalle*, ed. by Ziesche P., Lehmann G., Akademie Verlag, Berlin, 1983.
504. Suzuki T., Granato A. V., Thomas J. F., *Phys. Rev.* 175, p. 766 (1968).
505. Benckert S., *Phys. Stat. Sol. B* 43, p. 681 (1971).
506. Benckert S., *Phys. Stat. Sol. B* 69, p. 483 (1975).
507. Shimada K., *Phys. Stat. Sol. B* 61, p. 325 (1974).
508. Brovman E. G., Kagan Yu. M., *Zh. Exper. Teor. Fiz.*, 52, p. 557 (1967).
509. Brovman E. G., Kagan Yu. M., *Zh. Exper. Teor. Fiz.*, 57, p. 1329 (1969).
510. Vaks V. G., Kravchuk S. P., Trefilov A. V., *Fiz. Tv. Tela*, 19, p. 1271 (1977).
511. Ashcroft N. W., Langreth D. C., *Phys. Rev.* 155, p. 682 (1967).
512. Khanna K. N., Sharma P. K., *Acta Phys. Pol. A* 57, p. 335 (1980).
513. Srivastava S. K., Sharma P. K., *Sol. St. Comm.* 8, p. 703 (1970).
514. Geldart D. J. W., Taylor R., *Canad. J. Phys.* 48, p. 155 (1970).
515. Kushwaha S. S., Baiput J. S., *Phys. Stat. Sol. B* 69, p. 649 (1975).
516. Hafner J., *Sol. St. Comm.* 21, p. 179 (1977).
517. Prasad B., Srivastava R. S., *Phys. Stat. Sol. B* 87, p. 771 (1979).
518. Leibfried G., Ludwig W., in: *Solid State Physics*, vol. 12, ed. by Seitz F., Turnbull D., Academic Press, New York-London, 1969.
519. Belan-Geiko L. V., Bogdanov V. I., Fuks D. L., *Izv. Vuzov, Ser. Fiz.*, 4, p. 36 (1979).
520. Senoo M., Mu H., Fujishiro J., *J. Phys. Sol. Japan* 41, p. 1562 (1976).
521. Girifalco L. A., *Statistical Physics of Materials*, John Wiley and Sons, New York-London-San Francisco-Toronto, 1973.
522. Soma T., *Physica* 92B, p. 1 (1977).
523. Soma T., *Physica* 92B, p. 17 (1977).
524. Ziman J. M., *Phil. Mag.* 6, p. 1013 (1961).
525. Bradley C. C., Faber T. E., Wilson E. G., Ziman J. M., *Phil. Mag.* 7, p. 865 (1962).
526. Faber T. E., Ziman J. M., *Phil. Mag.* 11, p. 153 (1965).
527. Sinha A. K., *Phys. Rev. B* 1, p. 4541 (1970).
528. Evans R., Greenwood D. A., Lloyd P., *Phys. Lett. A* 35, p. 57 (1971).
529. Cote P. J., *Sol. St. Commun.* 18, p. 1311 (1976).

- 530. Chen A., Weisz G., Sher A., *Phys. Rev. B* 5, p. 2897 (1972).
- 531. Brouers F., Brawers M., *J. Phys. (Paris)* 36, p. 17 (1975).
- 532. Markowitz A., *Phys. Rev. B* 15, p. 3617 (1977).
- 533. Harris R., Shalmon H., Zuckermann M., *Phys. Rev. B* 18, p. 5906 (1978).
- 534. Cote P. J., Meisel L. V., *Phys. Rev. Lett.* 39, p. 102 (1977).
- 535. Ruppertsberg H., Egger H., *J. Chem. Phys.* 63, p. 4095 (1975).
- 536. Katsnelson A. A., Safronova L. A., *Izv. Vuzov, Ser. Fiz.*, 1, p. 18 (1976).
- 537. Ziman J. M., *Principles of the Theory of Solids*, Cambridge Univ. Press, 1972.
- 538. Khar'kov E. I., Lysov V. I., Fedorov V. E., *Physics of Liquid Metals*, Vyzcha Shkola, Kiev, 1979 (in Russian).
- 539. Dreirach O., Evans R., Gunterodt H. J., Künz H. U., *J. Phys. F* 2, p. 709 (1972).
- 540. Vasseda Y., Wright J. G., *Phys. Stat. Sol. B* 81, p. K37 (1977).
- 541. Katsnelson A. A., Silonov V. M., *Pseudopotential Theory of Liquid and Amorphous Metal Alloys*, MGU, Moscow, 1984 (in Russian).
- 542. Bhatia A. B., Thornton D. E., *Phys. Rev. B* 2, p. 3004 (1970).
- 543. Van Hove L., *Phys. Rev.* 96, p. 249 (1954).
- 544. Meisel L. V., Cote P. J., *Phys. Rev. B* 16, p. 2978 (1977).
- 545. Meisel L. V., Cote P. J., *Phys. Rev. B* 17, p. 4652 (1978).
- 546. Katsnelson A. A., Shevchuk L. M., *Fiz. Metall. Metalloved.*, 24, p. 683 (1967).
- 547. Wagner C. N., Ruppertsberg H., *Atomic Energy Review Suppl.*, 1, p. 101 (1981).
- 548. Katsnelson A. A., Aleshina L. A., Kruchinkina V. I., Popova I. I., Silonov V. M., Fofanov A. D., *Fiz. Tv. Tela*, 27, p. 807 (1985).
- 549. Bhatia A. B., Gupta O. P., *Phys. Lett.* A29, p. 358 (1969).
- 550. Katsnelson A. A., Kruchinkina V. I., Popova I. I., Silonov V. M., *Izv. Vuzov, Ser. Fiz.*, 6, p. 50 (1984).
- 551. Guntherodt H. J. and Beck H. (ed.) *Glassy Metals*, vol. 1, Springer, New York, 1981.
- 552. Gumbatov S. G., Pavlova G. Kh., Shikov A. A., *Fiz. Metall. Metalloved.*, 58, p. 292 (1984).
- 553. Aleksandrov B. N., Dalanova N. V., *Fiz. Metall. Metalloved.*, 59, p. 837 (1985).

Subject Index

Alloy

- charge flow in 129
- disordered 245, 246
- pseudopotential theory of 236, 241
- screening in 123
- total energy of 227

Andersen's radii 168

Approximation

- adiabatic (Born-Oppenheimer) 11, 267
- atomic sphere 113, 176, 204
- Born 5, 7, 62, 63-65, 67, 87, 104, 107, 163, 172
- Born-Begbie 282, 283
- coherent potential 129, 297
- Debye 278, 296, 304, 307
- effective field 11
- Fermi sphere 125, 135, 139, 143, 160, 162, 171
- Hartree 94, 98
- Hartree-Fock 71, 75-78
- Hubbard-Sham 285
- MT 107
- relaxation time 297
- Thomas-Fermi 71, 89, 92, 94-96, 104
- tight-binding (*see* model LCAO) 15, 297
- virtual (average) crystal 218, 241
- X_α - 73, 75, 77, 78, 81, 83, 106, 107, 117

Atomic displacement 179, 281, 182, 184, 304

Bloch's theorem 11, 12, 272

Born-Mayer repulsion 275

Brillouin zone 12, 77, 134, 141, 215-217, 228-230, 234, 242, 243, 261, 283, 284

Cell

- atomic 48
- Wigner-Seitz 12, 16, 17, 43, 103-106, 108, 111, 113, 114 121-123, 131, 157, 175, 176, 177-178, 180, 192

Criterion

- Bargmann's 54, 91, 98, 163
- convergence 98
- optimization 59, 60, 103, 104, 112, 114, 171
- Lindeman's 49
- minimum perturbation 128
- Pendry's 98
- smoothness 80

Debye-Waller factor 277, 278, 304-309

Depletion (orthogonalization) hole 153, 170, 239, 240

Dispersion law 12, 14, 15, 18-20, 49, 59, 119, 136-139, 167, 182, 216

Effective medium 129, 173-175, 179

Electrical resistivity 298-300, 302, 303, 310, 313, 314

Electronegativity 70, 76

Energy

- band structure 20, 211-213, 218, 228, 233, 235, 240, 241, 248, 250, 252, 257, 263, 267, 270, 272, 273, 279, 282, 289

Energy

- cohesion 49, 52, 134, 233, 261, 292, 294
- configurational part of 227, 232, 234, 241, 247, 254, 270, 275
- correlation 288
- electron-electron interaction 21
- electrostatic 211, 212, 223, 225, 226, 229, 233, 240, 241, 243, 249, 250, 252, 253, 257, 270, 272, 273, 277, 282, 289
- exchange 288
- Fermi 42, 45, 79, 90, 116, 125, 127, 128, 135, 139, 156, 171, 172, 180, 182
- free 273, 283, 298, 302
- internal 257, 261, 283
- kinetic 47, 205, 271, 282
- mixing 254-256
- ordering 246-248, 151, 253, 255, 256
- pairwise contribution to 233
- phonon contribution to 273, 275
- potential 271
- repulsion 252, 253
- self-diffusion activation 296
- short-range-order contribution 236
- structure-dependent contribution to 205, 213, 214
- structure-independent contribution to 213, 214
- total 19, 20, 189, 205, 211-213, 217-219, 223, 229, 234, 242, 243, 247, 248, 252, 254, 261, 279, 282-284, 287-290
- vacancy formation 296
- volume-dependent contribution to 289

Equation

- Hartree-Fock 69, 74
- Lippman-Schwinger 55
- of state 293, 294

Equation

- Poisson 86, 111, 113, 224
- Schrödinger 11-13, 23, 59, 60, 66, 68, 69, 109, 115, 149, 154, 168, 174, 176, 190, 237

Ewald

- method 223
- energy 250, 257

- Exchange-correlation interaction 96, 210, 215, 239, 241, 243, 245, 254, 256, 257, 285, 289, 293, 316
- Exchange interaction 20, 96, 106

- Fermi sphere 20, 21, 73, 116, 117, 136, 144, 151, 173, 179, 215, 217, 218, 233, 242, 243, 261, 262, 298, 300
- Formfactor 9, 16, 17, 21, 47, 61, 67, 68, 87, 91, 92, 95, 100, 104, 105
- APW 157-159, 167, 172, 178, 180
- definition 16
- E -dependence of 135, 162
- KKRZ 157, 165-167, 170, 175, 177, 178, 180
- long wavelength limit of 124, 170, 173, 179
- model 162
- nonlocal 17, 133
- nonlocality and energy dependence of 132
- OPW 144, 152, 155, 165-167
- phase-shift 157-159, 161, 163, 168, 170-172, 179, 180
- potential 86
- pseudopotential 32, 149, 151, 173, 214, 222, 223, 233
- q -dependence of 132, 161
- quasi-local 135
- t -matrix 302

- Friedel oscillations 46, 90, 91, 94, 103, 104, 214, 223, 230
- Friedel sum 49, 44, 45, 125, 126-131, 154, 155, 171, 172, 178-180
- definition of 44
- rule 43-45

Function

- Bessel 27, 28, 37, 161, 164, 165, 167, 170, 200
- characteristic (energy-wave-number function) 22, 210, 211, 213, 261, 263, 289, 290

Function

- characteristic function of alloying
 - 245, 246
 - dielectric 86, 88-90, 95, 123, 127, 130
- Green's 23-25, 27, 30, 31, 54, 55, 61, 87, 144, 152, 157, 158, 174, 181, 184, 185, 190, 191, 196, 283
- spectral expansion of 24
- Hankel 27, 29
- Lindhard's 21, 87, 95, 274, 209
- Neuman 17, 28, 66, 200
- phase 50-52, 55, 115
- pseudowave 146
- trial 13-15, 66, 157
- Wannier 120

Gaunt's coefficients 26, 161, 185

Grüneisen's constant 295, 296

Harmonics

- cubic (real) 26, 27, 161
- spherical 25-27

Hume-Rothery rules 215, 217, 240, 243, 263

Hybridization 15, 142, 147, 148, 156, 210, 215

Imperfections 266

- dynamic 267
- static 267, 279

Impurity 45, 131, 267, 281, 285, 286

effective radius 45

Laves phases 263, 264

Level

- quasi-stationary 40
- resonant 40
- width 37

Levinson's theorem 39, 40, 50

Logarithmic derivative 34-36, 53, 292

Long-range order 219, 221-224, 227, 232, 248, 249, 257

Method

- APW 106, 107, 113, 157, 158, 160, 161, 174, 183
- KKRZ 68, 144, 157, 158, 160, 168, 182, 183, 194
- KKR 31, 85, 106, 120, 144, 157, 160, 181, 183, 184, 194, 195
- LCAO 42, 106, 194
- Mattheis 110
- mixed basis 151
- OPW 85, 97, 113, 151, 152, 183
- phase-function 50
- Thomas-Fermi-Dirac-Weizsacker 94

Model

- atomic sphere 178

Model

- Drude-Lorentz-Sommerfeld 297
- empty lattice 17, 142, 184
- LCAO 15-17, 20, 38, 40, 54, 106, 139, 147, 149, 151, 156, 157, 185, 193, 196
- NFE 7, 8, 16, 42, 45, 47, 51, 53-55, 57, 71, 90, 112, 125, 136, 138, 139, 143, 149, 156, 157, 191-193, 301
- quasi-excited atom 118-120
- solitary cell 191

Normalization 27, 33, 43, 53, 62,

- at infinity 33
- at the origin 33
- factor 25, 26, 124
- integral 16, 39, 154
- plane wave 16, 33

Operator

- dielectric 84, 85, 106
- projection 30, 31, 58, 237
- t - 62, 63, 302

Optimization of a pseudopotential 59, 77, 113, 131, 168, 170-173, 177, 294

Orbital relaxation 70, 76, 78

- Phase shift 31-33, 38, 43, 45-48, 50,
 51, 115, 116, 128, 157, 163, 170,
 171, 173, 174
 Phase transition 8, 215, 244, 275
 Phonon spectra 293, 294
 Potential
 Ashcroft 94, 303
 atomic 16, 19, 43, 80, 84
 atomic sphere 114
 Born-Mayer 96
 centrifugal 42, 43
 chemical 70
 Coulomb 17, 46, 72, 74, 79, 88, 89,
 91, 92, 95, 97, 105, 112, 133,
 142, 213, 240
 crystal 11, 16, 21, 43, 75, 83-85, 91,
 100, 102, 103, 106, 108, 111, 114,
 120, 124, 125, 145, 159, 165,
 235, 239
 deformation 284, 285
 empty atom 94
 empty core 94
 exchange 69, 71-75, 77, 80, 81, 83,
 94, 106, 111, 112, 116
 exchange-correlation 88
 Gaspar-Kohn-Sham 73, 75, 81
 hard sphere 36, 54
 hybridization 223
 impurity 45, 130, 131, 284
 interaction 175, 185
 interatomic interaction 22, 90, 95,
 96, 223, 230, 263, 264, 285, 295
 linear screening 125, 127-129, 177
 local 75, 78, 87, 236, 240
 minimum perturbation 126-129
 MMT 116
 model 56, 109, 180, 236, 247, 253,
 254, 296, 315
 Potential
 muffin-tin 36, 107, 158, 173, 176,
 177, 180, 182, 195, 198
 nonlocal 17, 266, 275
 ordering 228, 230, 231, 234, 236, 259
 pairwise alloying 247
 perturbation 19, 86
 pseudoatom 91, 92, 95, 100
 repulsion 42, 103, 252
 screening 48, 84, 85, 101, 105-107,
 113, 114, 119, 120
 self-consistent 99, 102, 103,
 112
 single-site 12, 16, 92, 98, 100, 107,
 113, 114, 122, 128
 thermodynamic 273, 275, 277
 true 16, 37, 51, 181
 Wigner-Seitz cell 108
 Yukawa 90
 Pseudism 7, 8, 46, 49, 181
 definition 7
 Pseudoatom 83, 84, 92, 94, 95, 95, 97,
 98, 100, 102, 104, 113, 127,
 130
 definition 84
 Pseudopotential
 alloy 307
 Animalu 257, 259
 Ashcroft 92, 94
 modified Ashcroft 138
 crystal 105, 130, 284
 definition 7
 Harrison's 238
 Heine-Abarenkov-type 82, 95, 104,
 127, 296
 Pseudopotential
 KKRZ 160, 164, 177
 Lloyd 53, 54, 68, 177, 181
 local 137, 171, 245, 256, 294,
 302
 minimum perturbation 60
 model 59, 92, 94, 98, 138, 143, 156,
 292
 nonlocal 65, 124, 126, 133, 257
 OPW 7, 59, 63, 144, 152, 156, 236,
 237
 phase-shift 157, 170-172
 Phillipps-Kleinman 237
 R-matrix 65, 66
 screening 98
 Shaw 92, 93
 single-site 98
 "structural" 201
 total crystal 98

- Rennert oscillations 90
 "Repelled" solutions 139-144
 Repulsion, Coulomb 20, 21, 69, 74, 75, 78-80, 82
 Residual resistance 280
- Scattering 8, 9, 23, 40
 amplitude 61
 elastic 64
 hard-sphere 36, 39
 impurity 45
 on an isolated potential 31, 54
 Scattering
 partial amplitude 39
 resonance 55
- Screening
 additive 99, 101, 102, 104, 106, 111, 123, 128
 additive screening in the MT model 121, 122
 "background" 91
 dielectric 8, 21, 83, 86, 91, 92, 95, 98, 99-107, 109, 114, 121-125, 127-129
 in alloys 98, 123
 linear 8, 94, 98, 102, 125, 239
 mechanism 21
 nondiagonal 5, 86
 nonlinear 102
 potential 96
 Thomas-Fermi 94, 104
- Secular equation 8, 13, 26, 18, 31, 53
 KKR 183-190
 pseudism in 201
 pseudopotential 196
- Self-action 69, 74, 81
- Short-range order 219-221
 compositional 297, 304, 307, 309
 parameter 99, 223, 224, 226, 231, 232, 248, 249, 252, 256-259, 261
 definition of 220
 topological 297, 309
- Sphere
 atomic 104, 113, 122, 123, 131
 coordination 214, 231, 252, 284, 296
 Fermi sphere-Brillouin zone boundary relationship 215
 hard 36, 163, 195
 muffin-tin 43, 107, 111, 131, 173, 175, 197
 Wigner-Seitz 43, 79, 103, 104, 111-114, 122, 137, 176, 178, 210
- Stability 7-9, 96, 97, 210, 215, 218, 241, 261, 286
 of ordered alloys 228
- State
 bound 19, 39-41, 44, 46, 47, 49, 50, 54-56, 59, 60, 63, 64, 66, 83, 97, 98, 127, 164
 density of states 44
 quasi-bound 142, 183
 resonance 43, 49, 90
 virtual 49
- Statistical approach 71, 72, 74, 82
- Structure factor 17, 98, 124, 184, 238, 279, 285, 299, 300, 302-306, 308-309-312, 315
 Röntgen 241
- Theorem
 Austin-Heine-Sham 57, 59, 65
 Bargmann's 55
 Koopman's 70, 77
 Poisson 112
 virial 47
- Thermo-emf 280, 297, 300-303, 315, *t*-matrix 62, 63, 297, 302
- Transport properties 297, 300, 315
- Vegard's rule 261, 263

